

CR 151807

REPORT NO. CASD-NAS-78-007

CONTRACT NAS9-14095

(NASA-CR-151807) SPACE SHUTTLE ORBITER	N78-29142
REACTION CONTROL SYSTEM INTERACTIONS WITH	
THE VEHICLE FLOW FIELD Final Report	
(General Dynamics/Convair) 390 p	Unclas
HC A17/HF A01	CSSL 01A G3/16 28499

SPACE SHUTTLE ORBITER REACTION CONTROL SYSTEM INTERACTIONS WITH THE VEHICLE FLOW FIELD

FINAL REPORT

GENERAL DYNAMICS
Convair Division



REPORT NO. CASD-NAS-78-007

**SPACE SHUTTLE ORBITER REACTION
CONTROL SYSTEM INTERACTIONS
WITH THE VEHICLE FLOW FIELD**

FINAL REPORT

May 1978

J R Rausch

Prepared Under
Contract NAS9-14095

Prepared by
GENERAL DYNAMICS CONVAIR DIVISION
P O Box 80847
San Diego, California 92138

FOREWORD

The present study was undertaken by the Convair Division of General Dynamics under NASA Contract NAS9-14095 and this report covers work undertaken from 15 May 1977 through 1 May 1978. The contract monitor was Mr. Barney Roberts of the NASA Johnson Space Center, Houston, Texas and the author wishes to acknowledge his very valuable assistance, direction, and contributions to the successful completion of the study. The test data was obtained from models designed, built, and tested by Rockwell International personnel at NASA Langley Research Center and at Arnold Engineering Development Center. H. Dresser, J. Daileida, and J. Marroquin of Rockwell were most helpful and cooperative in providing test data and reports which greatly assisted in the completion of this study. Mr. D. Kanipe, NASA-JSC, also greatly assisted in providing test data and corrections for Test IA148, which is the primary source of data for the mated Orbiter plus tank.

CONTENTS

Section		Page
1	INTRODUCTION	1-1
2	TEST SUMMARY	2-1
2.1	Configurations and Reference Dimensions	2-1
2.1.1	Orbiter Configuration	2-1
2.1.2	Mated Configuration	2-1
2.2	RCS Data Base	2-2
2.2.1	MA22 Test Program Summary	2-2
2.2.2	IA148 Test Program Summary	2-3
2.3	Data Reduction Procedure	2-4
3	YAW ANGLE EFFECTS ON REAR-MOUNTED RCS DATA	3-1
3.1	Introduction	3-1
3.2	Yaw Effects on Rear-Mounted RCS Interaction	3-1
3.2.1	Pitch-Down RCS Interactions	3-2
3.2.1.1	Normal Force Increments	3-2
3.2.1.2	Pitching Moment Increments	3-2
3.2.1.3	Rolling Moment Increments	3-2
3.2.1.4	Yawing Moment Increments	3-2
3.2.1.5	Side Force Increments	3-3
3.2.2	Pitch-Up RCS Data	3-3
3.2.2.1	Normal Force Increments	3-3
3.2.2.2	Pitching Moment Increments	3-3
3.2.2.3	Rolling Moment Increments	3-3
3.2.2.4	Yawing Moment Increments	3-4
3.2.2.5	Side Force Increments	3-4
3.2.3	Yaw RCS Interactions	3-4
3.2.3.1	Normal Force Increments	3-4
3.2.3.2	Pitching Moment Increments	3-4
3.2.3.3	Rolling Moment Increments	3-4
3.2.3.4	Yawing Moment Increments	3-4
3.2.3.5	Side Force Increments	3-5
3.3	Conclusions	3-5

CONTENTS (Contd)

Section		Page
4	REAR-MOUNTED RCS CONTROL EFFECTIVENESS DURING RTLS	4-1
4.1	General	4-1
4.2	RTLS Flight Conditions	4-1
4.3	Symmetric Pitch-Down RCS	4-1
4.3.1	Effect of Angle of Attack	4-2
4.3.2	Effect of Altitude	4-2
4.3.3	Effect of Mach Number	4-2
4.3.4	Effect of Dynamic Pressure	4-2
4.3.5	Effect of Atmospheric Variation	4-2
4.3.6	Effect of Reynolds Number	4-2
4.3.7	Summary	4-3
4.4	RCS Roll Control	4-3
4.4.1	Effect of Altitude	4-4
4.4.2	Effect of Atmosphere Variation	4-4
4.4.3	Roll Control Effectiveness Maps	4-4
4.4.3.1	Pitch-Up RCS Roll Control Map	4-4
4.4.3.2	Pitch-Down RCS Roll Control Map	4-5
4.4.3.3	No RCS Roll Control Map	4-5
5	FORWARD-MOUNTED RCS CONTROL EFFECTIVENESS	5-1
5.1	General	5-1
5.2	Forward-Mounted Pitch-Up Jet Normal Force Model	5-2
5.3	Forward-Mounted Pitch-Up Jet Pitching Moment Model	5-2
5.4	Forward-Mounted Pitch-Up Jet Axial Force Model	5-2
6	MATED CONFIGURATION DATA ANALYSIS	6-1
6.1	IA148 Test Data	6-1
6.1.1	RC06 Test Data	6-2
6.1.2	RC38 Test Data	6-2
6.1.3	RC40 Test Data	6-2
6.1.4	RC51 Test Data	6-2
6.1.5	RC78 Test Data	6-3
6.1.6	RC82 Test Data	6-3

CONTENTS (Contd)

Section	Page	
6.2	Data Analysis	6-3
6.2.1	Effect of Yaw Angle	6-5
6.2.2	Superposition of Data	6-6
6.2.3	Correcting Jet-Off Differences from Data	6-7
7	TANK-ON INCREMENTAL EFFECTS	7-1
7.1	UZCMD = 0	7-1
7.1.1	UXCMD = 2	7-1
	7.1.1.1 UYCMD = 5	7-1
	7.1.1.2 UYCMD = 1	7-2
	7.1.1.3 UYCMD = 0	7-2
	7.1.1.4 UYCMD = -1	7-3
	7.1.1.5 UYCMD = -3	7-4
7.2.1	UXCMD = 0	7-4
	7.1.2.1 UYCMD = 5	7-4
	7.1.2.2 UYCMD = 1	7-5
	7.1.2.3 UYCMD = 0	7-5
	7.1.2.4 UYCMD = -1	7-5
	7.1.2.5 UYCMD = -3	7-6
7.1.3	UXCMD = -2	7-6
	7.1.3.1 UYCMD = 5	7-6
	7.1.3.2 UYCMD = 1	7-7
	7.1.3.3 UYCMD = 0	7-7
	7.1.3.4 UYCMD = -1	7-8
	7.1.3.5 UYCMD = -3	7-8
7.2	UZCMD = 1, -1	7-9
7.2.1	UXCMD = 2	7-9
	7.2.1.1 UYCMD = 5	7-9
	7.2.1.2 UYCMD = 1	7-10
	7.2.1.3 UYCMD = 0	7-10
	7.2.1.4 UYCMD = -1	7-11
	7.2.1.5 UYCMD = -3	7-11
7.2.2	UXCMD = 0	7-12
	7.2.2.1 UYCMD = 5	7-12
	7.2.2.2 UYCMD = 1	7-12
	7.2.2.3 UYCMD = 0	7-13
	7.2.2.4 UYCMD = -1	7-13
	7.2.2.5 UYCMD = -3	7-13

CONTENTS (Concl'd)

Section		Page
	7.2.3 UXCMD = -2	7-14
	7.2.3.1 UYCMD = 5	7-14
	7.2.3.2 UYCMD = 1	7-14
	7.2.3.3 UYCMD = 0	7-15
	7.2.3.4 UYCMD = -1	7-15
	7.2.3.5 UYCMD = -3	7-15
7.3	Mated Configuration Incremental Effects Prediction Routines	7-16
	7.3.1 - RCS Subroutine	7-16
	7.3.2 FITS Subroutine	7-17
8	CONCLUSIONS	8-1
	8.1 Study Conclusions	8-1
	8.2 Study Recommendations	8-2
9	REFERENCES	9-1
Appendix		
A	IA148 Curve Fit Coefficients at Zero Degrees Yaw	A-i
B	IA148 Curve Fit Coefficients at +4 Degrees Yaw	B-i
C	IA148 Curve Fit Coefficients at -4 Degrees Yaw	C-i
D	RCS and FITS Program Listings	D-i

ILLUSTRATIONS (Concl'd)

Figure		Page
6-1	Mated configuration reaction control combinations, UZCMD = 0	6-9
6-2	Mated configuration reaction control combinations, UZCMD = 1	6-9
6-3 } thru } 6-8 }	Jet-off sample data	6-10 thru 6-15
6-9 } thru } 6-13 }		RC06 sample data
6-14 } thru } 6-19 }	RC38 sample data	
6-20 } thru } 6-25 }		RC40 sample data
6-26 } thru } 6-31 }	RC51 sample data	
6-32 } thru } 6-37 }		RC78 sample data
6-39 } thru } 6-42 }	RC82 sample data	
6-43 } thru } 6-66 }		RC78 sample correlations
6-67 } thru } 6-72 }	RC78 yaw angle correlation samples	
6-73 } thru } 6-84 }		Superposition effect sample data
7-1	Schematic flow diagram for RCS subroutine	
7-2	Schematic flow diagram for FITS' subroutine	7-20
7-3	Body axis sign convention	7-21

ILLUSTRATIONS

Figure		Page
1-1	Reaction control subsystem elements	1-1
2-1	139B Orbiter configuration	2-7
2-2	OA169 Orbiter model	2-8
2-3	OA169 sting mount	2-9
2-4	Mated configuration sketch	2-10
2-5	Forward-mounted RCS jets simulated during Test IA148	2-11
2-6	Rear-mounted RCS jets simulated during Test IA148	2-12
3-1	Yaw effects on pitch-down RCS	3-5
thru		thru
3-15		3-19
3-16		3-20
thru		thru
3-30	Yaw effects on pitch-up RCS	3-34
3-31		3-35
thru	Yaw effects on yaw RCS	thru
3-45		3-49
4-1		4-6
4-2	Symmetric pitch-down error analysis	4-7
thru		thru
4-8		4-13
4-9	Typical roll interaction increment at low angles of attack for rear-mounted pitch-up jets	4-14
4-10	Symmetric roll error analysis	4-15
thru		thru
4-15		4-20
4-16	Roll control deadband for downward firing rear RCS units	4-21
4-17	Rear RCS roll control deadband	4-22
4-18	Symmetric rear RCS roll control deadband	4-23
5-1	Symmetric forward-mounted pitch-up jet data	5-3
thru		thru
5-3		5-6
5-4	Combined fore and aft jet data	5-7
thru		thru
5-6		5-9
5-7	Computed forward-mounted jet data	5-10
thru		thru
5-9		5-12
5-10	Forward-mounted jet correlation model data	5-13
thru		thru
5-12		5-16

TABLES

Table		Page
2-1	Test IA148 available RCS thruster locations	2-5
2-2	Summary of simulation parameters for RTLS abort simulation	2-6
4-1	Atmospheric variation	4-6

NOMENCLATURE

<u>Symbol</u>	<u>Definition</u>
A	area (ft ²)
b	lateral-directional reference length (ft)
\bar{c}	wing chord reference length (ft)
C_{ℓ}	body axis rolling moment coefficient = (rolling moment)/q S _{ref} b
C_m	body axis pitching moment coefficient = (pitching moment)/q S _{ref} \bar{c}
C_N	body axis normal force coefficient = (normal force)/q S _{ref}
C_n	body axis yaw moment coefficient = (yawing moment)/q S _{ref} b
C_P	pressure coefficient = (P - P _∞)/q
C_t	thrust coefficient = T/q S _{ref}
C_y	body axis side force coefficient = (side force)/q S _{ref}
C_D	nozzle discharge coefficient = measured thrust/ideal thrust
d	diameter (ft)
h	kinetic energy parameter (ft ² /sec ²)
K	force or moment amplification factor
ℓ_{ref}	longitudinal reference length (ft)
ℓ_B	body length (ft)
\dot{m}	mass flow (lbm/sec)
M	Mach number
n	number of jets in cluster
P	pressure (lbf/ft ²)
q	dynamic pressure (lbf/ft ²)
R	gas constant (ft ² /sec ² -°R)
r	radius (ft)
R_e	Reynolds number
S_{ref}	wing reference area (ft ²)
t	time (sec)

NOMENCLATURE (cont'd)

<u>Symbol</u>	<u>Definition</u>
T	thrust (lb)
T	temperature (°R)
V	velocity (ft/sec)
x	radial distance (ft)
α	angle of attack (deg)
β	angle of yaw (deg); also $\sqrt{M^2 - 1}$
θ_N	nozzle angle (deg)
θ	angular orientation in jet (deg)
ρ	density (lbm/ft ³)
γ	ratio of specific heat
Φ	momentum parameter (lbf) = $\gamma P M^2 A$
 <u>Subscripts</u>	
amb	ambient conditions
c	rocket chamber condition
i	initial condition or conditions at point i
j	jet exit conditions
l	local condition or rolling moment
MAC	mean aerodynamic chord
M	any force or moment coefficient
m	pitching moment
n	yawing moment
N	normal force
o	total conditions
y	side force
p	peak
∞	free stream condition
interaction	increment due to plume interaction

NOMENCLATURE (cont'd)

Symbol

Definition

Subscripts (cont'd)

impingement	increment due to plume impingement
cross coupling	increment due to combined jets interacting
thrust	thrust terms
total	sum of all terms

Superscripts

$\bar{\quad}$	mean value or averaged value
-	throat condition

SUMMARY

This is the final technical report and it documents the work performed through 1 May 1978 under NASA Contract NAS9-14095.

The Space Shuttle Orbiter has forward-mounted and rear-mounted Reaction Control Systems (RCS) which are used for orbital maneuvering and to provide control during entry and abort maneuvers in the atmosphere. RCS control effectiveness is critical to Orbiter flight performance and safety. The subject of this study is the effect of interaction between the RCS jets and the flow over the vehicle in the atmosphere.

Earlier reports from this study have documented the analysis of test data on the rear-mounted RCS units on the Orbiter alone and the resulting prediction techniques developed from these data.

This report documents the continuing analysis of the data for the rear-mounted RCS on the Orbiter alone, particularly in the examination of yaw angle effects. The report also documents mated tank-plus-Orbiter jet interactions resulting from combinations of forward and rear-mounted RCS units being fired prior to external tank staging. The primary RCS correlating parameter used for the mated data is a single-jet momentum ratioed to free-stream momentum.

An analytic model is also presented for computing RCS interactions for all control combinations used for mated vehicle coast.

1

INTRODUCTION

The Space Shuttle Orbiter has a large number of reaction-control jets clustered into three groups of controls, as shown in Figure 1-1. The group mounted in the nose of the vehicle consists of four yaw, four pitch-up/roll, three pitch-down/roll, and three translational thrusters (not including the vernier thrusters). The two rear-mounted groups are contained on the Orbital Maneuvering System (OMS) pods of the vehicle and consist of four yaw, three pitch-up/roll, three pitch-down/roll, and two translational

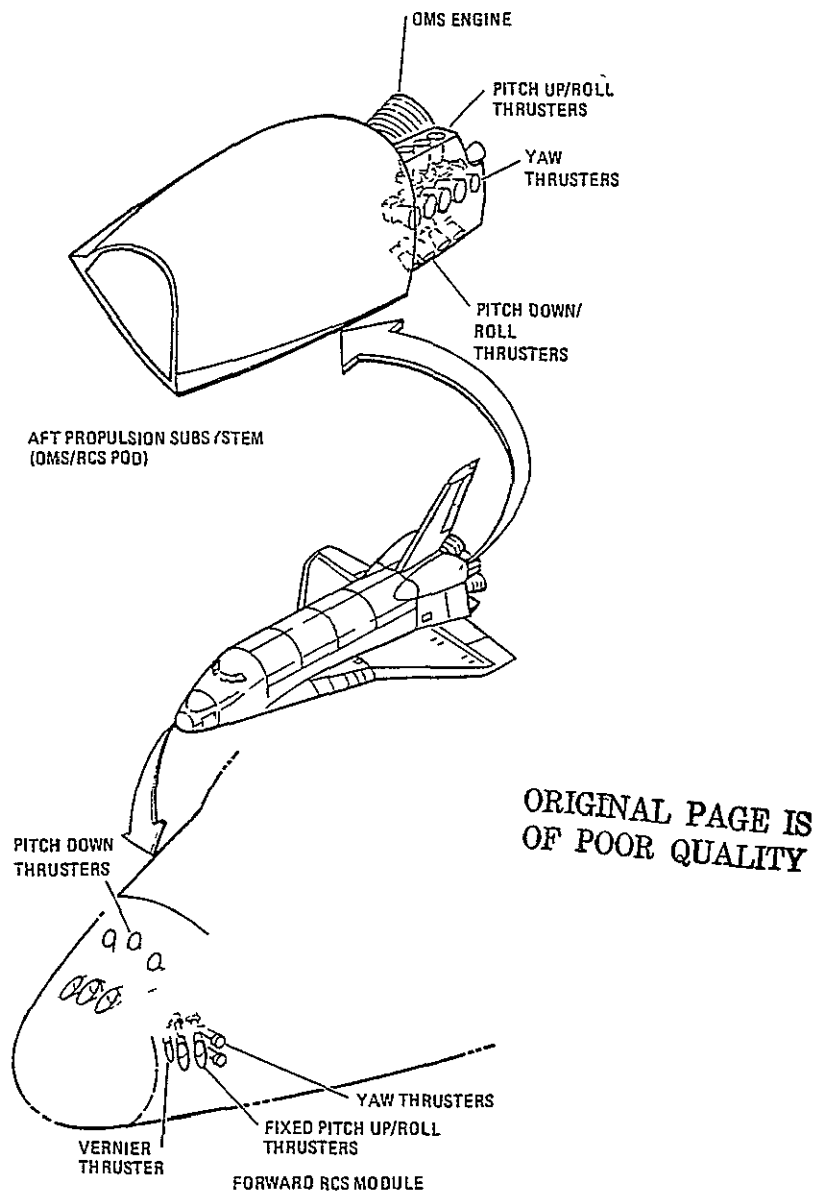


Figure 1-1. Reaction control subsystem elements.

thrusters per pod. These RCS units are used to provide orbital maneuvering control, control during entry, and control during staging. Orbital maneuvering control is outside the scope of this analysis.

The rear-mounted RCS units are required to provide control during entry until the aerodynamic control surfaces have sufficient effectiveness to assume full control of the vehicle. This entry case has been analyzed in detail in prior work on this contract and that work is presented in References 1 through 4. Both forward and rear-mounted RCS units are used during coasting flight to separate the Orbiter from the external tank in normal and abort staging maneuvers to stabilize the mated configuration and to separate the Orbiter from the tank. In addition, during abort the RCS units are used to pitch the vehicle up to entry attitude and to control it until aerodynamic control is established.

The studies performed in References 1 through 4, including wind tunnel data on the present baseline Orbiter, have shown that the control effectiveness of the RCS system is appreciably changed by the presence of air flow over and around the vehicle. These RCS/flow interactions have acted in directions such that the net RCS system effectiveness is much lower than the thrust moments alone, and it is critical to flight safety and performance to know what causes the induced RCS/flow interaction moments, and to develop methods to predict them. These are the basic purposes of the studies conducted under NASA Contract NAS9-14095. Reference 1 was the final report of the work performed on this contract through April 1977 and documented the data analysis and analytic model development for RCS flow interference prediction for the entry case.

This report extends the analysis presented in Reference 1 to the RTLS case for the rear-mounted jets and also includes investigated effects of yaw angle. In addition, test data for the mated Orbiter and tank have been analyzed and are presented. This report contains seven major sections:

<u>Section</u>	<u>Title</u>
2	Test Data Summary
3	Yaw Angle Effects on Rear-Mounted RCS Data
4	Rear-Mounted RCS Control Effectiveness During RTLS
5	Forward-Mounted RCS Control Effectiveness
6	Mated Configuration Data Analysis
7	Tank-On Incremental Effects
8	Conclusions



TEST SUMMARY

2.1 CONFIGURATIONS AND REFERENCE DIMENSIONS

2.1.1 ORBITER CONFIGURATION. Figure 2-1 presents the Space Shuttle Vehicle 102 Orbiter configuration used to develop the Orbiter-alone data base defined in Reference 1. The geometry of the model is defined in detail in Reference 7. The model was sting-mounted in all tests, in an arrangement similar to the AEDC VKF Tunnel B installation shown in Figure 2-2. The presence of the sting (Figure 2-3) prevented full simulation of the vehicle base geometry during all rear-mounted RCS tests. However, the major features were maintained as much as possible. Possible effects of sting mounting were shown in Reference 3, but no further data have been obtained to clarify this issue.

All Orbiter data used in this report are referenced to an axial location of 65% of body length and a vertical water line 25 inches below the fuselage reference line shown in Figure 2-1. In full scale vehicle dimension

- a. Vehicle nose Station 238
- b. (X) Moment reference center Station 1076.7
- c. (Z) Moment reference center waterline 375
- d. (Y) Moment reference center butt line 0

All data used in the analysis were reduced to coefficient form using the Orbiter wing area as the reference area, the wing mean aerodynamic chord (\bar{c}) as the longitudinal reference length, and the wing span (b) as the lateral-directional reference length.

- a. $S_{\text{ref}} = S_{\text{wing}} = 2690 \text{ ft}^2 (249.9 \text{ meters}^2)$
- b. $\bar{c} = 39.567 \text{ ft} (12.06 \text{ meters})$
- c. $b = 78.058 \text{ ft} (23.79 \text{ meters})$

2.1.2 MATED CONFIGURATION. The configuration shown in Figure 2-4 (Orbiter mated with external tank) was used to develop the data base. The external tank designated Model 70-OT is defined in Reference 7. The model test designated IA148, which forms the mated configuration data base, was tested with the balance in the Orbiter on the sting mount shown in Figure 2-2 and the external tank attached to the Orbiter.

All mated-configuration data presented in this report are referenced to an axial location 58.8% of body length aft of the Orbiter nose and on a vertical waterline 102.2

inches below the fuselage reference line. The reference location in full scale dimensions relative to the Orbiter coordinate system is:

- a. Moment reference center station = 993.64
- b. Moment reference center waterline = 297.8
- c. Moment reference center butt line = 0

All data were reduced to aerodynamic coefficient form, using Orbiter wing area as reference area and body length as the reference length for all moments.

- a. $S_{ref} = 2690 \text{ ft}^2$ (249.9 meters²)
- b. $\bar{c} = 107.53 \text{ ft}$ (32.774 meters)
- c. $b = 107.53 \text{ ft}$ (32.774 meters)

2.2 RCS DATA BASE

Data from all RCS tests conducted on the Space Shuttle have been provided to Convair by NASA-LBJSC for compilation and analysis under this contract. Reference 1 presents a summary of all of the data except test IA148. This data base was obtained primarily at zero yaw angle, except for a limited number of runs on tests MA22 and OA169. The effect of yaw on the rear-mounted RCS data was computed using MA22 test data, because the OA169 data did not include low angles of attack.

2.2.1 MA22 TEST PROGRAM SUMMARY. The rear-mounted RCS test designated MA22 was performed at the NASA Langley Research Center Continuous Flow Hypersonic Tunnel (CFHT) where it carried the test number CFHT 118 (Reference 5). The test was performed at a nominal Mach number of 10.3 using a 0.01 scale model of 139B Orbiter to obtain six-component force and moment data using a cold gas simulation of the RCS exhaust flow. The major test variables included:

- a. Tunnel dynamic pressure ($q = 125$ and 150 psia)
- b. RCS chamber pressure ($P_{oj} = 0$ to 700 psia)
- c. RCS control direction (pitch up, pitch down, yaw)
- d. RCS nozzle geometry
- e. Number of RCS nozzles
- f. Elevator angle ($\delta_e = +10^\circ, 0^\circ, -30^\circ$)
- g. Body flap angle ($\delta_{BF} = +13.5^\circ, 0^\circ, -14.25^\circ$)
- h. Combined RCS control directions
- i. Jet off repeat runs
- j. Yaw angle ($\pm 3^\circ$)

2.2.2 IA148 TEST PROGRAM SUMMARY

The test designated IA148 was performed at the Arnold Engineering Development Center von Karman Facility Continuous Flow Hypersonic Tunnel B where it carried a facility test number V41B-TOA (Reference 8). The test used the 0.0125 scale model defined below and was performed at a nominal Mach number 6.0. The primary purpose of the test was to provide data for Shuttle "Return to Launch Site" abort separation maneuvers from the external tank. The test thus included data of the forward-mounted, rear-mounted, and combined forward and rear-mounted RCS units firing both with and without the external tank attached to the Orbiter. The portion of the test analyzed in this portion of the study was the tank-on-mated configuration data. The principal test parameters for these runs are

- a. Yaw angle (-4, 0, +4°)
- b. RCS combinations
- c. RCS chamber pressure (0 - 1550 psia)

Data were taken at angles of attack from -14° to -12.5° and the nominal test conditions were

- a. $M_\infty = 5.89$
- b. $T_{0\infty} = 790^\circ\text{R}$
- c. $q_\infty = 100 \text{ psf}$
- d. $R_e = 1 \times 10^6 \text{ ft}^{-1}$

A steel model of the Space Shuttle Orbiter was used for this test using the preliminary lines for vehicle configuration 102 as the baseline. This configuration is shown in Figure 2-1 and defined in detail in Reference 7. The model contained an internal force balance and was sting-mounted through the base region of the Orbiter, as shown in Figure 2-2. The Orbiter main engine nozzles were partially simulated on the base of the model, as shown in Figure 2-3. Dummy nozzle holes were used to simulate the furthest aft side-firing nozzle and all vernier nozzles on the OMS pods. The external tank model used for mated Orbiter/external tank tests in OA169 and for tank separation tests in IA22 was also used for this test.

Twenty-seven RCS thrusters were simulated on this model. These include nine in the nose and nine in each of the two rear-mounted Orbital Maneuvering Systems (OMS) as sketched in Figures 2-5 and 2-6 and locations given in Table 2-1. The RCS simulation air-flow was ducted up the support sting and entered the model through a flow-through balance. The balance flow was then ducted to three plenums within the model: one in front to feed the forward RCS thrusters and one for each of the rear OMS pod assemblies. All nozzles within a pod are connected to the plenum and can be operated in any combination through nine ports which are plugged when a given nozzle is not

being used on a particular run. Individual nozzle geometry is fixed and the primary test variables are numbers of nozzles operating in a given direction, thrust direction, and combinations of nozzles. The nozzles were all metric (thrust measured in balance loads) when the flow-through balance was used. The nozzle simulation parameters are given in Table 2-2 for the nominal RTLS case.

2.3 DATA REDUCTION PROCEDURE

The test data from all tests were reduced into body axis force and moment coefficients (C_N , C_A , C_m , C_l , C_n , C_Y) with the RCS thrust forces and moments removed. The MA22 test data were obtained with non-metric RCS jets and reduced directly from measured balance data, since the RCS jet thrust was not included in the measured balance loads. The IA148 data obtained with the flow-through balance had metric jets and these data were reduced at the wind tunnel by removing thrust effects using wind-tunnel static calibrations of measured thrust effects, as defined in Reference 8.

The net result is that all data received from the wind tunnel represented the basic vehicle aerodynamic forces and moments plus any induced loads resulting either from RCS jet impingement or from changes to the vehicle flow caused by the RCS jet plumes. Therefore, the incremental induced effects are computed by removing the basic vehicle characteristics from the jet-on data:

$$\Delta C_{M_1} = C_{M_j} - C_{M_o} \quad (2-1)$$

where

$$\Delta C_{M_1} = \text{induced force or moment increment}$$

$$C_{M_j} = \text{measured force or moment coefficient with jet on}$$

$$C_{M_o} = \text{measured force or moment coefficient with jet off}$$

Angle-of-attack differences between the jet-on data and the jet-off data were accounted for by passing a third-degree polynomial through the jet-off base data with the nearest mean value angle-of-attack data as the midpoint of the curve fit, and the interpolation is made to the jet-on angle of attack. Interpolation of the baseline jet-off data was used since this method results in the same base value without regard to nozzle used, jet pressure, or possible jet-on angle-of-attack effects. Difference data was generated and analyzed for all six force and moment components.

The analysis of Reference 1 broke the total induced jet increment into an impingement component and a flow interaction component. The wind tunnel data for the rear-mounted RCS units were corrected for predicted values of jet impingement in the wind-tunnel as defined in Reference 1. The mated data from test IA148 were not corrected for jet impingement, since the data of test OA169 (Reference 6) showed very little impingement effects.

The nozzle flow parameters were corrected for model nozzle discharge coefficients in the same manner as described in Reference 1.

Table 2-1. Test IA148 available RCS thruster locations.

Thruster No.	Full Scale, in. *		
	X ₀	Y ₀	Z ₀
113	362.819	-69.538	373.634
115	350.542	-14.091	413.244
116	335.982	-63.481	356.600
123	364.814	-71.484	359.506
125	350.524	0.00	414.231
126	349.971	-67.581	357.543
135	350.542	14.091	413.244
136	335.982	63.481	356.600
146	349.971	67.581	357.543
215	1542.00	-132.00	498.56
223	1529.04	-149.55	459.04
225	1529.04	-132.00	498.56
226	1531.52	-115.28	452.40
233	1542.00	-149.55	459.04
236	1544.56	-114.40	430.72
243	1516.00	-149.55	459.04
245	1516.00	-132.00	498.56
246	1518.56	-115.92	425.52
315	1542.00	132.00	498.56
324	1529.04	149.55	459.04
325	1529.04	132.00	498.56
326	1531.52	115.28	452.40
334	1542.00	149.55	459.04
336	1544.56	114.40	430.72
344	1516.00	149.55	459.04
345	1516.00	132.00	498.56
346	1518.56	115.92	425.52

*X₀, Y₀, Z₀ referenced to Orbiter coordinates.

Table 2-2. Summary of simulation parameters for RTLS abort simulation.

	<u>Symbol</u>	<u>Free Flight</u>	<u>Wind Tunnel</u>
<u>A. Free-Stream Conditions</u>			
Dynamic Pressure	q	7.5 psf	93.6 psf
Mach Number	M	6.6	6.0
Reynolds Number*	Re	0.68×10^6	1×10^6
Ambient Pressure	P _∞	0.00171 psia	0.02579 psia
		<u>Prototype</u>	<u>Model</u>
<u>B. RCS Jet Characteristics</u>			
Chamber Pressure	P _c	152 psia	771.0
Chamber Temperature	T _c	4873 °R	520 °R
Average Specific Heat	γ _{avg}	1.3	1.4
Expansion Ratio	ε	22	12.5
Nozzle Lip Angle	θ _p	12°	12.01°
Exit Area	A _e	72.62 m ²	0.01470 m ²
Exit Mach Number	M _j	4.0	4.174
Exit Pressure	P _j	0.547 psia	4.039 psia
Mass Flow Rate	ṁ _j	3.01 lbm/sec	0.02099 lbm/sec
Momentum	ṁ _j u _j	839.71 lb	1.637 lb
Thrust	TH	870 lb	1.696 lb
		<u>Full Scale Free Flight</u>	<u>Simulation</u>
<u>C. Jet to Free-Stream Parameters for Single Nozzle (S_{ref} = S_{wing})</u>			
Thrust Ratio	$\frac{TH}{q S_{ref}}$	0.04312	0.04312
Momentum Ratio	$\frac{\gamma_j P_j M_j^2 A_j}{\gamma P_\infty M_\infty S_{ref}}$	0.02075	0.02098
Pressure Ratio	P _j /P	355.2	156.5
Plume Shape	(δ _j)	56.3°	44.4°

*Reynolds number based on Orbiter length L_{orb} = 107.5 ft.

2-7

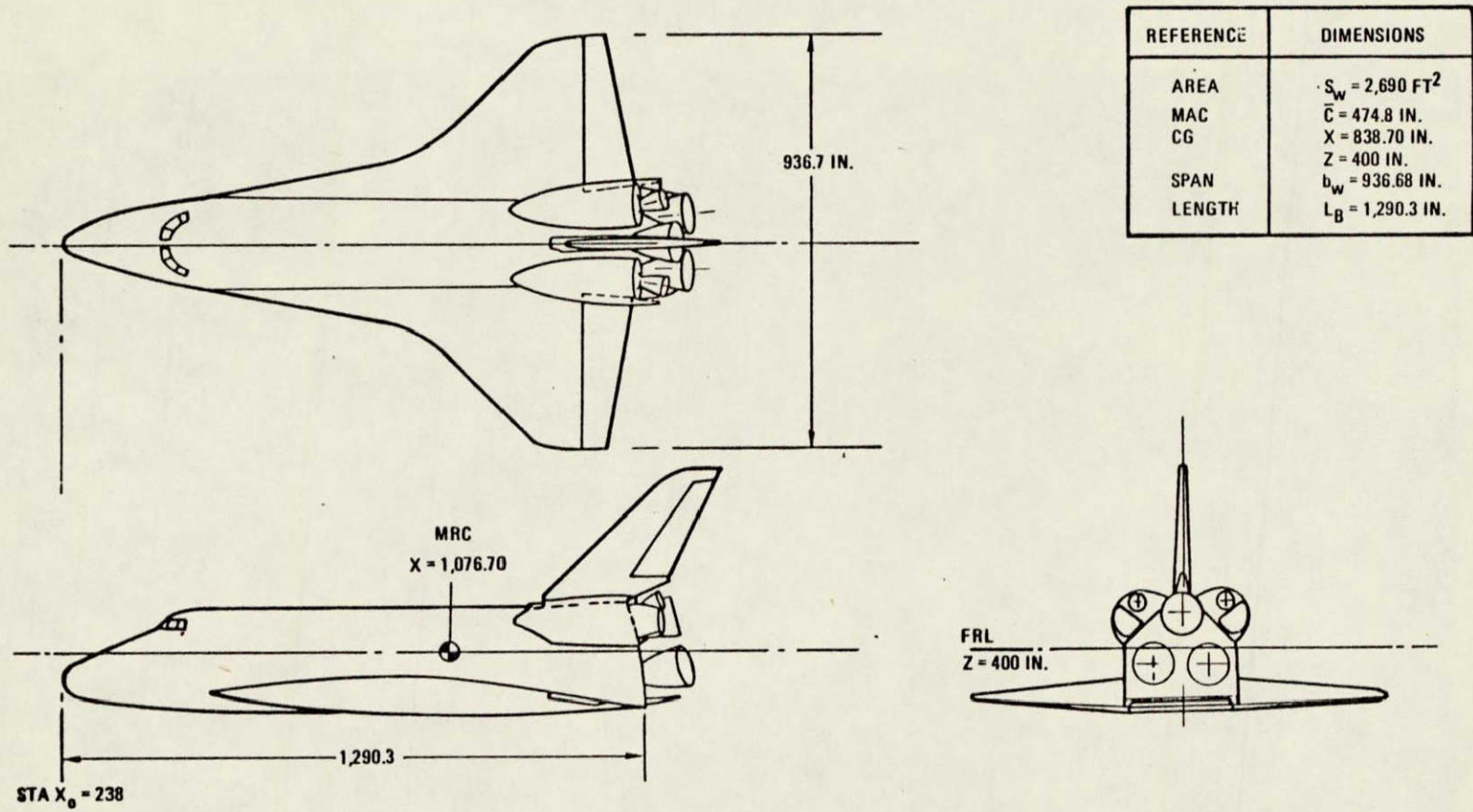


Figure 2-1. 139B Orbiter configuration.

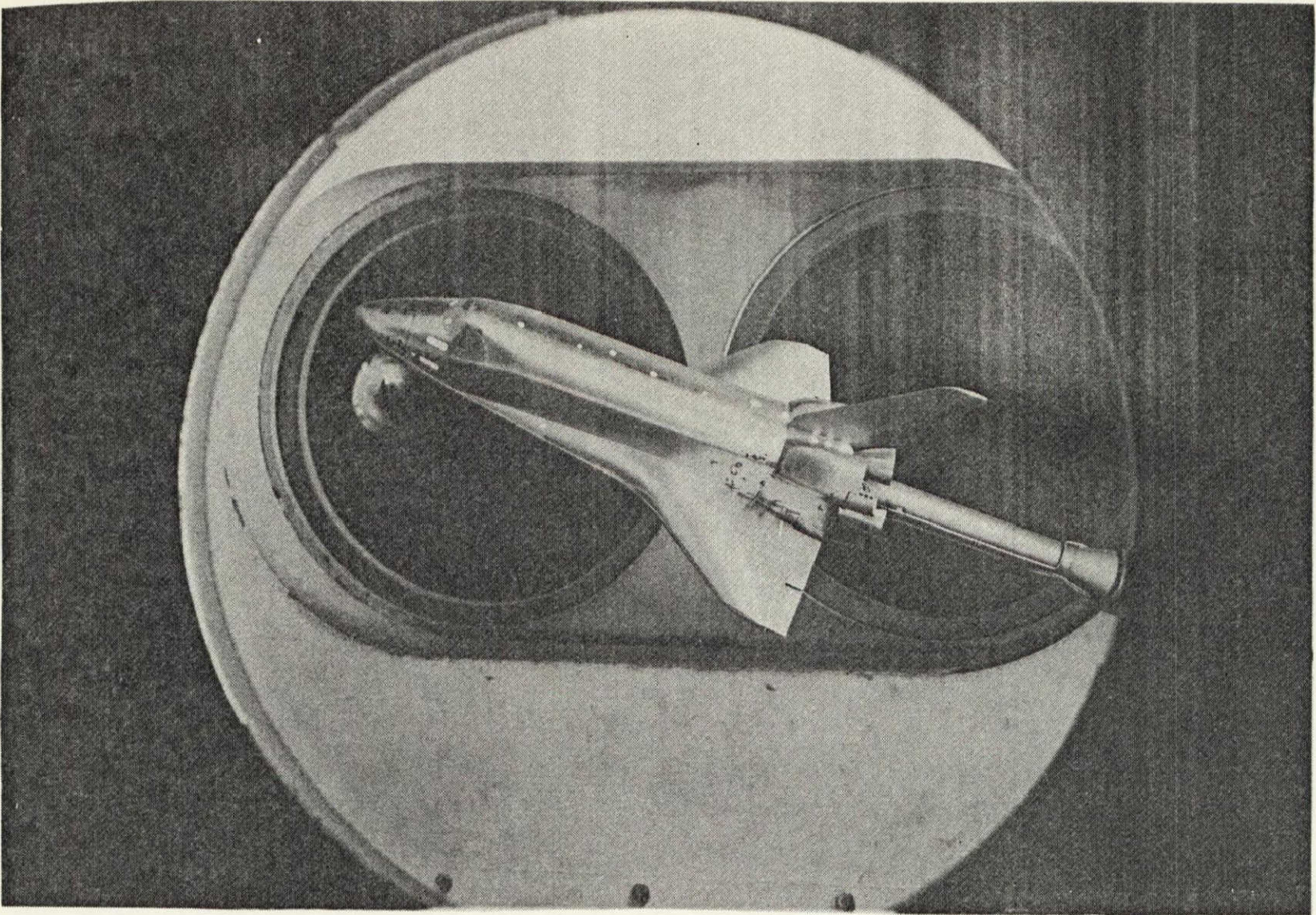


Figure 2-2. OA169 Orbiter model.

2-8

ORIGINAL PAGE IS
OF POOR QUALITY

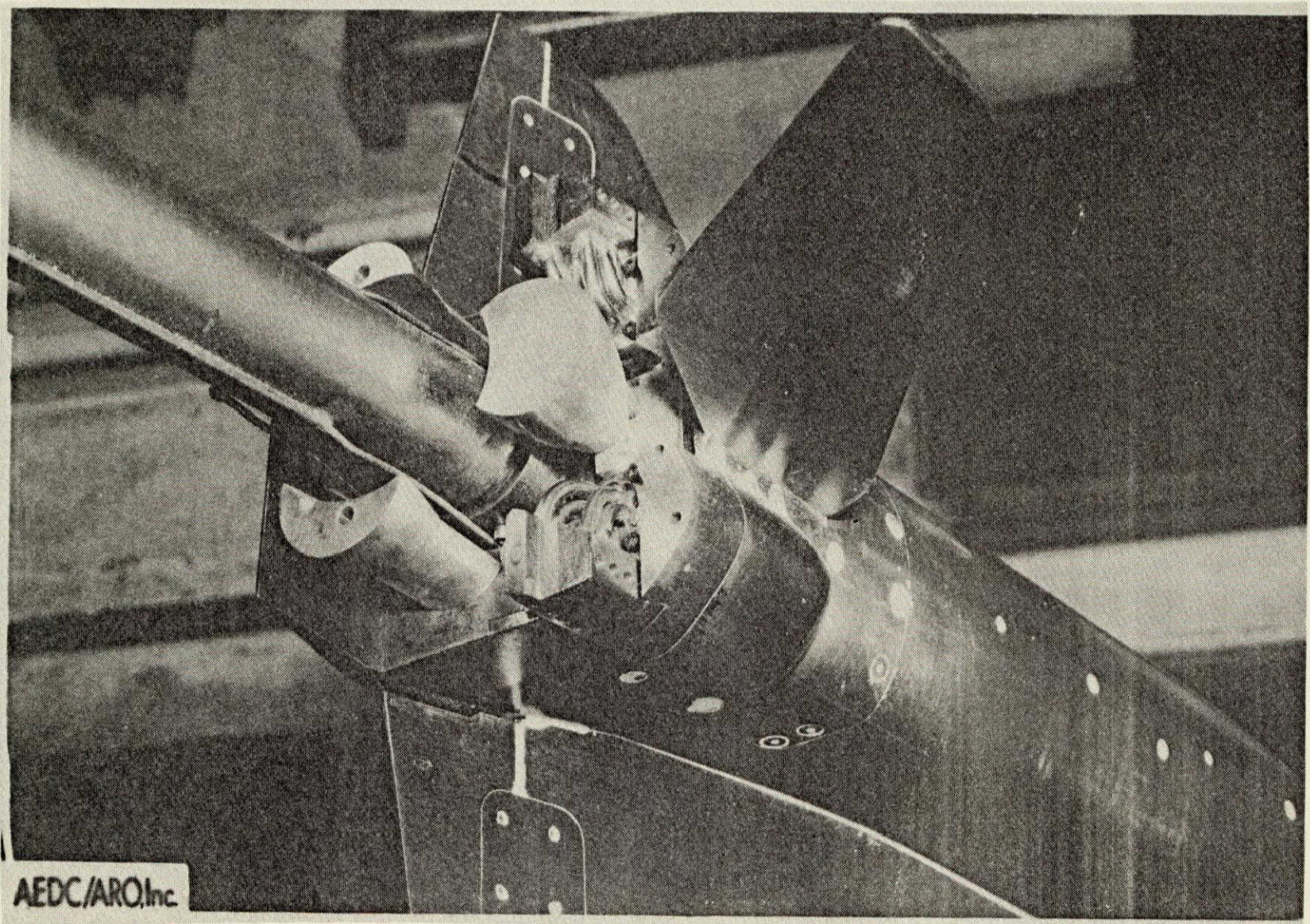


Figure 2-3. OA169 sting mount.

2-9

ORIGINAL PAGE IS
OF POOR QUALITY

AEDC/ARO, Inc

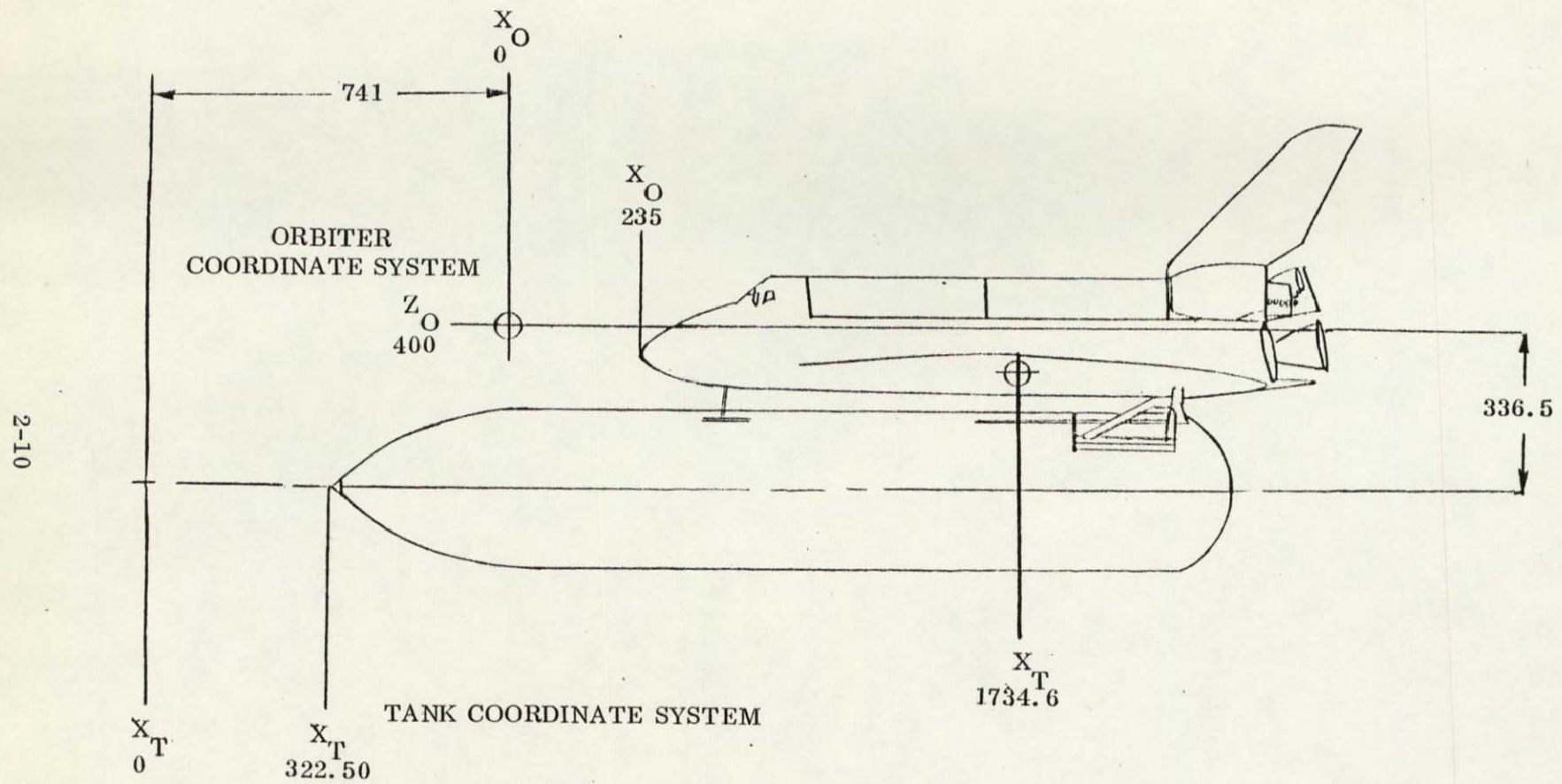


Figure 2-4. Mated configuration sketch.

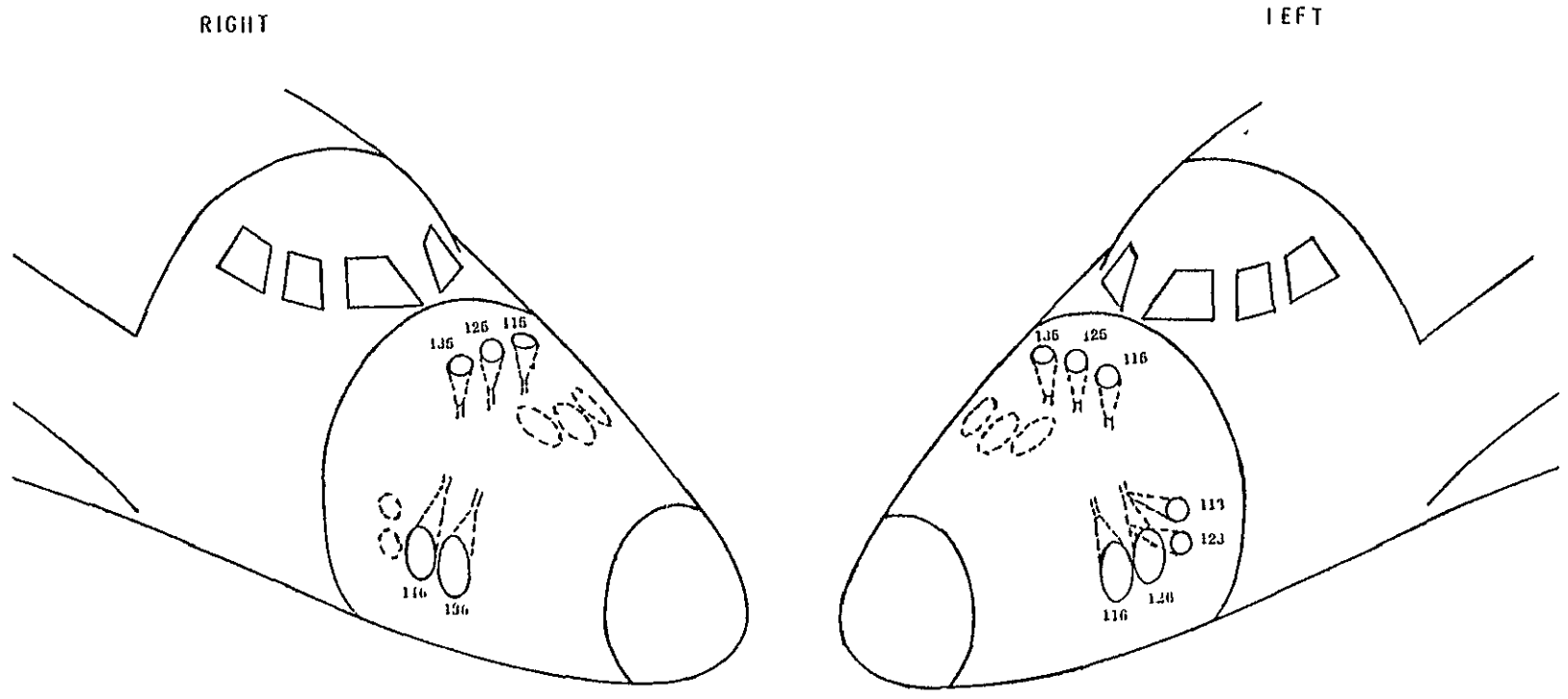
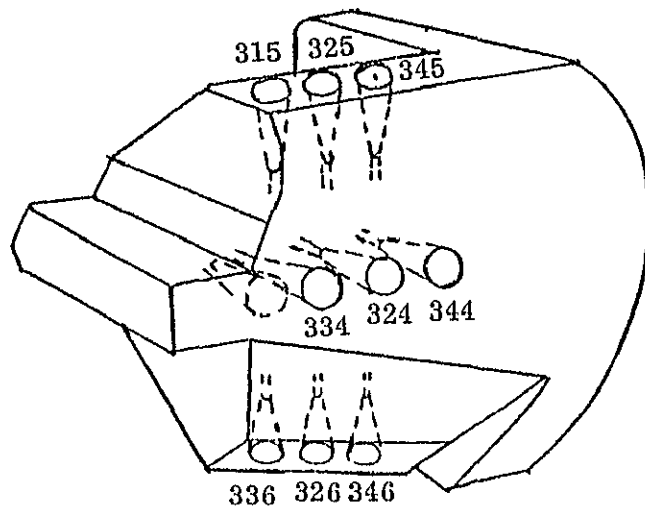
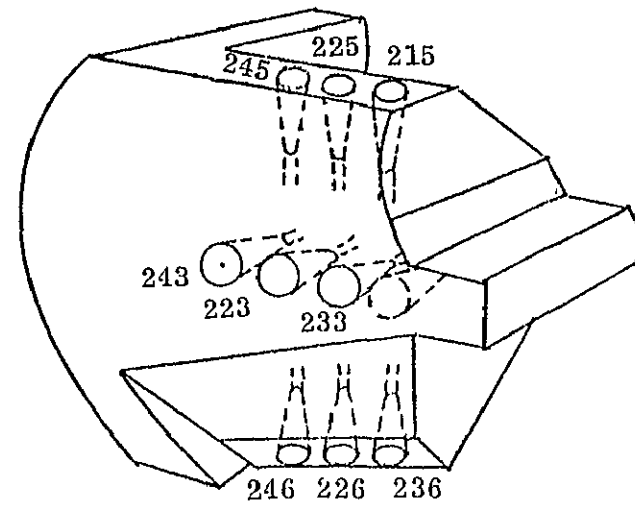


Figure 2-5. Forward-mounted RCS jets simulated during Test IA148.

RIGHT



LEFT



2-12

ORIGINAL PAGE IS
OF POOR QUALITY

Figure 2-6. Rear-mounted RCS jets simulated during Test IA148.

3

YAW ANGLE EFFECTS ON REAR-MOUNTED RCS DATA

3.1 INTRODUCTION

The rear-mounted Reaction Control System (RCS) interaction models presented in Reference 1 were developed from zero yaw data only. The assumption at that time was that yaw angle effects were small and could be added as increments if later analysis showed measureable effects. A yaw data base existed in a limited number of runs, as follows

<u>Test No.</u>	<u>Yaw Angle, deg</u>	<u>Angle of Attack, deg</u>
MA22	-3, -3	-10 to -35
OA169	+4	+15 to -45

The MA22 data were used because they represented a more complete set in terms of including different numbers of nozzles, nozzle directions, and because they include the more critical low angle-of-attack range. This section presents this analysis of yaw effects on the rear-mounted RCS interactions for the Orbiter alone. Mated configuration data are presented in Section 6 of this report.

3.2 YAW EFFECTS ON REAR-MOUNTED RCS INTERACTION

Data from Test MA22 at plus and minus three degrees yaw were compared to the zero yaw correlation models for rear-mounted RCS. The data included pitch-down RCS, pitch-up RCS, and yaw RCS simulations which were all correlated. The angle of attack increments used to obtain these data were larger than those of the zero yaw cases and deliberate correlations could not be made at each interval of the models. Sufficient yaw data were obtained to check correlations across the angle-of-attack range of the zero yaw model (-10° to 35° angle of attack).

The data set contained eight jet-off runs in addition to between six and nine jet-on runs for a given RCS direction. All yaw runs were treated as a set and differences were taken between this set and the basic zero yaw jet-off run used to obtain differences for the zero yaw models (i. e., MA22 Run 5). The differences thus obtained included both yaw and RCS effects. These differences were then fitted with least square curve fits of the form:

$$\Delta C = a_0 + a_1 x + a_2 x^2 + a_3 x^3 \quad (3-1)$$

where x = momentum ratio or mass flow ratio, depending on the data being fitted, and the a_0 term represents the best estimate of the jet-off yaw increment. This term was then to be added to the model for RCS effect to generate the data correlation plots. However, the correlation that was actually plotted was the curve:

$$\Delta C = a_{0_{\text{yaw}}} + (\Delta C_{\text{RCS}} - a_{0_{\text{RCS}}}) \quad (3-2)$$

where the intercept of the RCS model was replaced by the yaw effect intercept rather than being added to it. When the missing term is taken into account, most of the apparent effects of yaw on RCS effectiveness disappear. It was decided not to replot all of the data, since the difference is small on most plots and represents a shift of the entire curve.

3.2.1 PITCH-DOWN RCS INTERACTIONS. The data set contained three jet-on runs each for Nozzles N49, N79, and N83 (Reference 1 defines nozzles) which were combined with eight jet-off runs for a total yaw data base of 17 runs at +3 degrees yaw and 17 at -3 degrees yaw. The momentum ratios varied from zero to a maximum value of approximately 0.09. All three nozzle sets were located on the left side of the model.

3.2.1.1 Normal Force Increments. Figures 3-1, 3-2, and 3-3 show representative samples (at low angles of attack) of the effect of yaw angle on the normal force correlations. Most data are well within the zero yaw correlation and there is no discernible effect of yaw. It has been suggested that the data with yaw be incorporated into zero yaw data base and a new correlation and root-mean-square error be generated. However, since each basic curve was generated using 117 to 150 points, an additional 18 points which are within the basic data scatter are unlikely to change the curve significantly. It was decided that the resulting change was not worth the effort required to obtain it.

3.2.1.2 Pitching Moment Increments. Figures 3-4, 3-5, and 3-6 show the good correlation between yaw data and the zero yaw equations for pitching moment, showing that yaw does not affect the RCS pitch interaction.

3.2.1.3 Rolling Moment Increments. Figures 3-7, 3-8, and 3-9 show that yaw angle does change the rolling moment with no jets on. However, when the correlation is adjusted to the new value of rolling moment due to yaw, the data correlate very well with the zero yaw curves. The correction on the intercept for the -10 degree correlation (Figure 3-7) will bring all data points within the 2-sigma error boundaries.

3.2.1.4 Yawing Moment Increments. Figures 3-10, 3-11, and 3-12 present the incremental yawing moment correlations induced by pitch-down jets. There were large

differences which at first glance made it appear that there might be effects due to yaw angle. Further analysis showed that these differences were due to the missing intercept term discussed previously, and dashed lines were added to these plots to show where the true correlation line should appear. When the curves are corrected, no yaw effects are apparent.

3.2.1.5 Side Force Increments. The side force incremental data shown in Figures 3-13, 3-14, and 3-15 also appear to have some possible yaw effects in them. When the predicted curve intercept is corrected, the curve is brought into close agreement with the data and no yaw effects are seen.

3.2.2 PITCH-UP RCS DATA Data were obtained on three different pitch-up nozzle sets mounted on the right side of the vehicle. These were N78 (one nozzle), N52 (two nozzles), and N82 (three nozzles), where all nozzles had the same geometry as defined in Reference 1. Three runs were obtained with each set at different supply pressures which, combined with the eight jet-off yaw runs, gave a total data sample of 17 points at each angle of attack.

3.2.2.1 Normal Force Increments. Figures 3-16, 3-17, and 3-18 present the normal force correlations at the -10° , 0° , and $+10^\circ$ angles of attack. Most data are well within the zero yaw correlation 2-sigma error band and no consistent trend of yaw effects is seen at either positive or negative yaw angles.

3.2.2.2 Pitching Moment Increments. The pitching moment increment data presented in Figures 3-19, 3-20, and 3-21 show no effect of ± 3 degrees yaw.

3.2.2.3 Rolling Moment Increments. The lateral-directional data from pitch-up jet operation exhibited a peak value at low angles of attack, and four models are required to describe the data at low angles

- a. peak value
- b. angle of attack of peak value
- c. below peak value
- d. above peak value

These data are dependent on the angle of attack where the peak value occurs as well as on the jet exit momentum ratio. Data were only obtained at -10° , 0° , and $+10^\circ$ angle of attack for the yaw cases, so independent checks of each model were not possible. Thus, the data correlations shown for all lateral-directional data were done at a constant angle of attack and contain all four analytic model parts on each. Figure 3-22 presents data primarily in the below-peak-value range since the peak value at -10 degrees occurs at a momentum ratio slightly greater than 0.09. The data of Figure 3-23 present three points for the above-peak-value range while the data of Figure 3-24 are all above the value of the rolling moment. The data presented in Figures 3-22, 3-23, and 3-24 show there are no yaw effects on the low angle-of-attack rolling moments due to RCS jet operation.

3.2.2.4 Yawing Moment Increments. The yawing moment increments shown in Figures 3-25, 3-26, and 3-27 were correlated in the same manner as the rolling moments described in the preceding section. No yaw effects are evident in these data, as was shown in the other lateral-directional increments.

3.2.2.5 Side Force Increments. Figures 3-28, 3-29, and 3-30 present the side force increments correlated in the same manner as the rolling moment data. No yaw effects are evident in these data, as was shown in the other lateral-directional increments.

3.2.3 YAW RCS INTERACTIONS. Yaw effects on yaw jet interactions were obtained from data using two different yaw jet sets mounted on the left side of the model. The nozzle set designations were N51 and N85 and they differ only in the number of RCS nozzles being simulated; N51 contains four yaw nozzles while N85 contains two yaw nozzles. Reference 1 defines nozzle geometry. Three different supply pressures were tested with each, and the total data base is represented by 14 data points (8 jet-off) at each angle of attack.

3.2.3.1 Normal Force Increments. Figures 3-31, 3-32, and 3-33 present sample correlations of the effect of yaw angle on the normal force induced by yaw jets. The data for the -3° yaw case tend to fall outside of the plotted boundaries of the prediction. However, when the error in intercept is taken into account all data fall around the zero yaw curve.

3.2.3.2 Pitching Moment Increments. The pitching moment increments data are shown in Figures 3-34, 3-35, and 3-36. Most of the data are within the 2-sigma error band except for the data point at the highest mass flow ratio tested. This point is high for both positive and negative yaw and in close agreement with the data points used in the zero yaw correlation, so no effect of yaw is evident.

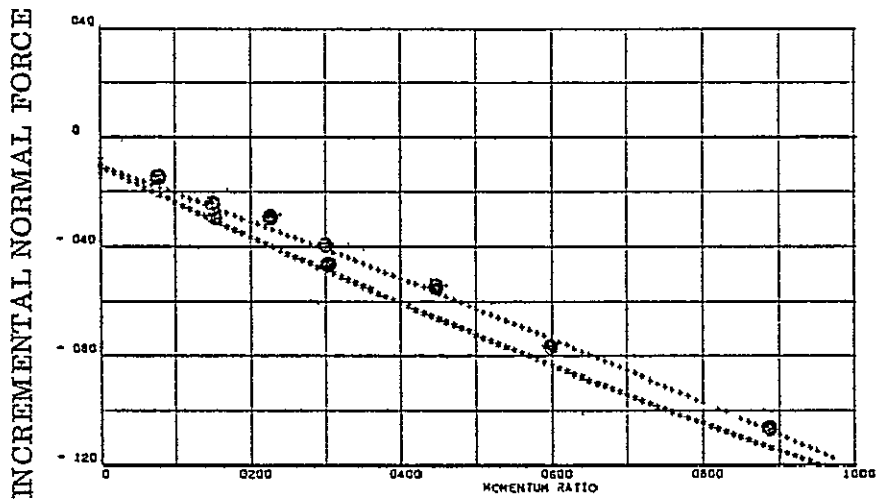
3.2.3.3 Rolling Moment Increments. Figures 3-37, 3-38, and 3-39 present the rolling moment increments at $\pm 3^\circ$ yaw compared to the analytic models for angles of from -10° to $+5^\circ$. All data appear to agree with zero yaw model with the exception of the points at the highest mass flow ratio. The positive yaw shows good agreement with the negative yaw point, however, and no yaw effect can be determined.

3.2.3.4 Yawing Moment Increments. The data shown in Figures 3-40, 3-41, and 3-42 are very interesting since there does appear to be a definite effect of yaw angle on RCS interaction. The positive yaw angle results in a decrease in induced yawing moment, while a negative yaw angle results in an increase. This was the only case of measurable yaw effects on the RCS model for Orbiter alone. The changes which come from yaw effects are not meaningful in the total RCS effectiveness, since the induced yaw component is small relative to the thrust.

3.2.3.5 Side Force Increments. Figures 3-43, 3-44, and 3-45 show that the side force data indicate a small decrease in RCS effectiveness at positive yaw angles. The negative yaw angle data, however, tend to remain within the 2-sigma scatter of the zero yaw model.

3.3 CONCLUSIONS

No significant yaw effects were found and it appears that the zero yaw models are adequate for non-zero yaw cases.

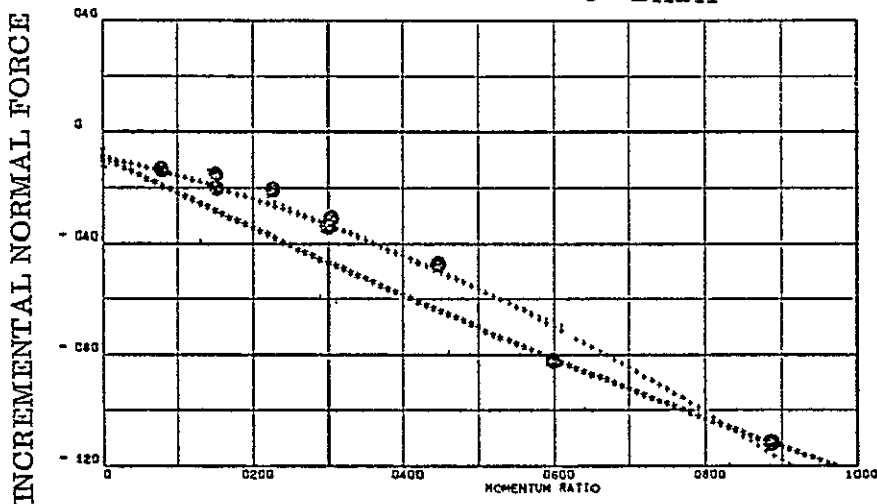


$$\beta = +3^\circ$$

$$a_0 \text{ error} = -.00358$$

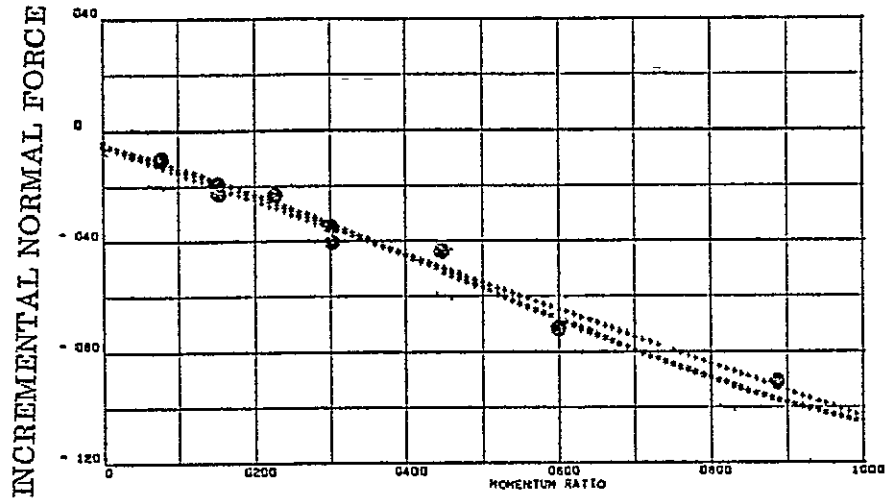
PLOT SYMBOLS

- * $\beta = 0$ MODEL
- . $\beta = 0 - 2\sigma$
- CURVE FIT OF DATA
- DATA



$$\beta = -3^\circ$$

Figure 3-1. Yaw effects on pitch-down RCS normal force at -10 to -5 degrees angle of attack.



$$\beta = +3^\circ$$

σ error = .00092

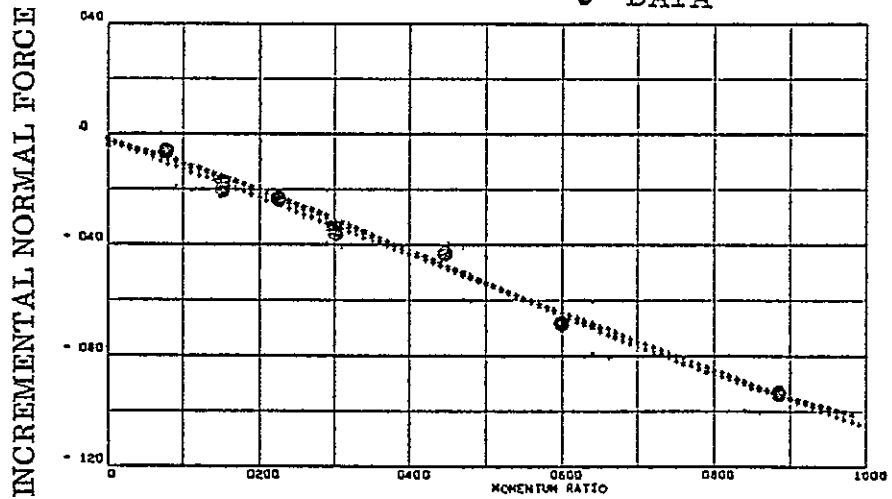
PLOT SYMBOLS

* $\beta = 0$ MODEL

. $\beta = 0 \pm 2\sigma$

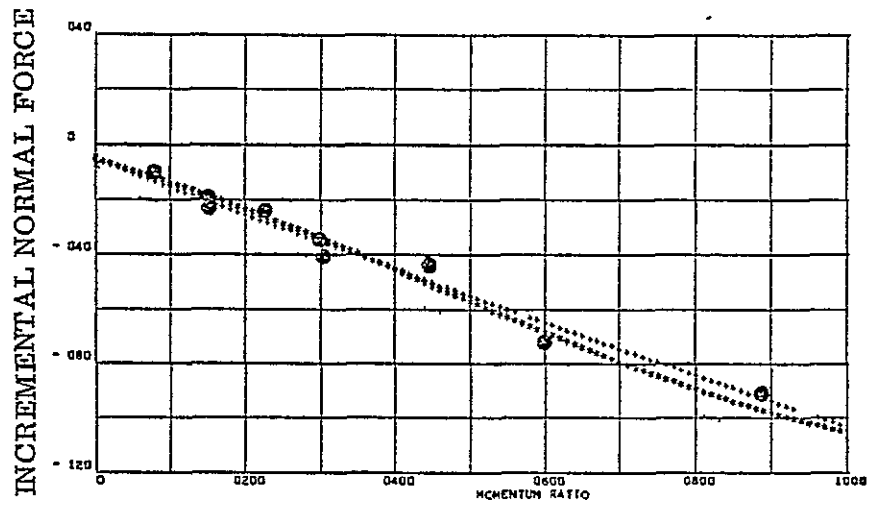
+ CURVE FIT OF DATA

• DATA



$$\beta = -3^\circ$$

Figure 3-2. Yaw effects on pitch-down RCS normal force at -5 to 0 degrees angle of attack.

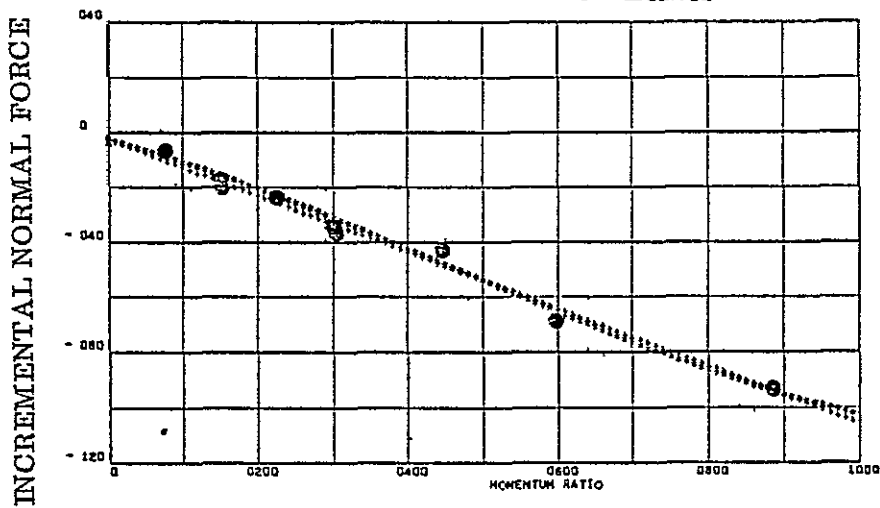


$$\beta = +3^\circ$$

σ error = -.00341

PLOT SYMBOLS

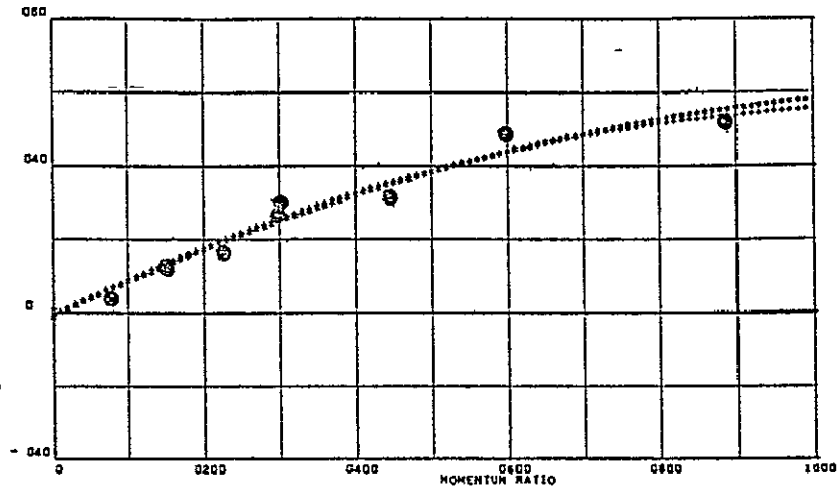
- * $\beta = 0$ MODEL
- . $\beta = 0 \pm 2\sigma$
- + CURVE FIT OF DATA
- DATA



$$\beta = -3^\circ$$

Figure 3-3. Yaw effects on pitch-down RCS normal force at 0 to 5 degrees angle of attack.

INCREMENTAL PITCHING MOMENT



$$\beta = +3^\circ$$

$$a_0 \text{ error} = -.00261$$

PLOT SYMBOLS

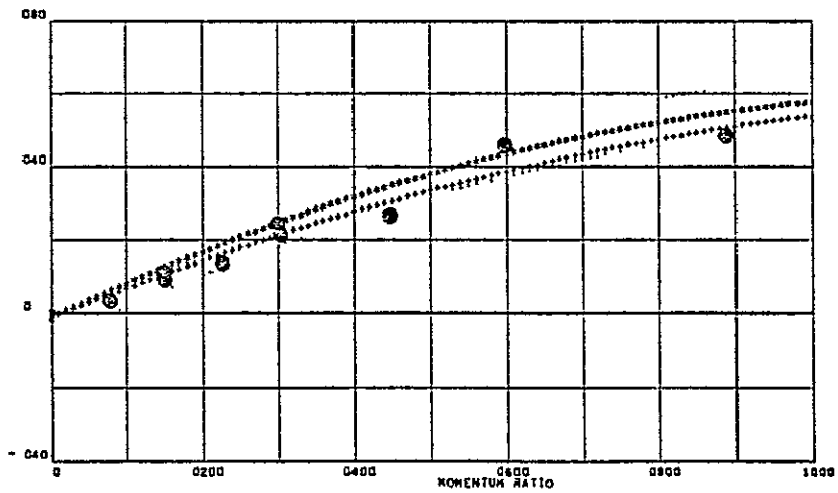
* $\beta = 0$ MODEL

. $\beta = 0 \pm 2\sigma$

+ CURVE FIT OF DATA

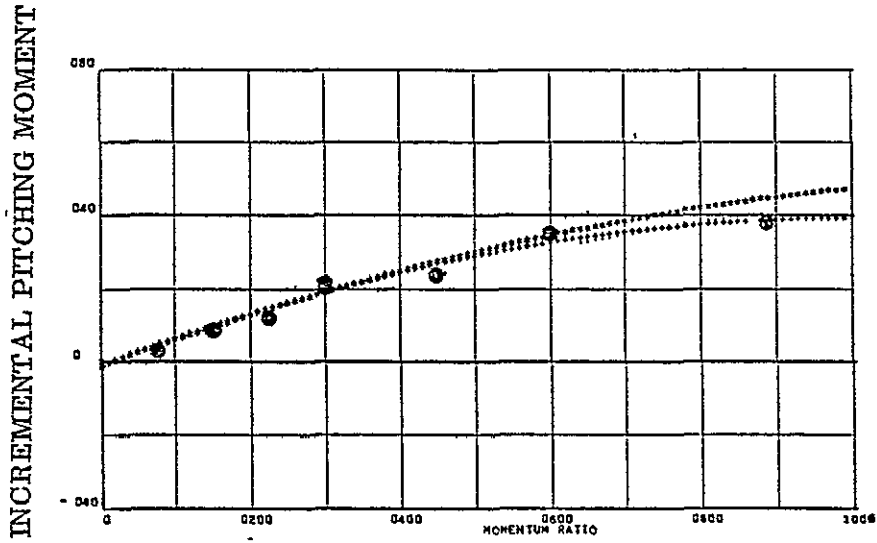
• DATA

INCREMENTAL PITCHING MOMENT



$$\beta = -3^\circ$$

Figure 3-4. Yaw effects on pitch-down RCS pitching moment at -10 to -5 degrees angle of attack.

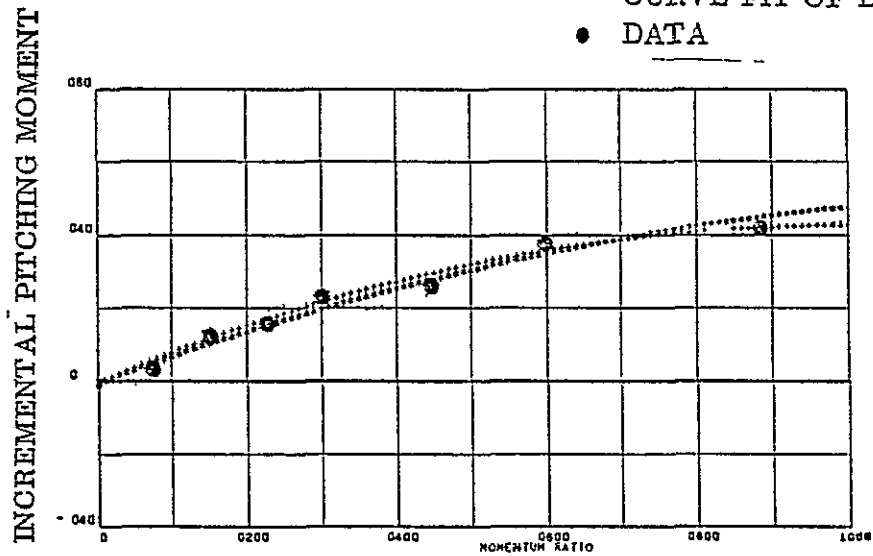


$$\beta = +3^\circ$$

a error = -.00171

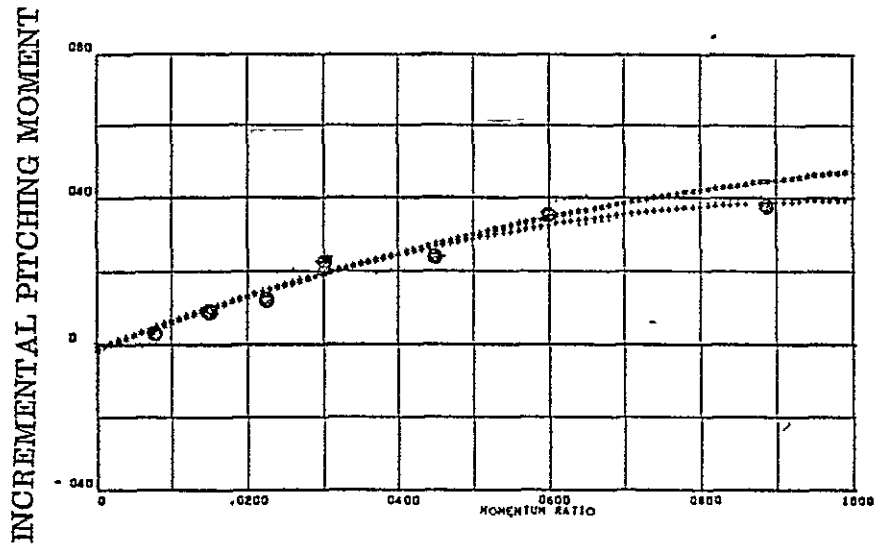
PLOT SYMBOLS

- * $\beta = 0$ MODEL
- . $\beta = 0 \pm 2\sigma$
- CURVE FIT OF DATA
- DATA



$$\beta = -3^\circ$$

Figure 3-5. Yaw effects on pitch-down RCS pitching moment at -5 to 0 degrees angle of attack.



$$\beta = +3^\circ$$

σ error = -.00206

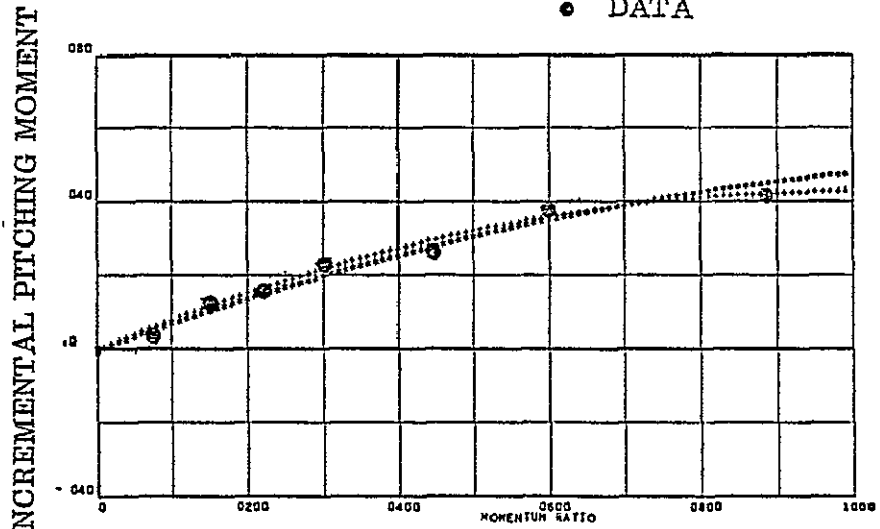
PLOT SYMBOLS

* $\beta = 0$ MODEL

. $\beta = 0 \pm 2\sigma$

+ CURVE FIT OF DATA

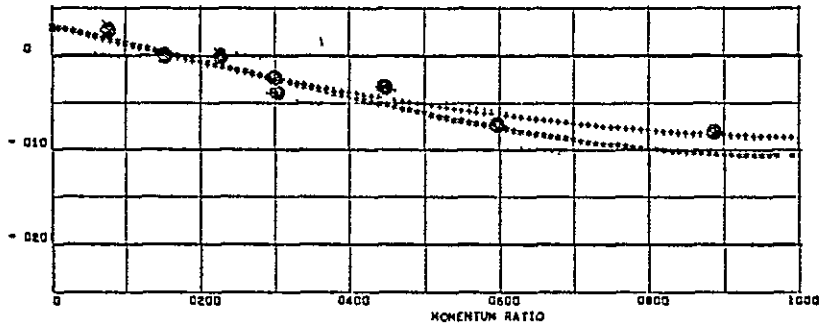
● DATA



$$\beta = -3^\circ$$

Figure 3-6. Yaw effects on pitch-down RCS pitching moment. at 0 to 5 degrees angle of attack.

INCREMENTAL ROLL MOMENT



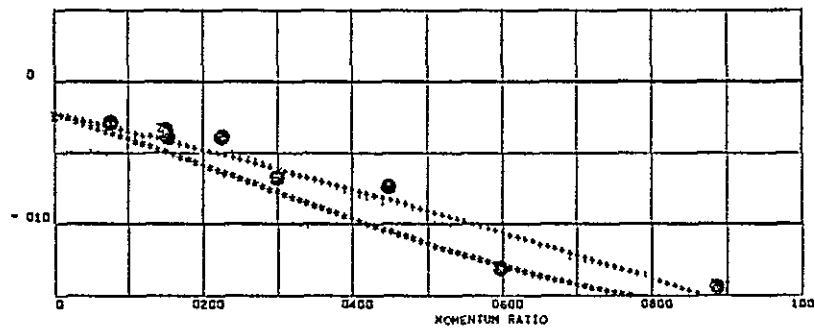
$$\beta = +3^\circ$$

a_0 error = 00105

PLOT SYMBOLS

- * $\beta = 0$ MODEL
- . $\beta = 0 \pm 2\sigma$
- + CURVE FIT OF DATA
- DATA

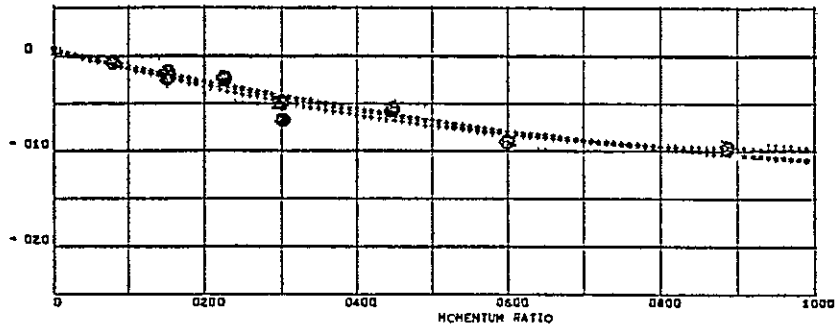
INCREMENTAL ROLL MOMENT



$$\beta = -3^\circ$$

Figure 3-7. Yaw effects on pitch-down RCS rolling moment at -10 to -5 degrees angle of attack.

INCREMENTAL ROLL MOMENT



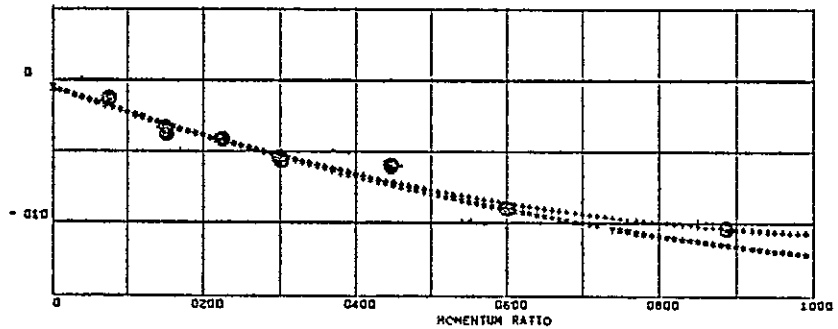
$$\beta = +3^\circ$$

a error = 00026

PLOT SYMBOLS

- * $\beta = 0$ MODEL
- . $\beta = 0 \pm 2\sigma$
- + CURVE FIT OF DATA
- DATA

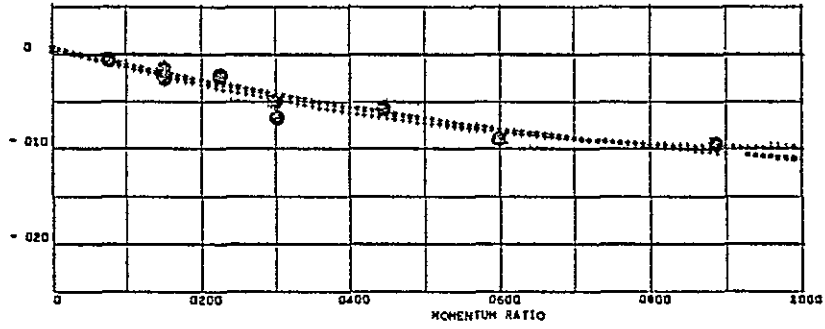
INCREMENTAL ROLL MOMENT



$$\beta = -3^\circ$$

Figure 3-8. Yaw effects on pitch-down RCS rolling moment at -5 to 0 degrees angle of attack.

INCREMENTAL ROLL MOMENT



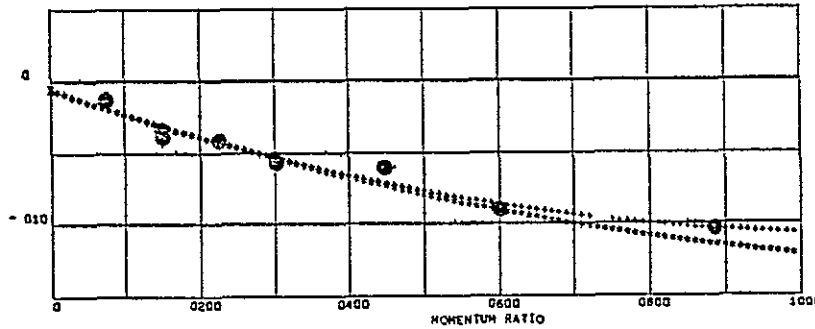
$\beta = +3^\circ$

a_o error = -.00010

PLOT SYMBOLS

- * $\beta = 0$ MODEL
- . $\beta = 0 + 2\sigma$
- + CURVE FIT OF DATA
- DATA

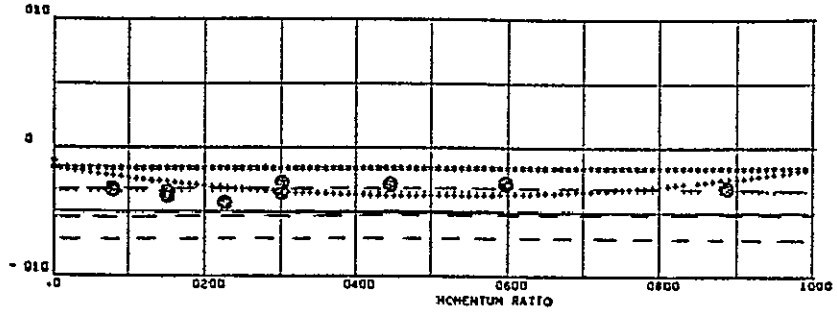
INCREMENTAL ROLL MOMENT



$\beta = -3^\circ$

Figure 3-9. Yaw effects on pitch-down RCS rolling moment at 0 to 5 degrees angle of attack.

INCREMENTAL YAWING MOMENT



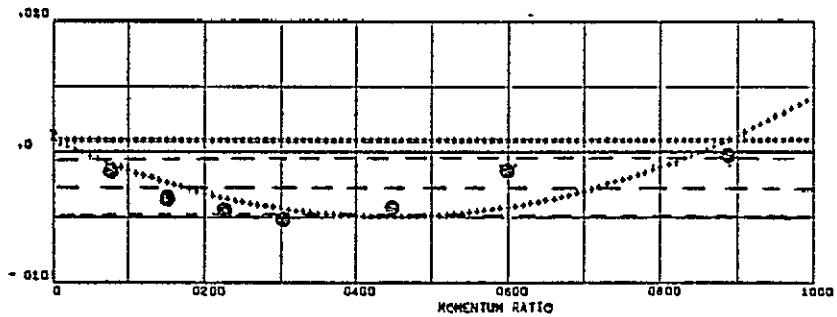
$$\beta = +3^\circ$$

a_0 error = -.0040

PLOT SYMBOLS

- * $\beta = 0$ MODEL
- . $\beta = 0 \pm 2\sigma$
- CURVE FIT OF DATA
- DATA

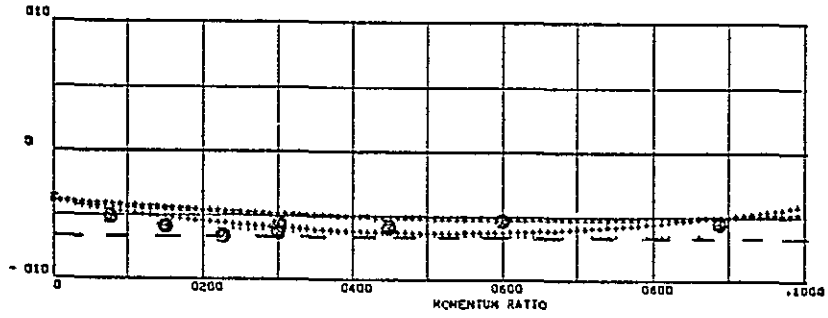
INCREMENTAL YAWING MOMENT



$$\beta = -3^\circ$$

Figure 3-10. Yaw effects on pitch-down RCS yawing moment at -10 to -5 degrees angle of attack.

INCREMENTAL YAWING MOMENT



$\beta = +3^\circ$

a_0 error = - 0025

PLOT SYMBOLS

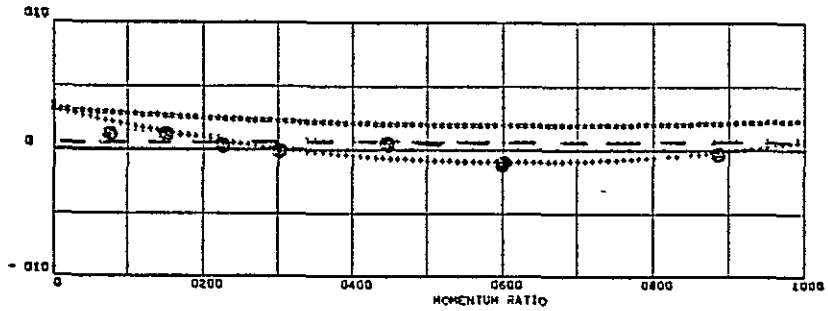
* $\beta = 0$ MODEL

. $\beta = 0 \pm 2\sigma$

+ CURVE FIT OF DATA

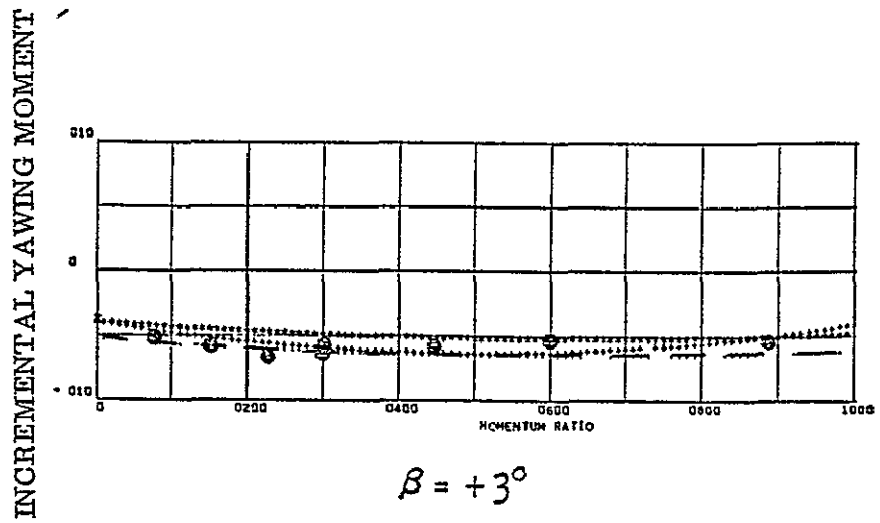
● DATA

INCREMENTAL YAWING MOMENT



$\beta = -3^\circ$

Figure 3-11. Yaw effects on pitch-down RCS yawing moment at -5 to 0 degrees angle of attack.



$a_{\text{error}} = -.0013$

PLOT SYMBOLS

- * $\beta = 0$ MODEL
- . $\beta = 0 \pm 2\sigma$
- CURVE FIT OF DATA
- DATA

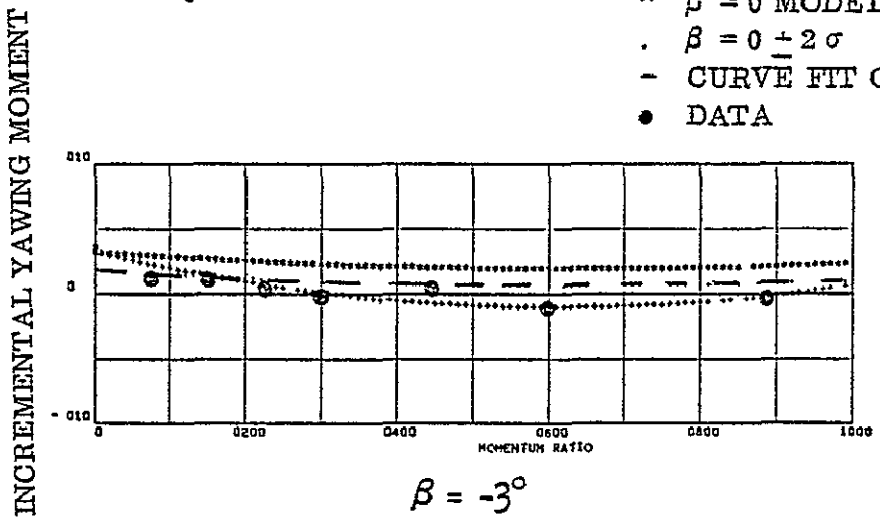
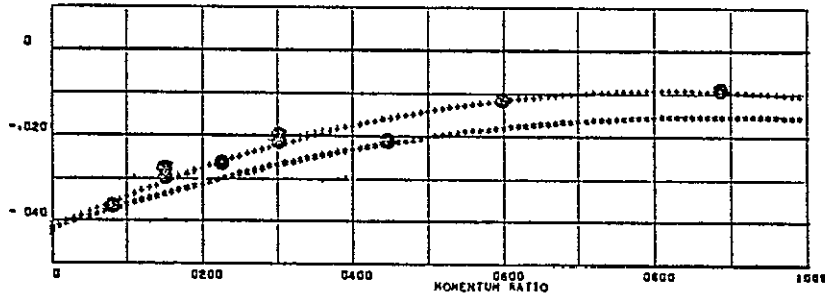


Figure 3-12. Yaw effects on pitch-down RCS yawing moment at 0 to 5 degrees angle of attack.

INCREMENTAL SIDE FORCE



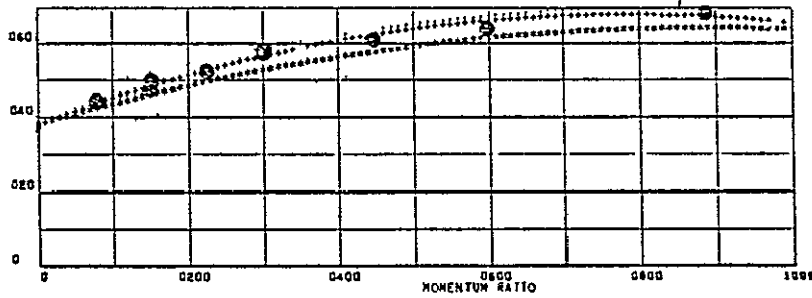
$\beta = +3^\circ$

$\sigma_{\text{error}} = .00245$

PLOT SYMBOLS

- x $\beta = 0$ MODEL
- . $\beta = 0 + 2\sigma$
- + CURVE FIT OF DATA
- DATA

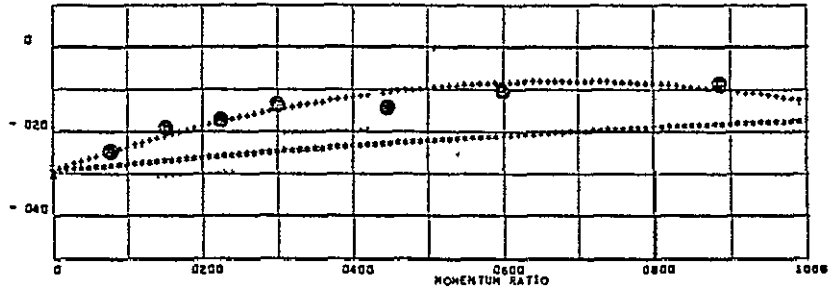
INCREMENTAL SIDE FORCE



$\beta = -3^\circ$

Figure 3-13. Yaw effects on pitch-down RCS side force at -10 to -5 degrees angle of attack.

INCREMENTAL SIDE FORCE



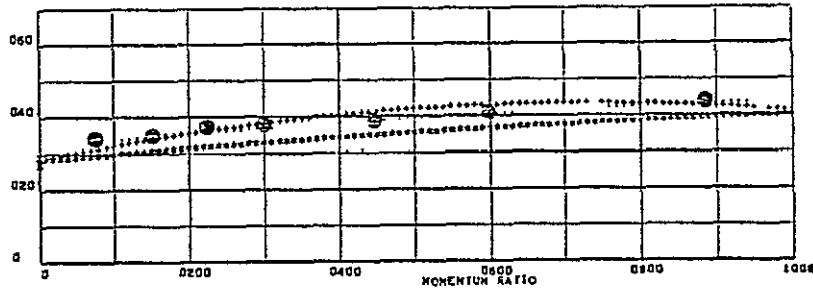
$\beta = +3^\circ$

σ error = .00417

PLOT SYMBOLS

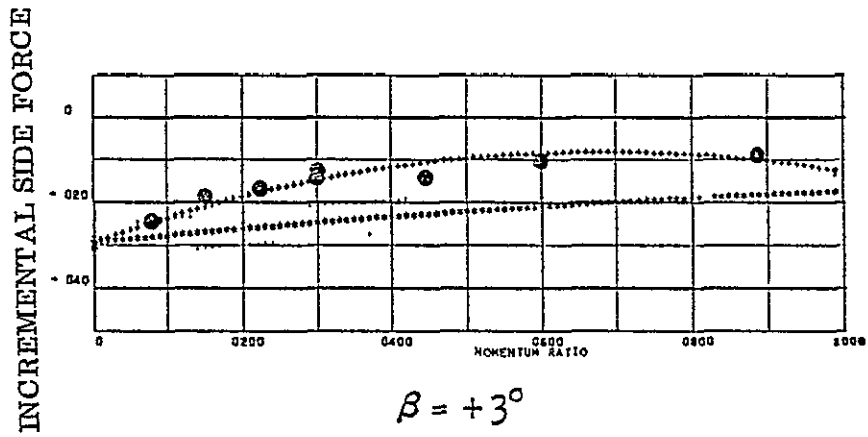
- * $\beta = 0$ MODEL
- . $\beta = 0 \pm 2\sigma$
- + CURVE FIT OF DATA
- DATA

INCREMENTAL SIDE FORCE



$\beta = -3^\circ$

Figure 3-14. Yaw effects on pitch-down RCS side force at -5 to 0 degrees angle of attack.



$\sigma_{\text{error}} = .00409$

PLOT SYMBOLS

- * $\beta = 0$ MODEL
- . $\beta = 0 \pm 2\sigma$
- + CURVE FIT OF DATA
- DATA

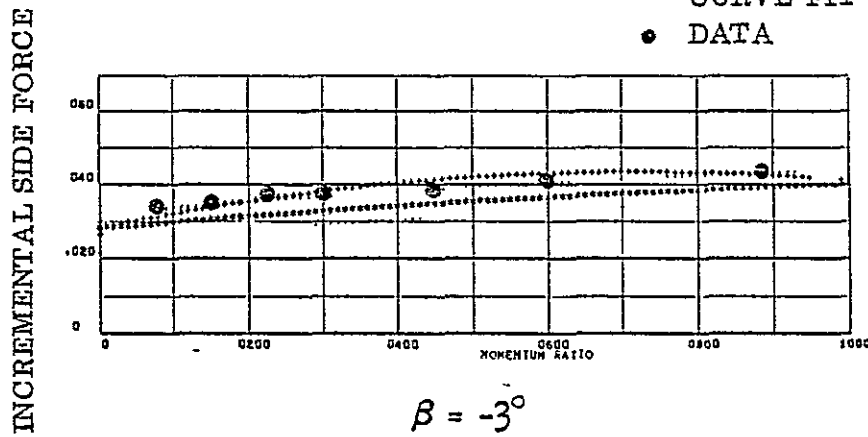
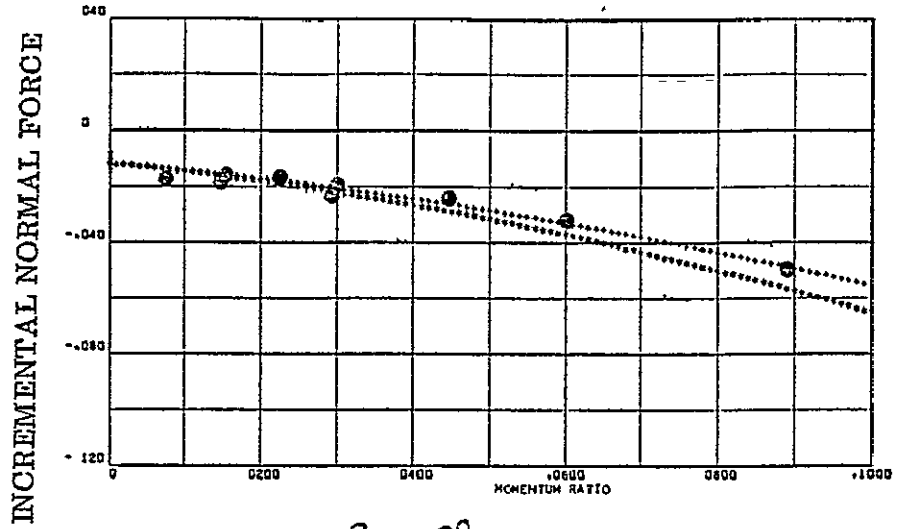


Figure 3-15. Yaw effects on pitch-down RCS side force at 0 to 5 degrees angle of attack.



a_0 error = -.01020

PLOT SYMBOLS
 * $\beta = 0$ MODEL
 . $\beta = 0 \pm 2\sigma$
 + CURVE FIT OF DATA
 ● DATA

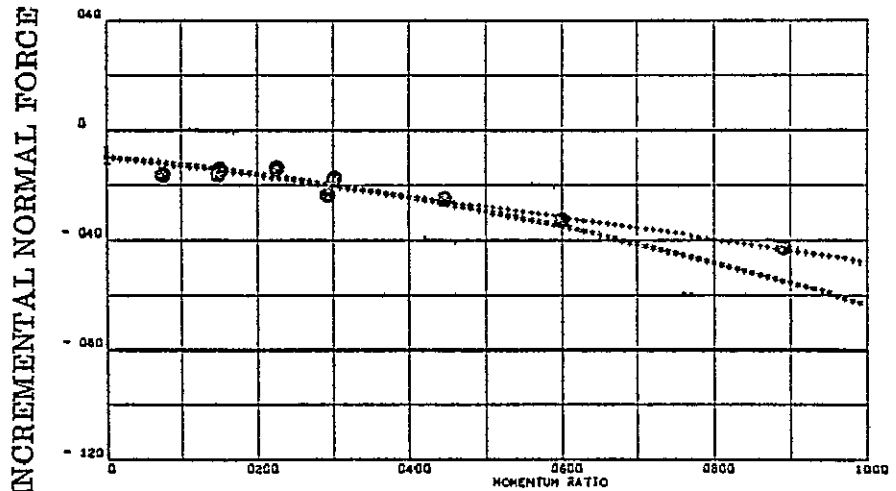
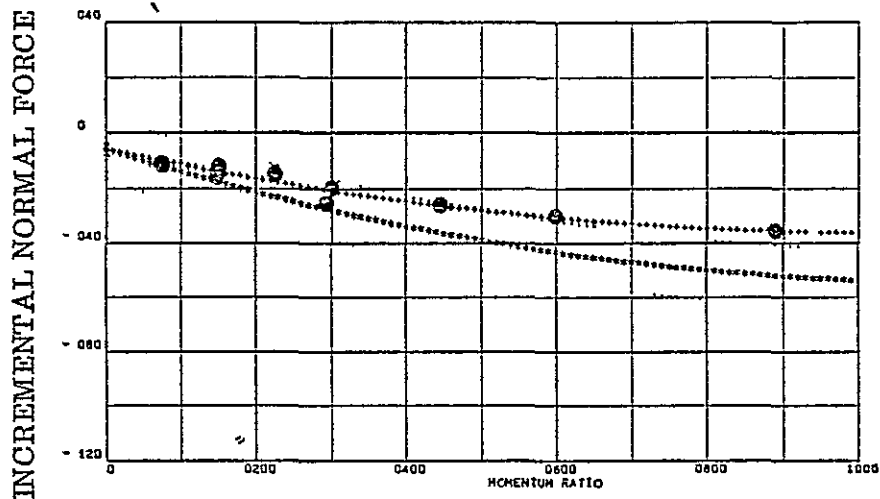


Figure 3-16. Yaw effects on pitch-up RCS normal force at -10 degrees angle of attack.



$$\beta = +3^\circ$$

$$a_0 \text{ error} = -.00216$$

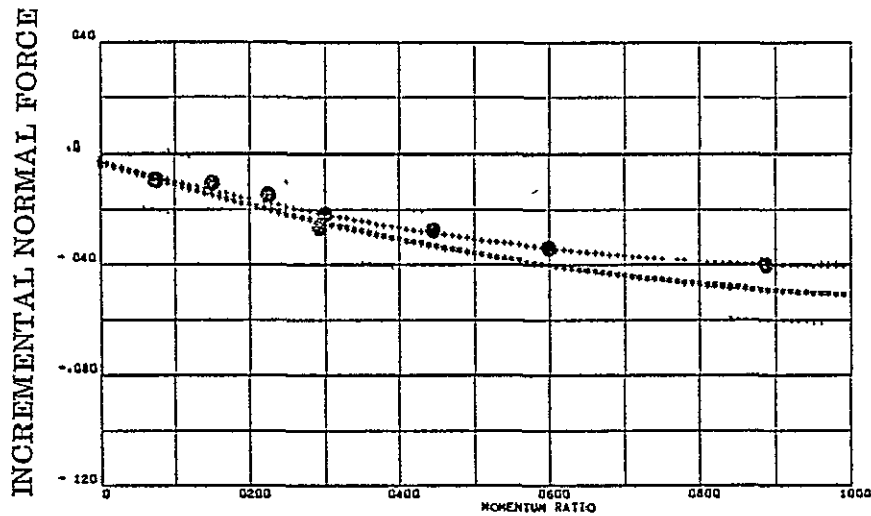
PLOT SYMBOLS

* $\beta = 0$ MODEL

. $\beta = 0 \pm 2\sigma$

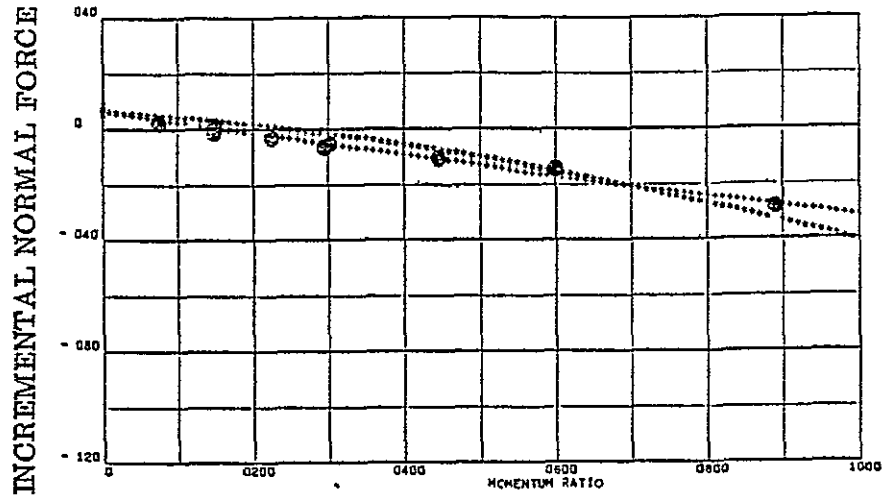
- CURVE FIT OF DATA

● DATA



$$\beta = -3^\circ$$

Figure 3-17. Yaw effects on pitch-up RCS normal force at 0 degrees angle of attack.



$$\beta = +3^\circ$$

σ error = -.00018

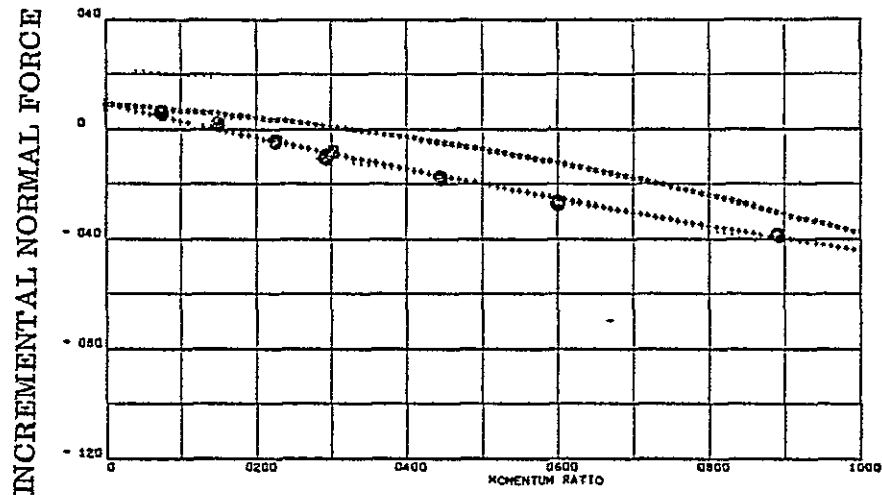
PLOT SYMBOLS

* $\beta = 0$ MODEL

. $\beta = 0 \pm 2\sigma$

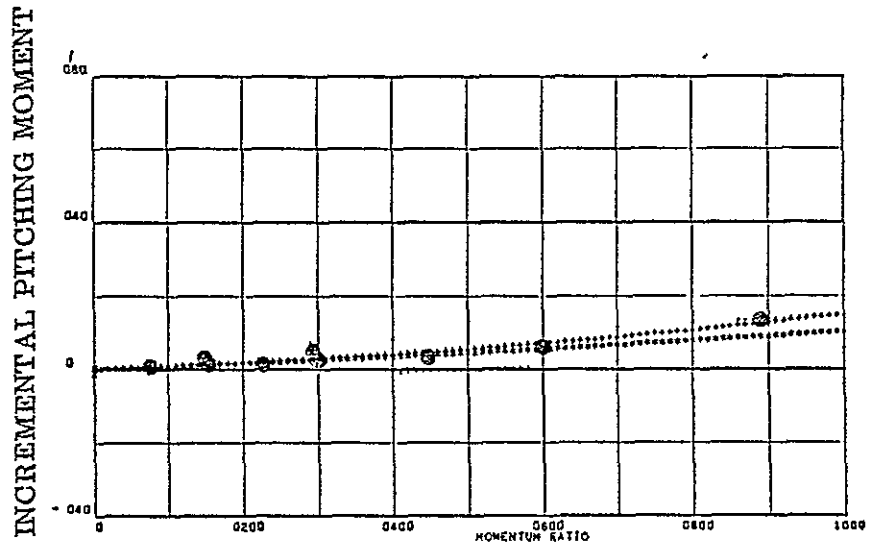
+ CURVE FIT OF DATA

● DATA



$$\beta = -3^\circ$$

Figure 3-18. Yaw effects on pitch-up RCS normal force at 10 degrees angle of attack.



$a_0 \text{ error} = .00207$

PLOT SYMBOLS

- * $\beta = 0$ MODEL
- . $\beta = 0 \pm 2\sigma$
- + CURVE FIT OF DATA
- DATA

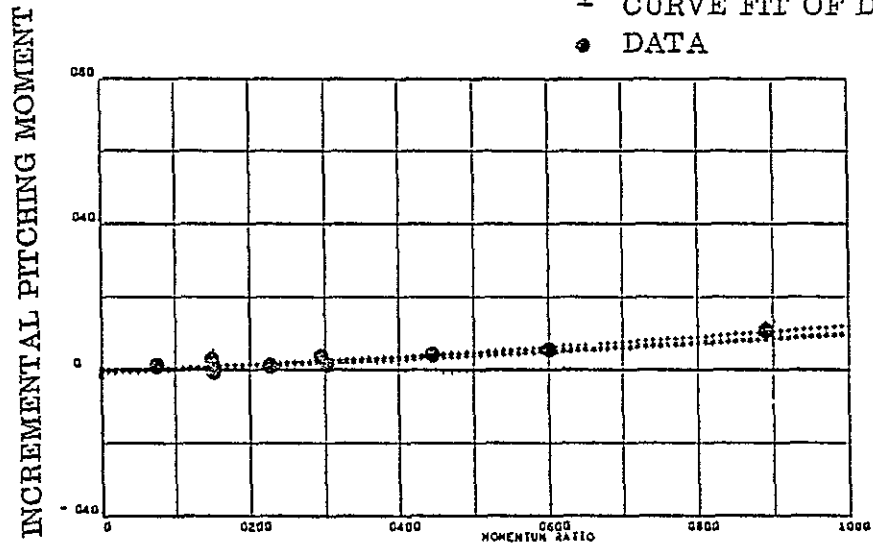
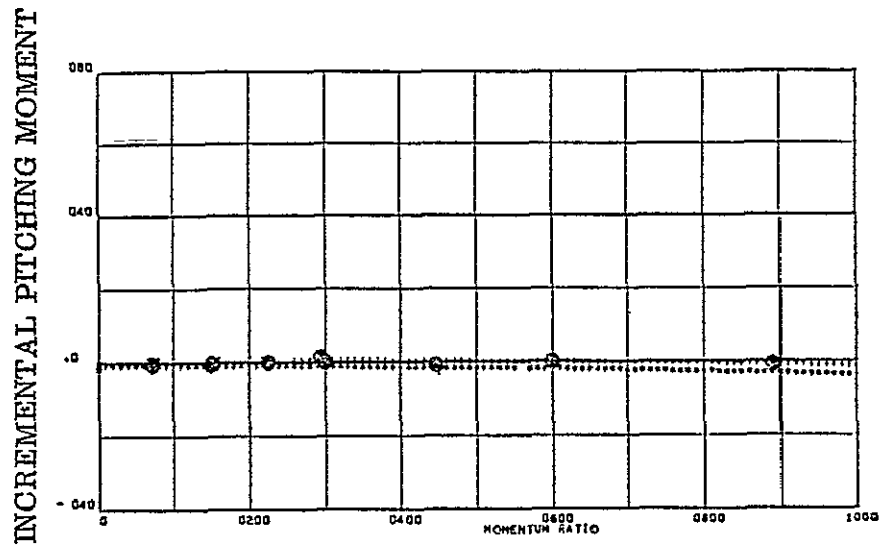


Figure 3-19. Yaw effects on pitch-up RCS pitching moment at -10 degrees angle of attack.

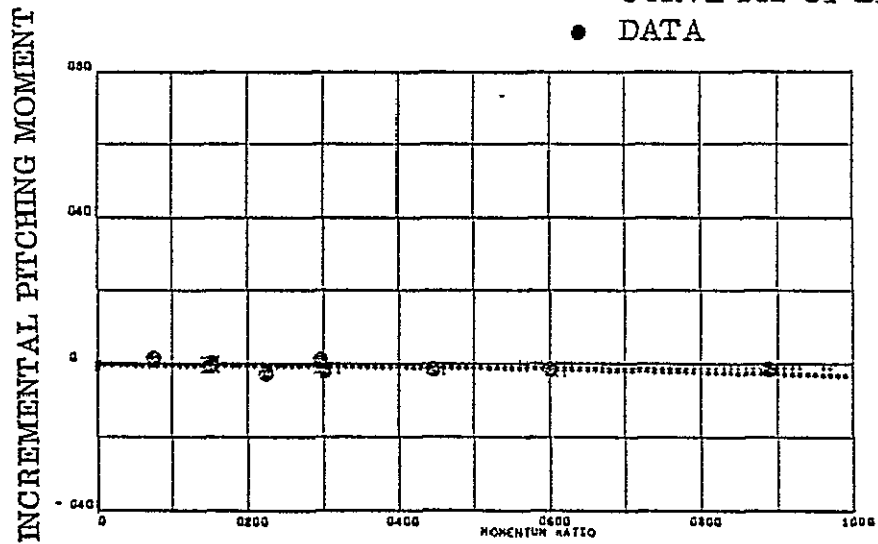


$$\beta = +3^\circ$$

a_0 error = 0.

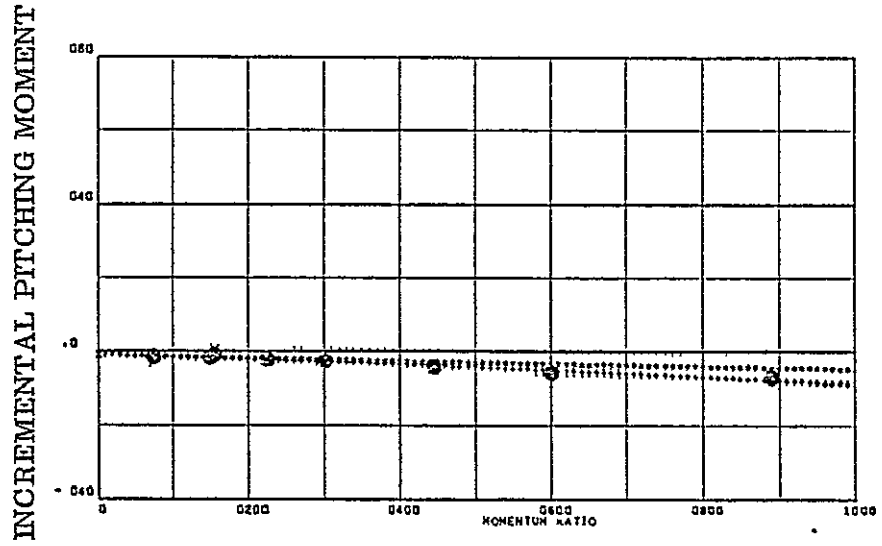
PLOT SYMBOLS

- * $\beta = 0$ MODEL
- . $\beta = 0 \pm 2\sigma$
- + CURVE FIT OF DATA
- DATA



$$\beta = -3^\circ$$

Figure 3-20. Yaw effects on pitch-up RCS pitching moment. at 0 degrees angle of attack.



$a_0 \text{ error} = -.00135$

PLOT SYMBOLS
 * $\beta = 0$ MODEL
 . $\beta = 0 \pm 2\sigma$
 + CURVE FIT OF DATA
 ● DATA

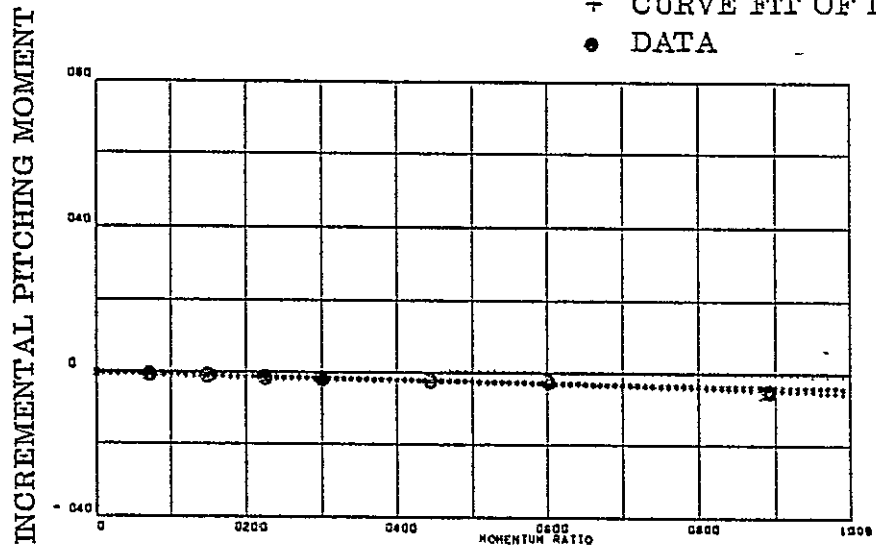
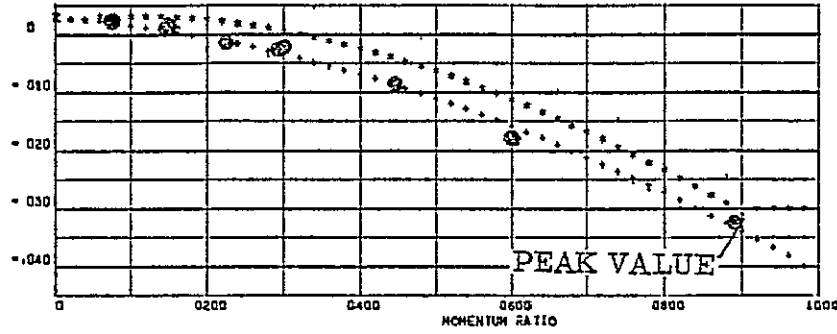


Figure 3-21. Yaw effects on pitch-up RCS pitching moment at 10 degrees angle of attack.

INCREMENTAL ROLL MOMENT



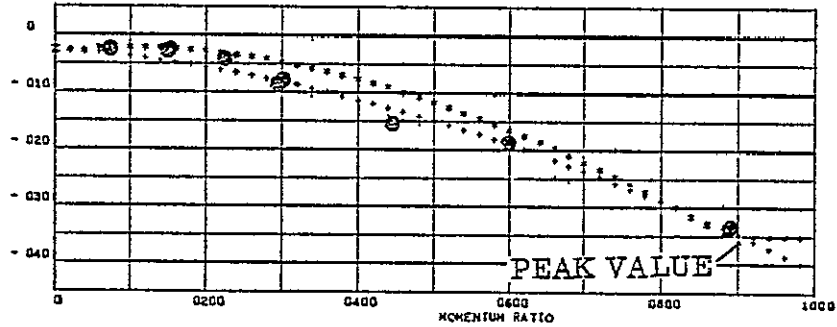
$$\beta = +3^\circ$$

$$\Delta C_{l_{max}} = -.0013$$

PLOT SYMBOLS

- * $\beta = 0$ MODEL
- . $\beta = 0 \pm 2\sigma$
- + CURVE FIT OF DATA
- DATA

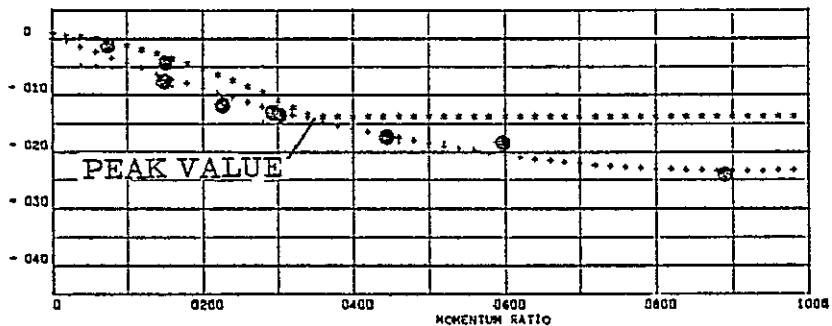
INCREMENTAL ROLL MOMENT



$$\beta = -3^\circ$$

Figure 3-22. Yaw effects on pitch-up RCS rolling moment at -10 degrees angle of attack.

INCREMENTAL ROLL MOMENT



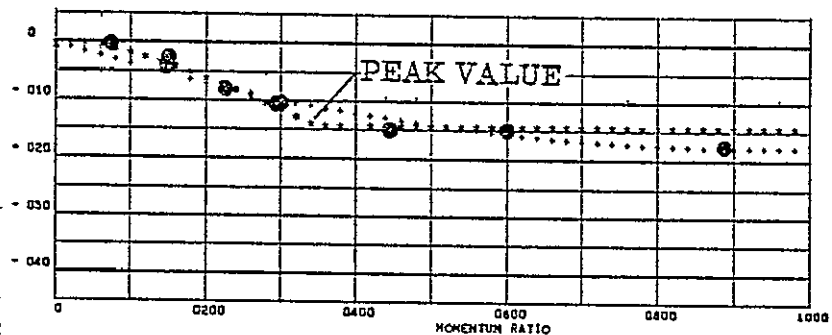
$$\beta = +3^\circ$$

$$\Delta C_{l \max} = -.00103$$

PLOT SYMBOLS

- * $\beta = 0$ MODEL
- . $\beta = 0 \pm 2\sigma$
- CURVE FIT OF DATA
- DATA

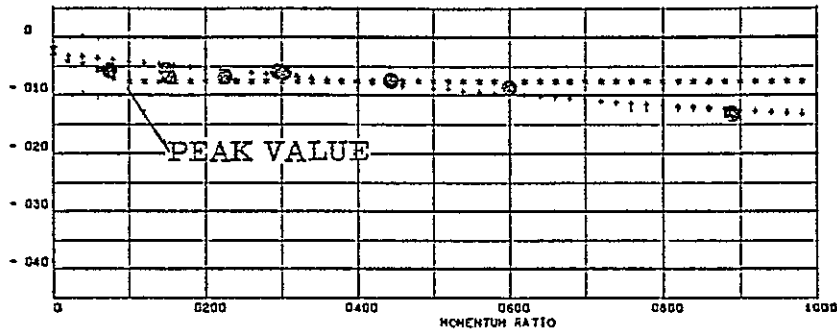
INCREMENTAL ROLL MOMENT



$$\beta = -3^\circ$$

Figure 3-23. Yaw effects on pitch-up RCS rolling moment at 0 degrees angle of attack.

INCREMENTAL ROLL MOMENT



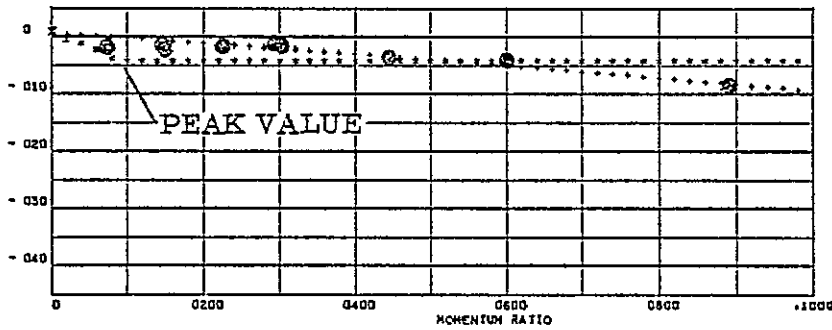
$$\beta = +3^\circ$$

$$\Delta C_{l_{\max}} = -.00103$$

PLOT SYMBOLS

- * $\beta = 0$ MODEL
- . $\beta = 0 - 2\sigma$
- + CURVE FIT OF DATA
- ⊙ DATA

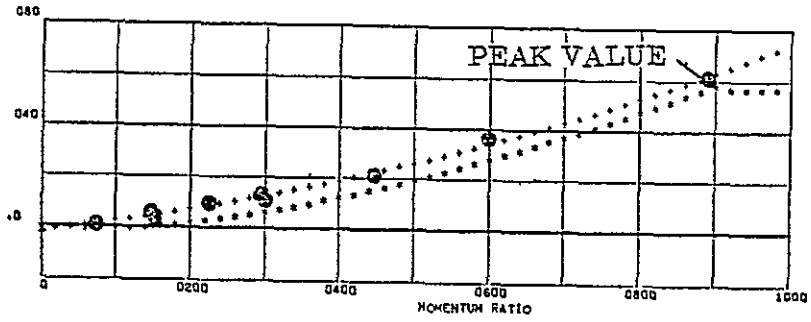
INCREMENTAL ROLL MOMENT



$$\beta = -3^\circ$$

Figure 3-24. Yaw effects on pitch-up RCS rolling moment at 10 degrees angle of attack.

INCREMENTAL YAWING MOMENT



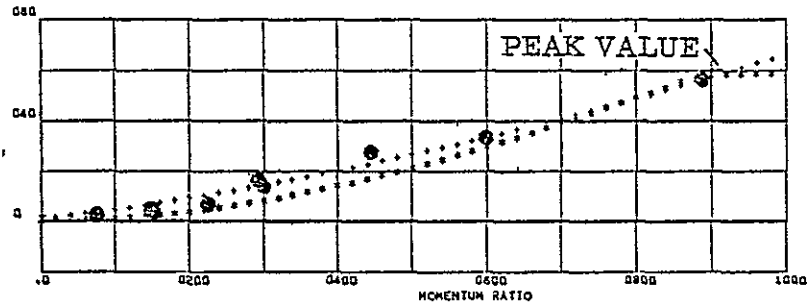
$$\beta = +3^\circ$$

$$\Delta C_{n \max} = .00105$$

PLOT SYMBOLS

- * $\beta = 0$ MODEL
- . $\beta = 0 - 2\sigma$
- + CURVE FIT OF DATA
- DATA

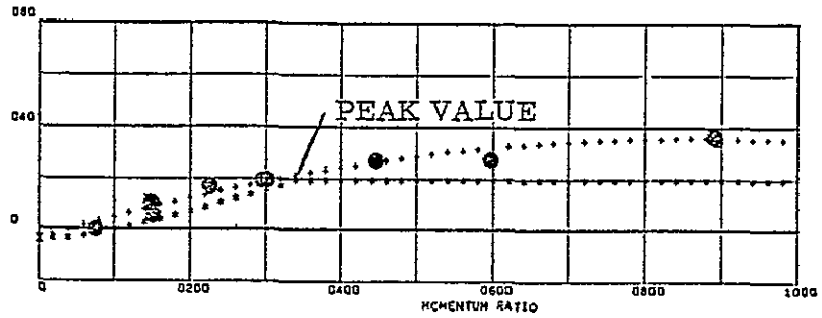
INCREMENTAL YAWING MOMENT



$$\beta = -3^\circ$$

Figure 3-25. Yaw effects on pitch-up RCS yawing moment at -10 degrees angle of attack.

INCREMENTAL YAWING MOMENT



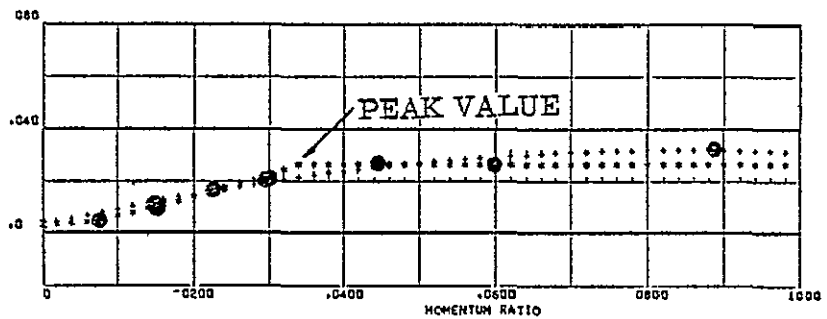
$$\beta = +3^\circ$$

$$\Delta C_{n \max} = .00105$$

PLOT SYMBOLS

- * $\beta = 0$ MODEL
- . $\beta = 0 \pm 2\sigma$
- CURVE FIT OF DATA
- DATA

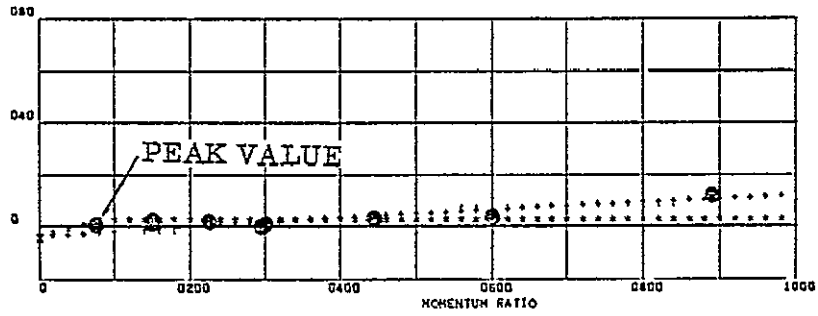
INCREMENTAL YAWING MOMENT



$$\beta = -3^\circ$$

Figure 3-26. Yaw effects on pitch-up RCS yawing moment at 0 degrees angle of attack.

INCREMENTAL YAWING MOMENT



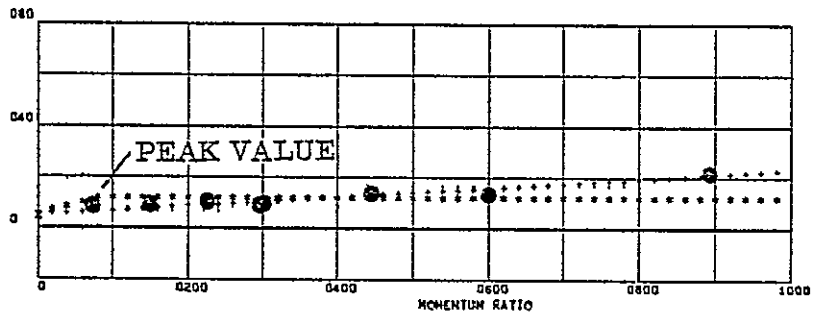
$$\beta = +3^\circ$$

$$\Delta C_{n \max} = .00105$$

PLOT SYMBOLS

- * $\beta = 0$ MODEL
- . $\beta = 0 \pm 2\sigma$
- CURVE FIT OF DATA
- DATA

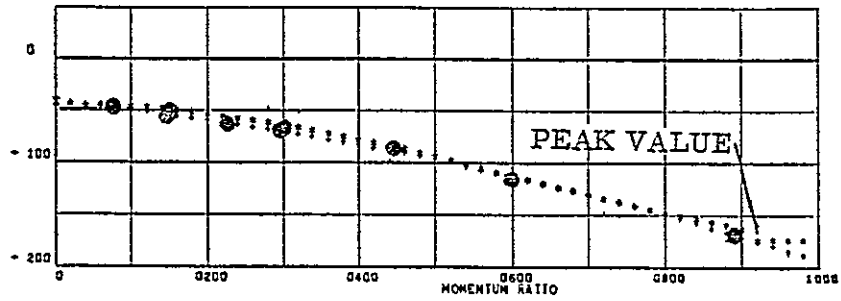
INCREMENTAL YAWING MOMENT



$$\beta = -3^\circ$$

Figure 3-27. Yaw effects on pitch-up RCS yawing moment at 10 degrees angle of attack.

INCREMENTAL SIDE FORCE



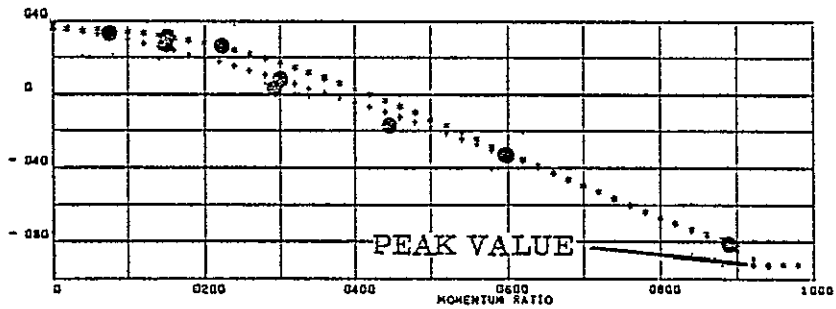
$$\beta = +3^\circ$$

$$\Delta C_{y \max} = -.00227$$

PLOT SYMBOLS

- * $\beta = 0$ MODEL
- . $\beta = 0 \pm 2\sigma$
- + CURVE FIT OF DATA
- DATA

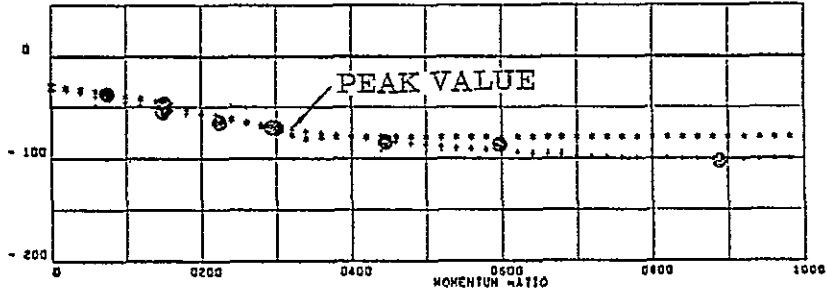
INCREMENTAL SIDE FORCE



$$\beta = -3^\circ$$

Figure 3-28. Yaw effects on pitch-up RCS side force at -10 degrees angle of attack.

INCREMENTAL SIDE FORCE



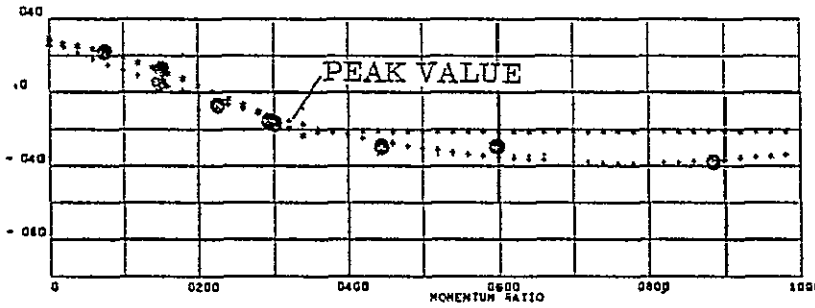
$$\beta = +3^\circ$$

$$\Delta C_{y \max} = -.00227$$

PLOT SYMBOLS

- * $\beta = 0$ MODEL
- . $\beta = 0 \pm 2\sigma$
- CURVE FIT OF DATA
- DATA

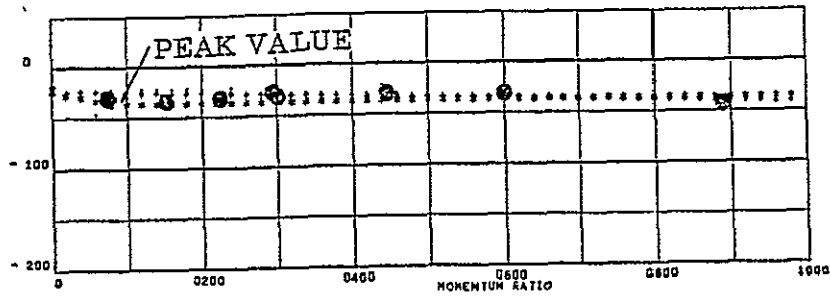
INCREMENTAL SIDE FORCE



$$\beta = -3^\circ$$

Figure 3-29. Yaw effects on pitch-up RCS side force at 0 degrees angle of attack.

INCREMENTAL SIDE FORCE

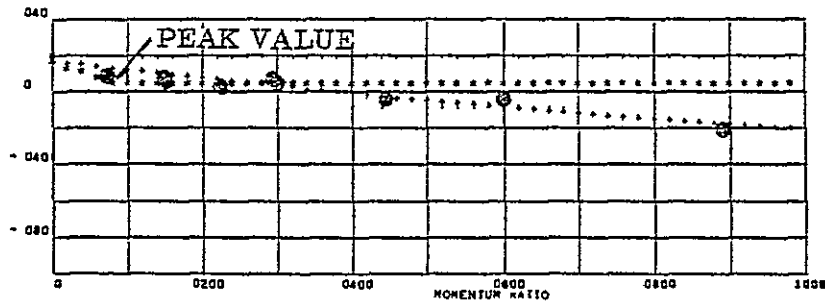


$$\beta = +3^\circ$$

PLOT SYMBOLS

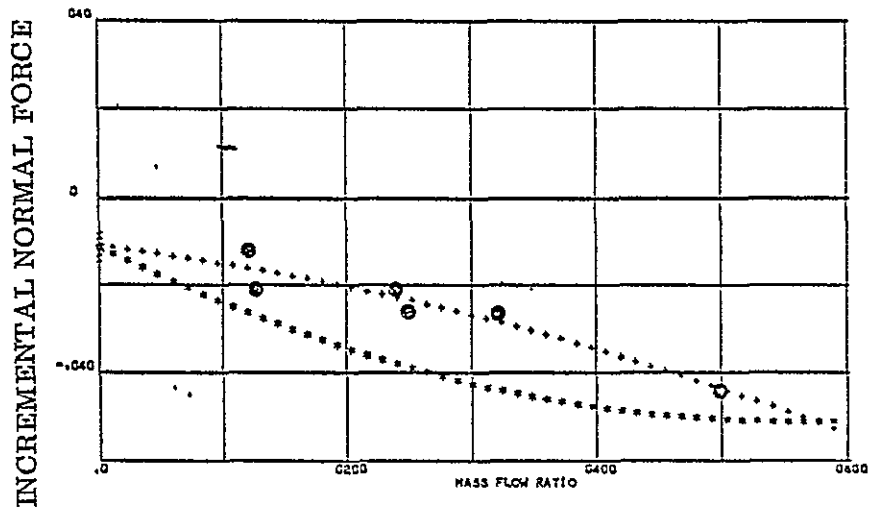
- * $\beta = 0$ MODEL
- . $\beta = 0 \pm 2\sigma$
- CURVE FIT OF DATA
- DATA

INCREMENTAL SIDE FORCE



$$\beta = -3^\circ$$

Figure 3-30. Yaw effects on pitch-up RCS side force at 10 degrees angle of attack.

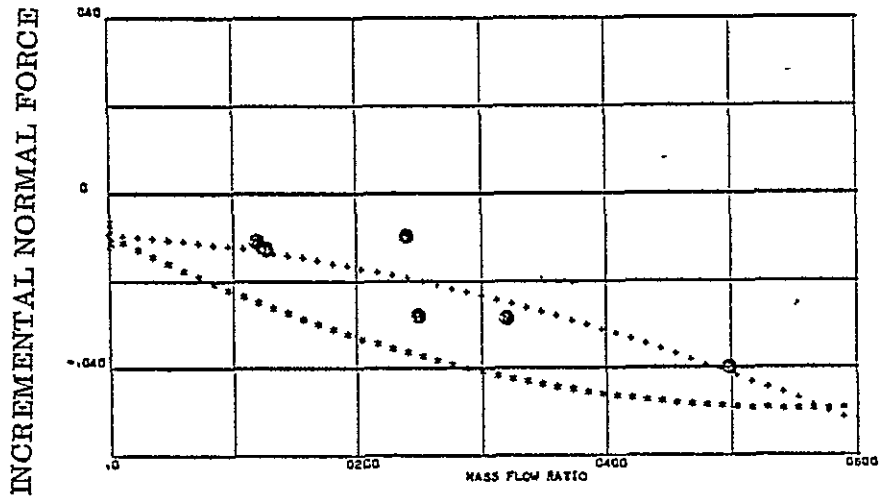


$$\beta = +3^\circ$$

a_0 error = .00327

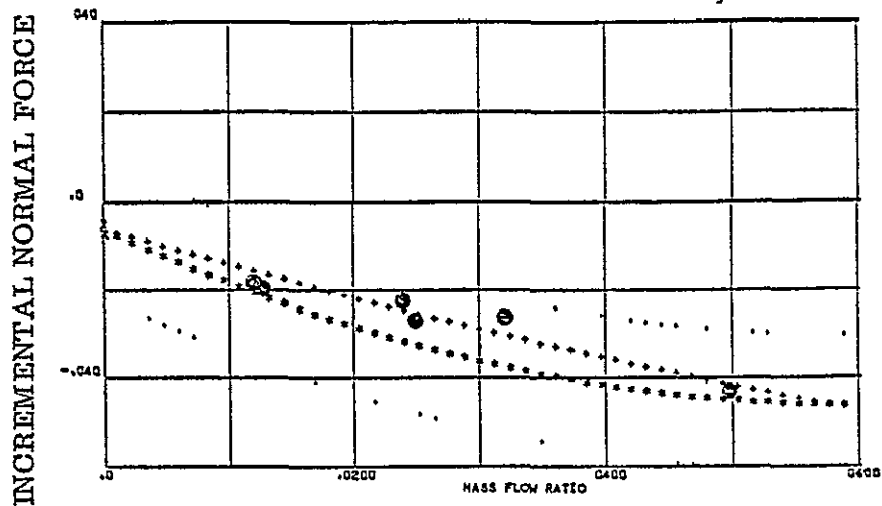
PLOT SYMBOLS

- * $\beta = 0$ MODEL
- . $\beta = 0 \pm 2\sigma$
- + CURVE FIT OF DATA
- DATA



$$\beta = -3^\circ$$

Figure 3-31. Yaw effects on yaw RCS normal force at -10 to -5 degrees angle of attack.

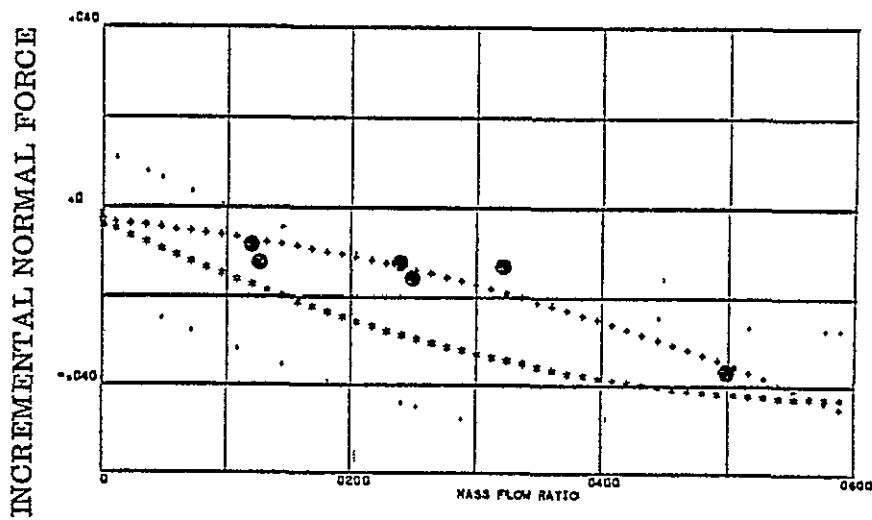


$$\beta = +3^\circ$$

σ error = .00414

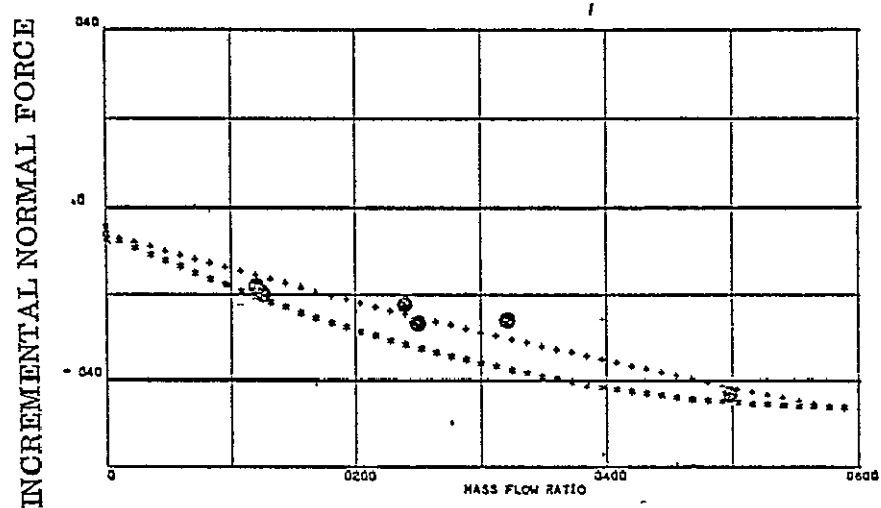
PLOT SYMBOLS

- * $\beta = 0$ MODEL
- . $\beta = 0 - 2\sigma$
- + CURVE FIT OF DATA
- DATA



$$\beta = -3^\circ$$

Figure 3-32. Yaw effects on yaw RCS normal force at -5 to 0 degrees angle of attack.



$\sigma_{\text{error}} = 0.0524$

- PLOT SYMBOLS
 * $\beta = 0$ MODEL
 . $\beta = 0 \pm 2\sigma$
 - CURVE FIT OF DATA
 ● DATA

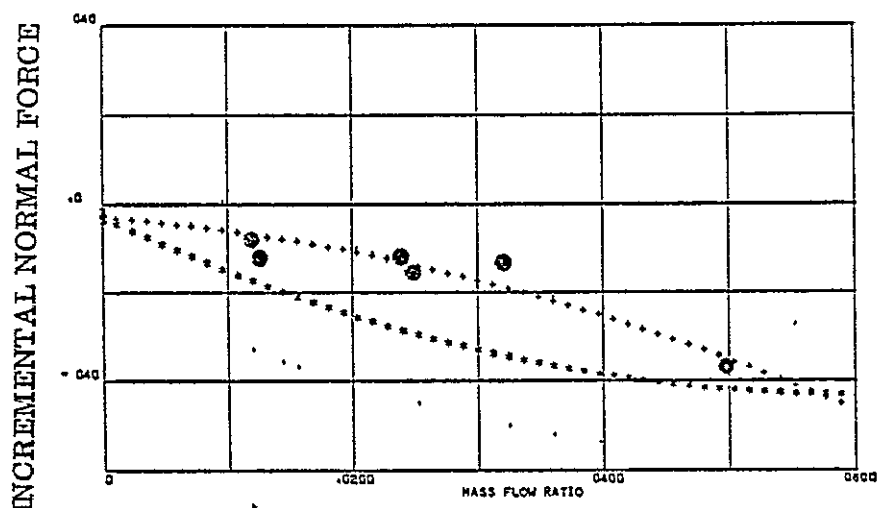
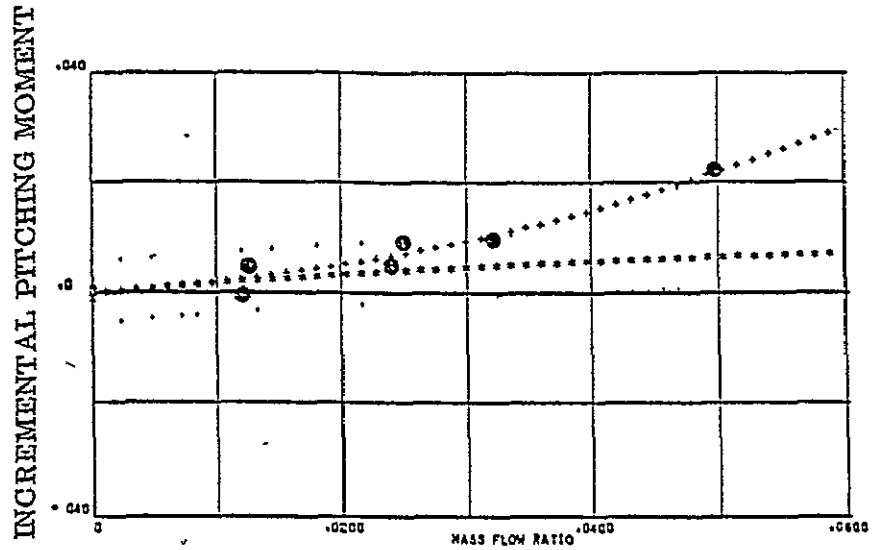


Figure 3-33. Yaw effects on yaw RCS normal force at 0 to 5 degrees angle of attack.

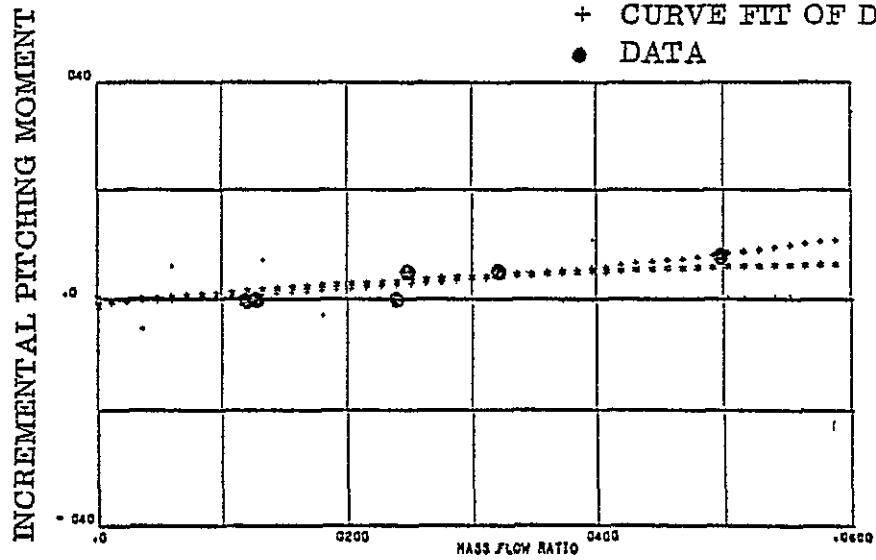


$$\beta = +3^\circ$$

σ error = .00006

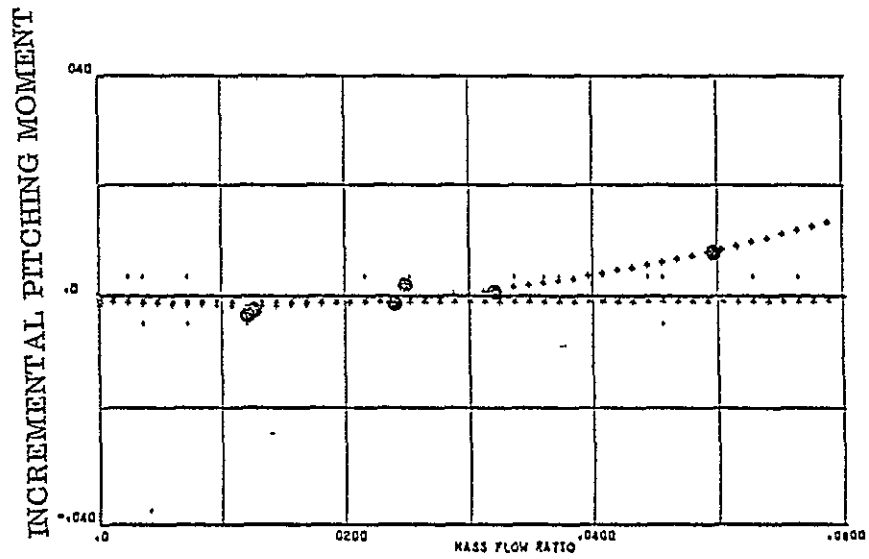
PLOT SYMBOLS

- * $\beta = 0$ MODEL
- . $\beta = 0 \pm 2\sigma$
- + CURVE FIT OF DATA
- DATA



$$\beta = -3^\circ$$

Figure 3-34. Yaw effects on yaw RCS pitching moment at -10 to -5 degrees angle of attack.



$$\beta = +3^\circ$$

a_0 error = 0.

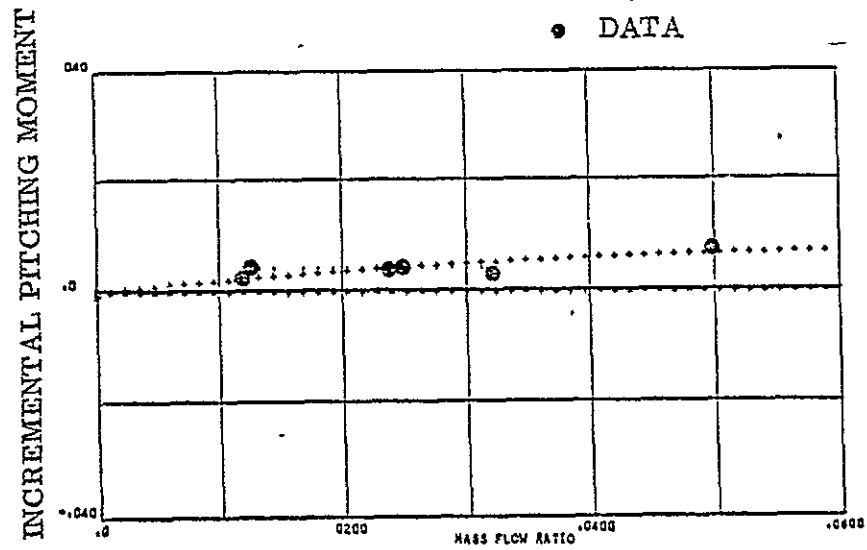
PLOT SYMBOLS

* $\beta = 0$ MODEL

. $\beta = 0 \pm 2\sigma$

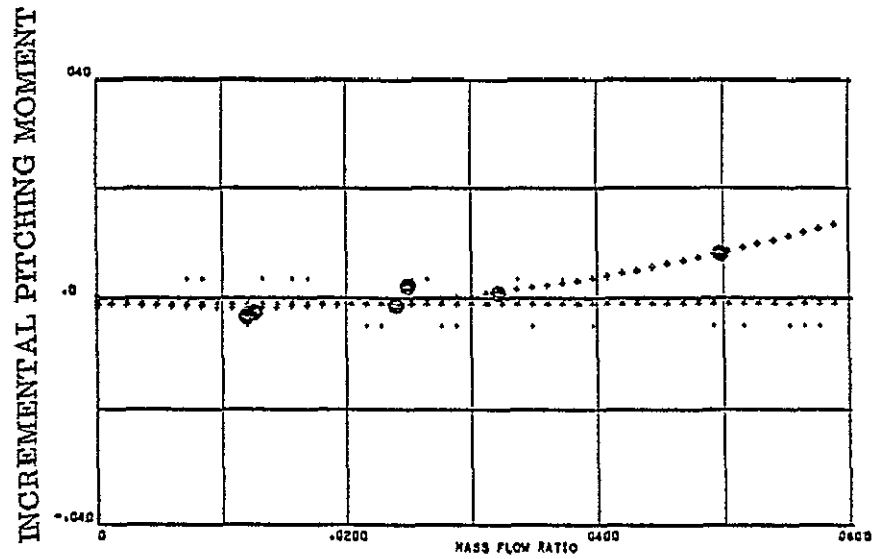
+ CURVE FIT OF DATA

● DATA



$$\beta = -3^\circ$$

Figure 3-35. Yaw effects on yaw RCS pitching moment at -5 to 0 degrees angle of attack.

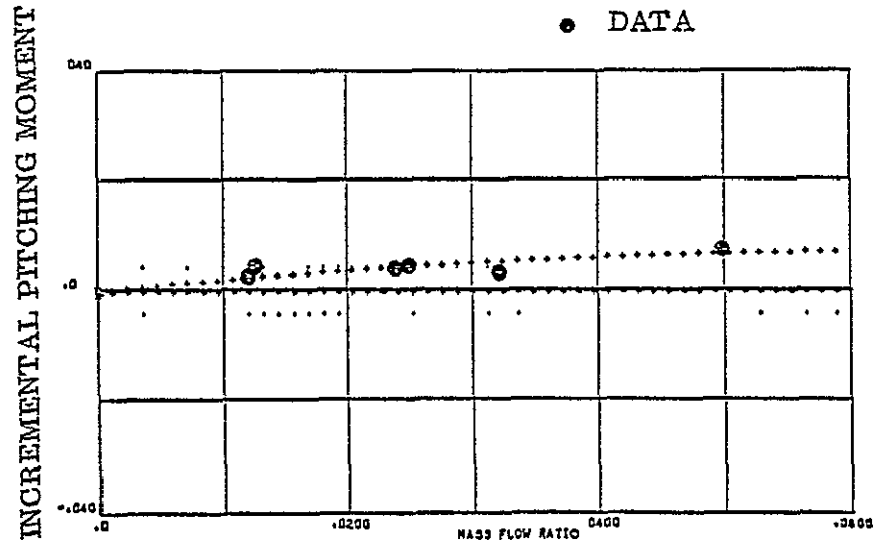


$$\beta = +3^\circ$$

a_0 error = 0.

PLOT SYMBOLS

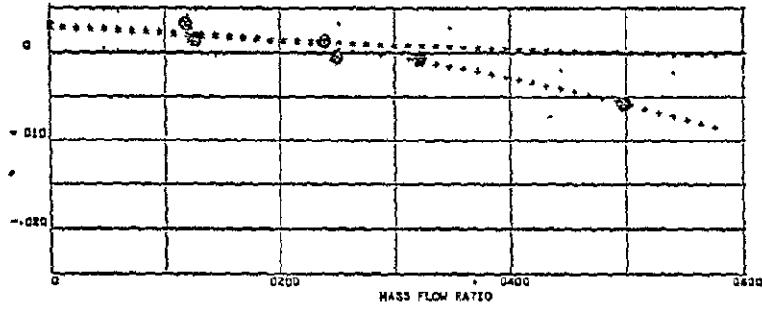
- * $\beta = 0$ MODEL
- . $\beta = 0 \pm 2\sigma$
- + CURVE FIT OF DATA
- DATA



$$\beta = -3^\circ$$

Figure 3-36. Yaw effects on yaw RCS pitching moment at 0 to 5 degrees angle of attack.

INCREMENTAL ROLL MOMENT



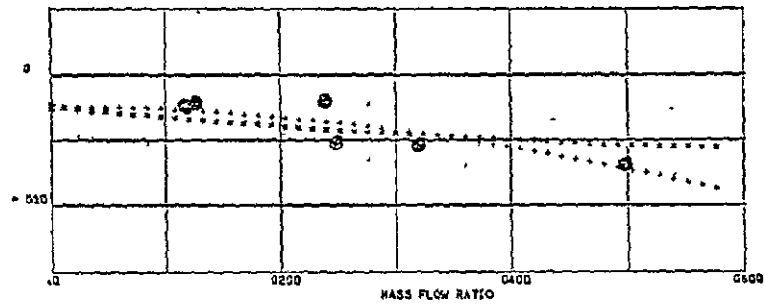
$$\beta = +3^\circ$$

σ error = .0005

PLOT SYMBOLS

- * $\beta = 0$ MODEL
- . $\beta = 0 \pm 2\sigma$
- + CURVE FIT OF DATA
- DATA

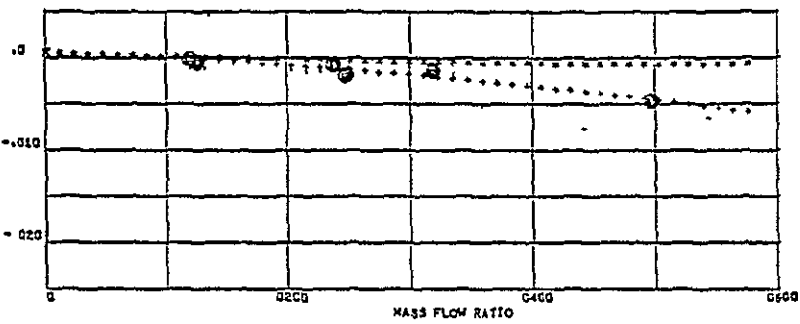
INCREMENTAL ROLL MOMENT



$$\beta = -3^\circ$$

Figure 3-37. Yaw effects on yaw RCS rolling moment at -10 to -5 degrees angle of attack.

INCREMENTAL ROLL MOMENT



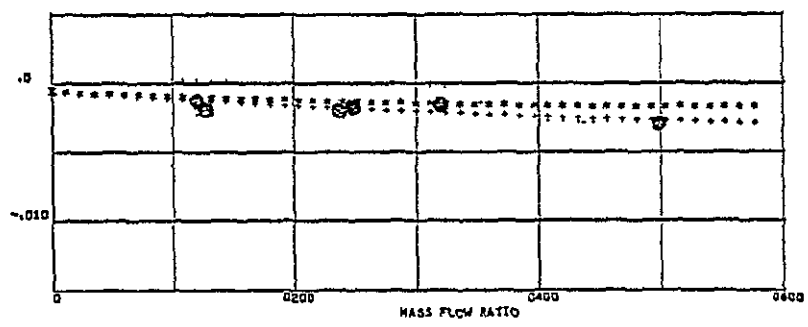
$\beta = +3^\circ$

σ error = 0.

PLOT SYMBOLS

- * $\beta = 0$ MODEL
- . $\beta = 0 \pm 2\sigma$
- + CURVE FIT OF DATA
- DATA

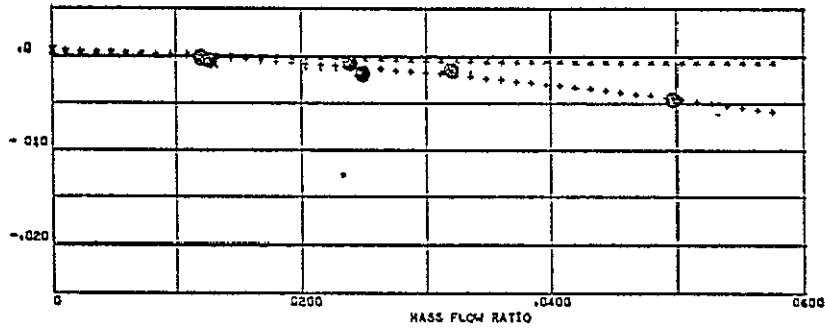
INCREMENTAL ROLL MOMENT



$\beta = -3^\circ$

Figure 3-38. Yaw effects on yaw RCS rolling moment at -5 to 0 degrees angle of attack.

INCREMENTAL ROLL MOMENT



$$\beta = +3^\circ$$

$$a_0 \text{ error} = -.00016$$

PLOT SYMBOLS

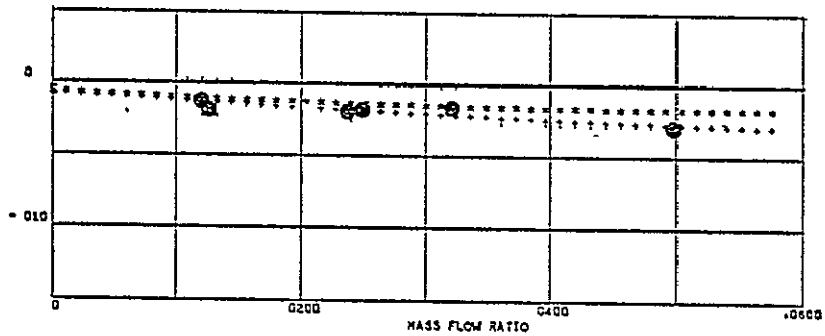
* $\beta = 0$ MODEL

. $\beta = 0 \pm 2\sigma$

+ CURVE FIT OF DATA

● DATA

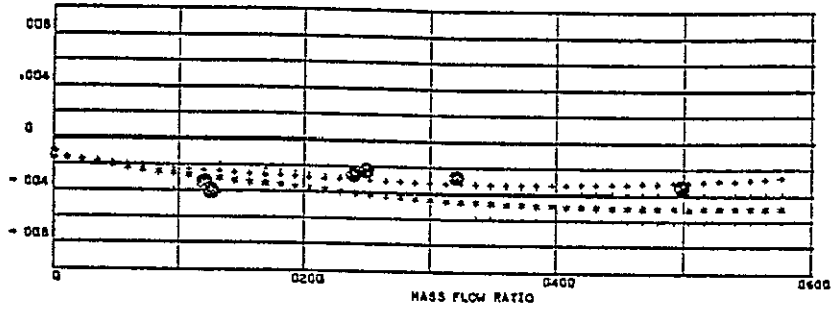
INCREMENTAL ROLL MOMENT



$$\beta = -3^\circ$$

Figure 3-39. Yaw effects on yaw RCS rolling moment at 0 to 5 degrees angle of attack.

INCREMENTAL YAWING MOMENT



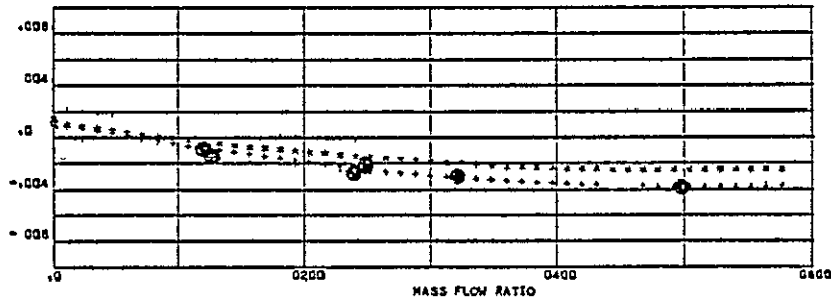
$$\beta = +3^\circ$$

$$\sigma_{\text{error}} = .00007$$

PLOT SYMBOLS

- * $\beta = 0$ MODEL
- . $\beta = 0 \pm 2\sigma$
- CURVE FIT OF DATA
- DATA

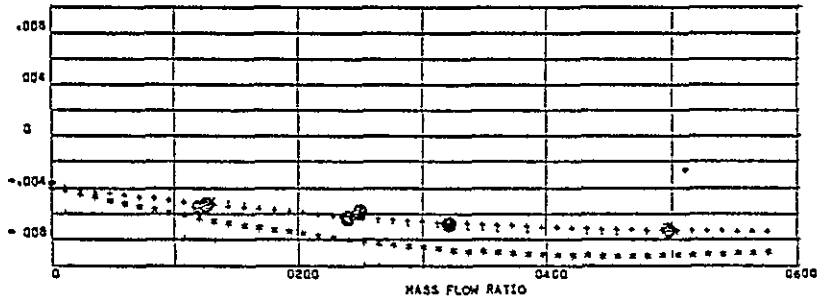
INCREMENTAL YAWING MOMENT



$$\beta = -3^\circ$$

Figure 3-40. Yaw effects on yaw RCS yawing moment at -10 to -5 degrees angle of attack.

INCREMENTAL YAWING MOMENT



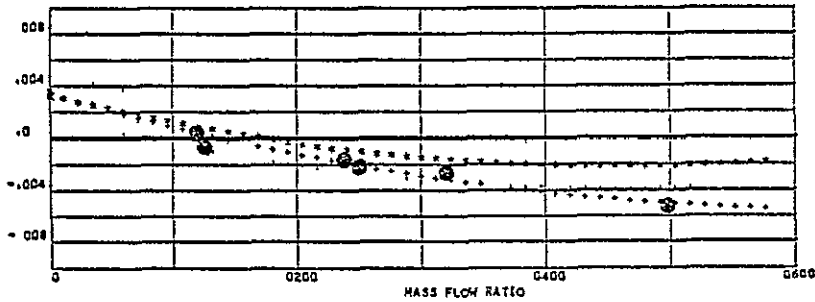
$$\beta = +3^\circ$$

$$a_0 \text{ error} = .00016$$

PLOT SYMBOLS

- * $\beta = 0$ MODEL
- . $\beta = 0 \pm 2\sigma$
- CURVE FIT OF DATA
- DATA

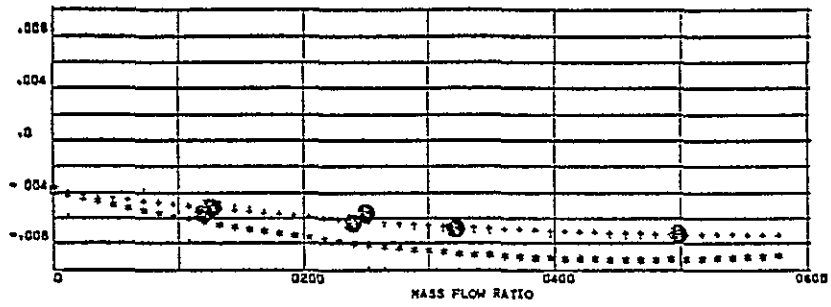
INCREMENTAL YAWING MOMENT



$$\beta = -3^\circ$$

Figure 3-41. Yaw effects on yaw RCS yawing moment at -5 to 0 degrees angle of attack.

INCREMENTAL YAWING MOMENT

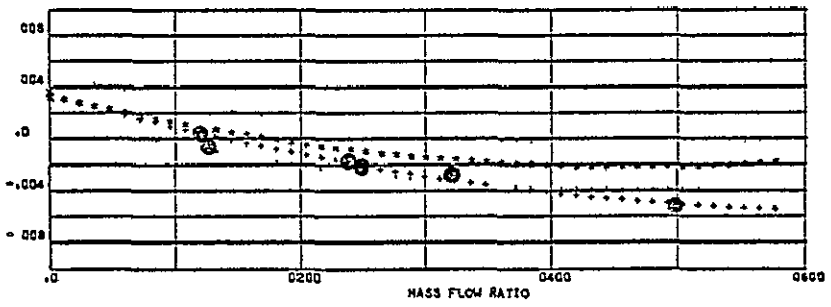


$\beta = +3^\circ$

$a_0 \text{ error} = -.00013$

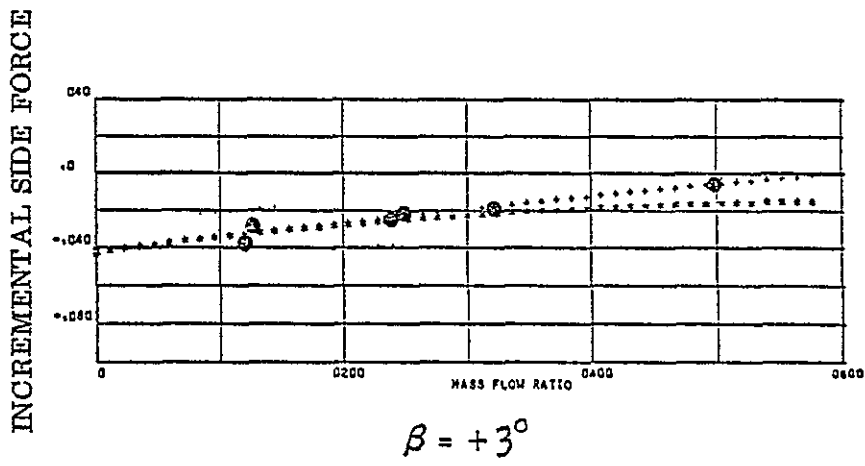
- PLOT SYMBOLS
 * $\beta = 0$ MODEL
 . $\beta = 0 \pm 2\sigma$
 + CURVE FIT OF DATA
 ● DATA

INCREMENTAL YAWING MOMENT



$\beta = -3^\circ$

Figure 3-42. Yaw effects on yaw RCS yawing moment at 0 to 5 degrees angle of attack.



a_{\circ} error = - 00245

PLOT SYMBOLS

- * $\beta = 0$ MODEL
- . $\beta = 0 \pm 2\sigma$
- + CURVE FIT OF DATA
- DATA

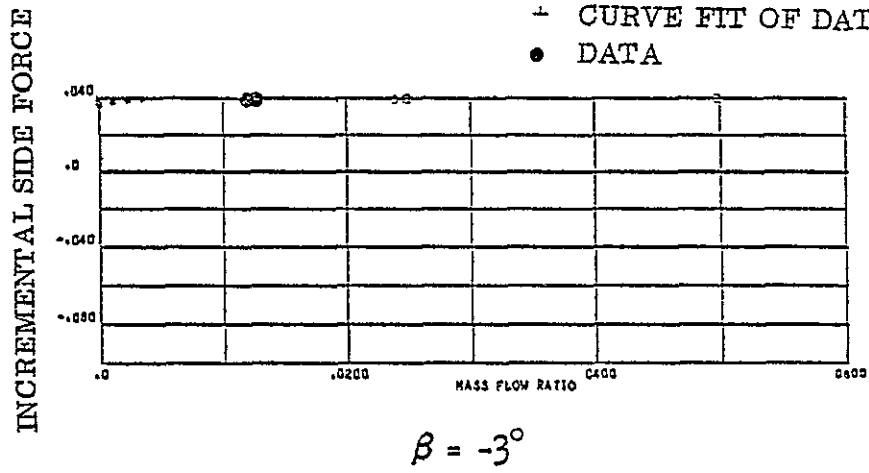
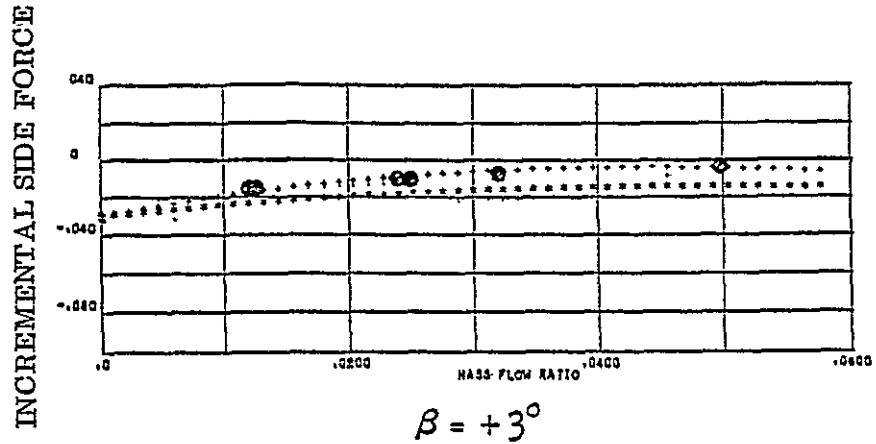


Figure 3-43. Yaw effects on yaw RCS side force at -10 to -5 degrees angle of attack.



$a_{\text{error}} = -.00038$

PLOT SYMBOLS
 * $\beta = 0$ MODEL
 . $\beta = 0 - 2\sigma$
 + CURVE FIT OF DATA
 ● DATA

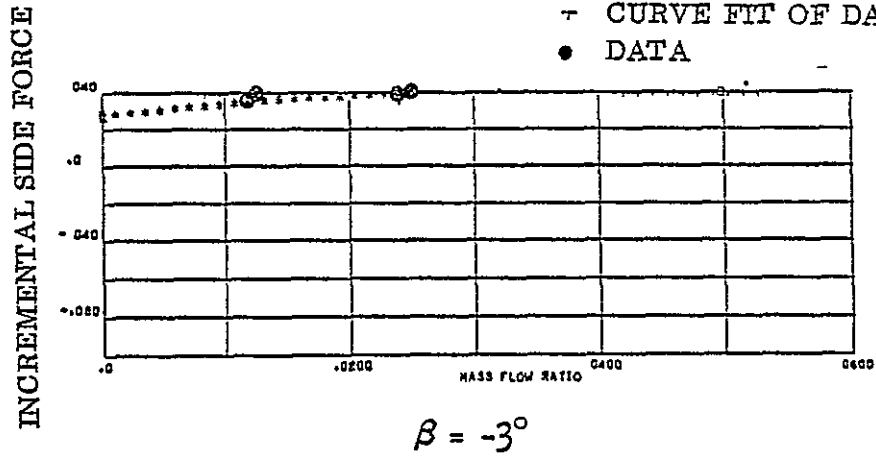
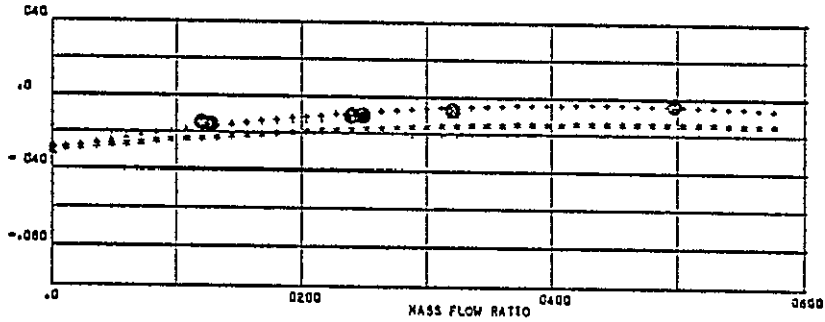


Figure 3-44. Yaw effects on yaw RCS side force at -5 to 0 degrees angle of attack.

INCREMENTAL SIDE FORCE



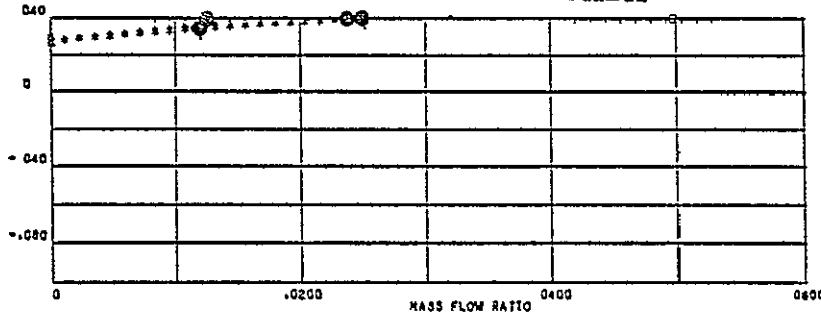
$$\beta = +3^\circ$$

a_0 error = -.00016

PLOT SYMBOLS

- * $\beta = 0$ MODEL
- . $\beta = 0 - 2\sigma$
- + CURVE FIT OF DATA
- DATA

INCREMENTAL SIDE FORCE



$$\beta = -3^\circ$$

Figure 3-45. Yaw effects on yaw RCS side force at 0 to 5 degrees angle of attack.

4

REAR-MOUNTED RCS CONTROL EFFECTIVENESS DURING RTLS

4.1 GENERAL

The estimated control effectiveness of the rear-mounted Reaction Control System (RCS) during reentry was presented in Reference 1, which showed the most critical cases occurred at the highest dynamic pressures. This section extends the analysis of the control effectiveness of the rear-mounted RCS to the flight regime which may be encountered in the return to landing site (RTLS) abort maneuvers using the analytic program described in Reference 1.

The RTLS flight regime is illustrated in Figure 4-1, which shows that the angles of attack are much lower and the dynamic pressure is higher than the reentry conditions analyzed previously.

The analysis was limited to two control cases (1) symmetric pitch down, and (2) combined pitch down and roll, since they represent the most critical problem at low angle of attack.

4.2 RTLS FLIGHT CONDITIONS

Figure 4-1 presented the reaction control system utilization and the representative flight conditions over which this maneuver may be performed. These conditions were used to define the velocity in 25,000 ft increments from 175,000 to 250,000 feet. The 1962 standard atmosphere was used as the nominal flight conditions at each of the four altitudes. The 1976 standard atmosphere (Reference 9) was used to define the seasonal maximum, minimum, and 2-sigma extremes at these altitudes. These data, shown in Table 4-1, were used to compute the effects of atmospheric uncertainty at a nominal Mach number of 8.

4.3 SYMMETRIC PITCH-DOWN RCS

Figure 4-1 shows that four-jet aft pitch control is to be used through the coast and pitch-up phases of the RTLS staging maneuver. The symmetric two-jet-on-each-side pitch-down RCS control is more critical than the pitch-up case, since the impingement, interaction, and across-the-base cross-coupling terms in the prediction model all act in opposition to the thrust moment. Thus, this study concentrated on the four-jet symmetric (two on each side) pitch-down case.

4.3.1 EFFECT OF ANGLE OF ATTACK. Figure 4-2 presents the normal force and pitching moment amplification as a function of angle of attack for a nominal Mach number of 8 at 200,000 feet, standard day conditions. Control amplification is defined as the total control force or moment divided by the thrust force or moment, so that a value of one represents no interference effects, while a value of zero is complete cancellation. The pitching moment is insensitive to angle of attack, while the normal force data are dependent on angle of attack up to five degrees. The two-sigma error curves show that there is no problem using the rear-mounted RCS units to obtain pitch control at any angle of attack. The two-sigma error band for normal force shows, however, that the rear-mounted RCS units may not generate any usable translation force to separate the Orbiter from the tank at angles of attack below -3 degrees.

4.3.2 EFFECT OF ALTITUDE. Figure 4-3 presents the effect of altitude on symmetric pitch-down control amplification at zero angle of attack using a Mach number of 8 and standard day conditions. The control amplification is not sensitive to effects of altitude when approached in this way. The expansion of the error envelope at lower altitudes is due to the fixed values of two-sigma error coefficients in the analytic model and the decreasing size of the thrust coefficient terms as dynamic pressure increases.

A more realistic way to look at the effect of altitude would be to assume constant velocity at the start of RTLs coast, since Mach No. is a function of atmospheric temperature. Figure 4-4 shows that the control amplification is still insensitive to altitude using this approach.

4.3.3 EFFECT OF MACH NUMBER. Figure 4-5 shows that control amplification is essentially independent of free-stream Mach No. at constant altitude and angle of attack. The expansion of the error boundaries at higher Mach No. represents the effect of increasing dynamic pressure.

4.3.4 EFFECT OF DYNAMIC PRESSURE. The preceding analyses show that, within the RTLs range of flight conditions, the principal parameters are angle of attack and free-stream dynamic pressure. Figure 4-6 shows that the only apparent effect of dynamic pressure is the expansion of the error boundaries for the symmetric pitch-down case.

4.3.5 EFFECT OF ATMOSPHERIC VARIATION. The atmospheric variation data presented in Table 4-1 were used to generate the data shown in Figure 4-7, where nominal lines are drawn for the various atmospheric conditions assumed. The data appear insensitive to atmosphere variation in the altitude range for RTLs separation maneuvers. The moment data show sensitivity only for the very high dynamic pressure cases, while the force amplification shows it only at the low dynamic pressures.

4.3.6 EFFECT OF REYNOLDS NUMBER. The worst case Reynolds number extrapolation described in Reference 1 was applied to data used to generate Figure 4-3, and Figure 4-8 presents the results. Reynolds number has no apparent effect on the control

moments generated by the pitch-down RCS; however, the worst case effect is strong on the translation force generated by the controls.

4.3.7 SUMMARY. It appears from these data that the confidence in useful rear-mounted RCS pitch control is high throughout the range of RTLS separation maneuvers. Conversely, the confidence in obtaining useful translation forces is low, since control is sensitive to the angle of attack and there is some possibility of Reynolds number effects. Increasing dynamic pressure reduces the Reynolds number effect but increases the error boundaries.

4.4 RCS ROLL CONTROL

The control schedule shown in Figure 4-1 shows that no rear-mounted RCS units are used for roll control at present. This schedule was developed based on the same wind tunnel data as the analytic models of Reference 1. These test results show that RCS roll control is a problem at low angles of attack. Most of the test data on which this conclusion is based were developed for symmetric roll cases (pitch-up plus pitch-down RCS, used together). However, analysis of the individual RCS components show that the problem is principally caused by the peak value of interaction (between the pitch-up jets and the external flow over the fin) shown in Figure 4-9. Thus, this analysis had two purposes: first, to determine if useful roll control could be obtained from the rear-mounted RCS at low angles of attack; and second, to show the effects of flight conditions on it.

The RCS component analysis was performed assuming that a combined control input of four pitch-down jets plus two roll jets was desired. This case was chosen because it represents the pitch control shown in Figure 4-1. There are a number of ways in which this total control requirement can be obtained (for a roll to the right) such as

- a. Three pitch-down left, two pitch-down right, one pitch-up right
- b. Three pitch-down left, one pitch-down right
- c. Three pitch-down left, three pitch-down right, two pitch-up right

Figure 4-10 shows that the roll control obtained with each combination is very sensitive to angle of attack but, if the Orbiter has knowledge of this angle and can control the selection of jets for roll control, it is possible to maintain some roll control throughout the angle-of-attack range of the RTLS separation maneuver.

The existence of the peak interaction is shown in the negative values of roll-control amplification for both cases which have pitch-up jets exhausting near the fin. Useful roll control is obtained both below the peak, where Figure 4-9 shows the interaction declines, and above the peak value of angle of attack, where the interaction also declines.

4.4.1 EFFECT OF ALTITUDE. Figure 4-11 presents the effect of altitude at constant Mach number and zero angle of attack for the three different control combinations. These data were only computed at 175,000, 200,000, 225,000, and 250,000 feet, and it is incorrect to connect the curves through these points for the rear-mounted RCS combinations which use pitch-up jets. The peak interaction is a function of jet momentum ratio as well as angle of attack and, as a result, the peak may be hidden between these computed points on these curves.

Figure 4-12 shows the relative magnitude of the error band as a function of altitude. The fixed value of the two-sigma error in rolling moment coefficient from the wind tunnel correlation (i. e., at $\alpha = 0^\circ$ $C_{l_{2\sigma}} \sim 0.00107$) causes the error to grow, relative to RCS thrust rolling coefficient primarily as a function of dynamic pressure rather than altitude.

4.4.2 EFFECT OF ATMOSPHERE VARIATION. Figure 4-13 and 4-14 present data on the rolling moment amplification at zero angle of attack as a function of changes in the atmospheric model presented in Table 4-1. Figure 4-13 shows clearly how the pitch-up peak value only appeared in the standard atmosphere case at the points computed and not in the other variations, and how dangerous it is not to examine all points on the trajectory. Figure 4-14 also shows significant effects of atmosphere model at the 225,000-foot point. These effects are primarily due to the range of dynamic pressure encountered in this flight regime.

4.4.3 ROLL CONTROL EFFECTIVENESS MAPS. Figure 4-10 showed how sensitive roll control effectiveness is to angle of attack, while Figures 4-11 to 4-14 demonstrate the sensitivity to flight dynamic pressure. Reference 1 showed that the interaction terms which are the primary reason for reduced control effectiveness are functions of jet momentum ratio defined as:

$$\frac{\phi_J}{\phi_\infty} = \frac{C_{d_j} \gamma_j P_j M_j^2 \Sigma A_j}{\gamma_\infty P_\infty M_\infty^2 S_{wing}} \quad (4-1)$$

In flight, everything is fixed except the number of nozzles (ΣA_j) and free-stream dynamic pressure ($\gamma/2 P_\infty M_\infty^2$). Thus, it should be possible to break the roll control models into parts and to obtain maps of control effectiveness on an angle-of-attack versus dynamic-pressure plot. The Orbiter can use such plots in its control selection logic, if the plots are computed on board.

4.4.3.1 Pitch-Up RCS Roll Control Map. The maps suggested above have been drawn to determine the deadband regions. These regions are mapped where the adverse roll control interactions equal or exceed the roll control moment of the thrusters. Figure 4-15 shows that these regions do occur at low angles of attack for the pitch-up RCS units. While there is an overlapping of the two-jet case with the one- and three-jet cases, the one- and three-jet cases do not overlap, implying that some roll control

can be maintained at all angles of attack in this dynamic pressure region. Impingement effects would only occur at the lower dynamic pressures and may change the curves around -10 degrees (lower limit of wind tunnel data).

The high-angle-of-attack models do have a deadband region but it does not occur until the dynamic pressure is high (15 pounds per square foot).

4.4.3.2 Pitch-Down RCS Roll Control Map. Figure 4-16 presents a similar map of roll-control deadbands for the pitch-down jets. The region of angle of attack at which no useful roll component is obtained is much more extensive than that of the pitch-up control. This suggests that more roll-control effectiveness is possible by using asymmetric (accepting the induced pitch) rather than symmetric roll control at all angles of attack.

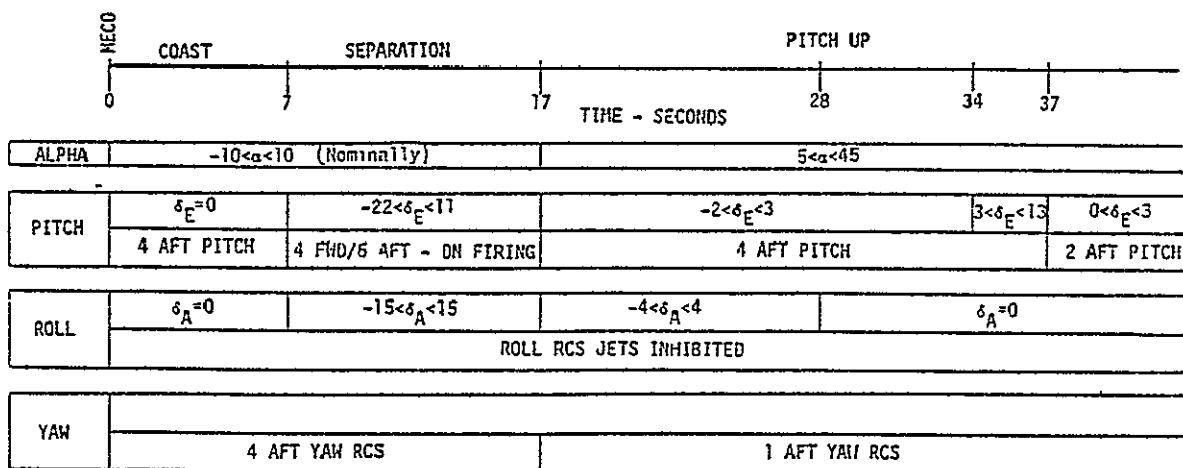
Both Figures 4-15 and 4-16 show that increasing the number of jets firing moves the deadband to higher dynamic pressures.

4.4.3.3 No RCS Roll Control Map. The regions of overlap between Figures 4-15 and 4-16 are regions where no useful roll control is possible from the rear-mounted RCS units. Figure 4-17 shows that this region is fairly extensive for a one-jet case, but can be delayed to dynamic pressures beyond the RTLS separation maneuver limit by using sufficient numbers of jets.

In contrast, Figure 4-18 presents the much larger regions of no roll control if symmetric (pitch-up and pitch-down) roll control is used. Figures 4-17 and 4-18 clearly show that use of nonsymmetrical roll RCS is the better way to go at low angles of attack.

Table 4-1. Atmospheric variation.

ATMOSPHERE		Seasonal Minimum -2σ	Seasonal Minimum	Seasonal Maximum	Seasonal Maximum +2σ
175,000 Ft V=8627.1 Ft/Sec	Δρ	$-6.82 \times 10^{-7} \frac{\text{lb}/\text{sec}^2}{\text{Ft}^4}$	-4.7×10^{-7}	4.37×10^{-7}	6.026×10^{-7}
	ΔT	-79°R	-38.7	32	60
	M	8.74	8.34	7.75	7.55
	P _∞	0031 psia	0045	0108	0125
	q _∞	23.9 psf	31.8	65.5	71.7
200,000 Ft V=8383.4 Ft/Sec	Δρ	$-3.162 \times 10^{-7} \frac{\text{lb}/\text{sec}^2}{\text{Ft}^4}$	-2.372×10^{-7}	2×10^{-7}	2.85×10^{-7}
	ΔT	-55°R	-22	33	73
	M	8.53	8.20	7.73	7.43
	P _∞	0010 psia	0015	0042	0051
	q _∞	7.41 psf	10.19	25.56	28.52
225,000 Ft V=7896.6 Ft/Sec	Δρ	$-1.25 \times 10^{-7} \frac{\text{lb}/\text{sec}^2}{\text{Ft}^4}$	-9.84×10^{-8}	7.28×10^{-8}	1.21×10^{-7}
	ΔT	-69°R	-30	31	94
	M	8.78	8.31	7.71	7.21
	P _∞	00032 psia	.00048	.00144	00194
	q _∞	2.49 psf	3.32	8.66	10.165
250,000 Ft V=7355.8 Ft/Sec	Δρ	$-4.67 \times 10^{-8} \frac{\text{lb}/\text{sec}^2}{\text{Ft}^4}$	-3.37×10^{-8}	1.79×10^{-8}	4.06×10^{-8}
	ΔT	-93°R	-54	44	101
	M	9.33	8.69	7.54	7.05
	P _∞	.00007 psia	.00013	00042	00060
	q _∞	.638 psf	.992	2.38	3.0



MACH RANGE 6-8
DYNAMIC PRESSURE RANGE. 2-10 PSF
FORWARD AND AFT JETS

ORIGINAL PAGE IS
OF POOR QUALITY

Figure 4-1. RCS utilization and control surface deflection for RTLS

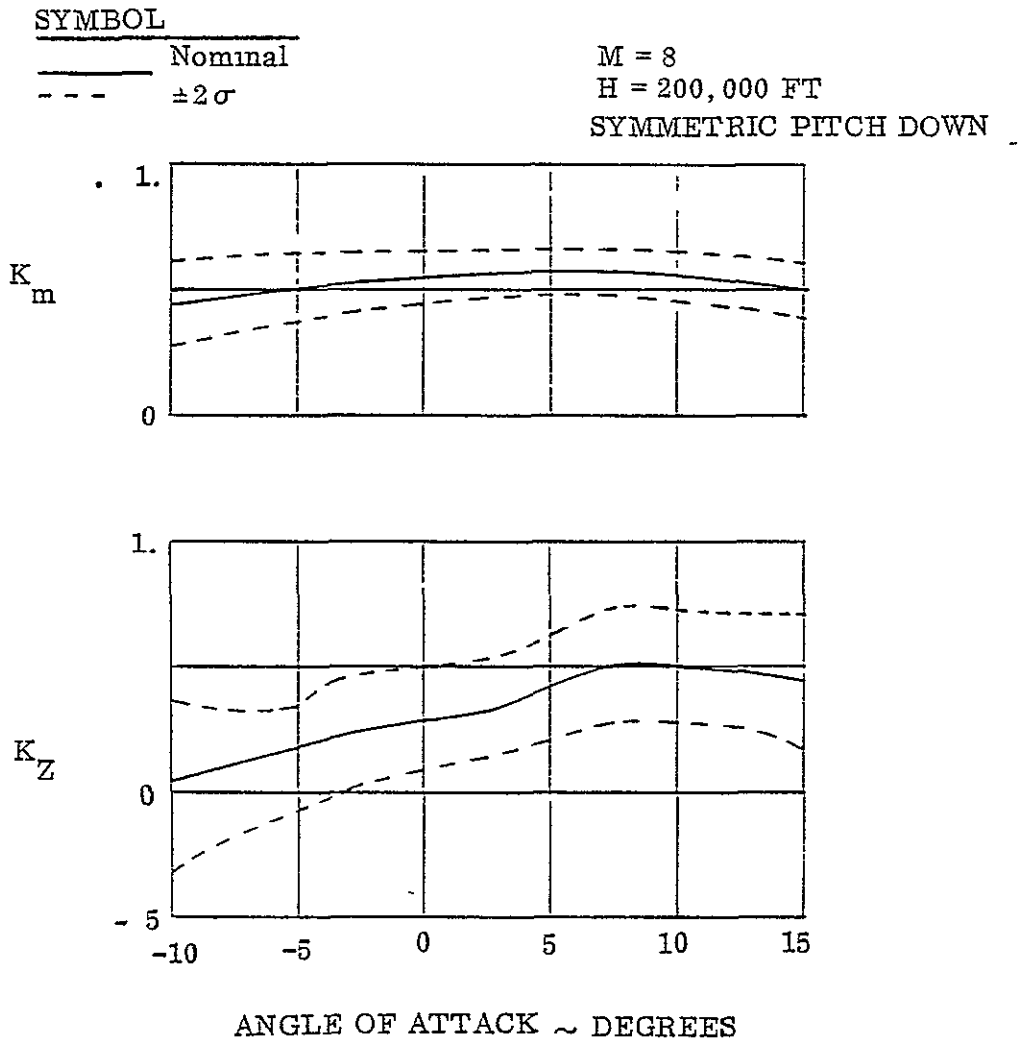


Figure 4-2. Effect of angle of attack at constant altitude and mach on rear 4 jet symmetric pitch down control amplification.

SYMBOL
 _____ NOMINAL
 - - - - $\pm 2\sigma$

$\alpha = 0^\circ$
 $M = 8$

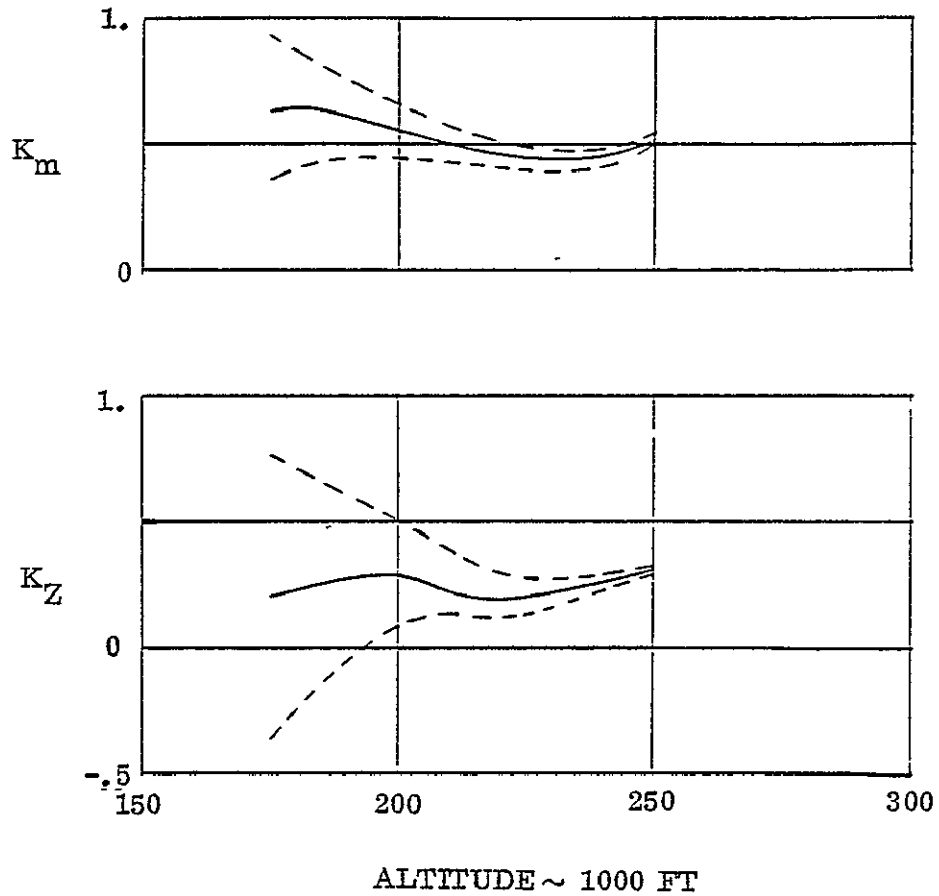


Figure 4-3. Effect of altitude at constant mach number on rear 4 jet symmetric pitch down control amplification.

SYMBOL
 _____ NOMINAL
 - - - $\pm 2\sigma$

$V = 7896.6 \text{ FT/SEC}$
 $\alpha = 0^\circ$
 SYMMETRIC PITCH DOWN

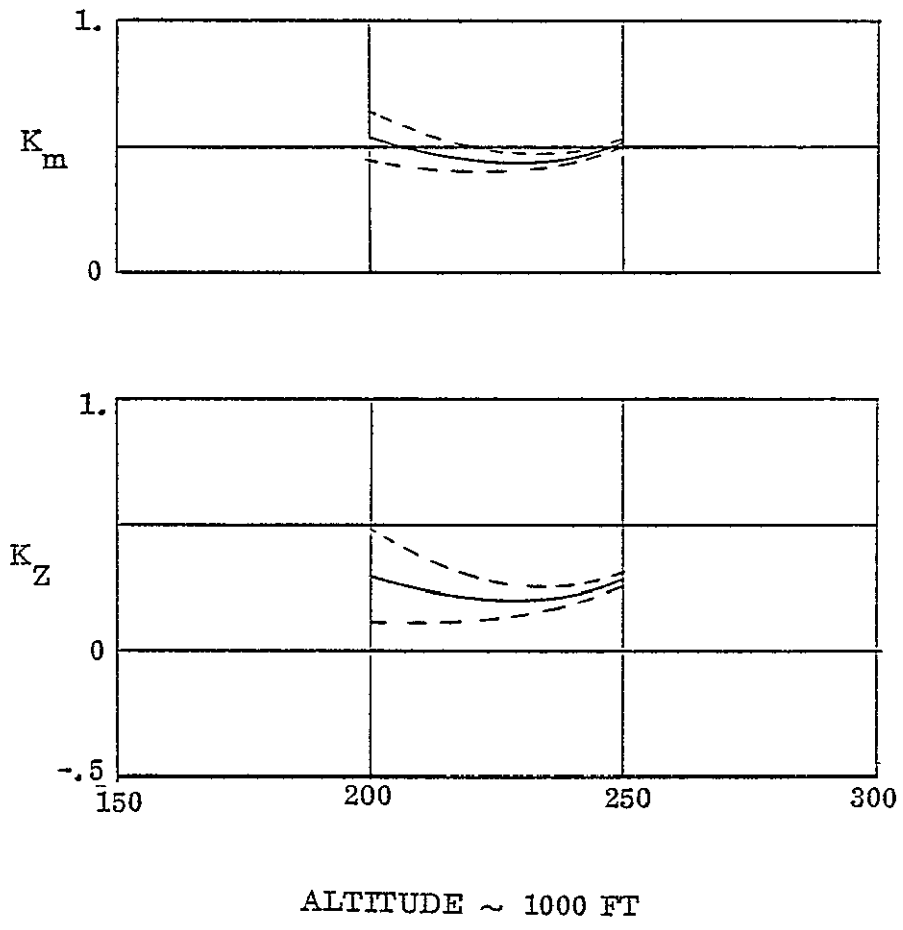


Figure 4-4. Effect of altitude at constant velocity on rear 4 jet symmetric pitch down control amplification.

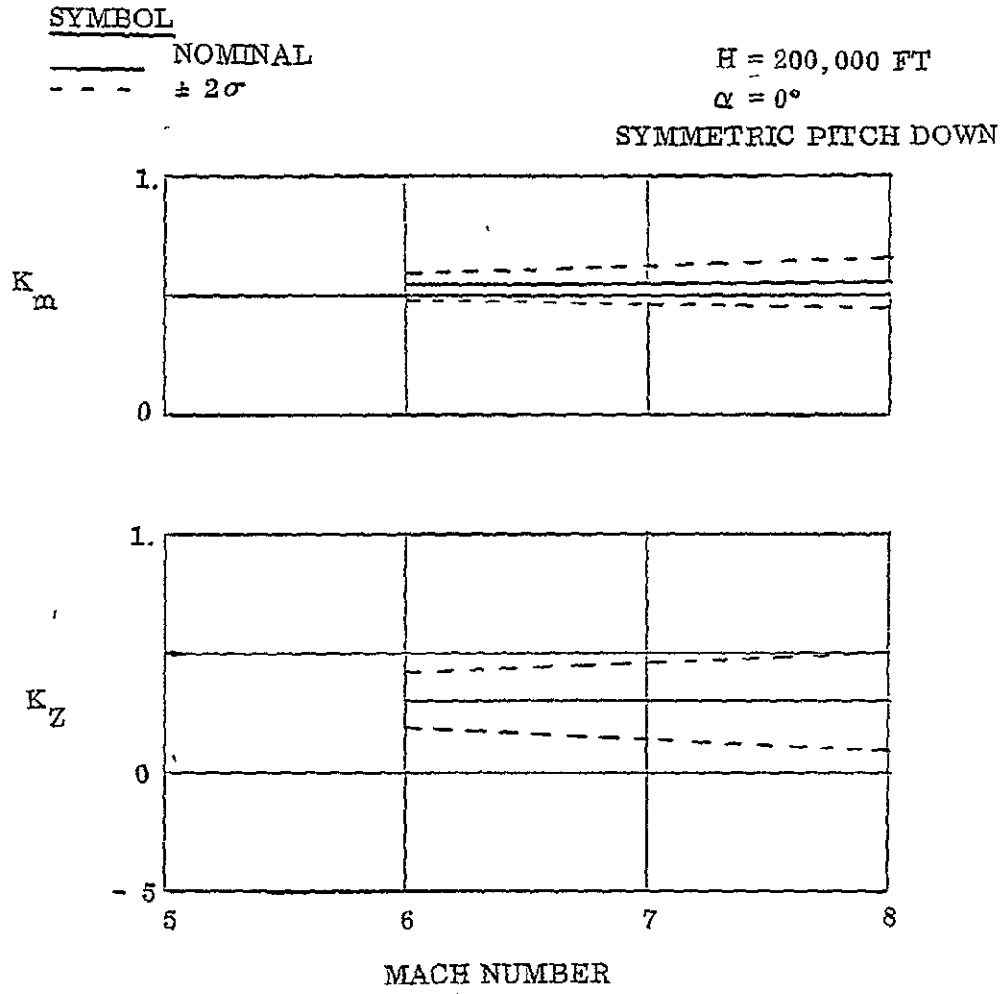


Figure 4-5. Effect of mach number at constant altitude on rear 4 jet symmetric pitch down control amplification.

SYMBOL
 _____ NOMINAL
 - - - $\pm 2\sigma$

H = 225,000 FT
 $\alpha = 0^\circ$
 SYMMETRIC PITCH DOWN

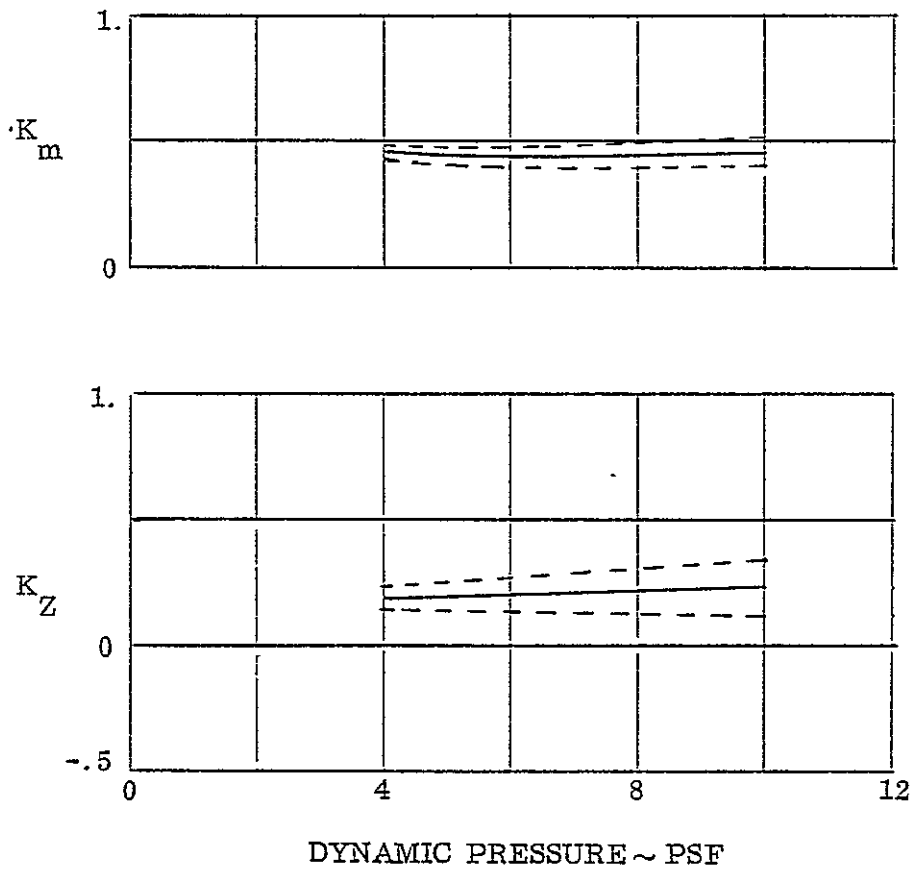


Figure 4-6. Effect of dynamic pressure at constant altitude on rear 4 jet symmetric pitch down control amplification.

SYMBOL	ATMOSPHERE
————	SEASONAL MINIMUM - 2σ
-----	SEASONAL MINIMUM
———	SEASONAL MAXIMUM
-----	SEASONAL MAXIMUM + 2σ

$\alpha = 0^\circ$
 $M = 8$ NOMINAL
 SYMMETRIC PITCH DOWN

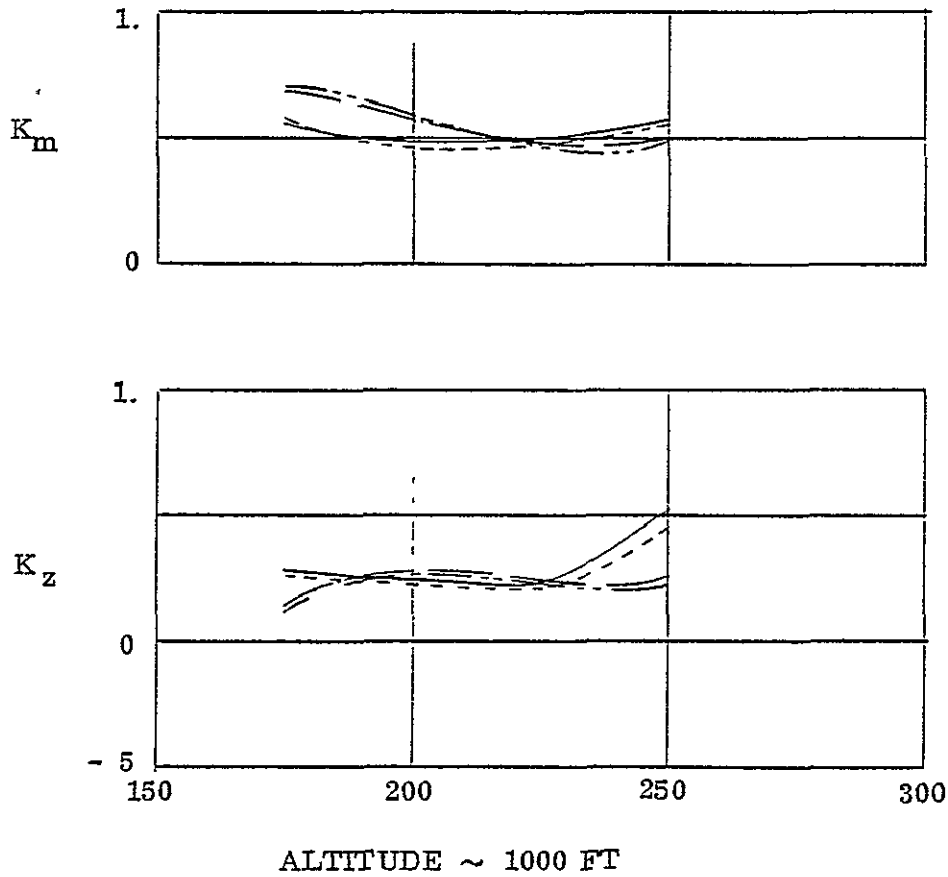


Figure 4-7. Effect of atmospheric variation on 4 jet symmetric rear pitch down control amplification.

$M = 8$
 $\alpha = 0^\circ$

SYMBOL
 _____ NO REYNOLDS EFFECT
 0---0 WORST CASE EFFECT

SYMMETRIC PITCH DOWN

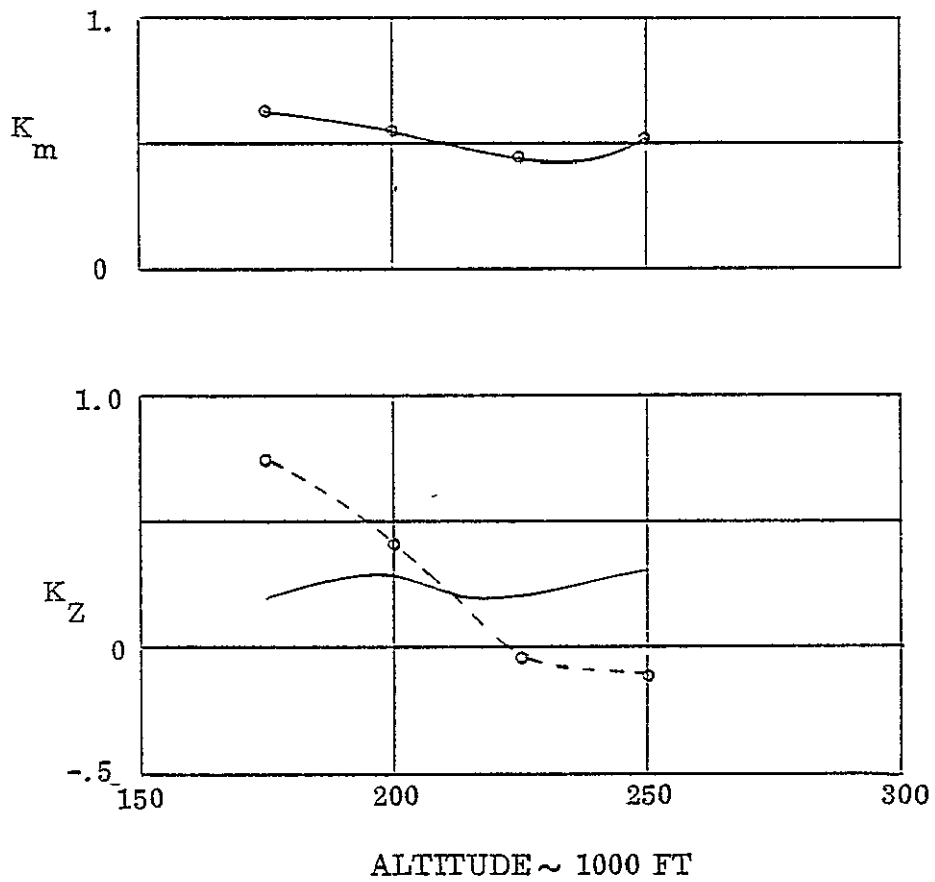


Figure 4-8. Worst case Reynolds number effects on rear 4 jet symmetric pitch down control amplification.

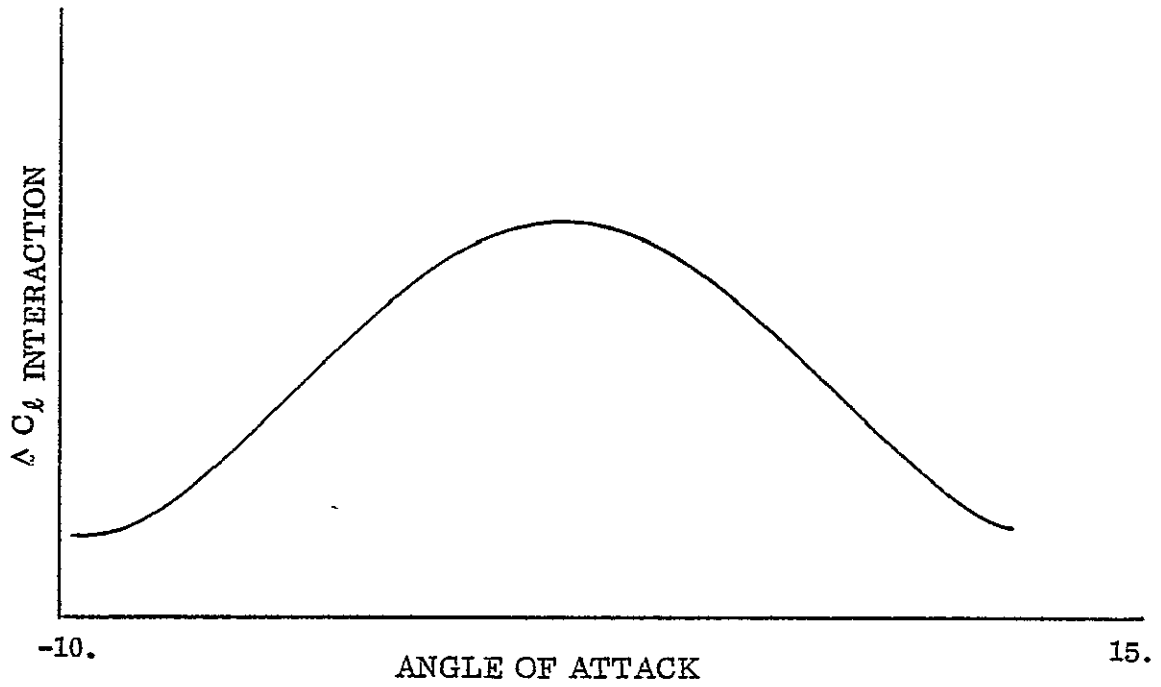


Figure 4-9. Typical roll interaction increment at low angles of attack for rear mounted pitch up jets.

SYMBOL	PITCH DOWN		PITCH UP	
	LEFT	RIGHT	LEFT	RIGHT
————	3	1	0	0
- - - - -	3	2	0	1
. - - . - - .	3	3	0	2

COMBINED 4 JETS PITCH DOWN PLUS
2 JETS ROLL

H = 200,000 FT
M = 8

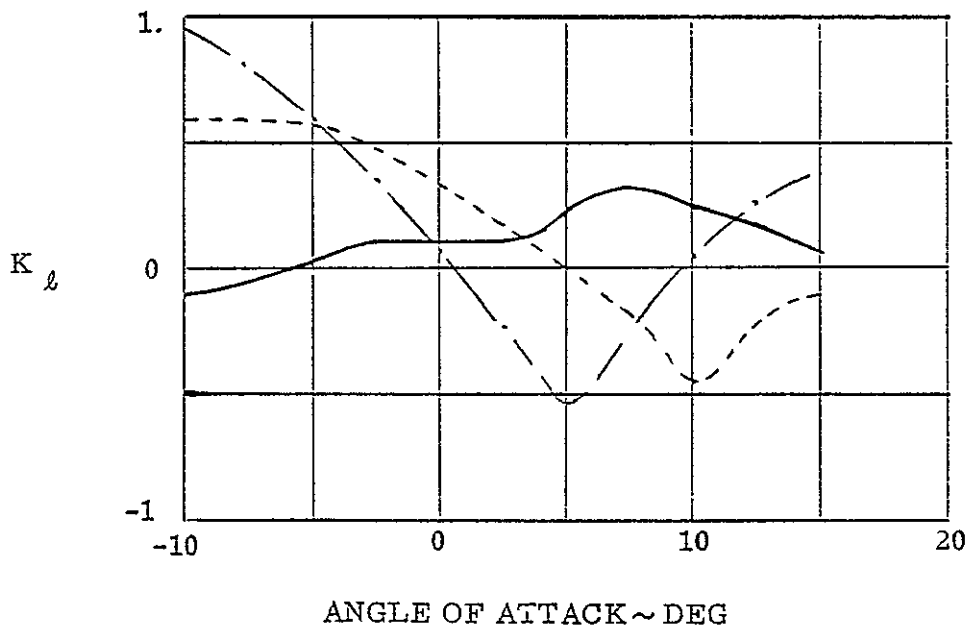


Figure 4-10. Effect of angle of attack on rear RCS roll control amplification.

SYMBOL	PITCH DOWN		PITCH UP	
	LEFT	RIGHT	LEFT	RIGHT
————	3	1	0	0
-----	3	2	0	1
·- - -	3	3	0	2

COMBINED 4 JETS PITCH DOWN
PLUS 2 JETS ROLL

$\alpha = 0$
 $M = 8$

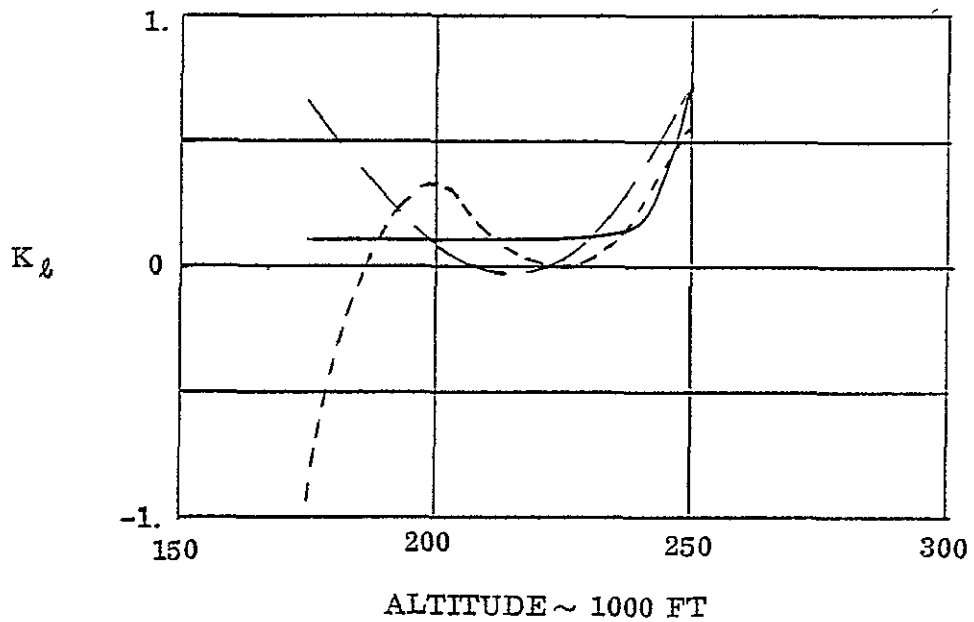


Figure 4-11. Effect of altitude on rear RCS roll control amplification at zero angle of attack.

COMBINED 4 JETS PITCH DOWN PLUS
 2 JETS ROLL (3 PITCH DOWN LEFT, 2 PITCH DOWN RIGHT,
 1 PITCH UP RIGHT)

$\alpha = 0^\circ$
 $M = 8$

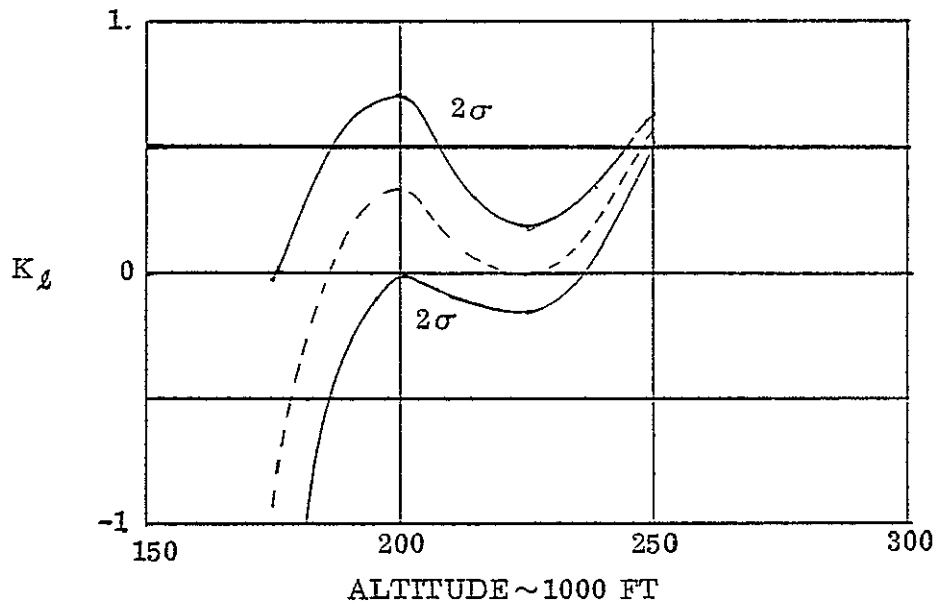
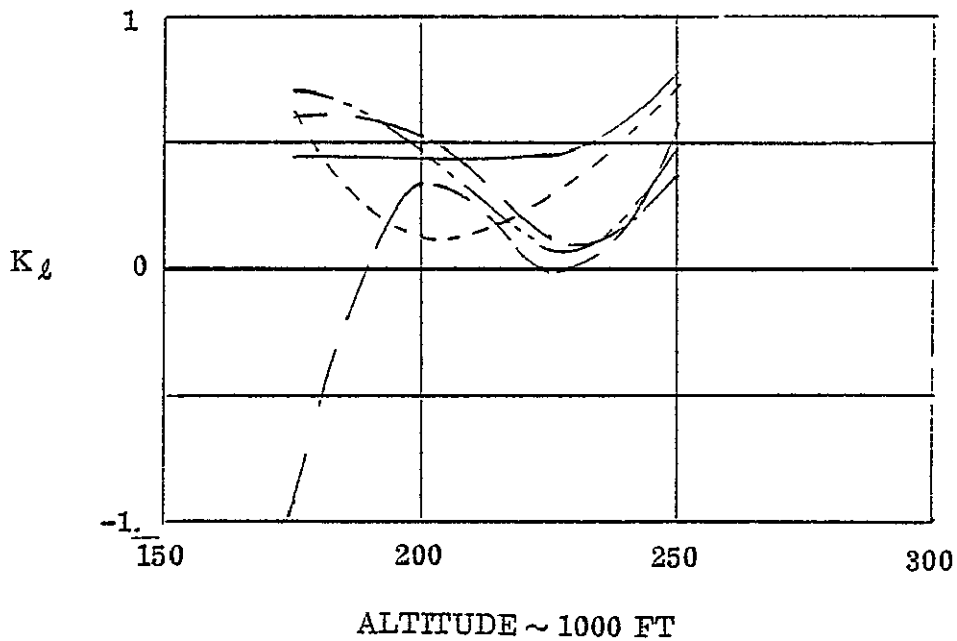


Figure 4-12. Error bands on rear RCS roll control amplification for zero angle of attack at mach 8 as a function of altitude.

SYMBOL	ATMOSPHERE
————	SEASONAL MINIMUM -2σ
- - - - -	SEASONAL MINIMUM
————	STANDARD ATMOSPHERE
—— — —	SEASONAL MAXIMUM
————	SEASONAL MAXIMUM $+2\sigma$

COMBINED 4 JETS PITCH DOWN PLUS 2 JETS ROLL
 (3 PITCH DOWN LEFT, 2 PITCH DOWN RIGHT,
 1 PITCH UP RIGHT)

$\alpha = 0$
 $M_{\text{NOMINAL}} = 8$



DATA COMPUTED ONLY AT 175, 200, 225, 250 KFT

Figure 4-13. Effect of atmospheric variation on rear RCS roll control amplification using two jets for roll (1 pitch up and 1 pitch down).

SYMBOL	ATMOSPHERE
—————	SEASONAL MINIMUM -2σ
- - - - -	SEASONAL MINIMUM
—————	SEASONAL MAXIMUM
- - - - -	SEASONAL MAXIMUM -2σ

COMBINED 4 JETS PITCH DOWN PLUS
 2 JETS ROLL (3 PITCH DOWN LEFT -
 1 PITCH DOWN RIGHT)

$\alpha = 0$
 $M_{\text{NOMINAL}} = 8$

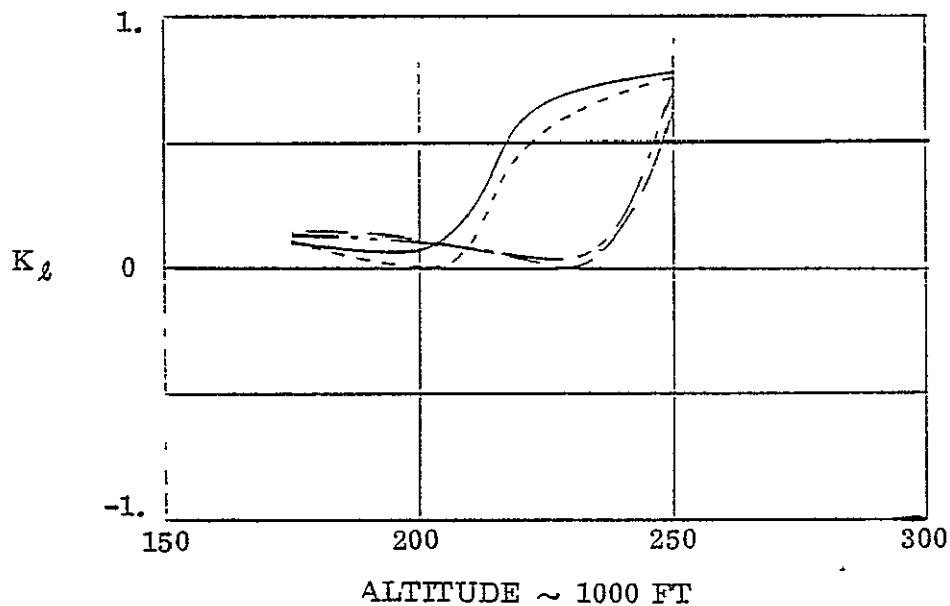


Figure 4-14. Effect of atmospheric variation on rear RCS roll control amplification using only pitch down jets.

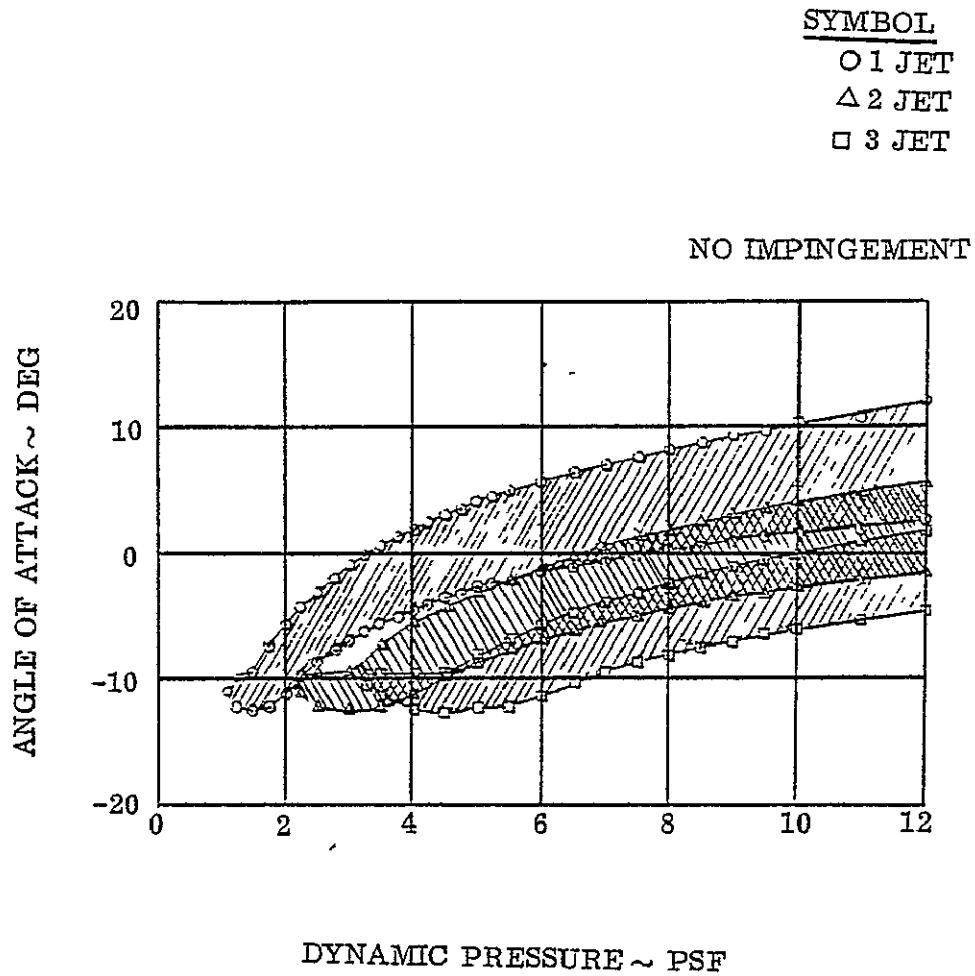


Figure 4-15. Roll control dead band for upward firing rear RCS units at low angle of attack.

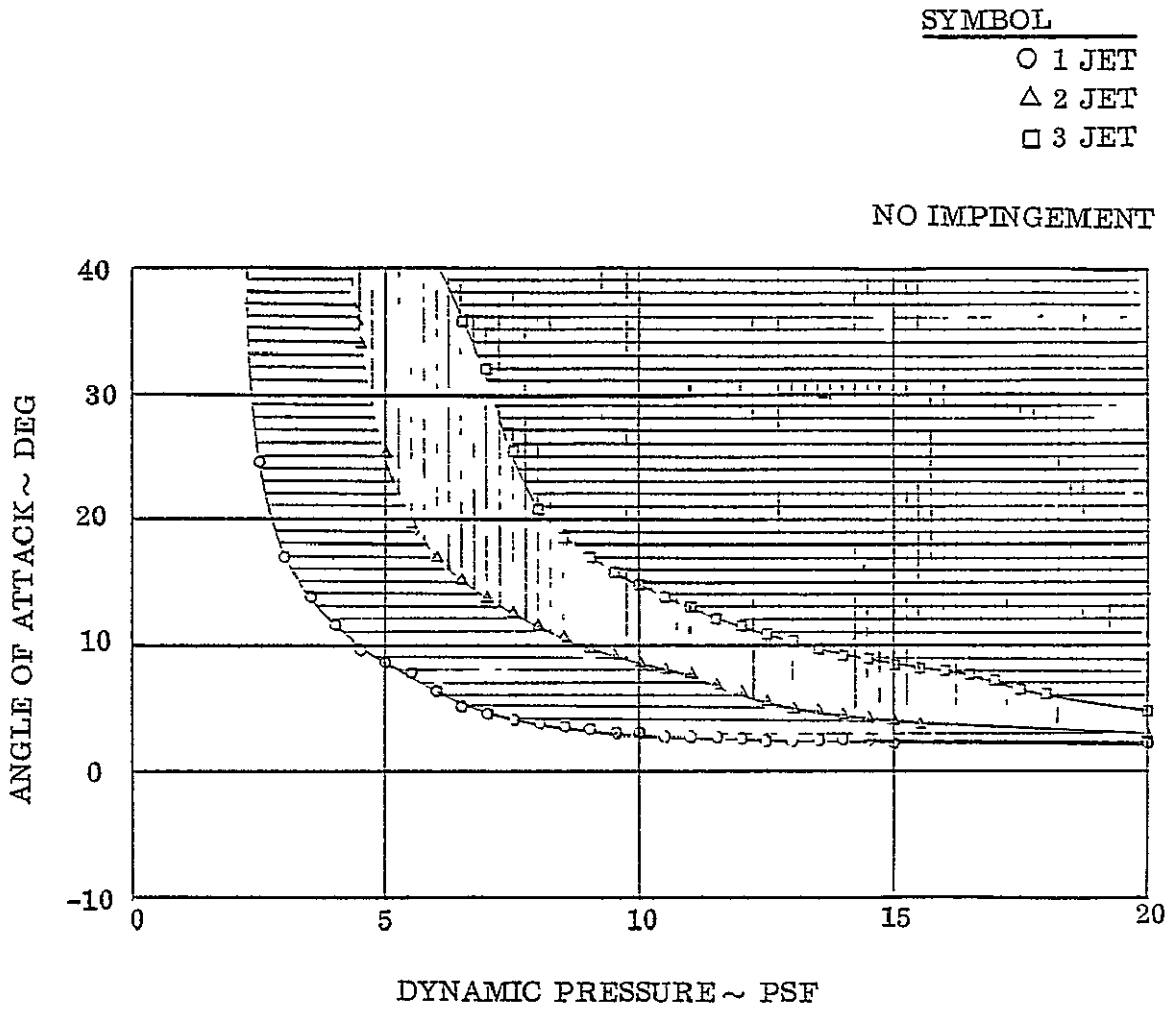


Figure 4-16. Roll control dead band for downward firing rear RCS units.

C-2

NO IMPINGEMENT

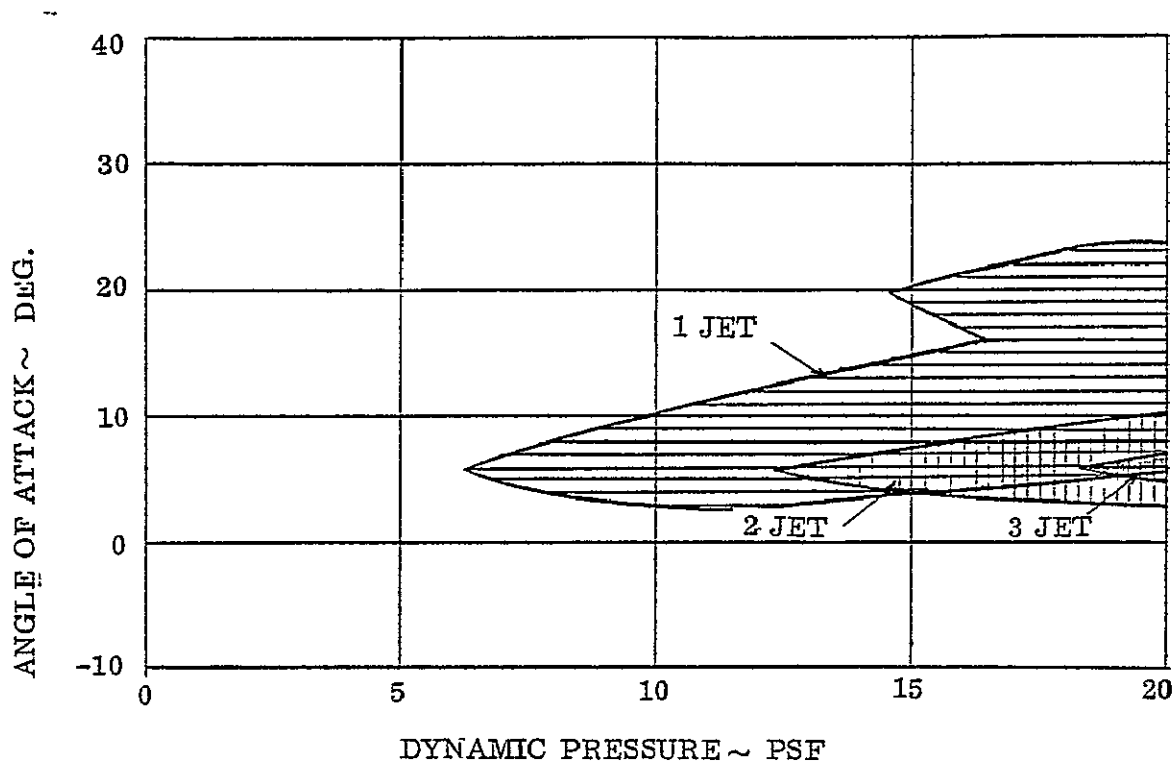


Figure 4-17. Rear RCS roll control dead band.

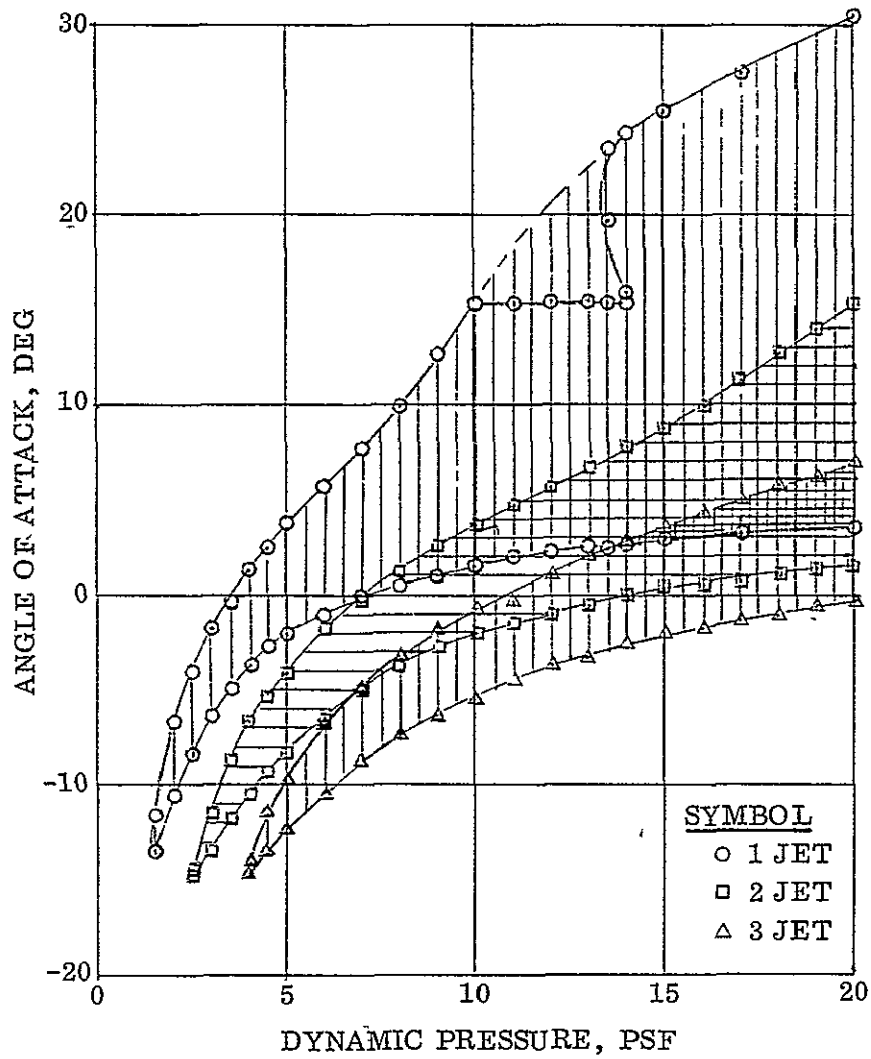


Figure 4-18. Symmetric rear RCS roll control deadband.

5

FORWARD-MOUNTED RCS CONTROL EFFECTIVENESS

5.1 GENERAL

The forward-mounted RCS units are not used during reentry, nor are they presently used alone after the Orbiter has separated from the tank during the RTLS abort maneuver. However, a forward-mounted jet model would be desirable, for analysis of the combined forward/aft RCS control combinations and for development of prediction models for the combination control.

There are only three runs of forward-mounted pitch jets alone during tests OA169, IA22, and IA148. All three runs occur within test OA169, and they provide data only in the high angle-of-attack range. Figures 5-1, 5-2, and 5-3 present these incremental effects for the two supply pressures tested. These data show that the forward pitch-up jet incremental effect appears to go from a peak value at low angles to an opposite peak value at higher angles. The peak values and the angles of attack at which these peaks occur appear to be functions of jet pressure.

Test OA169 also includes five runs at the same supply pressure of four forward and six rear-mounted jets combined. These data are shown in Figures 5-4, 5-5, and 5-6 compared to the six rear-mounted jet runs from test OA169 at the same supply pressure. The normal force (Figure 5-5) and pitching moment (Figure 5-6) incremental data are very interesting at low angles of attack since they show very close agreement between the combined jet data and the aft-only data. Also shown on these figures are the data that result from adding the forward-jet-only data to the aft-jet-only data. The close agreement between the sum of the two sets of data to the combined data, particularly at 12.5 degrees, indicates that the forward-mounted jets apparently have no effect on rear-mounted jet increments. This is a very small sample on which to base this conclusion, but it is the only test data available at this time and is consistent in all longitudinal data.

Based on this conclusion, the variation of forward-mounted jet increments with angle-of-attack were derived from the combined jet data minus the aft-jet-only data. Figures 5-7, 5-8, and 5-9 present these correlations and also show the forward-jet-only data for comparison. The data scatter results from subtracting all the aft-jet-only increments from the combined jet incremental data of test OA169. These data were used to derive tentative models for forward symmetric down-firing jets at lower angles of attack.

5.2 FORWARD-MOUNTED PITCH-UP JET NORMAL FORCE MODEL

The shape of the curve at low angles of attack was found to be best approximated by a sine curve raised to the third power, and the limit of its range is the angle of attack of the peak value.

$$\Delta C_N = C_{N_{PEAK}} \sin^3 \left(\frac{(\alpha + 2.5) 90.}{\alpha_{PEAK} + 2.5} \right) \quad (5-1)$$

where

$C_{N_{PEAK}}$ is given by Figure 5-10,

α_{PEAK} is given by Figure 5-11,

and momentum ratio is based on the sum of the nozzles firing.

5.3 FORWARD-MOUNTED PITCH-UP JET PITCHING MOMENT MODEL

The shape of the curve at low angles was approximated as a square of a sine wave. The correlation is limited to angles of attack up to the peak value.

$$\Delta C_m = C_{m_{PEAK}} \sin^2 \left(\frac{(\alpha + 10) 90.}{\alpha_{PEAK} + 10} \right) \quad (5-2)$$

where

$C_{m_{PEAK}}$ is given by Figure 5-12, and

α_{PEAK} is given by Figure 5-11.

5.4 FORWARD-MOUNTED PITCH-UP JET AXIAL FORCE MODEL

The axial force peak correlation with jet pressure or momentum ratio is not clear. The shape of the curve is a cosine

$$\Delta C_A = -0.016 \cos (3 \alpha - 30). \quad (5-3)$$

whose limit is 15 degrees.

ORIGINAL PAGE IS
OF POOR QUALITY

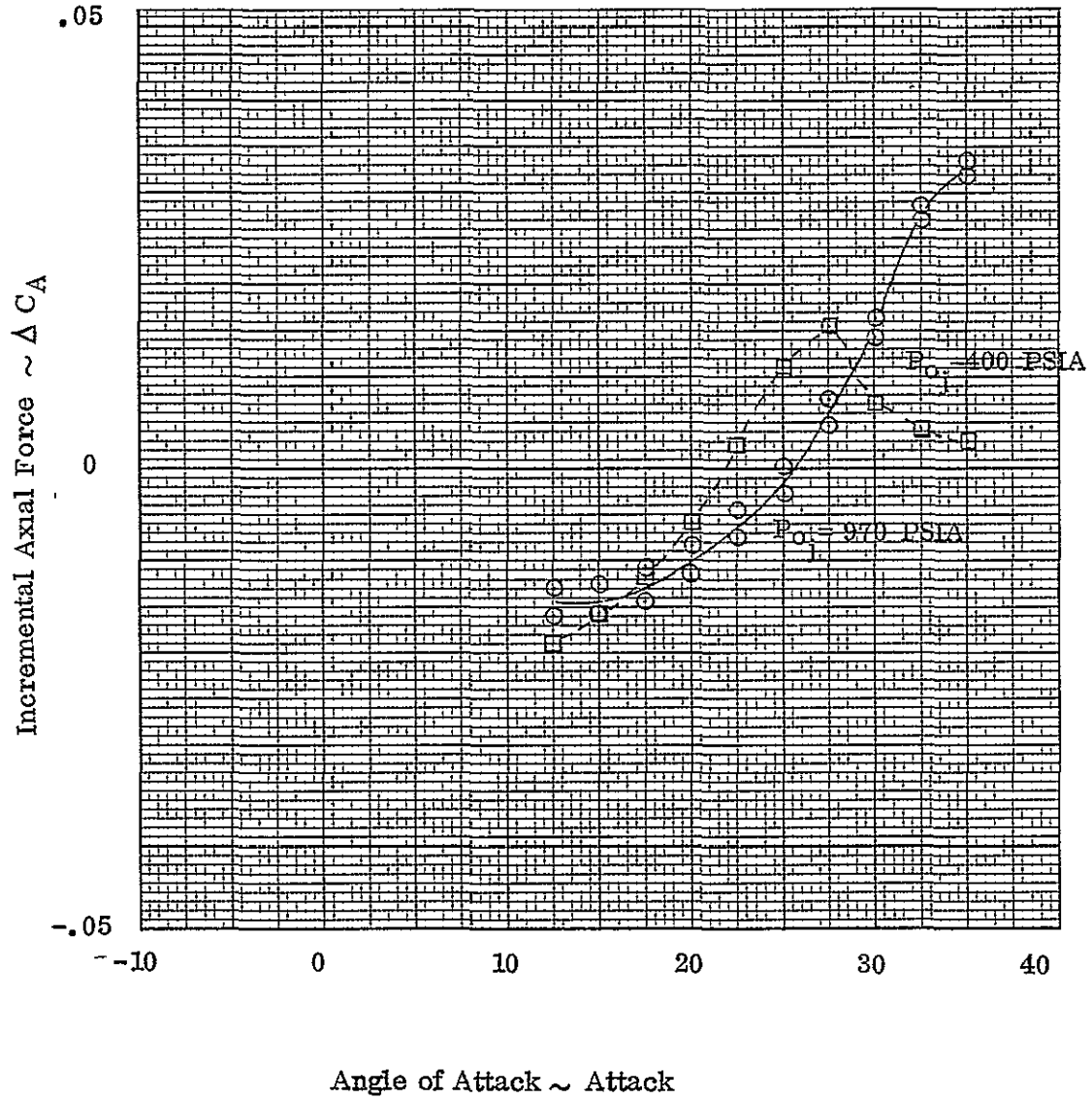


Figure 5-1. Axial force increments for symmetric fired four--
forward-mounted pitch-up jets.

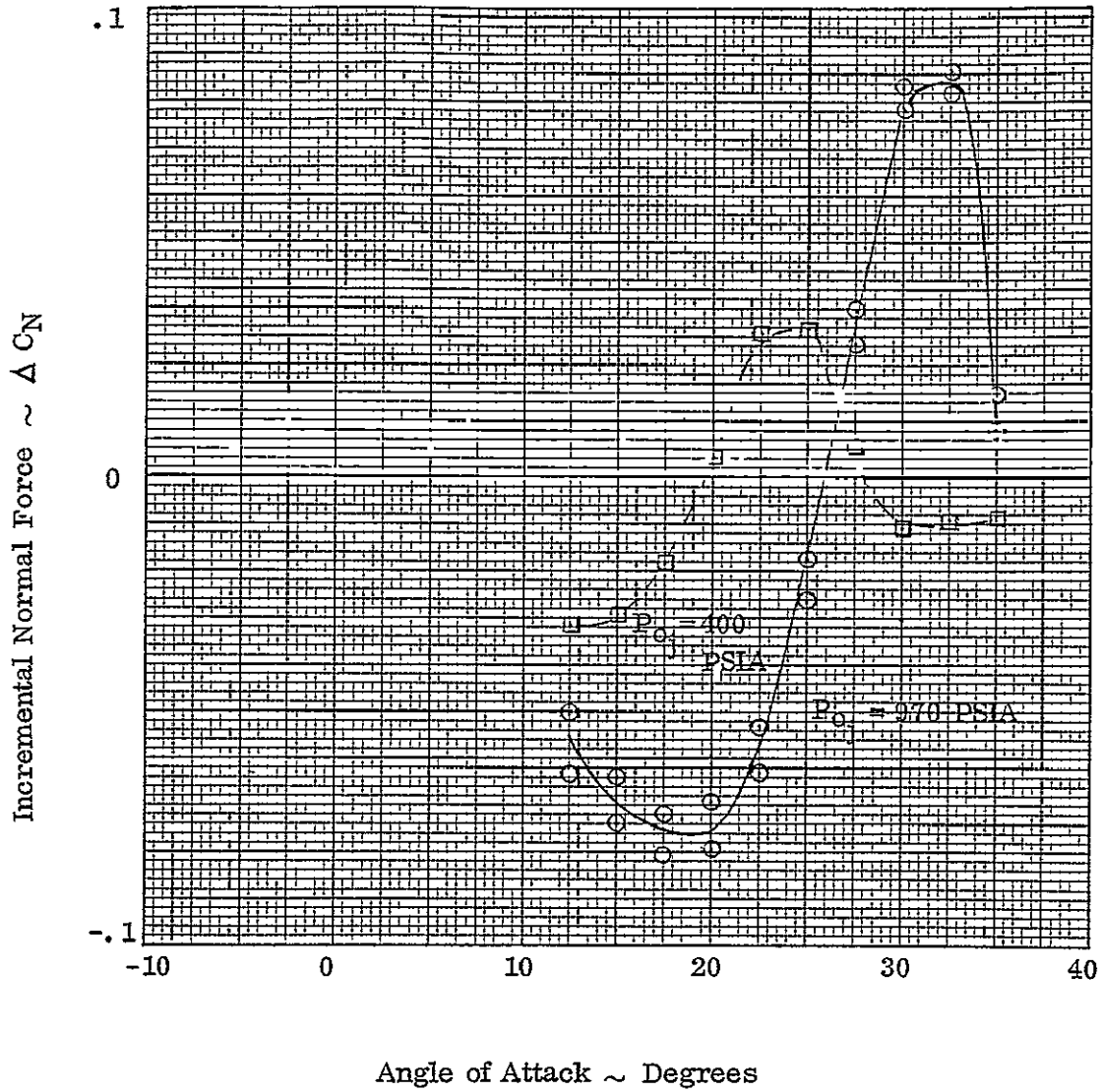


Figure 5-2. Normal force increments for symmetric fired four forward-mounted pitch-up jets.

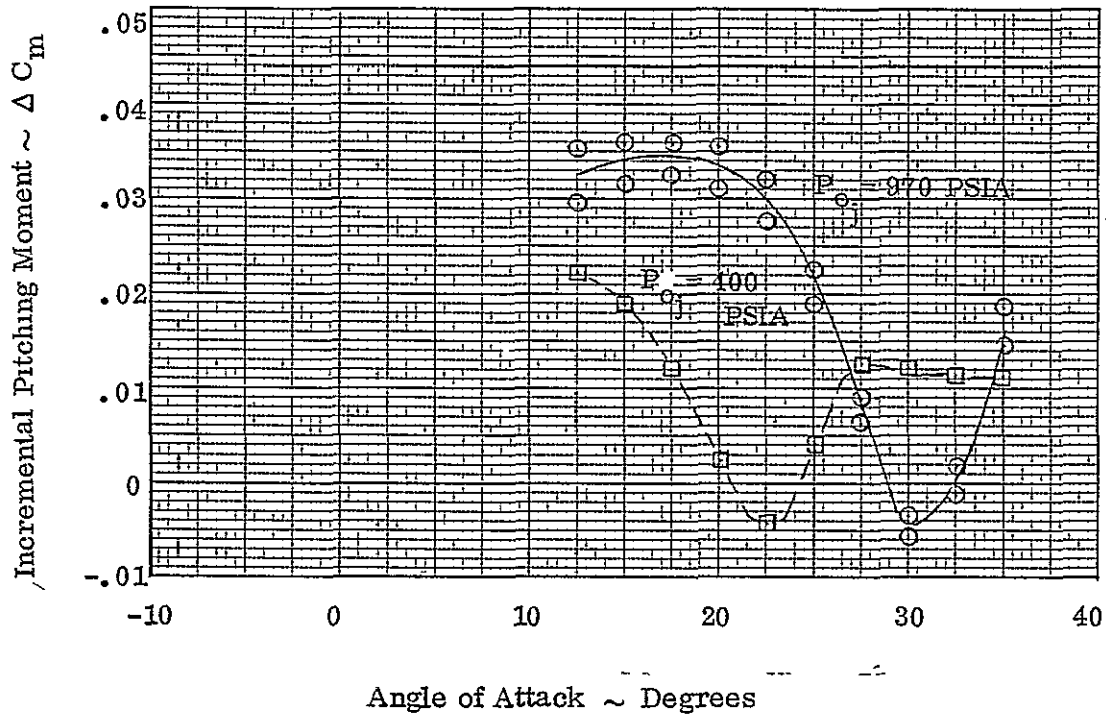


Figure 5-3. Pitching moment increment for symmetric fired four forward-mounted pitch-up jets.

SYMBOL	Data
○	4 Fwd & 6 Aft Data
□	6 Aft Data Only
▲	Sum of 4 Fwd Only Data & 6 Aft Only Data

$P_{0j} = 970 \text{ PSIA}$

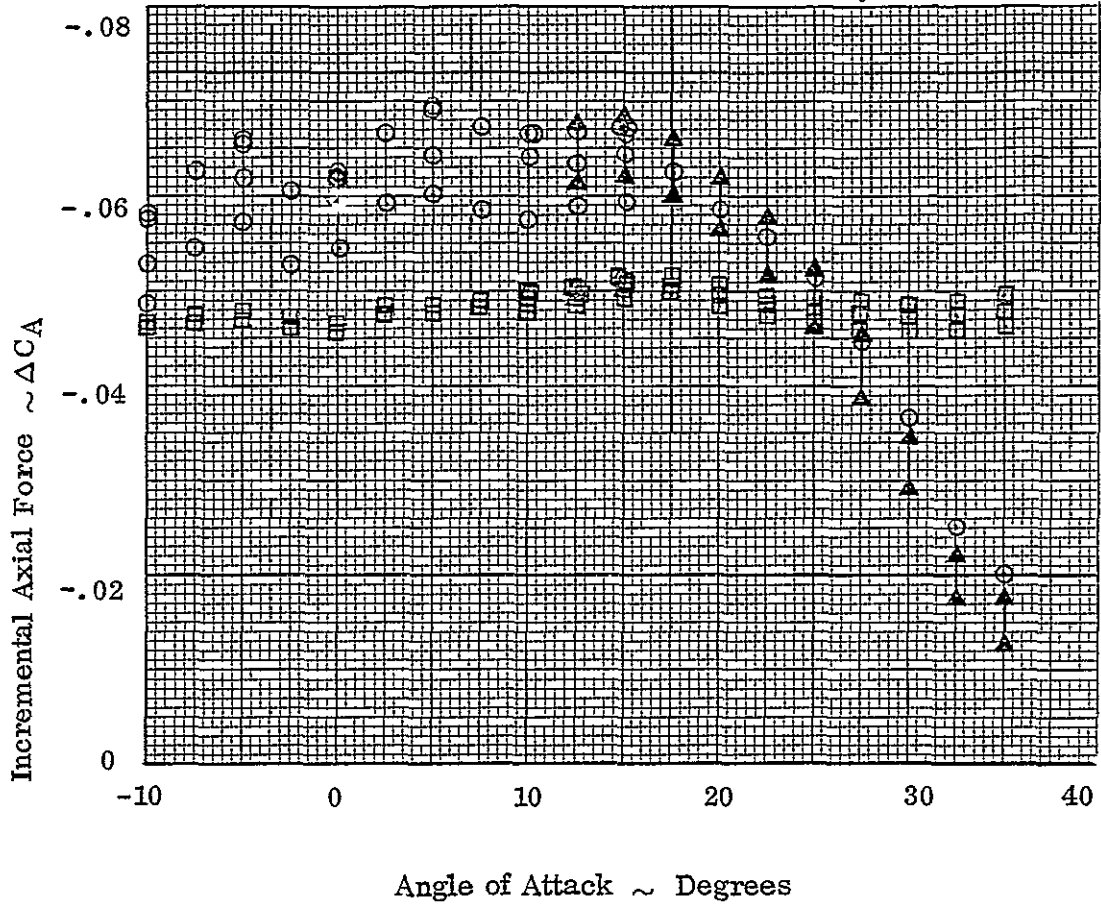


Figure 5-4. Axial force increments for combined four forward and six aft symmetric down firing RCS.

SYMBOL	Data
○	4 Fwd & 6 Aft Data
□	6 Aft Data Only
▲	Sum of 4 Fwd Only Data & 6 Aft Only Data

$P_{O_j} = 970$ PSIA

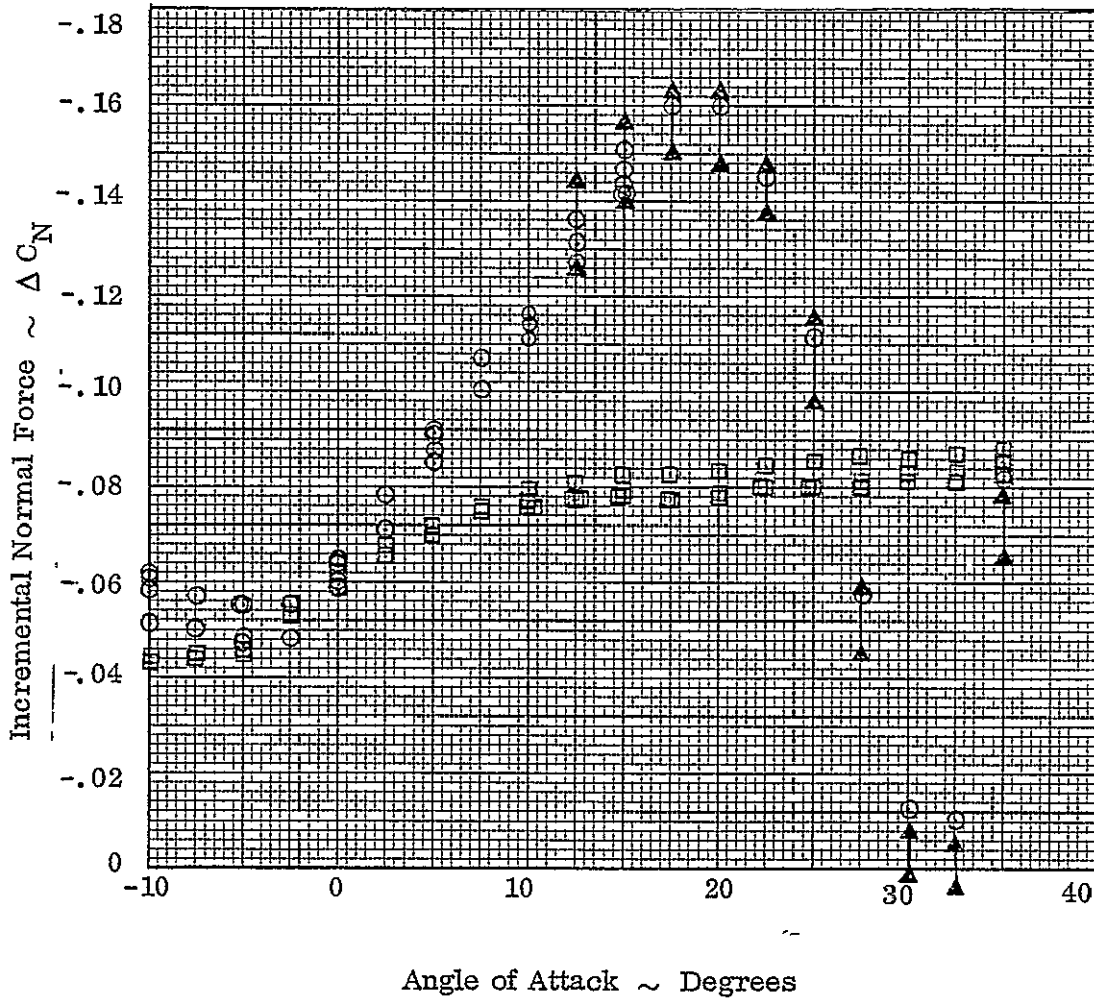


Figure 5-5. Normal force increments for combined four forward and six aft symmetric down firing RCS.

SYMBOL	Data
○	4 Fwd & 6 Aft Data
□	6 Aft Data Only
▲	Sum of 4 Fwd Only Data & 6 Aft Only Data

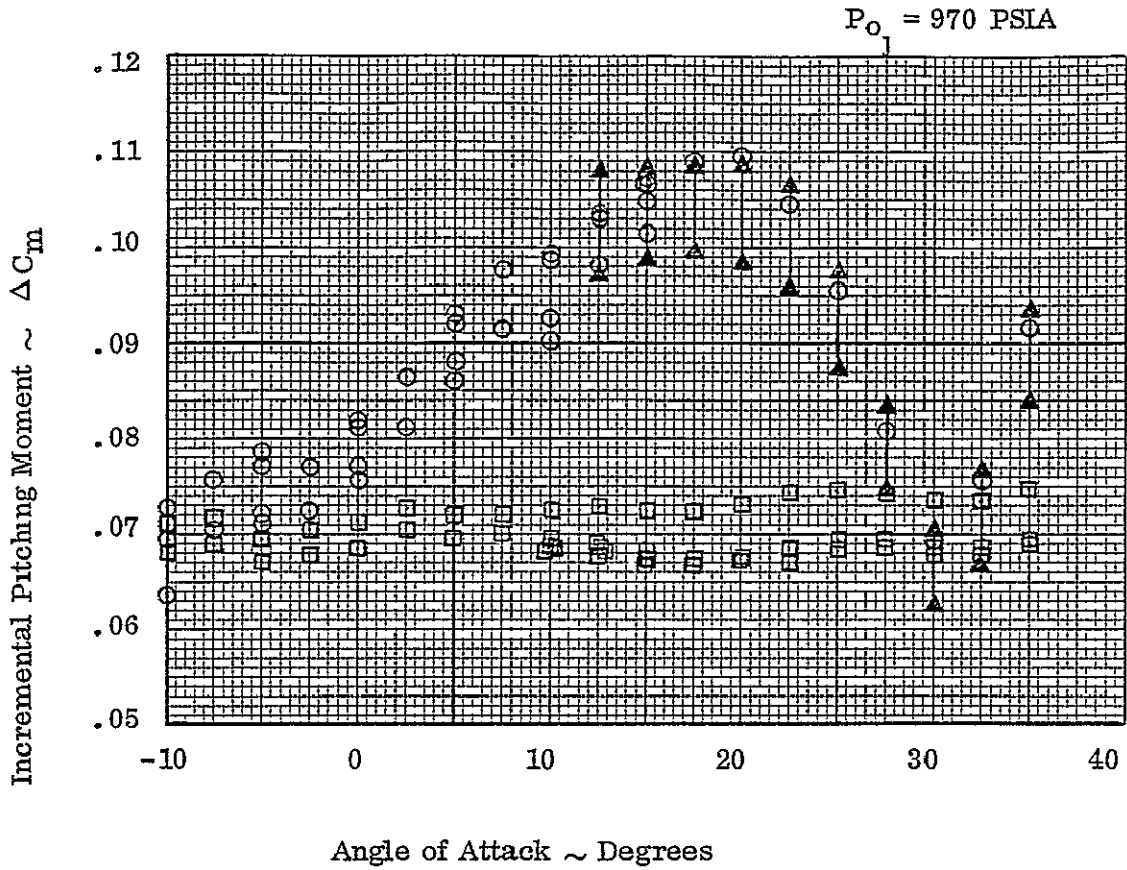


Figure 5-6. Pitching moment increments for four forward and six aft, symmetric down firing RCS.

SYMBOL	Data
○	4 Fwd/6 Aft Data - 6 Aft Data
□	4 Fwd Jet Data

$P_{O_j} = 970$ PSIA

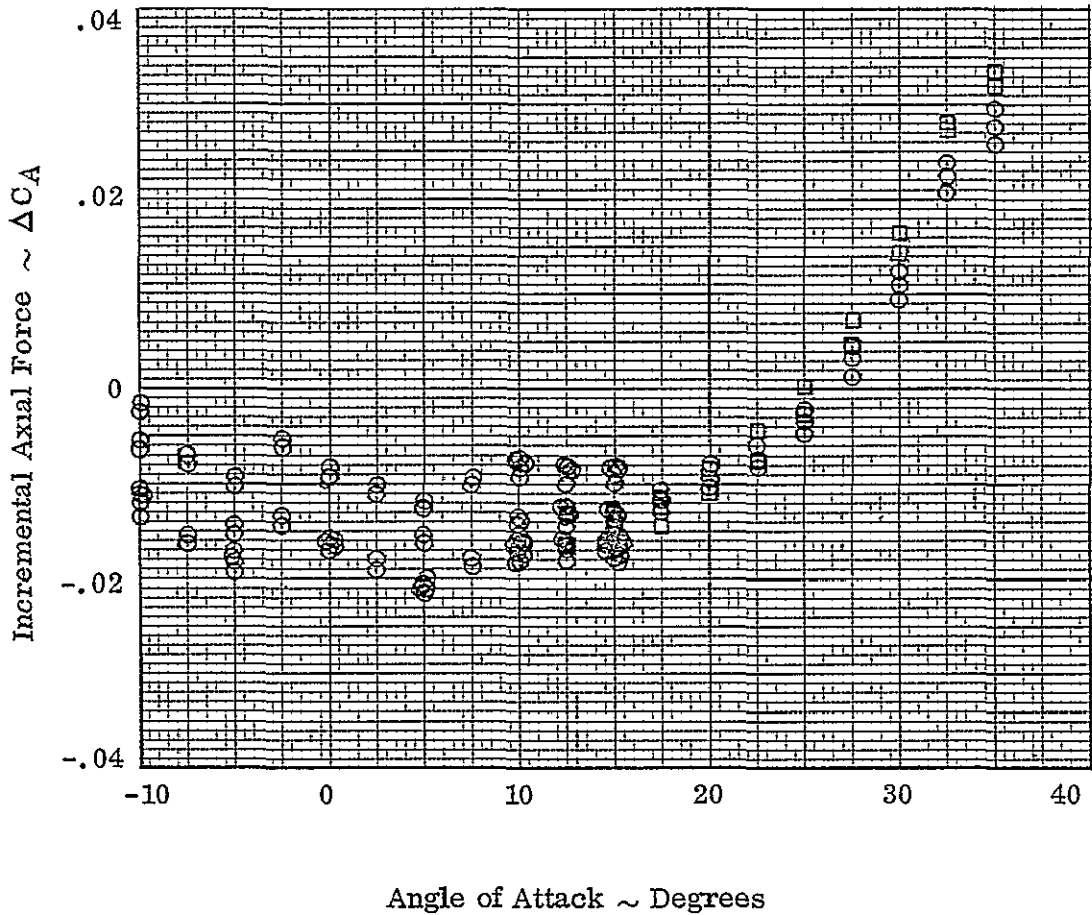


Figure 5-7. Axial force increment of forward down firing jets derived from four forward/six aft jet data.

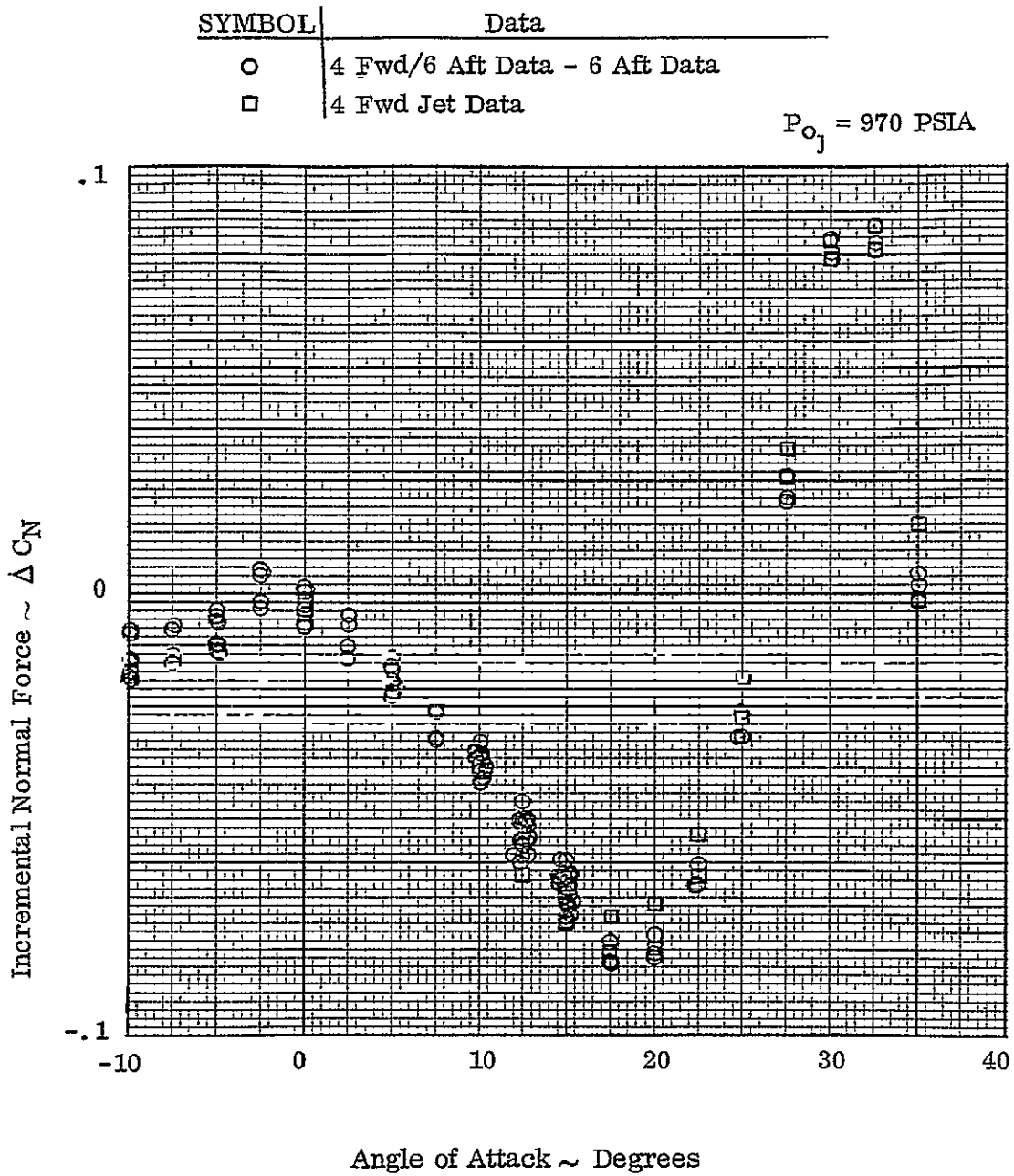


Figure 5-8. Normal force increment of forward down firing jets derived from four forward/six aft jet data.

SYMBOL	Data
○	4 Fwd/6Aft Data - 6 Aft Data
□	4 Fwd Jet Data

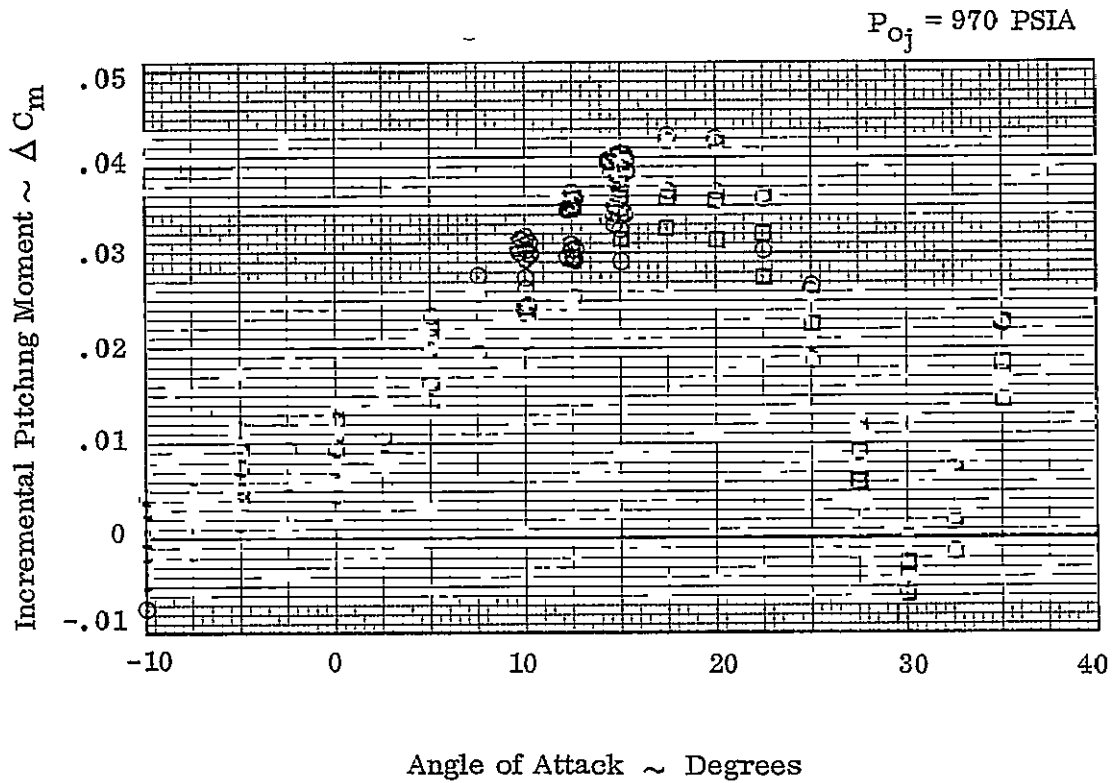


Figure 5-9. Pitch moment increment of forward down firing jets derived from four forward/six aft jet data.

ORIGINAL PAGE IS
OF POOR QUALITY

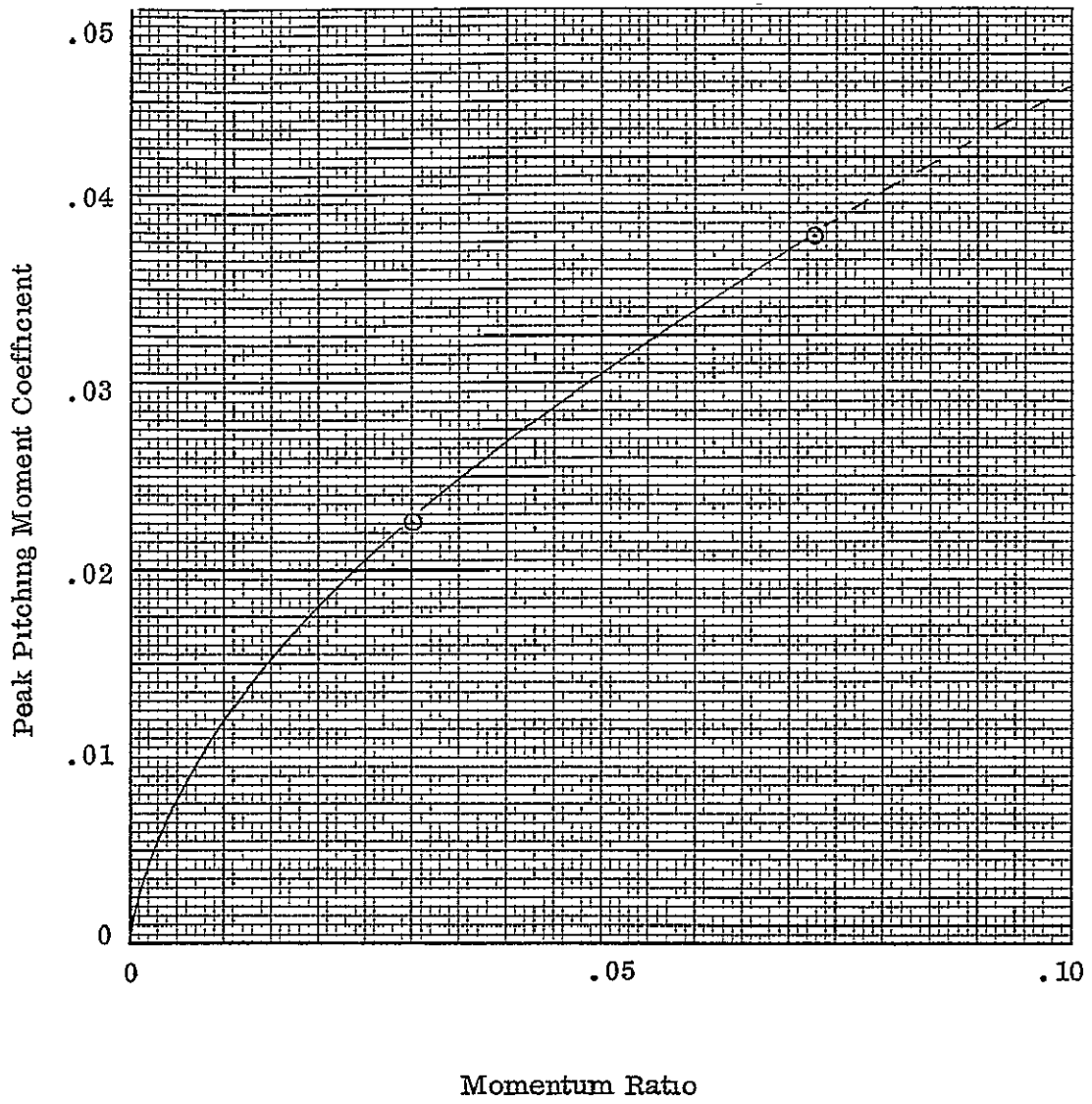


Figure 5-10. Peak pitching moment increment at low angles of attack for forward symmetric down firing RCS.

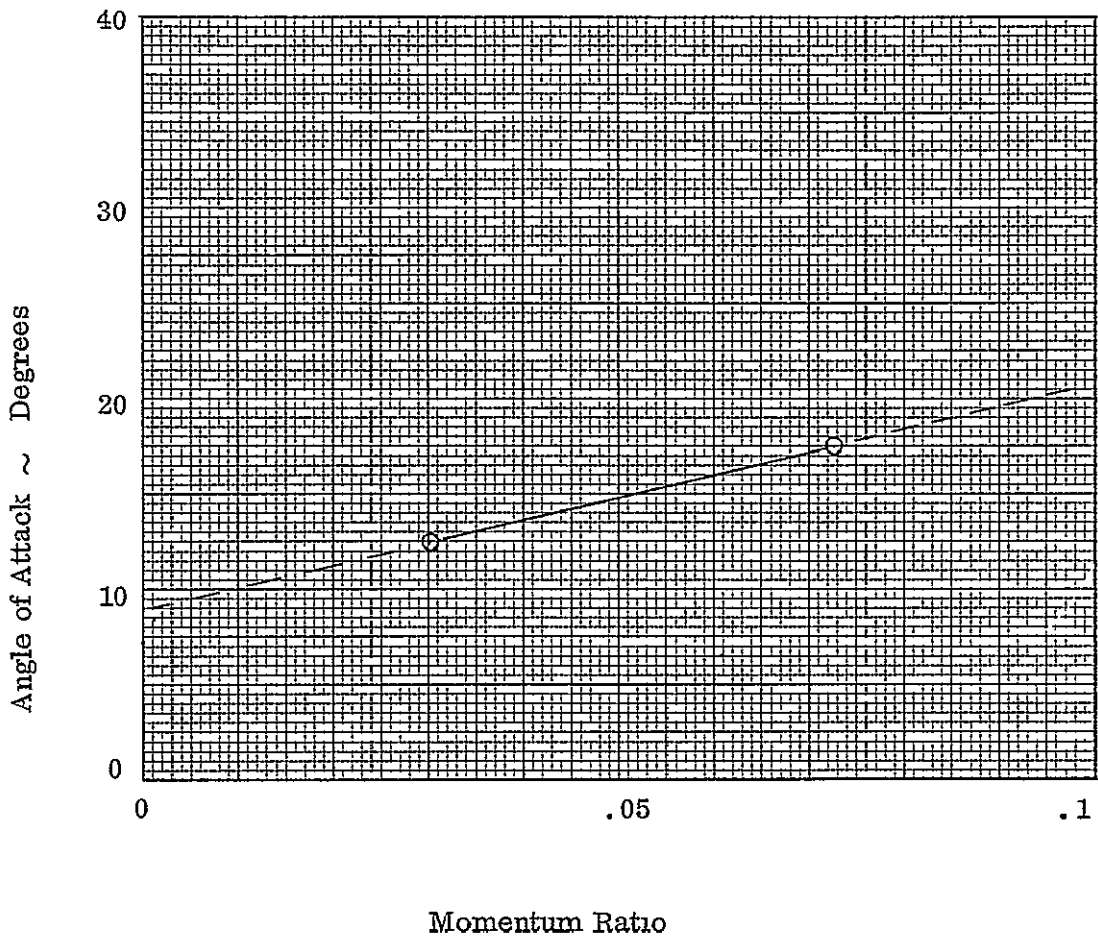


Figure 5-11. Angle of attack of peak value for forward symmetric down firing RCS.

ORIGINAL PAGE IS
OF POOR QUALITY

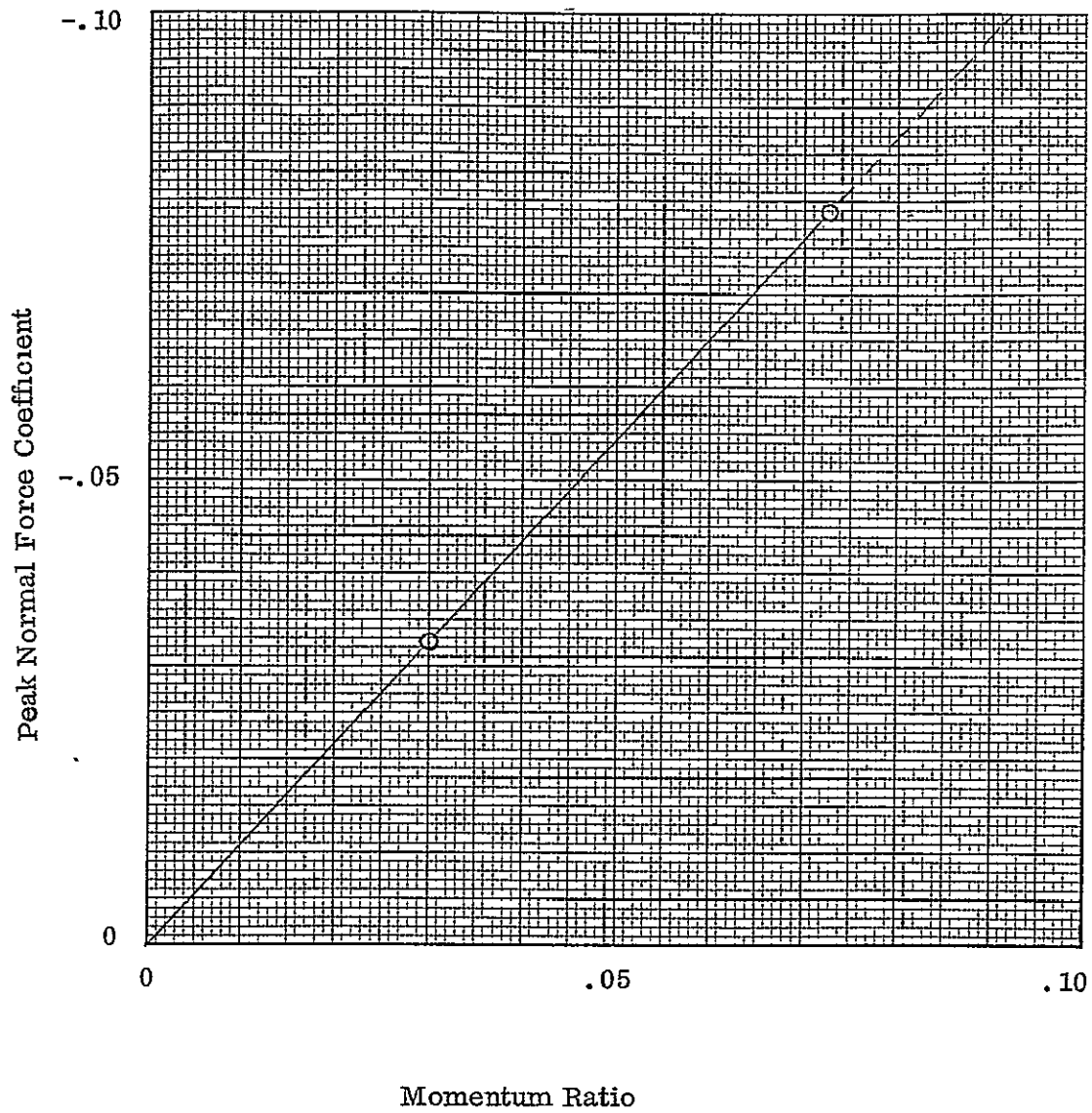


Figure 5-12. Peak normal force increment at low angles of attack for forward symmetric down firing RCS.

6

MATED CONFIGURATION DATA ANALYSIS

Figure 4-1 showed that there is a period of mated orbiter/tank coast prior to the RTLS abort staging maneuver, during which the vehicle establishes the correct attitude and rates to ensure a successful staging maneuver. Control during this time is maintained using combinations of both forward-mounted and rear-mounted reaction control jets. The jet combinations used are determined by three control parameters, UZCMD, UXCMD, and UYCMD. Figures 6-1 and 6-2 show the reaction control combinations selected by the allowable set of control parameters.

6.1 IA148 TEST DATA

Test IA148 was discussed briefly in Section 2 of this report and is also presented in Reference 8. Mated (tank-on) data were obtained for the nozzle combinations shown in Figures 6-1 and 6-2, where RC__ numbers are shown. Data were obtained at 0°, +4°, and -4° yaw for most (but not all) of the reaction control combinations tested.

Twenty-one different combinations were tested for the mated configuration during test IA148. Data increments were taken as jet-on data minus jet-off data, with no correction for impingement. The jet-off runs used to determine the differences were arbitrarily selected from the five repeat runs at zero yaw, the six repeat runs at -4 degrees yaw and the six repeat runs at +4 degrees yaw.

The differences between jet-off repeat runs are shown in Figures 6-3 through 6-8. The normal Force Data show a maximum difference of 0.015 between jet-off runs, while the axial force data show a scatter of 0.008 except at +4 degrees yaw, where there appears to be a problem in the jet-off data. The pitching moment data show a scatter of 0.004, while rolling moment data appear to repeat to 0.0005. The yawing moment shows its worst repeatability at +4 degrees yaw and the scatter is 0.0015. A similar trend is seen in side force data with a scatter of 0.005. Comparisons of repeat runs at $\beta = +4$ tend to show a problem may still exist in the IA148 data. The runs selected for the jet-off baselines were:

- a. $\beta = -4$, IA148 run 171
- b. $\beta = 0$, IA148 run 228
- c. $\beta = +4$, IA148 run 116

All jet-off differences were included in the jet-on analyses at each yaw angle for each RCS combination.

The jet-on data were obtained at three supply pressures for each jet combination, at angles of attack from -15 to +12.5 degrees. Selected data samples will be presented for the following jet combinations:

- a. RC06
- b. RC38
- c. RC40
- d. RC51
- e. RC78
- f. RC82

6.1.1 RC06 TEST DATA. RC06 represents the six rear-mounted symmetric pitch-down jets case (similar to the analysis of Reference 1 except for the external tank) with no forward jets firing. Data were obtained at zero and +4 degrees yaw, but the data presented in Figures 6-9 through 6-13 are for zero yaw only. The data show very small sensitivity to angle of attack. The longitudinal data appear to be nonlinear with jet pressure, while the lateral-directional data show some slight asymmetry. This was interpreted to be due to a nominal +0.2 degree yaw angle measured in the "zero yaw" data tests.

6.1.2 RC38 TEST DATA. The jet combination RC38 consists of the four symmetric forward-mounted down-firing jets, the six symmetric rear-mounted up-firing jets, and the three left side rear-mounted down-firing jets, all firing as a group. Data at 0, +4, and -4 degrees yaw are compared on Figures 6-14 through 6-19. The axial force incremental data appear to be sensitive to yaw angle and angles of attack above zero degrees. Normal force and pitching moment incremental data appear to be moderately sensitive to angle of attack and not very sensitive to yaw angle. The lateral-directional data appear more sensitive to yaw angle and angle of attack than to the different jet pressure ratios.

6.1.3 RC40 TEST DATA. The combination called RC40 has no forward-mounted jets firing but has the six symmetric rear-mounted up-firing jets coupled with three rear-mounted left side down-firing jets. The data are presented in Figures 6-20 through 6-25. Most interesting of these data are the reversal of normal force and pitching moment increments for a jet pressure of 1540 psi for the zero yaw case, compared to the two other jet pressures. The lateral-directional data also show a trend similar to the peak value seen in Reference 1 for the rear-mounted pitch-up jet data.

6.1.4 RC51 TEST DATA. The RC51 jet combination consists of:

- a. two left side forward-mounted yaw jets.
- b. four symmetric forward-mounted down-firing pitch jets.

- c. six symmetric rear-mounted up-firing pitch jets.
- d. one right side rear-mounted yaw jet.

Data obtained only at zero yaw angle for this combination are presented in Figures 6-26 through 6-31. The longitudinal data show moderate sensitivity to angle of attack while the lateral-directional data show reversed trends of supply pressure at positive and negative angles of attack.

6.1.5 RC78 TEST DATA. RC78 consists of two forward-mounted yaw jets on the left side and one rear-mounted yaw jet on the right side. It is an important case, since the derivation of most of the combinations not tested is the sum of RC78 plus some other combination. The test data are shown in Figures 6-32 through 6-37. As might be expected, this combination generates only small longitudinal force and moment increments, which appear not to be sensitive to jet supply pressure. The largest induced moment appears to be the induced yawing moment.

6.1.6 RC82 TEST DATA. The RC82 jet combination consists of:

- a. two left side forward-mounted yaw jets.
- b. four symmetric forward-mounted down-firing jets.
- c. six symmetric rear-mounted up-firing jets.
- d. three left side rear-mounted down-firing jets.
- e. one right side rear-mounted yaw jet.

The data for zero yaw are presented in Figures 6-38 through 6-42, where the longitudinal data show strong sensitivity to angle of attack and supply pressure. The principal lateral-directional induced moment is the incremental rolling moment. The RC82 combination could be achieved as the sum of RC38 and RC78, if superposition of data is possible. This will be discussed in the data analysis section.

6.2 DATA ANALYSIS

The mated configuration data base represented by the IA148 test data represents a large number of data runs with different control combinations. However, the data set for each combination was very small (three jet pressures at three yaw angles), with no systematic buildup of nozzle combinations, and increments between sets of nozzles could not be derived. It was necessary to reduce the data to obtain a form suitable for deriving other control combinations not tested and to allow interpolation in the data for differences in flight conditions. Figures 6-9 through 6-42 present samples of the existing data base for six different control combinations. These figures illustrate the need to smooth the data and to relate them to the flight condition. Most of the rear-mounted RCS data were correlated to a momentum ratio parameter (Reference 1);

however, yaw jet data were correlated to mass flow ratio. The equivalent nozzle momentum ratio used in Reference 1 is:

$$\frac{\Phi_j}{\Phi_\infty} = \frac{\gamma_j P_j M_j^2 \Sigma A_j}{\gamma_\infty P_\infty M_\infty^2 S_{wing}} \quad (6-1)$$

The related mass flow parameter is:

$$\frac{\dot{m}_j}{\dot{m}_\infty} = \left[\frac{\Phi_j \Sigma A_j P_j}{\Phi_\infty S_{Ref} P_\infty} \left(\frac{R_\infty T_\infty}{R_j T_j} \right)^{1/2} \right] \quad (6-2)$$

The use of these parameters was not practical for all jet combinations tested in IA148, since the many different nozzles used made it difficult to define the equivalent nozzle. Since sufficient data was not available to analyze the differences between combinations, it was decided to use a common parameter for all sets and to analyze each set separately. Single nozzle momentum ratio (equation 6-13) was chosen as the best parameter because insufficient data were available to differentiate between mass flow ratio and momentum ratio. Single-nozzle momentum ratio accurately reflects flight condition changes.

$$\frac{\phi_j}{\phi_\infty} = \frac{\gamma_j P_j M_j^2 A_j}{\gamma_\infty P_\infty M_\infty^2 S_{wing}} \quad (6-3)$$

The data presented in Figures 6-9 through 6-42 show that there are measurable effects of yaw with the external tank on, so the data was analyzed at zero, +4, and -4 degrees yaw as separate sets. A quadratic least-square-curve fit was generated for each set of data within a limited angle-of-attack range. This data set also used the jet-off differences in establishing the curve fit. The purpose of using the jet-off differences with the jet-on data is to account for run-to-run variation in the data, which is included in all jet-on differences.

Fourteen angle-of-attack ranges were chosen for curve fitting so that two or three test points are included in each range to help smooth the data and to give better fits versus momentum ratio. The ranges are

<u>Angle of Attack, α</u>	<u>Data Used</u>	<u>Angle of Attack, α</u>	<u>Data Used</u>
-14°	-14.6, -13.5	0°	-1.5, 0, 1.5
-12°	-13.5, -12, -10.5	1.5°	0, 1.5, 3
-9°	-10.5, -9, -7.5	3°	1.5, 3, 4.5
-6°	-7.5, -6, -4.5	4.5°	3, 4.5, 6
-4.5°	-6, -4.5, -3	6°	4.5, 6, 7.5
-3°	-4.5, -3, -1.5	9°	7.5, 9, 10.5
-1.5°	-3, -1.5, 0	12.35°	10.5, 12, 13.15

The data used to curve fit overlaps by at least one point in each range. Because of this overlap, linear interpolation between angles should be acceptable between fits. No corrections for impingement were made on the test data, since OA169 data showed no rear-mounted RCS impingement in the test data. Impingement corrections should be made for full scale predictions, but will probably be very small at dynamic pressures above 5 psf. Insufficient forward-mounted jet analysis has been made to predict impingement at this time.

Appendixes A, B, and C present the coefficients for all zero, +4, and -4 degree yaw angle fits, respectively. To present all data, 5300 plots are required for the twenty-one nozzle combinations at three yaw angles with fourteen angle-of-attack ranges for the six aerodynamic coefficients. These plots have been generated and examined to ensure the reliability of the curve fits; however, only sample data is presented in this report.

The sample chosen is RC78, and the correlations in four angle-of-attack ranges are presented in Figures 6-43 through 6-66. These data, presented as a function of angle of attack, were shown in Figures 6-32 through 6-37. The normal force increments show their largest values at the highest angles of attack presented. The normal-force jet-off (zero momentum ratio) intercept (a_0) is large compared to the incremental jet-on values at zero angle of attack. This raises the question of whether it is appropriate to remove this term when applying the data to the flight vehicle, because the term is related to wind tunnel repeatability, not to the induced effects. The axial force data also shows a large intercept value and the effects of least-square curve fit smoothing are seen in these samples.

The side force increments show a reversed sign between positive and negative angle of attack data. This trend is also seen in the rolling moment data.

Pitching moment increments appear to be sensitive to yaw angle, although this trend is largely due to the intercepts (a_0) at +4 degrees yaw. The incremental yawing moment data appear to be independent of angle of attack and yaw angle.

In all cases shown, the least-square curves fit the data very well. The good curve fit could be expected, since most of these curves were fit through only 18 points: nine jet-off data and three each at the three momentum ratios tested.

6.2.1 EFFECT OF YAW ANGLE. The data from the curve fits of the RC78 case were replotted as a function of yaw angle at constant angle of attack and at a single-nozzle momentum ratio of 0.02, to determine the best method of interpolating between curve fits for yaw angles other than 0, -4, or +4 degrees. Figures 6-67 through 6-72 present these comparisons (where the intercept a_0 has been left in the data).

A quadratic equation would appear to be a better fit than a linear interpolation for most data, since the "zero" yaw value is a maximum or minimum value for the three points available. It was pointed out in Subsection 6.1 that the zero yaw data was

actually obtained at a value of 0.2 degree yaw. Considering the small magnitude of many of the increments, it is important to include this in the data interpolation for yaw. The proposed interpolation assumes that all three yaw increments are first computed from angle of attack and momentum ratio. These then are used to compute the value of the given yaw angle using equation 6-4.

$$y_{\beta} = a \beta^2 + b\beta + c \quad (6-4)$$

where

$$a = .02976 y_{-4} + .03289 y_{+4} - .06266 y_0 \quad (6-5)$$

$$b = .125 (y_{+4} - y_{-4}) \quad (6-6)$$

$$c = 1.0025 y_0 - .02632 y_{+4} + .02381 y_{-4} \quad (6-7)$$

y_0 = solution of zero yaw curve fit

y_{+4} = solution of +4° yaw curve fit

y_{-4} = solution of -4° yaw curve fit

6.2.2 SUPERPOSITION OF DATA. Symmetry and superposition are the basic assumptions for generating the interaction models for RCS control combinations which were not tested in IA148.

Symmetry assumes that positive and negative yaw increments will be the same when the jets on the windward and leeward sides are matched. This appears to be a reasonable assumption, but no data exists on test IA148 to verify it.

Superposition is a much larger assumption, since it assumes that combinations of RCS jets can be assembled by simple addition (or subtraction) of the data from two or more other sets of control combinations. This assumption is extensively used in filling the mated tank-on control set data, especially the UZCMD = +1 combinations.

Figures 6-73 through 6-84 present comparison of the curve fits for RC51, RC55, RC82, and RC89 compared with the equivalent combination using RC78 summed with the appropriate other run. All data presented in these figures is for zero yaw angle. RC51 is compared to the sum of RC78 and RC62; RC55 is compared to RC78 plus RC06; RC82 is compared to RC78 plus RC38; and RC89 adds RC78 with RC61.

The normal-force increment comparisons shown in Figures 6-73 and 6-74 show that superposition over-predicts the increment for RC89, under-predicts the increment for RC51, but shows good agreement for the other two cases. The axial force increments (Figures 6-75 and 6-76) show that the two cases where forward-mounted jets are added (RC51 and RC82) result in a sum less than the measured data; for the cases where no forward-mounted jets are added, the sum over-predicts the effect.

The side force comparisons in Figures 6-77 and 6-78 show that the combinations which add forward-mounted jets (RC51 and RC82) show poorer correlation than the cases where only forward-mounted yaw jets are used.

Figures 6-79 and 6-80 present the incremental rolling moment data comparisons. The RC82 comparison looks much worse than that for RC51 but the difference in plot scales accounts for this. Figures 6-81 and 6-82 show that the sum of the two jet cases underestimates the induced pitching moment increment for all cases but RC82. The yawing moment data of Figures 6-83 and 6-84 show poorer agreement when forward-mounted jets must be added.

It appears that superposition of jet data to build up jet combinations works much better for aft-mounted jets than forward-mounted, particularly in the lateral-directional force and moment increments. If these increments are critical in terms of RCS control with the tank on, then more test data to fill in the jet combinations not tested in IA148 is very desirable.

6.2.3 CORRECTING JET-OFF DIFFERENCES FROM DATA. When the RCS jets are off, there will be no interaction increments, and it is reasonable to assume that the curve fit of the interaction data should go to zero. The curve fit expression

$$\Delta C = a_0 + a_1 X + a_2 X^2 \quad (6-8)$$

does contain a jet-off intercept (a_0) for which values were computed during the least-square curve fitting of the data. This term was never zero in all of the curve fits, and the nature and use of this term is being questioned. All of the jet-off differences were included in obtaining these curve fit coefficients, and these data represented nearly half of the data through which the curve was placed. Thus, the a_0 term represents the best estimate of the difference between the jet-off run used to derive jet-on increments and the "average" jet-off run. Average jet-off run is a relative term, since the sample size is small, but it is the only estimate available.

The best approximation to account for run-to-run variation in the test data would be to remove a_0 from the curve fit expression, leaving equation 6-9 as the best fit of the interaction increments.

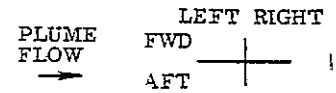
$$\Delta C = X (a_1 + a_2 X) \quad (6-9)$$

This in effect shifts all of the data so the curves pass through zero increment at zero momentum ratio. Most curve fit expressions (Appendixes A to C) already pass very close to zero, so the adjustment is small. However, the adjustment may well be significant, since many of the induced increments are small also. The largest adjustment appears to occur in the $\beta = +4$ degree axial force increments, for which the basic data appeared to have some problems.

This correction is particularly important to the data being summed to create new nozzle combinations where the a_0 terms are added to each other if left in the equations.

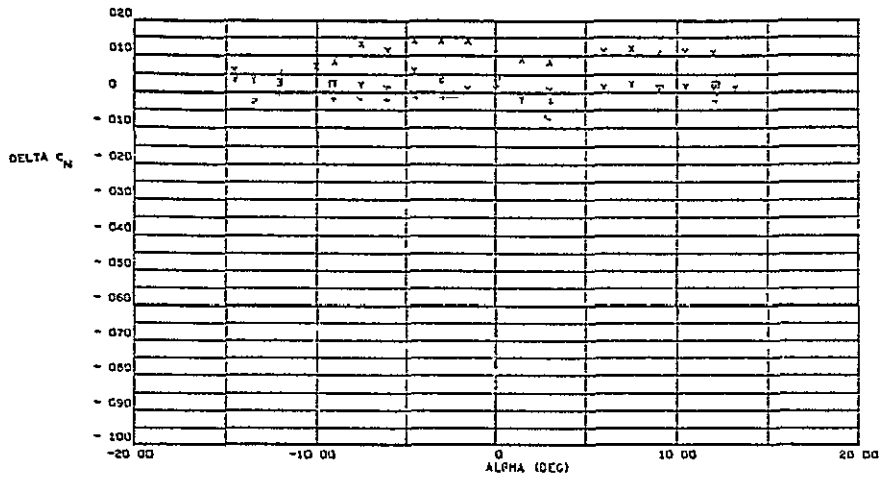
UYCMD	UXCMD = -2	UXCMD = 0	UXCMD = 2
5		RC62	RC38
4		RC59	RC38
3		RC11	RC39
2			RC40
1		RC37	
0		NO JETS FIRED	RC61
-1			
-2			
-3	RC06	RC06	RC06

Figure 6-1. Mated configuration reaction control combinations, UZCMD = 0.

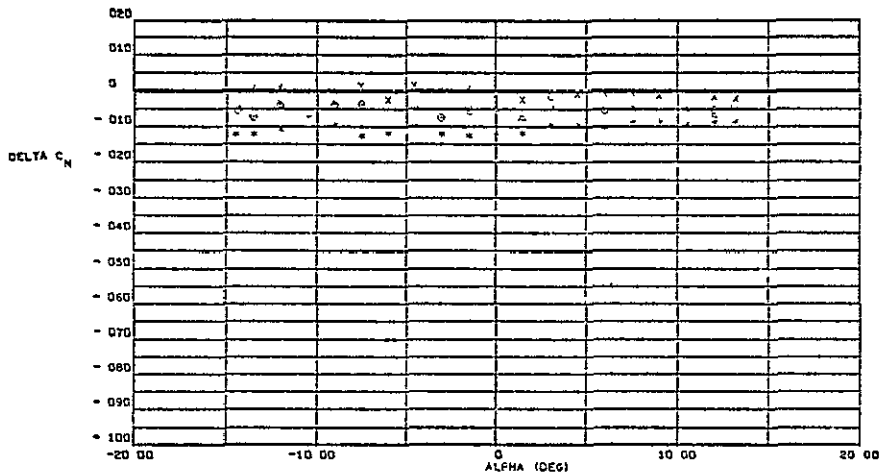


UYCMD	UXCMD = -2	UXCMD = 0	UXCMD = 2
5		RC51	RC32
4		RC45	RC32
3		RC42	RC36
2			RC37
1		RC77	
0	RC94	RC78	RC39
-1			
-2			
-3	RC55	RC55	RC55

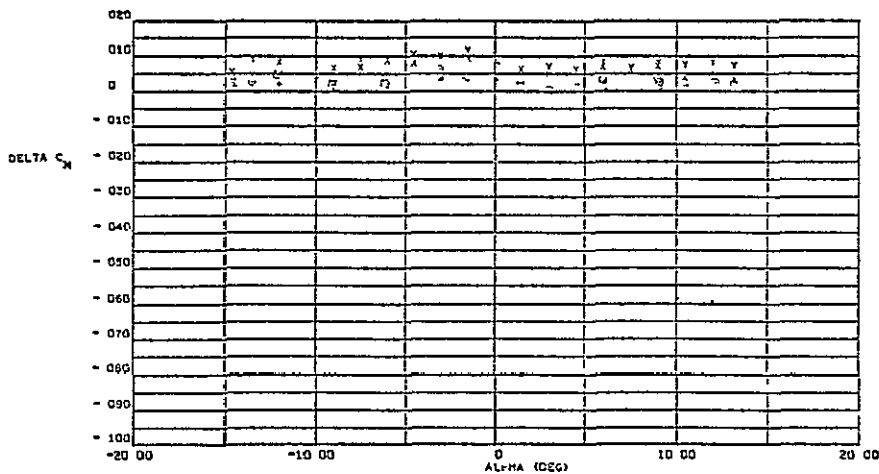
Figure 6-2. Mated configuration reaction control combinations, UZCMD = 1.



$$\beta = -4$$

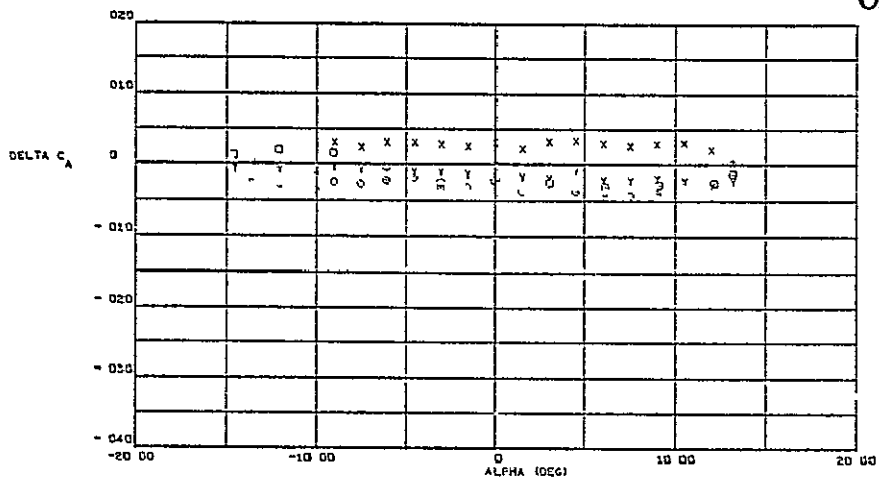


$$\beta = 0$$

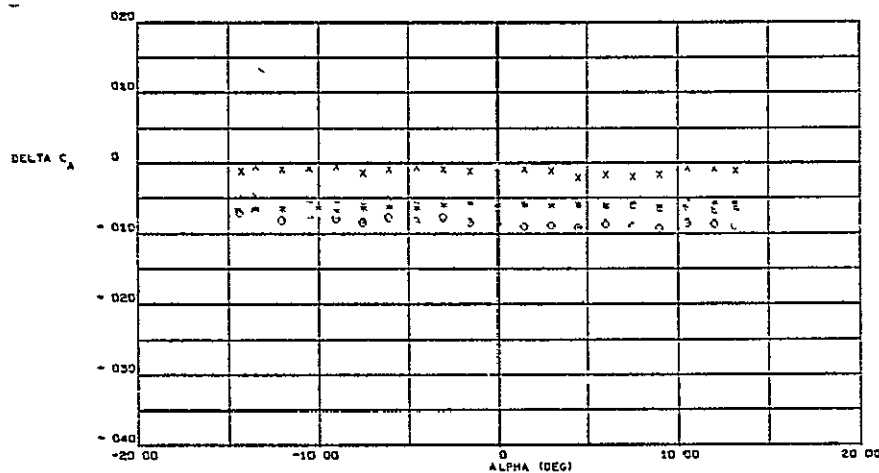


$$\beta = +4$$

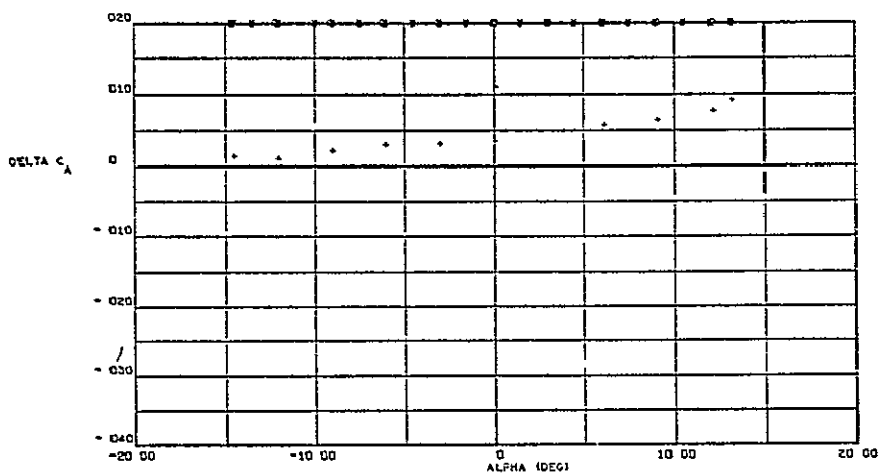
Figure 6-3. Variation in mated configuration jet-off normal force coefficients.



$\beta = -4$

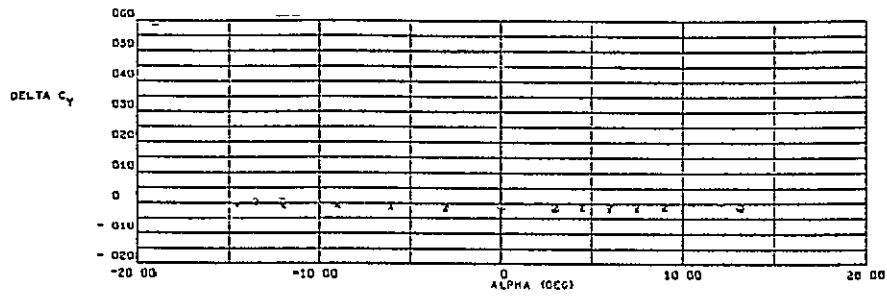


$\beta = 0$

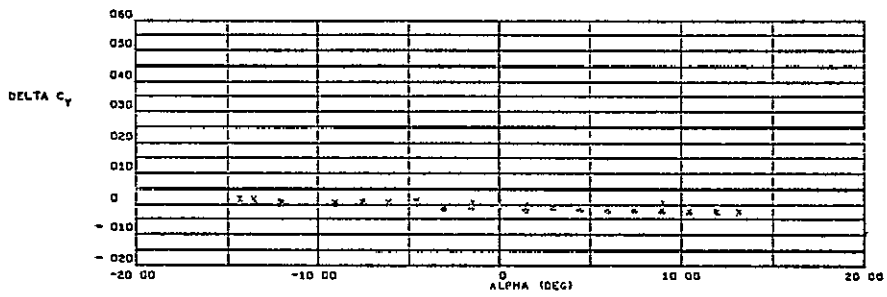


$\beta = +4$

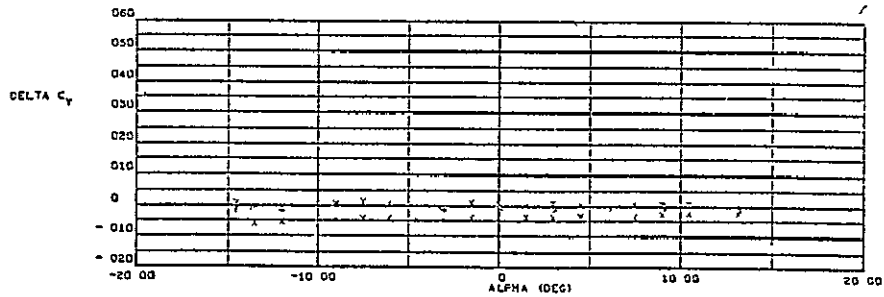
Figure 6-4. Variation in mated configuration jet-off axial force coefficients.



$$\beta = -4$$



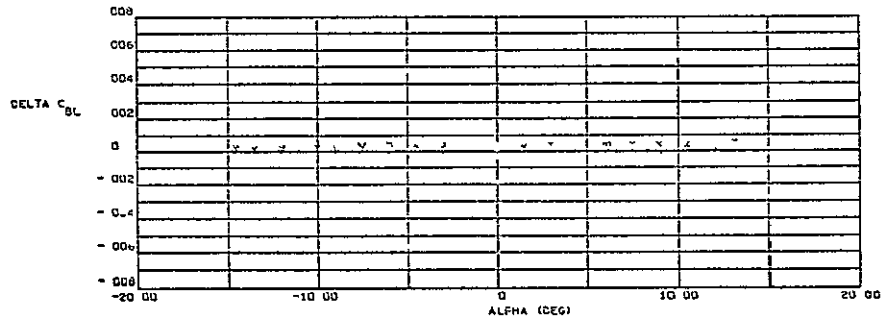
$$\beta = 0$$



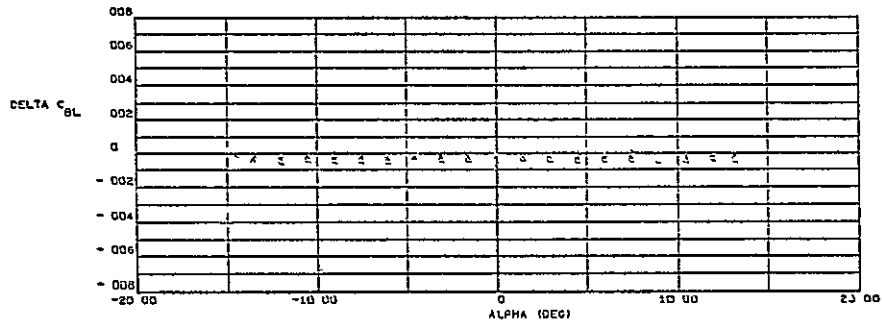
$$\beta = +4$$

Figure 6-5. Variation in mated configuration jet-off side force coefficients.

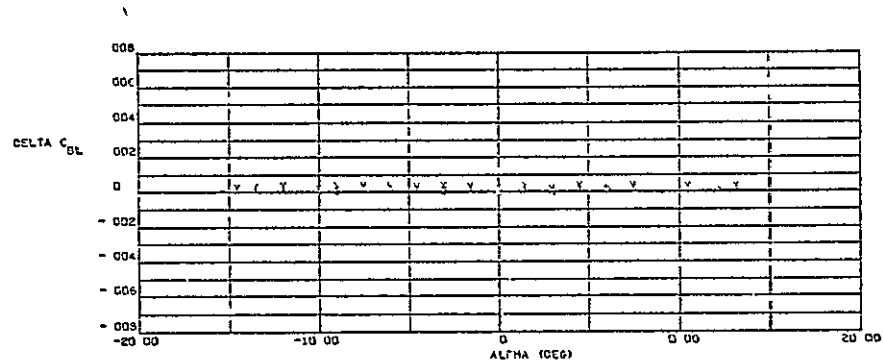
ORIGINAL PAGE IS
OF POOR QUALITY



$$\beta = -4$$

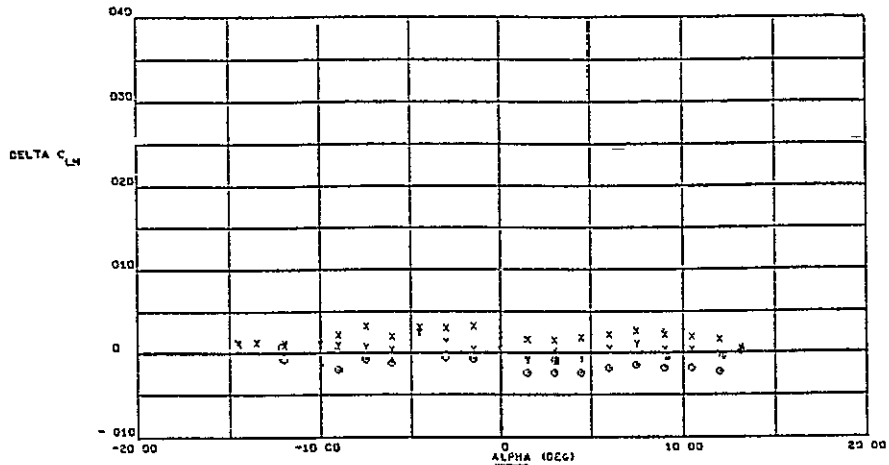


$$\beta = 0$$

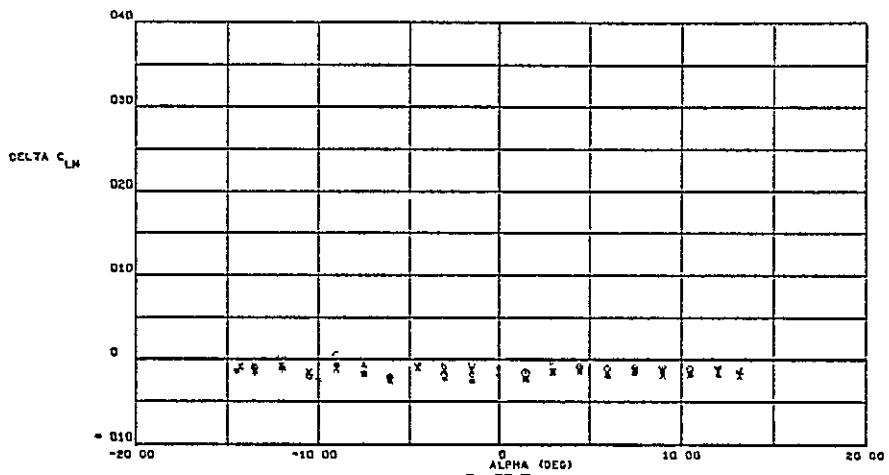


$$\beta = +4$$

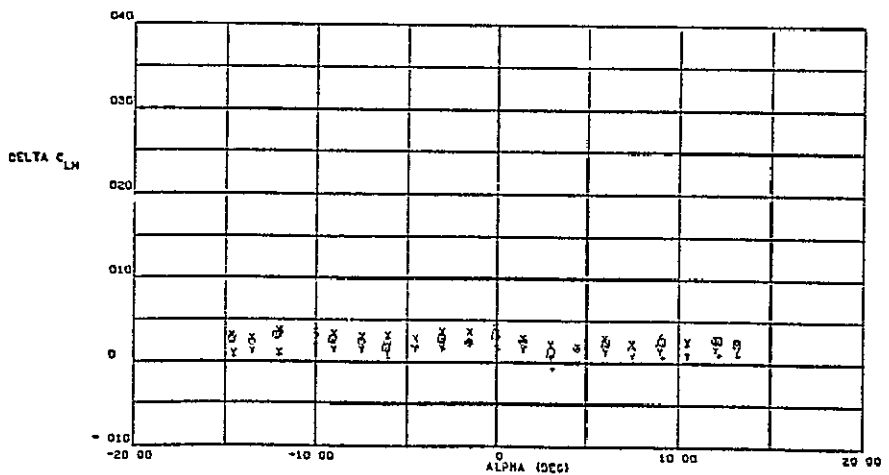
Figure 6-6. Variation in mated configuration jet-off rolling moment coefficients.



$$\beta = -4$$



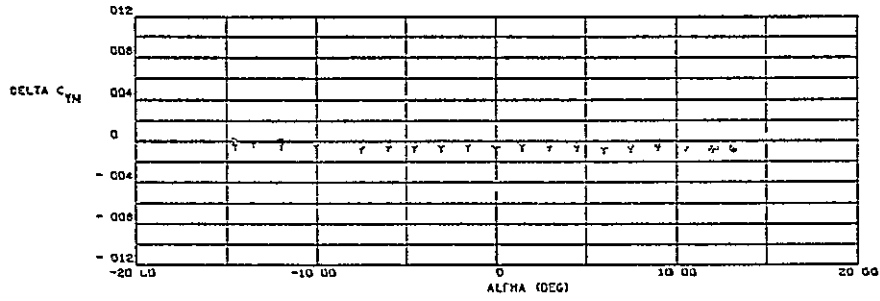
$$\beta = 0$$



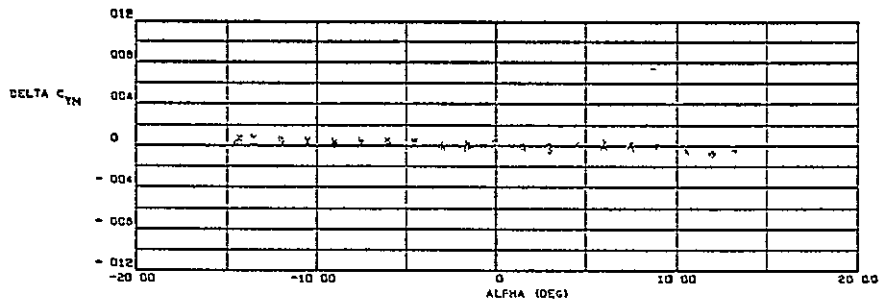
$$\beta = +4$$

Figure 6-7. Variation in mated configuration jet-off pitching moment coefficients.

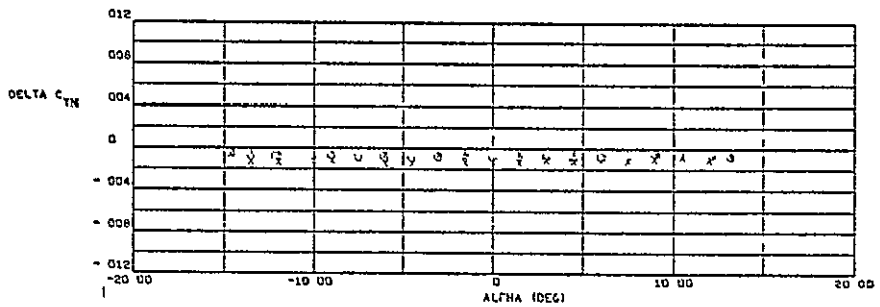
ORIGINAL PAGE IS
OF POOR QUALITY



$$\beta = -4$$



$$\beta = 0$$



$$\beta = +4$$

Figure 6-8. Variation in mated configuration jet-off yawing moment coefficients.

LEGEND	
SYMBOL	P_{0j}
Y L O	770 psia
+ X	1030
* □	1534

$$\beta = 0^\circ$$

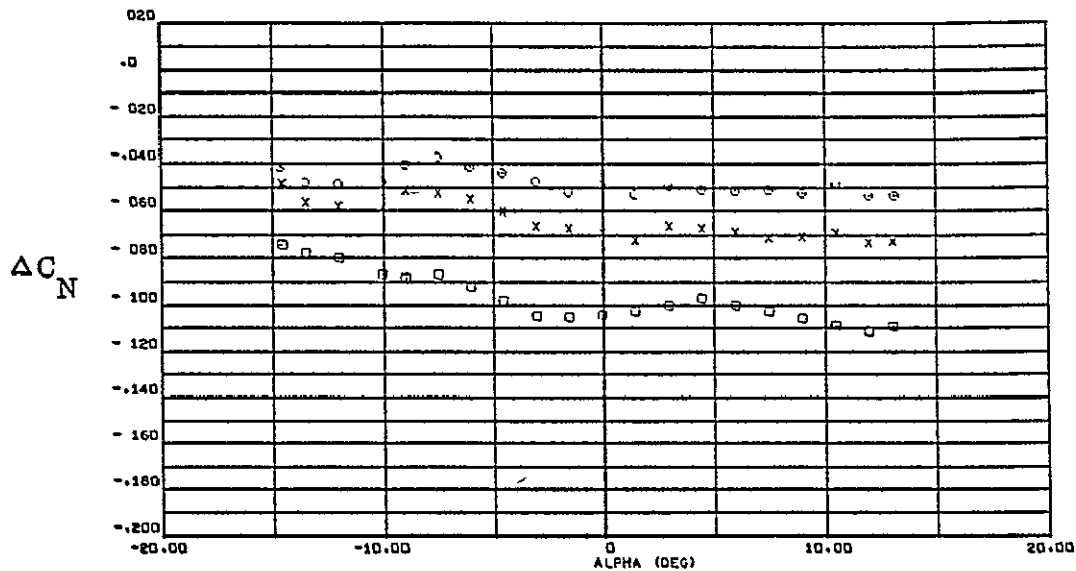


Figure 6-9. RC06 normal force increments.

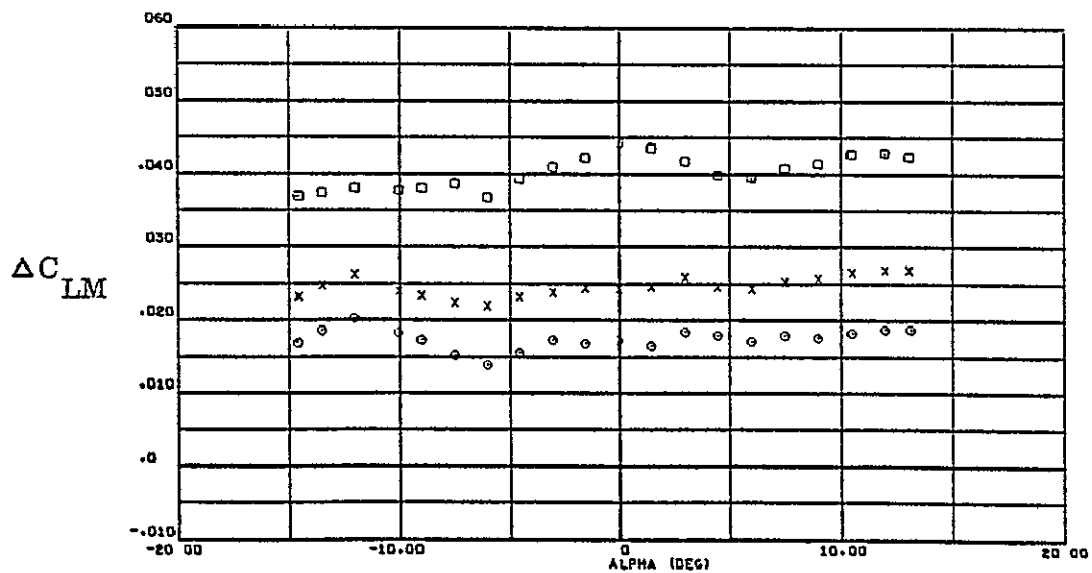


Figure 6-10. RC06 pitching moment increments.

ORIGINAL PAGE IS
OF POOR QUALITY

$$\beta = 0^\circ$$

LEGEND	
SYMBOL	P_{oj}
Y L O	770 psia
+ H X	1030
* □ □	1534

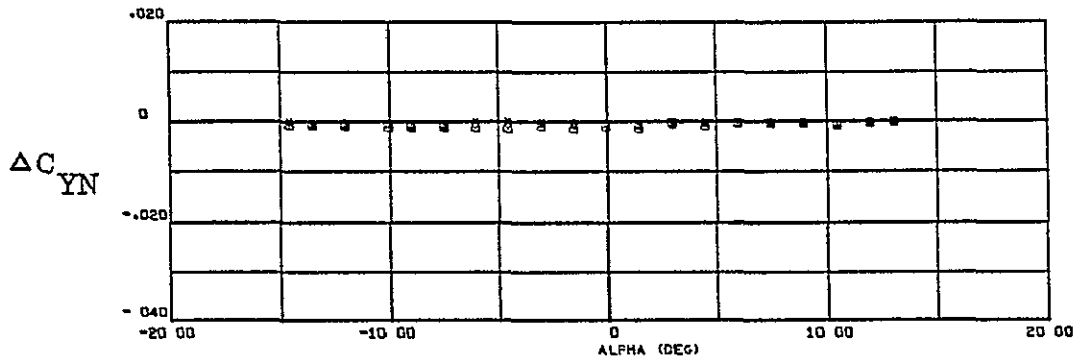


Figure 6-11. RC06 yawing moment increments.

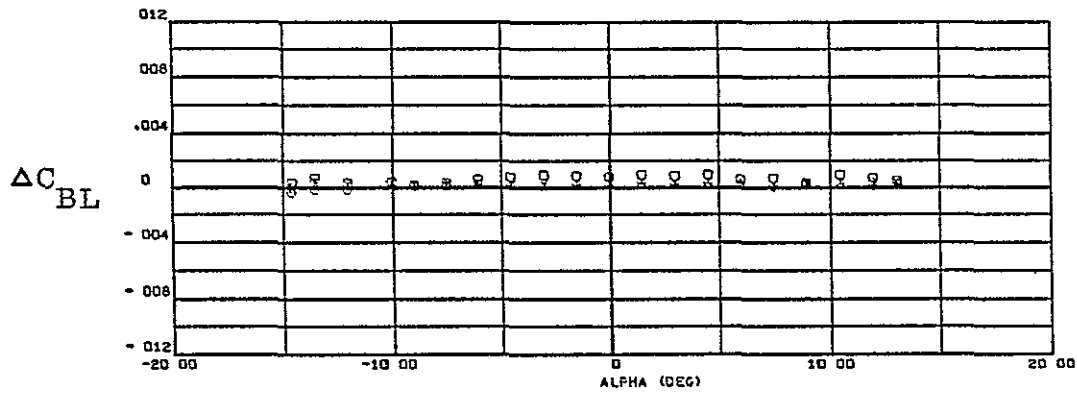


Figure 6-12. RC06 rolling moment increments.

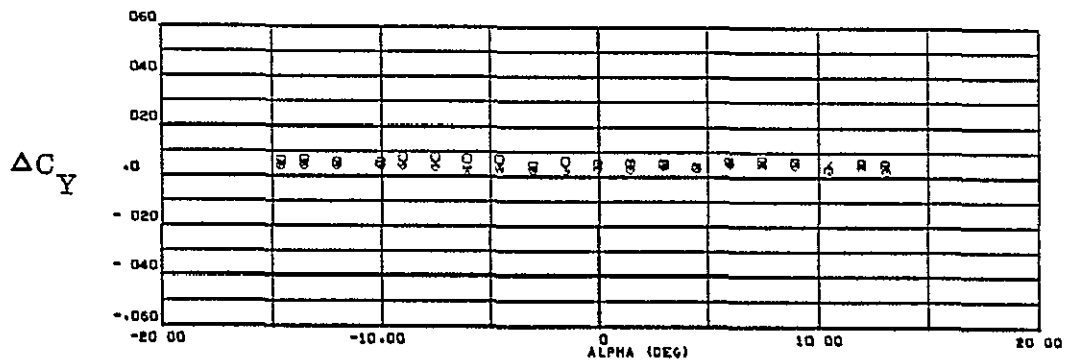
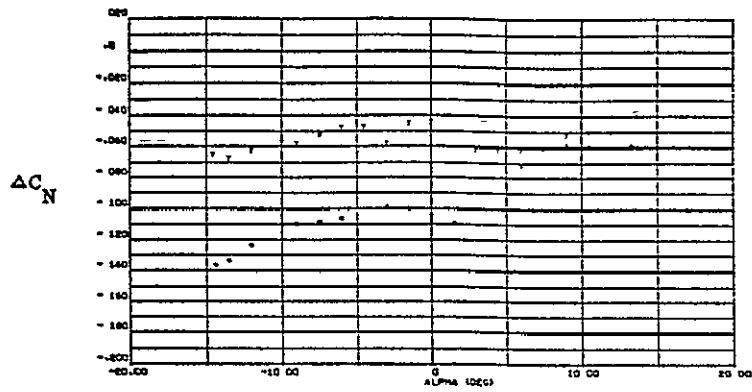
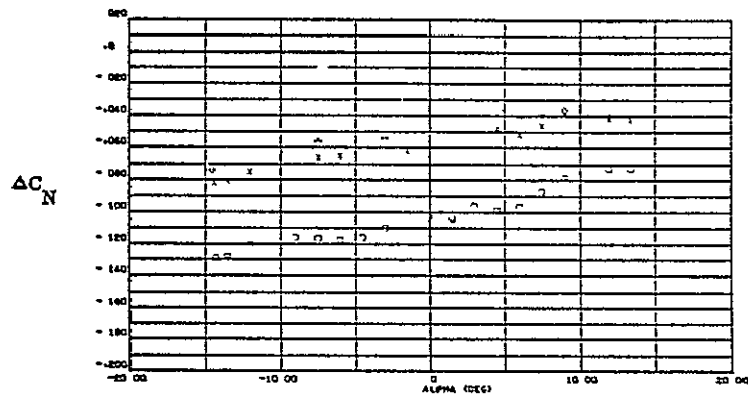


Figure 6-13. RC06 side force increments.

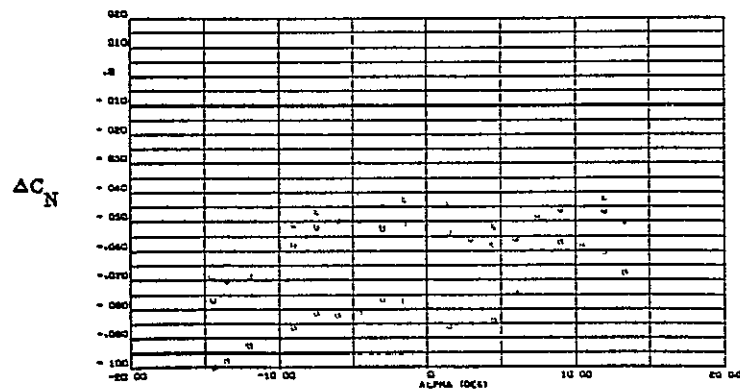
LEGEND	
SYMBOL	P_{Oj}
Y L O	770 psia
+ X	1030
+ □	1534



$\beta = +1^\circ$



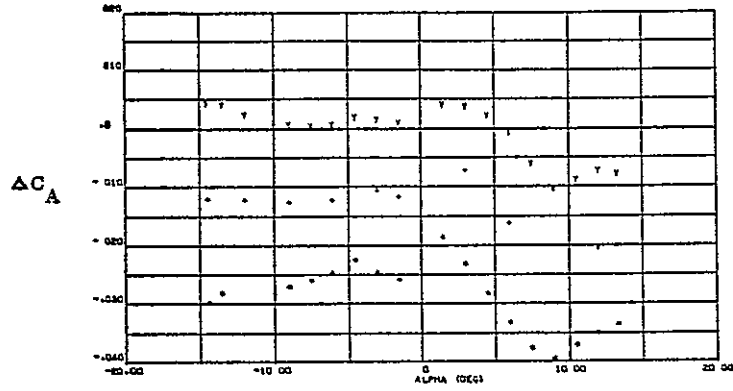
$\beta = 0^\circ$



$\beta = -1^\circ$

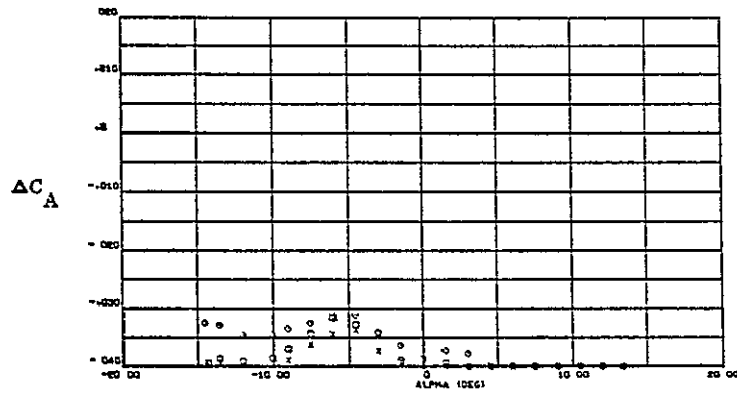
Figure 6-14. RC38 normal force increments.

LEGEND	
SYMBOL	P _{0j}
Y L O	770 psia
△ ▽ X	1030
+ □ □	1534

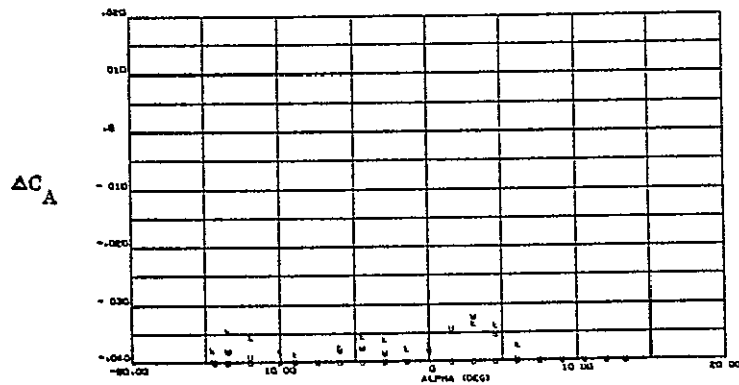


$\beta = +4^\circ$

ORIGINAL PAGE IS
OF POOR QUALITY



$\beta = 0^\circ$



$\beta = -4^\circ$

Figure 6-15. RC38 axial force increments.

LEGEND	
SYMBOL	P_{Oj}
Y L O	770 psia
+ u x	1030
* □ □	1534

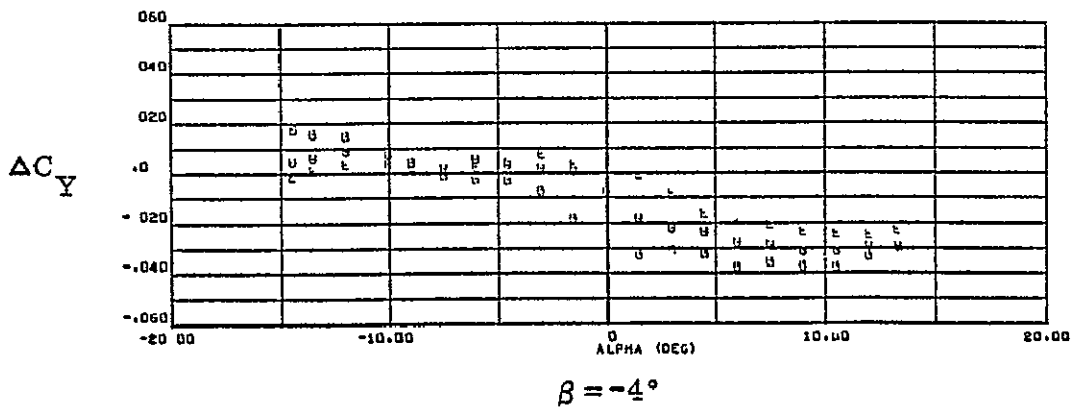
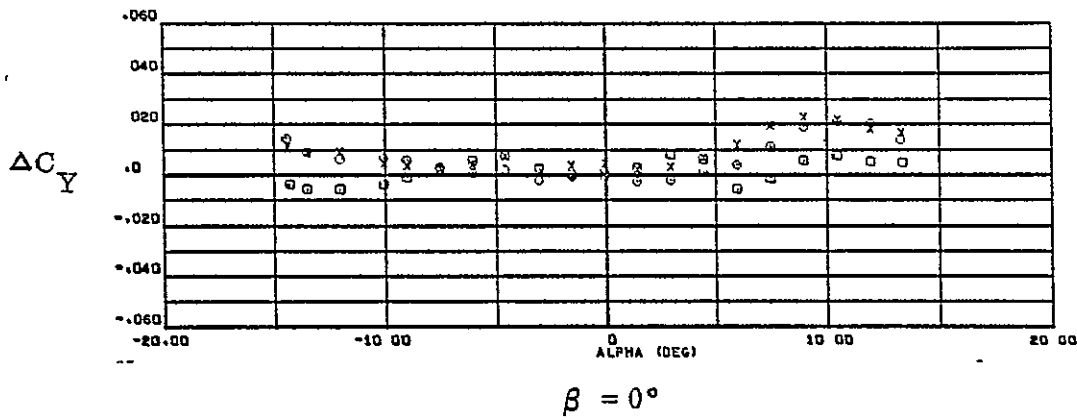
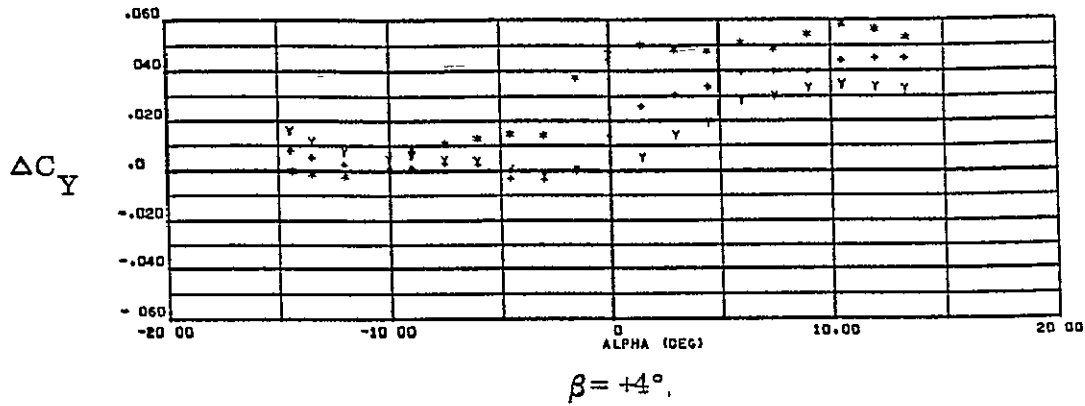


Figure 6-16. RC38 side force increments.

LEGEND	
SYMBOL	P_{01}
Y L O	770 psia
+ @ X	1030
+ □ □	1534

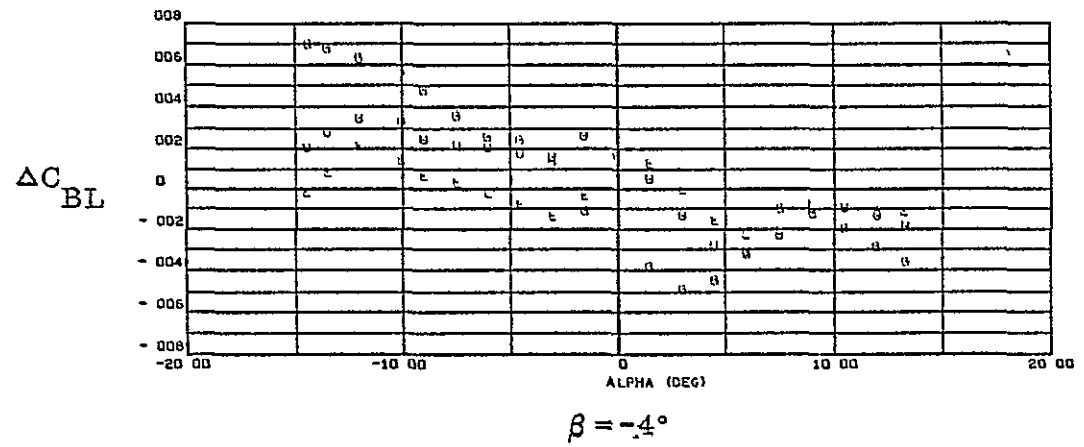
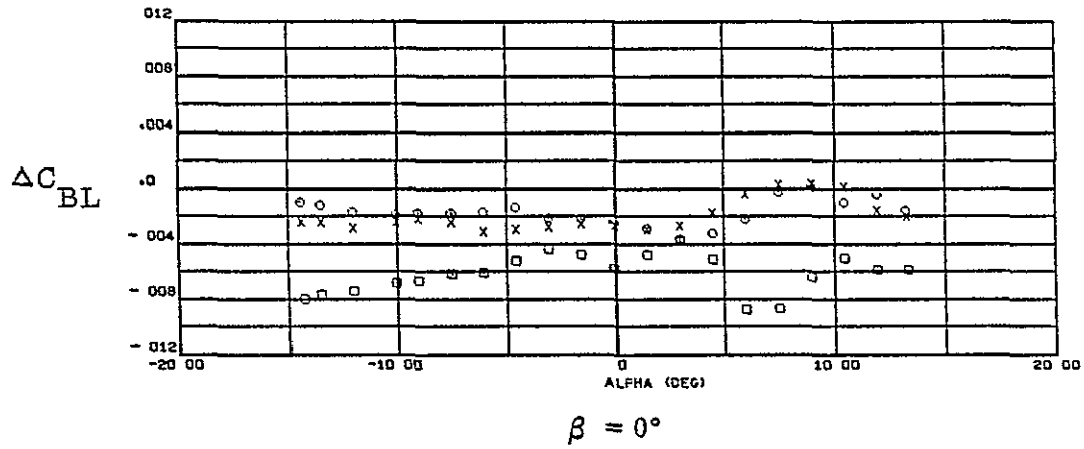
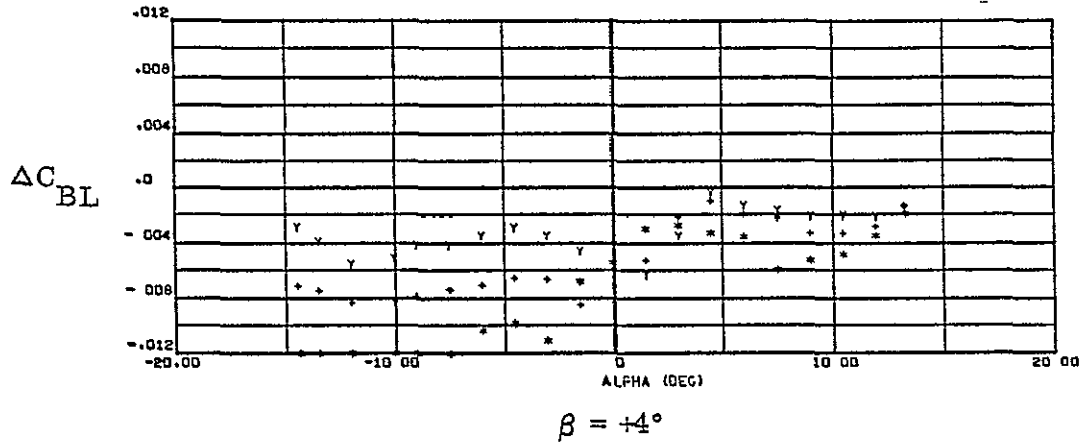
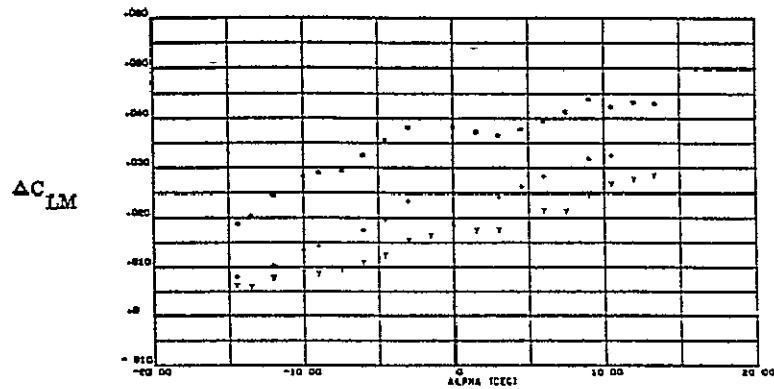
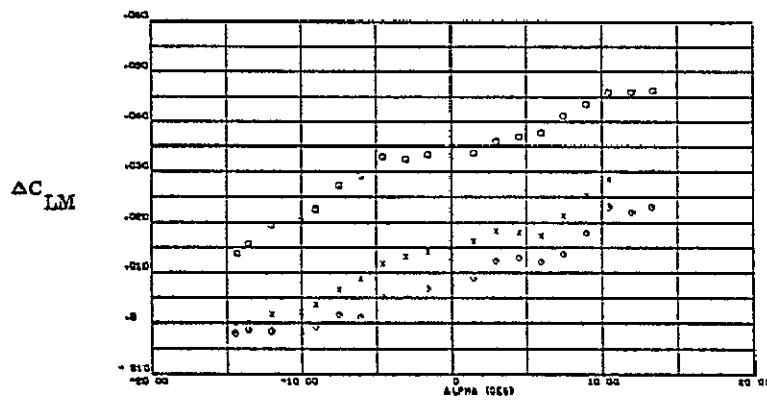


Figure 6-17. RC38 rolling moment increments.

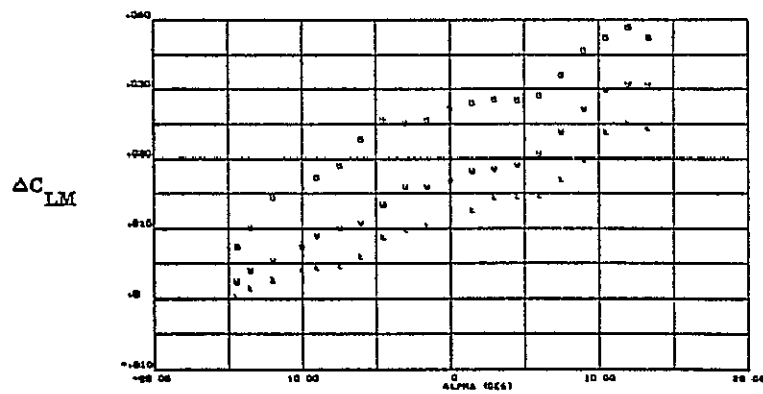
LEGEND	
SYMBOL	P_{01}
Y L O	770 psia
+ B X	1030
* □ □	1534



$\beta = +4^\circ$



$\beta = 0^\circ$



$\beta = -4^\circ$

Figure 6-18. RC38 pitching moment increments.

ORIGINAL PAGE IS
OF POOR QUALITY

LEGEND	
SYMBOL	P_{OJ}
Y L O	770 psia
+ U X	1030
* □	1534

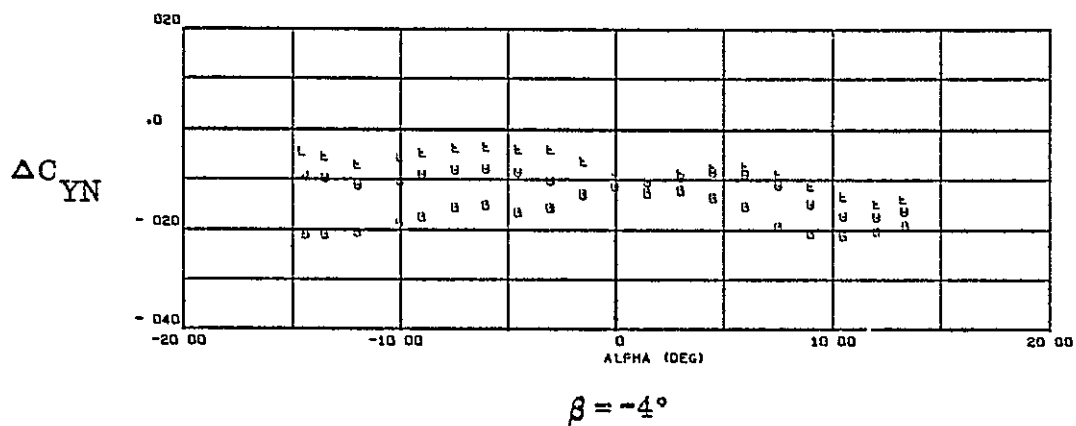
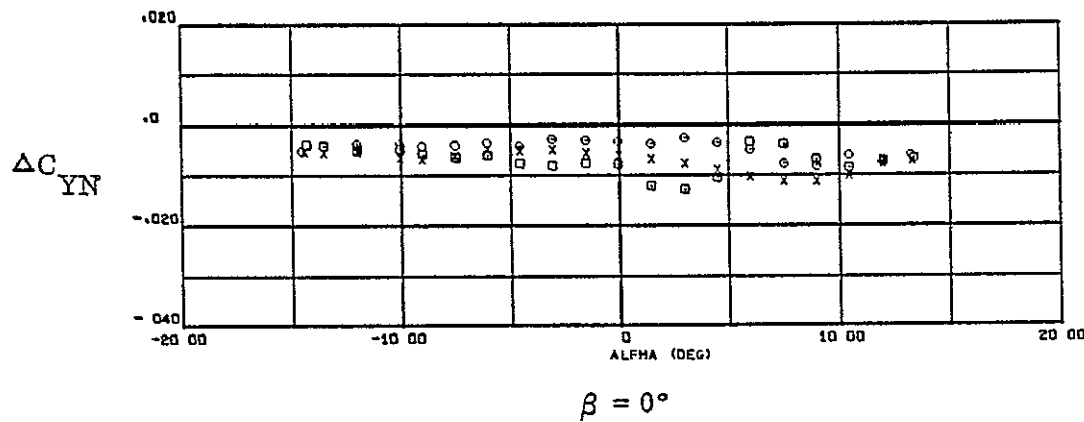
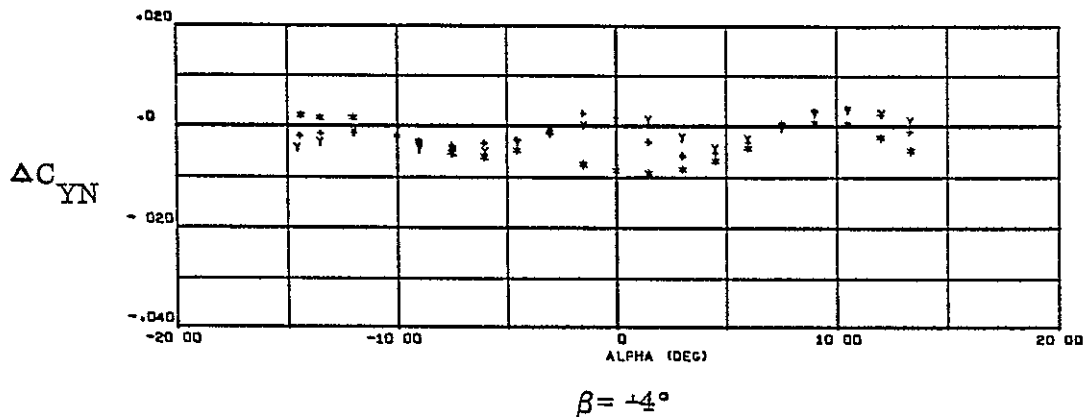
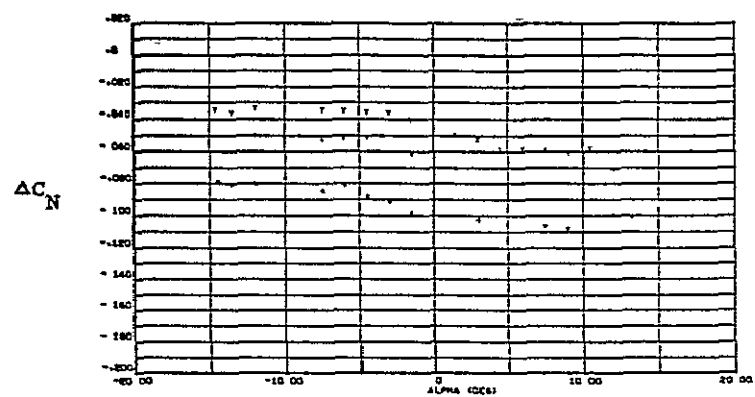
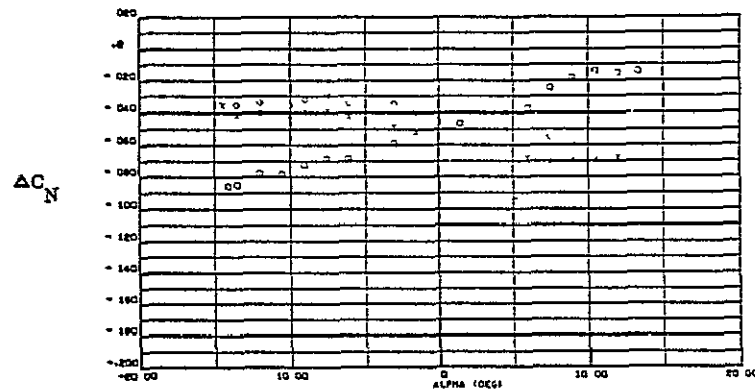


Figure 6-19. RC38 yawing moment increments.

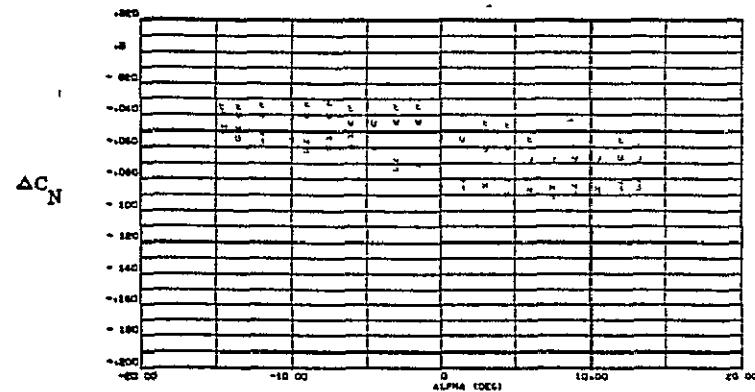
LEGEND	
SYMBOL	P_{Oj}
Y L O	770 psia
+ H X	1030
* □ □	1534



$\beta = +4^\circ$



$\beta = 0^\circ$



$\beta = -4^\circ$

Figure 6-20. RC40 normal force increments.

ORIGINAL PAGE IS
OF POOR QUALITY

LEGEND	
SYMBOL	P_{Oj}
Y L O	770 psia
+ u x	1020
+ □ □	1534

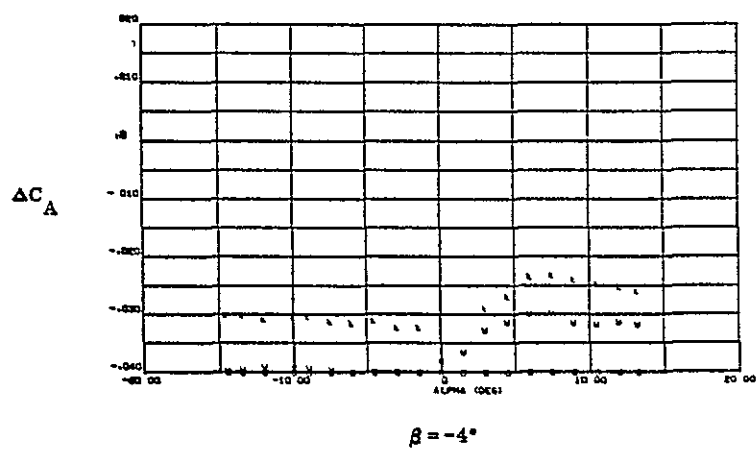
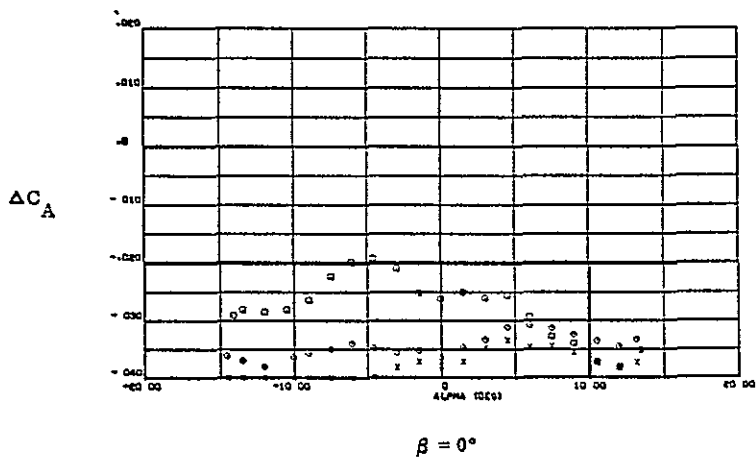
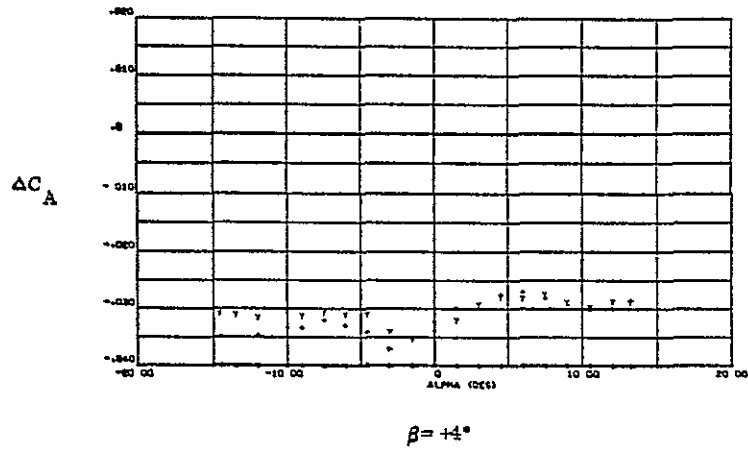


Figure 6-21. RC40 axial force increments.

LEGEND	
SYMBOL	P_{0j}
Y L O	770 psia
+ H X	1030
* □ □	1534

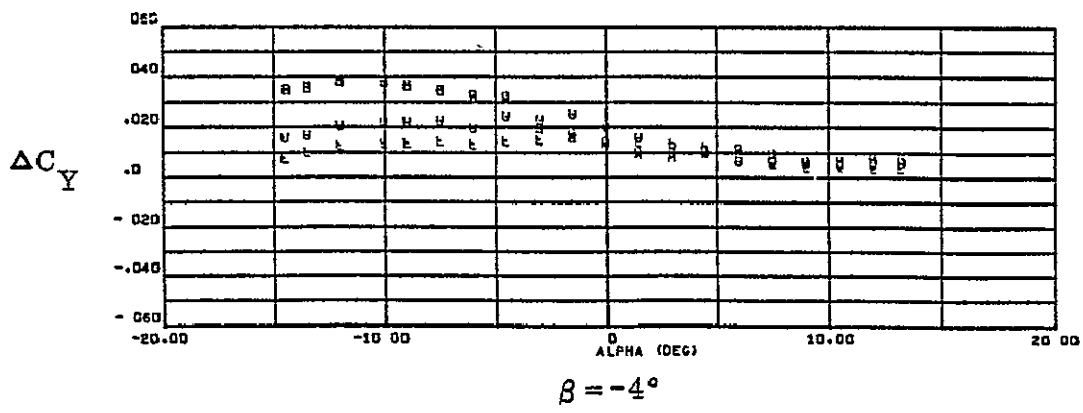
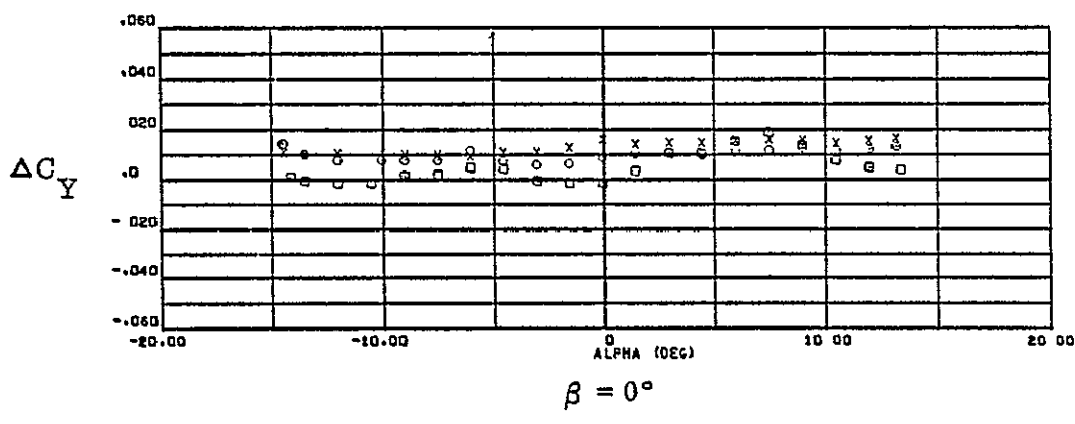
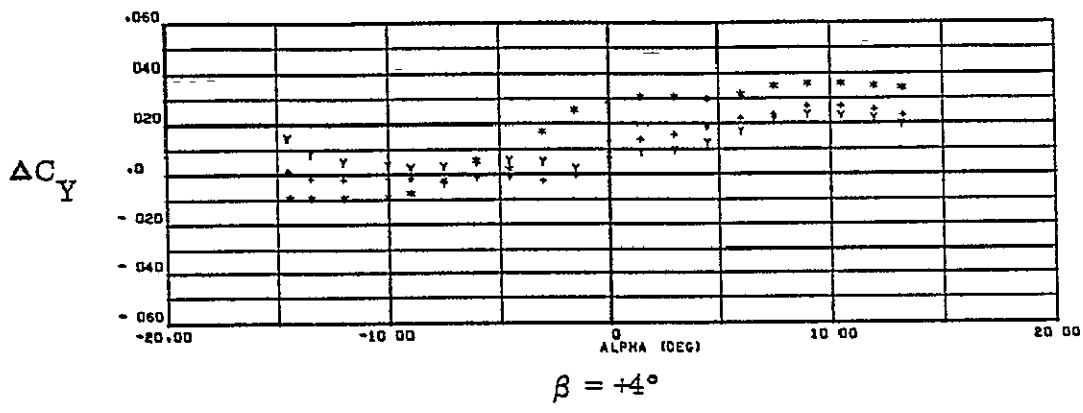
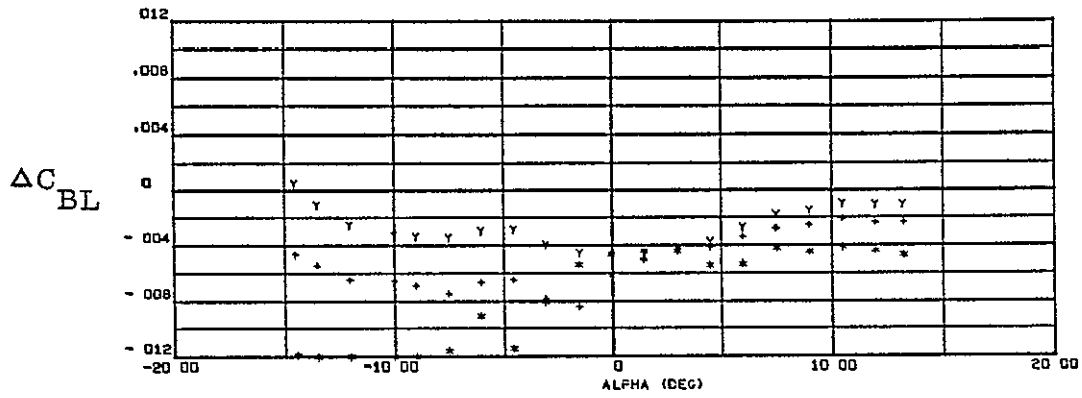


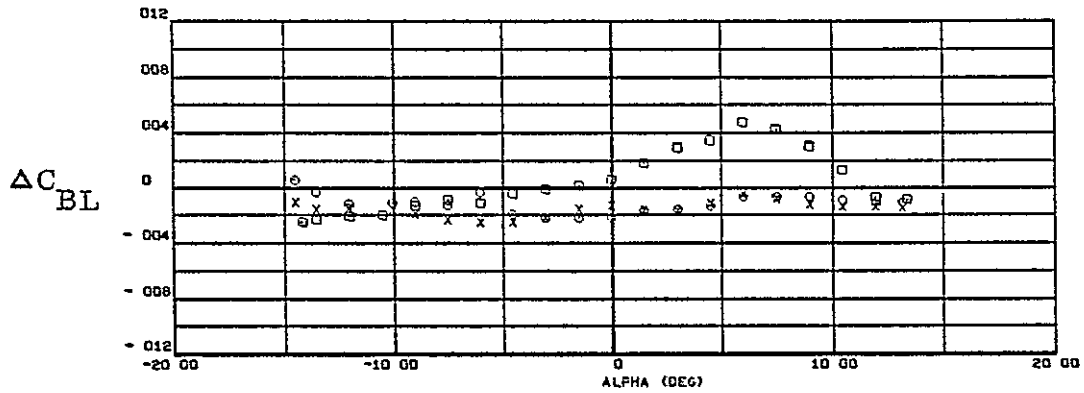
Figure 6-22. RC40 side force increments.

ORIGINAL PAGE IS
OF POOR QUALITY

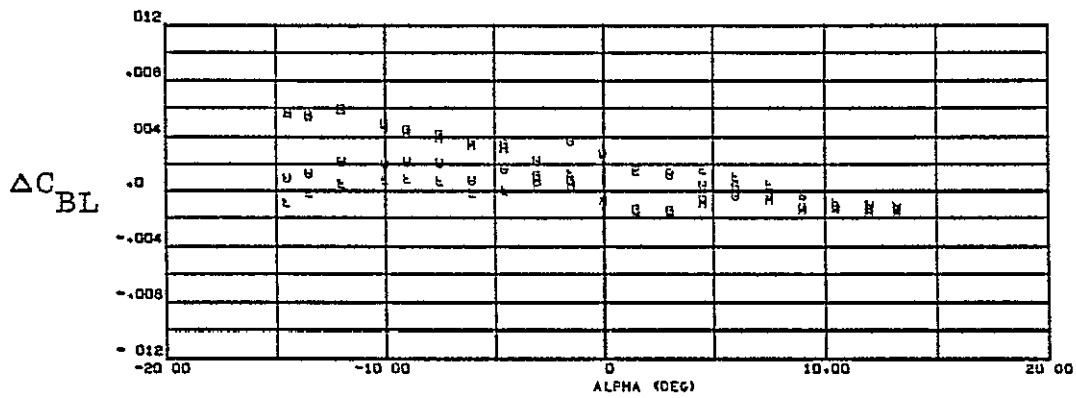
LEGEND	
SYMBOL	P_{Oj}
Y L O	770 psia
- U X	1030
+ □ □	1534



$\beta = +4^\circ$



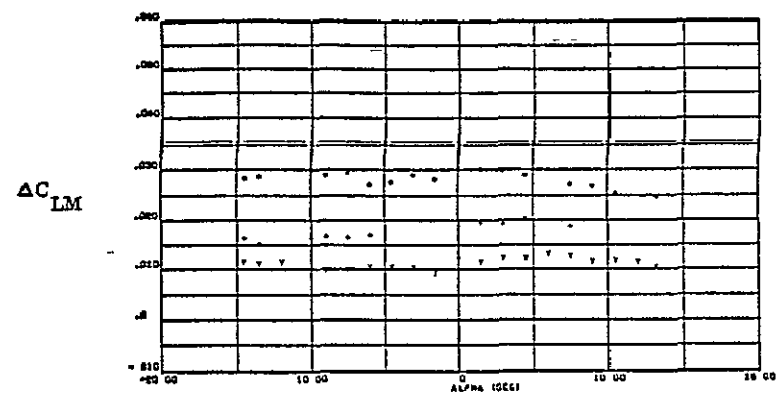
$\beta = 0^\circ$



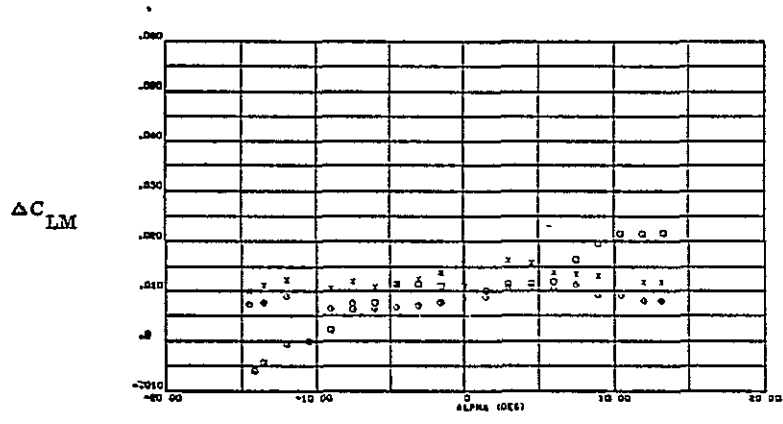
$\beta = -4^\circ$

Figure 6-23. RC40 rolling moment increments.

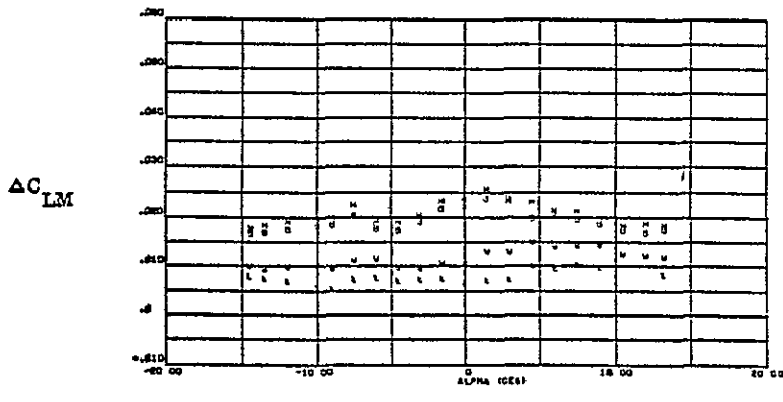
LEGEND	
SYMBOL	P_{OJ}
Y L O	770 psia
+ H X	1030
* □ □	1534



$\beta = +4^\circ$



$\beta = 0^\circ$



$\beta = -4^\circ$

Figure 6-24. RC40 pitching moment increments.

ORIGINAL PAGE IS
OF POOR QUALITY

LEGEND	
SYMBOL	P_{Oj}
Y L O	770 psia
+ X	1030
* □	1534

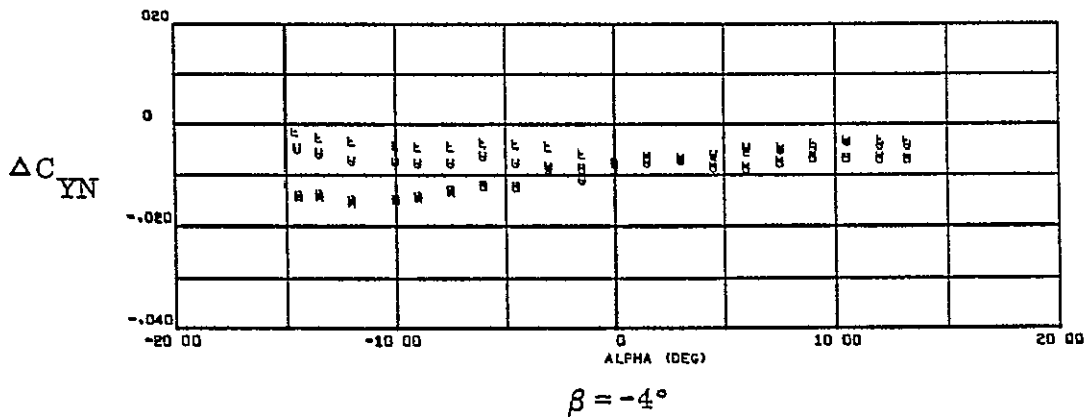
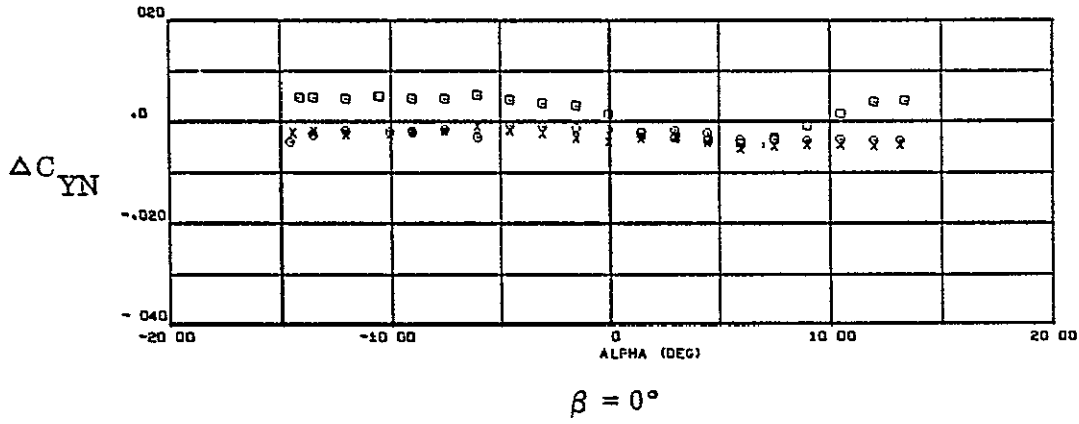
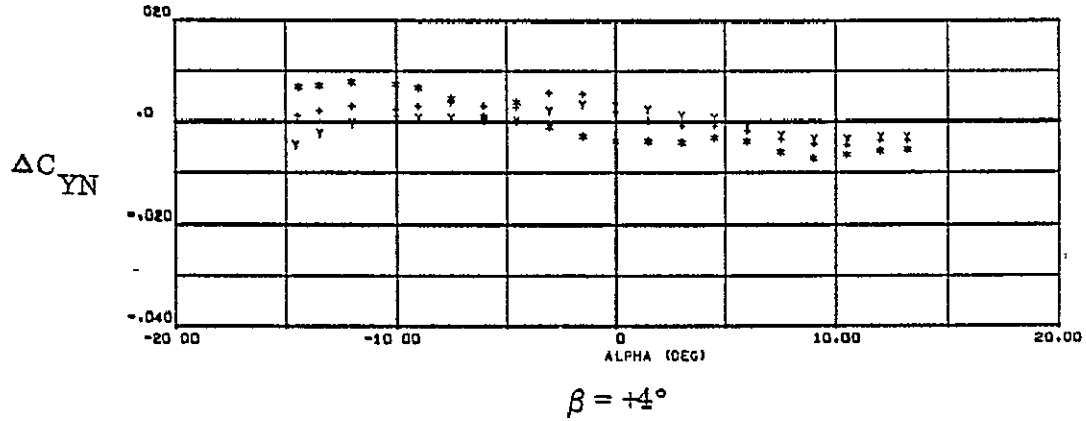


Figure 6-25. RC40 yawing moment increments.

LEGEND	
SYMBOL	P_{aj}
Y L O	770 psia
+ H X	1030
* □ □	1534

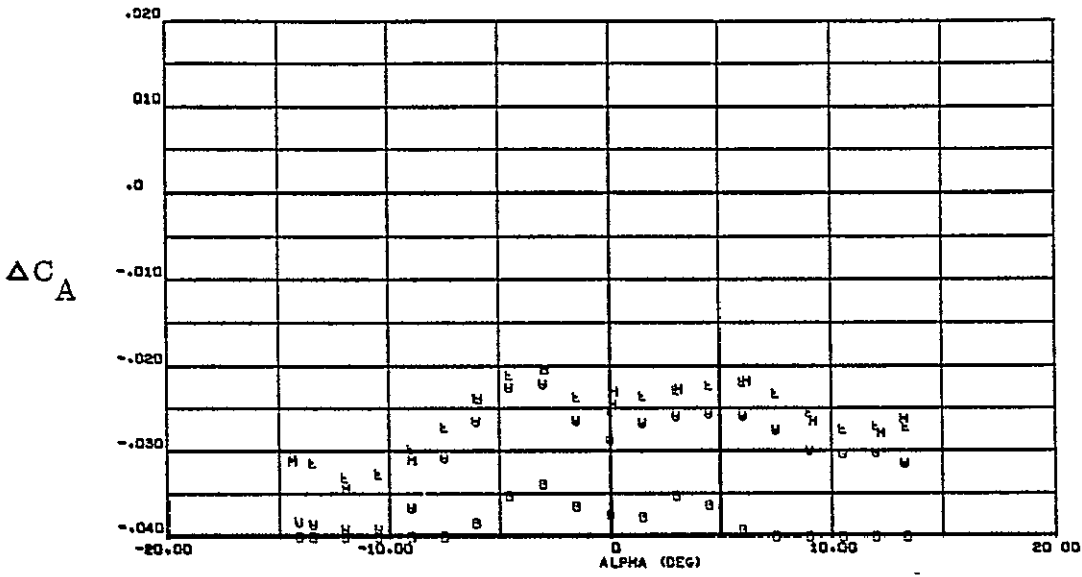


Figure 6-26. RC51 axial force increments.

LEGEND	
SYMBOL	P_{Oj}
Y L O	770 psia
+ U X	1030
* □ □	1534

ORIGINAL PAGE IS
OF POOR QUALITY

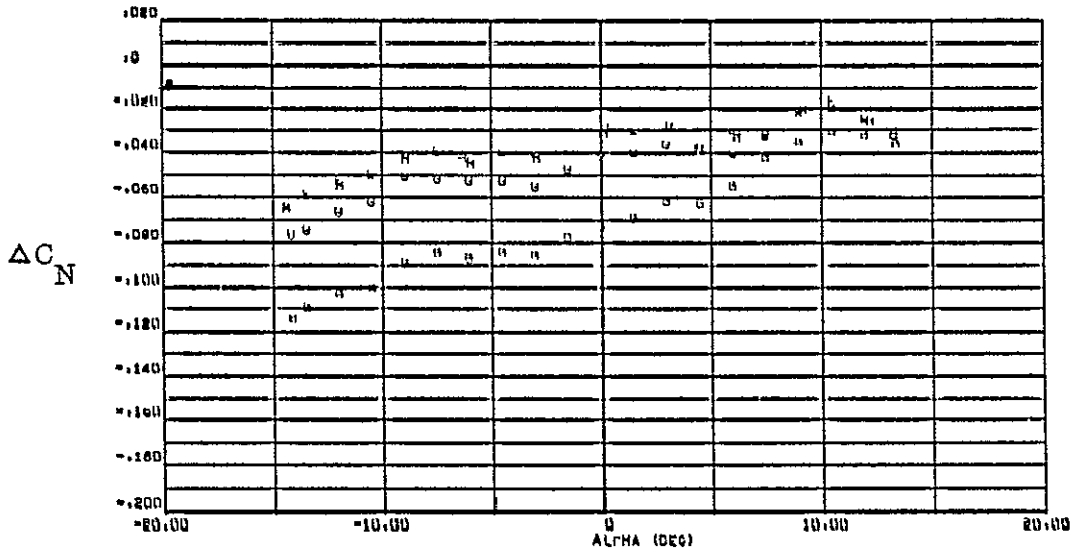


Figure 6-27. RC51 normal force increments.

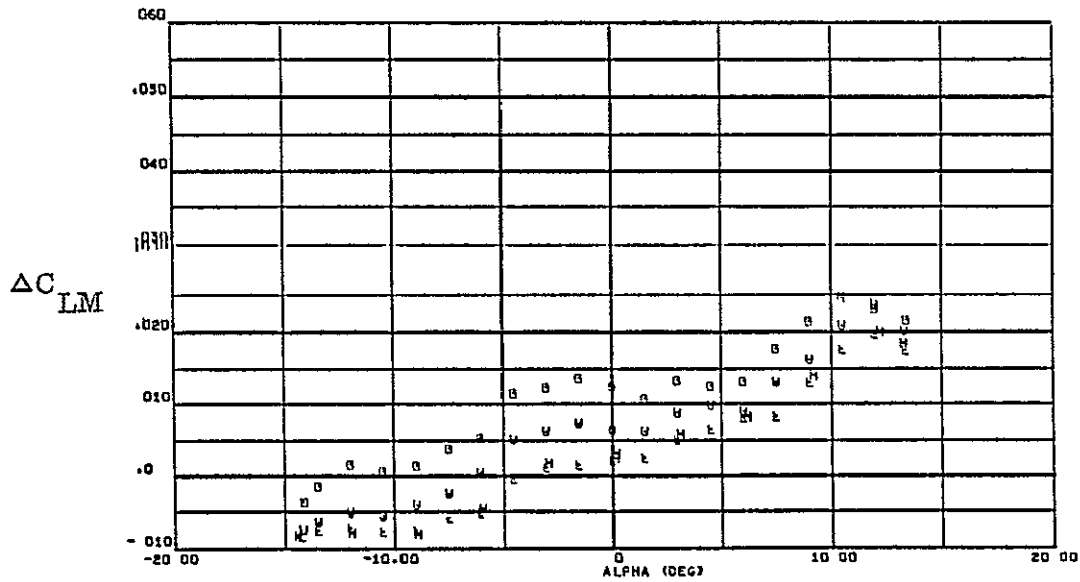


Figure 6-28. RC51 pitching moment increments.

LEGEND	
SYMBOL	P_{01}
Y L O	770 psia
+ H X	1030
* □ □	1534

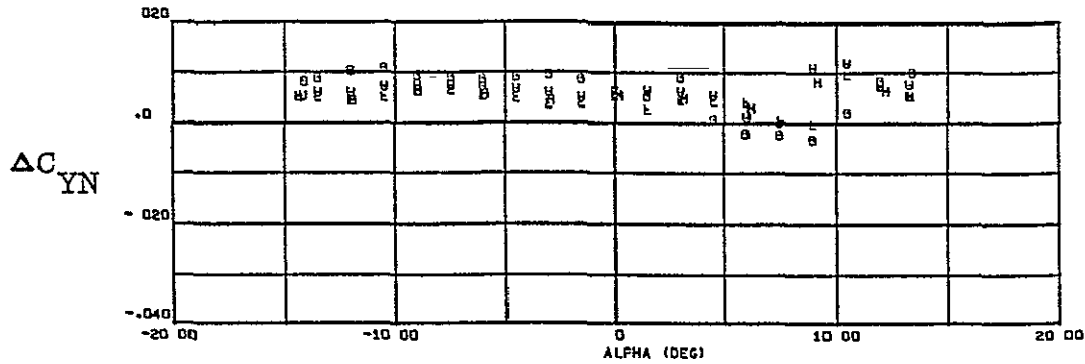


Figure 6-29. RC51 yawing moment increments.

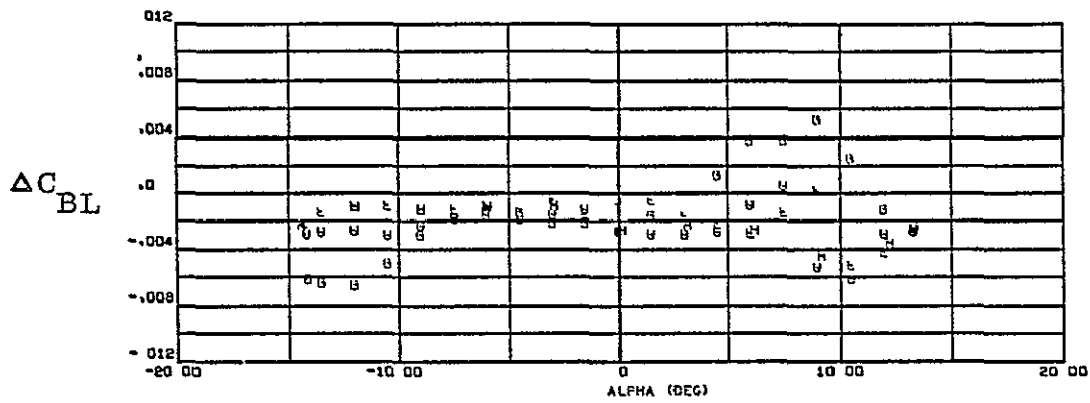


Figure 6-30. RC51 rolling moment increments.

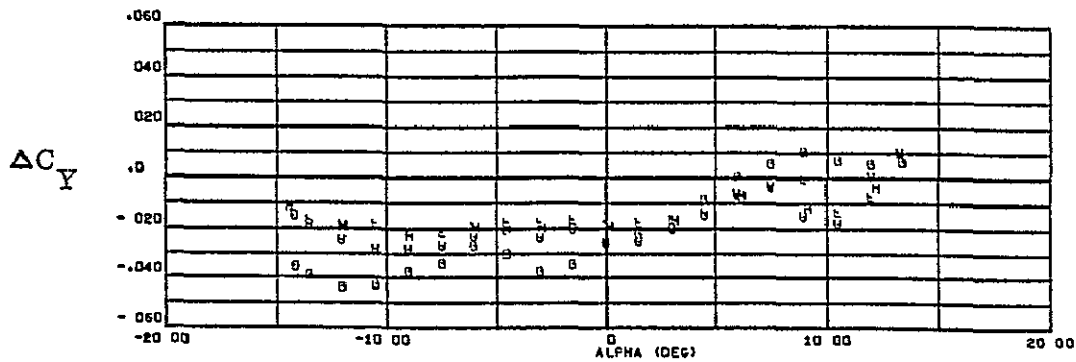


Figure 6-31. RC51 side force increments.

ORIGINAL PAGE IS
OF POOR QUALITY

LEGEND	
SYMBOL	P_{0j}
Y L O	770 psia
+ B X	1030
+ □ □	1534

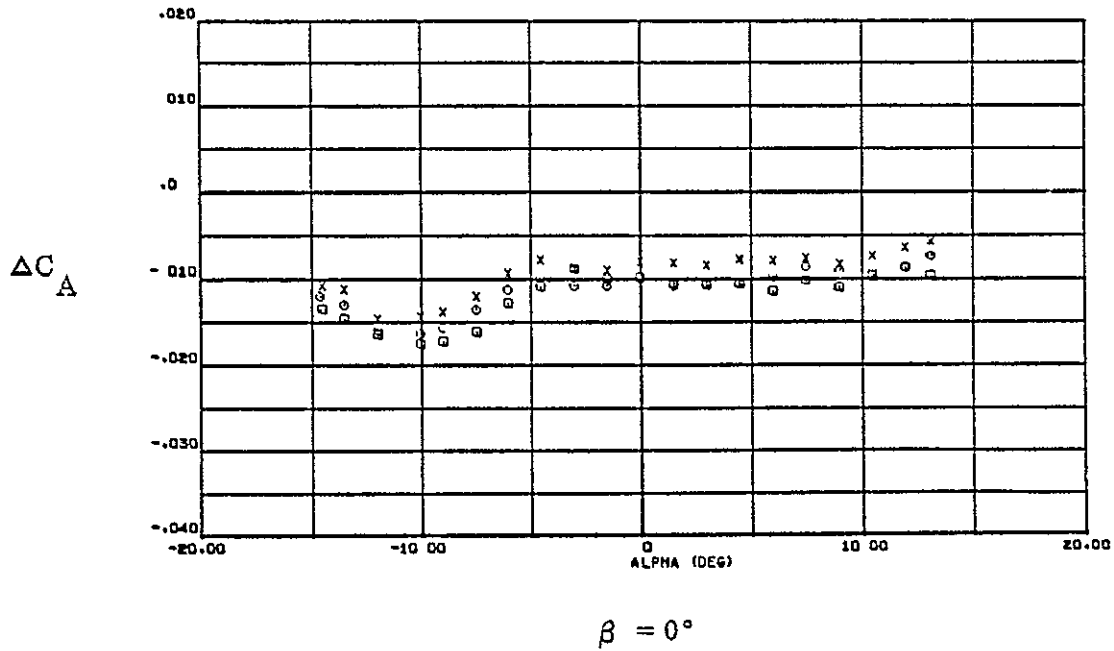
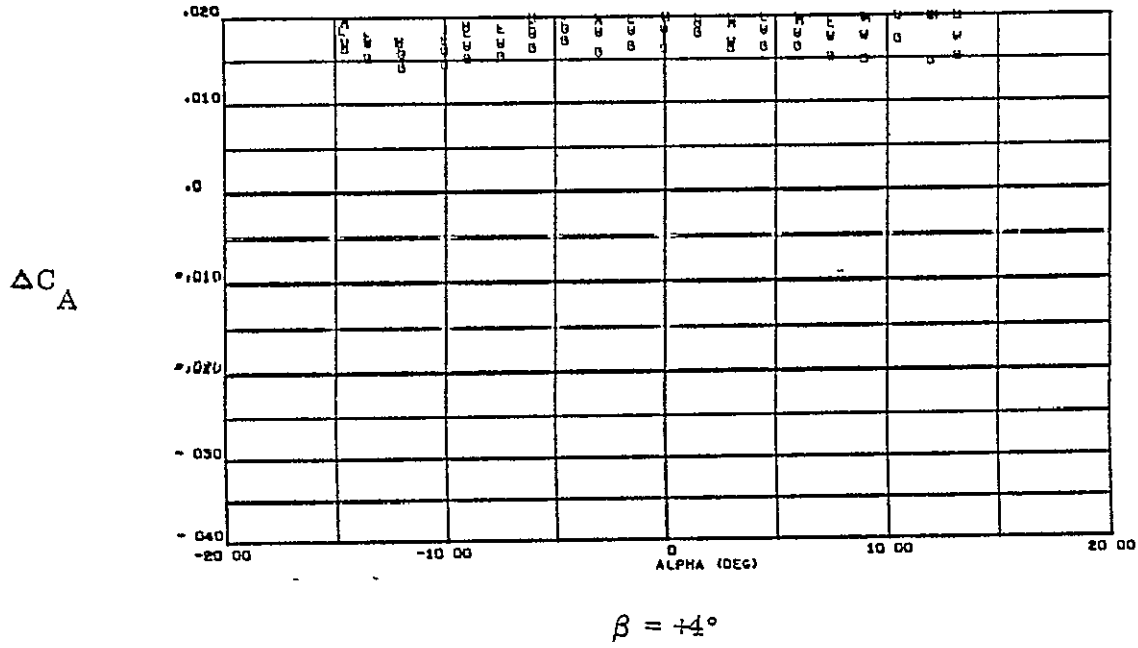
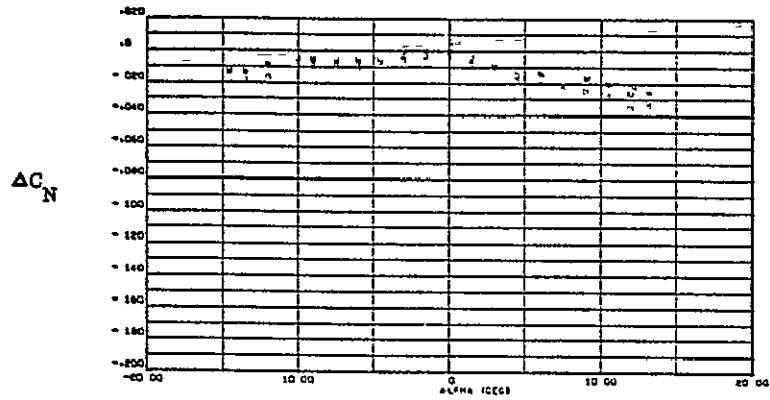
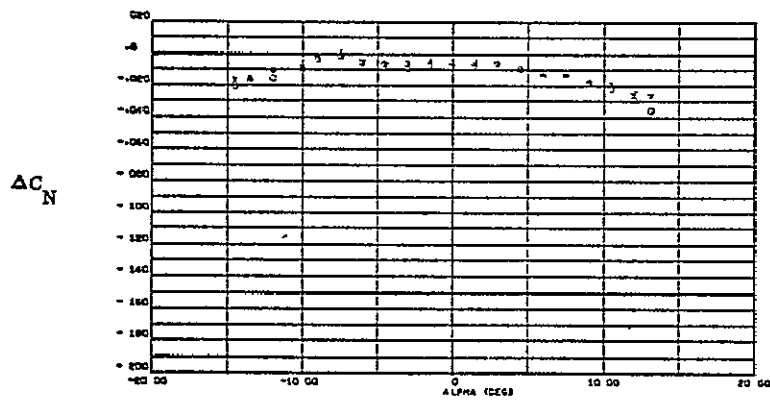


Figure 6-32. RC78 axial force increments.

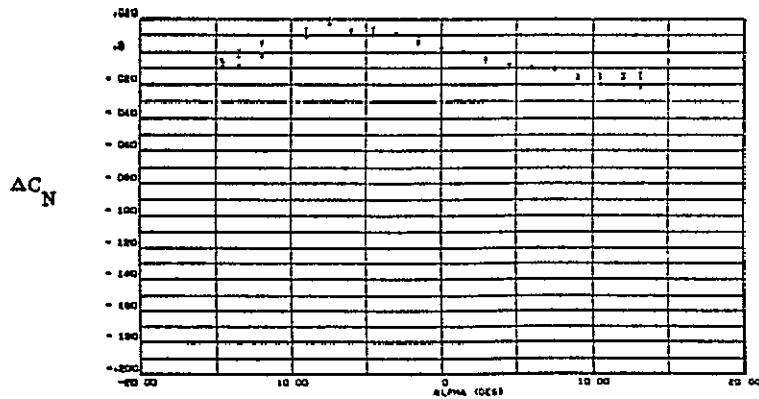
LEGEND	
SYMBOL	ρ_{0j}
Y t O	770 psia
+ u X	1030
* □ □	1534



$\beta = +4^\circ$



$\beta = 0^\circ$

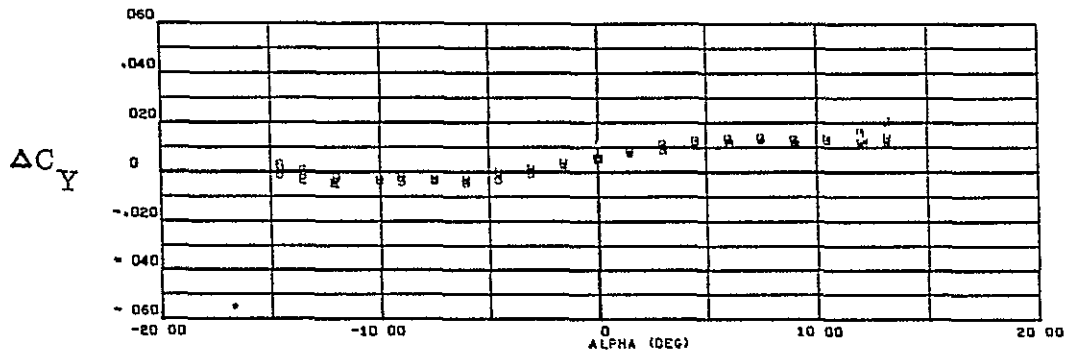


$\beta = -4^\circ$

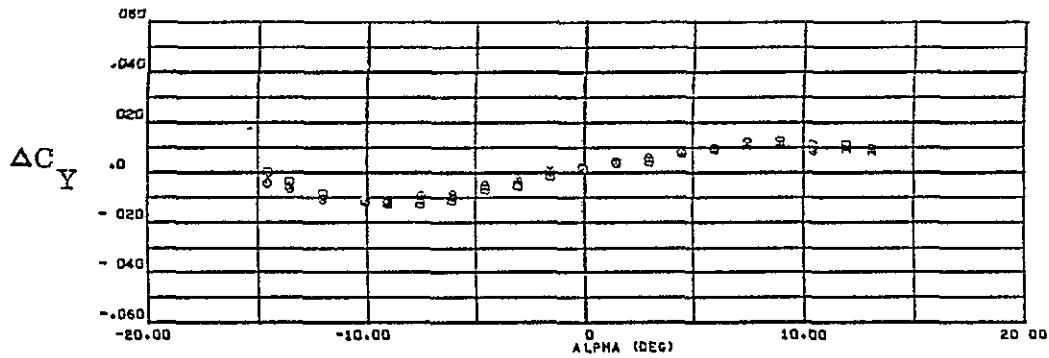
Figure 6-33. RC78 normal force increments.

ORIGINAL PAGE IS
OF POOR QUALITY

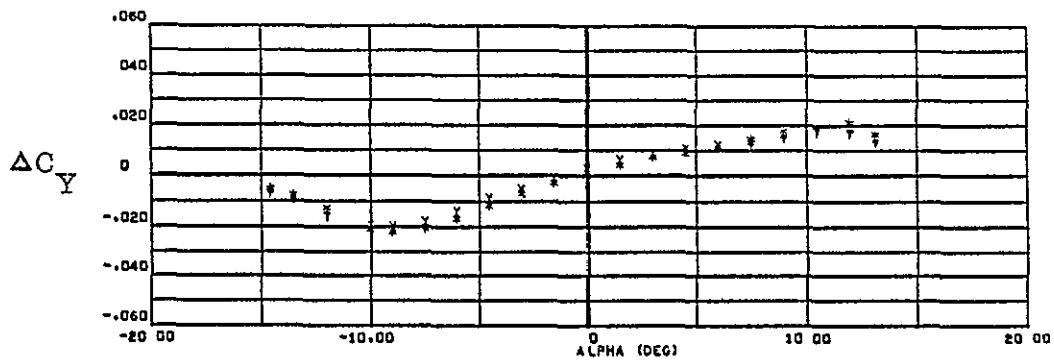
LEGEND	
SYMBOL	P_{0j}
Y L O	770 psia
+ X	1030
+ □	1534



$$\beta = +4^\circ$$



$$\beta = 0^\circ$$



$$\beta = -4^\circ$$

Figure 6-34. RC78 side force increments.

LEGEND	
SYMBOL	P_{01}
Y L O	770 psia
△ □ X	1030
* □ □	1534

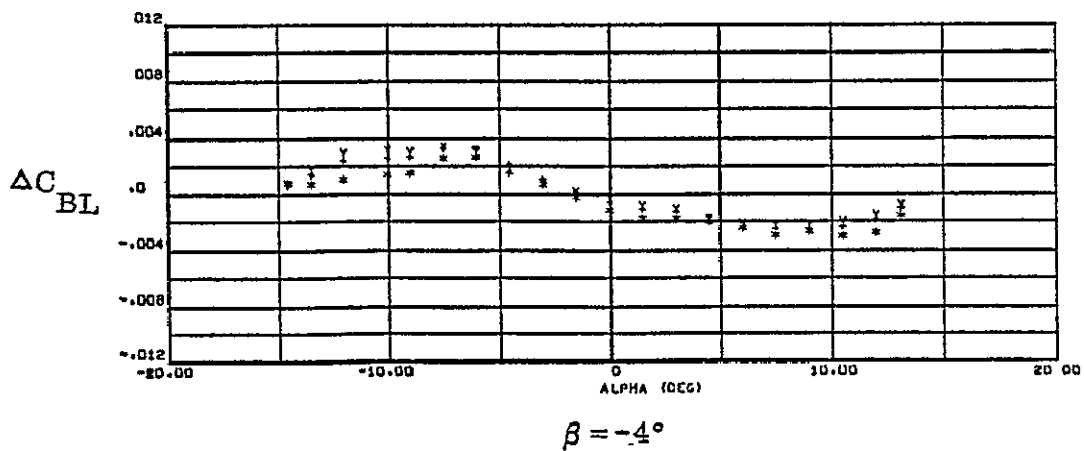
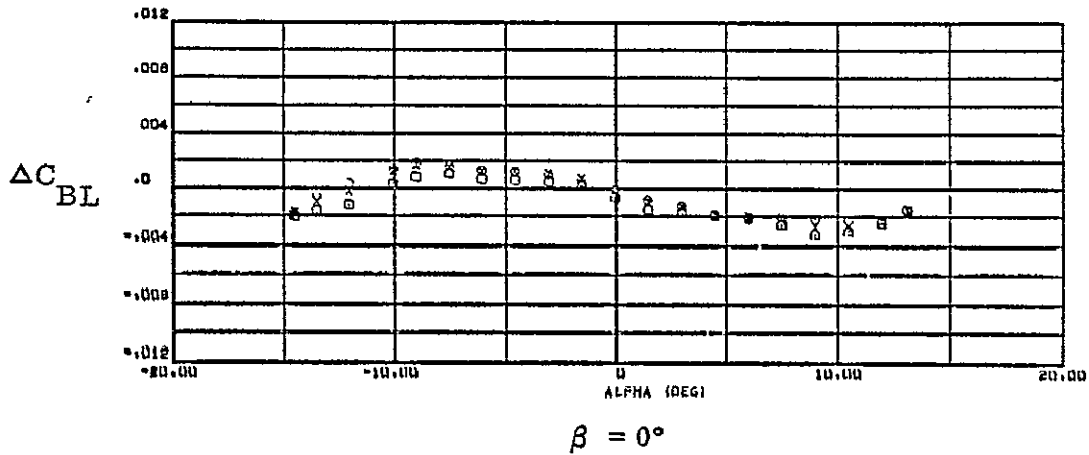
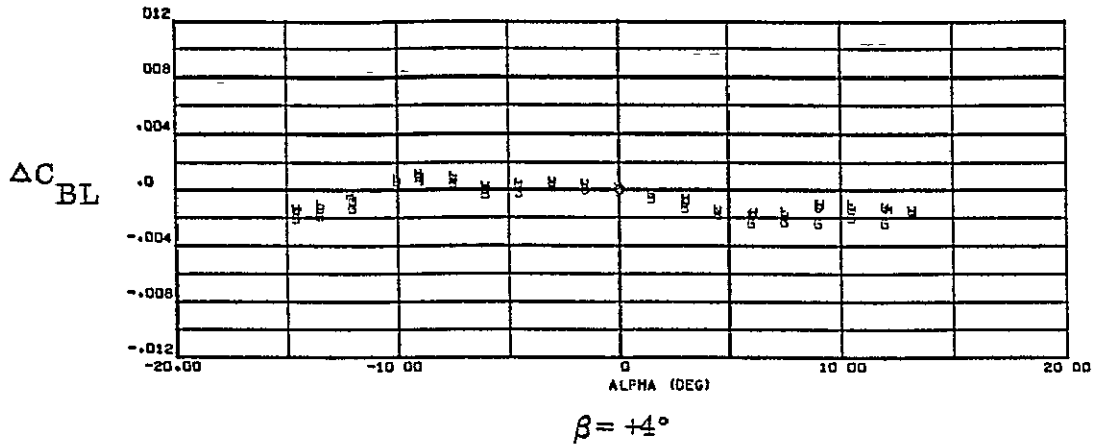
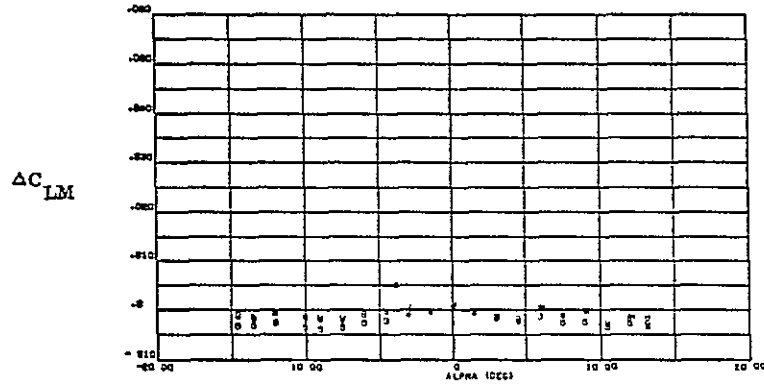


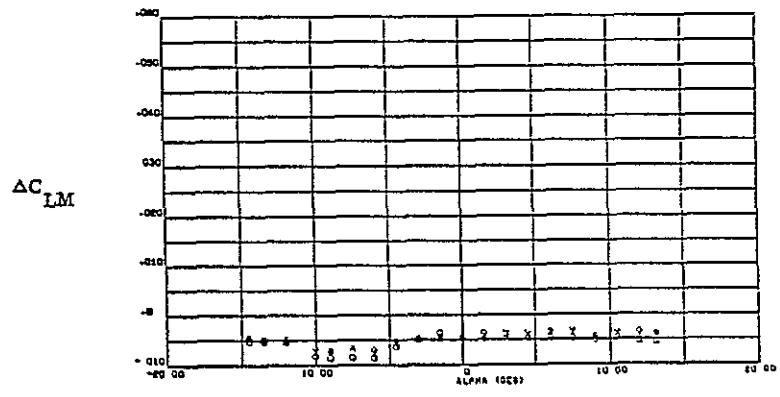
Figure 6-35. RC78 rolling moment increments.

LEGEND	
SYMBOL	P_{OJ}
Y L O	770 psia
+ @ X	1030
* □ □	1534

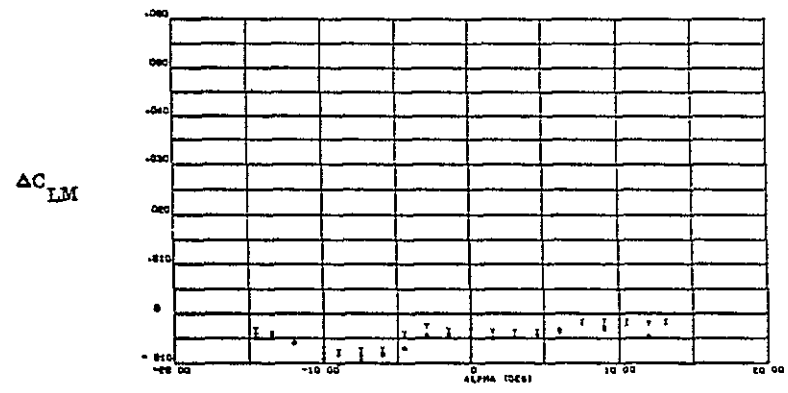


$\beta = +4^\circ$

ORIGINAL PAGE IS
OF POOR QUALITY



$\beta = 0^\circ$



$\beta = -4^\circ$

Figure 6-36. RC78 pitching moment increments.

LEGEND	
SYMBOL	P_{0j}
Y \square O	770 psia
+ \times X	1030
* \square \square	1534

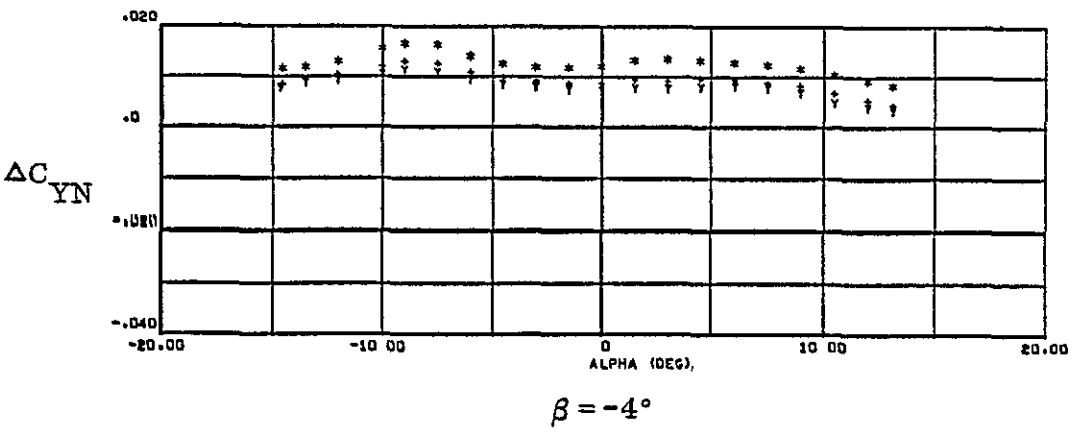
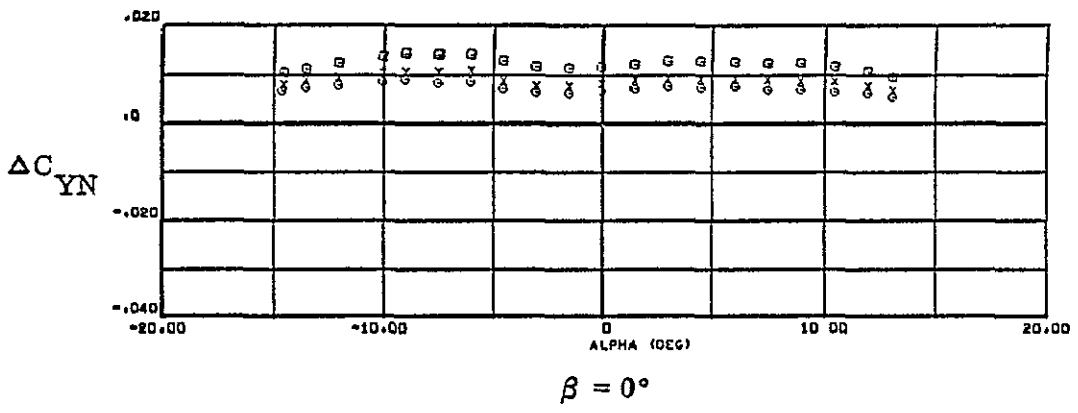
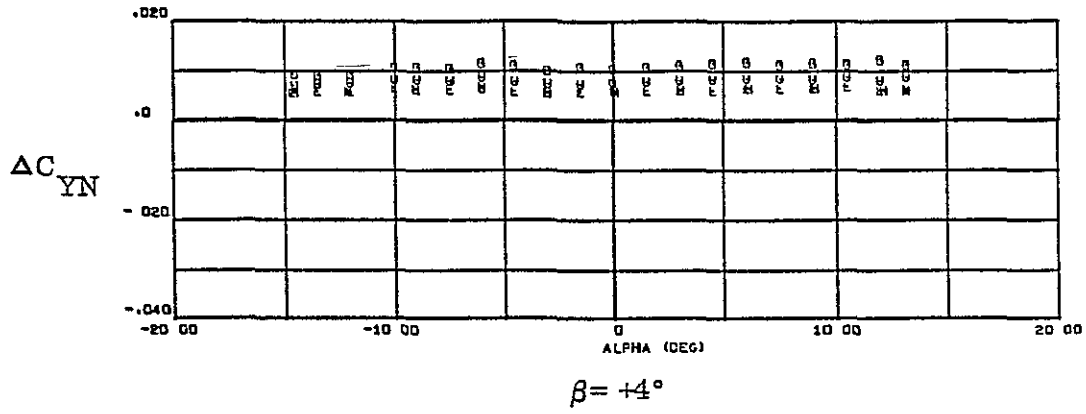


Figure 6-37. RC78 yawing moment increments.

ORIGINAL PAGE IS
OF POOR QUALITY

LEGEND	
SYMBOL	P ₀₁
Y	770 psia
+	1030
*	1534

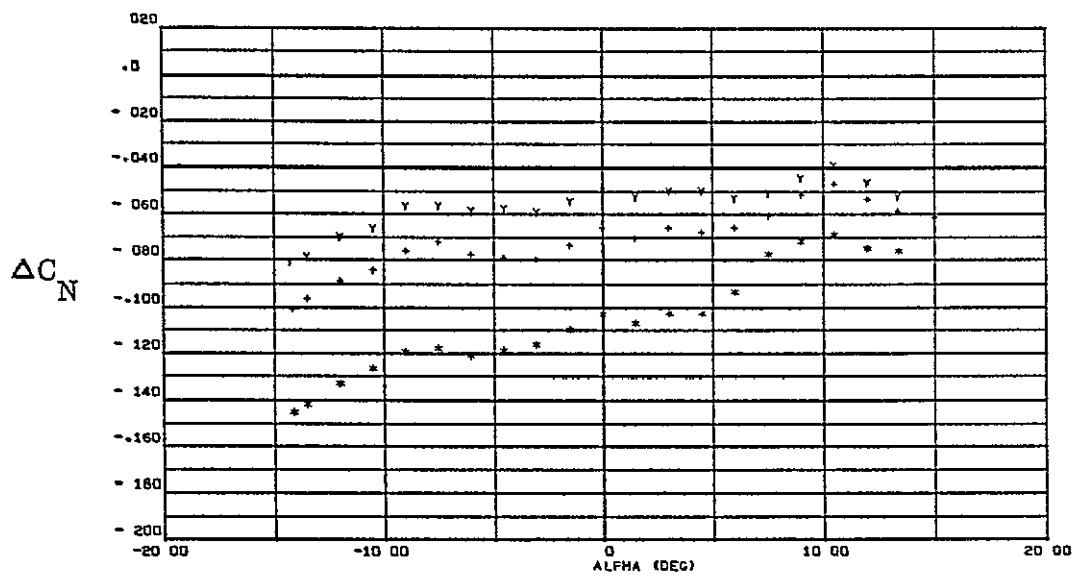


Figure 6-38. RC82 normal force increments.

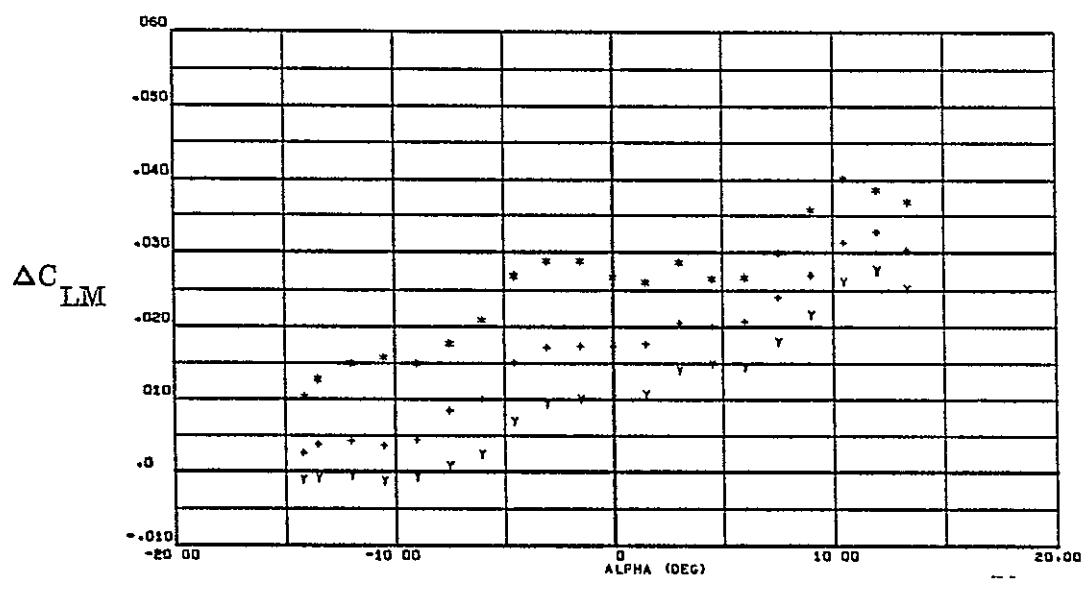


Figure 6-39. RC82 pitching moment increments.

LEGEND	
SYMBOL	P_{Oj}
Y L O	770 psia
+ U X	1030
* □ □	1534

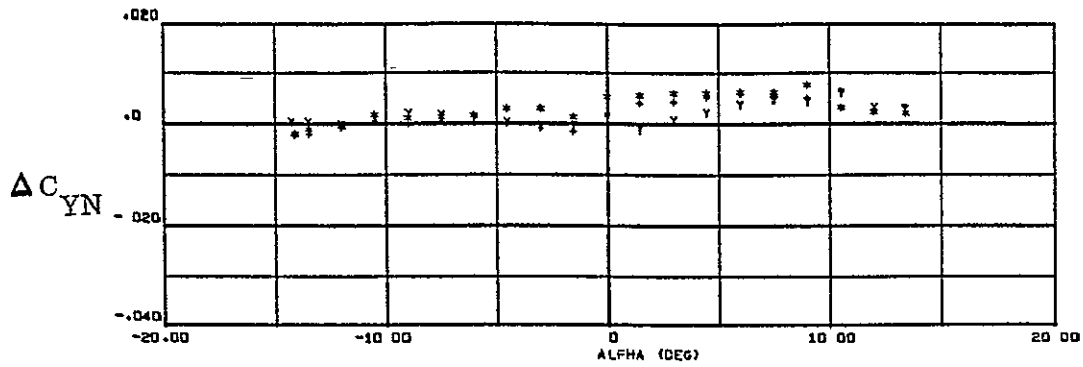


Figure 6-40. RC82 yaw moment increments.

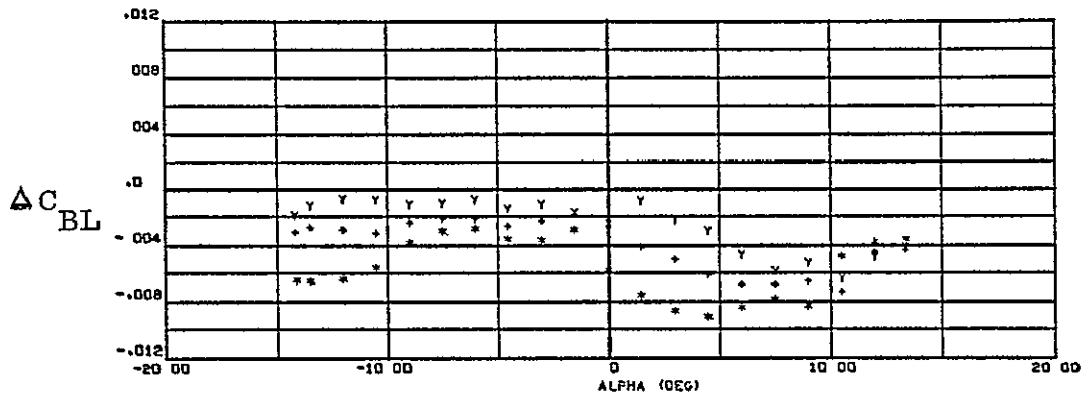


Figure 6-41. RC82 rolling moment increments.

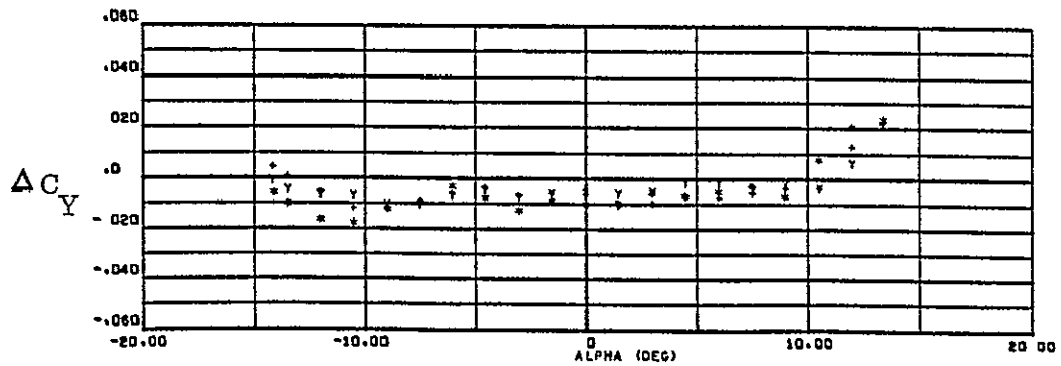


Figure 6-42. RC82 side force increments.

ORIGINAL PAGE IS
OF POOR QUALITY

LEGEND	
SYMBOL	$\frac{p_{0j}}{p_{01}}$
Y L O	770 psia
+ x X	1030
* □ □	1534

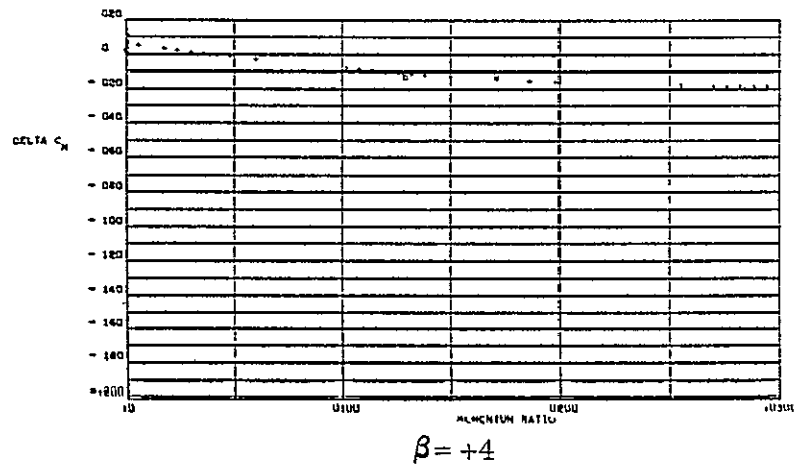
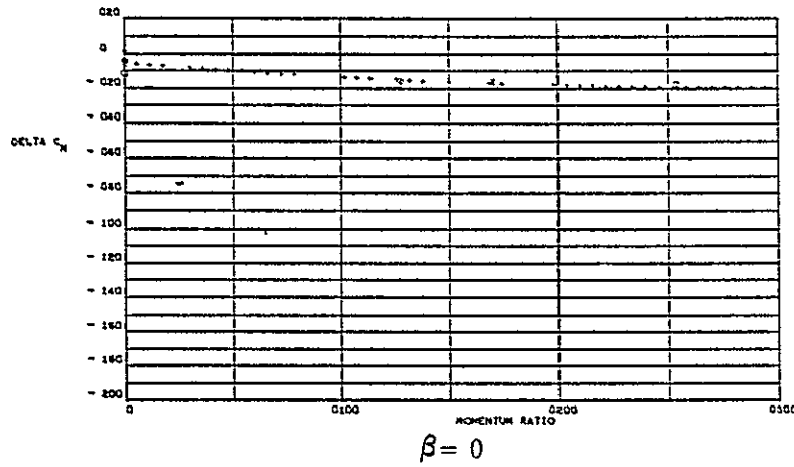
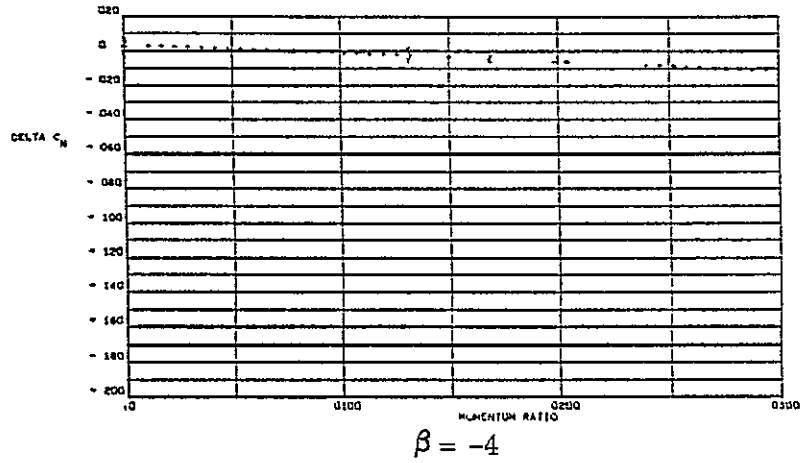


Figure 6-43. RC78 normal force correlation at $\alpha = -14^\circ$

LEGEND	
SYMBOL	P_{0j}
Y L O	770 psia
+ B X	1030
* □ □	1534

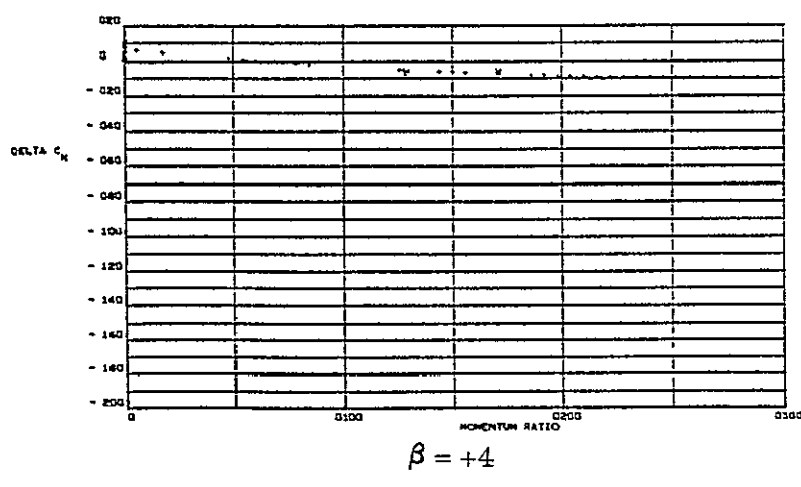
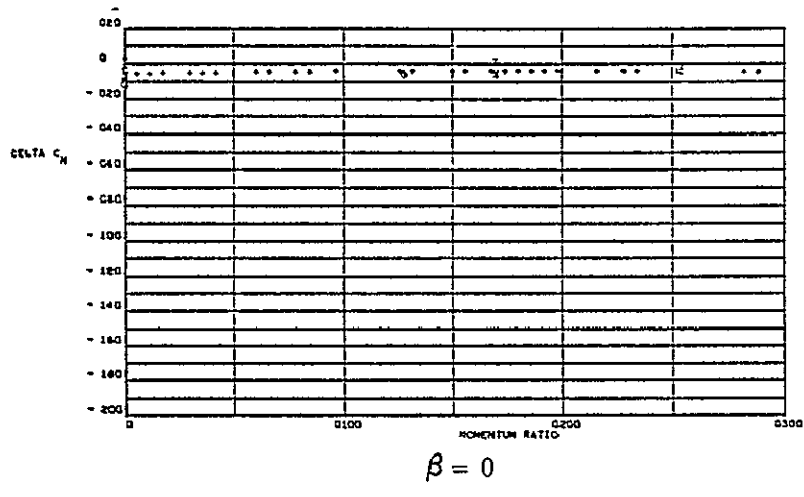
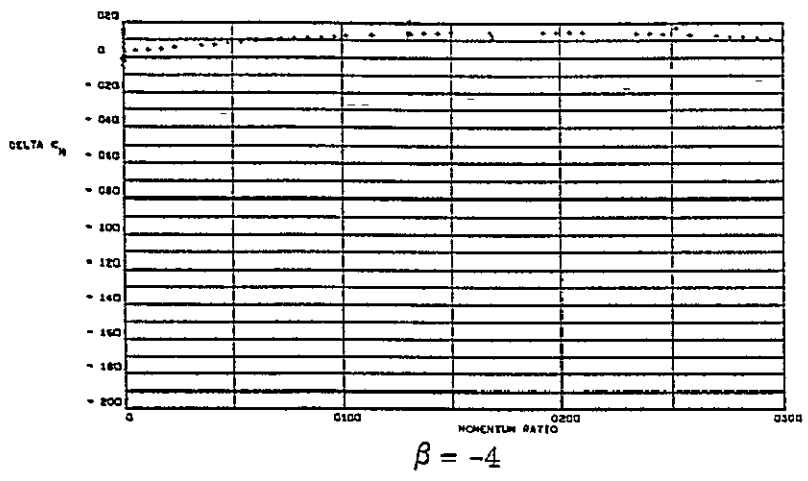
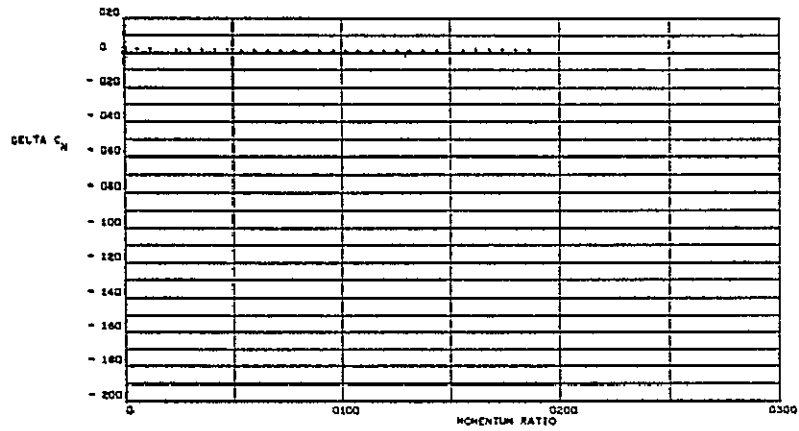
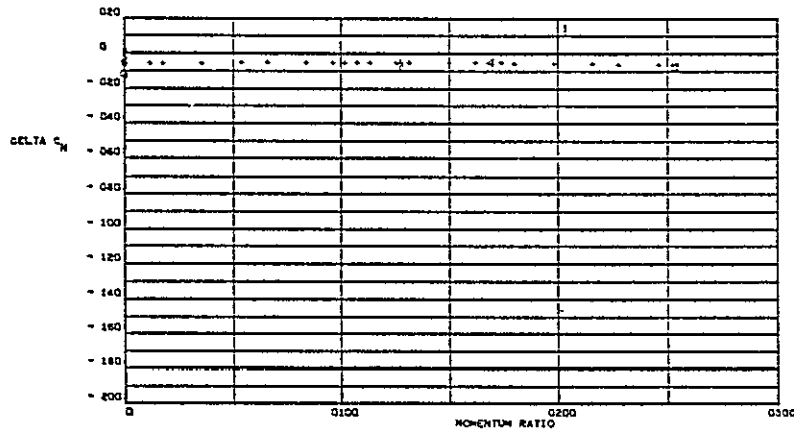


Figure 6-44. RC78 normal force correlation at $\alpha = -6^\circ$.

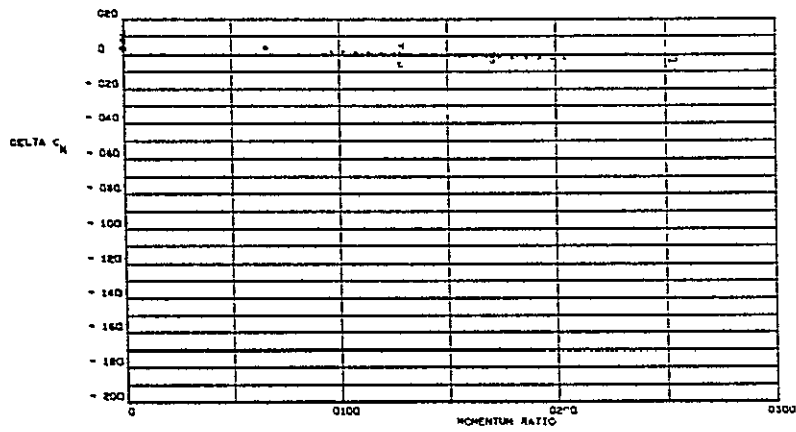
ORIGINAL PAGE IS
OF POOR QUALITY



$$\beta = -4$$



$$\beta = 0$$



$$\beta = +4$$

Figure 6-45. RC78 normal force correlation at $\alpha = 0^\circ$.

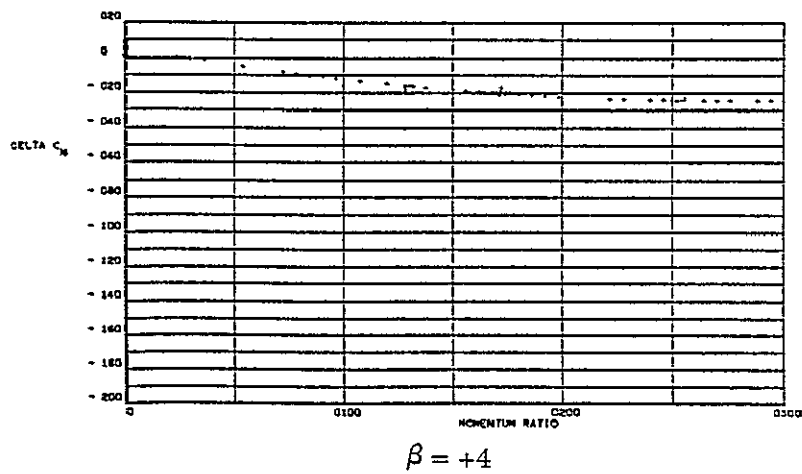
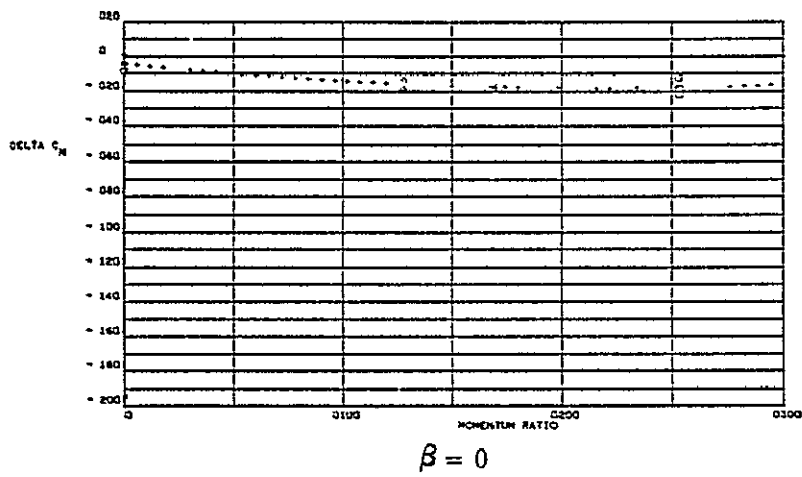
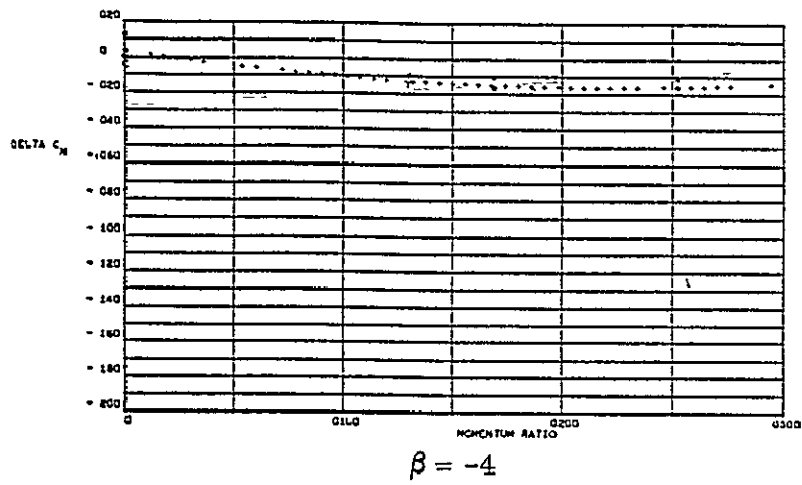


Figure 6-46. RC78 normal force correlation at $\alpha = +9^\circ$.

ORIGINAL PAGE IS
OF POOR QUALITY

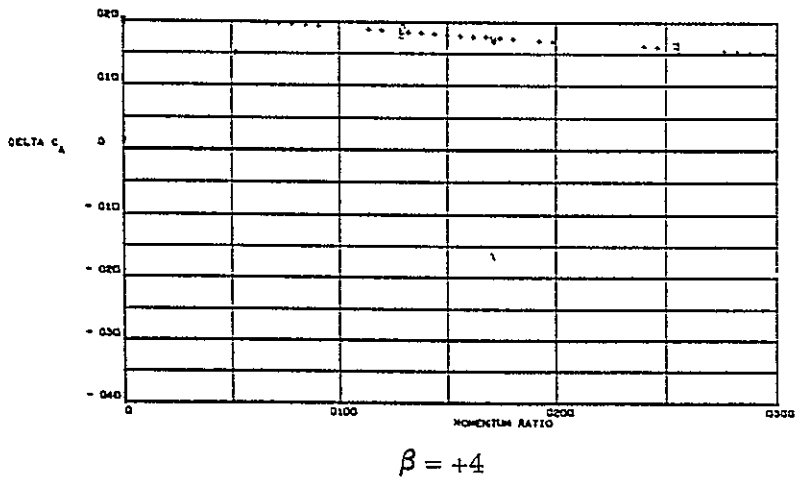
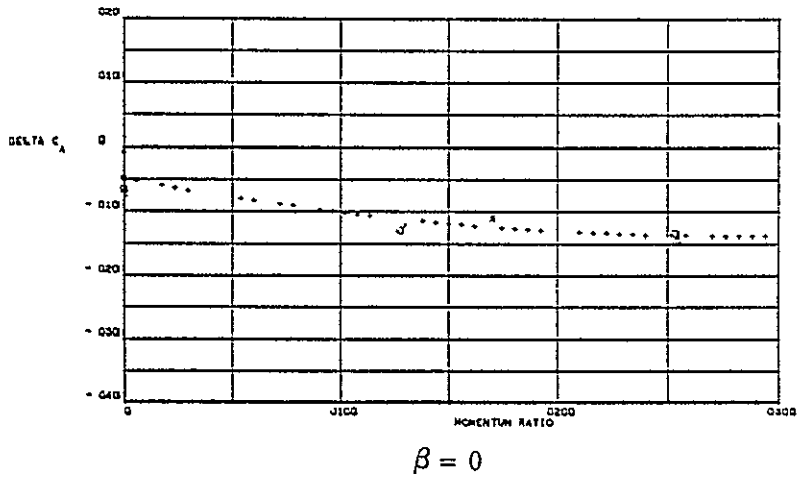
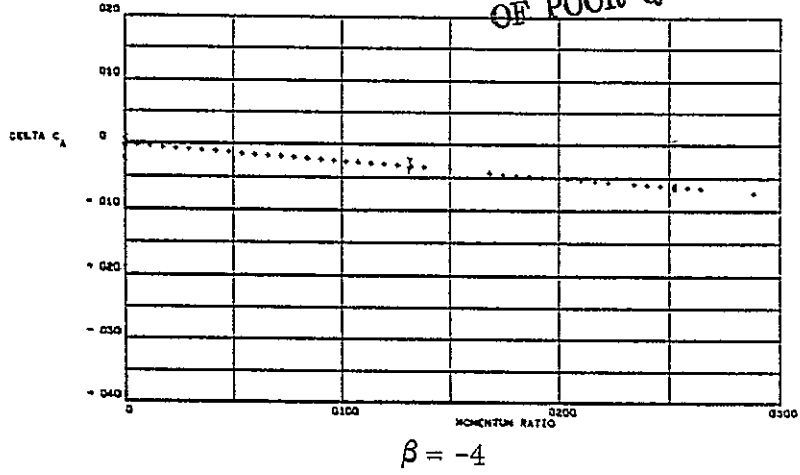


Figure 6-47. RC78 axial force correlation at $\alpha = -14^\circ$.

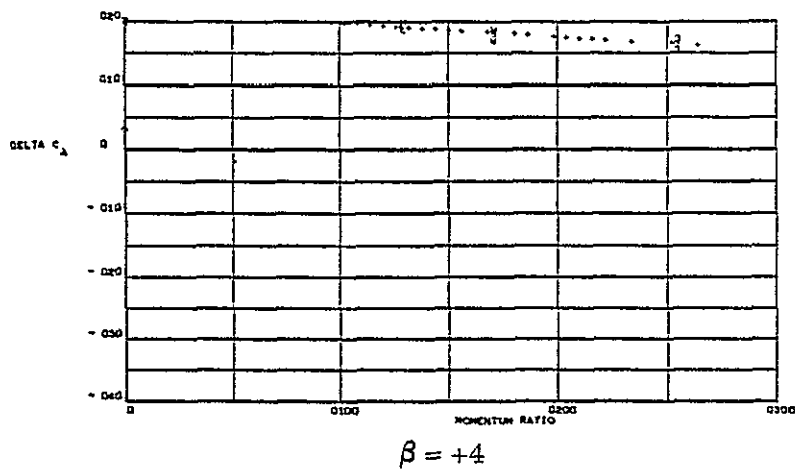
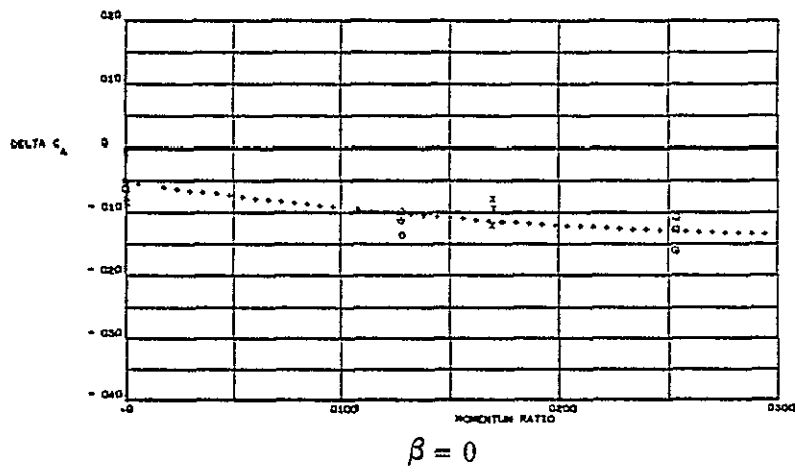
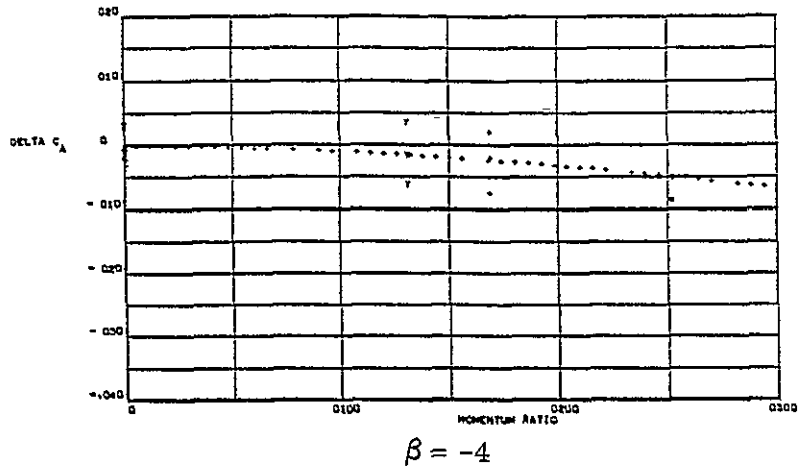


Figure 6-48. RC78 axial force correlation at $\alpha = -6^\circ$.

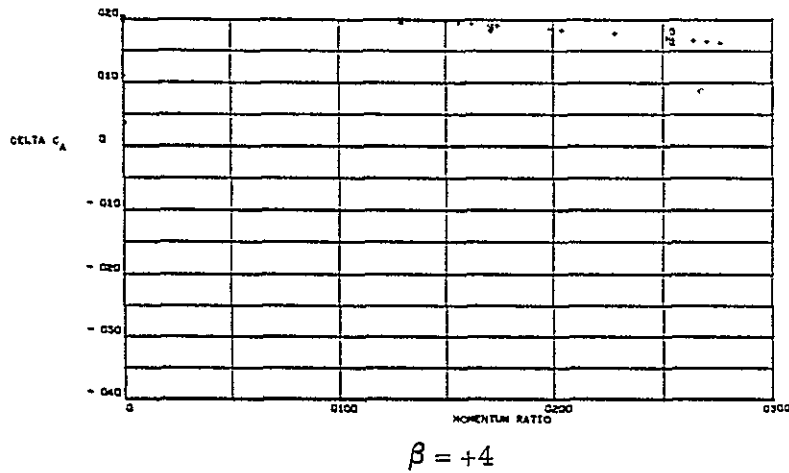
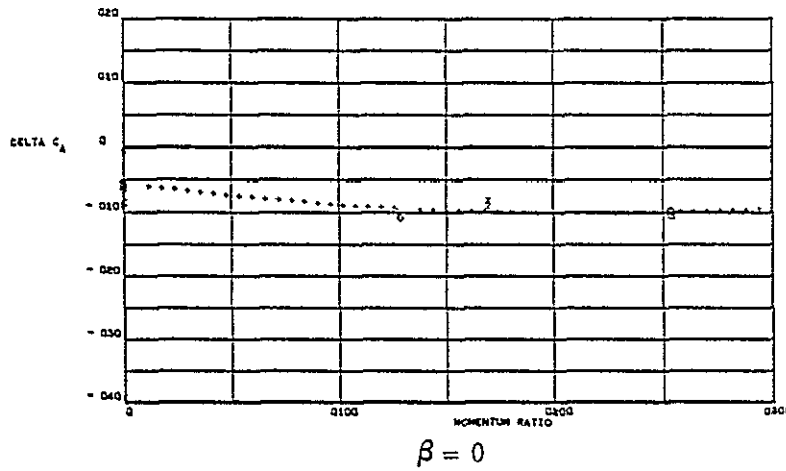
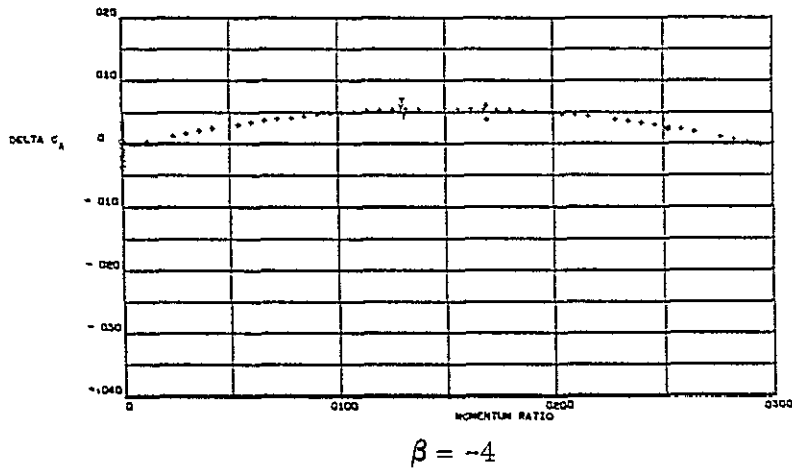


Figure 6-49. RC78 axial force correlation at $\alpha = 0^\circ$.

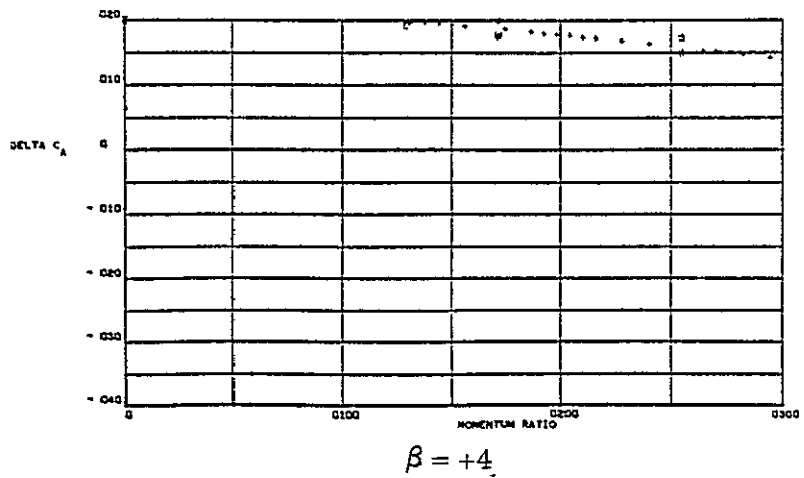
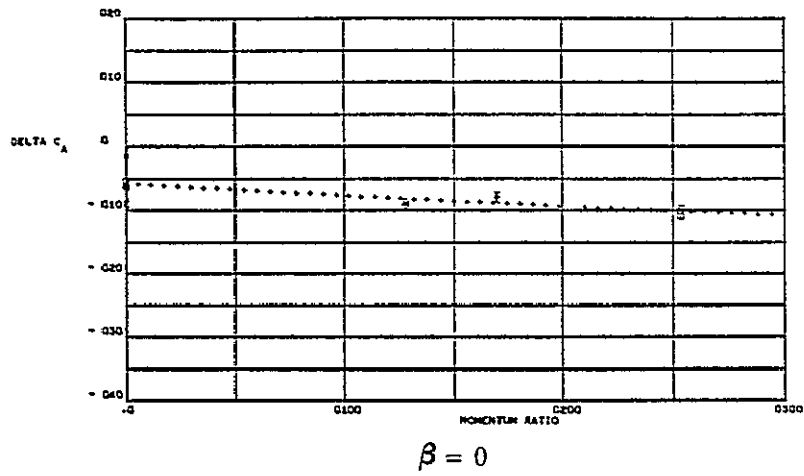
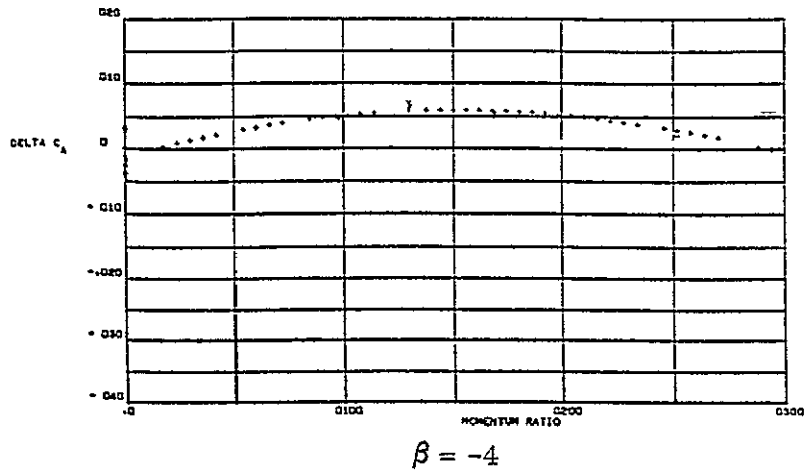


Figure 6-50. RC78 axial force correlation at $\alpha = +9^\circ$.

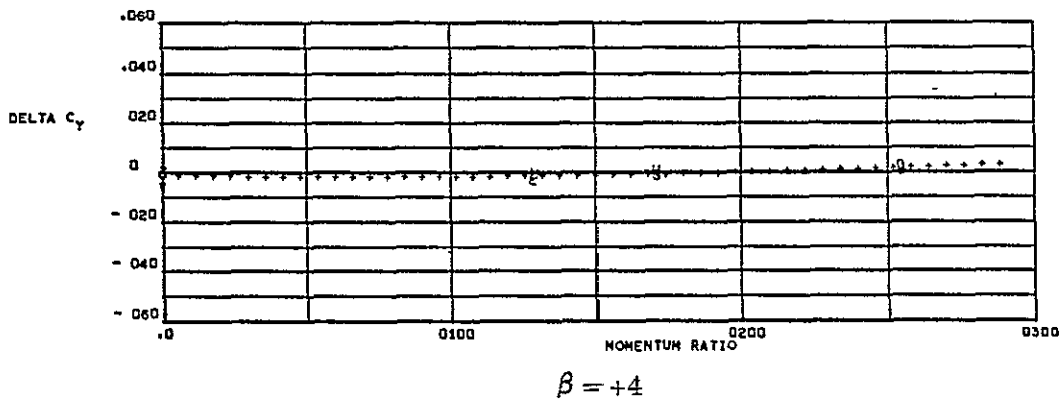
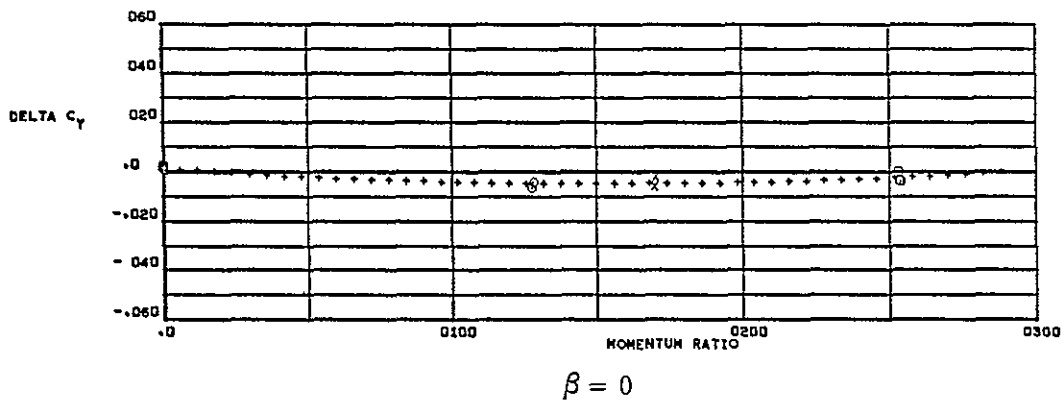
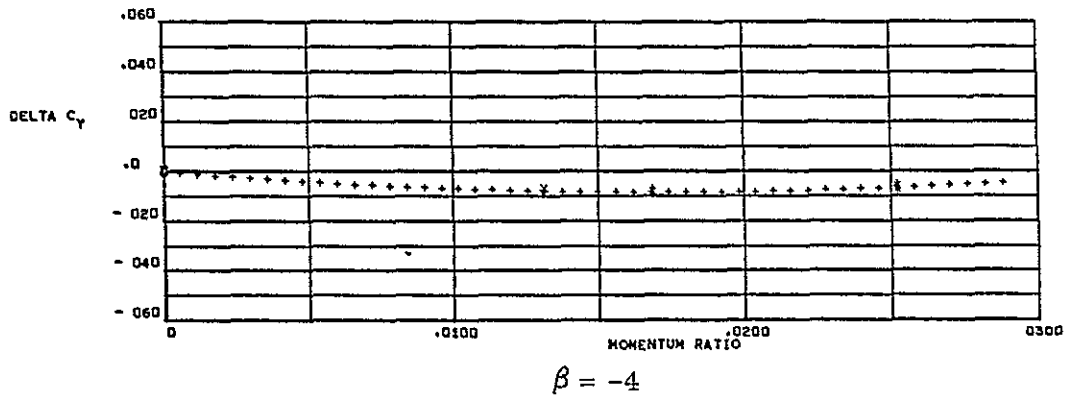


Figure 6-51. RC78 side force correlation at $\alpha = -14^\circ$.

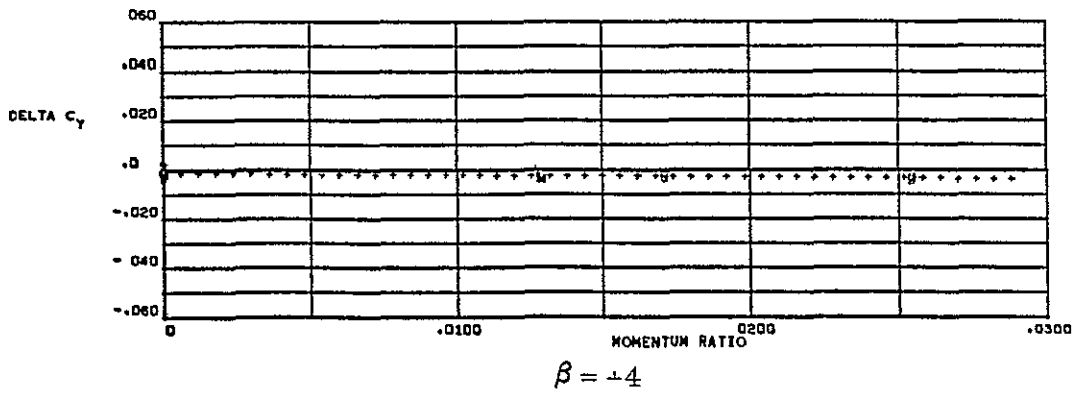
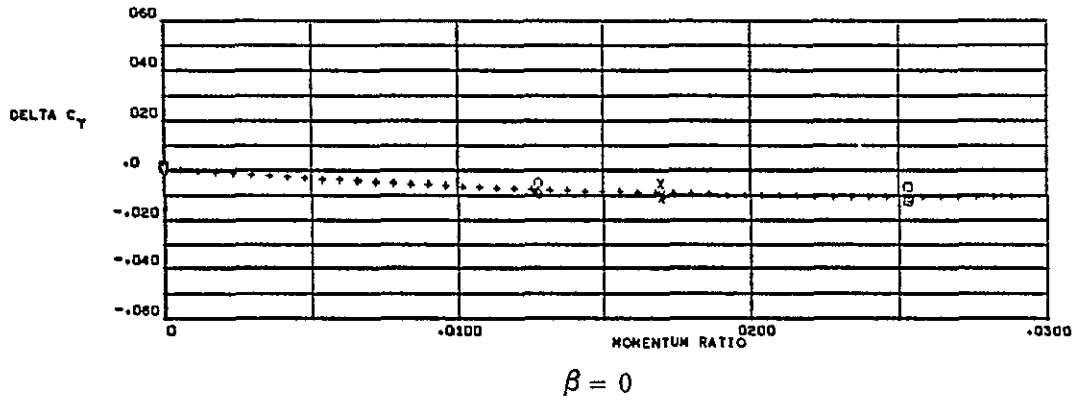
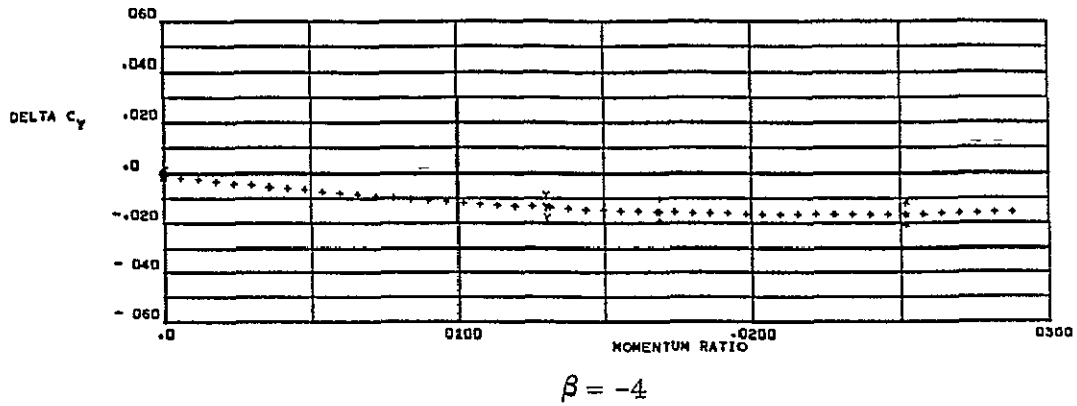
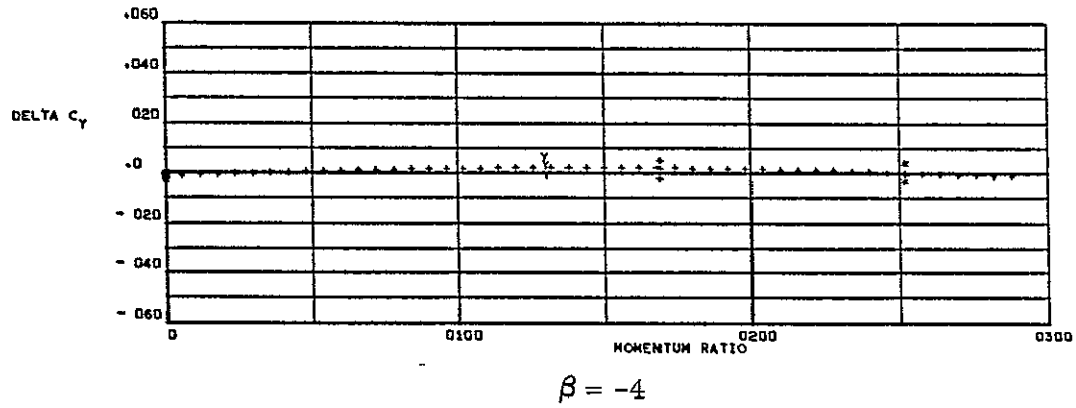


Figure 6-52. RC78 side force correlation at $\alpha = -6^\circ$.



ORIGINAL PAGE IS
OF POOR QUALITY

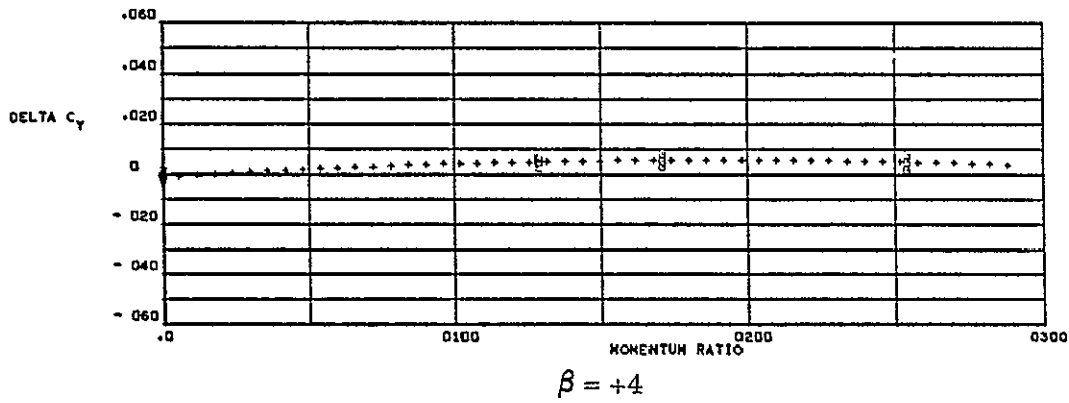
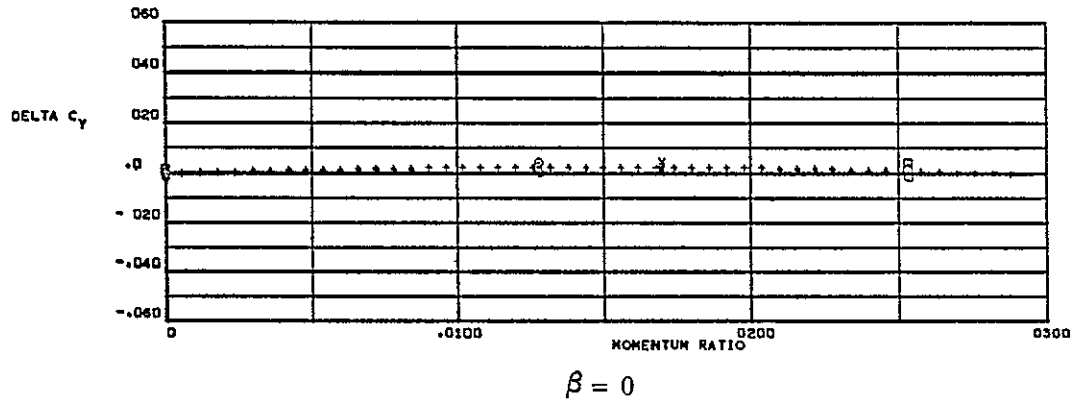


Figure 6-53. RC78 side force correlation at $\alpha = 0^\circ$.

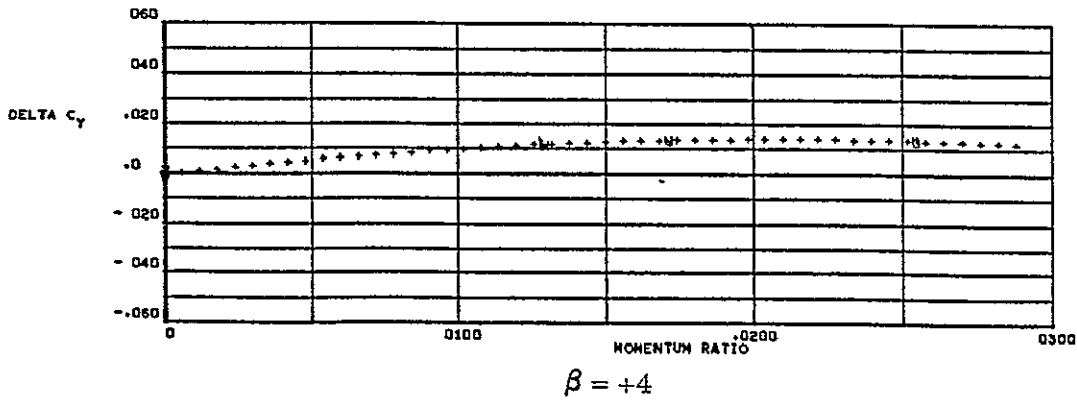
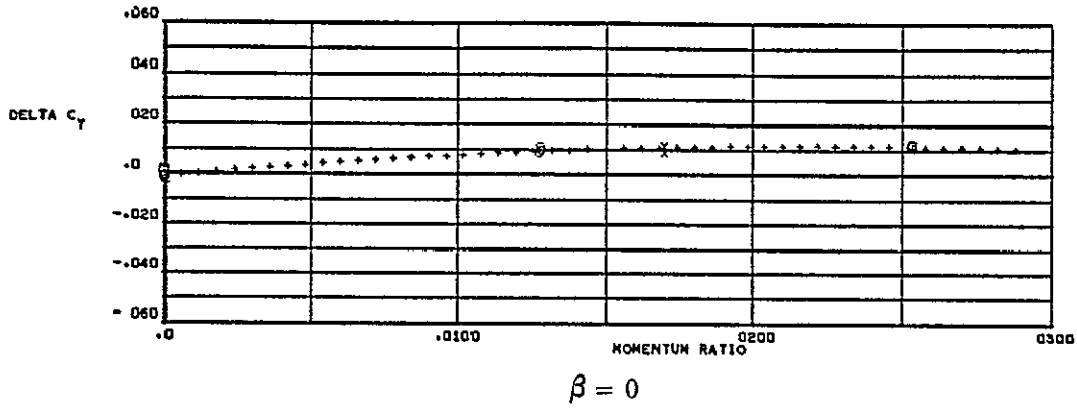
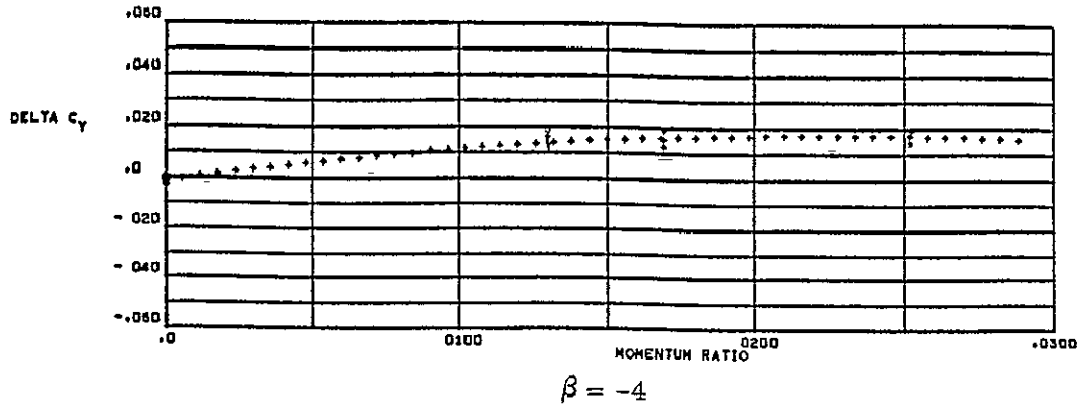
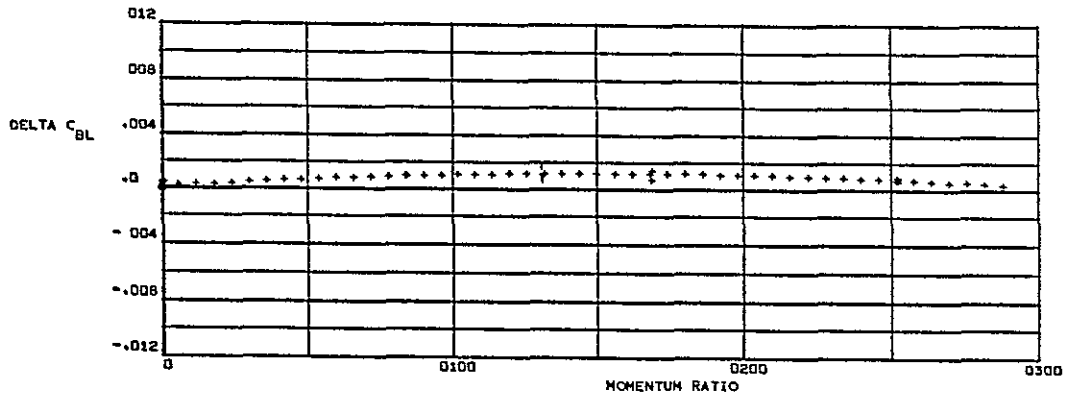
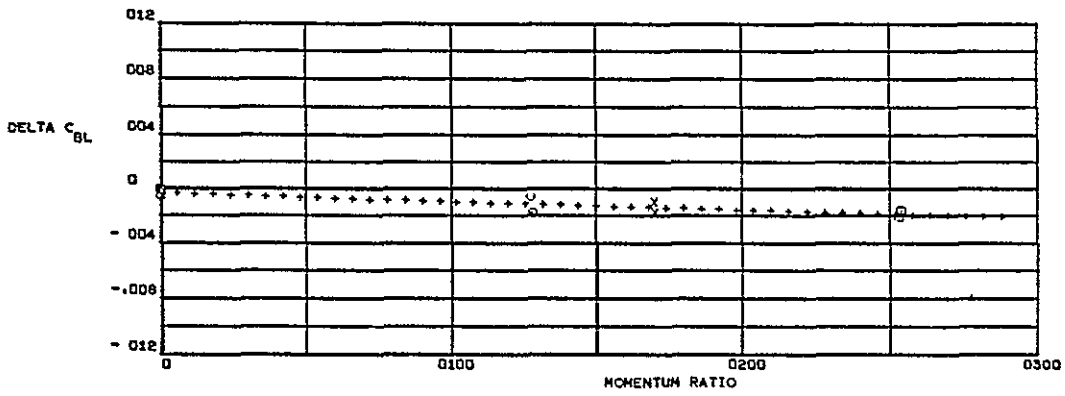


Figure 6-54. RC78 side force correlation at $\alpha = +9^\circ$.

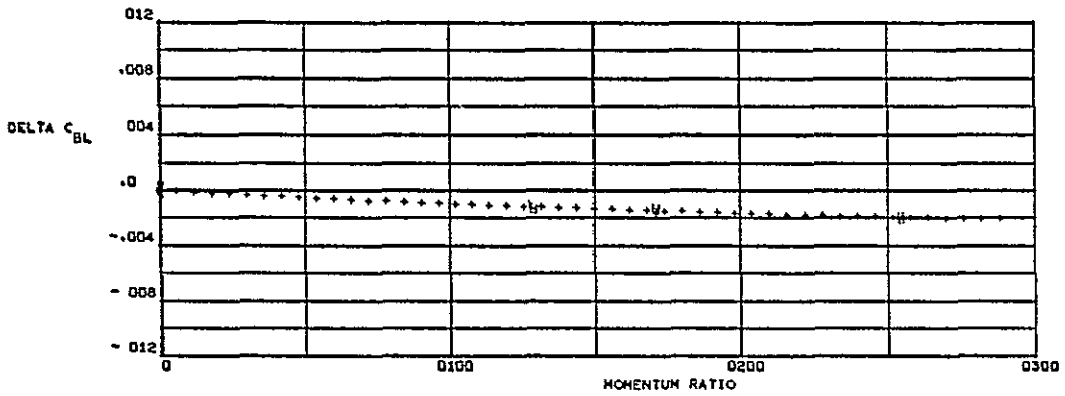


$$\beta = -4$$

ORIGINAL PAGE IS
OF POOR QUALITY

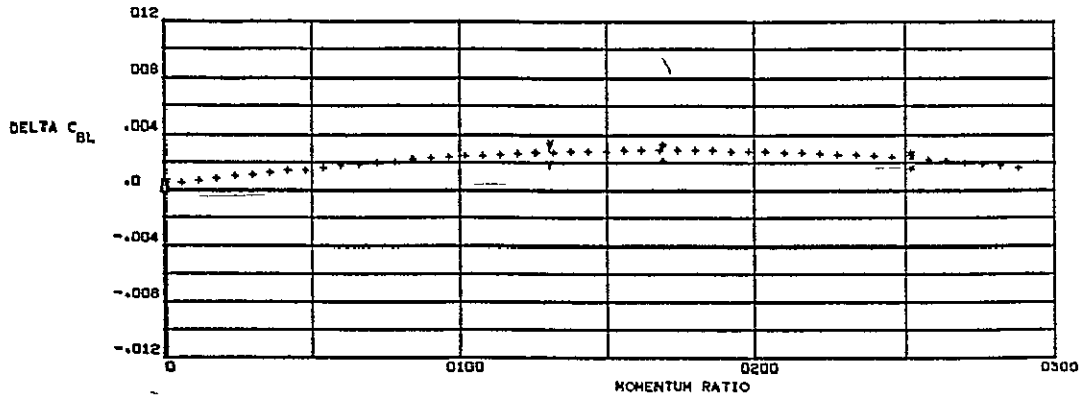


$$\beta = 0$$

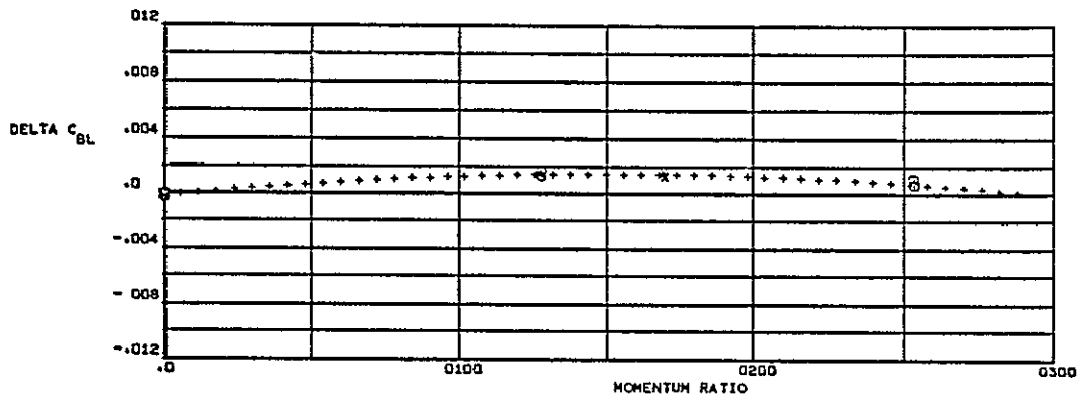


$$\beta = +4$$

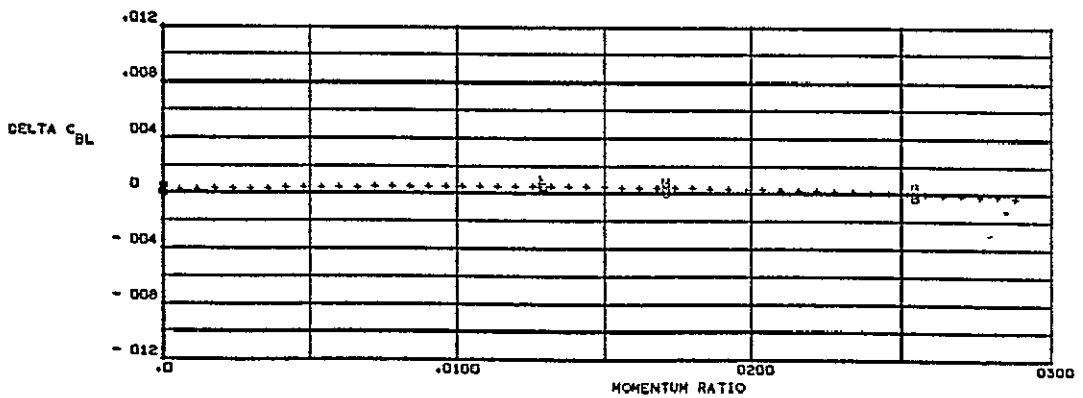
Figure 6-55. RC78 rolling moment correlation at -14° .



$$\beta = -4$$

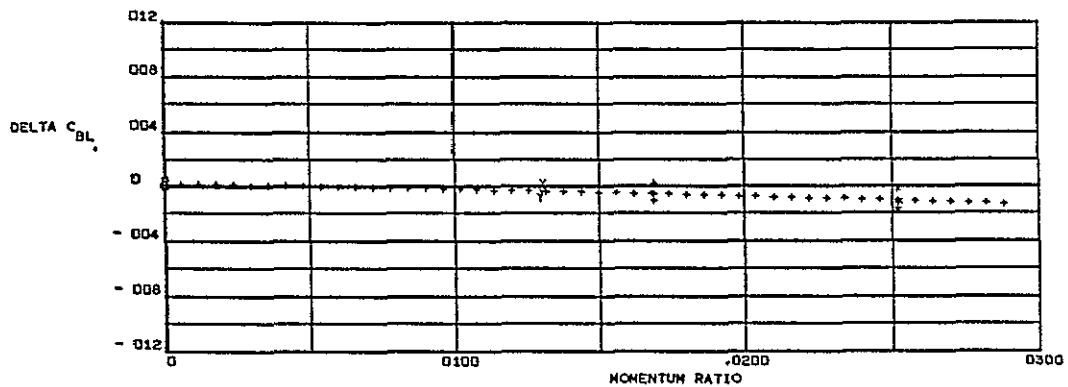


$$\beta = 0$$

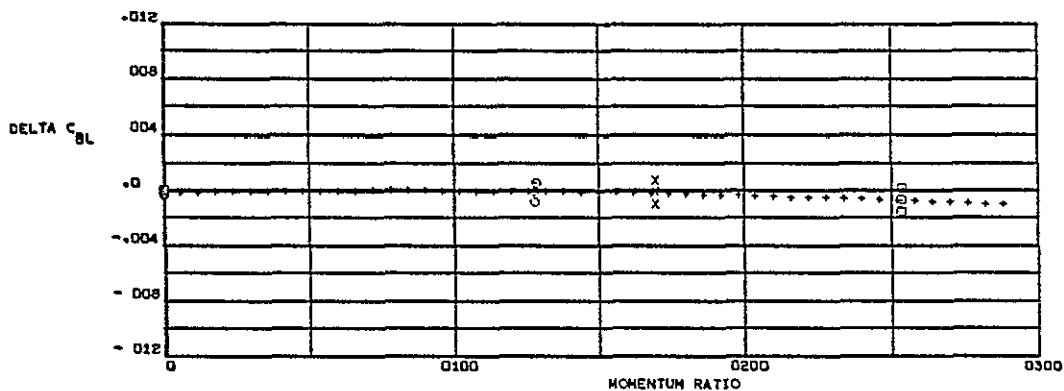


$$\beta = +4$$

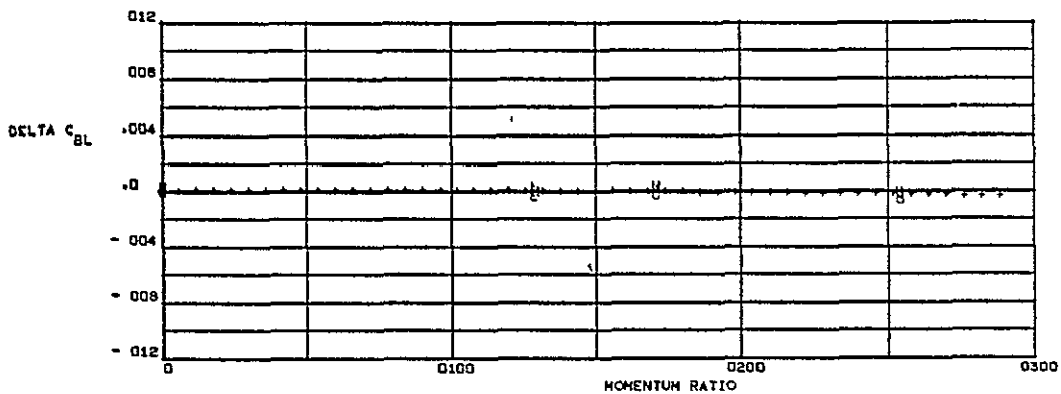
Figure 6-56. RC78 rolling moment correlation at $\alpha = -6^\circ$.



$$\beta = -4$$

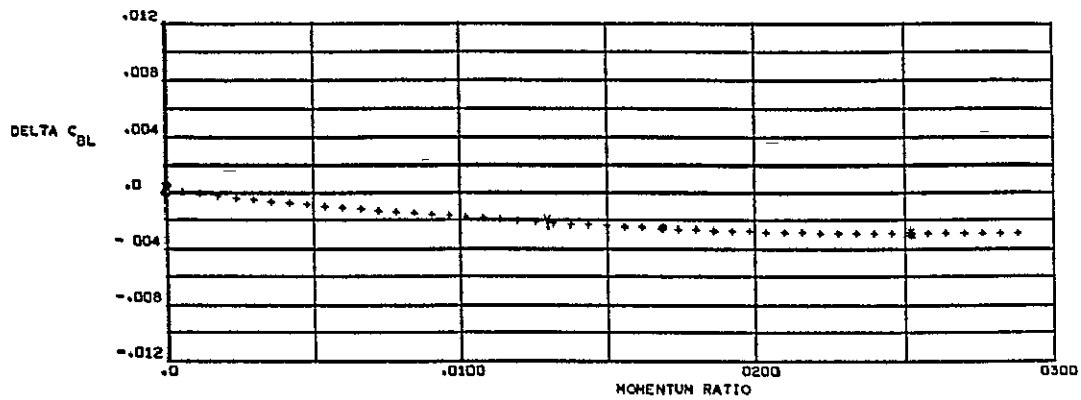


$$\beta = 0$$

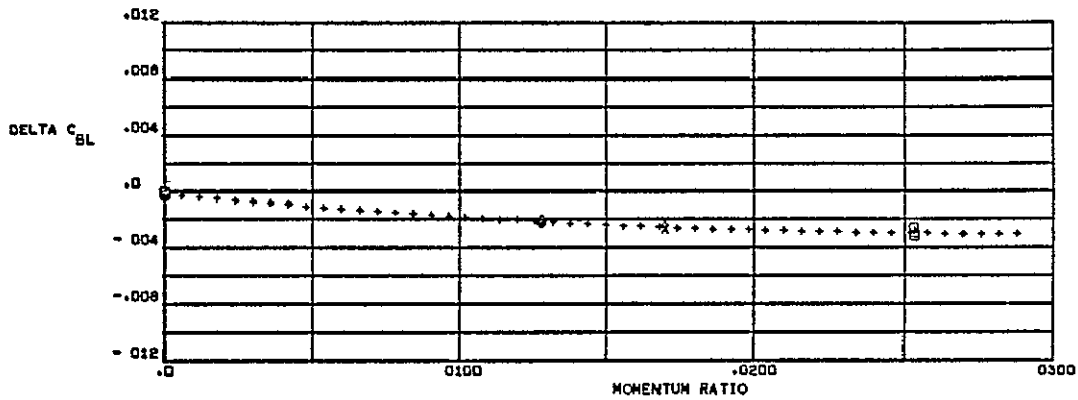


$$\beta = +4$$

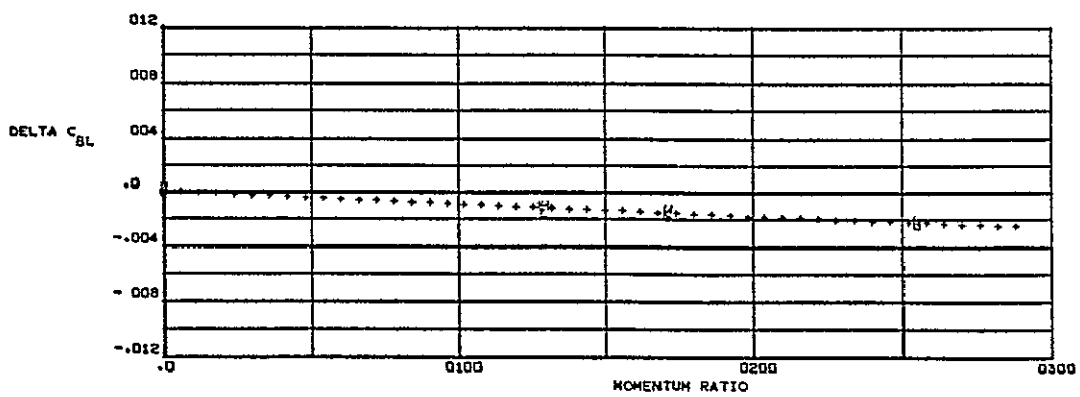
Figure 6-57. RC78 rolling moment correlation at $\alpha = 0^\circ$.



$$\beta = -4$$

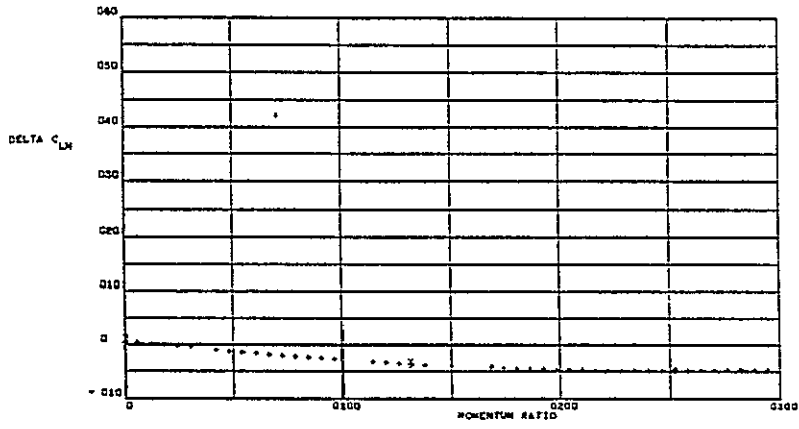


$$\beta = 0$$



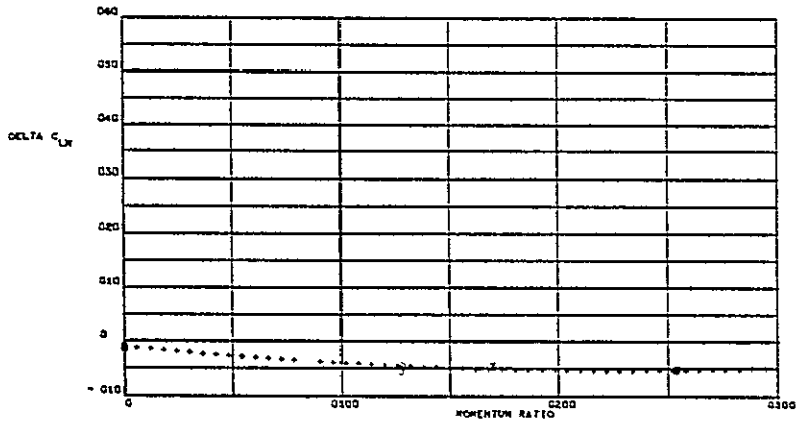
$$\beta = +4$$

Figure 6-58. RC78 rolling moment correlation at $\alpha = +9^\circ$.

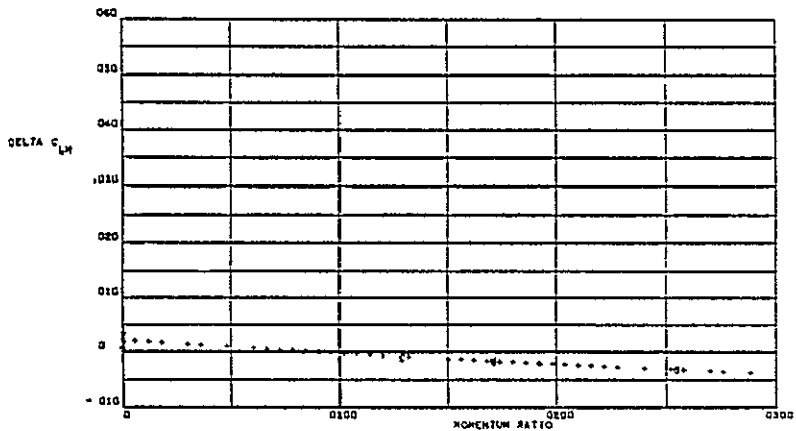


$\beta = -4$

ORIGINAL PAGE IS
OF POOR QUALITY



$\beta = 0$



$\beta = +4$

Figure 6-59. RC78 pitching moment correlation at $\alpha = -14^\circ$.

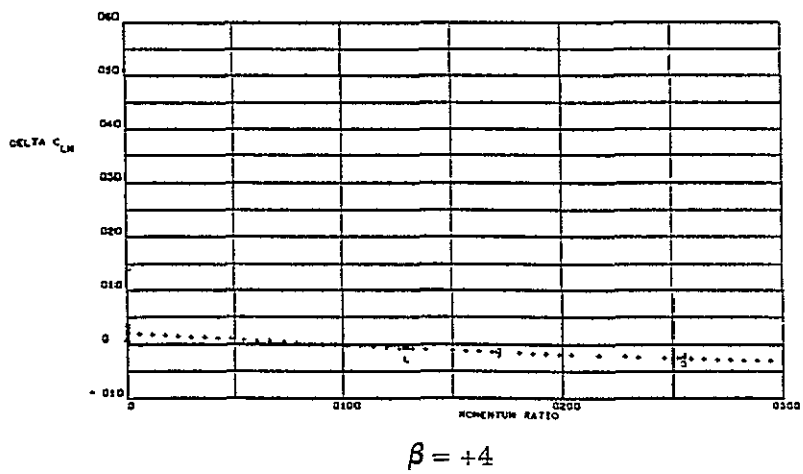
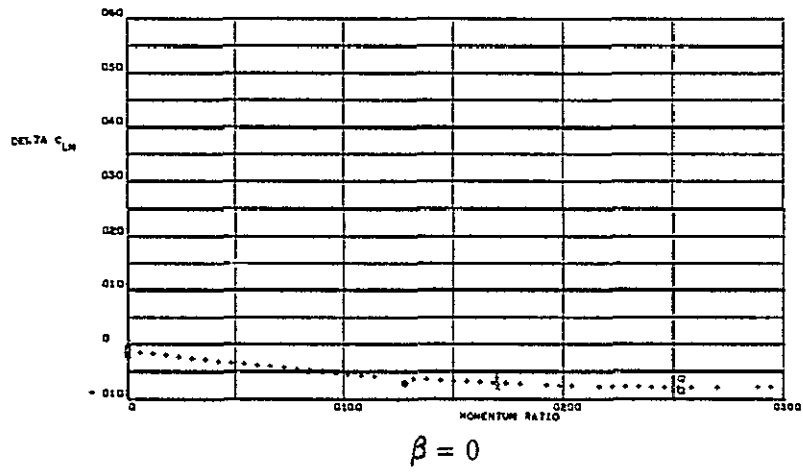
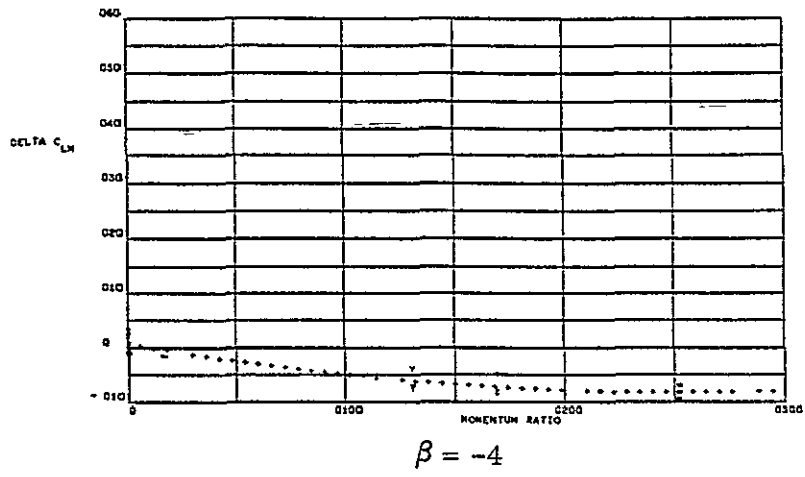


Figure 6-60. RC78 pitching moment correlation at $\alpha = -6^\circ$.

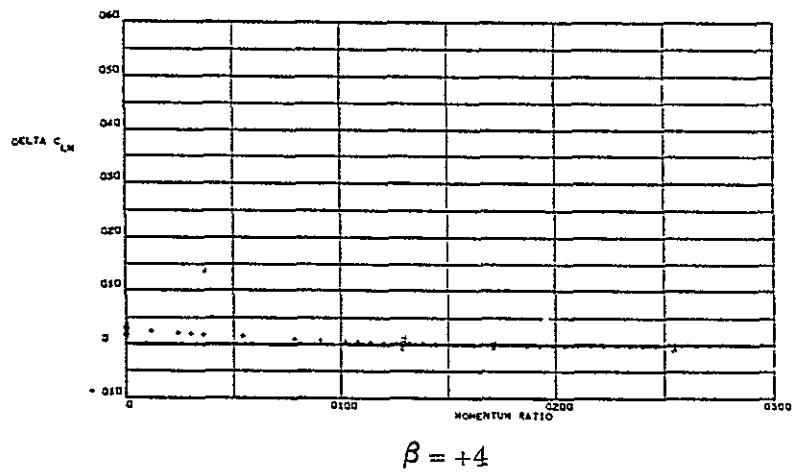
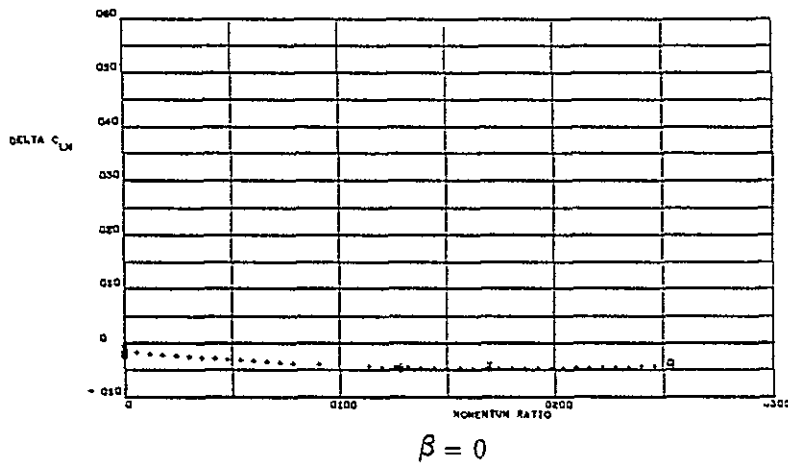
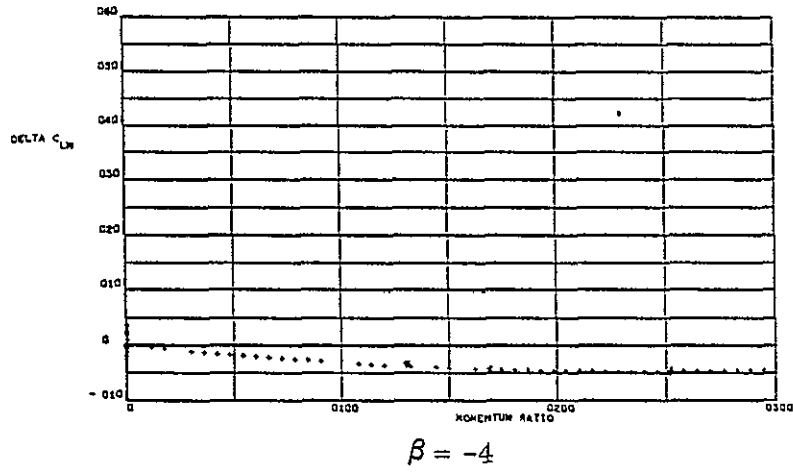
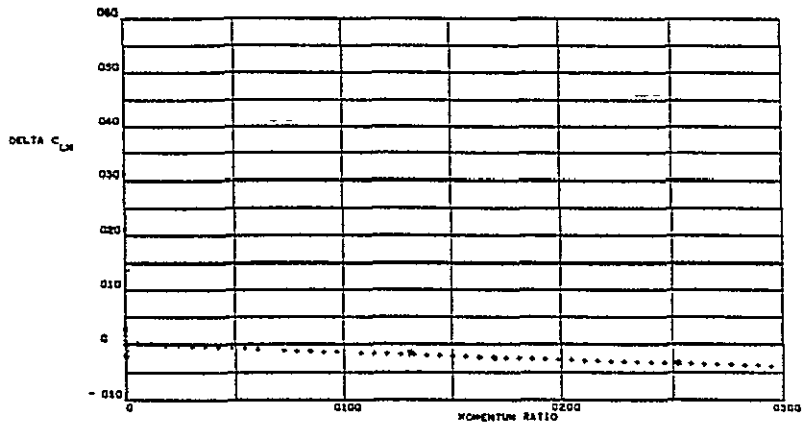
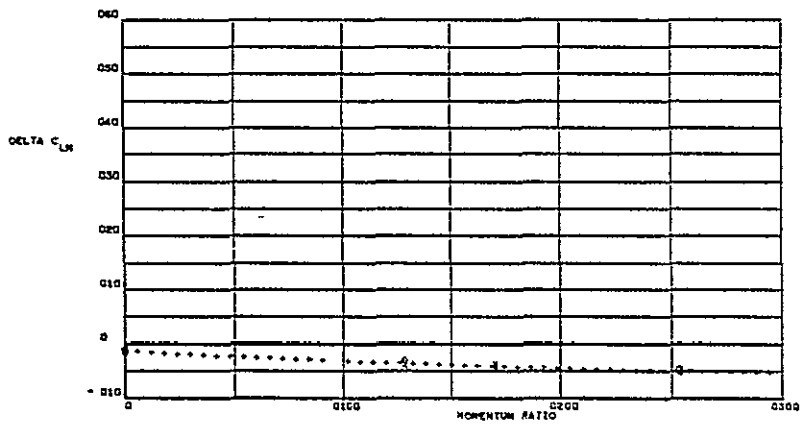


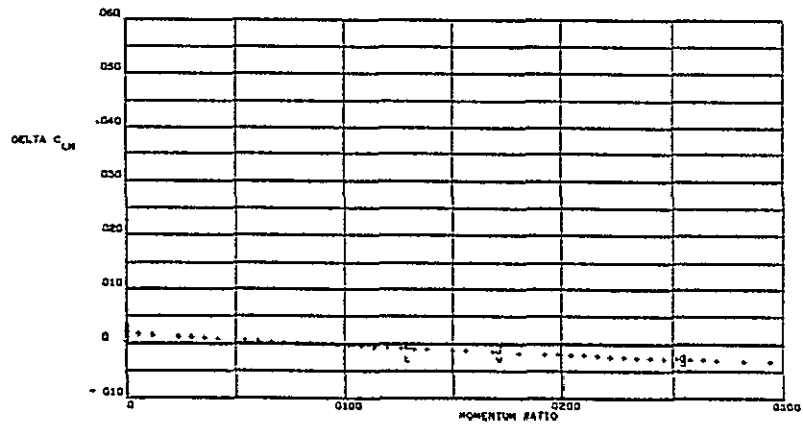
Figure 6-61. RC78 pitching moment correlation at $\alpha = 0^\circ$.



$$\beta = -4$$

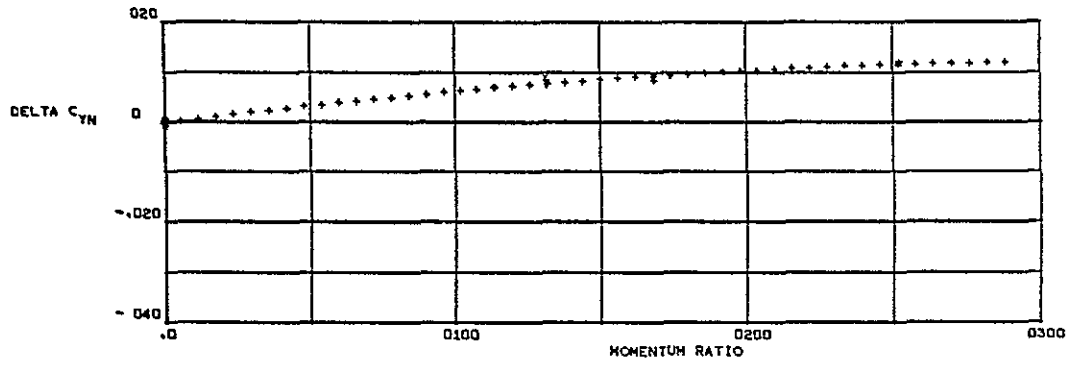


$$\beta = 0$$

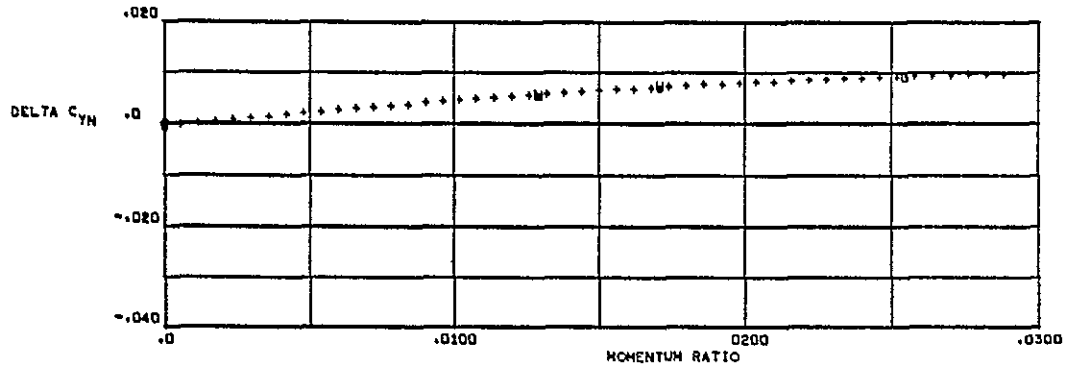


$$\beta = +4$$

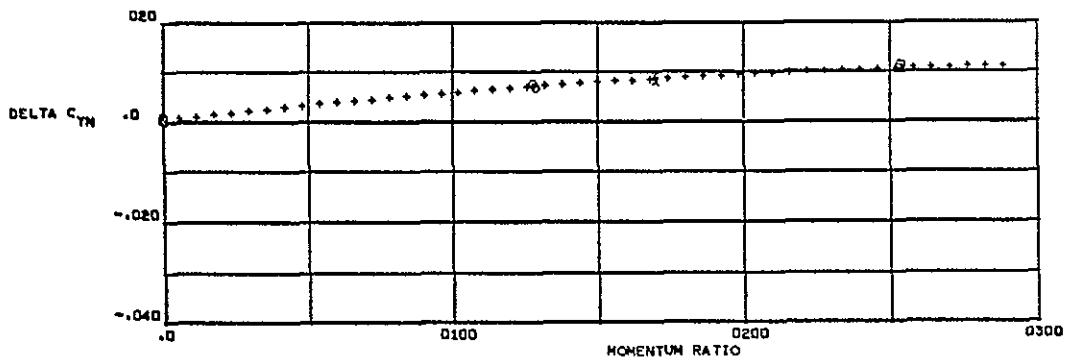
Figure 6-62. RC78 pitching moment correlation at $\alpha = +9^\circ$.



$$\beta = -4$$

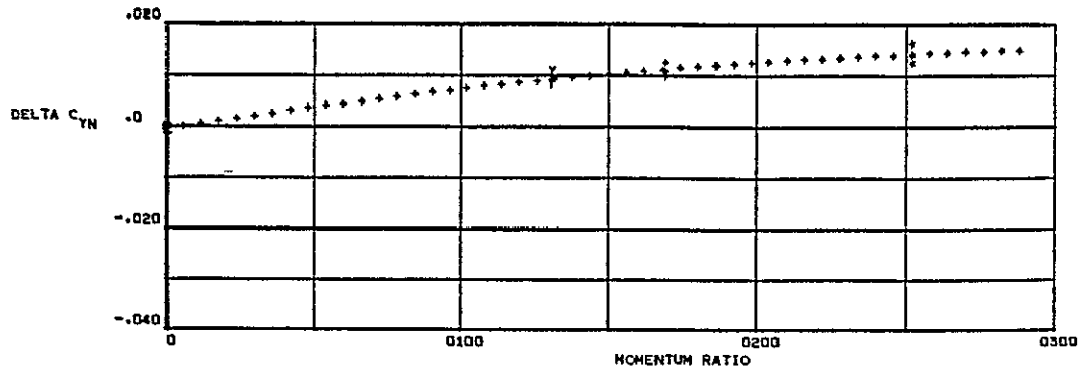


$$\beta = 0$$

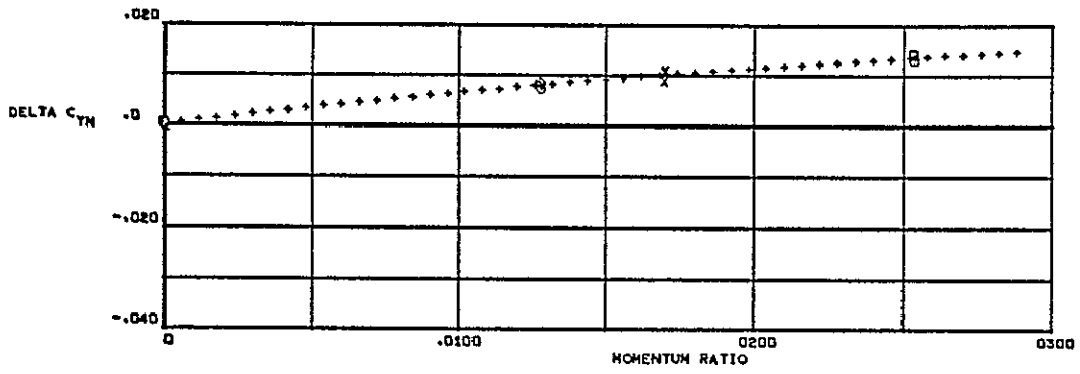


$$\beta = +4$$

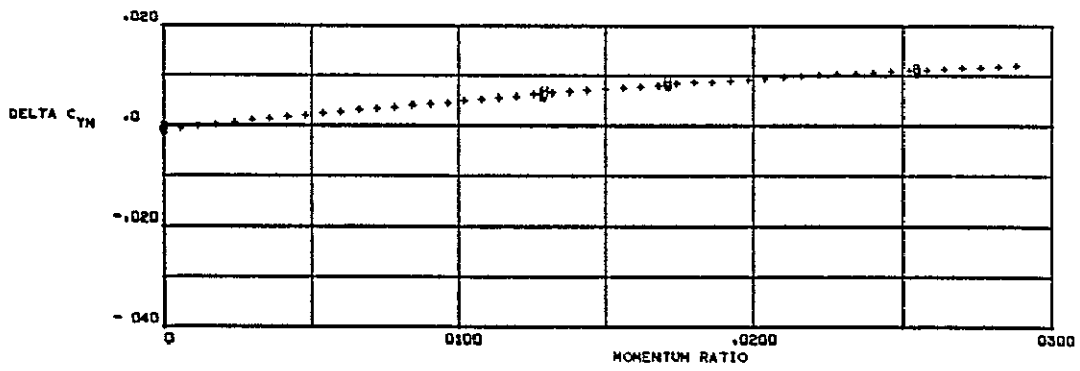
Figure 6-63. RC78 yawing moment correlation at $\alpha = -14^\circ$.



$$\beta = -4$$



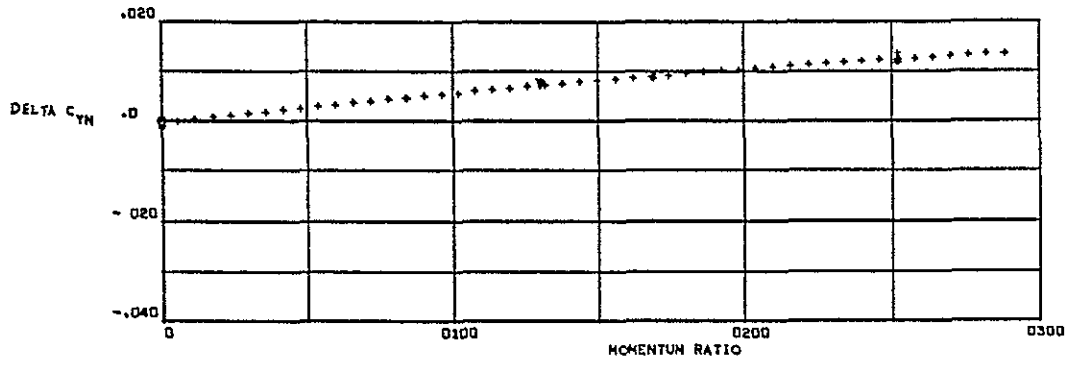
$$\beta = 0$$



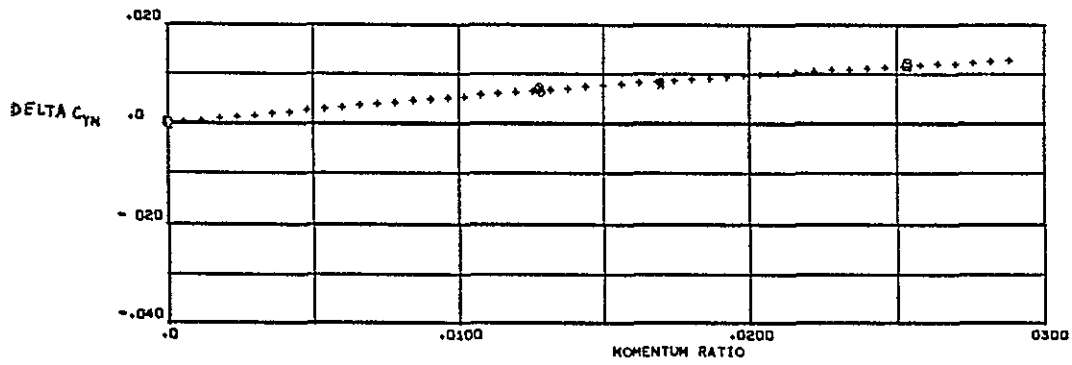
$$\beta = +4$$

Figure 6-64. RC78 yawing moment correlation at $\alpha = -6^\circ$.

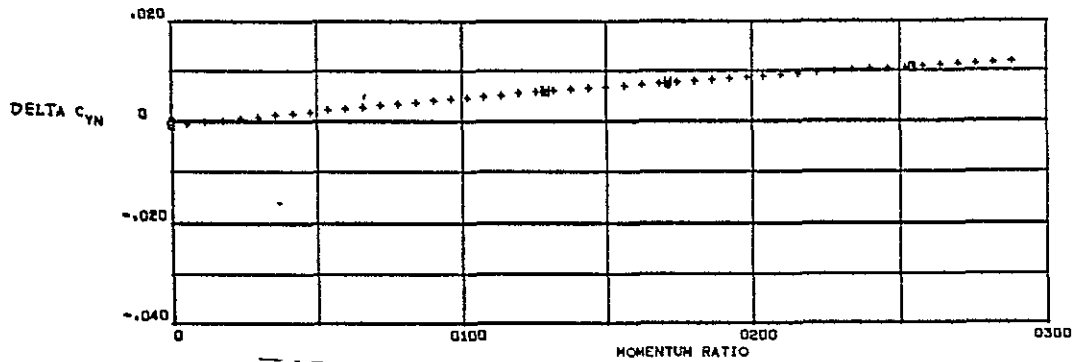
ORIGINAL PAGE IS
OF POOR QUALITY



$$\beta = -4$$

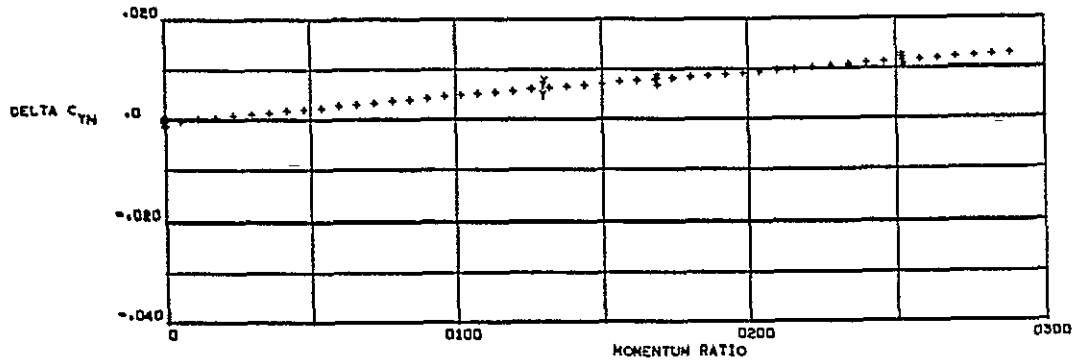


$$\beta = 0$$

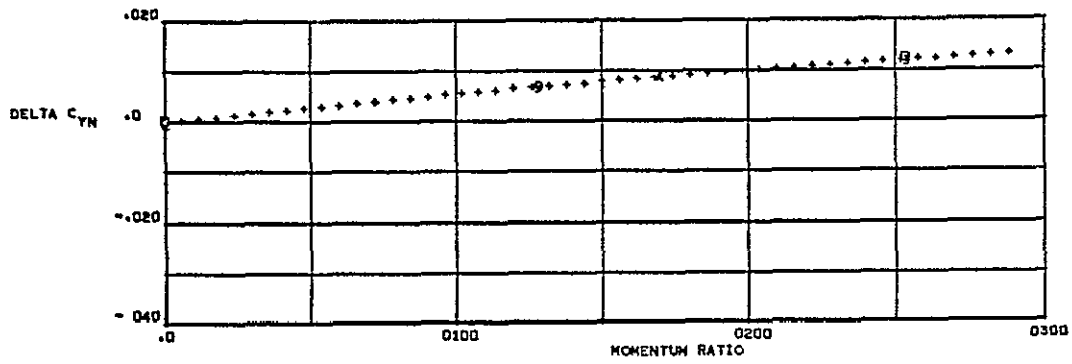


$$\beta = +4$$

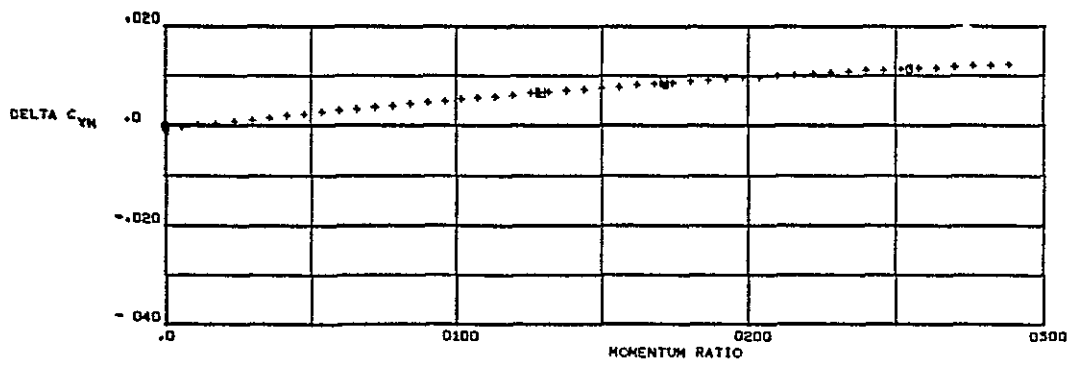
Figure 6-65. RC78 yawing moment correlation at $\alpha = 0^\circ$.



$$\beta = -4$$



$$\beta = 0$$



$$\beta = +4$$

Figure 6-66. RC78 yawing moment correlation at $\alpha = +9^\circ$.

ORIGINAL PAGE IS
OF POOR QUALITY

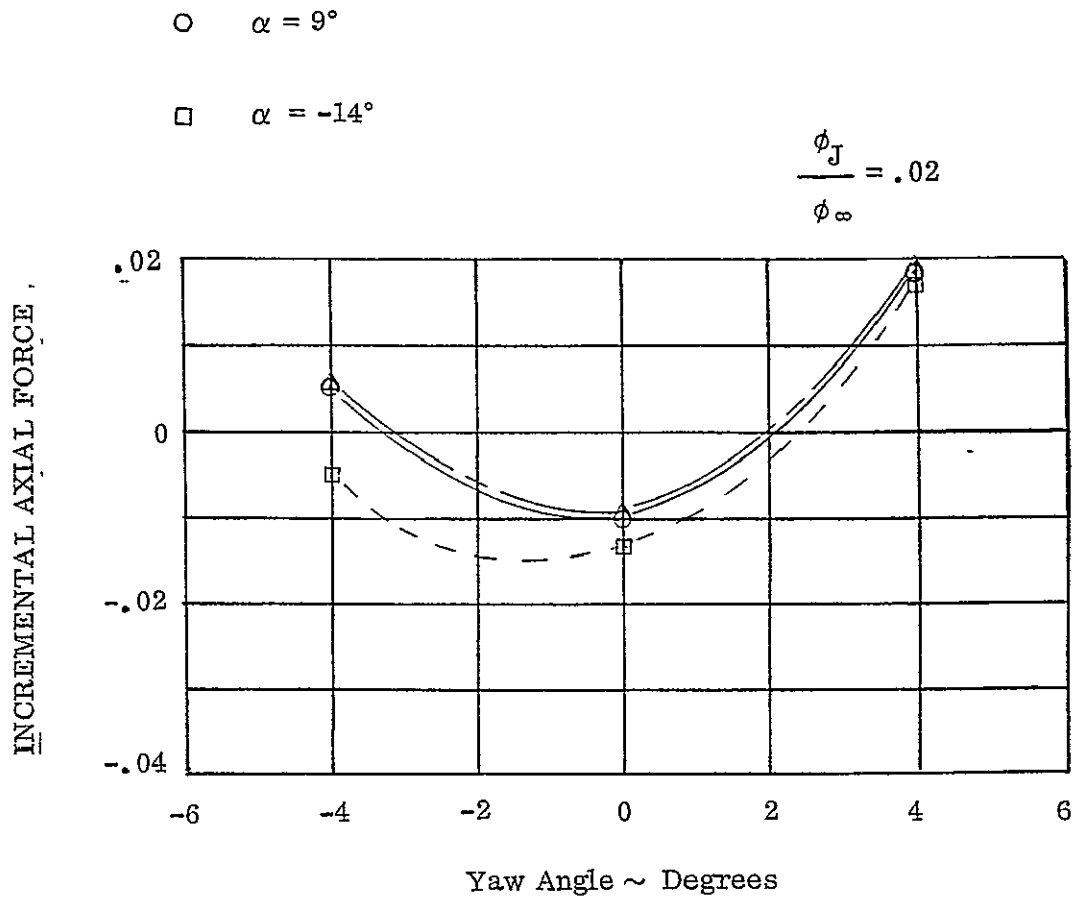


Figure 6-67. RC78 axial force increment changes due to yaw angle.

- $\alpha = -14^\circ$
- △ $\alpha = 0^\circ$
- $\alpha = 9^\circ$

$$\frac{\phi_J}{\phi_\infty} = .02$$

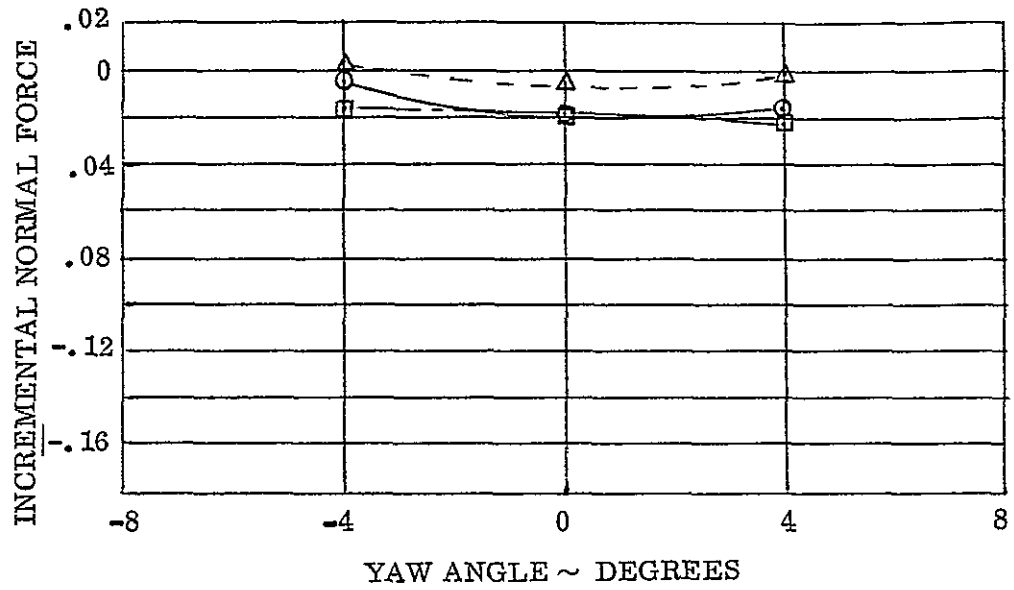


Figure 6-68. RC78 normal force increment due to yaw angle.

- $\alpha = -14^\circ$
- △ $\alpha = 0^\circ$
- $\alpha = 9^\circ$

$$\frac{\phi_J}{\phi_\infty} = .02$$

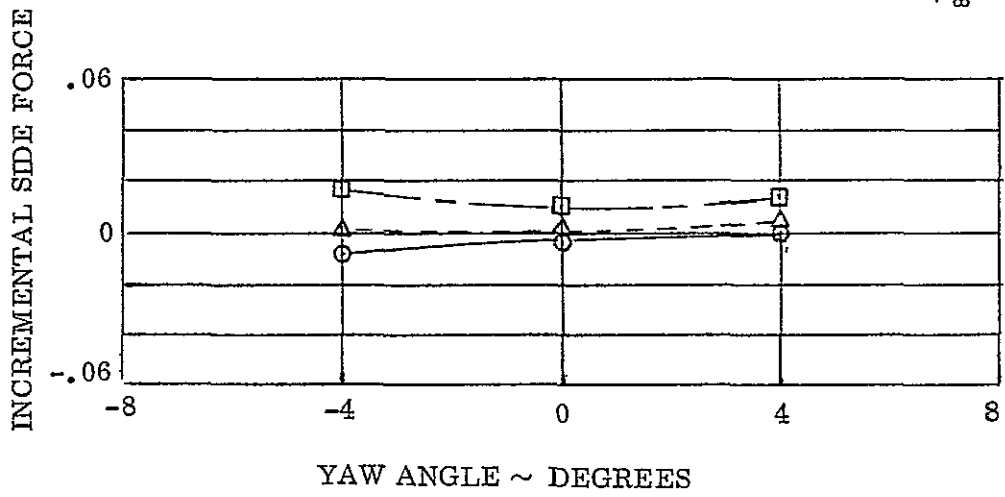


Figure 6-69. RC78 side force increment changes due to yaw angle.

- $\alpha = -14^\circ$
- △ $\alpha = 0^\circ$
- $\alpha = 9^\circ$

$$\frac{\phi_J}{\phi_\infty} = .02$$

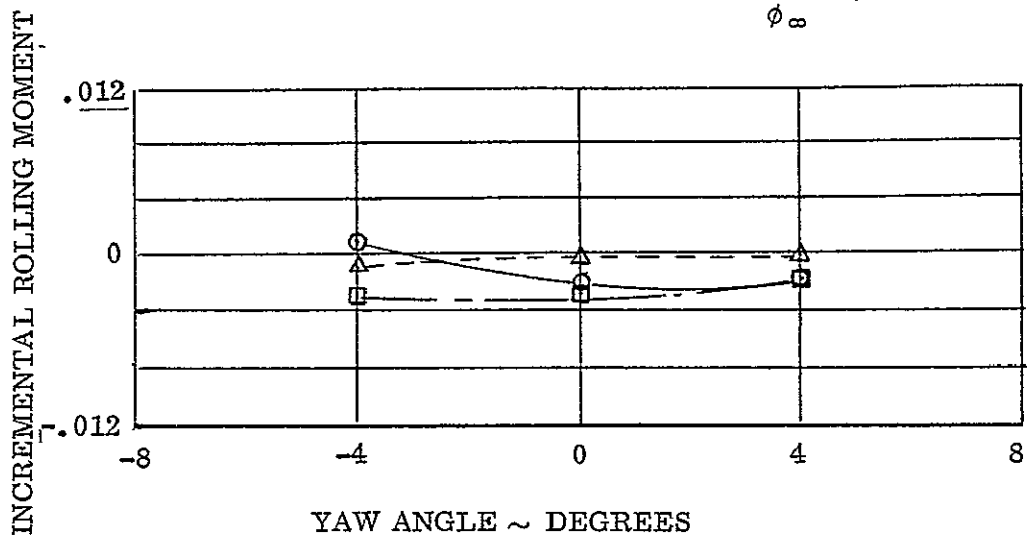


Figure 6-70. RC78 rolling moment increment change due to yaw angle.

- $\alpha = -14^\circ$
- △ $\alpha = 0^\circ$
- $\alpha = 9^\circ$

$$\frac{\phi_J}{\phi_\infty} = .02$$

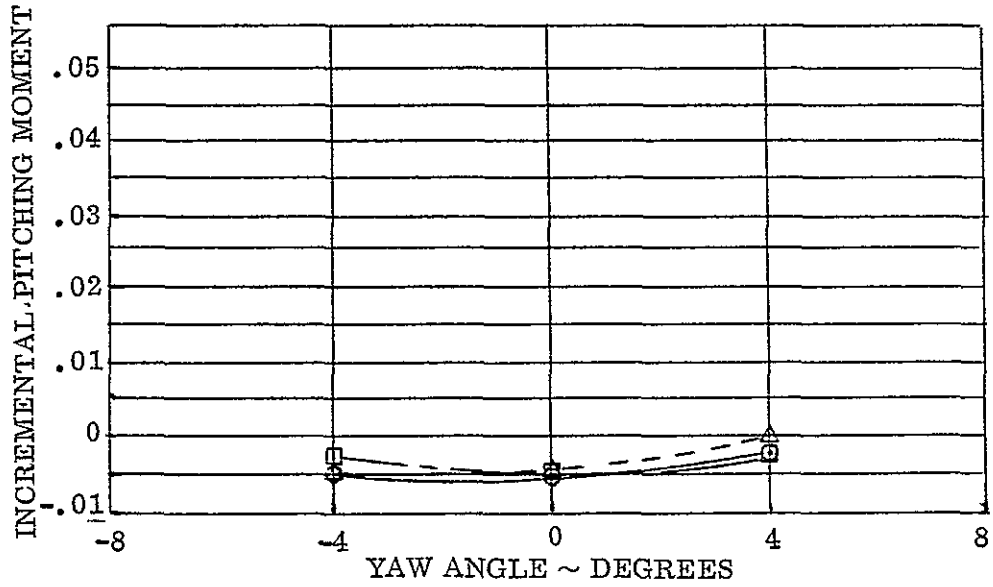


Figure 6-71. RC78 pitching moment increment changes due to yaw angle.

- $\alpha = -14^\circ$
- △ $\alpha = 0^\circ$
- $\alpha = 9^\circ$

$$\frac{\phi_J}{\phi_\infty} = .02$$

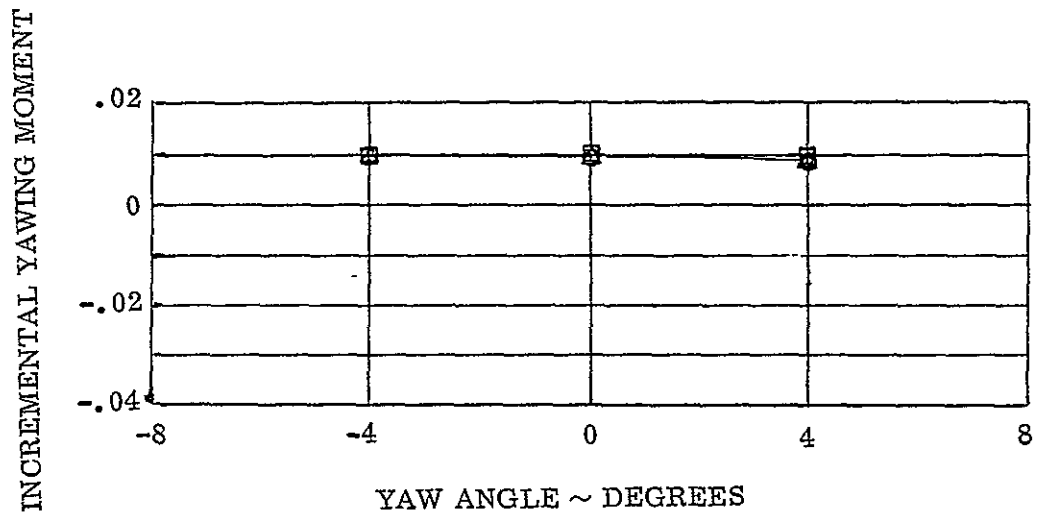


Figure 6-72. RC78 yawing moment increment changes due to yaw angle.

ORIGINAL PAGE IS
OF POOR QUALITY

$$\phi_J/\phi_\infty = 0.026$$

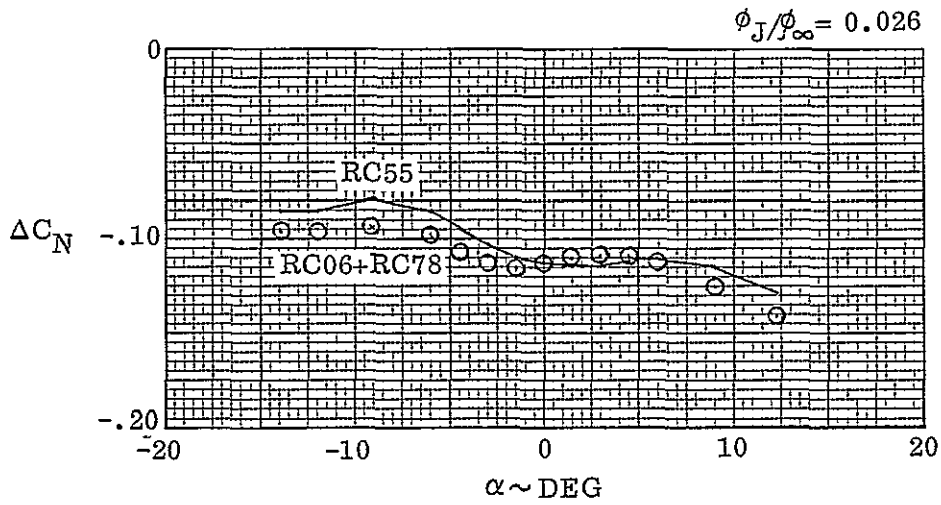
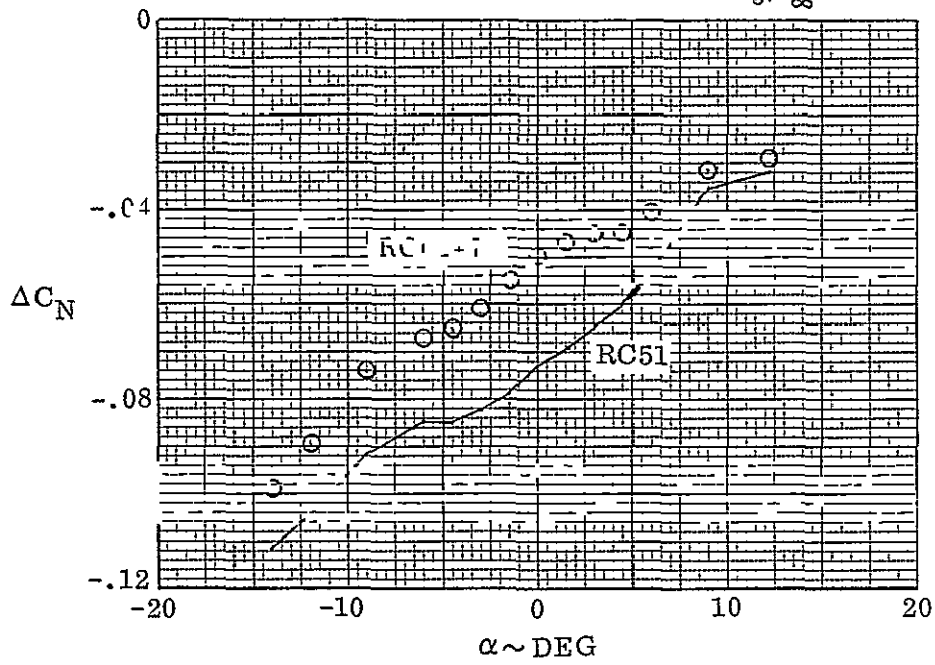


Figure 6-73. A comparison of the normal force increments for RC51 and RC55.

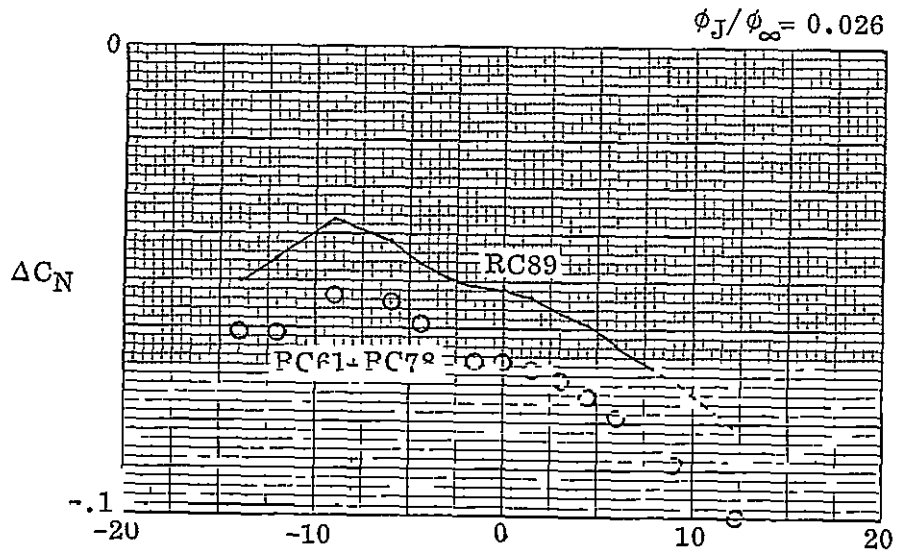
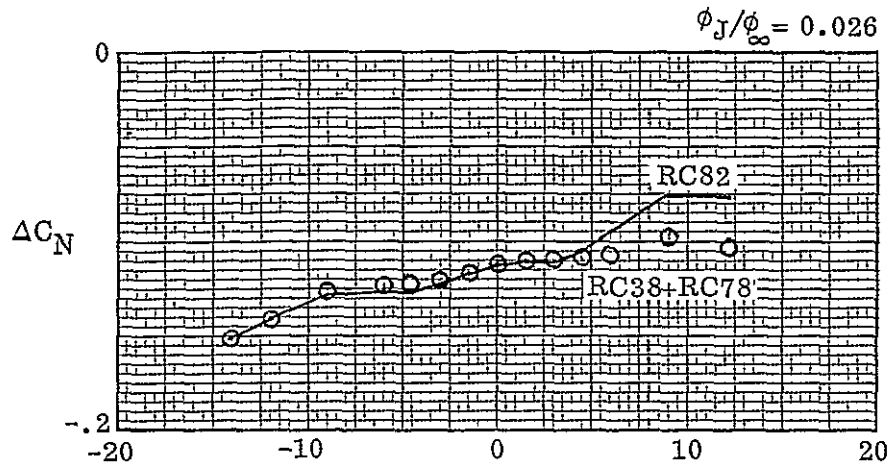


Figure 6-74. A comparison of the normal force increments for RC82 and RC89.

ORIGINAL PAGE IS
OF POOR QUALITY

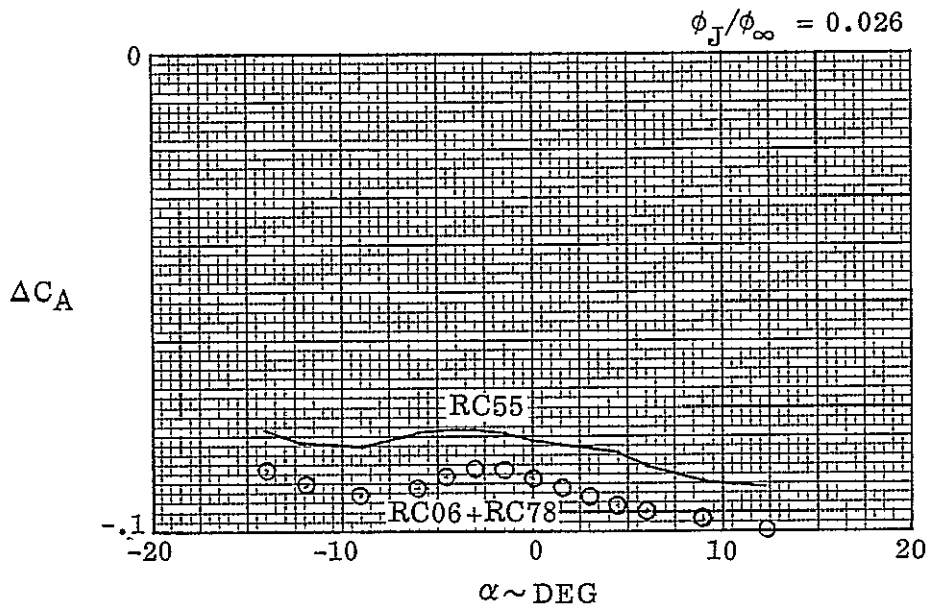
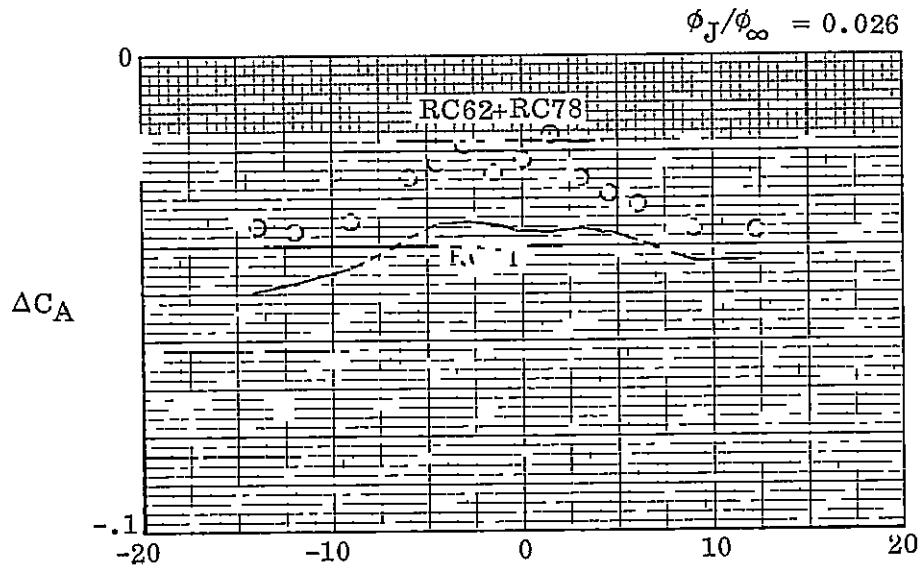


Figure 6-75. A comparison of axial force increments for RC51 and RC55.

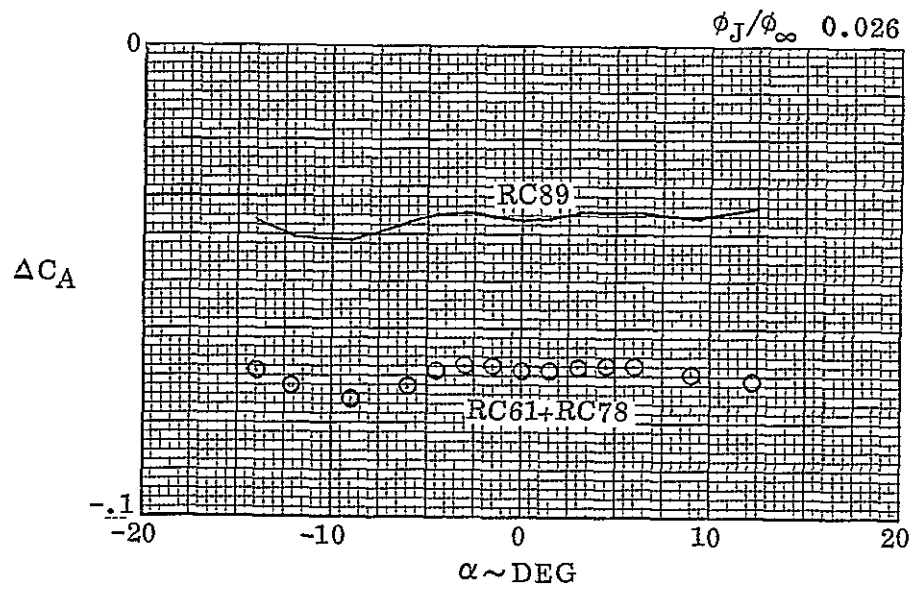
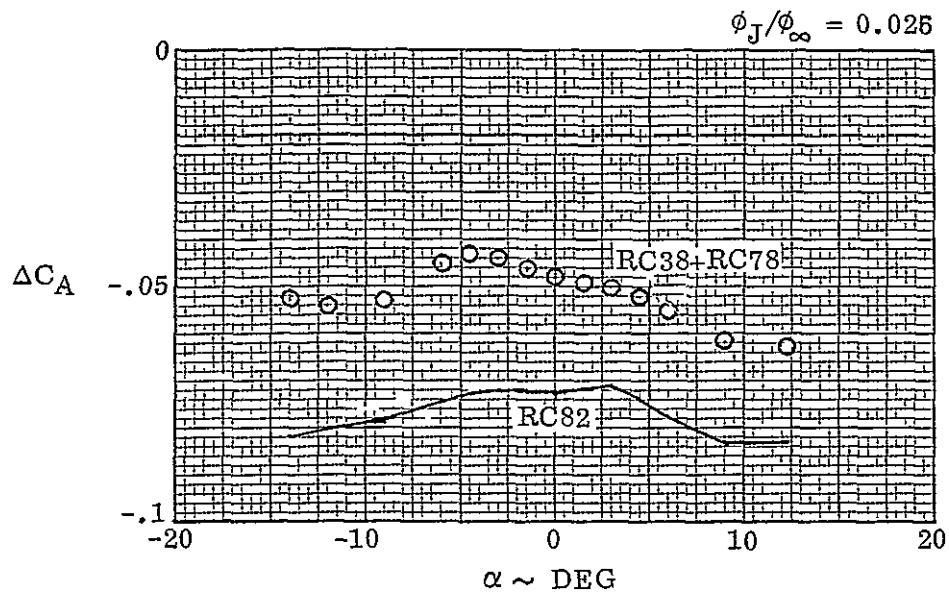
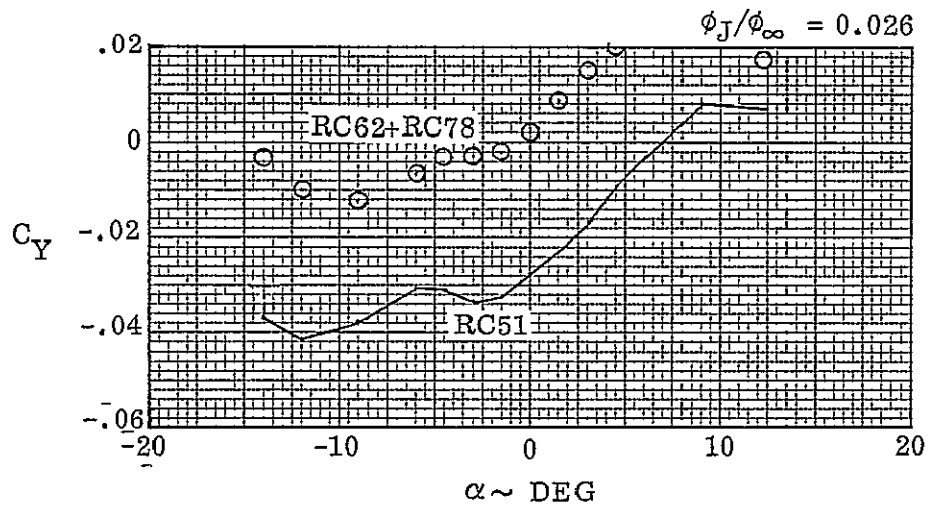


Figure 6-76. A comparison of axial force increments for RC82 and RC89.



ORIGINAL PAGE IS
OF POOR QUALITY

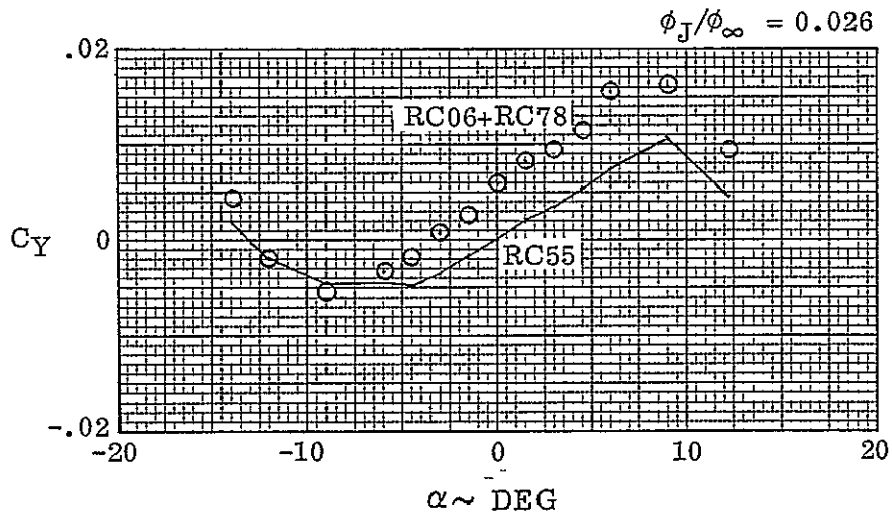


Figure 6-77. A comparison of side force increments for RC51 and RC55.

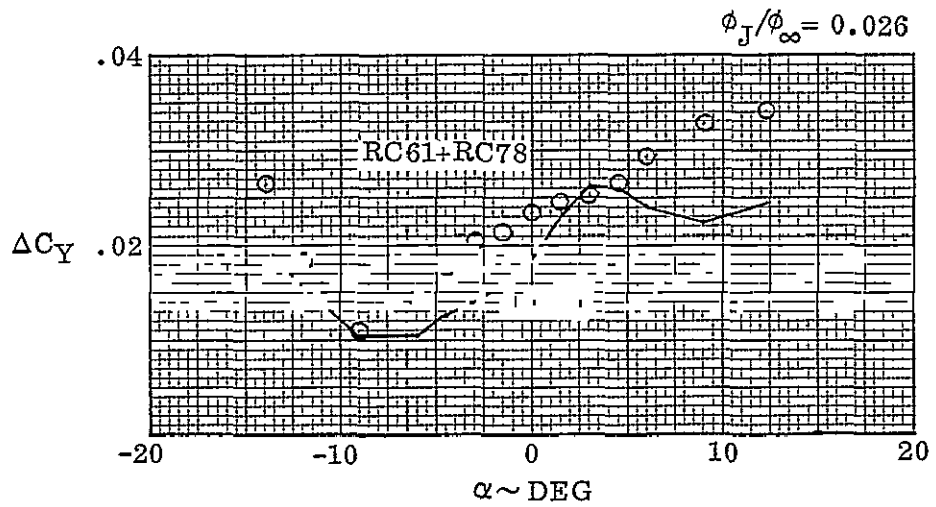
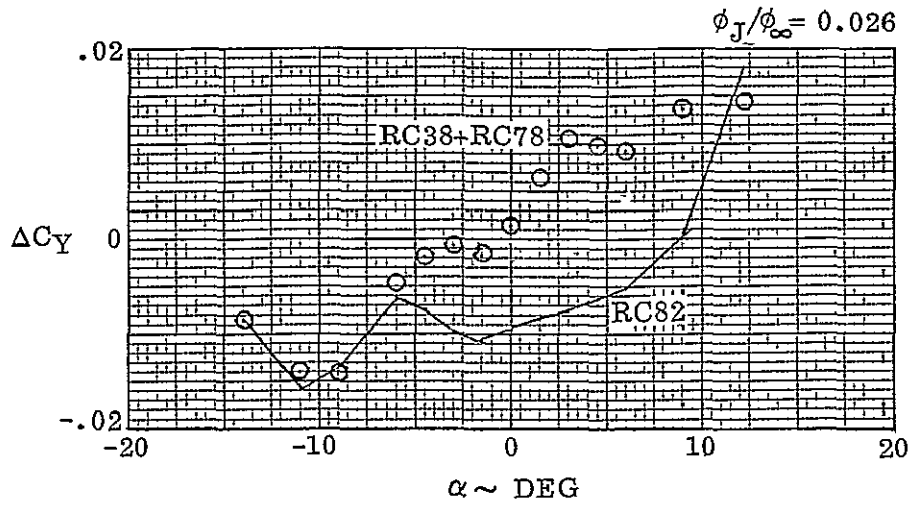
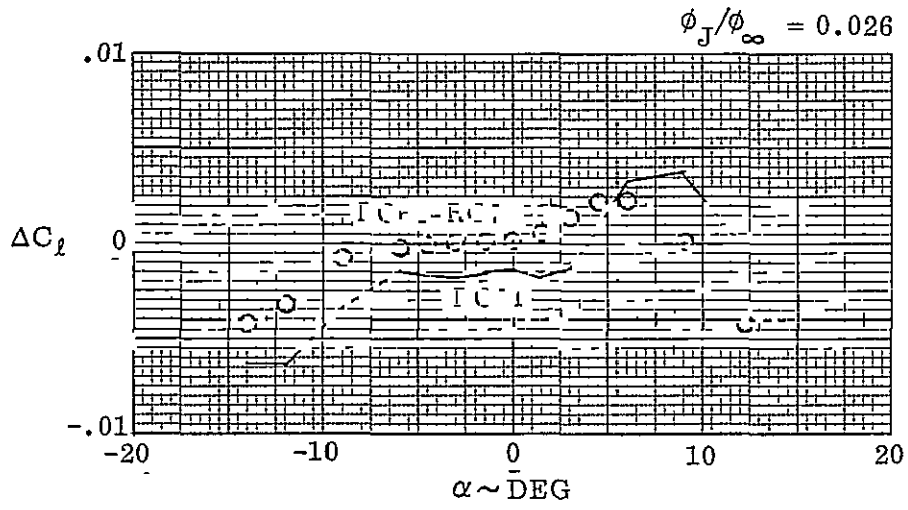


Figure 6-78. A comparison of side force increments for RC82 and RC89.



ORIGINAL PAGE IS
OF POOR QUALITY

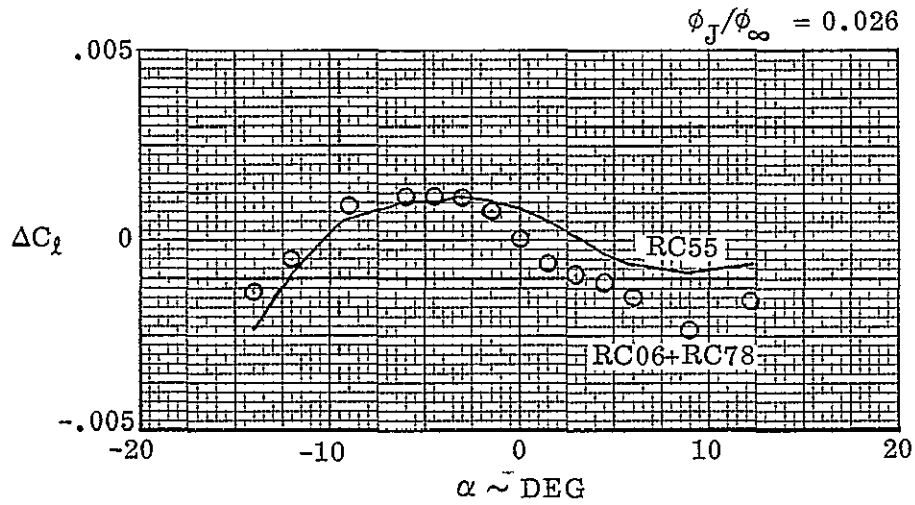


Figure 6-79. A comparison of rolling moment increments for RC51 and RC55.

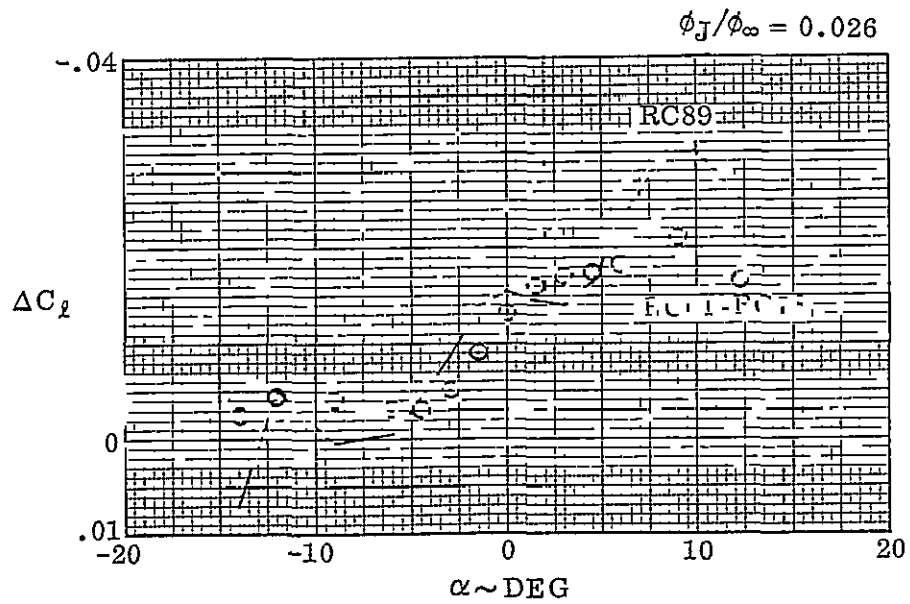
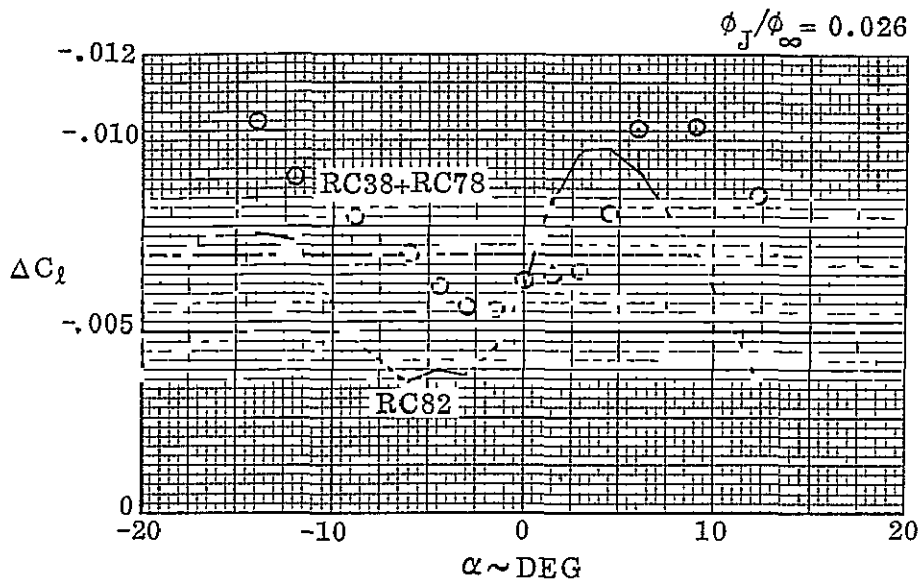


Figure 6-80. A comparison of rolling moment increments for RC82 and RC89.

ORIGINAL PAGE IS
OF POOR QUALITY

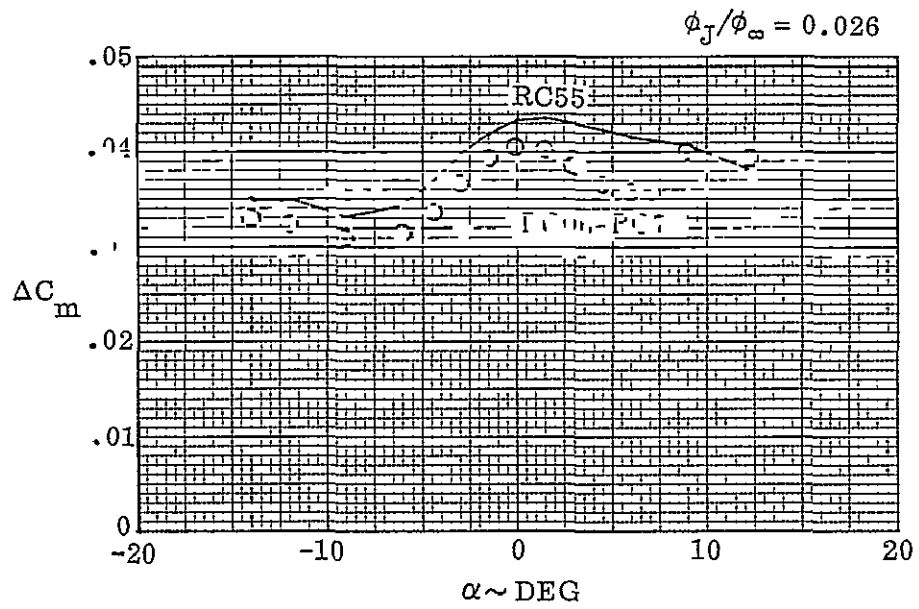
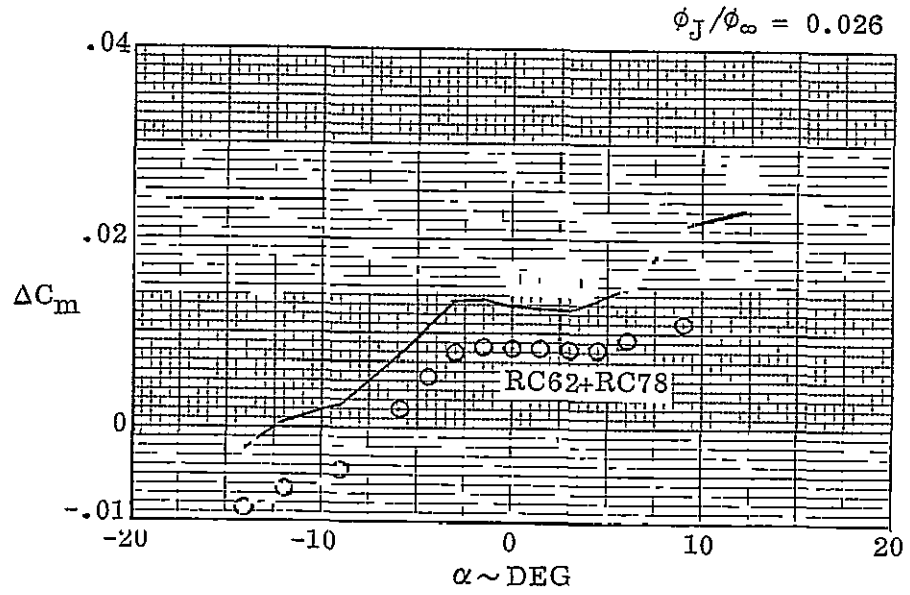


Figure 6-81. A comparison of pitching moment increments for RC51 and RC55.

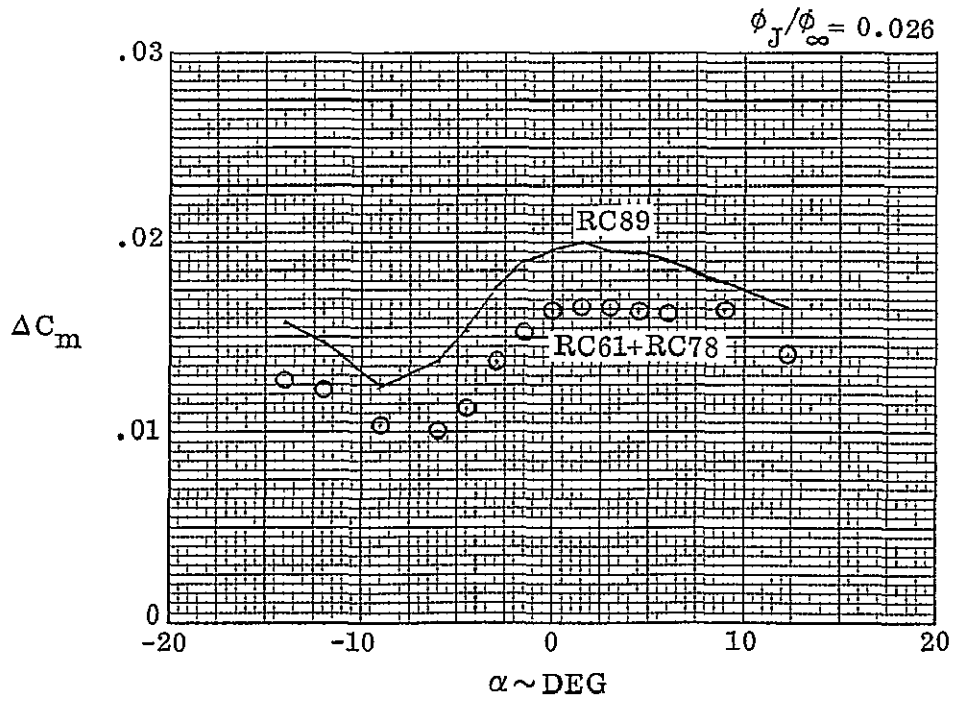
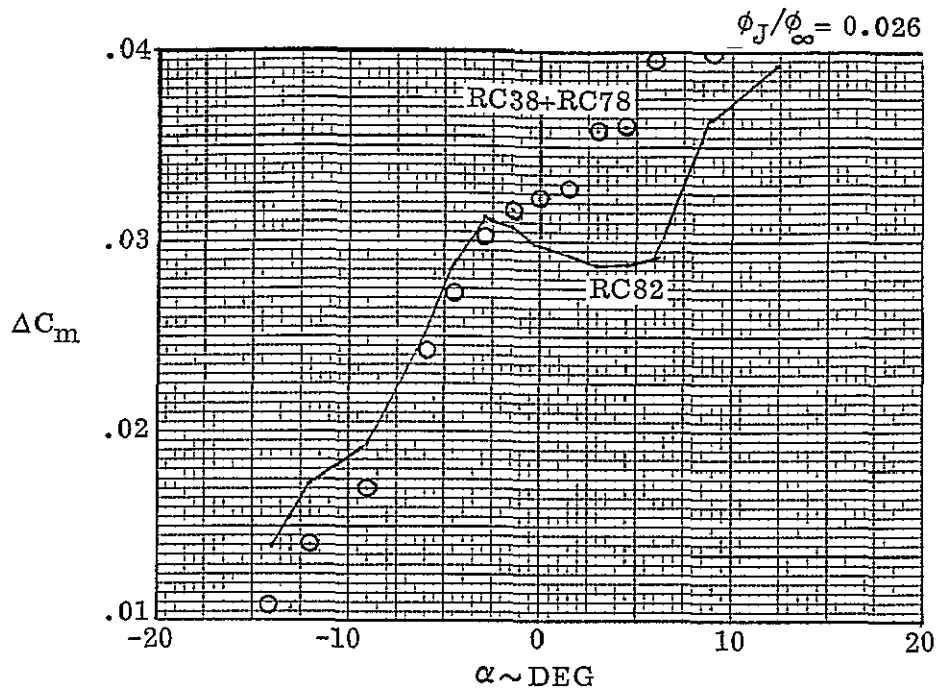


Figure 6-82. A comparison of pitching moment increments for RC82 and RC89.

ORIGINAL PAGE IS
OF POOR QUALITY

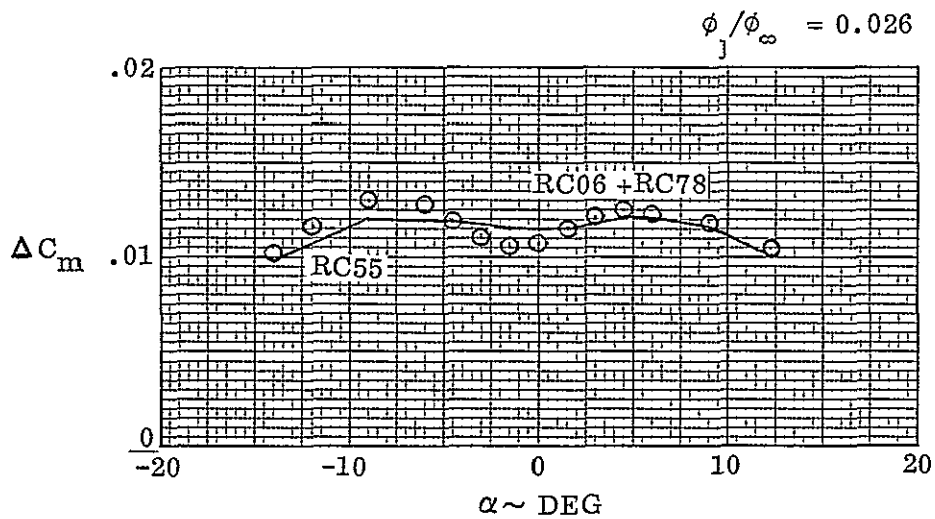
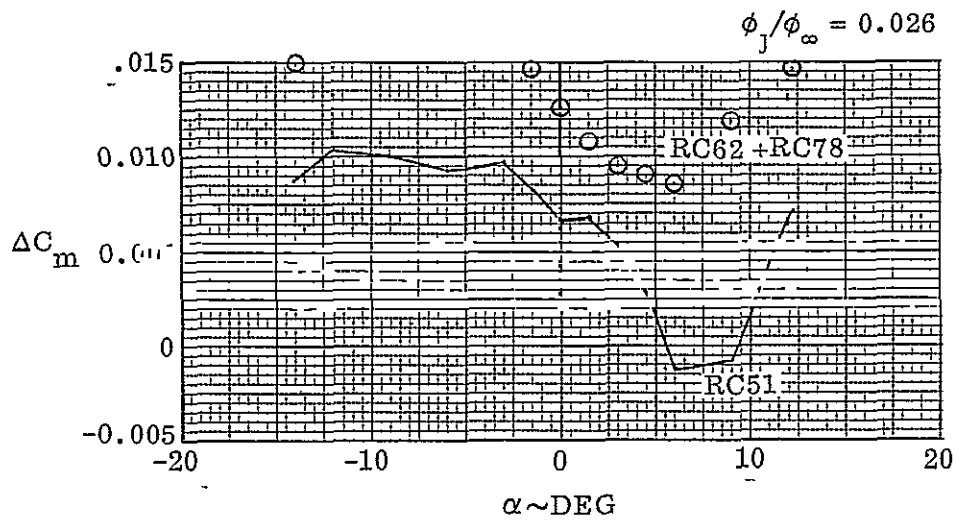


Figure 6-83. A comparison of yawing moment increments for RC51 and RC55.

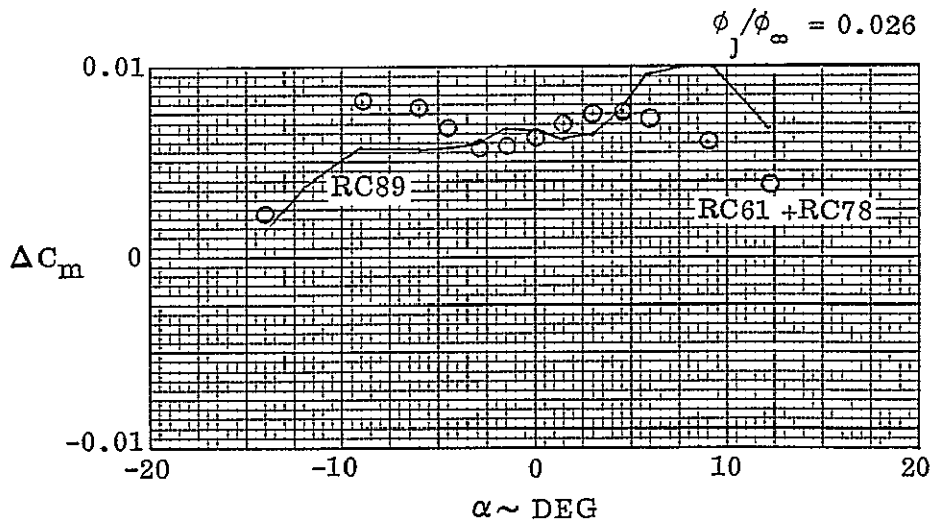
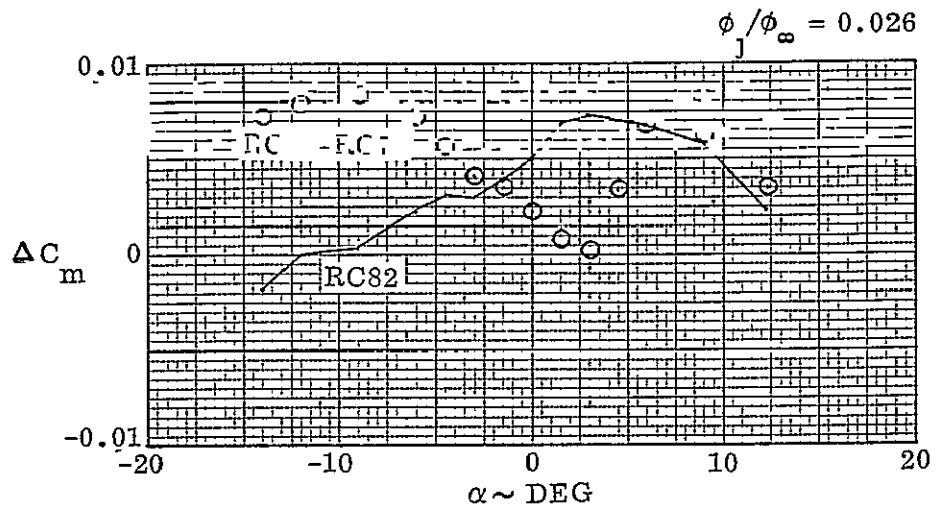


Figure 6-84. A comparison of yawing moment increments for RC82 and RC89.



ORIGINAL PAGE IS
OF POOR QUALITY

TANK-ON INCREMENTAL EFFECTS

Figures 6-1 and 6-2 presented diagrams of all RCS control combinations planned for use at the time of test IA148. The RC__ numbers shown in the two figures indicate the control combinations actually tested during IA148. The allowable range of control commands has been streamlined, and the only commands used at present are:

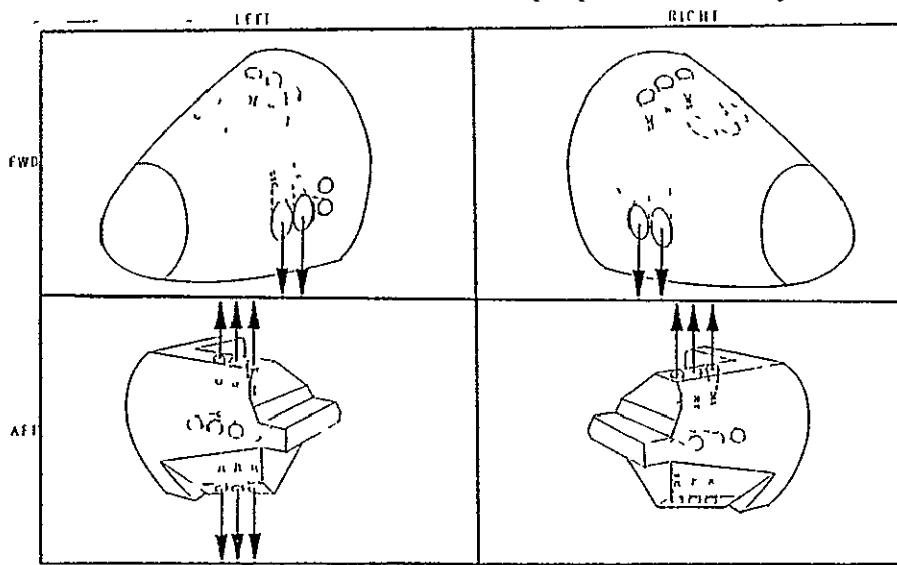
- a. UZCMD = 0, 1, -1
- b. UXCMD = +2, 0, -2
- c. UYCMD = 5, 1, 0, -1, -3

To define the induced RCS increments for the above control combinations, data were analyzed for all control combinations of test IA148 except RC42 and RC45. The resulting tables of curve fit coefficients are given in Appendices A to C. These curve fits do not provide RCS incremental effects for all of the allowable control combinations (UXCMD, UYCMD, UZCMD). Suitable methods to provide the rest of the data from the existing data were developed. These data were built up largely by symmetric and superposition assumptions. The methods used to define each block will be described briefly in the following paragraphs for each control command possible.

7.1 UZCMD = 0

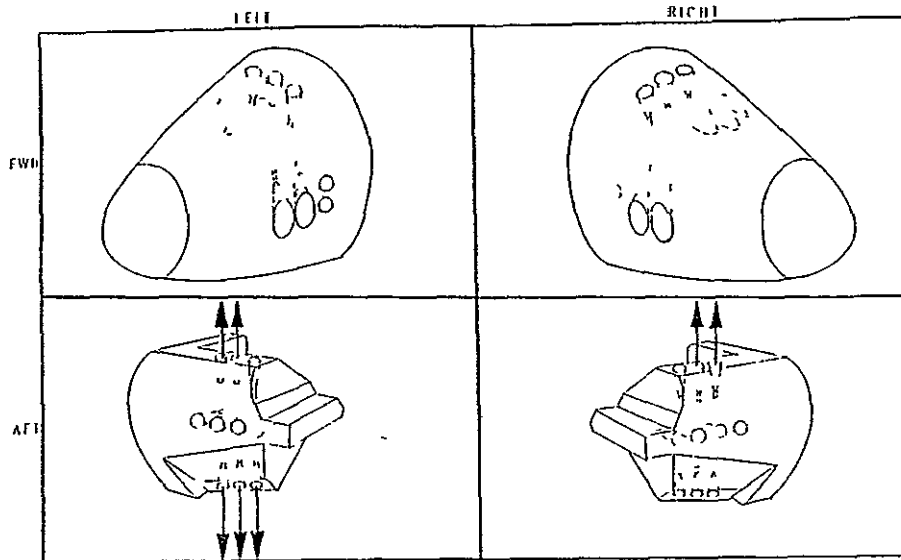
7.1.1 UXCMD = 2

7.1.1.1 UYCMD = 5



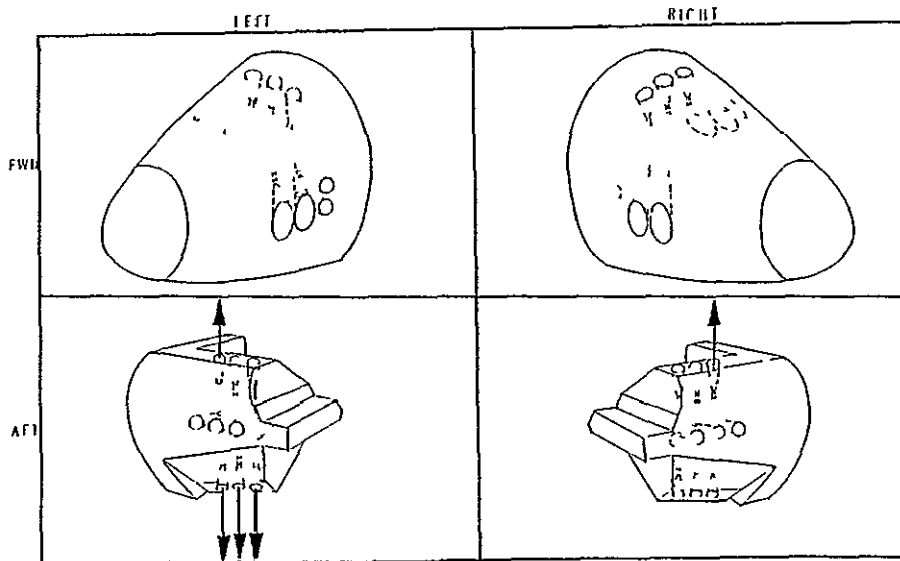
Data for this thirteen-jet combination are provided by the RC38 data of IA148. Data were obtained at all three yaw angles and curve fits are available directly for this case.

7.1.1.2 UYCMD = 1



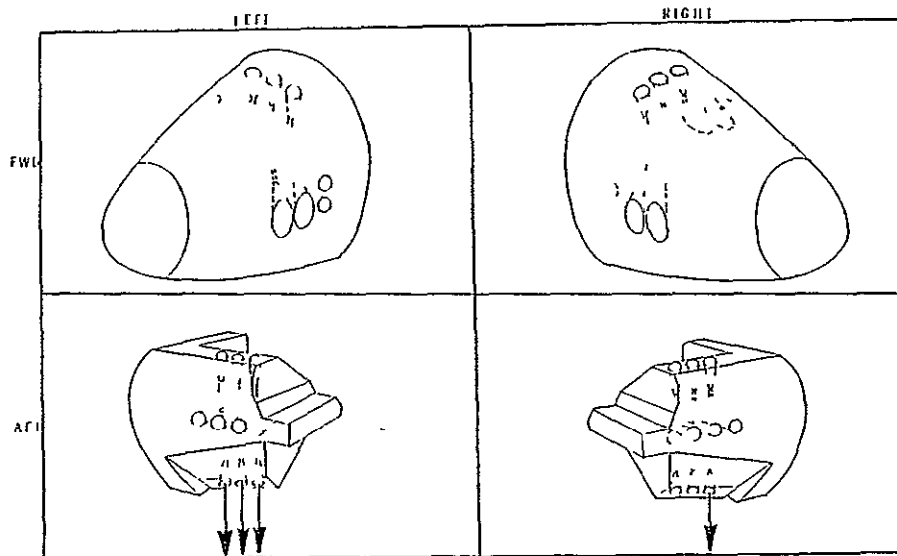
No test data were available for this control combination. However, data are available for the three-jet symmetric pitch-up case (RC40) and for the one-jet symmetric pitch-up case (RC61, Subsection 7.1.1.3). These two curve fit sets are averaged to produce the curve fits for this combination.

7.1.1.3 UYCMD = 0



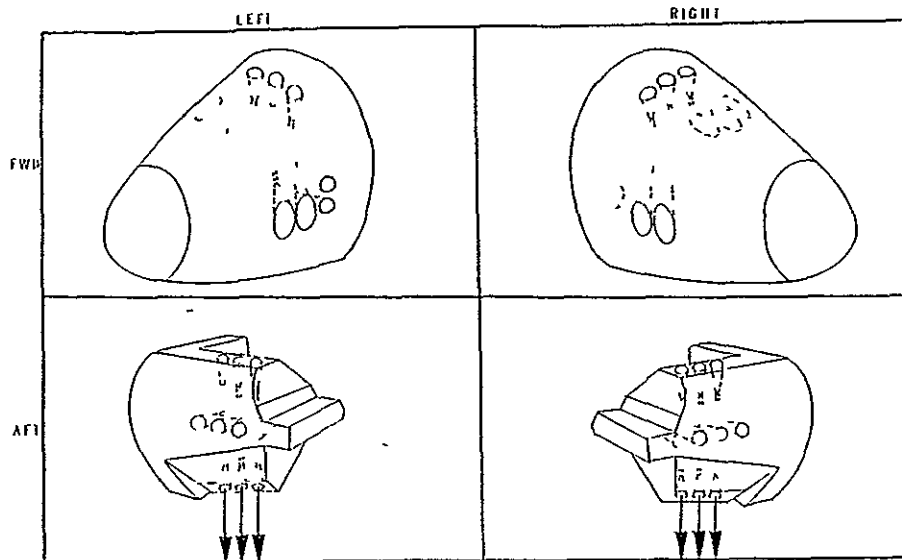
Data for this combination are provided as the curve fits of the RC61 data from test IA148.

7.1.1.4 UYCMD = -1



No data were available for any of the UYCMD = -1 control combinations, and no simple addition of jet combinations was available to derive this set. The approach taken was to define a two-jet symmetric down-firing set increment by interpolating the RC06 six-jet data using an equivalent single-nozzle momentum ratio which was 1/3 of the actual value. High dynamic pressure cases will result in an extrapolation of RC06 data back toward the jet-off limit, but extrapolation in this direction is controlled by zero increments of the jet-off limit. The increments for the remaining two down-firing jets on the left side were generated by taking differences between RC61 data and RC37 data to remove up-firing increments and derive a three-jet left side case. An equivalent momentum ratio of 2/3 of the actual single-nozzle momentum ratio is used to derive the two-jet increments, and these are added to the two-jet symmetric increments. The amount of data manipulation involved in these cases makes it desirable to obtain a better set of test data in the future.

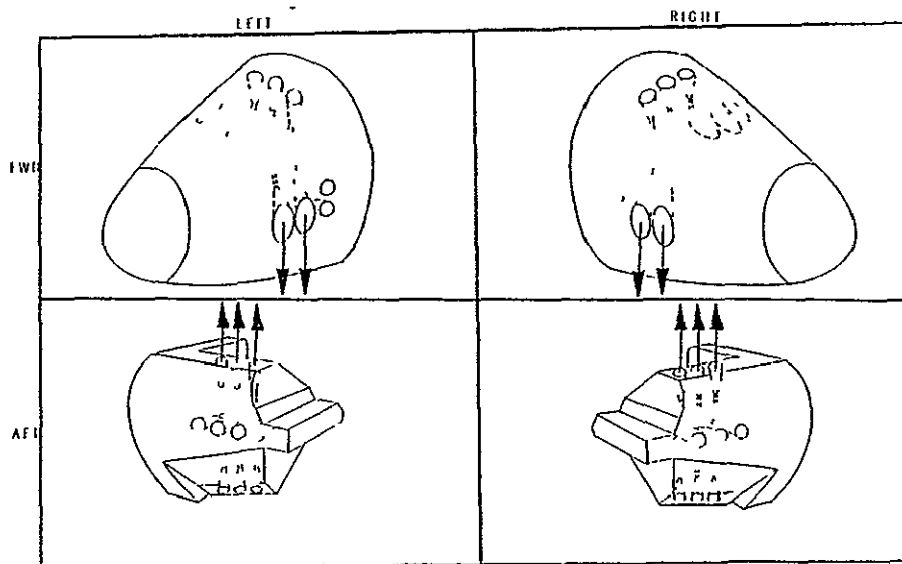
7.1.1.5 UYCMD = -3



The test data for RC06 provide the curve fits for this control combination. No data were taken for the -4 degree yaw case and it must be assumed that the yaw effects are symmetric. The longitudinal data (C_A, C_N, C_M) are assumed to be the same as the +4° values, but the signs are reversed for the lateral-directional (C_Y, C_ℓ, C_N) increments between the -4 and -4 degree yaw cases.

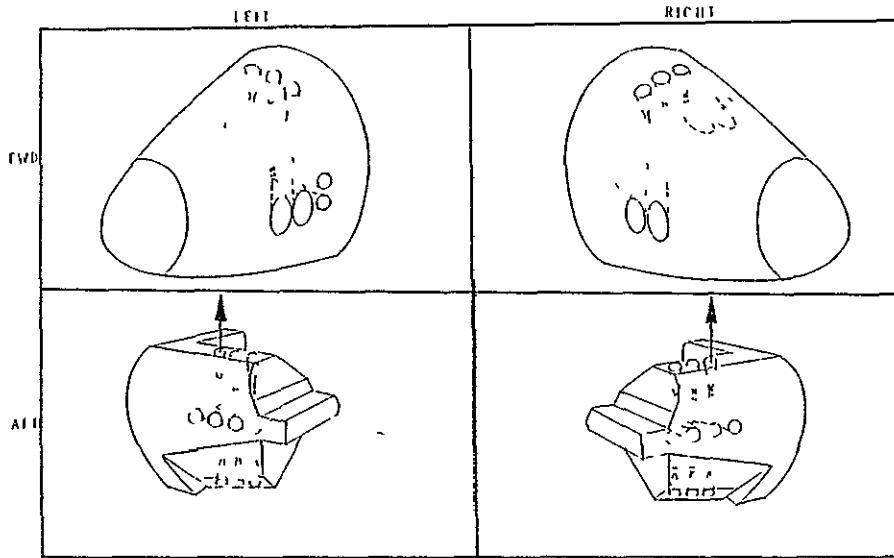
7.1.2 UXCMD = 0

7.1.2.1 UYCMD = 5



The curve fits of the RC62 test data provide the increments for this control combination. Since no -4 degree yaw data was obtained for this combination, symmetry was assumed for this data.

7.1.2.2 UYCMD = 1

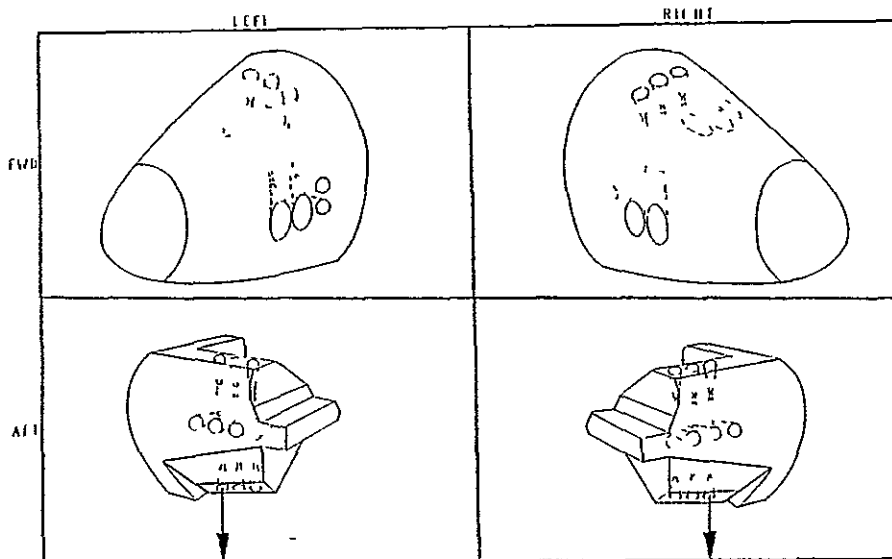


RC37 test data provide the curve fits to compute the increments for this combination. No -4 degree yaw data was obtained and symmetry was assumed.

7.1.2.3 UYCMD = 0

No jets are fired in this case.

7.1.2.4 UYCMD = -1



No test data were obtained for this combination, so the RC06 curve fits were interpolated to provide the required increments. This interpolation was accomplished by rationing the single-nozzle momentum ratio by the numbers of nozzles (2/6). The "effective" single-

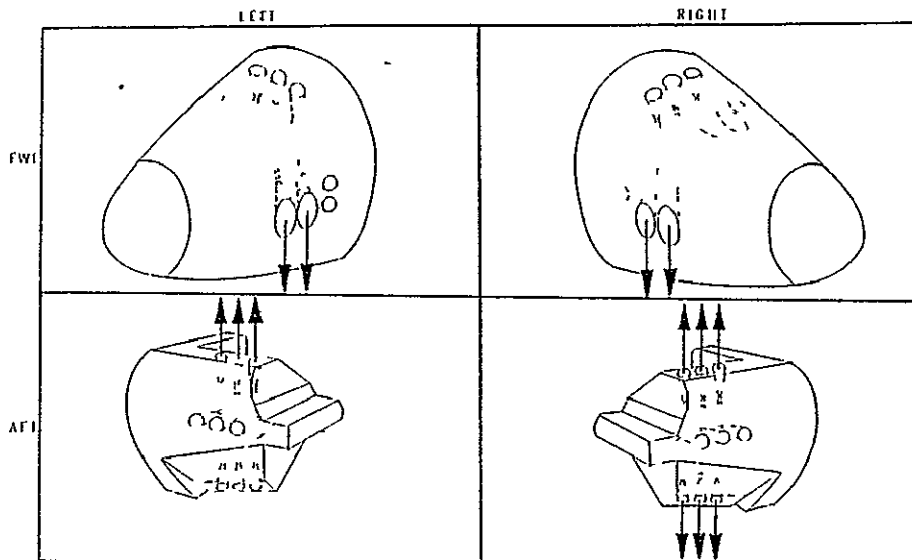
nozzle momentum ratio was then applied directly to the RC06 fits. Flight cases with high dynamic pressure may result in momentum ratios lower than those tested for RC06. This extrapolation is toward the limiting case of zero increments at the jet-off limit and the extrapolation is in the range of the curve fit applicability.

7.1.2.5 UYCMD = -3

This case is the RC06 data given in Subsection 7.1.1.5.

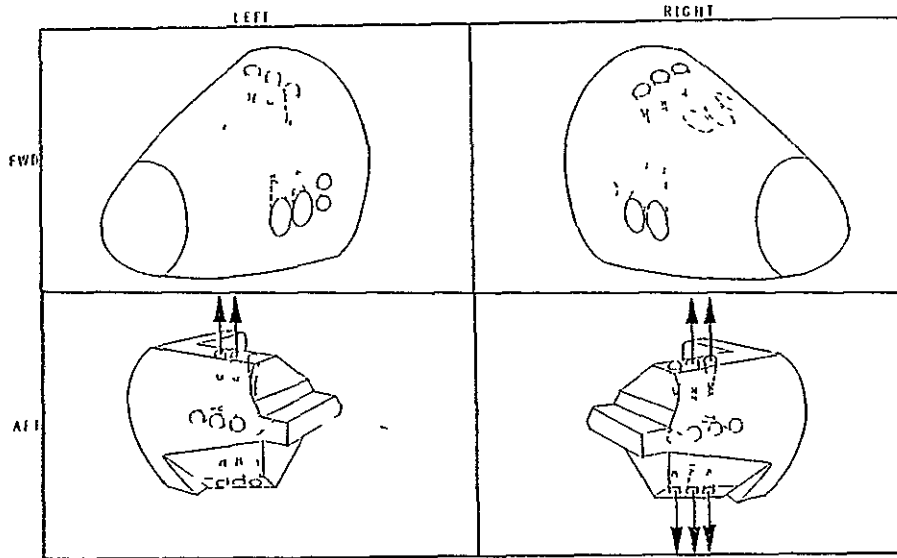
7.1.3 UXCMD = -2

7.1.3.1 UYCMD = 5



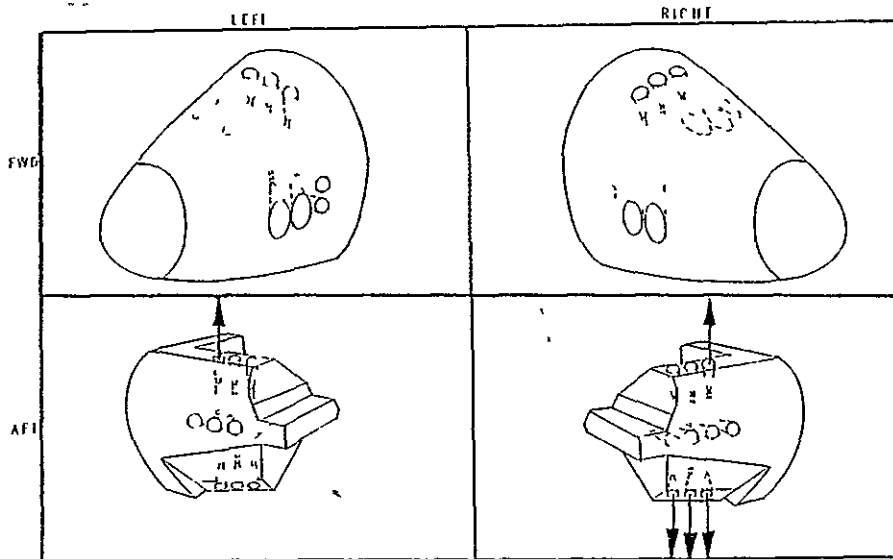
No data were generated for this combination. However, it is the same as RC38 (Subsection 7.1.1.1), except the three rear-mounted pitch-down jets are on the opposite side of the vehicle. These increments are derived by assuming symmetry with RC38 for the zero yaw case, which means that the signs of the lateral-directional data are reversed, while the longitudinal data are unchanged. The yaw data must account for windward and leeward positions of the asymmetric jets, which means a mirror image is assumed. Thus, the data for -4° yaw for this case uses the data for $+4^\circ$ yaw for RC38, and vice versa. The signs of the lateral-directional data must also be reversed, to complete the interchange.

7.1.3.2 UYCMD = 1



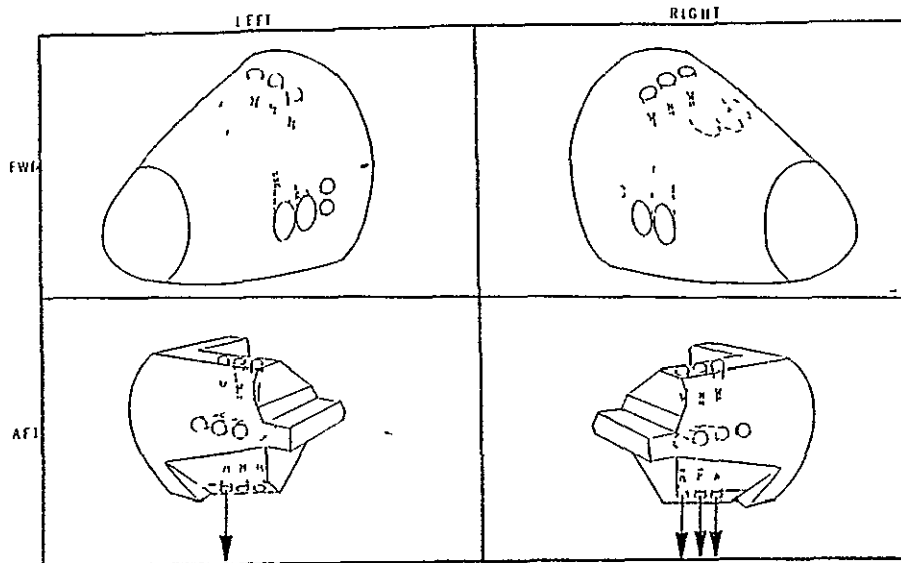
This case is the mirror image of the UXCMD = 2, UYCMD = 1 case described in Subsection 7.1.1.2. The data is derived as defined in that section, the lateral-directional signs are reversed, and the plus and minus yaw cases interchanged.

7.1.3.3 UYCMD = 0



This combination is a mirror image of RC61 which is defined in Subsection 7.1.1.3.

7.1.3.4 UYCMD = -1



This combination is a mirror image of the UXCMD = 2, UYCMD = -1 case defined in Subsection 7.1.1.4 and is derived from that data by using the interpolated RC06 case with the mirror image of (RC40 - RC11) interpolated by 2/3.

7.1.3.5 UYCMD = -3

This is the RC06 combination given in Subsection 7.1.1.5.

7.2 UZCMD = 1, -1

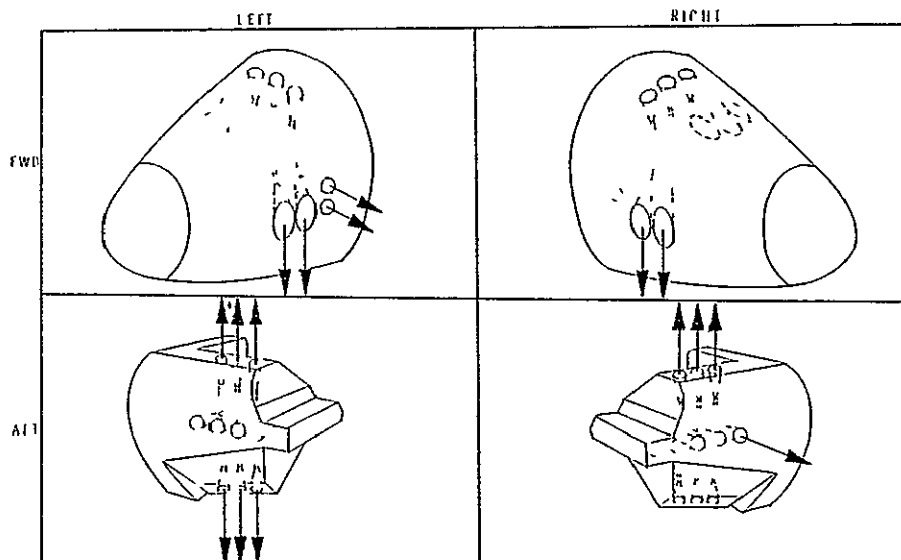
These combinations in general differ from the UZCMD = 0 cases by the addition of two forward-mounted yaw jets on the left side and one rear-mounted yaw jet on the right side, which is the RC78 combination. All of the missing curve fits were generated using RC78 combined with the UZCMD = 0 combinations.

The UZCMD = -1 combinations are exactly the same as the UZCMD = +1 combination, except that the forward-mounted right yaw thrusters and rear-mounted left yaw thrusters are used. These combinations are all generated by removing RC78 increments from the UZCMD = +1 combinations and adding reversed RC78 increments into the combinations.

7.2.1 UXCMD = 2

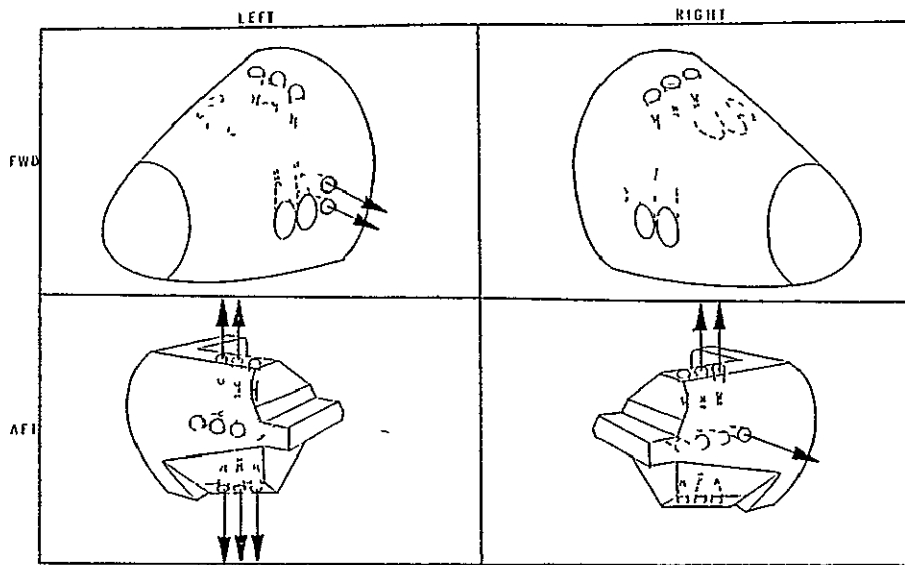
ORIGINAL PAGE IS
OF POOR QUALITY

7.2.1.1 UYCMD = 5



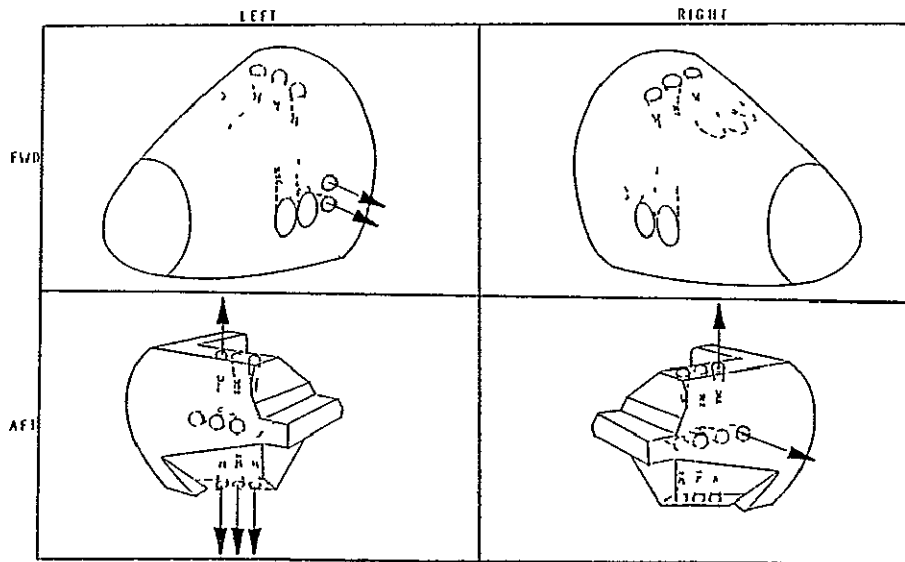
The zero yaw data is available as the RC82 data. However, no data was obtained at positive or negative yaw. The yaw increments were constructed as the sum of RC38 and RC78 data. A comparison of RC82 and the sum of RC38 and RC78 is given in Section 6 at zero yaw angle.

7.2.1.2 UYCMD = 1



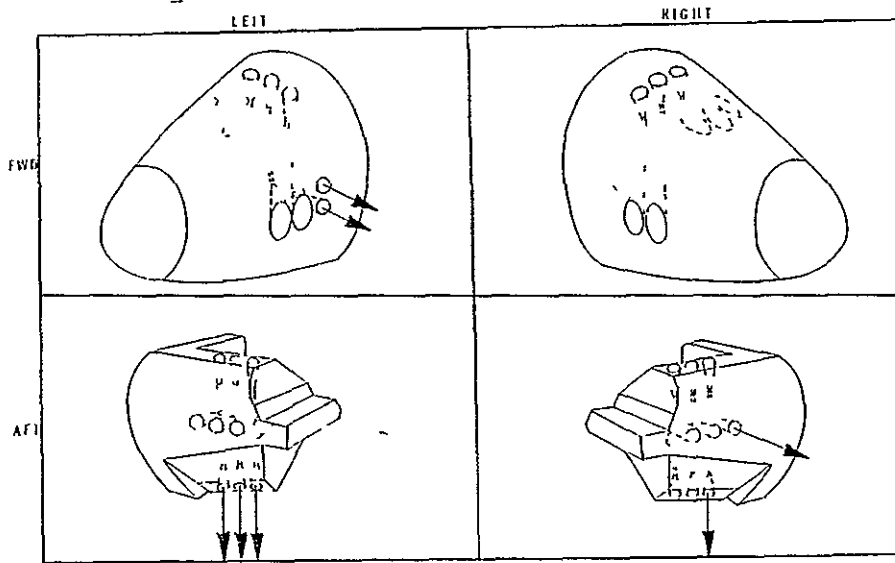
This control combination was generated as the sum of RC78 with the control combination of Subsection 7.1.1.2, which is the average of RC40 and RC61. The sum of RC87 plus RC89 was not used because RC87 had only zero yaw data.

7.2.1.3 UYCMD = 0



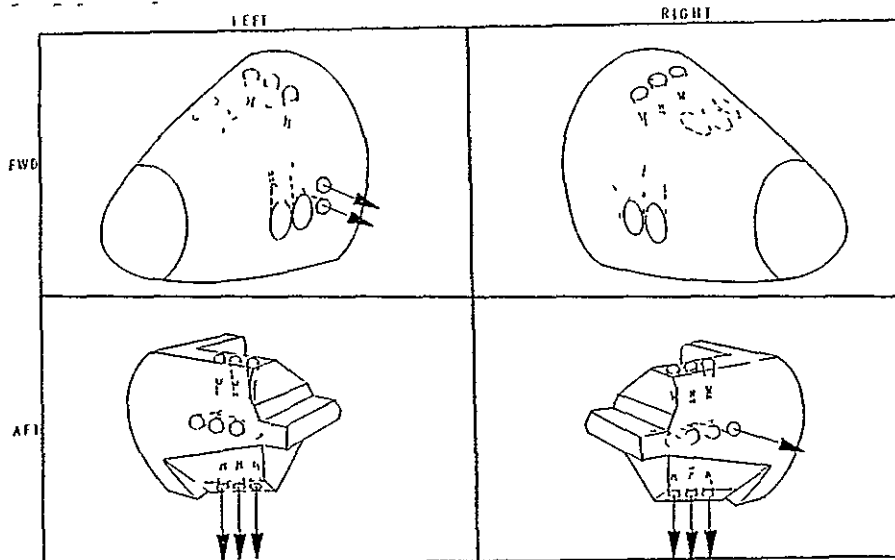
The RC89 data provide the models for this combination of reaction controls.

7.2.1.4 UYCMD = -1



These data are made up by summing RC78 data with the data discussed in Subsection 7.1.1.4. Thus the data from 4 test RCs are combined to generate this model, and the reliability of the estimates must be low compared to cases where test data are available.

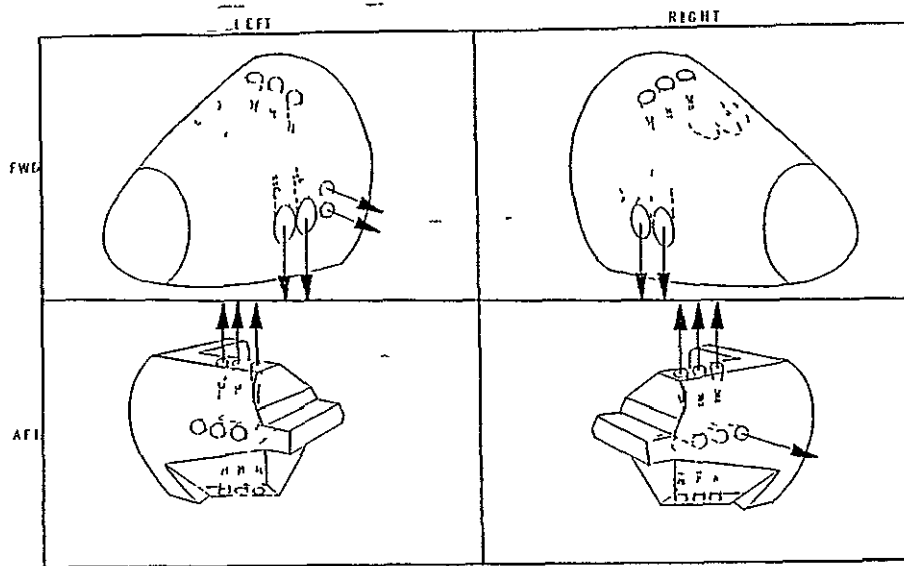
7.2.1.5 UYCMD = -3



The IA148 test data for RC55 are the basis of this model.

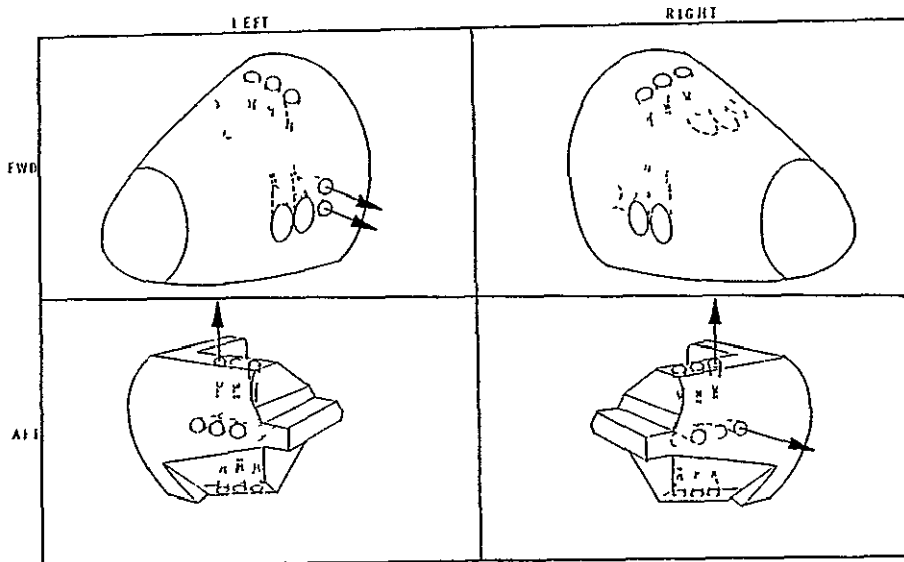
7.2.2 UXCMD = 0

7.2.2.1 UYCMD = 5



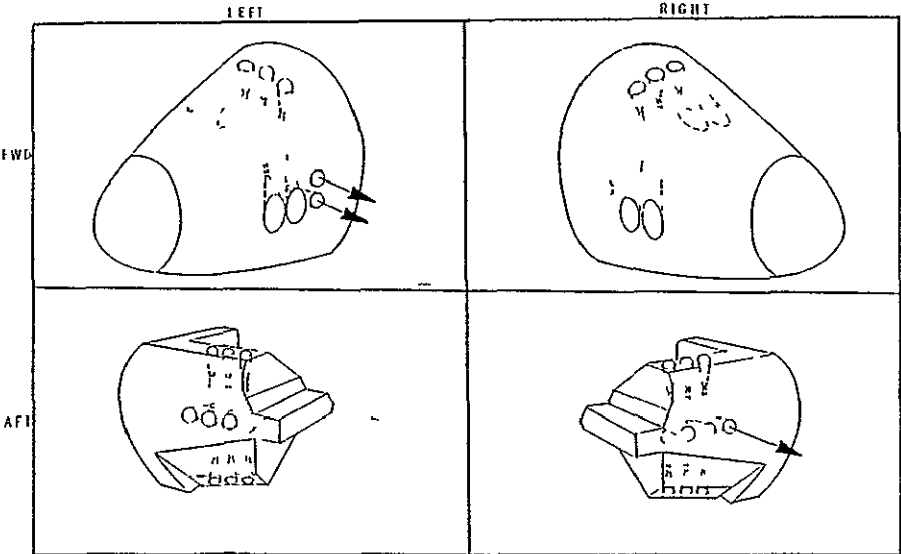
RC51 test data are available to define the zero yaw angle case for this combination. RC62 plus RC78 data must be used to define the $+4^\circ$ and -4° yaw cases. Section 6 presents a comparison of RC51 and the sum of RC78 plus RC62 at zero yaw.

7.2.2.2 UYCMD = 1



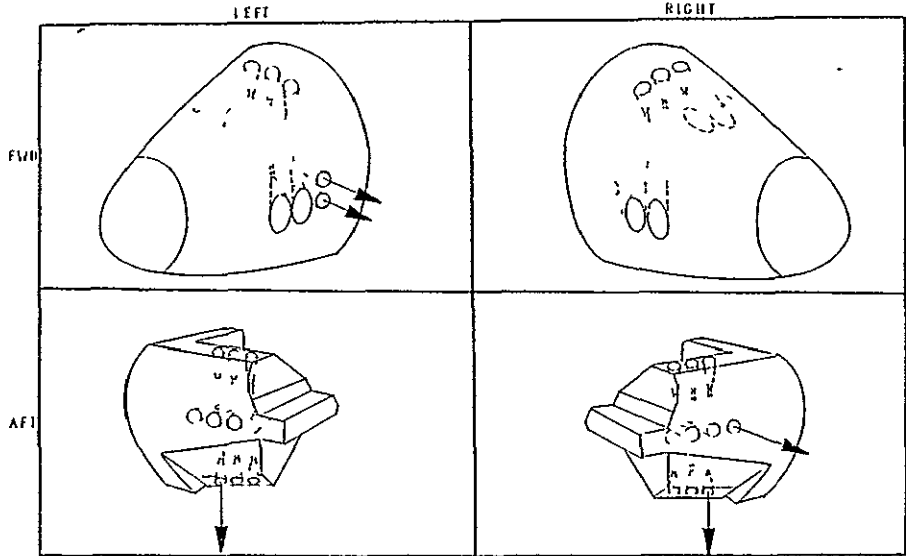
RC77 data are available for the zero yaw cases, while the sum of RC37 and RC78 is used to generate the models for $\pm 4^\circ$ yaw.

7.2.2.3 UYCMD = 0



This is the RC78 reaction control combination tested in test IA148 and the curve fits apply directly.

7.2.2.4 UYCMD = -1



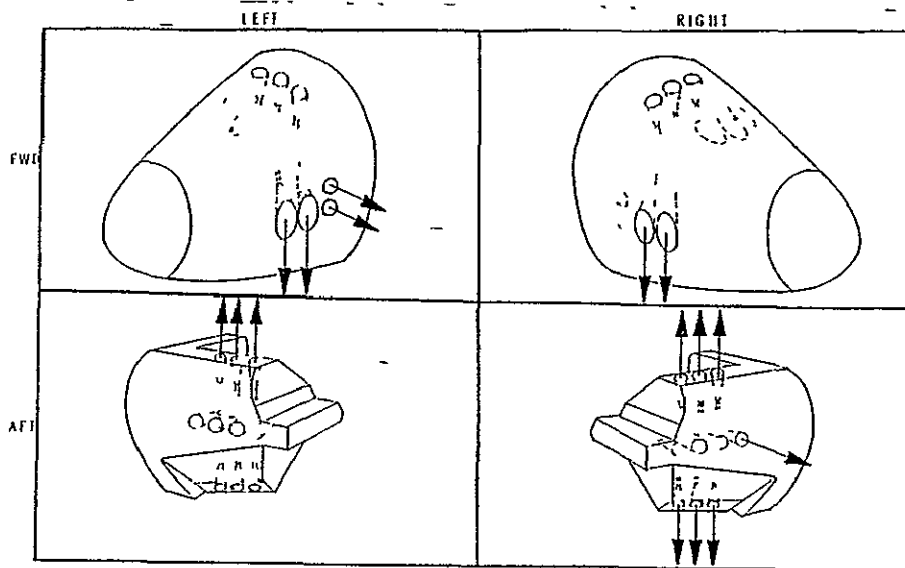
The summation of RC78 with the data developed in Subsection 7.1.2.4 is used to define this model.

7.2.2.5 UYCMD = -3

This case is the same as RC55 defined in Subsection 7.2.1.5.

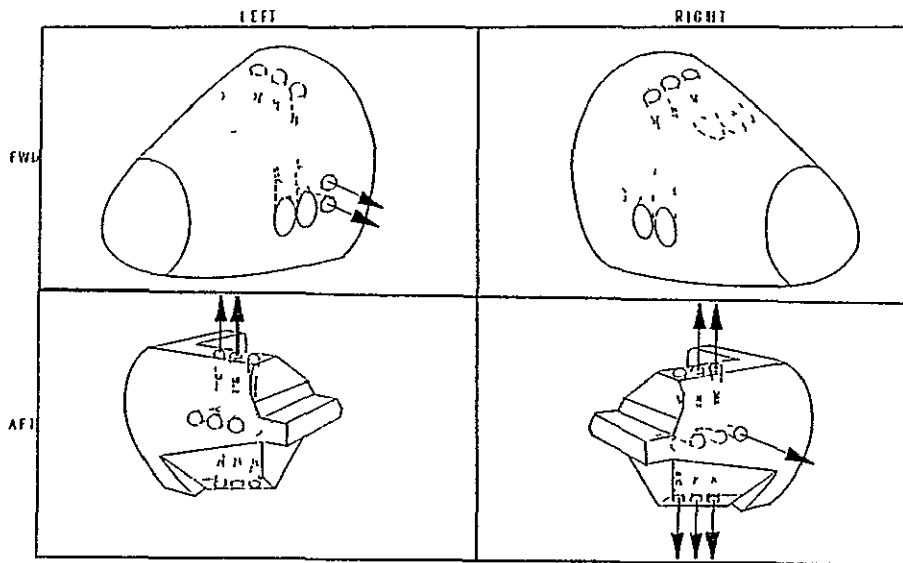
7.2.3 UXCMD = -2

7.2.3.1 UYCMD = 5



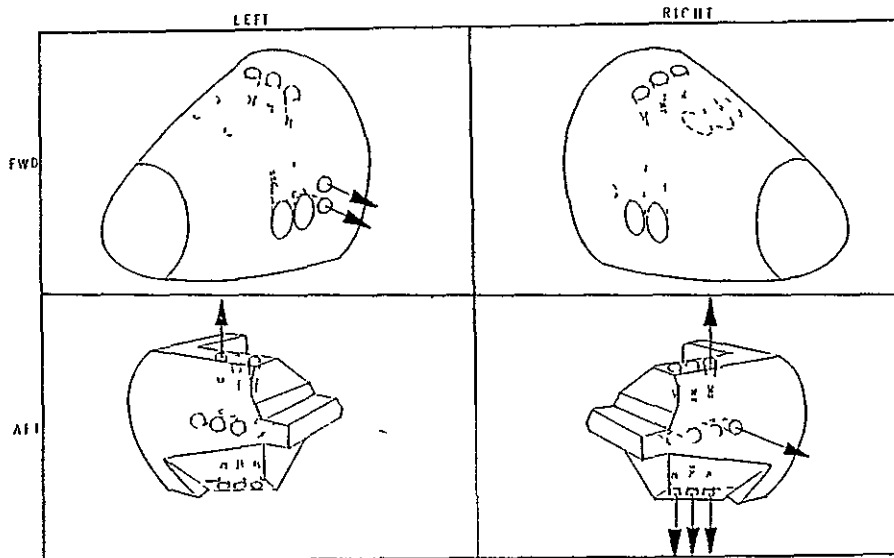
This combination was generated using the sum of RC78 with the mirror image of RC38.

7.2.3.2 UYCMD = 1



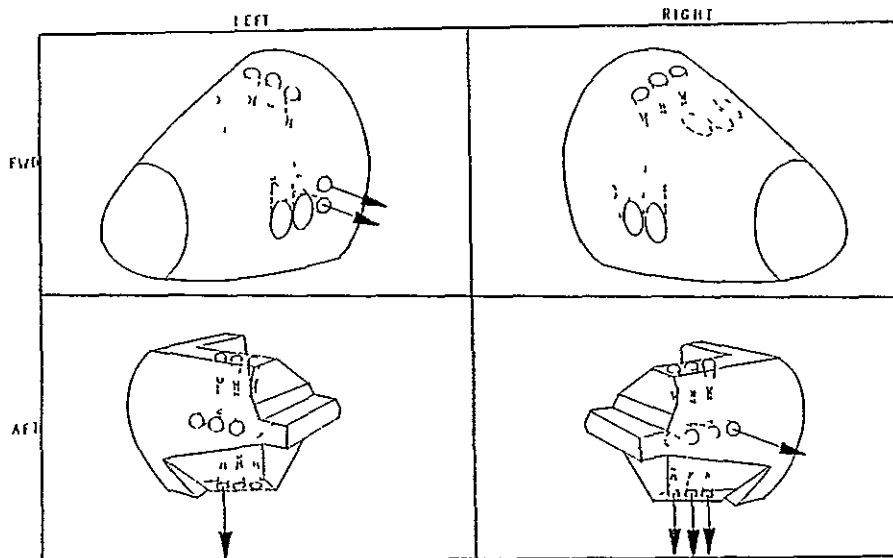
The required model was obtained as the sum of RC78 with the mirror image of the average between RC61 and RC40.

7.2.3.3 UYCMD = 0



RC94 data obtained in test IA148 provide the models for this control combination.

7.2.3.4 UYCMD = -1



This combination is the sum of RC78 with the model defined in Subsection 7.1.3.4.

7.2.3.5 UYCMD = -3

RC55 data defined in Subsection 7.2.1.5 is used for the control selection.

7.3 MATED CONFIGURATION INCREMENTAL EFFECTS PREDICTION ROUTINES

Subsections 7.1 and 7.2 define the methods used to generate data for all of the allowable control command combinations. A complete set of curve fit equations would be 25 combinations at 3 yaw angles at 14 angles of attack for the 6 aerodynamic force and moment coefficients, or 6300 curve fit equations. It was decided that a more efficient approach would be to use the existing set of curve fit data from IA148 and to develop a computer routine to define the others, based on the methods discussed in Subsections 7.1 and 7.2. Two subroutines, RCS and FITS, were written to perform these computations and are listed in Appendix D. The basic operations are shown schematically in Figures 7-1 and 7-2.

7.3.1 RCS SUBROUTINE. The six required inputs to the RCS subroutine are shown in Figure 7-1. They are:

- a. UZCMD - yaw control command
- b. UXCMD - roll control command
- c. UYCMD - pitch control command
- d. ALPHA - angle of attack in degrees
- e. BETA - yaw angle in degrees
- f. XMOM - single nozzle momentum ratio defined by equation 6-3

This subroutine performs all computations in assembling the required control combinations by calling the FITS subroutine to compute the incremental values at 0, +4, and -4 degrees yaw for each individual control combination. The routine uses the three command variables to branch to the correct combination of control requirements using UZCMD as the primary level. The proper branch is selected from the two available branches, based on UZCMD being zero or nonzero. Within each UZCMD path, the second level branching is based on the UXCMD command. Three paths exist and the selections are made for UXCMD less than zero, less than 1.0, and greater than 1.0. The third level branching occurs based on the value of UYCMD. Five different paths are selected by the following criteria:

- a. UYCMD = 5
- b. UYCMD < 5
- c. UYCMD < 1
- d. UYCMD < 0
- e. UYCMD < -1

After selection of a unique control case (defined in Subsections 7.1 or 7.2), the subroutine assembles the required combination by calling subroutine FITS with proper definitions of the RC combination ID, the momentum ratio, and the angle of attack.

FITS returns with values of the six aerodynamic increments computed at the correct momentum ratio and interpolated for angle of attack differences for 0, +4, and -4 degrees yaw. The subroutine RCS repeats these calls to FITS as many times as necessary to assemble increments for the desired control combination; it also corrects the increments for symmetry and mirror image computations as required.

When these operations are completed, the increments are corrected for yaw angle effects and are resolved into true body axis output. The output is the incremental aerodynamic coefficients due to interaction between the RCS exhaust plumes and the external flow over the vehicle for the mated orbiter-plus-tank configuration. Figure 7-3 shows the sign convention for the following

C_x = Incremental axial force coefficient

C_y = Incremental side force coefficient

ORIGINAL PAGE IS
OF POOR QUALITY

C_z = Incremental vertical force coefficient

C_ℓ = Incremental rolling moment coefficient

C_m = Incremental pitching moment coefficient

C_n = Incremental yawing moment coefficient

Thrust and impingement computations are not included in these data and must be made elsewhere to compute the total RCS effectiveness.

7.3.2 FITS SUBROUTINE. Subroutine FITS is used to store the existing curve fit data from test IA148 and to provide computed aerodynamic coefficients as called by subroutine RCS (Figure 7-2). Three sets of tables of curve fits are stored in FITS through data declaration statements. The first set represents the zero yaw data from IA148 and contains coefficients for RC06, RC11, RC37, RC38, RC40, RC51, RC55, RC61, RC62, RC77, RC78, RC82, RC87, RC89, and RC94. The second set represents the 4-degree yaw data and contains coefficients for RC06, RC11, RC37, RC38, RC40, RC55, RC61, RC62, RC78, RC89, and RC94. The third set representing the -4-degree yaw data contains fits for RC38, RC40, RC55, RC61, RC78, RC89, and RC94.

The data are stored in three-dimensional arrays of curve fit coefficients. AO0, AP0, and AM0 represent the a_0 term of equation 6-8 for the zero, +4, and -4 degree yaw cases. AO1, AP1, and AM1 are the a_1 terms of the curve fit equation while AO2, AP2, and AM2 represent the a_2 terms. The subscripts (for example AO0(I, IB, J)) of the curve fits are defined as:

I = ID for determining the RC data set to where it belongs

IB = Angle-of-attack index (14 values)

J = Aerodynamic force or moment
1 = normal force
2 = axial force
3 = pitching moment
4 = rolling moment
5 = yawing moment
6 = side force

The order of loading of coefficients is specified in the parameters JD, KD, and LD which specify the ID number order for 0, +4, and -4 degree yaw tables, respectively. The parameter AL specifies the order of tables in terms of angle of attack.

The required input to subroutine FITS includes:

- a. ID - RC code number from test IA148
- b. ALPH - Angle of attack in degrees
- c. XMR - Momentum Ratio

The subroutine first computes the index number for correct angle-of-attack sets. A linear interpolation/extrapolation term is also computed to correct the data between the angles of attack for which the curve fits are made. If the angle of attack exceeds the range of the curve fits, linear extrapolations are made.

Subroutine FITS then computes the index for the zero yaw curve fits and the program terminates if the proper ID is not found. The zero yaw coefficients for the six aerodynamic components are computed with interpolations due to angle of attack.

The index for the +4 degree data is then determined and the curve fit coefficients computed in a similar manner to the zero yaw coefficients. If the proper ID does not exist in the +4 degree yaw table, the last value of index is used. This is necessary because some cases, such as RC51 and RC82, have no data except at zero yaw. This approach allows dummy computations in FITS which are corrected in RCS where the yaw cases are generated by summing other sets.

The index for the negative yaw case is computed and the coefficients assembled, if the data exists. If the proper ID is not found, the negative yaw coefficients are computed from the positive yaw coefficients by assuming symmetry. If this is not true, it remains for subroutine RCS to correct the data.

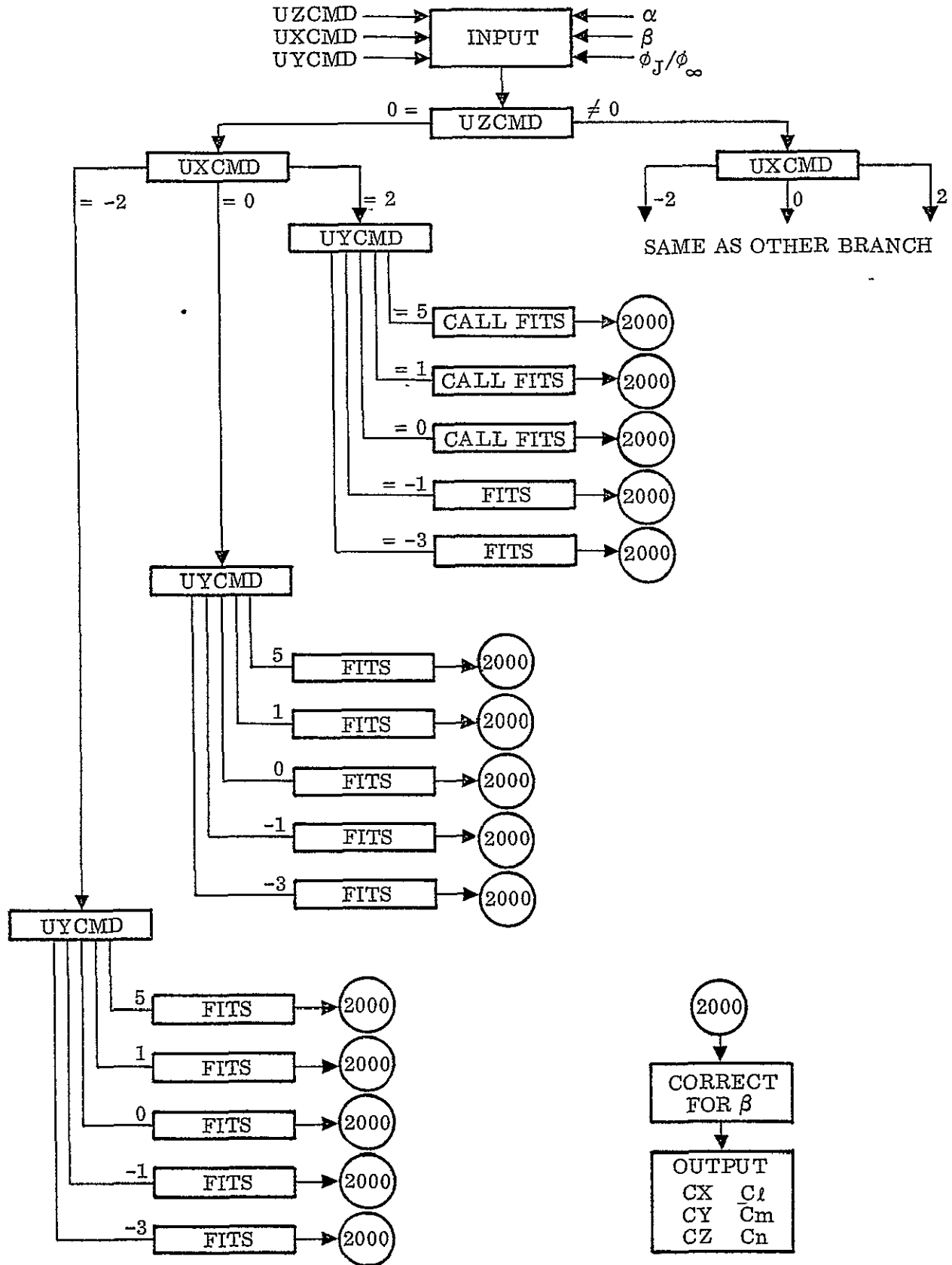


Figure 7-1. Schematic flow diagram for RCS subroutine.

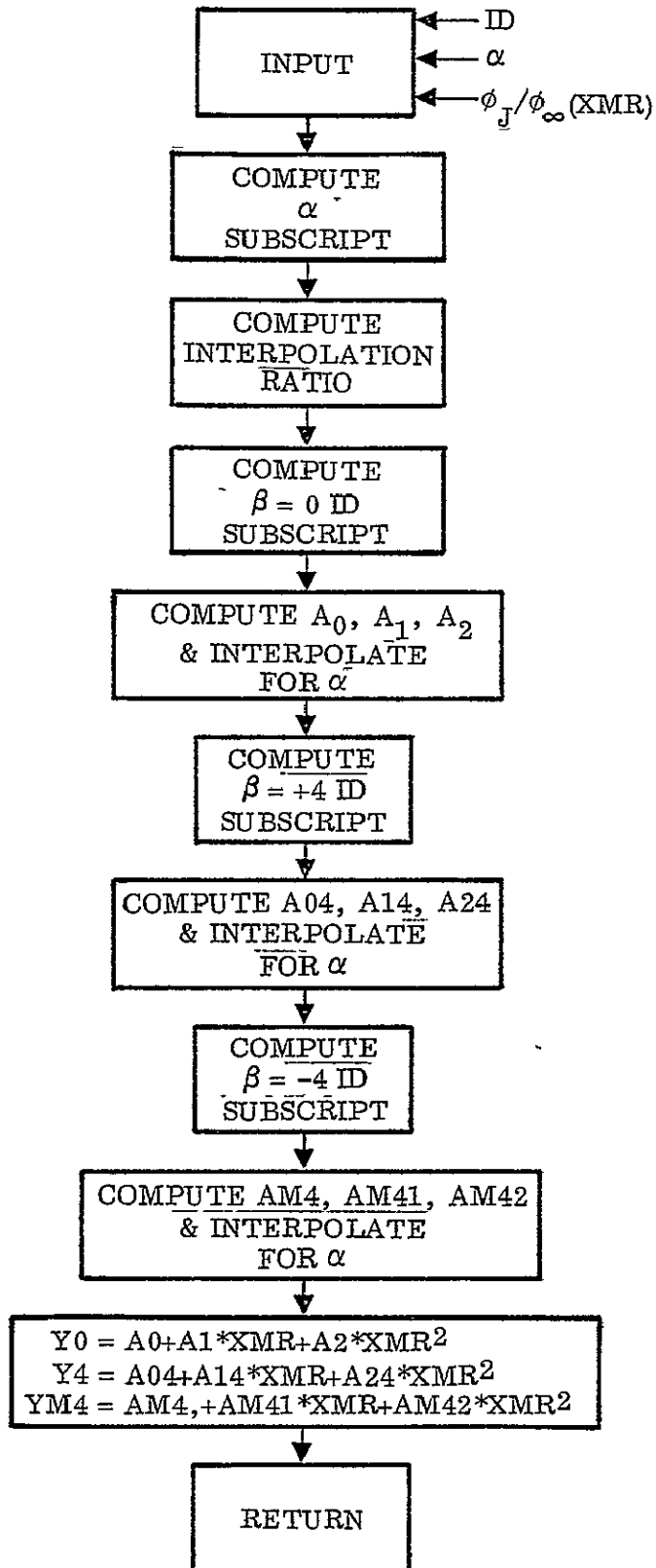
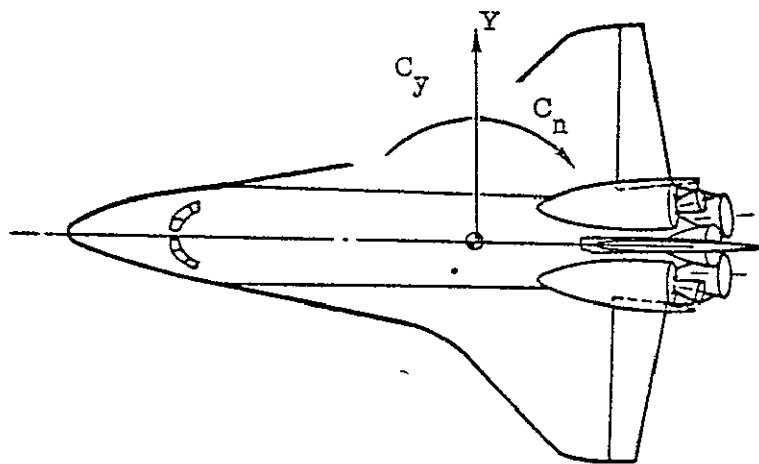
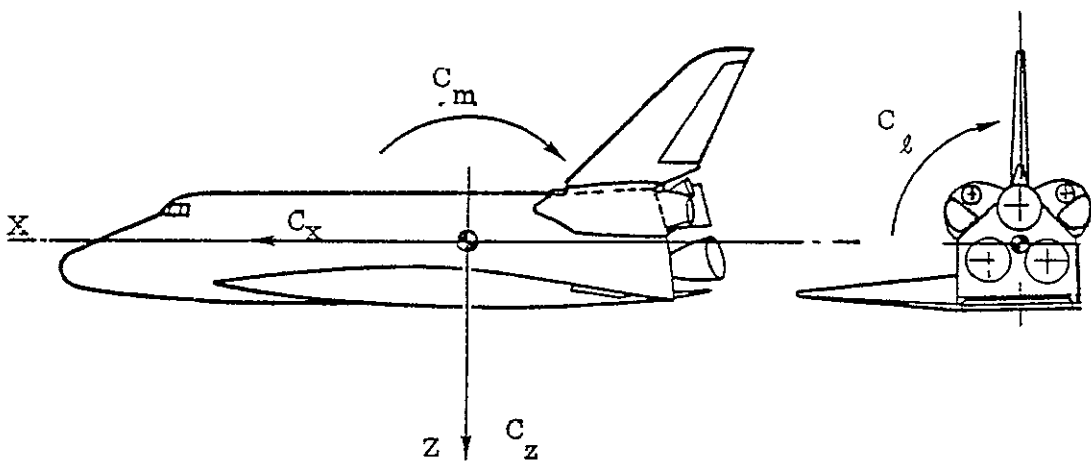


Figure 7-2. Schematic flow diagram for FITS subroutine.



ORIGINAL PAGE IS
OF POOR QUALITY



$$C_N = -C_z$$

$$C_A = -C_x$$

Figure 7-3. Body axis sign convention.

8

CONCLUSIONS

Analysis of wind-tunnel data has shown that aerodynamic interference exists between the reaction control system plumes and the flow over the Orbiter vehicle, with or without the external tank. These interference terms must be taken into account when computing vehicle control due to reaction controls, because they can be large relative to the thrust components. The interference terms have been correlated with the nozzle flow parameter (of which the most important is momentum ratio) and analytic models have been developed.

The present phase of the study concentrated on the following areas

- a. Yaw effects on RCS during entry
- b. RTLS error analysis
- c. Mated vehicle RCS interactions

8.1 STUDY CONCLUSIONS

- a. The effects of yaw on rear-mounted RCS interactions during entry were found to be within the accuracy bands of the zero yaw data.
- b. The most severe problem during RTLS abort is to maintain roll control, but this can be accomplished by the proper scheduling of pitch-up/pitch-down asymmetric roll control.
- c. RCS roll control can be maximized at any angle of attack or flight condition if the dynamic pressure can be computed and used to schedule asymmetric pitch-up or pitch-down roll control.
- d. Forward-mounted pitch jets were shown to have no interference with aft-mounted pitch jets for the Orbiter alone.
- e. Mated (tank-on) configuration data correlated very well using single-nozzle momentum ratio as the parameter which is used to correlate the data to flight conditions.
- f. There appear to be significant effects of yaw angle in the mated configuration data which were included in the analytic model.

- g. Superposition of jet combination data appears to work better for the cases where forward-mounted pitch and yaw jets are not combined.
- h. The intercept value, a_0 , of the curve fit-coefficients should be removed when applying the results to flight simulations because this term accounts for wind tunnel test repeatability.
- 1. All mated configuration control combinations can be generated from IA148 test data, but the confidence is lower for combinations where forward-mounted pitch and yaw jets are combined or where more than two data sets are used to generate the combination.

8.2 STUDY RECOMMENDATIONS

- a. A blade-mounted model should be built with a better representation of base geometry to evaluate sting interference.
- b. A vacuum chamber test of symmetric pitch-down RCS should be performed with a good base geometry representation (no sting) to evaluate symmetric pitch-down cross-coupling in the base region.
- c. Test data should be obtained on mated configuration RCS combinations not covered in test IA148.

9

REFERENCES

1. Rausch, J.R., "Space Shuttle Orbiter Rear Mounted Reaction Control System Jet Interaction Study Final Report," Convair Report CASD-NSC-77-003, May 1977.
2. Rausch, J.R. and Roberge, A.M., "RCS Jet-Flow Interaction Effects on the Aerodynamics of the Space Shuttle Orbiter," Convair Report CASD-NAS-73-020, November 1973.
3. Rausch, J.R. and Shih, K.T., "Space Orbiter Reaction Control System Jet Interaction Study Interim Report," Convair Report CASD-NSC-74-009, November 1974.
4. Rausch, J.R., "Space Shuttle Orbiter Reaction Control System Jet Interaction Study Final Report," Convair Report CASD-NSC-75-002, June 1975.
5. Chrysler DATAMAN: "Results of Test MA22 in the NASA/LaRC 31-inch CFHT On An 0.10-scale Model (32-0) of the Space Shuttle Configuration 3 to Determine RCS Jet Flow Field Interaction," Chrysler DATAMAN DMS-DR-2267, NASA CR-147, 604-7, May 1976.
6. Best, J.T., "Results of Tests to Determine the Interaction Effects of the Orbiter Reaction Control System Thruster Jet Plumes on the Space Shuttle Vehicle Aerodynamics at Mach number 6 (Test OA 169)," AEDC-DR-76-56, July 1976.
7. Daileda, J.J., "Pretest Information for RTLS Abort Separation Tests IA22/OA169 Using the .0125 Scale SSV Model In the AEDC VKF Tunnel B," Rockwell Report SD75-SH-0256, 16 February 1976.
8. Best, J.T. and Wagner, D.A., "Results of Tests to Determine the Interaction Effects of the Orbiter Reaction Control System Thruster Jet Plumes on the Space Shuttle Vehicle Aerodynamics during the RTLS Abort Maneuvers at Mach Number 6 (Test IA 148)" AEDC Report AEDC-DR-77-49, 17 June 1977.
9. "U.S. Standard Atmosphere, 1976," National Oceanic and Atmospheric Administration NOAA S/T76-1562, October 1976.

APPENDIX A

IA148 CURVE FIT COEFFICIENTS
AT ZERO DEGREES YAW

Table A1. RC06 Incremental Normal Force Coefficient at $\beta=0^\circ$.

$$\Delta C = a_0 + a_1 x + a_2 x^2$$

α	a_0	a_1	a_2	σ
-14	-.005567	- 3.0184	10.2744	.00400
-12	-.005590	- 3.3973	16.5761	.00390
- 9	-.005070	- 2.2595	- 38.4040	.00420
- 6	-.005170	- 2.0011	- 56.0651	.00400
- 4.5	-.005550	- 2.2795	- 53.4176	.00410
- 3	-.004980	- 2.7341	- 42.8578	.00390
- 1.5	-.005390	- 2.9763	- 35.7407	.00340
0	-.005900	- 3.2802	- 22.0907	.00330
1.5	-.005300	- 3.3460	- 17.9108	.00330
3	-.005170	- 3.4889	- 8.9492	.00320
4.5	-.004510	- 3.4920	- 8.3356	.00270
6	-.004750	- 3.5654	- 6.6444	.00270
9	-.004730	- 3.2982	- 25.8359	.00260
12.35	-.004860	- 3.2800	- 32.5296	.00260

Table A2. RC06 Incremental Axial Force Coefficient at $\beta=0^\circ$.

$$\Delta C = a_0 + a_1 x + a_2 x^2$$

α	a_0	a_1	a_2	σ
-14	-.00478	- 3.7849	43.8674	.00230
-12	-.00498	- 4.1283	56.2186	.00230
- 9	-.00514	- 3.7928	41.3972	.00240
- 6	-.00514	- 3.5113	27.5778	.00220
- 4.5	-.00502	- 3.5557	29.1527	.00210
- 3	-.00510	- 3.6096	31.7841	.00210
- 1.5	-.00518	- 3.6631	33.0481	.00220
0	-.00529	- 3.7019	32.5776	.00230
1.5	-.00543	- 3.8232	35.3675	.00240
3	-.00555	- 3.9370	37.4011	.00230
4.5	-.00564	- 4.0105	38.1869	.00220
6	-.00566	- 4.0000	35.7784	.00210
9	-.00559	- 3.9867	31.8521	.00230
12.35	-.00539	- 4.1724	34.6090	.00240

Table A3. RC06 Incremental Pitching Moment Coefficient at $\beta=0^\circ$.

$$\Delta C = a_0 + a_1 x + a_2 x^2$$

α	a_0	a_1	a_2	σ
-14	-.000909	1.4030	3.5154	.00049
-12	-.001068	1.5810	- 2.3386	.00071
- 9	-.000874	1.2046	12.8978	.00087
- 6	-.001096	.9807	22.1922	.00085
- 4.5	-.001390	1.0744	19.9636	.00103
- 3	-.001150	1.1039	21.1181	.00071
- 1.5	-.001260	1.1101	23.3810	.00072
0	-.001447	1.0815	26.0552	.00060
1.5	-.001238	1.1519	22.7509	.00077
3	-.001213	1.2571	16.3796	.00084
4.5	-.001040	1.3222	11.5527	.00062
6	-.001140	1.3257	11.0190	.00037
9	-.001250	1.3543	12.5760	.00049
12.35	-.001300	1.4327	11.2061	.00037

Table A4. RC06 Incremental Rolling Moment Coefficient at $\beta=0^\circ$.

$$\Delta C = a_0 + a_1 x + a_2 x^2$$

α	a_0	a_1	a_2	σ
-14	-.000301	.0022	1.1067	.00018
-12	-.000206	.0127	.5484	.00015
- 9	-.000168	.0288	- .4543	.00012
- 6	-.000205	.0284	- .0365	.00012
- 4.5	-.000192	.0139	.8404	.00012
- 3	-.000155	.0087	1.1322	.00011
- 1.5	-.000147	.0064	1.2332	.00011
0	-.000140	.0174	.7585	.00010
1.5	-.000137	.0161	.8112	.00010
3	-.000131	.0213	.6635	.00009
4.5	-.000154	.0189	.6446	.00011
6	-.000167	.0143	.7566	.00012
9	-.000166	.0210	.3811	.00013
12.35	-.000146	.0256	.2287	.00012

Table A5. RC06 Incremental Yawing Moment Coefficient at $\beta=0^\circ$.

$$\Delta C = a_0 + a_1 x + a_2 x^2$$

α	a_0	a_1	a_2	σ
-14	.000593	- .0797	1.0710	.00029
-12	.000401	- .0618	.2740	.00022
- 9	.000270	- .0547	- .0430	.00019
- 6	.000306	- .0109	- 1.8136	.00027
- 4.5	.000225	.0243	- 3.0036	.00024
- 3	.000110	.0270	- 3.0388	.00023
- 1.5	.000082	.0147	- 2.4545	.00019
0	.000055	- .0076	- 1.6786	.00019
1.5	.000028	- .0270	- .3550	.00025
3	-.000022	- .0203	- .3761	.00025
4.5	.000016	- .0143	- .1886	.00019
6	.000013	.0048	- 1.0545	.00019
9	-.000077	- .0018	- .7600	.00023
12.35	-.000183	.0051	- .6727	.00029

Table A6. RC06 Incremental Side Force Coefficient at $\beta=0^\circ$.

$$\Delta C = a_0 + a_1 x + a_2 x^2$$

α	a_0	a_1	a_2	σ
-14	.001439	.2694	- 3.6540	.00047
-12	.000927	.3429	- 6.2346	.00036
- 9	.000767	.2822	- 1.9325	.00048
- 6	.000738	.1197	4.7806	.00065
- 4.5	.000232	.1433	2.9372	.00087
- 3	.000003	.1809	1.4454	.00078
- 1.5	-.000297	.2634	- 2.1070	.00064
0	-.000382	.3357	- 4.3923	.00075
1.5	-.000410	.4685	- 9.9102	.00077
3	-.000706	.5227	- 12.2395	.00082
4.5	-.000728	.5963	- 14.4898	.00098
6	-.000924	.5873	- 13.1953	.00107
9	-.001160	.6356	- 15.4348	.00126
12.35	-.001380	.5609	- 13.3016	.00133

Table A7. RC11 Incremental Normal Force Coefficient at $\beta=0^\circ$.

$$\Delta C = a_0 + a_1 x + a_2 x^2$$

α	a_0	a_1	a_2	σ
-14	-.005554	.2555	- 27.2942	.00338
-12	-.005589	.2220	- 25.0938	.00369
- 9	-.005051	.2792	- 27.7104	.00370
- 6	-.005153	.2606	- 27.1202	.00357
- 4.5	-.005534	.3184	- 31.7682	.00339
- 3	-.004956	.2775	- 31.4307	.00358
- 1.5	-.005389	.2791	- 36.9901	.00364
0	-.005916	.1176	- 35.1237	.00387
1.5	-.005326	.0627	- 39.2109	.00323
3	-.005186	- .2695	- 28.8914	.00303
4.5	-.004510	- .6368	- 17.0588	.00329
6	-.004771	- 1.0710	- 1.5871	.00270
9	-.004776	- 1.6324	20.0767	.00230
12.35	-.004899	- 1.6923	25.0392	.00209

Table A8. RC11 Incremental Axial Force Coefficient at $\beta=0^\circ$.

$$\Delta C = a_0 + a_1 x + a_2 x^2$$

α	a_0	a_1	a_2	σ
-14	-.004733	- 1.0188	- 1.0624	.00190
-12	-.004940	- 1.0645	2.9413	.00208
- 9	-.005109	- 1.0848	7.4547	.00213
- 6	-.005129	- 1.1469	14.6263	.00214
- 4.5	-.005011	- 1.2058	18.1851	.00212
- 3	-.005102	- 1.2363	20.4603	.00216
- 1.5	-.005191	- 1.2352	21.5569	.00223
0	-.005293	- 1.2115	22.7242	.00231
1.5	-.005429	- 1.1620	23.2879	.00236
3	-.005552	- .9867	18.4666	.00230
4.5	-.005634	- .8003	13.1711	.00215
6	-.005633	- .6843	9.0189	.00195
9	-.005609	- .7981	11.1459	.00214
12.35	-.005367	- .9589	16.5190	.00221

Table A9. RC11 Incremental Pitching Moment Coefficient at $\beta=0^\circ$.

$$\Delta C = a_0 + a_1 x + a_2 x^2$$

α	a_0	a_1	a_2	σ
-14	-.000905	- .0050	9.2262	.00028
-12	-.001075	- .0160	10.3115	.00068
- 9	-.000884	- .0433	10.9559	.00080
- 6	-.001088	- .0585	14.6946	.00068
- 4.5	-.001391	- .0741	15.9073	.00058
- 3	-.001163	- .0721	15.4173	.00061
- 1.5	-.001285	.0148	11.6900	.00061
0	-.001464	.0617	10.1017	.00059
1.5	-.001255	.1240	7.1189	.00073
3	-.001227	.2663	.3939	.00090
4.5	-.001048	.4069	- 6.9787	.00069
6	-.001140	.5021	- 12.7204	.00053
9	-.001236	.3550	- 10.3439	.00076
12.35	-.001288	.1371	- 3.5460	.00035

Table A10. RC11 Incremental Rolling Moment Coefficient at $\beta=0^\circ$.

$$\Delta C = a_0 + a_1 x + a_2 x^2$$

α	a_0	a_1	a_2	σ
-14	-.000284	.0845	- 6.1793	.00035
-12	-.000200	.0022	- 2.6535	.00017
- 9	-.000165	- .0727	.2837	.00023
- 6	-.000201	- .0967	3.0307	.00059
- 4.5	-.000191	- .1126	4.2177	.00051
- 3	-.000156	- .1718	6.2484	.00028
- 1.5	-.000152	- .1734	7.2070	.00027
0	-.000144	- .1516	7.2720	.00025
1.5	-.000144	- .1024	5.6168	.00028
3	-.000140	- .0482	3.6826	.00026
4.5	-.000161	.0034	1.5613	.00020
6	-.000171	.0319	.4638	.00016
9	-.000166	.0588	- 1.3208	.00016
12.35	-.000146	.0109	.1199	.00011

Table A11. RC11 Incremental Yawing Moment Coefficient at $\beta=0^\circ$.

$$\Delta C = a_0 + a_1 x + a_2 x^2$$

α	a_0	a_1	a_2	σ
-14	.000576	.0610	6.0182	.00059
-12	.000401	.1806	.9730	.00028
- 9	.000270	.2953	- 3.6297	.00032
- 6	.000306	.3200	- 7.1635	.00091
- 4.5	.000230	.3396	- 8.5394	.00082
- 3	.000117	.4265	- 11.7135	.00059
- 1.5	.000091	.4009	- 12.0861	.00051
0	.000064	.3466	- 11.4349	.00039
1.5	.000040	.2542	- 7.7424	.00047
3	- .000006	.1951	- 5.4725	.00039
4.5	.000028	.1540	- 3.3620	.00028
6	.000022	.1518	- 3.1765	.00026
9	-.000074	.1174	- 1.0802	.00024
12.35	-.000182	.1631	- 2.5499	.00027

Table A12. RC11 Incremental Side Force Coefficient at $\beta=0^\circ$.

$$\Delta C = a_0 + a_1 x + a_2 x^2$$

α	a_0	a_1	a_2	σ
-14	.001472	- .0606	- 22.3510	.00119
-12	.000942	- .3172	- 9.7726	.00072
- 9	.000777	- .4996	- 1.1514	.00075
- 6	.000742	- .5216	5.8984	.00208
- 4.5	.000223	- .4903	7.1213	.00186
- 3	-.000004	- .6660	13.6677	.00115
- 1.5	-.000305	- .6108	15.3106	.00121
0	-.000382	- .5580	16.7995	.00092
1.5	-.000414	- .4145	12.5870	.00099
3	-.000713	- .2648	8.0022	.00102
4.5	-.000741	- .0879	1.2196	.00095
6	-.000929	.0378	- 3.5183	.00092
9	-.001147	.2471	- 12.6354	.00107
12.35	-.001364	.2471	- 11.5053	.00127

Table A13. RC37 Incremental Normal Force Coefficient at $\beta=0^\circ$.

$$\Delta C = a_0 + a_1 x + a_2 x^2$$

α	a_0	a_1	a_2	σ
-14	-.005550	- .7482	14.6076	.00340
-12	-.005590	- .7955	17.0759	.00360
- 9	-.005080	- .7308	15.7736	.00370
- 6	-.005190	- .5668	10.7221	.00350
- 4.5	-.005580	- .5716	10.9729	.00330
- 3	-.005010	- .5993	10.8404	.00350
- 1.5	-.005450	- .6276	9.8784	.00350
0	-.005960	- .5122	4.5676	.00330
1.5	-.005370	- .4991	2.4806	.00310
3	-.005220	- .4383	- 1.1469	.00290
4.5	-.004540	- .5396	- .4130	.00280
6	-.004800	- .6329	.3167	.00260
9	-.004790	- .9288	6.5481	.00230
12.35	-.004900	- 1.0784	10.8042	.00210

Table A14. RC37 Incremental Axial Force Coefficient at $\beta=0^\circ$.

$$\Delta C = a_0 + a_1 x + a_2 x^2$$

α	a_0	a_1	a_2	σ
-14	-.004720	- .3411	2.1741	.00200
-12	-.004920	- .2484	- 2.1433	.00210
- 9	-.005080	- .2274	- 3.4511	.00210
- 6	-.005100	- .2924	- .3260	.00210
- 4.5	-.004980	- .3091	- .7052	.00210
- 3	-.005060	- .3297	- 1.2225	.00210
- 1.5	-.005140	- .3903	.0385	.00210
0	-.005250	- .4564	2.5684	.00220
1.5	-.005380	- .5059	5.6757	.00220
3	-.005520	- .5188	8.2839	.00220
4.5	-.005620	- .4722	9.2922	.00210
6	-.005630	- .3626	6.8587	.00210
9	-.005560	- .1981	- 1.3045	.00220
12.35	-.005360	- .2858	- .0035	.00220

Table A15. RC37 Incremental Pitching Moment Coefficient at $\beta=0^\circ$.

$$\Delta C = a_0 + a_1 x + a_2 x^2$$

α	a_0	a_1	a_2	σ
-14	-.000916	.3042	- 1.8987	.00025
-12	-.001076	.3286	- 3.4805	.00066
- 9	-.000881	.2927	- 3.7715	.00066
- 6	-.001087	.2450	- 2.0979	.00071
- 4.5	-.001389	.1986	- .6161	.00061
- 3	-.001153	.1732	- .5235	.00053
- 1.5	-.001271	.1493	.2418	.00052
0	-.001447	.1408	1.1235	.00053
1.5	-.001236	.0562	4.6671	.00056
3	-.001209	.0292	6.8597	.00061
4.5	-.001037	.0343	7.5526	.00053
6	-.001145	.1449	3.7243	.00044
9	-.001244	.2724	- 3.1423	.00045
12.35	-.001286	.1540	- .6657	.00045

Table A16. RC37 Incremental Rolling Moment Coefficient at $\beta=0^\circ$.

$$\Delta C = a_0 + a_1 x + a_2 x^2$$

α	a_0	a_1	a_2	σ
-14	-.000299	- .0118	1.1039	.00013
-12	-.000204	.0201	- .8823	.00017
- 9	-.000169	.0374	- 2.6594	.00015
- 6	-.000206	.0471	- 3.2462	.00012
- 4.5	-.000190	.0448	- 3.3677	.00018
- 3	-.000152	.0293	- 3.1110	.00018
- 1.5	-.000142	- .0002	- 2.1891	.00017
0	-.000134	- .0333	- .8962	.00018
1.5	-.000132	- .0704	.6893	.00017
3	-.000129	- .1086	2.5267	.00017
4.5	-.000153	- .1317	4.0353	.00017
6	-.000168	- .1135	3.8837	.00024
9	-.000168	- .0285	1.1315	.00013
12.35	-.000148	- .0092	.4028	.00012

Table A17. RC37 Incremental Yawing Moment Coefficient at $\beta=0^\circ$.

$$\Delta C = a_0 + a_1 x + a_2 x^2$$

α	a_0	a_1	a_2	σ
-14	.000595	.0426	- 2.4734	.00027
-12	.000400	.0074	.3141	.00028
- 9	.000271	.0015	2.3682	.00024
- 6	.000311	- .0040	3.0536	.00020
- 4.5	.000226	.0055	3.0773	.00030
- 3	.000106	.0283	2.7049	.00028
- 1.5	.000073	.0817	.7272	.00028
0	.000046	.1322	- 1.5459	.00028
1.5	.000021	.1922	- 4.2015	.00025
3	-.000023	.2531	- 6.9912	.00023
4.5	.000018	.2804	- 8.5817	.00021
6	.000018	.2547	- 8.0452	.00032
9	-.000072	.1391	- 4.0420	.00028
12.35	-.000180	.1365	- 4.0758	.00028

Table A18. RC37 Incremental Side Force Coefficient at $\beta=0^\circ$.

$$\Delta C = a_0 + a_1 x + a_2 x^2$$

α	a_0	a_1	a_2	σ
-14	.001433	- .1922	3.7487	.00052
-12	.000918	- .0635	- 2.7695	.00052
- 9	.000758	.0550	- 10.1642	.00045
- 6	.000729	.0720	- 10.1003	.00062
- 4.5	.000229	.1144	- 11.2808	.00090
- 3	.000019	.0865	- 10.5917	.00092
- 1.5	-.000274	.0622	- 9.6999	.00073
0	-.000353	- .0347	- 5.9889	.00095
1.5	-.000382	- .1444	- 1.2138	.00096
3	-.000687	- .2730	4.7946	.00089
4.5	-.000722	- .3518	10.0263	.00088
6	-.000923	- .2973	9.5601	.00107
9	-.001159	- .0655	3.7525	.00108
12.35	-.001390	.0158	1.6123	.00122

Table A19. RC38 Incremental Normal Force Coefficient at $\beta=0^\circ$.

$$\Delta C = a_0 + a_1 x + a_2 x^2$$

α	a_0	a_1	a_2	σ
-14	-.005684	- 4.6993	- 4.7435	.00461
-12	-.005697	- 4.1014	- 20.4066	.00486
- 9	-.005182	- 3.2343	- 46.9895	.00483
- 6	-.005312	- 2.7922	- 61.8816	.00433
- 4.5	-.005675	- 2.8009	- 57.9836	.00412
- 3	-.005081	- 2.9519	- 44.8172	.00454
- 1.5	-.005507	- 2.6925	- 47.8652	.00442
0	-.006046	- 2.4027	- 54.9510	.00407
1.5	-.005461	- 2.1104	- 64.6451	.00421
3	-.005351	- 1.8656	- 72.0056	.00446
4.5	-.004655	- 1.6790	- 77.0703	.00373
6	-.004911	- 1.4736	- 80.0539	.00410
9	-.004882	- 1.3845	- 59.9822	.00405
12.35	-.005005	- 1.8763	- 29.9712	.00319

Table A20. RC38 Incremental Axial Force Coefficient at $\beta=0^\circ$.

$$\Delta C = a_0 + a_1 x + a_2 x^2$$

α	a_0	a_1	a_2	σ
-14	-.004685	- 3.1929	72.1151	.00198
-12	-.004903	- 3.3140	77.8627	.00208
- 9	-.005072	- 3.2727	79.8417	.00224
- 6	-.005097	- 3.0407	76.7470	.00210
- 4.5	-.004975	- 3.1270	80.0091	.00217
- 3	-.005070	- 3.2691	82.0468	.00252
- 1.5	-.005148	- 3.4646	86.7472	.00226
0	-.005258	- 3.5291	86.8990	.00213
1.5	-.005397	- 3.5695	87.5770	.00220
3	-.005523	- 3.6731	90.4554	.00217
4.5	-.005614	- 3.8175	93.5530	.00208
6	-.005627	- 3.9723	95.3005	.00242
9	-.005558	- 4.2923	96.9827	.00240
12.35	-.005350	- 4.6860	108.7361	.00224

Table A21. RC38 Incremental Pitching Moment Coefficient at $\beta=0^\circ$.

$$\Delta C = a_0 + a_1 x + a_2 x^2$$

α	a_0	a_1	a_2	σ
-14	-.000878	- .8821	58.7431	.00076
-12	-.001048	- .9761	68.8020	.00111
- 9	-.000864	- .9584	75.6480	.00158
- 6	-.001081	- .6718	74.9761	.00152
- 4.5	-.001386	- .4546	69.7344	.00130
- 3	-.001151	- .2546	63.5962	.00066
- 1.5	-.001275	- .1313	60.0474	.00073
0	-.001453	.0402	54.2055	.00072
1.5	-.001237	.2401	47.1787	.00110
3	-.001198	.4429	39.9040	.00104
4.5	-.001011	.4706	40.4345	.00070
6	-.001118	.5053	41.9746	.00112
9	-.001223	1.1944	22.6652	.00202
12.35	-.001265	1.7890	3.1306	.00056

Table A22. RC38 Incremental Rolling Moment Coefficient at $\beta=0^\circ$.

$$\Delta C = a_0 + a_1 x + a_2 x^2$$

α	a_0	a_1	a_2	σ
-14	-.000302	.2153	- 20.3183	.00017
-12	-.000209	.1127	- 15.5334	.00025
- 9	-.000177	.0593	- 12.2394	.00025
- 6	-.000205	.0056	- 9.0936	.00023
- 4.5	-.000190	- .0503	- 5.9819	.00032
- 3	-.000156	- .0810	- 4.1138	.00024
- 1.5	-.000154	- .1017	- 3.4943	.00028
0	-.000149	- .1223	- 2.8652	.00029
1.5	-.000150	- .1891	.3786	.00045
3	-.000153	- .2028	1.3627	.00051
4.5	-.000190	- .0421	- 6.8380	.00112
6	-.000209	.2333	- 20.2050	.00116
9	-.000197	.3919	- 25.3586	.00085
12.35	-.000161	.1659	- 14.9608	.00051

Table A23. RC38 Incremental Yawing Moment Coefficient at $\beta=0^\circ$.

$$\Delta C = a_0 + a_1 x + a_2 x^2$$

α	a_0	a_1	a_2	σ
-14	.000604	- .6642	19.1720	.00034
-12	.000419	- .5457	13.5119	.00047
- 9	.000296	- .5178	10.9238	.00059
- 6	.000386	- .3718	3.6871	.00039
- 4.5	.000234	- .2675	- 1.1453	.00044
- 3	.000121	- .2256	- 3.5702	.00035
- 1.5	.000098	- .2150	- 4.1496	.00040
0	.000072	- .2100	- 6.4133	.00088
1.5	.000053	- .1487	- 11.5643	.00101
3	.000015	- .1675	- 12.3202	.00084
4.5	.000075	- .4632	3.5392	.00195
6	.000077	- .8883	25.0250	.00188
9	.000033	- 1.0937	32.6807	.00120
12.35	-.000171	- .7554	18.3408	.00071

Table A24. RC38 Incremental Side Force Coefficient at $\beta=0^\circ$.

$$\Delta C = a_0 + a_1 x + a_2 x^2$$

α	a_0	a_1	a_2	σ
-14	.001419	1.9817	- 88.4667	.00114
-12	.000889	1.4729	- 67.4515	.00121
- 9	.000773	.7578	- 33.2048	.00118
- 6	.000698	.1700	.2973	.00143
- 4.5	.000181	- .0185	9.1201	.00182
- 3	-.000050	.0627	3.4038	.00211
- 1.5	-.000344	.1740	- 4.8729	.00147
0	-.000430	.2095	- 5.9582	.00155
1.5	-.000449	- .0092	6.9020	.00199
3	-.000752	- .0615	12.9511	.00187
4.5	-.000807	.5572	- 15.5405	.00334
6	-.001038	1.5789	- 60.2298	.00388
9	-.001230	3.0798	-113.1812	.00288
12.35	-.001395	2.9258	-104.5850	.00204

Table A25. RC40 Incremental Normal Force Coefficient at $\beta=0^\circ$.

$$\Delta C = a_0 + a_1 x + a_2 x^2$$

α	a_0	a_1	a_2	σ
-14	-.005669	- .3405	-108.1970	.00457
-12	-.005665	- .9612	- 76.0450	.00432
- 9	-.005107	- 1.1271	- 59.6023	.00421
- 6	-.005171	- 1.5023	- 35.5765	.00369
- 4.5	-.005524	- 2.0617	- 8.4840	.00375
- 3	-.004908	- 2.8996	32.7150	.00448
- 1.5	-.005326	- 3.6999	73.0021	.00437
0	-.005811	- 4.6063	115.1794	.00452
1.5	-.005196	- 5.2292	142.9434	.00458
3	-.005043	- 5.9101	171.8312	.00442
4.5	-.004363	- 6.4921	198.2057	.00456
6	-.004592	- 7.3192	238.9743	.00535
9	-.004538	- 8.7620	318.5676	.00534
12.35	-.004654	- 8.7750	326.1563	.00500

Table A26. RC40 Incremental Axial Force Coefficient at $\beta=0^\circ$.

$$\Delta C = a_0 + a_1 x + a_2 x^2$$

α	a_0	a_1	a_2	σ
-14	-.004643	- 4.4064	135.2430	.00239
-12	-.004848	- 4.4599	138.1980	.00250
- 9	-.005014	- 4.3143	136.8250	.00266
- 6	-.005016	- 4.4181	148.5670	.00264
- 4.5	-.004904	- 4.4246	149.5880	.00250
- 3	-.005018	- 4.2685	141.2650	.00241
- 1.5	-.005125	- 4.1364	133.0924	.00224
0	-.005235	- 3.9954	125.6538	.00215
1.5	-.005381	- 3.8479	119.7306	.00227
3	-.005503	- 3.5682	109.1801	.00223
4.5	-.005597	- 3.2927	96.2587	.00212
6	-.005608	- 3.0923	84.8517	.00221
9	-.005551	- 3.0300	73.9381	.00223
12.35	-.005348	- 3.1796	76.2553	.00221

Table A27. RC40 Incremental Pitching Moment Coefficient at $\beta=0^\circ$.

$$\Delta C = a_0 + a_1 x + a_2 x^2$$

α	a_0	a_1	a_2	σ
-14	-.000985	1.8971	- 79.9239	.00150
-12	-.001424	1.7501	- 68.5937	.00171
- 9	-.000943	1.3561	- 46.6669	.00173
- 6	-.001136	1.1141	- 28.3821	.00140
- 4.5	-.001431	1.0469	- 22.6991	.00124
- 3	-.001203	1.0651	- 21.9548	.00115
- 1.5	-.001336	1.2396	- 28.5206	.00144
0	-.001516	1.3714	- 34.0322	.00142
1.5	-.001304	1.5020	- 39.3591	.00145
3	-.001266	1.5607	- 41.6352	.00128
4.5	-.001081	1.5635	- 41.2464	.00100
6	-.001164	1.4271	- 33.4900	.00105
9	-.001237	.9091	- 43.6256	.00092
12.35	-.001238	.5676	12.6720	.00036

Table A28. RC40 Incremental Rolling Moment Coefficient at $\beta=0^\circ$.

$$\Delta C = a_0 + a_1 x + a_2 x^2$$

α	a_0	a_1	a_2	σ
-14	-.000285	- .0967	- 7.3295	.00035
-12	-.000197	- .0435	- 1.3655	.00021
- 9	-.000157	- .1471	3.7578	.00031
- 6	-.000188	- .2192	7.3733	.00046
- 4.5	-.000179	- .2596	9.4072	.00046
- 3	-.000153	- .3228	12.6525	.00022
- 1.5	-.000150	- .3206	13.1479	.00020
0	-.000140	- .3296	14.4470	.00031
1.5	-.000131	- .3674	17.3001	.00042
3	-.000120	- .3944	19.7866	.00038
4.5	-.000141	- .3879	21.0206	.00045
6	-.000153	- .3605	20.5832	.00039
9	-.000149	- .2925	15.8412	.00059
12.35	-.000139	- .1753	6.7934	.00040

Table A29. RC40 Incremental Yawing Moment Coefficient at $\beta=0^\circ$.

$$\Delta C = a_0 + a_1 x + a_2 x^2$$

α	a_0	a_1	a_2	σ
-14	.000603	- .7842	37.3467	.00395
-12	.000422	- .6701	32.8646	.00051
- 9	.000294	- .6021	30.2186	.00051
- 6	.000329	- .5597	28.5948	.00052
- 4.5	.000251	- .5329	27.1709	.00064
- 3	.000148	- .4773	23.7691	.00076
- 1.5	.000121	- .4907	22.8296	.00087
0	.000086	- .4342	17.6498	.00108
1.5	.000049	- .3252	10.4379	.00088
3	-.000006	- .2561	5.2746	.00042
4.5	.000035	- .3071	6.1669	.00059
6	.000034	- .3970	9.5163	.00051
9	-.000056	- .5960	21.8325	.00086
12.35	-.000151	- .8131	36.5509	.00082

Table A30. RC40. Incremental Side Force Coefficient at $\beta=0^\circ$.

$$\Delta C = a_0 + a_1 x + a_2 x^2$$

α	a_0	a_1	a_2	σ
-14	.001438	1.7453	- 71.1350	.00098
-12	.000878	1.5322	- 63.2140	.00102
- 9	.000715	1.3576	- 53.2736	.00112
- 6	.000702	1.2727	- 45.6489	.00108
- 4.5	.000182	1.3266	- 47.8647	.00158
- 3	-.000083	1.3829	- 52.1354	.00192
- 1.5	-.000404	1.6959	- 66.4678	.00231
0	-.000473	1.8511	- 70.5720	.00232
1.5	-.000476	1.8094	- 63.2682	.00250
3	-.000748	1.6170	- 49.4041	.00175
4.5	-.000767	1.4508	- 36.9412	.00144
6	-.000959	1.3842	- 29.6366	.00173
9	-.001179	1.6065	- 40.4477	.00213
12.35	-.001426	2.1316	- 72.8684	.00166

Table A31. RC42 Incremental Normal Force Coefficient at $\beta=0^\circ$.

$$\Delta C = a_0 - a_1 x + a_2 x^2$$

α	a_0	a_1	a_2	σ
-14	-.005973	- 1.7214	3.0795	.00363
-12	-.005941	- 1.1254	- 14.9304	.00428
- 9	-.005344	- .3689	- 34.0108	.00447
- 6	-.005310	- .5168	- 28.6531	.00409
- 4.5	-.005823	- .6816	- 24.8222	.00344
- 3	-.005227	- .5947	- 28.3864	.00370
- 1.5	-.005850	- .7093	- 22.8780	.00367
0	-.006181	- .8337	- 19.2624	.00383
1.5	-.005914	- .9244	- 20.6508	.00357
3	-.005695	- 1.0478	- 22.8093	.00379
4.5	-.005001	- 1.6070	- 6.5128	.00478
6	-.004973	- 2.3190	15.1888	.00417
9	-.004859	- 3.6440	63.5295	.00298
12.35	-.004916	- 4.0709	76.6844	.00313

Table A32. RC42 Incremental Axial Force Coefficient at $\beta=0^\circ$.

$$\Delta C = a_0 + a_1 x + a_2 x^2$$

α	a_0	a_1	a_2	σ
-14	-.004724	- 1.3270	7.4855	.00203
-12	-.004879	- 1.5947	18.6567	.00228
- 9	-.005112	- 1.5966	24.9481	.00254
- 6	-.005152	- 1.0657	15.0541	.00297
- 4.5	-.004990	- .9399	14.7556	.00238
- 3	-.005015	- .9989	18.4233	.00230
- 1.5	-.004993	- 1.0010	17.7833	.00230
0	-.005109	- .9229	14.7491	.00241
1.5	-.005213	- .7757	11.6061	.00260
3	-.005437	- .6757	11.9542	.00249
4.5	-.005501	- .4542	6.6709	.00246
6	-.005546	- .2478	- .0521	.00223
9	-.005324	- .0465	- 10.1936	.00221
12.35	-.005009	.0351	- 12.7473	.00239

Table A33. RC42 Incremental Pitch Moment Coefficient at $\beta=0^\circ$.

$$\Delta C = a_0 + a_1 x + a_2 x^2$$

α	a_0	a_1	a_2	σ
-14	-.000956	- .3172	13.9024	.00027
-12	-.001115	- .4155	17.1451	.00085
- 9	-.000904	- .6371	25.4868	.00081
- 6	-.001071	- .5230	23.8739	.00115
- 4.5	-.001457	- .4069	20.9346	.00113
- 3	-.001243	- .3569	20.1340	.00067
- 1.5	-.001432	- .4346	23.2963	.00071
0	-.001510	- .4534	23.9870	.00067
1.5	-.001393	- .3627	20.7794	.00113
3	-.001350	- .1202	11.3671	.00122
4.5	-.001153	.0701	3.6138	.00073
6	-.001191	.2214	- 4.3124	.00070
9	-.001266	.1931	- 8.2420	.00087
12.35	-.001276	.0042	- 5.5363	.00075

Table A34. RC42 Incremental Rolling Moment Coefficient at $\beta=0^\circ$.

$$\Delta C = a_0 + a_1 x + a_2 x^2$$

α	a_0	a_1	a_2	σ
-14	-.000216	- .1039	.7495	.00023
-12	-.000133	.0670	- 4.9961	.00049
- 9	-.000098	.1493	- 6.7116	.00021
- 6	-.000150	.1498	- 7.0722	.00069
- 4.5	-.000150	.1156	- 5.9438	.00077
- 3	-.000114	.0482	- 3.9218	.00106
- 1.5	-.000103	- .2084	6.0351	.00069
0	-.000095	- .2625	6.8073	.00049
1.5	-.000093	- .2011	2.2359	.00082
3	-.000097	- .1107	- 4.0842	.00072
4.5	-.000109	- .1189	- 6.2006	.00069
6	-.000111	- .2387	- 2.5700	.00071
9	-.000101	- .5841	14.5629	.00091
12.35	-.000094	- .3697	10.4996	.00078

Table A35. RC42 Incremental Yawing Moment Coefficient at $\beta=0^\circ$.

$$\Delta C = a_0 + a_1 x + a_2 x^2$$

α	a_0	a_1	a_2	σ
-14	.000448	.7032	- 8.3163	.00040
-12	.000297	.8044	- 9.1984	.00073
- 9	.000176	.9386	- 10.7041	.00034
- 6	.000254	.8324	- 6.4246	.00130
- 4.5	.000192	.7661	- 4.9424	.00136
- 3	.000068	.7324	- 4.3934	.00110
- 1.5	.000027	1.0084	- 16.9976	.00081
0	.000018	.9993	- 15.7634	.00081
1.5	-.000005	.8241	- 5.4642	.00154
3	-.000042	.6072	7.9504	.00124
4.5	-.000027	.6172	11.1481	.00098
6	-.000040	.8438	2.4039	.00111
9	-.000118	1.3119	- 24.0534	.00161
12.35	-.000209	.9161	- 15.9019	.00116

Table A36. RC42 Incremental Side Force Coefficient at $\beta=0^\circ$.

$$\Delta C = a_0 + a_1 x + a_2 x^2$$

α	a_0	a_1	a_2	σ
-14	.001305	- 1.3036	25.6781	.00124
-12	.000787	- 1.7321	33.2175	.00236
- 9	.000696	- 1.9200	31.5682	.00068
- 6	.000752	- 1.5328	19.1178	.00349
- 4.5	.000228	- 1.2882	14.3354	.00333
- 3	-.000003	- 1.0565	8.8482	.00223
- 1.5	-.000301	- 1.4385	31.0055	.00230
0	-.000278	- 1.1499	24.9852	.00305
1.5	-.000274	- .6499	9.5532	.00222
3	-.000568	- .0782	- 12.3873	.00122
4.5	-.000559	.0960	- 19.7667	.00139
6	-.000716	- .0315	- 12.5328	.00171
9	-.000968	- .6472	30.2161	.00345
12.35	-.001195	.1234	9.6709	.00198

Table A37. RC51 Incremental Normal Force Coefficient at $\beta=0^\circ$.

$$\Delta C = a_0 + a_1 x + a_2 x^2$$

α	a_0	a_1	a_2	σ
-14	-.005580	- 4.7544	25.6994	.00370
-12	-.005590	- 3.7936	- .1716	.00440
- 9	-.005090	- 2.6325	- 26.2446	.00510
- 6	-.005200	- 2.6336	- 16.3369	.00340
- 4.5	-.005560	- 2.6814	- 14.8966	.00310
- 3	-.004980	- 2.6063	- 14.2679	.00370
- 1.5	-.005400	- 1.9414	- 33.9465	.00510
0	-.005930	- 1.4941	- 42.2310	.00380
1.5	-.005340	- 1.3960	- 40.4129	.00340
3	-.005200	- 1.4235	- 33.2388	.00310
4.5	-.004520	- 1.8078	- 12.4581	.00300
6	-.004800	- 2.1415	10.8563	.00410
9	-.004810	- 1.3887	8.4775	.00430
12.35	-.004930	- 1.9571	35.4368	.00390

Table A38. RC51 Incremental Axial Force Coefficient at $\beta=0^\circ$.

$$\Delta C = a_0 + a_1 x + a_2 x^2$$

α	a_0	a_1	a_2	σ
-14	-.004710	- 2.5096	29.8390	.00180
-12	-.004930	- 2.7785	43.2342	.00200
- 9	-.005090	- 2.4322	35.0454	.00260
- 6	-.005140	- 1.5517	10.3237	.00280
- 4.5	-.005030	- 1.3315	5.8394	.00240
- 3	-.005100	- 1.2829	4.9126	.00230
- 1.5	-.005180	- 1.5236	13.1775	.00240
0	-.005280	- 1.6437	15.9405	.00210
1.5	-.005420	- 1.6017	15.1152	.00220
3	-.005540	- 1.4609	10.4097	.00210
4.5	-.005630	- 1.3538	5.5769	.00200
6	-.005640	- 1.2853	- .1568	.00210
9	-.005580	- 1.6184	6.8865	.00230
12.35	-.005380	- 1.8630	15.7441	.00220

Table A39. RC51 Incremental Pitching Moment Coefficient at $\beta=0^\circ$.

$$\Delta C = a_0 + a_1 x + a_2 x^2$$

α	a_0	a_1	a_2	σ
-14	-.000928	- .9980	36.4798	.00060
-12	-.001093	- .9902	40.8423	.00079
- 9	-.000916	- .9595	42.1345	.00116
- 6	-.001140	- .5455	34.1041	.00219
- 4.5	-.001443	- .2468	27.2540	.00223
- 3	-.001199	.0068	21.1097	.00106
- 1.5	-.001314	.0912	18.4669	.00085
0	-.001486	.1863	14.2061	.00089
1.5	-.001267	.3105	8.7717	.00111
3	-.001232	.5529	- .7791	.00108
4.5	-.001043	.7163	- 6.3121	.00070
6	-.001147	.8520	- 9.1731	.00114
9	-.001244	1.4436	- 21.8684	.00212
12.35	-.001284	2.1800	- 47.8053	.00086

Table A40. RC51 Incremental Rolling Moment Coefficient at $\beta=0^\circ$.

$$\Delta C = a_0 + a_1 x + a_2 x^2$$

α	a_0	a_1	a_2	σ
-14	-.000300	- .0248	- 7.9325	.00022
-12	-.000189	.0385	- 10.2764	.00035
- 9	-.000153	- .0780	- 1.7409	.00059
- 6	-.000198	- .1262	2.9617	.00022
- 4.5	-.000182	- .0957	1.5574	.00028
- 3	-.000152	- .0945	1.0673	.00025
- 1.5	-.000147	- .2000	5.6587	.00056
0	-.000132	- .2508	7.8100	.00055
1.5	-.000121	- .2694	7.9685	.00057
3	-.000110	- .2736	8.9666	.00081
4.5	-.000150	- .3818	16.1252	.00110
6	-.000174	- .4198	21.1976	.00072
9	-.000130	- .6705	31.8709	.00160
12.35	-.000137	- .5629	21.5665	.00108

Table A41. RC51 Incremental Yawing Moment Coefficient at $\beta=0^\circ$.

$$\Delta C = a_0 + a_1 x + a_2 x^2$$

α	a_0	a_1	a_2	σ
-14	.000613	.3807	- 2.6558	.00040
-12	.000401	.3418	1.5194	.00044
- 9	.000276	.5558	- 6.9625	.00039
- 6	.000313	.5290	- 7.1095	.00033
- 4.5	.000226	.4136	- 2.2233	.00046
- 3	.000112	.3440	.9751	.00040
- 1.5	.000084	.4461	- 5.2416	.00078
0	.000047	.5172	- 9.9827	.00079
1.5	.000016	.5408	- 10.5590	.00080
3	-.000039	.5472	- 12.9732	.00134
4.5	.000022	.5592	- 17.5421	.00192
6	.000023	.5018	- 21.0702	.00120
9	-.000140	1.0043	- 39.6644	.00304
12.35	-.000203	.9073	- 24.0349	.00169

Table A42. RC51 Incremental Side Force Coefficient at $\beta=0^\circ$.

$$\Delta C = a_0 + a_1 x + a_2 x^2$$

α	a_0	a_1	a_2	σ
-14	.001380	- .7034	- 29.4604	.00164
-12	.000905	- 1.3105	- 12.4395	.00173
- 9	.000785	- 2.0179	20.2834	.00157
- 6	.000720	- 1.9545	29.5523	.00163
- 4.5	.000205	- 1.7100	19.3259	.00180
- 3	-.000025	- 1.4343	5.3184	.00146
- 1.5	-.000289	- 1.6014	14.1171	.00198
0	-.000335	- 1.8310	30.3456	.00220
1.5	-.000333	- 2.0031	44.0938	.00176
3	-.000647	- 1.8629	47.8547	.00300
4.5	-.000697	- 1.4591	43.9149	.00421
6	-.000901	- 1.0897	42.6916	.00322
9	-.001023	- 1.7399	80.2853	.00405
12.35	-.001339	- .4031	27.7201	.0062

Table A43. RC55 Incremental Normal Force Coefficient at $\beta=0^\circ$.

$$\Delta C = a_0 + a_1 x + a_2 x^2$$

α	a_0	a_1	a_2	σ
-14	-.005542	- 2.1166	- 36.5922	.00350
-12	-.005574	- 1.4770	- 60.7751	.00430
- 9	-.005033	- .5177	- 87.7490	.00400
- 6	-.005137	- .6095	- 94.9053	.00480
- 4.5	-.005549	- .8488	-100.4455	.00530
- 3	-.005004	- 1.0217	-105.9124	.00460
- 1.5	-.005444	- 1.1196	-110.9256	.00360
0	-.005922	- 1.4196	-102.8726	.00390
1.5	-.005293	- 1.7130	- 95.0949	.00350
3	-.005166	- 2.1988	- 76.4831	.00320
4.5	-.004484	- 2.5802	- 59.5705	.00310
6	-.004745	- 2.8749	- 46.2922	.00260
9	-.004741	- 3.5877	- 23.9554	.00350
12.35	-.004880	- 3.5097	- 47.8799	.00370

Table A44. RC55 Incremental Axial Force Coefficient at $\beta=0^\circ$.

$$\Delta C = a_0 + a_1 x + a_2 x^2$$

α	a_0	a_1	a_2	σ
-14	-.004779	- 5.1833	90.0296	.00230
-12	-.004977	- 5.4600	96.4655	.00240
- 9	-.005134	- 5.2471	87.8254	.00230
- 6	-.005148	- 4.9022	78.7452	.00240
- 4.5	-.005021	- 4.7642	74.9063	.00220
- 3	-.005109	- 4.7010	72.6585	.00220
- 1.5	-.005189	- 4.6177	67.9980	.00220
0	-.005301	- 4.5689	63.9737	.00230
1.5	-.005445	- 4.5717	62.5949	.00240
3	-.005571	- 4.5783	61.7848	.00230
4.5	-.005657	- 4.6405	62.4776	.00230
6	-.005663	- 4.7438	63.4972	.00240
9	-.005587	- 4.9291	65.7792	.00220
12.35	-.005398	- 4.8692	61.1104	.00240

Table A45. RC55 Incremental Pitching Moment Coefficient at $\beta=0^\circ$.

$$\Delta C = a_0 + a_1 x + a_2 x^2$$

α	a_0	a_1	a_2	σ
-14	-.000915	.8407	20.8669	.00029
-12	-.001084	.7498	24.4986	.00110
- 9	-.000894	.4581	32.7159	.00077
- 6	-.001096	.5802	30.4675	.00109
- 4.5	-.001391	.6661	30.8149	.00140
- 3	-.001160	.7340	32.2591	.00113
- 1.5	-.001285	.7886	33.7521	.00091
0	-.001459	.8782	32.1808	.00061
1.5	-.001240	.9866	27.9943	.00069
3	-.001213	1.0654	24.3656	.00066
4.5	-.001039	1.1330	20.4892	.00049
6	-.001151	1.1300	20.2167	.00034
9	-.001248	1.1444	18.3773	.00041
12.35	-.001295	1.1501	14.0969	.00078

Table A46. RC55 Incremental Rolling Moment Coefficient at $\beta=0^\circ$.

$$\Delta C = a_0 + a_1 x + a_2 x^2$$

α	a_0	a_1	a_2	σ
-14	-.000301	- .0725	- .1958	.00036
-12	-.000201	.1121	- 5.4306	.00058
- 9	-.000165	.1759	- 5.6147	.00018
- 6	-.000207	.1313	- 3.2763	.00013
- 4.5	-.000195	.1404	- 3.6111	.00013
- 3	-.000158	.1174	- 2.7080	.00018
- 1.5	-.000152	.0680	- .8771	.00025
0	-.000145	- .0047	1.6111	.00028
1.5	-.000142	- .0584	3.2541	.00027
3	-.000136	- .1215	5.0397	.00028
4.5	-.000161	- .1664	6.1744	.00032
6	-.000176	- .1977	6.9896	.00022
9	-.000168	- .2100	7.1794	.00022
12.35	-.000146	- .2485	8.9494	.00026

Table A47. RC55 Incremental Yawing Moment Coefficient at $\beta=0^\circ$.

$$\Delta C = a_0 + a_1 x + a_2 x^2$$

α	a_0	a_1	a_2	σ
-14	.000605	.5010	- 5.7196	.00046
-12	.000402	.6432	- 9.5155	.00053
- 9	.000270	.7477	- 11.3829	.00021
- 6	.000317	.6781	- 8.9439	.00054
- 4.5	.000239	.5480	- 4.0384	.00070
- 3	.000121	.4577	- .9419	.00034
- 1.5	.000086	.4713	- 1.3146	.00035
0	.000056	.5561	- 4.5834	.00028
1.5	.000030	.6220	- 6.7944	.00024
3	-.000017	.6356	- 6.7796	.00019
4.5	.000020	.6171	- 5.8715	.00021
6	.000016	.5739	- 4.3907	.00027
9	-.000078	.5684	- 4.6235	.00025
12.35	-.000189	.5918	- 7.5135	.00071

Table A48. RC55 Incremental Side Force Coefficient at $\beta=0^\circ$.

$$\Delta C = a_0 + a_1 x + a_2 x^2$$

α	a_0	a_1	a_2	σ
-14	.001412	- .2166	9.0422	.00175
-12	.000909	- .7810	25.6796	.00137
- 9	.000750	- .7593	21.3023	.00054
- 6	.000708	- .4804	10.7358	.00116
- 4.5	.000200	- .1421	- 19.7981	.00144
- 3	-.000015	.1755	- 11.5068	.00124
- 1.5	-.000298	.3556	- 15.8979	.00138
0	-.000358	.4994	- 17.4094	.00115
1.5	-.000379	.7143	- 23.8067	.00122
3	-.000678	.9824	- 31.7234	.00117
4.5	-.000710	1.1879	- 36.7760	.00141
6	-.000905	1.3611	- 39.6737	.00143
9	-.001137	1.5492	- 42.1381	.00136
12.35	-.001361	1.5489	-. 50.8708	.00191

Table A49. RC59 Incremental Normal Force Coefficient at $\beta=0^\circ$.

$$\Delta C = a_0 + a_1 x + a_2 x^2$$

α	a_0	a_1	a_2	σ
-14	-.005570	- 2.1085	3.6034	.00360
-12	-.005620	- 1.8373	- .0624	.00410
- 9	-.005110	- 1.5799	- 2.5153	.00370
- 6	-.005210	- 1.5979	6.0418	.00360
- 4.5	-.005590	- 1.3838	3.6571	.00360
- 3	-.005030	- 1.5943	14.4011	.00400
- 1.5	-.005470	- 1.6699	23.3547	.00370
0	-.006010	- 1.6902	26.8601	.00370
1.5	-.005430	- 1.5379	20.5750	.00360
3	-.005310	- 1.4256	17.9392	.00360
4.5	-.004630	- 1.5476	25.2100	.00360
6	-.004880	- 1.5079	30.5123	.00350
9	-.004820	- 1.4483	41.4581	.00290
12.35	-.004930	- 1.4410	46.9635	.00220

Table A50. RC59 Incremental Axial Force Coefficient at $\beta=0^\circ$.

$$\Delta C = a_0 + a_1 x + a_2 x^2$$

α	a_0	a_1	a_2	σ
-14	-.004690	- 1.0915	- 1.6556	.00190
-12	-.004910	- 1.2290	5.7421	.00200
- 9	-.005070	- 1.2503	11.5021	.00230
- 6	-.005100	- 1.2631	19.3087	.00210
- 4.5	-.004980	- 1.3610	23.3715	.00210
- 3	-.005070	- 1.4112	24.1681	.00210
- 1.5	-.005170	- 1.4020	22.6428	.00210
0	-.005280	- 1.3425	21.3935	.00230
1.5	-.005420	- 1.3128	22.1526	.00230
3	-.005530	- 1.2704	20.6249	.00220
4.5	-.005620	- 1.2643	18.1796	.00220
6	-.005630	- 1.3232	16.6111	.00220
9	-.005570	- 1.6494	19.6903	.00270
12.35	-.005380	- 2.1229	32.7565	.00230

Table A51. RC59 Incremental Pitching Moment Coefficient at $\beta=0^\circ$.

$$\Delta C = a_0 + a_1 x + a_2 x^2$$

α	a_0	a_1	a_2	σ
-14	-.000916	-.5284	11.0179	.00032
-12	-.001084	-.5422	12.5943	.00074
-9	-.000897	-.7094	21.7107	.00100
-6	-.001010	-.6927	28.5141	.00037
-4.5	-.001401	-.6210	29.3508	.00082
-3	-.001179	-.6560	30.9176	.00077
-1.5	-.001302	-.5351	26.3726	.00085
0	-.001484	-.4095	22.0736	.00105
1.5	-.001276	-.3596	22.1624	.00114
3	-.001251	-.2493	19.9971	.00110
4.5	-.001074	-.0694	13.6102	.00114
6	-.001170	.2124	3.1605	.00095
9	-.001245	.8333	-15.4056	.00184
12.35	-.001283	1.2538	-24.7211	.00054

Table A52. RC59 Incremental Rolling Moment Coefficient at $\beta=0^\circ$.

$$\Delta C = a_0 + a_1 x + a_2 x^2$$

α	a_0	a_1	a_2	σ
-14	-.000265	.0912	-7.8638	.00064
-12	-.000195	.1132	.6136	.00044
-9	-.000171	.1769	4.0131	.00028
-6	-.000209	.1341	4.5535	.00029
-4.5	-.000192	.1440	5.7674	.00019
-3	-.000159	.1265	5.3899	.00028
-1.5	-.000151	.1149	5.2676	.00028
0	-.000146	.1301	6.8606	.00044
1.5	-.000137	.1683	9.9056	.00050
3	-.000137	.1920	12.5894	.00040
4.5	-.000167	.1638	12.6863	.00034
6	-.000187	.0853	10.6295	.00056
9	-.000172	.2505	-3.5854	.00065
12.35	-.000140	.2441	-7.2666	.00050

Table A53. RC59 Incremental Yawing Moment Coefficient at $\beta=0^\circ$.

$$\Delta C = a_0 + a_1 x + a_2 x^2$$

α	a_0	a_1	a_2	σ
-14	.000566	.0732	5.4582	.00065
-12	.000391	.2471	- 1.8731	.00037
- 9	.000269	.3351	- 6.5679	.00035
- 6	.000310	.3713	- 10.0911	.00024
- 4.5	.000232	.3635	- 10.1175	.00025
- 3	.000120	.3097	- 7.7762	.00033
- 1.5	.000088	.2923	- 7.8125	.00041
0	.000055	.3555	- 12.3148	.00083
1.5	.000026	.4404	- 18.3458	.00073
3	-.000016	.5082	- 23.4689	.00047
4.5	.000033	.4563	- 22.8080	.00051
6	.000041	.3456	- 19.5302	.00076
9	-.000069	- .1099	1.5008	.00109
12.35	-.000196	- .0821	5.7580	.00054

Table A54. RC59 Incremental Side Force Coefficient at $\beta=0^\circ$.

$$\Delta C = a_0 + a_1 x + a_2 x^2$$

α	a_0	a_1	a_2	σ
-14	.001320	.1042	- 12.1507	.00210
-12	.000879	.7293	- 38.1822	.00180
- 9	.000786	.7145	- 40.1938	.00100
- 6	.000750	- .0083	- 12.9057	.00130
- 4.5	.000243	- .2925	- .9554	.00120
- 3	.000001	- .4151	3.2808	.00110
- 1.5	-.000293	- .5328	10.8219	.00130
0	-.000372	- .6496	18.8359	.00170
1.5	-.000391	- .9153	34.7440	.00140
3	-.000699	- 1.0593	46.5078	.00200
4.5	-.000750	- .7174	37.6780	.00290
6	-.000942	- .0610	17.6002	.00280
9	-.001146	1.0144	- 22.7489	.00160
12.35	-.001371	1.0699	- 35.1806	.00250

Table A55. RC61 Incremental Normal Force Coefficient at $\beta=0^\circ$.

$$\Delta C = a_0 + a_1 x + a_2 x^2$$

α	a_0	a_1	a_2	σ
-14	-.005545	- 1.1589	- 8.1260	.00355
-12	-.005590	- 1.2163	- 13.7942	.00373
- 9	-.005065	- .8440	- 31.3342	.00378
- 6	-.005158	- .7210	- 38.5609	.00345
- 4.5	-.005539	- .9752	- 32.4354	.00370
- 3	-.004970	- 1.1545	- 30.2976	.00394
- 1.5	-.005395	- 1.4615	- 22.6230	.00345
0	-.005920	- 1.6071	- 19.5732	.00350
1.5	-.005339	- 1.6689	- 20.2656	.00320
3	-.005190	- 1.7001	- 22.1659	.00311
4.5	-.004514	- 1.7546	- 22.8338	.00305
6	-.004748	- 1.9856	- 17.7099	.00279
9	-.004755	- 2.2315	- 12.8547	.00231
12.35	-.004905	- 2.3792	- 6.1884	.00207

Table A56. RC61 Incremental Axial Force Coefficient at $\beta=0^\circ$.

$$\Delta C = a_0 + a_1 x + a_2 x^2$$

α	a_0	a_1	a_2	σ
-14	-.004757	- 2.4950	21.6695	.00197
-12	-.004957	- 2.4940	19.7225	.00215
- 9	-.005105	- 2.3477	11.5808	.00210
- 6	-.005116	- 2.3568	10.8406	.00202
- 4.5	-.004996	- 2.4155	13.6087	.00204
- 3	-.005085	- 2.5486	19.1436	.00213
- 1.5	-.005164	- 2.7051	24.6447	.00214
0	-.005262	- 2.8836	31.2412	.00214
1.5	-.005400	- 2.9504	34.7243	.00217
3	-.005535	- 2.9155	34.5155	.00214
4.5	-.005638	- 2.8504	33.2781	.00205
6	-.005658	- 2.7467	29.2659	.00199
9	-.005575	- 2.6307	21.3351	.00219
12.35	-.005372	- 2.7315	21.6981	.00220

Table A57. RC61 Incremental Pitching Moment Coefficient at $\beta=0^\circ$.

$$\Delta C = a_0 + a_1 x + a_2 x^2$$

α	a_0	a_1	a_2	σ
-14	-.000903	.7428	- .6900	.00040
-12	-.001069	.7883	- 1.4856	.00076
- 9	-.000884	.6078	5.6626	.00071
- 6	-.001088	.5968	5.1313	.00090
- 4.5	-.001379	.5609	6.6262	.00072
- 3	-.001148	.6103	5.8480	.00064
- 1.5	-.001267	.6087	7.1638	.00070
0	-.001451	.6048	8.8185	.00062
1.5	-.001248	.6034	9.1605	.0070
3	-.001213	.6101	8.8908	.00070
4.5	-.001044	.6733	6.6308	.00055
6	-.001143	.7215	5.2034	.00056
9	-.001245	.8364	- .2191	.00044
12.35	-.001291	.7269	2.4494	.00033

Table A58. RC61 Incremental Rolling Moment Coefficient at $\beta=0^\circ$.

$$\Delta C = a_0 + a_1 x + a_2 x^2$$

α	a_0	a_1	a_2	σ
-14	-.000304	.0114	- .9108	.00017
-12	-.000209	.0556	- 4.7062	.00037
- 9	-.000171	.1235	- 9.5100	.00023
- 6	-.000202	.0672	- 7.0272	.00030
- 4.5	-.000186	- .0073	- 3.8552	.00029
- 3	-.000149	- .0677	- 2.0303	.00031
- 1.5	-.000143	- .1096	- 1.0331	.00021
0	-.000137	- .1398	- .0777	.00014
1.5	-.000138	- .1641	.9284	.00012
3	-.000134	- .1965	2.3840	.00014
4.5	-.000158	- .2208	3.5095	.00013
6	-.000173	- .2265	3.8937	.00015
9	-.000171	- .1651	1.9303	.00019
12.35	-.000149	- .1631	2.0002	.00013

Table A59. RC61 Incremental Yawing Moment Coefficient at $\beta=0^\circ$.

$$\Delta C = a_0 + a_1 x + a_2 x^2$$

α	a_0	a_1	a_2	σ
-14	.000600	- .3032	- 2.2789	.00027
-12	.000404	- .3482	13.2571	.00037
- 9	.000274	- .4038	6.0787	.00037
- 6	.000305	- .3459	3.9407	.00042
- 4.5	.000219	- .2636	.3012	.00035
- 3	.000102	- .2162	- 1.1669	.00036
- 1.5	.000076	- .1846	- 1.8339	.00024
0	.000053	- .1704	- 2.0145	.00020
1.5	.000030	- .1358	- 3.0370	.00023
3	-.000017	- .0800	- 4.9492	.00027
4.5	.000022	- .0276	- 7.0458	.00021
6	.000022	- .0375	- 6.8956	.00029
9	-.000071	- .1595	- 3.2353	.00035
12.35	-.000182	- .1907	- 2.9647	.00029

Table A60. RC61 Incremental Side Force Coefficient at $\beta=0^\circ$.

$$\Delta C = a_0 + a_1 x + a_2 x^2$$

α	a_0	a_1	a_2	σ
-14	.001437	.8729	6.0380	.00069
-12	.000917	.9770	- .5676	.00057
- 9	.000758	1.1710	- 12.3403	.00068
- 6	.000743	1.1409	- 8.7908	.00125
- 4.5	.000240	1.0677	- 3.6572	.00109
- 3	.000018	.9947	- 1.3668	.00121
- 1.5	-.000282	1.0161	- 4.0931	.00062
0	-.000356	1.0003	- 4.4932	.00080
1.5	-.000389	.9880	- 5.3206	.00092
3	-.000693	.8996	- 3.2242	.00094
4.5	-.000730	.8296	- 1.6345	.00093
6	-.000934	.8145	- .7681	.00093
9	-.001168	1.1170	- 9.5406	.00126
12.35	-.001387	1.2484	- 10.6891	.00129

Table A61. RC62 Incremental Normal Force Coefficient at $\beta=0^\circ$.

$$\Delta C = a_0 + a_1 x + a_2 x^2$$

α	a_0	a_1	a_2	σ
-14	-.005609	- 3.0971	9.5526	.00392
-12	-.005628	- 2.4864	- 7.1336	.00442
- 9	-.005118	- 1.6916	- 29.6933	.00406
- 6	-.005209	- 1.2524	- 36.8912	.00393
- 4.5	-.005580	- .8985	- 43.3664	.00375
- 3	-.005018	- .9694	- 33.4187	.00440
- 1.5	-.005465	- .4665	- 43.2456	.00444
0	-.005992	- .0923	- 50.5489	.00409
1.5	-.005398	.1824	- 58.0241	.00334
3	-.005260	.3351	- 61.4943	.00320
4.5	-.004580	.2999	- 57.8434	.00302
6	-.004831	.3821	- 51.8671	.00381
9	-.004826	.5906	- 36.5363	.00338
12.35	-.004956	.3380	- 19.9146	.00265

Table A62. RC62 Incremental Axial Force Coefficient at $\beta=0^\circ$.

$$\Delta C = a_0 + a_1 x + a_2 x^2$$

α	a_0	a_1	a_2	σ
-14	-.004707	- .6008	- 3.1297	.00188
-12	-.004919	- .5818	- 1.6695	.00204
- 9	-.005079	- .4340	- 2.4901	.00243
- 6	-.005094	- .2682	- .9427	.00210
- 4.5	-.004975	- .3255	1.6288	.00208
- 3	-.005070	- .3378	- .0642	.00231
- 1.5	-.005153	- .4122	- .2457	.00218
0	-.005257	- .3901	- 2.4719	.00213
1.5	-.005391	- .3952	- 2.4414	.00217
3	-.005508	- .4580	.7171	.00211
4.5	-.005602	- .5753	3.0885	.00218
6	-.005618	- .7204	5.4270	.00237
9	-.005558	- 1.0837	11.2335	.00241
12.35	-.005357	- 1.3984	19.7655	.00222

Table A63. RC62 Incremental Pitching Moment Coefficient at $\beta=0^\circ$.

$$\Delta C = a_0 + a_1 x + a_2 x^2$$

α	a_0	a_1	a_2	σ
-14	-.000900	- .9788	32.8668	.00053
-12	-.001062	- .9945	39.2937	.00113
- 9	-.000877	- .9919	45.0750	.00111
- 6	-.001086	- .7260	44.1814	.00147
- 4.5	-.001385	- .5169	40.1231	.00095
- 3	-.001161	- .5012	40.2452	.00072
- 1.5	-.001284	- .3585	34.8206	.00075
0	-.001464	- .1841	27.5649	.00097
1.5	-.001248	.0586	17.7316	.00082
3	-.001215	.2465	10.6316	.00071
4.5	-.001033	.2932	9.0665	.00047
6	-.001132	.3505	9.7041	.00105
9	-.001231	.9865	- 6.1537	.00211
12.35	-.001280	1.5624	- 24.9211	.00036

Table A64. RC62 Incremental Rolling Moment Coefficient at $\beta=0^\circ$.

$$\Delta C = a_0 + a_1 x + a_2 x^2$$

α	a_0	a_1	a_2	σ
-14	-.000293	- .0507	- 1.1771	.00017
-12	-.000200	- .0986	.9269	.00014
- 9	-.000164	- .1104	2.4335	.00026
- 6	-.000199	- .1411	4.5463	.00022
- 4.5	-.000188	- .1436	5.0468	.00025
- 3	-.000152	- .1335	5.1813	.00018
- 1.5	-.000147	- .1622	6.8471	.00017
0	-.000140	- .2104	9.7479	.00032
1.5	-.000141	- .2860	14.2560	.00043
3	-.000142	- .3060	16.6512	.00042
4.5	-.000170	- .2479	16.0002	.00066
6	-.000183	- .0683	9.6091	.00076
9	-.000178	.2627	- 5.5066	.00056
12.35	-.000152	.1878	- 7.2821	.00073

Table A65. RC62 Incremental Yawing Moment Coefficient at $\beta=0^\circ$.

$$\Delta C = a_0 + a_1 x + a_2 x^2$$

α	a_0	a_1	a_2	σ
-14	.000584	.3794	- 8.5442	.00038
-12	.000396	.4291	- 10.1173	.00027
- 9	.000267	.4109	- 9.1575	.00034
- 6	.000300	.4970	- 12.5314	.00037
- 4.5	.000222	.5443	- 14.6594	.00037
- 3	.000106	.5806	- 16.7991	.00034
- 1.5	.000080	.6335	- 20.3353	.00042
0	.000054	.6871	- 25.5571	.00096
1.5	.000037	.7470	- 31.1624	.00089
3	-.000001	.7527	- 34.0075	.00054
4.5	.000042	.6470	- 31.0210	.00081
6	.000033	.4049	- 21.4906	.00090
9	-.000062	.0185	- 1.4873	.00095
12.35	-.000180	.1958	- 1.7776	.00092

Table A66. RC62 Incremental Side Force Coefficient at $\beta=0^\circ$.

$$\Delta C = a_0 + a_1 x + a_2 x^2$$

α	a_0	a_1	a_2	σ
-14	.001435	.4600	- 21.5453	.00106
-12	.000936	.0984	- 8.4487	.00088
- 9	.000794	- .3662	12.8843	.00123
- 6	.000732	- .7388	32.7346	.00073
- 4.5	.000221	- .7833	34.9426	.00112
- 3	-.000009	- .6798	28.6419	.00113
- 1.5	-.000301	- .6244	24.5849	.00078
0	-.000377	- .7650	32.3655	.00144
1.5	-.000397	- 1.1492	53.4475	.00217
3	-.000710	- 1.2898	66.5101	.00193
4.5	-.000750	- .9976	61.4044	.00249
6	-.000957	- .2453	37.3629	.00314
9	-.001173	1.5082	- 33.0076	.00248
12.35	-.001364	1.7613	- 55.2229	.00226

Table A67. RC77 Incremental Normal Force Coefficient at $\beta=0^\circ$.

$$\Delta C = a_0 + a_1 x + a_2 x^2$$

α	a_0	a_1	a_2	σ
-14	-.005550	- 1.0488	7.0034	.00340
-12	-.005570	- .4556	- 8.5892	.00440
- 9	-.005050	.3365	- 24.5113	.00410
- 6	-.005170	.2006	- 17.5255	.00360
- 4.5	-.005530	.1122	- 18.0424	.00340
- 3	-.004970	.1474	- 21.8162	.00340
- 1.5	-.005410	.3520	- 29.7039	.00350
0	-.005950	.2179	- 22.8233	.00350
1.5	-.005370	.0810	- 18.6311	.00340
3	-.005240	- .2933	- 5.4905	.00300
4.5	-.004560	- .5771	1.2932	.00350
6	-.004820	- .9042	9.8990	.00320
9	-.004790	- 1.4775	17.3056	.00340
12.35	-.004920	- 2.1323	25.7223	.00350

Table A68. RC77 Incremental Axial Force Coefficient at $\beta=0^\circ$.

$$\Delta C = a_0 + a_1 x + a_2 x^2$$

α	a_0	a_1	a_2	σ
-14	-.004740	- .9381	11.9082	.00190
-12	-.004940	- 1.1464	17.2930	.00220
- 9	-.005100	- 1.1262	16.3720	.00220
- 6	-.005110	- .7646	9.0755	.00240
- 4.5	-.004990	- .7118	10.2761	.00210
- 3	-.005070	- .7441	13.0783	.00200
- 1.5	-.005160	- .7903	14.8151	.00200
0	-.005260	- .7361	12.2192	.00210
1.5	-.005410	- .6848	10.3746	.00220
3	-.005540	- .6185	8.7135	.00210
4.5	-.005620	- .5541	7.5749	.00200
6	-.005630	- .5153	7.8858	.00200
9	-.005560	- .4382	7.0192	.00210
12.35	-.005370	- .1868	- 1.4898	.00230

Table A69. RC77 Incremental Pitching Moment Coefficient at $\beta=0^\circ$.

$$\Delta C = a_0 + a_1 x + a_2 x^2$$

α	a_0	a_1	a_2	σ
-14	-.000924	-.0612	3.8532	.00039
-12	-.001081	-.1077	3.3549	.00100
-9	-.000886	-.2993	6.5284	.00070
-6	-.001086	-.2645	6.4159	.00099
-4.5	-.001376	-.1986	5.7912	.00092
-3	-.001148	-.2102	8.0587	.00055
-1.5	-.001268	-.1795	7.6087	.00059
0	-.001459	-.1788	7.7416	.00070
1.5	-.001249	-.1597	6.5265	.00070
3	-.001222	-.1597	6.8349	.00074
4.5	-.001040	-.1279	5.9983	.00043
6	-.001147	-.1006	5.7149	.00033
9	-.001242	-.0087	1.1121	.00046
12.35	-.001279	.0571	-3.6154	.00038

Table A70. RC77 Incremental Rolling Moment Coefficient at $\beta=0^\circ$.

$$\Delta C = a_0 + a_1 x + a_2 x^2$$

α	a_0	a_1	a_2	σ
-14	-.000300	-.0723	-.3057	.00031
-12	-.000201	.1117	-6.5164	.00051
-9	-.000164	.2439	-9.6860	.00020
-6	-.000204	.1793	-6.5826	.00030
-4.5	-.000190	.1531	-5.5139	.00027
-3	-.000153	.1544	-6.4714	.00056
-1.5	-.000143	.1259	-7.3340	.00067
0	-.000136	.0550	-6.3967	.00043
1.5	-.000137	-.0804	-1.1031	.00045
3	-.000135	-.2254	5.1164	.00041
4.5	-.000165	-.2624	6.9057	.00033
6	-.000178	-.1631	1.5592	.00064
9	-.000164	-.1672	-2.0020	.00067
12.35	-.000148	-.3664	7.9512	.00055

Table A71. RC77 Incremental Yawing Moment Coefficient at $\beta=0^\circ$.

$$\Delta C = a_0 + a_1 x + a_2 x^2$$

α	a_0	a_1	a_2	σ
-14	.000602	.6345	- 7.8846	.00037
-12	.000406	.7158	- 7.8857	.00061
- 9	.000275	.7978	- 8.1334	.00026
- 6	.000314	.7826	- 8.6520	.00078
- 4.5	.000232	.6879	- 6.3835	.00103
- 3	.000113	.5376	- .8044	.00055
- 1.5	.000075	.4868	2.5652	.00060
0	.000048	.5481	1.7107	.00043
1.5	.000027	.7036	- 4.5400	.00052
3	-.000015	.8368	- 10.2911	.00039
4.5	.000030	.8179	- 9.6028	.00049
6	.000025	.6550	- 1.5740	.00075
9	-.000081	.6600	1.0027	.00068
12.35	-.000187	.8628	- 11.5746	.00086

Table A72. RC77 Incremental Side Force Coefficient at $\beta=0^\circ$.

$$\Delta C = a_0 + a_1 x + a_2 x^2$$

α	a_0	a_1	a_2	σ
-14	-.001410	- 1.0029	27.9282	.00117
-12	.000898	- 1.4028	34.6355	.00199
- 9	.000753	- 1.3738	26.3732	.00058
- 6	.000723	- 1.1316	21.5616	.00221
- 4.5	.000211	- .8127	14.3981	.00245
- 3	-.000006	- .3390	- 1.1145	.00119
- 1.5	-.000286	.0290	- 14.9772	.00127
0	-.000356	.3044	- 24.5138	.00138
1.5	-.000380	.2656	- 16.2668	.00195
3	-.000686	.2016	- 6.1790	.00206
4.5	-.000738	.3372	- 5.6641	.00177
6	-.000937	.8684	- 26.1729	.00199
9	-.001126	.9902	- 33.1208	.00198
12.35	-.001378	.4248	- 6.8888	.00144

Table A73. RC78 Incremental Normal Force Coefficient at $\beta=0^\circ$.

$$\Delta C = a_0 + a_1 x + a_2 x^2$$

α	a_0	a_1	a_2	σ
-14	-.005550	- .9596	16.8534	.00330
-12	-.005570	- .4186	3.1925	.00420
- 9	-.005050	.3534	- 13.2736	.00420
- 6	-.005170	.1798	- 5.3027	.00370
- 4.5	-.005550	.0146	- 2.2787	.00330
- 3	-.004980	.0849	- 7.7856	.00330
- 1.5	-.005420	.1898	- 11.7154	.00330
0	-.005940	.1437	- 6.9364	.00320
1.5	-.005340	- .0241	- .9063	.00310
3	-.005200	- .2324	6.4255	.00300
4.5	-.004530	- .5207	13.5936	.00320
6	-.004810	- .7603	20.5162	.00270
9	-.004810	- 1.2165	28.5020	.00310
12.35	-.004910	- 1.6520	27.8637	.00350

Table A74. RC78 Incremental Axial Force Coefficient at $\beta=0^\circ$.

$$\Delta C = a_0 + a_1 x + a_2 x^2$$

α	a_0	a_1	a_2	σ
-14	-.004760	- .6452	11.6025	.00200
-12	-.004970	- .9155	19.2794	.00240
- 9	-.005130	- .8696	16.5189	.00230
- 6	-.005140	- .4709	6.5477	.00240
- 4.5	-.005010	- .4565	9.4310	.00220
- 3	-.005100	- .4798	11.8525	.00210
- 1.5	-.005180	- .5018	13.3727	.00210
0	-.005290	- .4398	10.2946	.00230
1.5	-.005430	- .3838	7.9313	.00230
3	-.005560	- .3650	7.0661	.00230
4.5	-.005650	- .3013	4.2555	.00210
6	-.005660	- .2373	2.0193	.00200
9	-.005580	- .2133	1.4406	.00210
12.35	-.005390	- .1422	- .1707	.00230

Table A75. RC78 Incremental Pitching Moment Coefficient at $\beta=0^\circ$.

$$\Delta C = a_0 + a_1 x + a_2 x^2$$

α	a_0	a_1	a_2	σ
-14	-.000924	- .3912	8.7395	.00036
-12	-.001084	- .4672	10.3710	.00093
- 9	-.000893	- .5840	11.3466	.00070
- 6	-.001096	- .5195	10.1263	.00090
- 4.5	-.001388	- .4420	9.3179	.00097
- 3	-.001154	- .4069	10.0841	.00064
- 1.5	-.001278	- .3714	9.7128	.00054
0	-.001458	- .3635	10.3020	.00055
1.5	-.001247	- .3265	8.3302	.00062
3	-.001213	- .2859	6.6416	.00057
4.5	-.001036	- .2263	3.4564	.00036
6	-.001142	- .1783	1.3379	.00081
9	-.001244	- .2078	2.4923	.00036
12.35	-.001289	- .1932	1.4084	.00030

Table A76. RC78 Incremental Rolling Moment Coefficient at $\beta=0^\circ$.

$$\Delta C = a_0 + a_1 x + a_2 x^2$$

α	a_0	a_1	a_2	σ
-14	-.000299	- .0668	.2219	.00030
-12	-.000199	.1143	- 5.6114	.00057
- 9	-.000164	.2486	- 8.4723	.00020
- 6	-.000205	.2161	- 7.0853	.00017
- 4.5	-.000193	.1882	- 6.2877	.00012
- 3	-.000158	.1558	- 5.3153	.00018
- 1.5	-.000150	.1064	- 4.0110	.00033
0	-.000142	.0367	- 2.3121	.00044
1.5	-.000139	- .0330	- .5394	.00033
3	-.000134	- .1080	1.7356	.00024
4.5	-.000157	- .1651	3.7652	.00023
6	-.000171	- .1919	4.3947	.00016
9	-.000166	- .1959	3.3725	.00017
12.35	-.000148	- .1953	4.2613	.00033

Table A77. RC78 Incremental Yawing Moment Coefficient at $\beta=0^\circ$.

$$\Delta C = a_0 + a_1 x + a_2 x^2$$

α	a_0	a_1	a_2	σ
-14	.000600	.6350	- 9.1150	.00037
-12	.000404	.7353	- 10.2555	.00053
- 9	.000276	.8042	- 10.3678	.00024
- 6	.000316	.7204	- 7.6204	.00050
- 4.5	.000237	.6379	- 5.5283	.00073
- 3	.000121	.5619	- 3.7685	.00041
- 1.5	.000089	.5553	- 4.0329	.00023
0	.000059	.5994	- 5.3682	.00031
1.5	.000032	.6491	- 6.5450	.00033
3	-.000016	.6778	- 6.9767	.00021
4.5	.000024	.6838	- 7.1026	.00020
6	.000020	.6657	- 6.6255	.00023
9	-.000075	.6289	- 5.6860	.00025
12.35	-.000182	.5777	- 5.7701	.00053

Table A78. RC78 Incremental Side Force Coefficient at $\beta=0^\circ$.

$$\Delta C = a_0 + a_1 x + a_2 x^2$$

α	a_0	a_1	a_2	σ
-14	.001410	- .8080	26.5169	.00120
-12	.000906	- 1.2162	34.1713	.00180
- 9	.000755	- 1.2286	28.2557	.00050
- 6	.000721	- .8531	16.6284	.00150
- 4.5	.000208	- .5268	8.2728	.00180
- 3	-.000014	- .1530	- 1.1893	.00160
- 1.5	-.000306	.1431	- 8.3397	.00160
0	-.000376	.3736	- 12.7347	.00130
1.5	-.000391	.5598	- 16.9796	.00110
3	-.000684	.8057	- 23.1785	.00120
4.5	-.000710	.9817	- 26.9923	.00140
6	-.000193	1.1039	- 27.5101	.00120
9	-.001133	1.1538	- 25.8705	.00120
12.35	-.001363	1.0255	- 22.2963	.00120

Table A79. RC82 Incremental Normal Force Coefficient at $\beta=0^\circ$.

$$\Delta C = a_0 + a_1 x + a_2 x^2$$

α	a_0	a_1	a_2	σ
-14	-.005830	- 5.6849	3.8565	.00373
-12	-.005615	- 4.8279	- 14.4495	.00518
- 9	-.005092	- 3.5777	- 45.5677	.00476
- 6	-.005199	- 3.3386	- 49.8544	.00363
- 4.5	-.005555	- 3.6432	- 38.4264	.00323
- 3	-.004973	- 3.7091	- 30.6436	.00385
- 1.5	-.005412	- 3.4069	- 33.1982	.00464
0	-.005933	- 3.1060	- 39.2504	.00356
1.5	-.005352	- 2.9927	- 40.6527	.00323
3	-.005212	- 3.0807	- 36.9642	.00302
4.5	-.004546	- 3.3505	- 19.4757	.00317
6	-.004803	- 3.7241	9.8117	.00477
9	-.004815	- 3.3250	24.0683	.00388
12.35	-.004948	- 3.4172	27.5234	.00378

Table A80. RC82 Incremental Axial Force Coefficient at $\beta=0^\circ$.

$$\Delta C = a_0 + a_1 x + a_2 x^2$$

α	a_0	a_1	a_2	σ
-14	-.004675	- 3.5428	22.7967	.00207
-12	-.004885	- 3.6649	29.6263	.00218
- 9	-.005066	- 3.2246	15.5883	.00263
- 6	-.005105	- 2.3603	- 11.4684	.00251
- 4.5	-.004992	- 2.1396	- 17.7428	.00217
- 3	-.005075	- 2.2244	- 13.6245	.00228
- 1.5	-.005153	- 2.5163	- 3.0151	.00246
0	-.005244	- 2.7498	6.6174	.00221
1.5	-.005379	- 2.7354	6.9461	.00229
3	-.005506	- 2.7409	8.1745	.00215
4.5	-.005612	- 2.7296	4.3388	.00234
6	-.005627	- 2.8089	1.5672	.00254
9	-.005415	- 3.1224	5.2658	.00218
12.35	-.005342	- 3.3971	15.4990	.00217

Table A81. RC82 Incremental Pitching Moment Coefficient at $\beta=0^\circ$.

$$\Delta C = a_0 + a_1 x + a_2 x^2$$

α	a_0	a_1	a_2	σ
-14	-.000928	- .4954	41.1815	.00066
-12	-.001090	- .5874	50.0041	.00078
- 9	-.000907	- .5411	50.7334	.00128
- 6	-.001129	- .0751	41.7158	.00228
- 4.5	-.001419	.2271	35.9293	.00219
- 3	-.001181	.4697	29.8899	.00105
- 1.5	-.001299	.6488	22.6784	.00082
0	-.001478	.7834	15.9317	.00086
1.5	-.001267	.9689	7.9627	.00121
3	-.001234	1.1961	- 1.5149	.00113
4.5	-.001058	1.3542	- 7.8714	.00067
6	-.001161	1.5523	- 14.9638	.00118
9	-.001243	2.1433	- 26.5592	.00234
12.35	-.001281	2.6870	- 43.3722	.00080

Table A82. RC82 Incremental Rolling Moment Coefficient at $\beta=0^\circ$.

$$\Delta C = a_0 + a_1 x + a_2 x^2$$

α	a_0	a_1	a_2	σ
-14	-.000298	.0644	- 12.8031	.00020
-12	-.000193	.0981	- 13.9837	.00028
- 9	-.000157	- .0114	- 6.2004	.00050
- 6	-.000199	- .0607	- 2.4208	.00026
- 4.5	-.000185	- .0571	- 2.9462	.00027
- 3	-.000153	- .0841	- 1.8582	.00023
- 1.5	-.000155	- .0807	- 3.0389	.00057
0	-.000142	- .0382	- 7.0347	.00089
1.5	-.000133	- .0124	- 11.3556	.00070
3	-.000114	- .0402	- 12.2965	.00062
4.5	-.000141	- .2130	- 5.6152	.00058
6	-.000160	- .3940	2.2652	.00055
9	-.000164	- .6394	14.7145	.00064
12.35	-.000147	- .6409	19.6673	.00066

Table A83. RC82 Incremental Yawing Moment Coefficient at $\beta=0^\circ$.

$$\Delta C = a_0 + a_1 x + a_2 x^2$$

α	a_0	a_1	a_2	σ
-14	.000621	- .1033	.3913	.00057
-12	.000411	- .0892	3.1412	.00072
- 9	.000287	.0576	- .1998	.00045
- 6	.000328	- .0476	4.6662	.00050
- 4.5	.000246	- .1761	10.9713	.00050
- 3	.000130	- .2367	13.4132	.00055
- 1.5	.000099	- .2015	13.3893	.00095
0	.000047	- .1495	13.0857	.00125
1.5	.000004	- .0684	12.8450	.00084
3	-.000059	.0418	9.0677	.00098
4.5	-.000009	.2367	1.2962	.00080
6	-.000001	.3945	- 5.2317	.00058
9	-.000077	.5772	- 13.4945	.00082
12.35	-.000189	.5820	- 18.7600	.00088

Table A84. RC82 Incremental Side Force Coefficient at $\beta=0^\circ$.

$$\Delta C = a_0 + a_1 x + a_2 x^2$$

α	a_0	a_1	a_2	σ
-14	.001331	.2403	- 23.6123	.00247
-12	.000871	- .2259	- 15.8905	.00252
- 9	.000753	- .9923	17.1409	.00148
- 6	.000695	- .8903	24.0262	.00179
- 4.5	.000182	- .6471	13.6612	.00187
- 3	-.000039	- .4812	4.2039	.00139
- 1.5	-.000341	- .5077	4.6611	.00124
0	-.000388	- .5995	9.8781	.00123
1.5	-.000386	- .7137	15.9138	.00150
3	-.000647	- .6082	13.2259	.00164
4.5	-.000668	- .4525	8.9516	.00161
6	-.000884	- .3878	8.7451	.00157
9	-.001145	- .5380	22.8626	.00256
12.35	-.001378	.6166	5.5694	.00629

Table A85. RC86 Incremental Normal Force Coefficient at $\beta=0^\circ$.

$$\Delta C = a_0 + a_1 x + a_2 x^2$$

α	a_0	a_1	a_2	σ
-14	-.005540	- 4.8187	2.5619	.00350
-12	-.005570	- 4.5990	7.2313	.00510
- 9	-.005030	- 3.7247	- 4.4522	.00430
- 6	-.005130	- 4.0320	16.0168	.00360
- 4.5	-.005510	- 4.3140	24.6113	.00380
- 3	-.004960	- 4.4968	30.8812	.00380
- 1.5	-.005420	- 4.3897	30.0792	.00410
0	-.005960	- 4.1356	25.1866	.00330
1.5	-.005350	- 4.3690	29.5090	.00400
3	-.005210	- 4.7790	42.8093	.00380
4.5	-.004530	- 5.4441	70.5732	.00320
6	-.004800	- 5.9540	101.7579	.00320
9	-.004780	- 6.2382	133.2190	.00330
12.35	-.004920	- 5.2158	99.3000	.00270

Table A86. RC86 Incremental Axial Force Coefficient at $\beta=0^\circ$.

$$\Delta C = a_0 + a_1 x + a_2 x^2$$

α	a_0	a_1	a_2	σ
-14	-.004720	- 3.6560	49.8544	.00210
-12	-.004930	- 4.1884	72.1854	.00210
- 9	-.005080	- 4.1998	79.6754	.00260
- 6	-.005120	- 3.7581	73.3386	.00250
- 4.5	-.005020	- 3.5644	67.7252	.00230
- 3	-.005110	- 3.5190	66.5745	.00230
- 1.5	-.005190	- 3.5426	66.7655	.00230
0	-.005280	- 3.7525	78.1565	.00240
1.5	-.005420	- 3.7562	82.9082	.00260
3	-.005560	- 3.6160	80.0650	.00240
4.5	-.005650	- 3.2973	64.5993	.00240
6	-.005650	- 3.1503	52.1759	.00260
9	-.005570	- 3.5672	57.3757	.00250
12.35	-.005380	- 3.8302	64.5985	.00250

Table A87. RC86 Incremental Pitching Moment Coefficient at $\beta=0^\circ$.

$$\Delta C = a_0 + a_1 x + a_2 x^2$$

α	a_0	a_1	a_2	σ
-14	-.000909	- .5694	41.4068	.00036
-12	-.001073	- .7506	49.3426	.00059
- 9	-.000880	- 1.0747	64.2508	.00086
- 6	-.001099	- .8418	62.7532	.00160
- 4.5	-.001406	- .6406	59.6522	.00129
- 3	-.001176	- .4607	54.8605	.00103
- 1.5	-.001296	- .3738	53.1222	.00082
0	-.001473	- .2557	49.9734	.00080
1.5	-.001271	- .2485	50.5131	.00099
3	-.001248	- .0175	42.7545	.00130
4.5	-.001074	.3589	27.2839	.00161
6	-.001165	.7480	12.6945	.00112
9	-.001244	1.2397	.4004	.00193
12.35	-.001287	1.9571	- 17.9080	.00146

Table A88. RC86 Incremental Rolling Moment Coefficient at $\beta=0^\circ$.

$$\Delta C = a_0 + a_1 x + a_2 x^2$$

α	a_0	a_1	a_2	σ
-14	-.000302	- .1010	- 1.3366	.00015
-12	-.000205	- .0699	- 2.6981	.00018
- 9	-.000172	- .0003	- 4.6248	.00029
- 6	-.000207	.0809	- 7.6066	.00026
- 4.5	-.000187	.0960	- 8.4655	.00023
- 3	-.000158	.0214	- 5.1583	.00037
- 1.5	-.000162	.0010	- 5.1416	.00062
0	-.000159	.0274	- 7.5021	.00068
1.5	-.000139	.1264	- 13.8138	.00062
3	-.000119	.1477	- 16.8310	.00077
4.5	-.000138	- .0240	- 11.5739	.00102
6	-.000159	- .3258	.6549	.00088
9	-.000164	- .5813	15.4049	.00069
12.35	-.000151	- .4651	13.5826	.00053

Table A89. RC86 Incremental Yawing Moment Coefficient at $\beta=0^\circ$.

$$\Delta C = a_0 + a_1 x + a_2 x^2$$

α	a_0	a_1	a_2	σ
-14	.000598	.1727	- 11.9899	.00047
-12	.000405	.1996	- 8.0398	.00086
- 9	.000280	.3705	- 10.9254	.00044
- 6	.000313	.3273	- 11.0997	.00052
- 4.5	.000225	.1169	- 1.3554	.00076
- 3	.000123	.0501	2.0297	.00088
- 1.5	.000114	- .0387	8.7136	.00112
0	.000098	- .0403	10.3760	.00121
1.5	.000045	- .0592	13.0880	.00087
3	-.000028	.0502	8.9390	.00084
4.5	.000001	.3222	- 2.4915	.00096
6	.000010	.6067	- 15.6540	.00083
9	-.000071	.6280	- 21.3569	.00077
12.35	-.000177	.4347	- 15.8876	.00090

Table A90. RC86 Incremental Side Force Coefficient at $\beta=0^\circ$.

$$\Delta C = a_0 + a_1 x + a_2 x^2$$

α	a_0	a_1	a_2	σ
-14	.001380	.5535	1.2652	.00145
-12	.000905	.3866	- 3.0188	.00234
- 9	.000764	- .0030	- 1.1819	.00126
- 6	.000721	- .1174	2.0667	.00063
- 4.5	.000249	.0393	- 2.2878	.00133
- 3	.000008	- .2411	12.2214	.00211
- 1.5	-.000319	- .4320	18.4752	.00269
0	-.000422	- .3330	11.7381	.00260
1.5	-.000403	- .1512	.9087	.00200
3	-.000673	.0425	- 3.1365	.00173
4.5	-.000690	.0711	- .2343	.00205
6	-.000890	.2690	- .8587	.00235
9	-.001118	.4311	7.2793	.00172
12.35	-.001386	.7941	2.2087	.00283

Table A91. RC87 Incremental Normal Force Coefficient at $\beta=0^\circ$.

$$\Delta C = a_0 + a_1 x + a_2 x^2$$

α	a_0	a_1	a_2	σ
-14	-.005560	- 2.0935	- 18.9428	.00350
-12	-.005590	- 1.1937	- 53.0562	.00420
- 9	-.005060	- .6564	- 63.5491	.00380
- 6	-.005170	- .9968	- 55.0068	.00410
- 4.5	-.005550	- 1.1059	- 59.6272	.00380
- 3	-.004990	- 1.1286	- 66.6108	.00360
- 1.5	-.005420	- 1.0220	- 75.9542	.00340
0	-.005950	- 1.2521	- 71.9523	.00420
1.5	-.005360	- 1.3453	- 74.1554	.00380
3	-.005230	- 2.0706	- 49.5480	.00370
4.5	-.004530	- 2.6555	- 28.9505	.00410
6	-.004790	- 3.6797	9.8160	.00330
9	-.004790	- 4.7243	47.5784	.00240
12.35	-.004930	- 4.8845	45.2958	.00280

Table A92. RC87 Incremental Axial Force Coefficient at $\beta=0^\circ$.

$$\Delta C = a_0 + a_1 x + a_2 x^2$$

α	a_0	a_1	a_2	σ
-14	-.004700	- 3.1948	33.4761	.00190
-12	-.004910	- 3.5604	48.7740	.00220
- 9	-.005070	- 3.6987	59.5163	.00230
- 6	-.005090	- 3.2503	51.8905	.00270
- 4.5	-.004980	- 3.1256	51.1080	.00220
- 3	-.005060	- 3.1770	54.9020	.00210
- 1.5	-.005150	- 3.1924	55.3891	.00210
0	-.005250	- 3.1467	55.2577	.00230
1.5	-.005400	- 3.0613	54.8094	.00230
3	-.005520	- 2.9540	53.3790	.00210
4.5	-.005600	- 2.7555	45.8075	.00210
6	-.005620	- 2.5523	36.7917	.00200
9	-.005560	- 2.4508	29.6021	.00210
12.35	-.005350	- 2.3771	27.3193	.00220

Table A93. RC87 Incremental Pitching Moment Coefficient at $\beta=0^\circ$.

$$\Delta C = a_0 + a_1 x + a_2 x^2$$

α	a_0	a_1	a_2	σ
-14	-.000909	.0076	22.8418	.00032
-12	-.001073	- .0978	27.9640	.00076
- 9	-.000888	- .2557	34.2912	.00083
- 6	-.001103	- .1295	33.7795	.00116
- 4.5	-.001403	- .0177	31.7945	.00112
- 3	-.001172	.0072	32.2043	.00062
- 1.5	-.001287	.0868	29.6843	.00071
0	-.001464	.1335	28.2584	.00071
1.5	-.001247	.3120	21.3610	.00090
3	-.001222	.4525	14.9017	.00096
4.5	-.001042	.7597	.4615	.00088
6	-.001149	.8105	- 3.3721	.00077
9	-.001240	.7254	- 3.7321	.00062
12.35	-.001293	.5856	- 1.8222	.00056

Table A94. RC87 Incremental Rolling Moment Coefficient at $\beta=0^\circ$.

$$\Delta C = a_0 + a_1 x + a_2 x^2$$

α	a_0	a_1	a_2	σ
-14	-.000303	- .0340	- 3.3976	.00023
-12	-.000204	.1434	- 10.1285	.00041
- 9	-.000165	.1815	- 10.5906	.00025
- 6	-.000209	.1506	- 10.3791	.00064
- 4.5	-.000203	.1004	- 8.8890	.00073
- 3	-.000167	.0003	- 5.6685	.00106
- 1.5	-.000159	- .2806	5.2646	.00069
0	-.000151	- .3108	4.0742	.00076
1.5	-.000150	- .2238	- 2.1451	.00086
3	-.000148	- .1615	- 7.6193	.00060
4.5	-.000158	- .2368	- 5.8735	.00063
6	-.000159	- .4452	2.9510	.00071
9	-.000164	- .7657	20.2572	.00060
12.35	-.000154	- .4968	11.8808	.00060

Table A95. RC87 Incremental Yawing Moment Coefficient at $\beta=0^\circ$.

$$\Delta C = a_0 + a_1 x + a_2 x^2$$

α	a_0	a_1	a_2	σ
-14	.000605	.3271	- 7.1207	.00047
-12	.000409	.4765	- 10.8158	.00081
- 9	.000276	.6730	- 14.2682	.00045
- 6	.000318	.5860	- 9.5735	.00115
- 4.5	.000246	.5192	- 7.7577	.00122
- 3	.000130	.5004	- 8.1173	.00099
- 1.5	.000101	.7611	- 19.9844	.00064
0	.000074	.6237	- 10.6028	.00157
1.5	.000050	.3743	4.1950	.99178
3	-.000002	.1965	16.7371	.00086
4.5	.000008	.3600	10.8380	.00107
6	-.000012	.7389	- 6.5109	.00132
9	-.000076	1.1678	- 32.7939	.00120
12.35	-.000173	.6555	- 17.5792	.00103

Table A96. RC87 Incremental Side Force Coefficient at $\beta=0^\circ$.

$$\Delta C = a_0 + a_1 x + a_2 x^2$$

α	a_0	a_1	a_2	σ
-14	.001397	- .0318	26.8579	.00142
-12	.000883	- .6750	46.2289	.00263
- 9	.000739	- .9570	44.8698	.00097
- 6	.000704	- .5631	28.1121	.00306
- 4.5	.000175	- .3116	23.0607	.00320
- 3	-.000043	- .1203	20.3832	.00230
- 1.5	-.000335	- .4577	41.2729	.00186
0	-.000404	.0219	22.9670	.00270
1.5	-.000428	.7715	- 7.1002	.00246
3	-.000727	1.3388	- 31.8401	.00123
4.5	-.000718	1.3115	- 28.5198	.00156
6	-.000886	.8782	- 5.2026	.00225
9	-.001145	.3237	35.2496	.00241
12.35	-.001400	1.4418	- 6.3643	.00195

Table A97. RC89 Incremental Normal Force Coefficient at $\beta=0^\circ$.

$$\Delta C = a_0 + a_1 x + a_2 x^2$$

α	a_0	a_1	a_2	σ
-14	-.005520	- .7012	- 38.6354	.00330
-12	-.005550	- .0808	- 55.7759	.00450
- 9	-.005030	.4119	- 62.2908	.00380
- 6	-.005180	.1354	- 56.9765	.00450
- 4.5	-.005560	- .0744	- 57.0485	.00370
- 3	-.004990	- .0026	- 65.4618	.00350
- 1.5	-.005420	- .0491	- 64.6022	.00340
0	-.005940	- .1944	- 60.2241	.00360
1.5	-.005340	- .6976	- 44.2070	.00360
3	-.005180	- 1.0928	- 34.2475	.00330
4.5	-.004500	- 1.5441	- 21.8076	.00330
6	-.004750	- 1.7281	- 21.0061	.00310
9	-.004760	- 2.5450	.3919	.00290
12.35	-.004900	- 3.2956	13.2377	.00410

Table A98. RC89 Incremental Axial Force Coefficient at $\beta=0^\circ$.

$$\Delta C = a_0 + a_1 x + a_2 x^2$$

α	a_0	a_1	a_2	σ
-14	-.004770	- 1.2621	.3297	.00210
-12	-.004970	- 1.5465	7.3438	.00250
- 9	-.005120	- 1.6528	9.8885	.00220
- 6	-.005120	- 1.3771	4.9044	.00230
- 4.5	-.005000	- 1.3226	5.1355	.00210
- 3	-.005080	- 1.3741	7.5366	.00210
- 1.5	-.005150	- 1.4202	8.8805	.00210
0	-.005250	- 1.4145	8.2085	.00210
1.5	-.005400	- 1.3877	7.8827	.00220
3	-.005530	- 1.3655	7.7674	.00210
4.5	-.005630	- 1.3445	7.6989	.00200
6	-.005640	- 1.3483	7.4320	.00190
9	-.005560	- 1.2998	4.0221	.00210
12.35	-.005360	- 1.1160	- 2.4398	.00230

Table A99. RC89 Incremental Pitching Moment Coefficient at $\beta=0^\circ$.

$$\Delta C = a_0 + a_1 x + a_2 x^2$$

α	a_0	a_1	a_2	σ
-14	-.000913	.3912	9.6768	.00024
-12	-.001074	.3699	9.2568	.00070
- 9	-.000878	.2590	9.7493	.00090
- 6	-.001095	.3604	8.0158	.00099
- 4.5	-.001389	.4001	9.5286	.00113
- 3	-.001151	.4385	10.8842	.00087
- 1.5	-.001268	.5025	10.6732	.00073
0	-.001449	.5684	9.1770	.00056
1.5	-.001238	.4985	12.0648	.00060
3	-.001208	.5787	8.4329	.00065
4.5	-.001035	.6702	4.4631	.00072
6	-.001146	.8365	- 2.3915	.00036
9	-.001242	.8227	- 3.3854	.00049
12.35	-.001286	.8095	- 4.8745	.0050

Table A100. RC89 Incremental Rolling Moment Coefficient at $\beta=0^\circ$.

$$\Delta C = a_0 + a_1 x + a_2 x^2$$

α	a_0	a_1	a_2	σ
-14	-.000304	1.1677	- 4.9205	.00031
-12	-.000203	.1935	- 11.5984	.00042
- 9	-.000163	.2706	- 13.0417	.00020
- 6	-.000203	.1746	- 9.5643	.00031
- 4.5	-.000192	.1636	- 10.2347	.00040
- 3	-.000155	.1576	- 11.4267	.00068
- 1.5	-.000142	.0755	- 9.7712	.00049
0	-.000133	- .0588	- 5.1224	.00041
1.5	-.000134	- .2145	1.2223	.00043
3	-.000133	- .3481	6.5346	.00034
4.5	-.000167	- .3525	5.9170	.00052
6	-.000179	- .2528	.1543	.00073
9	-.000163	- .3271	.4100	.00061
12.35	-.000149	- .4936	8.9159	.00055

Table A101. RC89 Incremental Yawing Moment Coefficient at $\beta=0^\circ$.

$$\Delta C = a_0 + a_1 x + a_2 x^2$$

α	a_0	a_1	a_2	σ
-14	.000610	.1720	- 5.2911	.00049
-12	.000412	.2898	- 6.4607	.00078
- 9	.000273	.4468	- 9.1883	.00026
- 6	.000314	.4278	- 8.5831	.00081
- 4.5	.000233	.3095	- 3.7561	.00094
- 3	.000112	.1507	2.9106	.00062
- 1.5	.000073	.1450	4.2014	.00039
0	.000044	.2411	.3972	.00046
1.5	.000024	.4005	- 6.4385	.00050
3	-.000018	.4927	- 9.4800	.00042
4.5	.000034	.4228	- 4.8684	.00082
6	.000027	.2691	3.7794	.00086
9	-.000084	.4210	- .8398	.00077
12.35	-.000185	.5736	- 11.7231	.00090

Table A102. RC89 Incremental Side Force Coefficient at $\beta=0^\circ$.

$$\Delta C = a_0 + a_1 x + a_2 x^2$$

α	a_0	a_1	a_2	σ
-14	-.001389	.0923	28.0028	.00120
-12	-.000873	- .3365	37.1740	.00229
- 9	.000731	- .5175	34.4778	.00095
- 6	.000716	- .3190	27.0008	.00185
- 4.5	.000207	.1140	13.4560	.00236
- 3	-.000008	.5790	- 1.7578	.00130
- 1.5	-.000281	.8827	- 10.8831	.00144
0	-.000353	1.0352	- 11.4192	.00234
1.5	-.000383	1.0176	- 4.0520	.00159
3	-.000695	1.0900	- 2.0186	.00099
4.5	-.000751	1.3283	- 11.5209	.00173
6	-.000948	1.7901	- 31.9298	.00194
9	-.001128	1.6453	- 28.2280	.00194
12.35	-.001382	1.1697	- 6.5931	.00142

Table A103. RC94 Incremental Normal Force Coefficient at $\beta=0^\circ$.

$$\Delta C = a_0 + a_1 x + a_2 x^2$$

α	a_0	a_1	a_2	σ
-14	-.005550	- 1.6883	- 12.6211	.00340
-12	-.005570	- 1.1138	- 31.0176	.00460
- 9	-.005050	.0057	- 66.7175	.00390
- 6	-.005160	- .2773	- 60.9514	.00450
- 4.5	-.005560	- .4365	- 64.7981	.00390
- 3	-.005000	- .2474	- 80.8450	.00370
- 1.5	-.005430	- .2751	- 82.4494	.00350
0	-.005940	- .6635	- 57.7838	.00400
1.5	-.005350	- 1.1799	- 52.1857	.00380
3	-.005240	- 1.5848	- 43.2749	.00350
4.5	-.004560	- 1.8339	- 39.4888	.00320
6	-.004800	- 2.2070	- 29.9899	.00320
9	-.004750	- 3.2625	2.1065	.00290
12.35	-.004910	- 3.8782	16.7458	.00310

Table A104. RC94 Incremental Axial Force Coefficient at $\beta=0^\circ$.

$$\Delta C = a_0 + a_1 x + a_2 x^2$$

α	a_0	a_1	a_2	σ
-14	-.004760	- 1.2638	.1647	.00210
-12	-.004970	- 1.5039	5.8693	.00230
- 9	-.005130	- 1.2860	- 3.6043	.00230
- 6	-.005130	- .8865	- 13.9888	.00230
- 4.5	-.005010	- .8666	- 11.5467	.00220
- 3	-.005090	- .9555	- 6.7572	.00210
- 1.5	-.005170	- 1.0043	- 5.3237	.00210
0	-.005270	- .9598	- 8.3848	.00220
1.5	-.005410	- .8960	- 10.3927	.00220
3	-.005530	- .8700	- 9.7622	.00210
4.5	-.005630	- .8270	- 9.8650	.00200
6	-.005650	- .8211	- 9.7838	.00200
9	-.005580	- .8415	- 10.9282	.00220
12.35	-.005370	- .7996	- 13.5472	.00230

Table A105. RC94 Incremental Pitching Moment Coefficient at $\beta=0^\circ$.

$$\Delta C = a_0 + a_1 x + a_2 x^2$$

α	a_0	a_1	a_2	σ
-14	-.000916	.5090	3.9822	.00027
-12	-.001076	.4965	3.5699	.00072
- 9	-.000878	.1566	13.8735	.00093
- 6	-.001089	.1667	16.0634	.00093
- 4.5	-.001386	.2244	17.4867	.00121
- 3	-.001150	.2434	20.2666	.00101
- 1.5	-.001273	.2887	21.9166	.00084
0	-.001460	.3899	19.0883	.00067
1.5	-.001250	.4577	16.3575	.00071
3	-.001224	.5319	12.8017	.00064
4.5	-.001049	.5842	11.3199	.00062
6	-.001160	.6134	11.0411	.00058
9	-.001244	.7919	2.6223	.00063
12.35	-.001286	.8056	- 1.5734	.00048

Table A106. RC94 Incremental Rolling Moment Coefficient at $\beta=0^\circ$.

$$\Delta C = a_0 + a_1 x + a_2 x^2$$

α	a_0	a_1	a_2	σ
-14	-.000298	- .0795	1.0248	.00030
-12	-.000197	.1029	- 4.2259	.00068
- 9	-.000160	.2034	- 4.6041	.00030
- 6	-.000205	.1722	- 1.6055	.00038
- 4.5	-.000191	.1874	- 2.2456	.00039
- 3	-.000151	.2073	- 3.8937	.00059
- 1.5	-.00141	.2000	- 5.5198	.00048
0	-.000138	.1719	- 5.6196	.00022
1.5	-.000144	.1323	- 4.3547	.00024
3	-.000142	.0649	- 1.6054	.00029
4.5	-.000163	.0098	.5623	.00025
6	-.000167	- .0163	1.1780	.00026
9	-.000159	- .0705	1.9119	.00031
12.35	-.000145	- .2107	8.6121	.00040

Table A107. RC94 Incremental Yawing Moment Coefficient at $\beta=0^\circ$.

$$\Delta C = a_0 + a_1 x + a_2 x^2$$

α	a_0	a_1	a_2	σ
-14	.000606	.8230	- 1.4788	.00040
-12	.000404	.9777	- 5.6940	.00052
- 9	.000274	1.0979	- 8.5397	.00020
- 6	.000318	1.0493	- 7.8640	.00091
- 4.5	.000236	.9102	- 2.2685	.00103
- 3	.000115	.7402	5.1998	.00076
- 1.5	.000073	.7077	8.8505	.00049
0	.000046	.7773	6.8423	.00037
1.5	.000031	.8769	2.6942	.00038
3	-.000008	.9472	- .4248	.00031
4.5	.000024	.9874	- 2.9624	.00041
6	.000006	.9694	- 2.2798	.00047
9	-.000089	1.0528	- 5.1076	.00048
12.35	-.000188	1.1339	- 11.2599	.00072

Table A108. RC94 Incremental Side Force Coefficient at $\beta=0^\circ$.

$$\Delta C = a_0 + a_1 x + a_2 x^2$$

α	a_0	a_1	a_2	σ
-14	.001408	- 1.4791	6.9671	.00086
-12	.000891	- 1.9249	20.9558	.00146
- 9	.000739	- 2.0244	19.5248	.00071
- 6	.000710	- 1.7789	11.3548	.00187
- 4.5	.000202	- 1.2572	- 7.4178	.00235
- 3	-.000007	- .6647	- 31.1743	.00166
- 1.5	-.000275	- .3139	- 46.8694	.00094
0	-.000344	- .1524	- 50.6958	.00177
1.5	-.000382	- .0820	- 47.8968	.00186
3	-.000693	.0341	- 45.3614	.00149
4.5	-.000717	.0410	- 39.2249	.00184
6	-.000887	.1239	- 37.5513	.00165
9	-.001102	- .0742	- 23.7946	.00177
12.35	-.001371	- .3549	- 11.0894	.00153

APPENDIX B

IA148 CURVE FIT COEFFICIENTS
AT +4 DEGREES YAW

Table B1. RC06 Incremental Normal Force Coefficient at $\beta=+4^\circ$.

$$\Delta C = a_0 + a_1 x + a_2 x^2$$

α	a_0	a_1	a_2	σ
-14	.005220	- 4.6744	43.2277	.00433
-12	.006238	- 4.7346	37.0045	.00373
- 9	.005558	- 4.5947	23.9799	.00366
- 6	.006185	- 4.8690	27.1566	.00380
- 4.5	.006315	- 4.9066	26.3658	.00381
- 3	.007263	- 5.0149	25.8730	.00380
- 1.5	.007289	- 4.8927	19.7319	.00358
0	.007231	- 5.0747	24.0039	.00398
1.5	.005280	- 5.0765	24.6309	.00442
3	.003689	- 5.0952	24.5731	.00337
4.5	.003435	- 4.9489	18.3577	.00334
6	.004615	- 4.7953	9.2469	.00305
9	.004626	- 4.5473	- .2065	.00319
12.35	.003967	- 4.6754	- 1.1012	.00441

Table B2. RC06 Incremental Axial Force Coefficient at $\beta=+4^\circ$.

$$\Delta C = a_0 + a_1 x + a_2 x^2$$

α	a_0	a_1	a_2	σ
-14	.021098	- 6.5925	124.4801	.00554
-12	.021536	- 6.6325	123.6747	.00519
- 9	.021887	- 6.7439	126.2752	.00448
- 6	.022054	- 6.8058	126.6940	.00437
- 4.5	.020724	- 6.6915	123.3574	.00521
- 3	.022049	- 6.7675	123.5653	.00445
- 1.5	.020557	- 6.5771	117.3451	.00534
0	.021732	- 6.6316	117.1839	.00461
1.5	.020549	- 6.4697	111.8948	.00519
3	.022152	- 6.7036	117.5858	.00423
4.5	.021164	- 6.6885	117.1054	.00488
6	.022546	- 6.9158	121.9566	.00413
9	.022483	- 6.9778	118.5692	.00419
12.35	.022017	- 6.9064	115.3235	.00434

Table B3. RC06 Incremental Pitching Moment Coefficient at $\beta=+4^\circ$.

$$\Delta C = a_0 + a_1 x + a_2 x^2$$

α	a_0	a_1	a_2	σ
-14	.002192	1.2941	10.4615	.00131
-12	.002565	1.1952	14.4305	.00146
- 9	.002402	1.2263	13.6238	.00115
- 6	.002020	1.3250	9.3995	.00115
- 4.5	.002176	1.2963	10.1709	.00118
- 3	.002514	1.1781	13.7965	.00118
- 1.5	.002858	1.1084	16.9303	.00116
0	.002851	1.0677	18.8825	.00108
1.5	.002225	1.1395	18.1512	.00116
3	.001423	1.2286	16.3231	.00116
4.5	.001392	1.2362	16.1200	.00114
6	.001682	1.1762	18.1002	.00116
9	.001843	1.1258	19.5071	.00113
12.35	.001985	1.1345	19.5920	.00117

Table B4. RC06 Incremental Rolling Moment Coefficient at $\beta=+4^\circ$.

$$\Delta C = a_0 + a_1 x + a_2 x^2$$

α	a_0	a_1	a_2	σ
-14	.000010	.0076	- 3.0815	.00037
-12	.000112	.0029	- 2.5089	.00041
- 9	.000148	.0274	- 2.7913	.00040
- 6	.000165	.0466	- 2.9205	.00028
- 4.5	.000137	.0444	- 2.7100	.00028
- 3	.000139	.0405	- 2.1921	.00031
- 1.5	.000097	.0357	- 1.4373	.00032
0	.000090	.0317	- .7647	.00030
1.5	.000065	.0363	- .5172	.00030
3	.000105	.0382	- .2992	.00033
4.5	.000109	.0528	- .6463	.00030
6	.000163	.0780	- 1.8548	.00033
9	.000107	.1331	- 4.6844	.00030
12.35	.000056	.0490	- 2.1732	.00047

Table B5. RC06 Incremental Yawing Moment Coefficient at $\beta = \pm 4^\circ$.

$$\Delta C = a_0 + a_1 x + a_2 x^2$$

α	a_0	a_1	a_2	σ
-14	-.000484	.0796	- 2.6616	.00065
-12	-.000740	.0639	- 2.3862	.00071
- 9	-.000720	.0388	- 2.4575	.00062
- 6	-.000803	.0442	- 2.7635	.00060
- 4.5	-.000797	.0722	- 3.5043	.00062
- 3	-.000790	.0856	- 3.9973	.00064
- 1.5	-.000722	.0945	- 4.9211	.00066
0	-.000714	.0851	- 4.9904	.00067
1.5	-.000666	.0548	- 4.0032	.00067
3	-.000704	.0574	- 3.4361	.00077
4.5	-.000694	.0485	- 2.5806	.00076
6	-.000760	.0641	- 2.8247	.00075
9	-.000566	.0314	- 1.2200	.00075
12.35	-.000667	.0721	- 1.4214	.00067

Table B6. RC06 Incremental Side Force Coefficient at $\beta = \pm 4^\circ$.

$$\Delta C = a_0 - a_1 x + a_2 x^2$$

α	a_0	a_1	a_2	σ
-14	-.001051	.3927	- 6.2890	.00193
-12	-.001793	.4519	- 3.8385	.00210
- 9	-.001205	.2730	6.2799	.00181
- 6	-.001251	.3303	4.0269	.00186
- 4.5	-.001270	.3900	1.1613	.00185
- 3	-.001274	.4217	- 1.0731	.00189
- 1.5	-.000944	.3788	.9348	.00184
0	-.000916	.3624	3.4687	.00217
1.5	-.000884	.3632	5.7941	.00199
3	-.001040	.4175	4.8197	.00187
4.5	-.000910	.4177	4.4828	.00176
6	-.000965	.4131	5.2604	.00184
9	-.000648	.3565	7.9481	.00179
12.35	-.001010	.8203	- 5.6932	.00237

Table B7. RC11 Incremental Normal Force Coefficient at $\beta=+4^\circ$.

$$\Delta C = a_0 + a_1 x + a_2 x^2$$

α	a_0	a_1	a_2	σ
-14	.005235	- 1.9636	18.0149	.00215
-12	.006211	- 1.9650	17.1936	.00214
- 9	.005586	- 1.8562	14.5108	.00223
- 6	.006255	- 1.9363	18.4891	.00240
- 4.5	.006380	- 1.7496	10.2077	.00268
- 3	.007395	- 1.8312	6.8087	.00307
- 1.5	.007419	- 1.7450	- 2.6525	.00289
0	.007392	- 2.0958	4.8265	.00281
1.5	.005390	- 2.2831	13.8266	.00360
3	.003811	- 2.7236	33.4330	.00286
4.5	.003546	- 3.1360	50.4834	.00266
6	.004741	- 3.5350	61.0070	.00227
9	.004701	- 3.9172	71.0928	.00214
12.35	.004005	- 3.8249	75.0820	.00222

Table B8. RC11 Incremental Axial Force Coefficient at $\beta=+4^\circ$.

$$\Delta C = a_0 + a_1 x + a_2 x^2$$

α	a_0	a_1	a_2	σ
-14	.021421	- 3.3921	57.0051	.00581
-12	.021920	- 3.5387	65.0236	.00501
- 9	.022143	- 3.6357	73.5529	.00480
- 6	.022290	- 3.5220	68.6533	.00471
- 4.5	.020941	- 3.4838	68.5907	.00599
- 3	.022329	- 3.8622	83.9522	.00471
- 1.5	.020754	- 3.8640	90.2840	.00615
0	.021933	- 3.9709	97.7034	.00522
1.5	.020704	- 3.6513	91.7892	.00608
3	.022346	- 3.5834	89.1466	.00468
4.5	.021328	- 3.1986	76.1996	.00562
6	.022763	- 3.1376	70.8378	.00425
9	.022743	- 3.0425	65.5267	.00400
12.35	.022223	- 3.0290	66.7827	.00465

Table B9. RC11 Incremental Pitching Moment Coefficient at $\beta=+4^\circ$.

$$\Delta C = a_0 - a_1 x + a_2 x^2$$

α	a_0	a_1	a_2	σ
-14	.002172	- .0085	10.0064	.00072
-12	.002533	- .1196	14.0529	.00076
- 9	.002456	- .2609	20.0757	.00071
- 6	.002061	- .1580	14.1577	.00080
- 4.5	.002192	- .1203	11.5101	.00068
- 3	.002536	- .2171	14.5725	.00060
- 1.5	.002881	- .2443	15.9362	.00081
0	.002872	- .2750	17.3634	.00082
1.5	.002239	- .1702	15.2076	.00109
3	.001428	- .0573	12.1126	.00090
4.5	.001402	.0904	5.9058	.00092
6	.001708	.1801	.3914	.00090
9	.001897	.2037	- 5.1421	.00082
12.35	.002022	.0514	- 1.5495	.00069

Table B10. RC11 Incremental Rolling Moment Coefficient at $\beta=+4^\circ$.

$$\Delta C = a_0 + a_1 x + a_2 x^2$$

α	a_0	a_1	a_2	σ
-14	.000038	.2446	- 22.7420	.00069
-12	.000127	.0161	- 14.3705	.00049
- 9	.000159	- .1369	- 8.0896	.00038
- 6	.000189	- .2397	- .7373	.00065
- 4.5	.000156	- .3112	4.1362	.00061
- 3	.000157	- .4193	9.3915	.00081
- 1.5	.000103	- .6059	18.7875	.00062
0	.000089	- .6667	22.4529	.00053
1.5	.000057	- .6232	21.8633	.00042
3	.000091	- .5065	17.4211	.00037
4.5	.000097	- .3853	12.5724	.00032
6	.000149	- .3100	9.6568	.00039
9	.000102	- .1503	5.0148	.00047
12.35	.000055	.0025	- .3667	.00017

Table B11. RC11 Incremental Yawing Moment Coefficient at $\beta=+4^\circ$.

$$\Delta C = a_0 + a_1 x + a_2 x^2$$

α	a_0	a_1	a_2	σ
-14	-.000521	- .2168	31.4568	.00108
-12	-.000773	.1762	17.2017	.00078
- 9	-.000738	.3934	7 5909	.00064
- 6	-.000844	.5592	- 3.7881	.00094
- 4.5	-.000835	.6837	- 11.7014	.00101
- 3	-.000838	.8496	- 19.9539	.00132
- 1.5	-.000746	1.1180	- 33.9357	.00096
0	-.000731	1.1824	- 38.1675	.00081
1.5	-.000668	1.0815	- 35.6389	.00071
3	-.000704	.8830	- 27.8028	.00067
4.5	-.000693	.6840	- 20.2339	.00060
6	-.000757	.5510	- 15 8291	.00083
9	-.000568	.3008	- 9.3166	.00056
12.35	-.000668	.1845	- 3.7041	.00032

Table B12. RC11 Incremental Side Force Coefficient at $\beta=+4^\circ$.

$$\Delta C = a_0 + a_1 x + a_2 x^2$$

α	a_0	a_1	a_2	σ
-14	-.001020	.5238	- 65.8527	.00261
-12	-.001799	- .0894	- 41.0320	.00215
- 9	-.001182	- .6581	- 17.0903	.00198
- 6	-.001185	- .9325	6.1718	.00267
- 4.5	-.001199	- 1.1698	25.7800	.00313
- 3	-.001184	- 1.5469	49.6453	.00413
- 1.5	-.000908	- 2.1192	84.0583	.00262
0	-.000912	- 2.1186	91.2201	.00243
1.5	-.000910	- 1.6961	78.7824	.00252
3	-.001080	- 1.0315	55.2574	.00229
4.5	-.000923	- .4391	33.5556	.00202
6	-.000973	.0648	16.3379	.00231
9	-.000683	.7672	- 5.5313	.00160
12.35	-.001036	.9934	- 13.7311	.00101

Table B13. RC37 Incremental Normal Force Coefficient at $\beta=+4^\circ$.

$$\Delta C = a_0 + a_1 x + a_2 x^2$$

α	a_0	a_1	a_2	σ
-14	.005257	- 2.1850	40.9390	.00208
-12	.006211	- 2.2928	46.0385	.00224
- 9	.005593	- 2.1179	42.3368	.00222
- 6	.006227	- 2.0597	38.5165	.00267
- 4.5	.006361	- 1.9536	35.4465	.00283
- 3	.007379	- 2.0829	37.2579	.00260
- 1.5	.007377	- 2.1364	41.5098	.00262
0	.007348	- 2.2604	43.9324	.00262
1.5	.005365	- 2.0649	38.5349	.00329
3	.003811	- 1.6966	22.2193	.00265
4.5	.003519	- 1.6236	17.8328	.00261
6	.004688	- 1.7780	17.9486	.00229
9	.004721	- 2.2363	26.5390	.00254
12.35	.004032	- 2.8485	50.3817	.00196

Table B14. RC37 Incremental Axial Force Coefficient at $\beta=+4^\circ$.

$$\Delta C = a_0 + a_1 x + a_2 x^2$$

α	a_0	a_1	a_2	σ
-14	.021417	- 3.3937	78.8697	.00582
-12	.021922	- 3.4378	79.0447	.00497
- 9	.022144	- 3.4491	78.6978	.00476
- 6	.022302	- 3.4606	79.4149	.00465
- 4.5	.020950	- 3.3587	76.7630	.00595
- 3	.022324	- 3.5867	82.7426	.00466
- 1.5	.020750	- 3.4330	78.1367	.00605
0	.021940	- 3.5398	81.2693	.00503
1.5	.020721	- 3.3443	76.1977	.00594
3	.022384	- 3.5465	82.8206	.00447
4.5	.021371	- 3.5282	84.9173	.00552
6	.022813	- 3.7767	94.2612	.00412
9	.022762	- 3.7902	96.0678	.00394
12.35	.022225	- 3.5838	89.0360	.00463

Table B15. RC37 Incremental Pitching Moment Coefficient at $\beta=+4^\circ$.

$$\Delta C = a_0 + a_1 x + a_2 x^2$$

α	a_0	a_1	a_2	σ
-14	.002156	.1547	.9401	.00072
-12	.002521	.1143	1.2234	.00081
- 9	.002457	.0815	.5327	.00075
- 6	.002058	.1270	- 2.2889	.00073
- 4.5	.002193	.1167	- 1.9656	.00079
- 3	.002529	.0658	- 1.1095	.00065
- 1.5	.002868	.0426	.2585	.00078
0	.002863	.0390	- .0006	.00079
1.5	.002246	.0780	- .5242	.00111
3	.001460	.1738	- 3.7780	.00082
4.5	.001417	.0808	.6592	.00086
6	.001708	- .0260	4.8406	.00071
9	.001881	- .0321	4.7641	.00063
12.35	.002011	- .0281	3.7848	.00060

Table B16. RC37 Incremental Rolling Moment Coefficient at $\beta=+4^\circ$.

$$\Delta C = a_0 + a_1 x + a_2 x^2$$

α	a_0	a_1	a_2	σ
-14	.000007	.0001	1.6637	.00013
-12	.000107	.0715	- 2.8660	.00029
- 9	.000144	.1446	- 7.5628	.00018
- 6	.000168	.1413	- 7.6883	.00012
- 4.5	.000135	.1435	- 7.7769	.00013
- 3	.000128	.1588	- 8.8139	.00019
- 1.5	.000086	.1911	- 11.1002	.00027
0	.000082	.2140	- 13.0971	.00032
1.5	.000063	.2098	- 13.6007	.00019
3	.000107	.1710	- 12.4028	.00021
4.5	.000112	.1207	- 10.2992	.00020
6	.000169	.0350	- 6.1702	.00041
9	.000119	- .0686	.1489	.00018
12.35	.000068	- .1976	6.2578	.00031

Table B17. RC37 Incremental Yawing Moment Coefficient at $\beta=+4^\circ$.

$$\Delta C = a_0 + a_1 x + a_2 x^2$$

α	a_0	a_1	a_2	σ
-14	-.000480	.0930	- 4.7222	.00033
-12	-.000745	.0148	1.4877	.00054
- 9	-.000718	- .1028	8.8949	.00038
- 6	-.000813	- .0929	8.9739	.00035
- 4.5	-.000802	- .0859	8.6720	.00032
- 3	-.000790	- .1054	9.8709	.00036
- 1.5	-.000716	- .1565	13.2142	.00046
0	-.000718	- .1934	16.3012	.00056
1.5	-.000677	- .1968	17.4195	.00038
3	-.000729	- .1380	15.6595	.00040
4.5	-.000717	- .0532	11.8697	.00043
6	-.000788	.0936	4.8173	.00070
9	-.000594	.2991	- 6.6643	.00031
12.35	-.000682	.5346	- 16.1297	.00037

Table B18. RC37 Incremental Side Force Coefficient at $\beta=+4^\circ$.

$$\Delta C = a_0 + a_1 x + a_2 x^2$$

α	a_0	a_1	a_2	σ
-14	-.001151	- .1202	7.7359	.00158
-12	-.001885	.2177	- 9.8550	.00190
- 9	-.001251	.4284	- 24.8358	.00164
- 6	-.001270	.4233	- 24.2318	.00163
- 4.5	-.001274	.4809	- 25.1092	.00147
- 3	-.001287	.5775	- 29.2167	.00152
- 1.5	-.000956	.6767	- 35.4351	.00148
0	-.000918	.7669	- 41.4105	.00145
1.5	-.000873	.7331	- 40.8968	.00130
3	-.001021	.6583	- 36.4317	.00138
4.5	-.000878	.4615	- 26.2029	.00128
6	-.000921	.2278	- 11.7492	.00203
9	-.000650	- .0651	8.9783	.00119
12.35	-.001018	- .3562	22.6220	.00115

Table B19. RC38 Incremental Normal Force Coefficient at $\beta=+4^\circ$.

$$\Delta C = a_0 + a_1 x + a_2 x^2$$

α	a_0	a_1	a_2	σ
-14	.005245	- 5.6018	8.2808	.00213
-12	.006240	- 5.6932	28.8734	.00475
- 9	.005575	- 5.0436	24.4312	.00304
- 6	.006225	- 4.1350	- 6.0067	.00278
- 4.5	.006356	- 3.9506	- 8.6894	.00306
- 3	.007367	- 3.9812	- 6.4210	.00277
- 1.5	.007365	- 3.7680	- 14.9589	.00269
0	.007347	- 4.0600	- 8.9788	.00352
1.5	.005350	- 4.5993	12.2773	.00464
3	.003767	- 5.3012	42.3479	.00336
4.5	.003491	- 5.8291	70.6529	.00324
6	.004638	- 6.0469	87.2689	.00375
9	.004605	- 5.3621	77.9067	.00363
12.35	.003993	- 4.7252	52.3508	.00227

Table B20. RC38 Incremental Axial Force Coefficient at $\beta=+4^\circ$.

$$\Delta C = a_0 + a_1 x + a_2 x^2$$

α	a_0	a_1	a_2	σ
-14	.021533	- 1.2501	- 27.8151	.00611
-12	.022031	- 1.5533	- 15.8938	.00528
- 9	.022255	- 1.8761	- 17.4719	.00501
- 6	.022408	- 1.9243	3.8630	.00495
- 4.5	.021029	- 1.6910	- 2.3476	.00611
- 3	.022420	- 1.7930	- 1.0050	.00483
- 1.5	.020811	- 1.6434	- 4.1781	.00618
0	.022012	- 1.7217	.0132	.00531
1.5	.020780	- 1.4456	- 7.4798	.00699
3	.022467	- 1.4845	- 11.5078	.00488
4.5	.021441	- 1.4706	- 17.9033	.00602
6	.022904	- 1.9959	- 7.1330	.00505
9	.022852	- 1.2785	16.1699	.00413
12.35	.022306	- 2.7429	19.6608	.00470

Table B21. RC38 Incremental Pitching Moment Coefficient at $\beta=+4^\circ$.

$$\Delta C = a_0 + a_1 x + a_2 x^2$$

α	a_0	a_1	a_2	σ
-14	.002179	- .1414	31.1738	.00081
-12	.002549	- .1271	37.4057	.00176
- 9	.002451	0472	37.7117	.00083
- 6	.002046	.2932	34.3483	.00139
- 4.5	.002176	.4723	31.6452	.00159
- 3	.002517	.6289	27.1863	.00114
- 1.5	.002861	.8517	19.2616	.00095
0	.002859	.9527	14.8745	.00087
1.5	.002232	1.1136	9.4827	.00108
3	.001429	1.2572	5.0337	.00096
4.5	.001398	1.4423	- .9645	.00128
6	.001690	1.555	- 3.3786	.00112
9	.001881	1.9413	- 14.1412	.00128
12.35	.002023	2.3778	- 30.8953	.00065

Table B22. RC38 Incremental Rolling Moment Coefficient at $\beta=+4^\circ$.

$$\Delta C = a_0 + a_1 x + a_2 x^2$$

α	a_0	a_1	a_2	σ
-14	.000020	.0052	- 23.6905	.00035
-12	.000114	- .2094	- 14.9518	.00034
- 9	.000160	- .2695	- 9.9719	.00056
- 6	.000189	- .2619	- 6.4954	.00062
- 4.5	.000153	- .2411	- 6.7039	.00046
- 3	.000157	- .3730	6.5674	.00098
- 1.5	.000106	- .5864	10.6010	.00109
0	.000094	- .7830	22.4234	.00090
1.5	.000053	- .6688	20.3655	.00110
3	.000083	- .3624	9.6252	.00121
4.5	.000096	- .1238	.0301	.00056
6	.000158	- .0207	- 5.7189	.00055
9	.000114	- .1170	- 3.5781	.00029
12.35	.000058	- .1784	1.7443	.00056

Table B23. RC38 Incremental Yawing Moment Coefficient at $\beta=+4^\circ$.

$$\Delta C = a_0 + a_1 x + a_2 x^2$$

α	a_0	a_1	a_2	σ
-14	-.000495	- .5209	24.0514	.00055
-12	-.000753	- .3140	15.1260	.00053
- 9	-.000742	- .3632	11.2175	.00110
- 6	-.000843	- .2697	4.0306	.00076
- 4.5	-.000821	- .1764	2.3942	.00112
- 3	-.000823	.1475	- 10.7454	.00157
- 1.5	-.000741	.4290	- 23.6209	.00148
0	-.000731	.6089	- 34.7512	.00103
1.5	-.000661	.3467	- 25.5037	.00119
3	-.000697	- .0036	- 11.0629	.00119
4.5	-.000701	- .2012	- .9073	.00088
6	-.000781	- .1502	1.7021	.00160
9	-.000596	.3550	- 11.9230	.00089
12.35	-.000678	.5023	- 21.5229	.00113

Table B24. RC38 Incremental Side Force Coefficient at $\beta=+4^\circ$.

$$\Delta C = a_0 + a_1 x + a_2 x^2$$

α	a_0	a_1	a_2	σ
-14	-.001045	1.8625	- .0072	.00230
-12	-.001788	1.1160	- .0042	.00241
- 9	-.001512	.2901	.0462	.00264
- 6	-.001185	- .2344	28.8833	.00241
- 4.5	-.001202	- .6448	46.2601	.00243
- 3	-.001180	- 1.2435	81.3172	.00488
- 1.5	-.000934	- 1.5737	111.2433	.00585
0	-.000971	- 1.2873	119.0705	.00476
1.5	-.000987	- .3623	89.6955	.00424
3	-.001182	.7960	45.2309	.00372
4.5	-.000973	1.7577	8.0190	.00328
6	-.000996	2.4570	- 18.8935	.00271
9	-.000657	3.0503	- 36.2091	.00215
12.35	-.001070	3.3125	- 42.3183	.00142

Table B25. RC40 Incremental Normal Force Coefficient at $\beta=+4^\circ$.

$$\Delta C = a_0 + a_1 x + a_2 x^2$$

α	a_0	a_1	a_2	σ
-14	.005303	- 3.0102	- 10.0648	.00232
-12	.006312	- 3.1493	- 5.9334	.00231
- 9	.005670	- 2.8858	- 18.4647	.00272
- 6	.006311	- 2.9731	- 20.8230	.00260
- 4.5	.006428	- 2.9500	- 25.1396	.00294
- 3	.007457	- 3.1238	- 28.5884	.00341
- 1.5	.007458	- 3.4012	- 23.5854	.00321
0	.007441	- 4.0005	- 6.6110	.00333
1.5	.005433	- 4.3419	7.5336	.00392
3	.003849	- 4.7630	23.3436	.00296
4.5	.003570	- 5.1199	35.8109	.00292
6	.004748	- 5.4690	45.9553	.00199
9	.004708	- 5.4765	46.5630	.00213
12.35	.004026	- 5.1860	42.8635	.00204

Table B26. RC40 Incremental Axial Force Coefficient at $\beta=+4^\circ$.

$$\Delta C = a_0 + a_1 x + a_2 x^2$$

α	a_0	a_1	a_2	σ
-14	.021333	- 4.6711	69.8411	.00612
-12	.021819	- 4.7478	73.5278	.00543
- 9	.022044	- 4.8578	82.3352	.00525
- 6	.022195	- 4.8248	79.2116	.00522
- 4.5	.020864	- 4.8711	82.0433	.00632
- 3	.022230	- 5.3280	101.1584	.00520
- 1.5	.020668	- 5.3710	109.6386	.00649
0	.021830	- 5.4096	113.6132	.00572
1.5	.020620	- 4.9859	101.3942	.00654
3	.022253	- 4.8886	95.9908	.00529
4.5	.021256	- 4.5812	85.1783	.00606
6	.022685	- 4.6472	84.0265	.00483
9	.022663	- 4.7371	84.8359	.00458
12.35	.022149	- 4.7507	86.0579	.00512

Table B27. RC40 Incremental Pitching Moment Coefficient at $\beta=+4^\circ$.

$$\Delta C = a_0 + a_1 x + a_2 x^2$$

α	a_0	a_1	a_2	σ
-14	.002164	.3645	25.3087	.00073
-12	.002526	.2501	30.4180	.00085
- 9	.002433	.2008	32.9616	.00087
- 6	.002035	.3779	24.6166	.00070
- 4.5	.002172	.3699	24.5081	.00087
- 3	.002507	.2535	29.0459	.00077
- 1.5	.002852	.2597	29.7750	.00107
0	.002835	.3546	26.7562	.00123
1.5	.002214	.5638	20.3967	.00123
3	.001401	.7246	14.7463	.00117
4.5	.001382	.8018	10.5930	.00107
6	.001675	.8219	8.0122	.00101
9	.001860	.7366	8.6792	.00091
12.35	.002000	.6065	11.7571	.00075

Table B28. RC40 Incremental Rolling Moment Coefficient at $\beta=+4^\circ$.

$$\Delta C = a_0 + a_1 x + a_2 x^2$$

α	a_0	a_1	a_2	σ
-14	.000037	.2694	- 29.0603	.00070
-12	.000129	.0472	- 21.7577	.00056
- 9	.000164	- .1303	- 14.4133	.00048
- 6	.000192	- .2106	- 8.4414	.00070
- 4.5	.000159	- .2956	- 3.3729	.00080
- 3	.000163	- .4539	4.5438	.00125
- 1.5	.000109	- .6260	14.7025	.00084
0	.000095	- .6441	17.3877	.00064
1.5	.000059	- .5514	14.5079	.00030
3	.000094	- .4575	10.5081	.00031
4.5	.000100	- .3458	5.7359	.00036
6	.000161	- .2437	1.7535	.00044
9	.000118	- .0929	- 3.0064	.00021
12.35	.000063	- .0282	- 5.6603	.00017

Table B29. RC40 Incremental Yawing Moment Coefficient at $\beta=+4^\circ$.

$$\Delta C = a_0 + a_1 x + a_2 x^2$$

α	a_0	a_1	a_2	σ
-14	-.000523	- .5363	32.5260	.00110
-12	-.000773	- .2149	20.9129	.00073
- 9	-.000742	.0117	10.2067	.00071
- 6	-.000848	.1700	- .1295	.00099
- 4.5	-.000840	.3534	- 9.9105	.00128
- 3	-.000840	.5748	- 20.3219	.00160
- 1.5	-.000746	.7667	- 31.8251	.00106
0	-.000726	.6986	- 30.9465	.00091
1.5	-.000664	.5041	- 24.3826	.00057
3	-.000705	.3643	- 18.5328	.00053
4.5	-.000700	.2155	- 12.7457	.00051
6	-.000776	.0774	- 8.1758	.00088
9	-.000590	- .1737	- 2.0186	.00035
12.35	-.000679	- .1818	- .7314	.00026

Table B30. RC40 Incremental Side Force Coefficient at $\beta=+4^\circ$.

$$\Delta C = a_0 + a_1 x + a_2 x^2$$

α	a_0	a_1	a_2	σ
-14	-.001002	1.6116	- 76.2421	-.00307
-12	-.001781	1.0321	- 51.7156	.00222
- 9	-.001169	0.5439	- 28.9176	.00215
- 6	-.001163	0.2685	- 7.0226	.00266
- 4.5	-.001169	- .0148	13.4353	.00354
- 3	-.001153	- .4577	40.4272	.00471
- 1.5	-.000879	- .7318	64.2061	.00333
0	-.000883	- .4642	60.9648	.00301
1.5	-.000884	- .0680	43.4433	.00175
3	-.003570	- .0512	35.8109	.00292
4.5	-.000901	.9385	10.9760	.00193
6	-.000924	1.4011	- 4.9736	.00217
9	-.000623	1.9814	- 22.6163	.00137
12.35	-.001013	1.9182	- 20.5202	.00124

Table B31. RC55 Incremental Normal Force Coefficient at $\beta=+4^\circ$.

$$\Delta C = a_0 + a_1 x + a_2 x^2$$

α	a_0	a_1	a_2	σ
-14	.005280	- 4.8150	2.4523	.00216
-12	.006258	- 4.8567	5.8298	.00253
- 9	.005573	- 4.3818	- 10.0820	.00263
- 6	.006253	- 4.7224	- 10.3138	.00307
- 4.5	.006369	- 4.9082	- 5.0124	.00278
- 3	.007350	- 4.6939	- 15.5328	.00299
- 1.5	.007362	- 4.3758	- 23.3029	.00278
0	.007341	- 4.3418	- 33.2152	.00284
1.5	.005353	- 4.4210	- 31.4598	.00369
3	.003781	- 4.7249	- 23.5614	.00346
4.5	.003518	- 4.9147	- 23.7162	.00341
6	.00472	- 5.4359	- 13.3771	.00307
9	.004737	- 6.1088	14.5343	.00242
12.35	.004046	- 6.6749	15.7228	.00241

Table B32. RC55 Incremental Axial Force Coefficient at $\beta=+4^\circ$.

$$\Delta C = a_0 + a_1 x + a_2 x^2$$

α	a_0	a_1	a_2	σ
-14	.021449	- 3.3438	42.6487	.00585
-12	.021955	- 3.7079	54.6952	.00501
- 9	.022176	- 3.7233	55.4779	.00478
- 6	.022335	- 3.6580	51.9109	.00466
- 4.5	.020972	- 3.4578	46.5085	.00595
- 3	.022350	- 3.4940	44.9392	.00465
- 1.5	.020771	- 3.1468	31.8595	.00607
0	.021970	- 3.1672	29.6748	.00501
1.5	.020750	- 3.0492	24.9968	.00597
3	.022420	- 3.2888	30.0891	.00456
4.5	.021398	- 3.2754	28.2754	.00554
6	.022850	- 3.5155	- 33.3243	.00418
9	.022820	- 3.6500	34.6482	.00394
12.35	.022280	- 3.5602	29.7463	.00465

04

Table B33. RC55 Incremental Pitching Moment Coefficient at $\beta = -4^\circ$.

$$\Delta C = a_0 + a_1 x + a_2 x^2$$

α	a_0	a_1	a_2	σ
-14	.002155	1.3290	15.2181	.00070
-12	.002532	1.4099	10.8607	.00080
- 9	.002464	1.4101	11.0241	.00074
- 6	.002053	1.5636	8.7457	.00095
- 4.5	.002191	1.5855	9.4942	.00089
- 3	.002548	1.5694	11.6176	.00086
- 1.5	.002891	1.4764	17.1765	.00096
0	.002890	1.4175	20.0786	.00092
1.5	.002257	1.4547	18.3815	.00126
3	.001456	1.4665	17.5538	.00085
4.5	.001414	1.4816	17.5711	.00089
6	.001708	1.4446	19.2793	.00078
9	.001885	1.4867	15.7268	.00089
12.35	.002022	1.4757	12.8406	.00065

Table B34. RC55 Incremental Rolling Moment Coefficient at $\beta = +4^\circ$.

$$\Delta C = a_0 + a_1 x + a_2 x^2$$

α	a_0	a_1	a_2	σ
-14	.000008	- .2078	- 2.2215	.00027
-12	.000115	- .1119	- 3.2450	.00073
- 9	.000156	- .0099	- 4.6344	.00025
- 6	.000170	- .0622	- 3.4245	.00025
- 4.5	.000137	- .0683	- 2.6840	.00031
- 3	.000133	- .0595	- 2.0110	.00031
- 1.5	.000091	- .0860	1.8865	.00026
0	.000083	- .1362	2.7003	.00019
1.5	.000058	- .1737	4.1885	.00018
3	.000096	- .2222	5.7165	.00021
4.5	.000100	- .2671	7.2887	.00019
6	.000155	- .2991	8.3098	.00018
9	.000106	- .1833	4.1106	.00040
12.35	.000054	- .1039	.7691	.00029

Table B35. RC55 Incremental Yawing Moment Coefficient at $\beta=+4^\circ$.

$$\Delta C = a_0 + a_1 x + a_2 x^2$$

α	a_0	a_1	a_2	σ
-14	-.000471	.5997	- 5.5987	.00039
-12	-.000742	.6452	- 8.0863	.00041
- 9	-.000716	.6859	- 7.8741	.00041
- 6	-.000800	.7379	- 8.9881	.00046
- 4.5	-.000704	.7421	- 9.8814	.00046
- 3	-.000787	.7184	- 9.2643	.00036
- 1.5	-.000717	.7094	- 8.8760	.00032
0	-.000713	.7173	- 8.9006	.00029
1.5	-.000668	.7073	- 8.4565	.00029
3	-.000717	.7308	- 8.9194	.00035
4.5	-.000707	.7428	- 9.2010	.00030
6	-.000777	.7700	- 10.5421	.00033
9	-.000587	.6961	- 8.6732	.00026
12.35	-.000678	.6180	- 3.4571	.00044

Table B36. RC55 Incremental Side Force Coefficient at $\beta=+4^\circ$.

$$\Delta C = a_0 + a_1 x + a_2 x^2$$

α	a_0	a_1	a_2	σ
-14	-.001150	.0081	2.6215	.00154
-12	-.001903	.0416	- 1.8673	.00185
- 9	-.001263	- .0432	- 1.9172	.00175
- 6	-.001286	- .2948	7.8107	.00182
- 4.5	-.001290	- .2579	7.8953	.00179
- 3	-.001289	- .0441	1.1606	.00155
- 1.5	-.000961	.1418	- 5.3816	.00160
0	-.000933	.4373	- 14.2219	.00199
1.5	-.000895	.7043	- 20.4025	.00188
3	-.001050	.9136	- 24.5607	.00155
4.5	-.000898	1.0260	- 26.1956	.00133
6	-.000943	1.1737	- 30.2096	.00141
9	-.000640	1.3936	- 34.0085	.00149
12.35	-.001007	1.2786	- 26.5349	.00132

Table B37. RC59 Incremental Normal Force Coefficient at $\beta=+4^\circ$.

$$\Delta C = a_0 - a_1 x - a_2 x^2$$

α	a_0	a_1	a_2	σ
-14	.005268	- 3.1708	10.3512	.00195
-12	.006279	- 2.8217	4.7942	.00327
- 9	.005637	- 2.2274	- 9.1231	.00240
- 6	.006275	- 2.4521	10.7544	.00288
- 4.5	.006402	- 2.5692	23.6541	.00318
- 3	.007422	- 2.7426	34.6774	.00266
- 1.5	.007411	- 2.7317	35.8124	.00238
0	.007367	- 3.0742	45.1577	.00316
1.5	.005355	- 3.2854	49.7895	.00402
3	.003780	- 3.7035	65.0726	.00316
4.5	.003517	- 4.0272	78.7446	.00274
6	.004696	- 4.3936	94.6835	.00193
9	.004657	- 4.8446	128.0453	.00373
12.35	.003928	- 4.1021	115.5795	.00373

Table B38. RC59 Incremental Axial Force Coefficient at $\beta=+4^\circ$.

$$\Delta C = a_0 + a_1 x + a_2 x^2$$

α	a_0	a_1	a_2	σ
-14	.021502	- 1.0150	- 4.9112	.00597
-12	.021998	- 1.3176	7.2081	.00513
- 9	.022230	- 1.4877	15.5867	.00491
- 6	.022380	- 1.4429	14.2839	.00479
- 4.5	.021011	- 1.3349	11.3165	.00605
- 3	.022400	- 1.5868	19.4121	.00477
- 1.5	.020797	- 1.6649	28.2018	.00617
0	.021982	- 1.8103	38.0954	.00535
1.5	.020747	- 1.5879	35.4782	.00612
3	.022423	- 1.4844	30.2988	.00452
4.5	.021397	- 1.1755	16.1293	.00559
6	.022851	- 1.3020	13.4806	.00447
9	.022815	- 1.5456	13.3592	.00398
12.35	.022290	- 1.6620	18.7461	.00464

Table B39. RC59 Incremental Pitching Moment Coefficient at $\beta=+4^\circ$.

$$\Delta C = a_0 + a_1 x + a_2 x^2$$

α	a_0	a_1	a_2	σ
-14	.002176	- .4250	9.3675	.00078
-12	.002549	- .3909	9.9553	.00093
- 9	.002464	- .4776	16.9888	.00077
- 6	.002065	- .4548	19.1419	.00064
- 4.5	.002196	- .4395	19.9361	.00082
- 3	.002537	- .4437	20.7353	.00083
- 1.5	.002877	- .4246	22.2005	.00089
0	.002868	- .3692	21.6669	.00090
1.5	.002238	- .2289	18.8007	.00109
3	.001430	- .0253	12.4915	.00100
4.5	.001404	.1117	7.4334	.00089
6	.001702	.2068	3.0806	.00070
9	.001879	.0050	15.0770	.00120
12.35	.001995	.2823	10.8362	.00146

Table B40. RC59 Incremental Rolling Moment Coefficient at $\beta=+4^\circ$.

$$\Delta C = a_0 + a_1 x + a_2 x^2$$

α	a_0	a_1	a_2	σ
-14	.000024	.0037	- 17.7723	.00039
-12	.000126	- .1347	- 12.5487	.00039
- 9	.000172	- .3178	- 2.2849	.00080
- 6	.000194	- .4828	11.1520	.00103
- 4.5	.000154	- .5415	17.0108	.00079
- 3	.000148	- .6266	22.8250	.00067
- 1.5	.000094	- .7187	28.2695	.00040
0	.000080	- .6790	28.0389	.00060
1.5	.000049	- .5308	23.8827	.00080
3	.000081	- .3323	18.2735	.00100
4.5	.000088	- .0702	8.3052	.00092
6	.000144	.0890	1.1715	.00077
9	.000108	.1381	4.4144	.00043
12.35	.000050	- .0408	2.8178	.00033

Table B41. RC59 Incremental Yawing Moment Coefficient at $\beta=+4^\circ$.

$$\Delta C = a_0 + a_1 x - a_2 x^2$$

α	a_0	a_1	a_2	σ
-14	-.000511	-.0778	27.4380	.00089
-12	-.000772	.2565	13.3674	.00066
-9	-.000759	.5039	- 2.3962	.00131
-6	-.000854	.7829	- 21.5146	.00112
-4.5	-.000836	.9265	- 29.8286	.00092
-3	-.000833	1.1349	- 39.9033	.00115
-1.5	-.000736	1.3529	- 51.4367	.00102
0	-.000712	1.3548	- 54.2944	.00118
1.5	-.000646	1.0586	- 45.0871	.00140
3	-.000677	.6519	- 39.0688	.00150
4.5	-.000675	.2242	- 11.2315	.00130
6	-.000750	.0540	- .7407	.00148
9	-.000577	.1206	5.4035	.00095
12.35	-.000658	.4215	- 6.5720	.00067

Table B42. RC59 Incremental Side Force Coefficient at $\beta=+4^\circ$.

$$\Delta C = a_0 + a_1 x - a_2 x^2$$

α	a_0	a_1	a_2	σ
-14	-.001036	1.8209	- 96.6859	.00262
-12	-.001845	1.0098	- 66.7314	.00235
-9	-.001216	.4059	- 40.3719	.00216
-6	-.001173	-.2639	- 1.5748	.00260
-4.5	-.001172	-.8155	26.5650	.00303
-3	-.001150	- 1.4539	60.1606	.00386
-1.5	-.000900	- 1.8237	85.3614	.00352
0	-.000922	- 1.7144	93.4697	.00367
1.5	-.000913	- 1.2947	84.3139	.00250
3	-.001116	-.8865	73.0822	.00230
4.5	-.000948	-.4825	60.9802	.00300
6	-.000998	.0785	43.6601	.00345
9	-.000690	.8597	15.8615	.00149
12.35	-.001084	.1358	40.5577	.00250

Table B43. RC61 Incremental Normal Force Coefficient at $\beta=+4^\circ$.

$$\Delta C = a_0 - a_1 x - a_2 x^2$$

α	a_0	a_1	a_2	σ
-14	.005244	- 2.8621	5.8547	.00227
-12	.006234	- 2.6081	- 9.0899	.00222
- 9	.005594	- 2.6222	- 9.0685	.00243
- 6	.006232	- 3.0058	1.6112	.00267
- 4.5	.006371	- 2.9498	- 2.1769	.00275
- 3	.007409	- 3.1186	- .1347	.00249
- 1.5	.007414	- 3.0921	- 3.5715	.00255
0	.007381	- 3.2120	- 5.7197	.00298
1.5	.005376	- 3.1395	- 11.5653	.00357
3	.003814	- 3.1481	- 14.0927	.00267
4.5	.003547	- 3.1984	- 14.7731	.00254
6	.004729	- 3.3933	- 11.6473	.00191
9	.004700	- 3.8356	2.7544	.00204
12.35	.004043	- 3.8816	8.6046	.00195

Table B44. RC61 Incremental Axial Force Coefficient at $\beta=+4^\circ$.

$$\Delta C = a_0 + a_1 x - a_2 x^2$$

α	a_0	a_1	a_2	σ
-14	.021430	- 4.9962	95.5659	.00582
-12	.021929	- 5.0021	93.5227	.00498
- 9	.022166	- 4.9133	89.6974	.00475
- 6	.022325	- 4.8866	86.5713	.00465
- 4.5	.020962	- 4.8841	86.7104	.00598
- 3	.022348	- 5.1862	94.9652	.00469
- 1.5	.020764	- 5.1236	93.4741	.00605
0	.021956	- 5.2087	94.7462	.00500
1.5	.020739	- 5.1064	93.8368	.00595
3	.022412	- 5.4166	105.3949	.00451
4.5	.021384	- 5.4459	109.7549	.00551
6	.022812	- 5.6419	115.6526	.00411
9	.022775	- 5.5500	111.6610	.00391
12.35	.022249	- 5.5163	111.6802	.00459

Table B45. RC61 Incremental Pitching Moment Coefficient at $\beta=+4^\circ$.

$$\Delta C = a_0 + a_1 x - a_2 x^2$$

α	a_0	a_1	a_2	σ
-14	.002173	.5087	19.3477	.00071
-12	.002544	.4757	20.0188	.00078
- 9	.002462	.3960	21.6682	.00075
- 6	.002060	.4109	20.3411	.00064
- 4.5	.002194	.4357	18.9352	.00070
- 3	.002537	.3560	20.9524	.00062
- 1.5	.002879	.3869	19.6126	.00079
0	.002876	.3788	20.1504	.00079
1.5	.002251	.4382	20.2238	.00110
3	.001460	.4407	22.7905	.00093
4.5	.001418	.4233	24.7994	.00082
6	.001711	.3863	26.1162	.00066
9	.001888	.4060	23.7777	.00062
12.35	.002017	.4127	21.4072	.00058

Table B46. RC61 Incremental Rolling Moment Coefficient at $\beta=+4^\circ$.

$$\Delta C = a_0 + a_1 x + a_2 x^2$$

α	a_0	a_1	a_2	σ
-14	.000001	.0008	- 4.1013	.00022
-12	.000102	.0809	- 9.8299	.00038
- 9	.000141	.1477	- 14.4214	.00017
- 6	.000166	.1468	- 14.6713	.00010
- 4.5	.000134	.1463	- 14.9621	.00020
- 3	.000126	.1493	- 15.6340	.00020
- 1.5	.000084	.1482	- 16.0715	.00010
0	.000078	.1342	- 15.8085	.00015
1.5	.000058	.1195	- 16.0275	.00028
3	.000107	.0487	- 13.9645	.00043
4.5	.000123	- .0736	- 9.0479	.00062
6	.000187	- .1921	- 3.1898	.00065
9	.000122	- .2822	3.4372	.00029
12.35	.000062	- .3184	5.1735	.00020

Table B47. RC61 Incremental Yawing Moment Coefficient at $\beta=+4^\circ$.

$$\Delta C = a_0 - a_1 x - a_2 x^2$$

α	a_0	a_1	a_2	σ
-14	-.000471	-.1924	- 1.1342	.00034
-12	-.000736	-.2957	6.1023	.00058
- 9	-.000710	-.4566	14.8447	.00042
- 6	-.000810	-.4351	14.8230	.00035
- 4.5	-.000803	-.4068	14.5585	.00050
- 3	-.000792	-.3973	15.2072	.00050
- 1.5	-.000717	-.3976	15.9556	.00028
0	-.000715	-.3960	16.1460	.00031
1.5	-.000671	-.4048	17.3443	.00042
3	-.000730	-.3172	15.0258	.00065
4.5	-.000730	-.1411	7.8502	.00091
6	-.000808	.0568	- 2.0214	.00102
9	-.000592	.2245	- 13.6716	.00034
12.35	-.000675	.3272	- 17.2965	.00021

Table B48. RC61 Incremental Side Force Coefficient at $\beta=+4^\circ$.

$$\Delta C = a_0 + a_1 x - a_2 x^2$$

α	a_0	a_1	a_2	σ
-14	-.001113	1.4800	- 15.9313	.00153
-12	-.001856	1.9045	- 36.0899	.00177
- 9	-.001224	2.1558	- 51.8456	.00158
- 6	-.001245	2.2659	- 56.0365	.00164
- 4.5	-.001261	2.3731	- 60.6113	.00156
- 3	-.001268	2.3947	- 62.7160	.00159
- 1.5	-.000950	2.4168	- 64.9437	.00134
0	-.000918	2.3925	- 63.4394	.00130
1.5	-.000879	2.3900	- 64.4730	.00133
3	-.001010	2.2700	- 60.2771	.00169
4.5	-.000834	1.9117	- 44.9626	.00214
6	-.000854	1.5866	- 26.5687	.00246
9	-.000620	1.1668	- .0132	.00136
12.35	-.001023	.8546	13.4099	.00102

Table B49. RC62 Incremental Normal Force Coefficient at $\beta=+4^\circ$.

$$\Delta C = a_0 + a_1 x + a_2 x^2$$

α	a_0	a_1	a_2	σ
-14	.005231	- 4.9282	64.8791	.00217
-12	.006210	- 4.6099	68.3567	.00536
- 9	.005542	- 3.7419	58.7025	.00318
- 6	.006198	- 2.9637	35.7218	.00311
- 4.5	.006360	- 2.6608	29.4361	.00329
- 3	.007378	- 2.5009	26.5945	.00319
- 1.5	.007395	- 2.2543	21.6878	.00250
0	.007352	- 2.8750	16.7824	.00372
1.5	.005354	- 2.7852	36.4024	.00496
3	.003752	- 3.4164	60.7197	.00364
4.5	.003483	- 3.9458	90.3967	.00345
6	.004643	- 4.1000	103.6805	.00365
9	.004605	- 3.4962	96.4398	.00349
12.35	.004004	- 2.8534	7.1548	.00218

Table B50. RC62 Incremental Axial Force Coefficient at $\beta=+4^\circ$.

$$\Delta C = a_0 + a_1 x + a_2 x^2$$

α	a_0	a_1	a_2	σ
-14	.021423	- .6530	- 25.2308	.00582
-12	.021921	- 1.0455	- 8.7892	.00503
- 9	.022149	- 1.3307	4.2181	.00477
- 6	.022282	- 1.3023	8.6473	.00478
- 4.5	.020915	- 1.0546	3.1375	.00601
- 3	.022291	- 1.1125	2.7167	.00473
- 1.5	.020722	- .8652	- 5.2529	.00611
0	.021916	- .9440	- 1.3804	.00524
1.5	.020696	- .7229	- 5.8600	.00606
3	.022356	- .8252	- 4.5302	.00463
4.5	.021340	- .7682	- 10.4012	.00573
6	.022775	- 1.2116	- 1.1380	.00478
9	.022732	- 1.7306	11.3663	.00404
12.35	.022207	- 1.6128	9.3597	.00470

Table B51. RC62 Incremental Pitching Moment Coefficient at $\beta=+4^\circ$.

$$\Delta C = a_0 + a_1 x + a_2 x^2$$

α	a_0	a_1	a_2	σ
-14	.002165	- 1.0291	22.3881	.00072
-12	.002538	- 1.1101	32.3421	.00162
- 9	.002439	- 1.1023	39.3758	.00091
- 6	.002034	- .8498	35.5633	.00154
- 4.5	.002177	- .6894	33.5278	.00141
- 3	.002512	- .5008	26.5898	.00115
- 1.5	.002861	- .2654	17.1832	.00114
0	.002855	- .0600	7.0369	.00084
1.5	.002236	.0093	5.6135	.00114
3	.001430	.1038	3.2709	.00100
4.5	.001395	.2098	1.4859	.00138
6	.001684	.3621	- 2.3440	.00121
9	.001867	.8885	- 18.3110	.00156
12.35	.002016	1.3576	- 35.9758	.00063

Table B52. RC62 Incremental Rolling Moment Coefficient at $\beta=+4^\circ$.

$$\Delta C = a_0 + a_1 x + a_2 x^2$$

α	a_0	a_1	a_2	σ
-14	.000024	.1107	- 24.0734	.00040
-12	.000116	- .1239	- 13.7479	.00040
- 9	.000163	- .2078	- 6.9900	.00066
- 6	.000196	- .2233	- 1.3048	.00081
- 4.5	.000157	- .1657	- 2.3148	.00058
- 3	.000160	- .2357	2.1955	.00085
- 1.5	.000113	- .4195	11.0141	.00097
0	.000102	- .6619	24.2728	.00098
1.5	.000059	- .6408	26.4459	.00119
3	.000081	- .3965	19.3852	.00133
4.5	.000092	- .1207	8.8559	.00073
6	.000158	.0293	1.6801	.00042
9	.000108	.0158	.9381	.00026
12.35	.000052	.0018	4.1117	.00047

Table B53. RC62 Incremental Yawing Moment Coefficient at $\beta = \pm 4^\circ$.

$$\Delta C = a_0 + a_1 x + a_2 x^2$$

α	a_0	a_1	a_2	σ
-14	-.000503	.0363	28.9379	.00065
-12	-.000752	.3076	16.4855	.00063
-9	-.000741	.3512	7.8659	.00122
-6	-.000843	.4533	- 1.5391	.00069
-4.5	-.000819	.5060	- 2.6554	.00084
-3	-.000819	.7377	- 12.1718	.00124
-1.5	-.000748	1.0004	- 23.6789	.00127
0	-.000740	1.2848	- 39.1453	.00118
1.5	-.000666	1.1722	- 37.2360	.00133
3	-.000688	.8955	- 27.7296	.00136
4.5	-.000690	.6408	- 15.9971	.00089
6	-.000773	.6374	- 12.0348	.00141
9	-.000581	.9738	- 18.6796	.00070
12.35	-.000670	1.0910	- 26.0762	.00103

Table B54. RC62 Incremental Side Force Coefficient at $\beta = \pm 4^\circ$.

$$\Delta C = a_0 + a_1 x + a_2 x^2$$

α	a_0	a_1	a_2	σ
-14	-.001035	1.8119	- 97.3141	.00241
-12	-.001790	.8443	- 55.9730	.00265
-9	-.001156	- .3464	4.6516	.00281
-6	-.001180	- .9873	42.3355	.00234
-4.5	-.001196	- 1.2794	57.2479	.00228
-3	-.001182	- 1.6957	84.2939	.00421
-1.5	-.000923	- 2.0281	113.3828	.00506
0	-.000969	- 1.9208	128.4325	.00464
1.5	-.000993	- 1.2558	111.9177	.00432
3	-.001220	- .1919	74.1411	.00430
4.5	-.001002	.8142	36.4765	.00379
6	-.001009	1.5906	8.5571	.00307
9	-.000699	2.5447	- 22.1640	.00245
12.35	-.001104	2.8294	- 28.2930	.00175

Table B55. RC78 Incremental Normal Force Coefficient at $\beta=+4^\circ$.

$$\Delta C = a_0 + a_1 x + a_2 x^2$$

α	a_0	a_1	a_2	σ
-14	.005241	- 1.6479	29.3288	.00200
-12	.006219	- 1.3267	20.9421	.00289
- 9	.005568	- 1.0866	21.5411	.00229
- 6	.006237	- 1.1640	21.7549	.00248
- 4.5	.006380	- .9349	13.7713	.00296
- 3	.007398	- .8001	10.5980	.00313
- 1.5	.007404	- .6335	8.9049	.00238
0	.007378	- .6635	8.8594	.00267
1.5	.005377	- .7744	11.0226	.00407
3	.003798	- 1.1642	21.1515	.00359
4.5	.003525	- 1.4147	25.5128	.00281
6	.004717	- 1.8978	37.6068	.00248
9	.004684	- 2.1626	40.5798	.00220
12.35	.004011	- 2.6558	49.6748	.00301

Table B56. RC78 Incremental Axial Force Coefficient at $\beta=+4^\circ$.

$$\Delta C = a_0 + a_1 x - a_2 x^2$$

α	a_0	a_1	a_2	σ
-14	.021443	- .2488	1.3443	.00563
-12	.021933	- .4270	5.8315	.00486
- 9	.022175	- .3461	2.7344	.00464
- 6	.022326	- .2533	.9335	.00454
- 4.5	.020967	- .0538	- 4.6078	.00569
- 3	.022349	- .2044	- .7241	.00450
- 1.5	.020770	.0244	- 7.8673	.00571
0	.021965	- .0928	- 3.9923	.00480
1.5	.020751	.0156	- 6.5826	.00562
3	.022423	- .1919	- .8925	.00439
4.5	.021398	- .1066	- 3.5341	.00528
6	.022836	- .2496	- .6245	.00402
9	.022802	- .1714	- 3.9749	.00387
12.35	.022271	.0296	- 11.1543	.00443

Table B57. RC78 Incremental Pitching Moment Coefficient at $\beta=+4^\circ$.

$$\Delta C = a_0 - a_1 x + a_2 x^2$$

α	a_0	a_1	a_2	σ
-14	.002164	- .2368	1.3202	.00068
-12	.002527	- .2897	3.0187	.00077
- 9	.002445	- .3635	5.2844	.00074
- 6	.002057	- .2374	2.2207	.00080
- 4.5	.002186	- .2042	2.2452	.00074
- 3	.002523	- .2502	4.7034	.00064
- 1.5	.002869	- .2801	6.5525	.00072
0	.002869	- .2790	6.4354	.00069
1.5	.002243	- .2554	5.7193	.00112
3	.001447	- .2409	5.0211	.00085
4.5	.001417	- .1595	1.4880	.00090
6	.001718	- .1274	- .7249	.00079
9	.001888	- .2248	1.7952	.00086
12.35	.002021	- .3941	7.6477	.00062

Table B58. RC78 Incremental Rolling Moment Coefficient at $\beta=+4^\circ$.

$$\Delta C = a_0 + a_1 x - a_2 x^2$$

α	a_0	a_1	a_2	σ
-14	.000005	- .1073	1.2763	.00014
-12	.000111	- .0119	- 1.2066	.00054
- 9	.000150	.1172	- 4.2553	.00015
- 6	.000167	5.4011	- 2.4168	.00023
- 4.5	.000134	.0485	- 2.2496	.00015
- 3	.000127	.0584	- 2.4399	.00011
- 1.5	.000083	.0343	- 1.3392	.00015
0	.000077	.0112	- .8537	.00019
1.5	.000057	- .0186	- .3349	.00027
3	.000098	- 7.6193	1.0168	.00031
4.5	.000104	- .1239	2.0021	.00030
6	.000161	- .1654	3.0456	.00015
9	.000115	- .0100	.3805	.00018
12.35	.000056	- .1209	1.6539	.00018

Table B59. RC78 Incremental Yawing Moment Coefficient at $\beta=+4^\circ$.

$$\Delta C = a_0 + a_1 \lambda + a_2 x^2$$

α	a_0	a_1	a_2	σ
-14	-.000473	.5999	- 8.2579	.00028
-12	-.000747	.6632	- 9.4162	.00044
- 9	-.000721	.6707	- 8.2816	.00030
- 6	-.000808	.6701	- 7.6658	.00040
- 4.5	-.000799	.6281	- 6.2166	.00046
- 3	-.000788	.5792	- 4.7078	.00034
- 1.5	-.000713	.5858	- 5.3359	.00030
0	-.000711	.5996	- 5.5719	.00029
1.5	-.000670	.6093	- 5.8166	.00028
3	-.000719	.6216	- 5.7626	.00031
4.5	-.000707	.6322	- 5.7276	.00029
6	-.000777	.6570	- 6.5123	.00026
9	-.000587	.6689	- 7.4731	.00022
12.35	-.000680	.6259	- 5.1842	.00027

Table B60. RC78 Incremental Side Force Coefficient at $\beta=+4^\circ$.

$$\Delta C = a_0 + a_1 \lambda + a_2 x^2$$

α	a_0	a_1	a_2	σ
-14	-.001124	- .1429	10.1772	.00165
-12	-.001864	- .2951	13.0301	.00166
- 9	-.001217	- .1398	2.4840	.00150
- 6	-.001263	- .0451	- 1.2235	.00169
- 4.5	-.001275	.1137	- 5.9747	.00184
- 3	-.001277	.3443	- 11.8007	.00177
- 1.5	-.000946	.5420	- 16.1444	.00186
0	-.000918	.7244	- 18.9090	.00184
1.5	-.000887	.8833	- 20.5817	.00172
3	-.001038	1.1287	- 26.3452	.00155
4.5	-.000888	1.2344	- 27.9854	.00130
6	-.000922	1.3274	- 30.0083	.00119
9	-.000636	1.3647	- 31.9953	.00113
12.35	-.001003	1.2667	- 22.6789	.00151

Table B61. RC89 Incremental Normal Force Coefficient at $\beta=+4^\circ$.

$$\Delta C = a_0 - a_1 x - a_2 x^2$$

α	a_0	a_1	a_2	σ
-14	.005266	- 2.9216	- 14.8668	.00205
-12	.006279	- 2.6394	- 23.2558	.00302
- 9	.005630	- 2.1838	- 30.3077	.00221
- 6	.006279	- 2.3674	- 25.7211	.00257
- 4.5	.006410	- 2.3632	- 27.0245	.00263
- 3	.007421	- 2.4713	- 24.4941	.00242
- 1.5	.007423	- 2.3745	- 27.7670	.00229
0	.007386	- 2.5203	- 24.4469	.00247
1.5	.005369	- 2.5808	- 25.1122	.00390
3	.003780	- 2.8717	- 20.0355	.00427
4.5	.003516	- 3.2424	- 13.1768	.00326
6	.004725	- 3.8020	.0607	.00264
9	.004740	- 4.3820	14.1436	.00236
12.35	.004052	- 4.9668	28.4202	.00263

Table B62. RC89 Incremental Axial Force Coefficient at $\beta=+4^\circ$.

$$\Delta C = a_0 - a_1 x + a_2 x^2$$

α	a_0	a_1	a_2	σ
-14	.021469	- .7888	- 18.2902	.00585
-12	.021975	- .9903	- 13.3116	.00505
- 9	.022213	- 1.0801	- 10.2437	.00483
- 6	.022368	- 1.0274	- 11.3733	.00473
- 4.5	.020998	- .8899	- 15.1463	.00600
- 3	.022383	- .9810	- 15.5093	.00471
- 1.5	.020786	- .7738	- 23.0538	.00608
0	.021985	- .8293	- 22.6026	.00505
1.5	.020766	- .7971	- 22.1444	.00601
3	.022448	- 1.1078	- 12.1492	.00459
4.5	.021419	- 1.1576	- 7.7208	.00559
6	.022862	- 1.4098	1.8105	.00419
9	.022820	- 1.2406	- 3.7995	.00403
12.35	.022290	- .9685	- 13.5633	.00467

Table B63. RC89 Incremental Pitching Moment Coefficient at $\beta=+4^\circ$.

$$\Delta C = a_0 - a_1 x - a_2 x^2$$

α	a_0	a_1	a_2	σ
-14	.002159	.8474	5.2103	.00070
-12	.002527	.8447	4.5522	.00079
-9	.002456	.7879	4.9463	.00075
-6	.002069	.8632	5.4822	.00100
-4.5	.002202	.9259	4.7771	.00070
-3	.002539	.9231	4.4706	.00053
-1.5	.002878	.9514	2.9759	.00073
0	.002870	1.0016	1.0470	.00073
1.5	.002244	1.0540	-.3794	.00113
3	.001443	1.0202	1.8319	.00097
4.5	.001411	.9469	4.8706	.00084
6	.001703	.9174	5.9134	.00072
9	.001881	.9190	4.1244	.00087
12.35	.002017	.8208	6.4583	.00064

Table B64. RC89 Incremental Rolling Moment Coefficient at $\beta=+4^\circ$.

$$\Delta C = a_0 + a_1 x + a_2 x^2$$

α	a_0	a_1	a_2	σ
-14	.000006	-.1534	-3.4036	.00014
-12	.000111	-.0035	-9.9143	.00041
-9	.000148	.1682	-16.6088	.00023
-6	.000169	.0974	-15.5943	.00035
-4.5	.000135	.0605	-14.4159	.00017
-3	.000125	.0575	-14.1649	.00013
-1.5	.000083	.0559	-14.5314	.00019
0	.000078	.0168	-13.8114	.00033
1.5	.000060	-5.1846	-12.1807	.00044
3	.000105	-.1388	-10.3169	.00052
4.5	.000112	-.2144	-9.1292	.00055
6	.000177	-.3207	-5.5156	.00050
9	.000131	-.4810	3.9447	.00059
12.35	.000062	-.4990	5.8227	.00029

Table B65. RC89 Incremental Yawing Moment Coefficient at $\beta=+4^\circ$.

$$\Delta C = a_0 - a_1 x - a_2 x^2$$

α	a_0	a_1	a_2	σ
-14	-.000474	.2598	- 4.5044	.00031
-12	-.000743	.2426	- .1573	.00091
- 9	-.000717	.1994	5.6241	.00035
- 6	-.000809	.2306	6.5946	.00051
- 4.5	-.000801	.2352	6.9604	.00036
- 3	-.000788	.2147	7.8413	.00037
- 1.5	-.000716	.1825	9.7009	.00035
0	-.000717	.1929	10.3129	.00039
1.5	-.000677	.2288	10.0400	.00058
3	-.000735	.3030	8.7130	.00063
4.5	-.000721	.3599	8.2513	.00058
6	-.000801	.4881	3.0847	.00073
9	-.000607	.7836	- 13.4580	.00076
12.35	-.000678	.7825	- 13.7965	.00051

Table B66. RC89 Incremental Side Force Coefficient at $\beta=+4^\circ$.

$$\Delta C = a_0 - a_1 x - a_2 x^2$$

α	a_0	a_1	a_2	σ
-14	-.001143	.8364	5.8310	.00192
-12	-.001886	.8583	- 4.5375	.00256
- 9	-.001237	1.0753	- 23.0280	.00161
- 6	-.001252	1.0031	- 23.2237	.00174
- 4.5	-.001264	1.0236	- 24.8752	.00157
- 3	-.001274	1.1922	- 30.3053	.00155
- 1.5	-.000945	1.3967	- 37.5614	.00174
0	-.000906	1.6425	- 44.8536	.00180
1.5	-.000863	1.7762	- 47.9219	.00138
3	-.001010	1.8742	- 50.3696	.00138
4.5	-.000855	1.8200	- 48.2365	.00140
6	-.000872	1.6968	- 39.8689	.00205
9	-.000598	1.2802	- 11.4930	.00200
12.35	-.001012	1.0708	7.3226	.00118

Table B67. RC94 Incremental Normal Force Coefficient at $\beta=+4^\circ$.

$$\Delta C = a_0 - a_1 x + a_2 x^2$$

α	a_0	a_1	a_2	σ
-14	.005278	- 2.9398	20.2431	.00208
-12	.006256	- 2.8213	17.6866	.00267
- 9	.005597	- 2.1522	- 1.8671	.00235
- 6	.006268	- 2.2054	- 5.4728	.00269
- 4.5	.006408	- 2.2976	- 2.4788	.00261
- 3	.007407	- 2.2480	- 5.5304	.00255
- 1.5	.007373	- 2.0048	- 14.8330	.00266
0	.007320	- 2.0390	- 16.9167	.00298
1.5	.005332	- 1.9344	- 23.9350	.00404
3	.003788	- 2.1222	- 24.5984	.00412
4.5	.003542	- 2.2734	- 31.1651	.00428
6	.004749	- 2.9132	- 20.5918	.00412
9	.004763	- 3.7755	- 3.8680	.00293
12.35	.004055	- 4.6590	25.9664	.00231

Table B68. RC94 Incremental Axial Force Coefficient at $\beta=+4^\circ$.

$$\Delta C = a_0 + a_1 x - a_2 x^2$$

α	a_0	a_1	a_2	σ
-14	.021495	- 1.4234	- 12.3647	.00595
-12	.021998	- 1.6636	- 6.3141	.00512
- 9	.022229	- 1.6996	- 4.4148	.00489
- 6	.022392	- 1.6975	- 3.2110	.00483
- 4.5	.021016	- 1.5102	- 8.5955	.00606
- 3	.022400	- 1.5689	- 8.9949	.00475
- 1.5	.020802	- 1.3084	- 17.9560	.00613
0	.022013	- 1.3611	- 16.6427	.00516
1.5	.020791	- 1.2960	- 17.7996	.00611
3	.022475	- 1.5493	- 9.0843	.00470
4.5	.021437	- 1.5859	- 5.5272	.00566
6	.022885	- 1.8222	3.5808	.00426
9	.022844	- 1.8746	6.8603	.00406
12.35	.022296	- 1.5967	- 3.5811	.00467

Table B69. RC94 Incremental Pitching Moment Coefficient at $\beta=+4^\circ$.

$$\Delta C = a_0 + a_1 x - a_2 x^2$$

α	a_0	a_1	a_2	σ
-14	.002166	.6321	- 3.4400	.00072
-12	.002535	.6491	- 4.8198	.00080
- 9	.002463	.5083	- .3685	.00073
- 6	.002067	.6140	- 2.0700	.00088
- 4.5	.002203	.6611	- 2.2285	.00081
- 3	.002551	.5615	3.1572	.00078
- 1.5	.002879	.4712	8.6221	.00098
0	.002866	.4123	11.8168	.00084
1.5	.002235	.4556	10.5895	.00119
3	.001446	.4785	10.0812	.00083
4.5	.001408	.4764	11.4853	.00101
6	.001697	.4191	15.1608	.00087
9	.001868	.5194	11.0445	.00093
12.35	.002010	.6267	4.4294	.00079

Table B70. RC94 Incremental Rolling Moment Coefficient at $\beta=+4^\circ$.

$$\Delta C = a_0 + a_1 x - a_2 x^2$$

α	a_0	a_1	a_2	σ
-14	.000005	- .1054	2.1462	.00016
-12	.000111	.0840	- 4.8316	.00058
- 9	.000153	.2625	- 10.0287	.00026
- 6	.000171	.2147	- 7.8282	.00025
- 4.5	.000138	.2310	- 8.0414	.00033
- 3	.000134	.2610	- 8.2190	.00029
- 1.5	.000090	.3016	- 9.7814	.00025
0	.000080	.3103	- 11.2138	.00049
1.5	.000059	.2767	- 11.6063	.00051
3	.000110	.1435	- 7.7004	.00063
4.5	.000123	- .0453	.0253	.00066
6	.000185	- .1775	6.6054	.00070
9	.000114	- .1553	9.9669	.00045
12.35	.000055	- .0634	6.0889	.00035

Table B71. RC94 Incremental Yawing Moment Coefficient at $\beta=+4^\circ$.

$$\Delta C = a_0 + a_1 \lambda - a_2 x^2$$

α	a_0	a_1	a_2	σ
-14	-.000477	.8877	- 7.9395	.00030
-12	-.000751	.8495	- 3.3333	.00080
- 9	-.000726	.7663	2.9551	.00036
- 6	-.000815	.7770	2.3434	.00044
- 4.5	-.000804	.7460	3.3154	.00044
- 3	-.000791	.7034	4.4028	.00030
- 1.5	-.000715	.6163	8.8292	.00047
0	-.000709	.5574	12.8151	.00060
1.5	-.000669	.5465	15.0506	.00050
3	-.000734	.6854	10.5094	.00077
4.5	-.000735	.9058	.9784	.00094
6	-.000815	1.0948	- 8.8441	.00111
9	-.000596	1.2268	- 20.3481	.00049
12.35	-.000675	1.1300	- 16.2235	.00051

Table B72 RC94 Incremental Side Force Coefficient at $\beta=+4^\circ$.

$$\Delta C = a_0 + a_1 x - a_2 x^2$$

α	a_0	a_1	a_2	σ
-14	-.001153	- .9518	5.7517	.00192
-12	-.001882	- .9204	- 2.4663	.00222
- 9	-.001234	- .6401	- 20.6360	.00162
- 6	-.001263	- .6041	- 21.8431	.00175
- 4.5	-.001280	- 5.1957	- 24.1403	.00182
- 3	-.001299	- .2356	- 32.1737	.00187
- 1.5	-.000976	.1274	- 46.1115	.00195
0	-.000949	.5568	- 62.3753	.00175
1.5	-.000902	.7843	- 69.6289	.00151
3	-.001024	.7203	- 64.1129	.00174
4.5	-.000845	.3438	- 43.2521	.00220
6	-.000864	.0572	- 24.2312	.00289
9	-.000624	- .2131	3.4330	.00186
12.35	-.001024	- .2787	14.8559	.00160

APPENDIX C

IA148 CURVE FIT COEFFICIENTS
AT -4 DEGREES YAW

Table C1. RC38 Incremental Normal Force Coefficient at $\beta=-4^\circ$.

$$\Delta C = a_0 + a_1 x + a_2 x^2$$

α	a_0	a_1	a_2	σ
-14	.003266	- 6.2695	88.0602	.00357
-12	.002489	- 5.3643	65.1187	.00414
- 9	.003110	- 4.3280	35.6295	.00469
- 6	.003595	- 3.5544	11.3856	.00518
- 4.5	.003563	- 3.5550	13.5254	.00495
- 3	.004923	- 3.7882	22.9891	.00481
- 1.5	.003373	- 3.7686	25.3907	.00444
0	.002396	- 3.5524	13.7658	.00487
1.5	.001086	- 3.5600	11.8781	.00458
3	.000337	- 3.8223	21.0708	.00487
4.5	.000606	- 4.3663	47.6937	.00502
6	.001660	- 4.7687	73.7905	.00635
9	.002532	- 4.5674	86.0642	.00490
12.35	.002581	- 4.2150	67.1135	.00385

Table C2 RC38 Incremental Axial Force Coefficient at $\beta=-4^\circ$.

$$\Delta C = a_0 + a_1 x + a_2 x^2$$

α	a_0	a_1	a_2	σ
-14	-.000184	- 3.1703	41.5192	.00187
-12	-.000983	- 3.1001	42.4693	.00188
- 9	-.000565	- 3.5741	61.7099	.00214
- 6	-.000203	- 3.5054	63.0629	.00236
- 4.5	-.000482	- 3.3062	55.2960	.00227
- 3	-.000681	- 3.3002	53.3221	.00234
- 1.5	-.000674	- 3.3778	56.6771	.00223
0	-.000626	- 3.4050	62.2962	.00279
1.5	-.000731	- 3.1840	57.6131	.00269
3	-.000900	- 2.9733	49.1371	.00286
4.5	-.001085	- 2.9767	44.4787	.00311
6	-.001199	- 3.2315	48.3424	.00333
9	-.001189	- 3.7658	59.9650	.00276
12.35	-.001162	- 4.0104	66.4322	.00247

Table C3. RC38 Incremental Pitching Moment Coefficient at $\beta=-4^\circ$.

$$\Delta C = a_0 + a_1 x + a_2 x^2$$

α	a_0	a_1	a_2	σ
-14	.000902	- .2607	22.2686	.00077
-12	.000515	- .1350	25.0284	.00131
- 9	.000479	.0383	24.4566	.00129
- 6	.000875	.0991	29.0905	.00176
- 4.5	.000856	.2896	24.7415	.00151
- 3	.001247	.4572	19.0222	.00117
- 1.5	.000558	.6255	14.5023	.00115
0	.000159	.7530	11.6093	.00131
1.5	- .000210	.9282	6.7995	.00123
3	- .000410	.1117	.2284	.00119
4.5	- .000215	1.2010	- 2.7769	.00115
6	.000165	1.2952	- 5.0995	.00158
9	.000323	1.8506	- 19.0894	.00204
12.35	.000121	2.3454	- 33.8605	.00092

Table C4. RC38 Incremental Rolling Moment Coefficient at $\beta=-4^\circ$.

$$\Delta C = a_0 + a_1 x + a_2 x^2$$

α	a_0	a_1	a_2	σ
-14	.000093	- .1814	17.5451	.00029
-12	.000107	.0119	9.0099	.00033
- 9	.000174	- .0142	7.6095	.00050
- 6	.000216	- .0606	6.7292	.00054
- 4.5	.000167	- .0801	6.5478	.00062
- 3	.000144	- .0002	1.7223	.00096
- 1.5	.000141	.1633	- 7.2971	.00095
0	.000152	.3122	- 15.8726	.00073
1.5	.000160	.2957	- 17.3799	.00061
3	.000184	.1216	- 11.5755	.00072
4.5	.000201	- .0867	- 3.2339	.00054
6	.000241	- .2466	4.9018	.00059
9	.000213	- .1626	4.0224	.00038
12.35	.000226	- .0599	- 2.1200	.00031

Table C5. RC38 Incremental Yawing Moment Coefficient at $\beta=-4^\circ$.

$$\Delta C = a_0 + a_1 x + a_2 x^2$$

α	a_0	a_1	a_2	σ
-14	-.000101	.0295	- 32.6946	.00034
-12	-.000145	- .1976	- 22.2800	.00061
- 9	-.000218	- .1304	- 20.3919	.00084
- 6	-.000351	- .0267	- 21.9919	.00055
- 4.5	-.000284	- .0927	- 19.6185	.00077
- 3	-.000269	- .3428	- 8.9766	.00138
- 1.5	-.000268	- .6680	6.2740	.00130
0	-.000287	- .8902	16.5754	.00081
1.5	-.000308	- .8920	17.2479	.00038
3	-.000347	- .7343	10.2271	.00052
4.5	-.000414	- .5763	2.8314	.00061
6	-.000497	- .4820	4.2726	.00112
9	-.000440	- .8894	4.6190	.00125
12.35	-.000631	- 1.3182	21.9178	.00048

Table C6. RC38 Incremental Side Force Coefficient at $\beta=-4^\circ$.

$$\Delta C = a_0 + a_1 x + a_2 x^2$$

α	a_0	a_1	a_2	σ
-14	-.000036	- .5593	47.6141	.00079
-12	-.000380	.0644	19.2701	.00129
- 9	-.000431	.3500	- 5.6314	.00212
- 6	-.000740	.6875	- 28.2002	.00109
- 4.5	-.000933	1.0133	- 43.9339	.00136
- 3	-.001169	1.2569	- 61.2446	.00263
- 1.5	-.001317	1.4832	- 82.6692	.00352
0	-.001334	1.2031	- 84.9683	.00407
1.5	-.001342	.5201	- 65.1974	.00373
3	-.001278	- .4327	- 30.1286	.00329
4.5	-.001371	- 1.1236	- 4.9532	.00249
6	-.001380	- 1.5612	9.9261	.00163
9	-.001218	- 2.1518	30.6117	.00110
12.35	-.001354	- 2.3861	44.7419	.00133

Table C7. RC40 Incremental Normal Force Coefficient at $\beta=-4^\circ$.

$$\Delta C = a_0 + a_1 x + a_2 x^2$$

α	a_0	a_1	a_2	σ
-14	.003350	- 3.5177	55.8112	.00228
-12	.002604	- 3.2575	40.6484	.00278
- 9	.003234	- 3.0245	25.6822	.00358
- 6	.003703	- 3.4682	41.3330	.00509
- 4.5	.003625	- 3.3914	31.6935	.00543
- 3	.004960	- 3.1283	10.4506	.00495
- 1.5	.003420	- 2.8838	- 6.1325	.00502
0	.002466	- 3.0263	- 5.8386	.00522
1.5	.001172	- 3.4263	6.1521	.00421
3	.000454	- 3.6714	15.0621	.00454
4.5	.000722	- 4.3167	37.9001	.00464
6	.001798	- 4.8323	54.0769	.00496
9	.002624	- 5.4524	76.3582	.00418
12.35	.002633	- 5.5477	84.1407	.00322

Table C8. RC40 Incremental Axial Force Coefficient at $\beta=-4^\circ$.

$$\Delta C = a_0 + a_1 x + a_2 x^2$$

α	a_0	a_1	a_2	σ
-14	- .000108	- 2.3661	4.0562	.00076
-12	- .000903	- 2.3702	7.7854	.00113
- 9	- .000477	- 2.5473	16.7176	.00143
- 6	- .000103	- 2.6404	17.4071	.00168
- 4.5	- .000388	- 2.7404	22.5541	.00198
- 3	- .000573	- 2.9168	34.2860	.00212
- 1.5	- .000592	- 3.0146	43.4565	.00213
0	- .000537	- 2.9887	46.8083	.00207
1.5	- .000655	- 2.8061	43.5201	.00188
3	- .000813	- 2.5611	35.3903	.00206
4.5	- .001016	- 2.1986	22.5512	.00212
6	- .001116	- 1.9319	12.1319	.00206
9	- .001085	- 1.8614	7.3012	.00196
12.35	- .001076	- 1.9893	11.2135	.00156

Table C9. RC40 Incremental Pitching Moment Coefficient at $\beta = -4^\circ$.

$$\Delta C = a_0 + a_1 x + a_2 x^2$$

α	a_0	a_1	a_2	σ
-14	.000924	.3583	11.1182	.00059
-12	.000523	.2773	16.3115	.00080
- 9	.000492	.1759	22.6810	.00125
- 6	.000887	.3041	16.2339	.00137
- 4.5	.000871	.2924	15.8591	.00114
- 3	.001277	.1472	22.9516	.00141
- 1.5	.000588	.1343	26.9523	.00127
0	.000176	.1715	28.7064	.00126
1.5	- .000210	.2420	27.1911	.00113
3	- .000431	.5088	16.3973	.00149
4.5	- .000228	.6471	8.8869	.00136
6	.000164	.7813	1.4236	.00126
9	.000327	.7818	- 1.6373	.00127
12.35	.000117	.6856	.4173	.00086

Table C10. RC40 Incremental Rolling Moment Coefficient at $\beta = -4^\circ$.

$$\Delta C = a_0 + a_1 x + a_2 x^2$$

α	a_0	a_1	a_2	σ
-14	.000098	- .2873	19.5348	.00018
-12	.000111	- .1472	13.8123	.00032
- 9	.000182	- .0398	8.0379	.00023
- 6	.000234	- .0966	9.0084	.00035
- 4.5	.000184	- .0419	5.4140	.00068
- 3	.000159	.1317	- 2.7135	.00087
- 1.5	.000149	.3061	- 11.4342	.00062
0	.000154	.3792	- 15.5586	.00065
1.5	.000157	.3673	- 16.2818	.00040
3	.000181	.2831	- 13.1877	.00033
4.5	.000206	.1758	- 8.2377	.00048
6	.000249	.0815	- 4.0643	.00039
9	.000217	- .0349	- .4281	.00036
12.35	.000227	- .1253	2.4621	.00016

Table C11. RC40 Incremental Yawing Moment Coefficient at $\beta=-4^\circ$.

$$\Delta C = a_0 + a_1 x + a_2 x^2$$

α	a_0	a_1	a_2	σ
-14	-.000107	.2260	- 29.7134	.00032
-12	-.000151	.0358	- 23.1643	.00047
- 9	-.000229	- .1243	- 15.9532	.00046
- 6	-.000359	- .1483	- 12.4697	.00048
- 4.5	-.000294	- .2603	- 6.0234	.00097
- 3	-.000280	- .5027	5.0083	.00126
- 1.5	-.000274	- .7332	16.3382	.00089
0	-.000284	- .8175	20.8608	.00088
1.5	-.000302	- .7753	20.3079	.00048
3	-.000342	- .6399	14.7651	.00054
4.5	-.000419	- .4849	7.7807	.00062
6	-.000502	- .3687	3.1775	.00055
9	-.000447	- .2521	.4875	.00045
12.35	-.000636	- .1439	- 3.3329	.00027

Table C12. RC40 Incremental Side Force Coefficient at $\beta=-4^\circ$.

$$\Delta C = a_0 + a_1 x + a_2 x^2$$

α	a_0	a_1	a_2	σ
-14	-.000017	.0004	53.6573	.00055
-12	-.000357	.4735	38.8702	.00125
- 9	-.000440	.8792	21.9293	.00096
- 6	-.000752	1.0990	8.6709	.00129
- 4.5	-.000976	1.4194	- 11.0078	.00315
- 3	-.001269	1.9940	- 40.8268	.00368
- 1.5	-.001394	2.4165	- 66.3181	.00179
0	-.001440	2.4068	- 70.9807	.00225
1.5	-.001436	2.1466	- 65.0537	.00188
3	-.001372	1.7208	- 50.4029	.00115
4.5	-.001388	1.3366	- 34.8932	.00146
6	-.001379	.9447	- 19.5644	.00157
9	-.001246	.5092	- 6.3456	.00084
12.35	-.001371	.4294	- 3.4067	.00063

Table C13. RC55 Incremental Normal Force Coefficient at $\beta=-4^\circ$.

$$\Delta C = a_0 + a_1 \lambda - a_2 x^2$$

α	a_0	a_1	a_2	σ
-14	.003315	- 3.7537	.4755	.00258
-12	.002592	- 2.5880	- 36.8803	.00417
- 9	.003252	- 2.1864	- 36.2311	.00382
- 6	.003694	- 3.0713	- 6.4724	.00594
- 4.5	.003614	- 3.5154	- 1.2417	.00540
- 3	.004967	- 3.8541	.2293	.00544
- 1.5	.003418	- 4.0021	- 4.9830	.00530
0	.002440	- 4.2082	- 7.1402	.00576
1.5	.001111	- 4.5489	- 3.4090	.00499
3	.000370	- 4.8936	4.7532	.00502
4.5	.000633	- 5.4761	24.7251	.00470
6	.001731	- 5.9631	42.4129	.00485
9	.002638	- 6.3658	54.8978	.00442
12.35	.002627	- 5.5358	8.4616	.00412

Table C14. RC55 Incremental Axial Force Coefficient at $\beta=-4^\circ$.

$$\Delta C = a_0 - a_1 x - a_2 x^2$$

α	a_0	a_1	a_2	σ
-14	-.000176	- 4.6263	74.4119	.00163
-12	-.000971	- 4.6770	71.9129	.00206
- 9	-.000542	- 4.6598	66.2734	.00191
- 6	-.000176	- 4.2055	53.1048	.00274
- 4.5	-.000458	- 3.8653	43.8248	.00219
- 3	-.000658	- 3.6928	40.3892	.00206
- 1.5	-.000651	- 3.5382	35.7240	.00196
0	-.000586	- 3.4329	31.6026	.00185
1.5	-.000675	- 3.2939	25.2610	.00185
3	-.000817	- 3.2374	21.8077	.00197
4.5	-.001024	- 3.2268	21.1569	.00207
6	-.001144	- 3.3266	23.5946	.00231
9	-.001130	- 3.5613	28.7655	.00225
12.35	-.001099	- 3.4077	26.6318	.00214

Table C15. RC55 Incremental Pitching Moment Coefficient at $\beta = -4^\circ$.

$$\Delta C = a_0 - a_1 x + a_2 x^2$$

α	a_0	a_1	a_2	σ
-14	.000912	.7110	24.1638	.00047
-12	.000504	.4773	31.7816	.00123
-9	.000478	.3551	32.1784	.00115
-6	.000879	.5476	25.8018	.00153
-4.5	.000862	.7495	20.6164	.00161
-3	.001258	.8522	19.0389	.00124
-1.5	.000574	.9382	18.4755	.00109
0	.000173	.8840	22.6471	.00115
1.5	-.000204	.8520	25.6975	.00107
3	-.000408	.9571	23.1421	.00132
4.5	-.000215	1.0386	20.4041	.00122
6	.000173	1.1291	15.9222	.00121
9	.000333	1.1057	13.9999	.00119
12.35	.000118	1.0038	17.1766	.00091

Table C16. RC55 Incremental Rolling Moment Coefficient at $\beta = -4^\circ$.

$$\Delta C = a_0 + a_1 x + a_2 x^2$$

α	a_0	a_1	a_2	σ
-14	.000102	.0852	.0567	.00030
-12	.000116	.2647	- 5.7975	.00038
-9	.000189	.3319	- 8.1207	.00019
-6	.000243	.2361	- 4.2325	.00047
-4.5	.000195	.1235	- .6978	.00059
-3	.000186	.0091	2.1569	.00056
-1.5	.000166	-.0510	2.8089	.00046
0	.000169	-.1031	3.8730	.00026
1.5	.000161	-.1371	5.2597	.00022
3	.000178	-.1632	6.4276	.00018
4.5	.000193	-.1627	5.9436	.00027
6	.000232	-.1785	5.3240	.00032
9	.000209	-.3108	9.7322	.00026
12.35	.000226	-.2446	7.6218	.00048

Table C17. RC55 Incremental Yawing Moment Coefficient at $\beta=-4^\circ$.

$$\Delta C = a_0 + a_1 x + a_2 x^2$$

α	a_0	a_1	a_2	σ
-14	-.000112	.7154	- 11.0911	.00027
-12	-.000161	.8862	- 15.7559	.00077
- 9	-.000239	1.0470	- 18.4924	.00032
- 6	-.000367	.9317	- 16.2920	.00087
- 4.5	-.000311	.7840	- 12.6427	.00068
- 3	-.000321	.6646	- 9.2015	.00044
- 1.5	-.000302	.5638	- 5.0622	.00030
0	-.000309	.5544	- 3.5412	.00050
1.5	-.000306	.5726	- 3.0113	.00040
3	-.000332	.6237	- 4.6061	.00025
4.5	-.000397	.6426	- 5.7174	.00029
6	-.000474	.6455	- 6.3590	.00030
9	-.000439	.5429	- 3.4840	.00050
12.35	-.000640	.3507	.8593	.00083

Table C18. RC55 Incremental Side Force Coefficient at $\beta=-4^\circ$.

$$\Delta C = a_0 + a_1 x + a_2 x^2$$

α	a_0	a_1	a_2	σ
-14	-.000021	- .7298	19.3997	.00097
-12	-.000373	- 1.5191	39.6394	.00351
- 9	-.000438	- 2.2050	56.3187	.00069
- 6	-.000739	- 1.5338	34.5269	.00262
- 4.5	-.000956	- .8741	14.1039	.00266
- 3	-.001217	- .2302	- 4.3843	.00263
- 1.5	-.001360	.2203	- 14.7371	.00233
0	-.001401	.5687	- 23.0076	.00167
1.5	-.001427	.7516	- 26.4332	.00093
3	-.001383	.9240	- 31.1133	.00103
4.5	-.001428	1.0194	- 31.8396	.00102
6	-.001426	1.1194	- 32.6661	.00080
9	-.001268	1.7658	- 60.7863	.00161
12.35	-.001359	1.8011	- 70.7490	.00228

Table C19. RC61 Incremental Normal Force Coefficient at $\beta=-4^\circ$.

$$\Delta C = a_0 - a_1 x - a_2 x^2$$

α	a_0	a_1	a_2	σ
-14	.003383	- 1.7917	18.7902	.00202
-12	.002611	- 1.5334	2.8532	.00228
- 9	.003233	- 1.3367	- 8.6488	.00355
- 6	.003711	- 1.7889	6.9078	.00508
- 4.5	.003634	- 1.7664	2.3515	.00476
- 3	.004976	- 1.6585	- 6.3467	.00473
- 1.5	.003424	- 1.3181	- 19.8033	.00440
0	.002457	- 1.2978	- 21.1863	.00459
1.5	.001157	- 1.3148	- 25.3909	.00450
3	.000456	- 1.3008	- 27.7998	.00480
4.5	.000748	- 1.4415	- 29.7860	.00452
6	.001838	- 1.7750	- 21.3708	.00501
9	.002691	- 2.4012	- 5.5482	.00441
12.35	.002673	- 2.8686	12.7522	.00328

Table C20. RC61 Incremental Axial Force Coefficient at $\beta=-4^\circ$.

$$\Delta C = a_0 + a_1 x + a_2 x^2$$

α	a_0	a_1	a_2	σ
-14	-.000101	- 1.5029	- 8.8815	.00076
-12	-.000892	- 1.3559	- 15.6325	.00117
- 9	-.000470	- 1.3963	- 17.3299	.00156
- 6	-.000098	- 1.5820	- 12.9550	.00149
- 4.5	-.000395	- 1.5351	- 15.1149	.00159
- 3	-.000590	- 1.4770	- 16.8398	.00166
- 1.5	-.000602	- 1.4018	- 19.4336	.00166
0	-.000534	- 1.3512	- 21.0970	.00166
1.5	-.000640	- 1.3232	- 21.0643	.00172
3	-.000779	- 1.4218	- 16.6779	.00195
4.5	-.000986	- 1.4985	- 10.8844	.00209
6	-.001082	- 1.5831	- 5.4676	.00219
9	-.001072	- 1.5687	- 5.2984	.00204
12.35	-.001060	- 1.4442	- 11.7325	.00165

Table C21. RC61 Incremental Pitching Moment Coefficient at $\beta=-4^\circ$.

$$\Delta C = a_0 + a_1 x - a_2 x^2$$

α	a_0	a_1	a_2	σ
-14	.000911	.6621	- .4169	.00043
-12	.000516	.5962	3.5393	.00072
- 9	.000493	.4954	7.9152	.00114
- 6	.000892	.5719	3.2842	.00126
- 4.5	.000875	.5639	3.6044	.00119
- 3	.001272	.5056	6.7327	.00134
- 1.5	.000582	.5991	5.6029	.00111
0	.000173	.6391	5.5831	.00116
1.5	-.000203	.6285	6.0565	.00107
3	-.000411	.6415	7.1927	.00124
4.5	-.000211	.5769	10.0363	.00121
6	.000169	.5021	13.5020	.00121
9	.000323	.5746	9.2233	.00119
12.35	.000113	.7313	1.7432	.00088

Table C22. RC61 Incremental Rolling Moment Coefficient at $\beta=-4^\circ$.

$$\Delta C = a_0 + a_1 x + a_2 x^2$$

α	a_0	a_1	a_2	σ
-14	.000096	- .0251	1.0113	.00014
-12	.000112	- .0047	- 1.1353	.00030
- 9	.000187	- .0259	- 1.5527	.00013
- 6	.000243	- .0750	.2861	.00013
- 4.5	.000196	- .0823	.5586	.00013
- 3	.000186	- .0996	1.3192	.00011
- 1.5	.000169	- .1504	3.7403	.00024
0	.000174	- .2024	6.3433	.00024
1.5	.000165	- .2393	8.2615	.00013
3	.000177	- .2173	7.4442	.00018
4.5	.000186	- .1635	5.2384	.00032
6	.000223	- .1421	3.9743	.00034
9	.000208	- .1534	3.1211	.00019
12.35	.000217	- .0385	- 1.9982	.00033

Table C23. RC61 Incremental Yawing Moment Coefficient at $\beta=-4^\circ$.

$$\Delta C = a_0 + a_1 x + a_2 x^2$$

α	a_0	a_1	a_2	σ
-14	-.000110	- .2290	- 3.5550	.00018
-12	-.000160	- .2132	- 3.4385	.00025
- 9	-.000240	- .1666	- 4.7408	.00025
- 6	-.000378	- .1603	- 4.6521	.00027
- 4.5	-.000318	- .1742	- 4.4424	.00024
- 3	-.000325	- .1423	- 6.2199	.00021
- 1.5	-.000307	- .0536	- 10.5209	.00040
0	-.000313	.0053	- 13.5066	.00036
1.5	-.000310	.0292	- 14.8693	.00027
3	-.000330	- .0542	- 11.4258	.00036
4.5	-.000390	- .1583	6.9689	.00053
6	-.000464	- .2152	- 4.1052	.00050
9	-.000435	- .2451	- 1.2468	.00032
12.35	-.000624	- .4078	6.0395	.00047

Table C24. RC61 Incremental Side Force Coefficient at $\beta=-4^\circ$.

$$\Delta C = a_0 + a_1 x + a_2 x^2$$

α	a_0	a_1	a_2	σ
-14	-.000005	.9902	- .5675	.00056
-12	-.000350	1.0770	- 2.8834	.00042
- 9	-.000417	1.0675	- 2.5223	.00060
- 6	-.000710	1.1941	- 5.7103	.00076
- 4.5	-.000925	1.1887	- 4.7799	.00065
- 3	-.001173	1.1472	- 1.9717	.00059
- 1.5	-.001340	.9881	5.6137	.00085
0	-.001395	.8606	11.6249	.00080
1.5	-.001438	.8131	12.5008	.00090
3	-.001408	.9790	3.7768	.00092
4.5	-.001464	1.2177	- 7.7512	.00104
6	-.001459	1.3466	- 15.4661	.00130
9	-.001258	1.2115	- 17.0106	.00076
12.35	-.001392	1.5746	- 34.7687	.00080

Table C25. RC78 Incremental Normal Force Coefficient at $\beta=-4^\circ$.

$$\Delta C = a_0 - a_1 x - a_2 x^2$$

α	a_0	a_1	a_2	σ
-14	.003398	- .4349	- 1.6775	.00212
-12	.002656	.4399	- 24.0344	.00425
- 9	.003280	1.3595	- 42.2515	.00434
- 6	.003743	1.2259	- 33.6878	.00512
- 4.5	.003666	.8175	- 20.5515	.00475
- 3	.005022	.4017	- 7.8333	.00484
- 1.5	.003453	.0355	5.4018	.00473
0	.002487	- .2553	13.0350	.00492
1.5	.001166	- .4897	17.9282	.00437
3	.000441	- .7972	27.7952	.00466
4.5	.000692	- 1.1504	38.5655	.00436
6	.001777	- 1.4062	42.8626	.00470
9	.002644	- 1.7129	39.4748	.00467
12.35	.002641	- 1.6424	28.8521	.00322

Table C26. RC78 Incremental Axial Force Coefficient at $\beta=-4^\circ$.

$$\Delta C = a_0 - a_1 x - a_2 x^2$$

α	a_0	a_1	a_2	σ
-14	-.000106	- .2478	.1059	.00080
-12	-.000905	- .4238	5.3162	.00155
- 9	-.000475	- .5459	7.0618	.00155
- 6	-.000106	- .0234	- 6.5318	.00288
- 4.5	-.000402	.3793	- 17.1077	.00215
- 3	-.000592	.5806	- 20.8178	.00175
- 1.5	-.000607	.7152	- 23.9927	.00178
0	-.000545	.8339	- 27.9819	.00169
1.5	-.000646	.9852	- 33.7856	.00171
3	-.000783	.9930	- 33.7753	.00192
4.5	-.000985	1.0444	- 35.0919	.00198
6	-.001091	1.0074	- 33.3518	.00205
9	-.001073	.9304	- 30.5453	.00204
12.35	-.001050	1.2697	- 39.7578	.00219

Table C27. RC78 Incremental Pitching Moment Coefficient at $\beta=-4^\circ$.

$$\Delta C = a_0 + a_1 x + a_2 x^2$$

α	a_0	a_1	a_2	σ
-14	.000902	- .4617	9.4550	.00047
-12	.000507	- .6515	14.8706	.00126
- 9	.000487	- .8095	16.3799	.00109
- 6	.000879	- .7205	14.3378	.00148
- 4.5	.000863	- .5646	10.7095	.00152
- 3	.001260	- .4666	8.3296	.00117
- 1.5	.000577	- .4185	8.6518	.00106
0	.000175	- .4152	8.9148	.00113
1.5	- .000203	- .3653	6.5078	.00105
3	- .000412	- .3349	5.8417	.00117
4.5	- .000221	- .3390	6.5119	.00119
6	.000171	- .3098	6.2347	.00129
9	.000341	- .1683	1.0725	.00111
12.35	.000121	- .1449	- .3947	.00090

Table C28. RC78 Incremental Rolling Moment Coefficient at $\beta=-4^\circ$.

$$\Delta C = a_0 + a_1 x + a_2 x^2$$

α	a_0	a_1	a_2	σ
-14	.000103	.1373	- 4.4353	.00024
-12	.000120	.3230	- 11.3545	.00035
- 9	.000193	.3779	- 12.4134	.00028
- 6	.000242	.3123	- 9.1135	.00040
- 4.5	.000194	.2150	- 6.1277	.00058
- 3	.000183	.1045	- 3.2591	.00052
- 1.5	.000166	.0254	- 1.6028	.00042
0	.000170	- .0317	- .6550	.00035
1.5	.000162	- .0769	.3795	.00020
3	.000178	- .1336	2.1791	.00022
4.5	.000192	- .1867	3.9301	.00026
6	.000230	- .2353	5.1490	.00025
9	.000211	- .2418	4.7524	.00014
12.35	.000226	- .1483	1.7018	.00038

Table C29. RC78 Incremental Yawing Moment Coefficient at $\beta = -4^\circ$.

$$\Delta C = a_0 + a_1 x + a_2 x^2$$

α	a_0	a_1	a_2	σ
-14	-.000103	.7688	- 11.8214	.00035
-12	-.000152	.9088	- 14.5465	.00080
- 9	-.000236	1.0341	- 15.2868	.00035
- 6	-.000372	.9252	- 13.4467	.00083
- 4.5	-.000313	.8266	- 11.8630	.00051
- 3	-.000321	.7601	- 10.3599	.00033
- 1.5	-.000302	.7014	- 8.2996	.00024
0	-.000308	.6735	- 6.4054	.00034
1.5	-.000304	.6665	- 5.3280	.00032
3	-.000332	.6916	- 5.6503	.00021
4.5	-.000399	.7228	- 7.0808	.00025
6	-.000479	.7399	- 8.1654	.00029
9	-.000442	.5747	- 3.8830	.00071
12.35	-.000635	.3080	3.6457	.00057

Table C30. RC78 Incremental Side Force Coefficient at $\beta = -4^\circ$.

$$\Delta C = a_0 - a_1 x + a_2 x^2$$

α	$-a_0$	a_1	a_2	σ
-14	-.000025	- .9889	29.0474	.00076
-12	-.000373	- 1.6726	45.4322	.00338
- 9	-.000432	- 2.0554	48.6614	.00083
- 6	-.000728	- 1.3746	29.9003	.00255
- 4.5	-.000941	- .9023	18.5213	.00240
- 3	-.001188	- .4252	7.1864	.00232
- 1.5	-.001351	.0412	- 5.0388	.00205
0	-.001401	.4815	- 16.5829	.00198
1.5	-.001437	.8365	- 25.2311	.00172
3	-.001390	1.1087	- 31.2388	.00144
4.5	-.001424	1.3004	- 35.2041	.00102
6	-.001411	1.3947	- 35.2407	.00107
9	-.001239	1.6396	- 36.0032	.00157
12.35	-.001361	1.7143	- 36.0610	.00138

Table C31. RC89 Incremental Normal Force Coefficient at $\beta = -4^\circ$.

$$\Delta C = a_0 + a_1 x + a_2 x^2$$

α	a_0	a_1	a_2	σ
-14	.003388	- 2.5772	18.7245	.00203
-12	.002628	- 1.5496	- 10.1864	.00435
- 9	.003254	- .5377	- 36.1930	.00389
- 6	.003699	- 1.0095	- 20.3298	.00559
- 4.5	.003607	- 1.6315	- 1.8369	.00492
- 3	.004955	- 2.0105	6.5588	.00490
- 1.5	.003395	- 2.1210	5.4207	.00487
0	.002418	- 2.1093	- 4.0710	.00552
1.5	.001116	- 2.2762	- 6.3056	.00490
3	.000398	- 2.5489	- 4.1589	.00526
4.5	.000702	- 3.0164	7.1823	.00475
6	.001788	- 3.5640	20.0935	.00500
9	.002649	- 4.9369	61.3709	.00492
12.35	.002641	- 4.9565	55.3231	.00334

Table C32. RC89 Incremental Axial Force Coefficient at $\beta = -4^\circ$.

$$\Delta C = a_0 + a_1 x + a_2 x^2$$

α	a_0	a_1	a_2	σ
-14	-.000160	- 3.8839	69.8369	.00129
-12	-.000961	- 4.0511	72.4132	.00204
- 9	-.000551	- 4.1275	70.7370	.00200
- 6	-.000173	- 3.6008	55.7882	.00308
- 4.5	-.000448	- 3.1843	45.0272	.00240
- 3	-.000648	- 2.9777	40.8140	.00195
- 1.5	-.000644	- 2.7983	35.1481	.00184
0	-.000584	- 2.7223	32.4032	.00181
1.5	-.000678	- 2.6678	30.9782	.00181
3	-.000822	- 2.7250	34.3943	.00205
4.5	-.001030	- 2.6552	33.1905	.00216
6	-.001147	- 2.5945	31.6618	.00222
9	-.001131	- 2.4466	25.3206	.00215
12.35	-.001091	- 2.2937	21.1794	.00192

Table C33. RC89 Incremental Pitching Moment Coefficient at $\beta=-4^\circ$.

$$\Delta C = a_0 + a_1 x - a_2 x^2$$

α	a_0	a_1	a_2	σ
-14	.000905	.3080	7.1205	.00047
-12	.000509	.1708	9.9556	.00128
-9	.000498	.0387	13.4089	.00112
-6	.000880	.0197	13.1423	.00147
-4.5	.000858	.1337	11.6856	.00154
-3	.001256	.2238	10.3385	.00123
-1.5	.000574	.2787	12.7687	.00128
0	.000174	.3099	13.8565	.00124
1.5	-.000198	.3466	13.9485	.00110
3	-.000405	.3804	12.3682	.00117
4.5	-.000210	.3714	13.1585	.00119
6	.000165	.4427	9.8527	.00131
9	.000325	.6874	- 1.4787	.00115
12.35	.000116	.6634	- 2.3495	.00094

Table C34. RC89 Incremental Rolling Moment Coefficient at $\beta=-4^\circ$.

$$\Delta C = a_0 + a_1 x - a_2 x^2$$

α	a_0	a_1	a_2	σ
-14	.000105	.1084	- 4.8528	.00024
-12	.000122	.2325	- 9.1300	.00027
-9	.000195	.2131	- 7.7532	.00027
-6	.000242	.0690	- .6478	.00040
-4.5	.000191	-.0540	3.9002	.00056
-3	.000179	-.1529	6.3847	.00053
-1.5	.000161	-.2004	7.2598	.00035
0	.000158	-.1946	5.7691	.00038
1.5	.000148	-.2007	5.0619	.00050
3	.000163	-.1947	1.9953	.00087
4.5	.000188	-.2091	- .0497	.00078
6	.000231	-.2576	- .6062	.00040
9	.000210	-.4018	4.8589	.00020
12.35	.000222	-.2863	2.0963	.00059

Table C35. RC89 Incremental Yawing Moment Coefficient at $\beta=-4^\circ$.

$$\Delta C = a_0 - a_1 x + a_2 x^2$$

α	a_0	a_1	a_2	σ
-14	-.000115	.5248	- 16.1425	.00036
-12	-.000158	.7535	- 22.1900	.00093
- 9	-.000238	.9567	- 26.6754	.00031
- 6	-.000366	.8441	- 26.9421	.00118
- 4.5	-.000304	.7256	- 25.4836	.00072
- 3	-.000311	.5994	- 21.7607	.00052
- 1.5	-.000292	.4428	- 15.9507	.00059
0	-.000291	.2843	- 8.6433	.00063
1.5	-.000284	.1850	- 2.8850	.00082
3	-.000314	.1393	3.0102	.00114
4.5	-.000397	.1499	5.7526	.00084
6	-.000486	.1780	6.9865	.00028
9	-.000443	.1507	6.2023	.00072
12.35	-.000632	- .0964	11.3766	.00085

Table C36. RC89 Incremental Side Force Coefficient at $\beta=-4^\circ$.

$$\Delta C = a_0 + a_1 x + a_2 x^2$$

α	a_0	a_1	a_2	σ
-14	-.000032	- .3905	40.8300	.00071
-12	-.000376	- 1.2408	63.4745	.00379
- 9	-.000441	- 1.8152	74.8682	.00088
- 6	-.000741	- 1.2162	63.5095	.00312
- 4.5	-.000968	- .7170	53.2551	.00278
- 3	-.001226	- .1268	37.4399	.00266
- 1.5	-.001379	.4848	22.7810	.00330
0	-.001439	1.1908	1.6752	.00317
1.5	-.001475	1.7629	- 17.3712	.00147
3	-.001420	2.1627	- 38.1263	.00184
4.5	-.001420	2.3525	- 51.2806	.00154
6	-.001392	2.3959	- 57.7121	.00091
9	-.001230	2.4159	- 55.8101	.00134
12.35	-.001358	2.6160	- 59.1014	.00085

Table C37. RC94 Incremental Normal Force Coefficient at $\beta=-4^\circ$.

$$\Delta C = a_0 - a_1 x - a_2 x^2$$

α	a_0	a_1	a_2	σ
-14	.003421	- 2.0744	- 21.9163	.00192
-12	.002661	- 1.0950	- 47.1764	.00516
- 9	.003293	- .5153	- 51.4954	.00413
- 6	.003728	- .7537	- 41.3046	.00487
- 4.5	.003641	- 1.3660	- 21.9258	.00464
- 3	.004987	- 1.7615	- 11.4574	.00447
- 1.5	.003410	- 1.8378	- 12.0642	.00459
0	.002427	- 1.8784	- 19.3231	.00633
1.5	.001107	- 2.1358	- 21.1504	.00630
3	.000401	- 2.7327	- 9.0279	.00566
4.5	.000689	- 3.3045	5.2745	.00454
6	.001794	- 4.0509	28.2141	.00444
9	.002645	- 5.0959	57.6029	.00441
12.35	.002655	- 4.4612	29.9136	.00327

Table C38. RC94 Incremental Axial Force Coefficient at $\beta=-4^\circ$.

$$\Delta C = a_0 + a_1 x - a_2 x^2$$

α	a_0	a_1	a_2	σ
-14	-.000175	- 2.5940	39.1290	.00141
-12	-.000964	- 2.6657	37.6917	.00210
- 9	-.000526	- 2.7674	37.6105	.00158
- 6	-.000158	- 2.3716	27.6744	.00277
- 4.5	-.000440	- 2.0436	19.6593	.00217
- 3	-.000638	- 1.9369	18.8453	.00163
- 1.5	-.000634	- 1.8555	16.4114	.00153
0	-.000567	- 1.8544	16.8279	.00150
1.5	-.000662	- 1.7933	16.3775	.00180
3	-.000816	- 1.7807	18.5831	.00206
4.5	-.001033	- 1.6747	16.4742	.00191
6	-.001154	- 1.5755	12.2655	.00200
9	-.001119	- 1.6043	11.5321	.00188
12.35	-.001089	- 1.3771	7.1324	.00220

Table C39. RC94 Incremental Pitching Moment Coefficient at $\beta=-4^\circ$.

$$\Delta C = a_0 + a_1 x + a_2 x^2$$

α	a_0	a_1	a_2	σ
-14	.000894	.0714	22.5172	.00048
-12	.000494	- .0283	23.6156	.00145
- 9	.000478	- .2045	24.8197	.00113
- 6	.000884	- .1480	23.0749	.00142
- 4.5	.000865	- .0774	22.9822	.00149
- 3	.001259	- .0453	23.6795	.00112
- 1.5	.000567	.0600	21.5385	.00097
0	.000162	.0530	23.0914	.00107
1.5	-.000215	.0563	25.4846	.00140
3	-.000424	.1308	25.2284	.00151
4.5	-.000227	.3115	19.3963	.00117
6	.000169	.5181	10.2846	.00121
9	.000335	.6671	1.8763	.00108
12.35	.000122	.5181	4.9303	.00103

Table C40. RC94 Incremental Rolling Moment Coefficient at $\beta=-4^\circ$.

$$\Delta C = a_0 + a_1 x + a_2 x^2$$

α	a_0	a_1	a_2	σ
-14	.000105	.0175	1.2992	.00032
-12	.000122	.1803	- 3.2305	.00055
- 9	.000196	.2478	- 3.3553	.00057
- 6	.000241	.1842	1.9568	.00039
- 4.5	.000188	.0996	5.5998	.00039
- 3	.000174	.0093	8.2629	.00054
- 1.5	.000160	- .0039	7.5331	.00051
0	.000160	.0350	4.1690	.00062
1.5	.000149	.0924	.4406	.00060
3	.000162	.0905	- 1.1592	.00057
4.5	.000187	.0512	- .9210	.00058
6	.000234	- .0201	.5762	.00040
9	.000213	- .1302	4.5984	.00021
12.35	.000223	- .0706	3.8502	.00047

Table C41. RC94 Incremental Yawing Moment Coefficient at $\beta=-4^\circ$.

$$\Delta C = a_0 + a_1 x - a_2 x^2$$

α	a_0	a_1	a_2	σ
-14	-.000123	1.2886	- 15.7272	.00034
-12	-.000164	1.4782	- 22.7941	.00067
- 9	-.000244	1.6519	- 27.7343	.00040
- 6	-.000366	1.5331	- 28.6509	.00160
- 4.5	-.000301	1.3549	- 25.1276	.00103
- 3	-.000303	1.2346	- 22.0992	.00061
- 1.5	-.000289	1.0590	- 14.8223	.00060
0	-.000294	.9440	- 7.6082	.00134
1.5	-.000287	.8328	.3090	.00130
3	-.000315	.8473	2.8101	.00075
4.5	-.000395	.9038	1.7342	.00046
6	-.000489	.9854	- 1.6056	.00039
9	-.000451	.9840	- 5.7572	.00106
12.35	-.000637	.6470	2.8847	.00091

Table C42. RC94 Incremental Side Force Coefficient at $\beta=-4^\circ$.

$$\Delta C = a_0 + a_1 x - a_2 x^2$$

α	a_0	a_1	a_2	σ
-14	-.000006	- 2.2757	19.8724	.00049
-12	-.000366	- 3.1648	51.2204	.00305
- 9	-.000430	- 3.7809	70.2886	.00124
- 6	-.000747	- 3.0680	56.9803	.00408
- 4.5	-.000973	- 2.5308	44.9827	.00310
- 3	-.001229	- 2.0102	31.9272	.00240
- 1.5	-.001383	- 1.4011	13.0778	.00254
0	-.001439	- .7014	- 11.5480	.00212
1.5	-.001477	- .1301	- 33.0573	.00107
3	-.001421	.0992	- 41.6456	.00080
4.5	-.001425	.1379	- 41.7445	.00104
6	-.001382	.0570	- 35.3300	.00149
9	-.001205	- .0401	- 20.5340	.00245
12.35	-.001344	.3824	- 33.2344	.00185

APPENDIX D

RCS AND FITS PROGRAM LISTINGS

```

SUBROUTINE RCS(UZCMD,UYCMD,UXCMD,ALPHA,BETA,XMOM,CX,CY,CZ,CL,CM,CN
1)
C** COMPUTE TANK ON RCS INTERACTIONS ***
C*** ALPHA = ANGLE OF ATTACK ***
C*** BETA = YAW ANGLE ***
C*** XMOM = SINGLE JET MOMENTUM RATIO BASED ON WING AREA ***
C*** UZCMD = 0 OR NOT 0 = CONTROL COMMANDS ***
C*** UXCMD = -2, 0, +2 CONTROL COMMANDS ***
C*** UYCMD = 5, 1, 0, -1, -3 CONTROL COMMANDS ***
DIMENSION Y51(6),Y52(6),Y53(6)
DIMENSION Y54(6),Y55(6),Y56(6)
COMMON/FIT/ALPH,XMR,Y0(6),Y4(6),YM4(6)
ALPH=ALPHA
XMR=XMOM
IF(UZCMD.NE.0.) GO TO 1000
C*** **UZCMD=0.
IF(UXCMD.LT.0.) GO TO 750
IF(UXCMD.LT.1.) GO TO 500
C*** **UXCMD=2.
IF(UYCMD.LT.5.) GO TO 100
C*** **UYCMD=5.*RC38 CURVE FITS*
CALL FITS(38)
GO TO 2000
100 IF(UYCMD.LT.1.) GO TO 200
C*** **UYCMD=1.*RC40+RC61 DATA AVERAGE*
CALL FITS(40)
DO 120 I=1,6
Y51(I)=Y0(I)
Y52(I)=Y4(I)
Y53(I)=YM4(I)
120 CONTINUE
CALL FITS(61)
DO 150 I=1,6
Y0(I)=(Y0(I)+Y51(I))/2.
Y4(I)=(Y4(I)+Y52(I))/2.
YM4(I)=(YM4(I)+Y53(I))/2.
150 CONTINUE
GO TO 2000
200 IF(UYCMD.LT.0.) GO TO 300
C*** **UYCMD=0.*RC61 DATA*
CALL FITS(61)
GO TO 2000
300 IF(UYCMD.LT.-1.) GO TO 400
C*** **UYCMD=-1.* **INTERPOLATE RC06/3.+(RC40-RC11)2/3 ***
XMR=XMR*2./3.
CALL FITS(40)
DO 301 I=1,6
Y51(I)=Y0(I)
Y52(I)=Y4(I)
301 Y53(I)=YM4(I)

```



```

CALL FITS(11)
DO 302 I=1,6
Y51(I)=Y51(I)-Y0(I)
Y52(I)=Y52(I)-Y4(I)
302 Y53(I)=Y53(I)-YM4(I)
XMR=XMR/2.
CALL FITS(6)
DO 303 I=1,6
Y0(I)=Y0(I)+Y51(I)
Y4(I)=Y4(I)+Y52(I)
303 YM4(I)=YM4(I)+Y53(I)
GO TO 2000
C****UYCMD=-3.*RC06 DATA*
400 CALL FITS(6)
GO TO 2000
500 IF(UYCMD.LT.5.) GO TO 600
C****UYCMD=0.
C****UYCMD=5.*RC02 DATA*
CALL FITS(62)
GO TO 2000
600 IF(UYCMD.LT.1.) GO TO 650
C****UYCMD=1.*RC37 DATA*
CALL FITS(37)
GO TO 2000
650 IF(UYCMD.LT.0.) GO TO 600
C****UYCMD=0.*NO JETS ON*
DO 655 I=1,6
Y0(I)=0.
Y4(I)=0.
655 YM4(I)=0.
GO TO 2000
C** UYCMD=-3. * USE RC06 DATA*
660 IF(UYCMD.LT.-1.)GO TO 400
C****UYCMD=-1. * INTERPOLATE RC06 DATA*
XMR=XMR/3.
GO TO 400
750 CONTINUE
C****UYCMD=-2.
IF(UYCMD.LT.5.) GO TO 775
C****UYCMD=5.*MIRROR IMAGE OF RC38 *
CALL FITS(30)
DO 760 I=1,6
Y51(I)=Y4(I)
Y4(I)=YM4(I)
YM4(I)=Y51(I)
IF(1.LT.4) GO TO 760
Y0(I)=-Y0(I)
Y4(I)=-Y4(I)
YM4(I)=-YM4(I)
760 CONTINUE

```

```

GO TO 2000
775 IF(UYCMD.LT.1.) GO TO 800
C****UYCMD=1.*MIRROR IMAGE OF (RC40+RC61)/2.*
CALL FITS(40)
DO 780 I=1,6
Y51(I)=Y0(I)
Y52(I)=Y4(I)
Y53(I)=YM4(I)
780 CONTINUE
CALL FITS(61)
DO 790 I=1,6
Y0(I)=(Y0(I)+Y51(I))/2.
Y4(I)=(Y4(I)+Y52(I))/2.
YM4(I)=(YM4(I)+Y53(I))/2.
Y51(I)=Y4(I)
Y4(I)=YM4(I)
YM4(I)=Y51(I)
IF(I.LT.4) GO TO 790
Y0(I)=-Y0(I)
Y4(I)=-Y4(I)
YM4(I)=-YM4(I)
790 CONTINUE
GO TO 2000
800 IF(UYCMD.LT.0.)GO TO 900
C****UYCMD=0.*MIRROR IMAGES OF RC61 *
CALL FITS(61)
DO 820 I=1,6
Y51(I)=Y4(I)
Y4(I)=YM4(I)
YM4(I)=Y51(I)
IF(I.LT.4) GO TO 820
Y0(I)=-Y0(I)
Y4(I)=-Y4(I)
YM4(I)=-YM4(I)
820 CONTINUE
GO TO 2000
900 IF(UYCMD.LT.-1.)GO TO 400
C*** IF(UYCMD=-3. * RC06 DATA *
C*** UYCMD=-1. *INTERPOLATE (RC06)/3 + MIRROR IMAGE OF (RC40-RC11)2/3
XMR=XMR/3.
CALL FITS(6)
DO901 I=1,6
Y51(I)=Y0(I)
Y52(I)=Y4(I)
901 Y53(I)=YM4(I)
XMR=2.*XMR
CALL FITS(40)
DO902 I=1,6
Y54(I)=Y0(I)
Y55(I)=Y4(I)

```

ORIGINAL PAGE IS
OF POOR QUALITY

```

902 Y56(I)=YM4(I)
CALL FITS(11)
DO905 I=1,6
Y54(I)=Y54(I)-Y0(I)
Y55(I)=Y55(I)-Y4(I)
Y56(I)=Y56(I)-YM4(I)
Y4(I)=Y56(I)
Y56(I)=Y55(I)
Y55(I)=Y4(I)
IF(I.LT.4)GO TO 903
Y54(I)=-Y54(I)
Y55(I)=-Y55(I)
Y56(I)=-Y56(I)
903 Y0(I)=Y51(I)+Y54(I)
Y4(I)=Y52(I)+Y55(I)
905 YM4(I)=Y53(I)+Y56(I)
GO TO 2000
1000 CONTINUE
C****KUZCMD=1,OR2.*
IF(UXCMD.LT.2.) GO TO 1300
C****UXCMD=2.
IF(UYCMD.LT.5.) GO TO 1100
C****UYCMD=5.* USE RC82 DATA AND(RC38+RC78)FOR YAW CASES*
CALL FITS(82)
DO 1010 I=1,6
Y51(I)=Y0(I)
1010 CONTINUE
CALL FITS(30)
DO1011 I=1,6
Y52(I)=Y4(I)
1011 Y53(I)=YM4(I)
CALL FITS(78)
DO1012 I=1,6
Y0(I)=Y51(I)
Y4(I)=Y52(I)+Y4(I)
1012 YM4(I)=Y53(I)+YM4(I)
GO TO 2000
1100 IF(UYCMD.LT.1.) GO TO 1150
C****UYCMD=1.*SUM OF RC78+(RC40+RC61)/2.*
CALL FITS(40)
DO 1101 I=1,6
Y51(I)=Y0(I)
Y52(I)=Y4(I)
Y53(I)=YM4(I)
1101 CONTINUE
CALL FITS(61)
DO 1102 I=1,6
Y51(I)=(Y51(I)+Y0(I))/2.
Y52(I)=(Y52(I)+Y4(I))/2.
Y53(I)=(Y53(I)+YM4(I))/2.

```

```

1102 CONTINUE
    CALL FITS(78)
    DO 1103 I=1,6
    Y0(I)=Y0(I)+Y51(I)
    Y4(I)=Y4(I)+Y52(I)
    YM4(I)=YM4(I)+Y53(I)
1103 CONTINUE
    GO TO 2000
1150 IF(UYCMD.LT.0.) GO TO 1200
C****UYCMD=0.*RC09 DATA*
    CALL FITS(89)
    GO TO 2000
1200 IF(UYCMD.LT.-1.) GO TO 1250
C****UYCMD=-1.* RC78+(RC61-RC37)2/3+RC06/3
    CALL FITS(78)
    DO 1201 I=1,6
    Y51(I)=Y0(I)
    Y52(I)=Y4(I)
    Y53(I)=YM4(I)
1201 CONTINUE
    XMR=XMR/3.
    CALL FITS(00)
    DO 1202 I=1,6
    Y51(I)=Y51(I)+Y0(I)
    Y52(I)=Y52(I)+Y4(I)
    Y53(I)=Y53(I)+YM4(I)
1202 CONTINUE
    XMR=XMR*2.
    CALL FITS(61)
    DO 1203 I=1,6
    Y51(I)=Y51(I)+Y0(I)
    Y52(I)=Y52(I)+Y4(I)
    Y53(I)=Y53(I)+YM4(I)
1203 CONTINUE
    CALL FITS(37)
    DO 1204 I=1,6
    Y0(I)=Y51(I)-Y0(I)
    Y4(I)=Y52(I)-Y4(I)
    YM4(I)=Y53(I)-YM4(I)
1204 CONTINUE
    GO TO 2000
1250 CALL FITS(55)
C***UYCMD=-3 * RC55 DATA*
    GO TO 2000
1300 IF(UXCMD.LT.0.) GO TO 1600
C*** UXCMD = 0. *
    IF(UYCMD.LT.5.) GO TO 1400
C*** UYCMD = 5 * RC51 AT B=0 RC62+RC78 AT B=+4 AND -4 *
    CALL FITS(51)
    DO 1301 J=1,6

```

ORIGINAL PAGE IS
OF POOR QUALITY

```

1301 Y51(J) = Y0(J)
    CALL FITS(70)
    DO 1302 J=1,6
    Y52(J)=Y4(J)
1302 Y53(J)=YM4(J)
    CALL FITS(62)
    DO 1303 J=1,6
    Y0(J) = Y51(J)
    Y4(J)=Y4(J)+Y52(J)
1303 YM4(J)=YM4(J)+Y53(J)
    GO TO 2000
1400 IF(UYCMD.LT.1.) GO TO 1450
C*** UYCMD = 1. *RC77 DATA +(RC37+RC78) AT B=+4 OR -4 *
    CALL FITS(77)
    DO 1401 J=1,6
1401 Y51(J)=Y0(J)
    CALL FITS(37)
    DO 1402 J=1,6
    Y52(J)=Y4(J)
1402 Y53(J)=YM4(J)
    CALL FITS(70)
    DO 1403 J=1,6
    Y0(J) = Y51(J)
    Y4(J)=Y4(J)+Y52(J)
1403 YM4(J)=YM4(J)+Y53(J)
    GO TO 2000
1450 IF(UYCMD.LT.0.) GO TO 1500
C*** UYCMD = 0 *RC78 DATA*
    CALL FITS(70)
    GO TO 2000
1500 IF(UYCMD.LT.-1.) GO TO 1250
C*** IF UYCMD=-3 *RC55 DATA *
C*** UYCMD = -1. * RC78 +(RC06)/3. ***
    CALL FITS(70)
    DO 1501 J=1,6
    Y51(J)=Y0(J)
    Y52(J)=Y4(J)
1501 Y53(J) = YM4(J)
    XMR=XMR/3.
    CALL FITS(00)
    DO 1502 J=1,6
    Y0(J)=Y0(J)+Y51(J)
    Y4(J)=Y4(J)+Y52(J)
1502 YM4(J)=YM4(J)+Y53(J)
    GO TO 2000
1600 IF(UYCMD.LT.5.) GO TO 1700
C*** UYCMD=-2 *
C*** UYCMD=5 *RC78 + A MIRROR IMAGE OF RC38 *
    CALL FITS(78)
    DO 1601 J=1,6

```

ORIGINAL PAGE IS
OF POOR QUALITY

```
Y51(J)=Y0(J)
Y52(J)=Y4(J)
1601 Y53(J)=YM4(J)
CALL FITS(36)
DO 1602 J=1,6
Y54(J)=Y4(J)
Y4(J)=YM4(J)
YM4(J)=Y54(J)
IF(J.LT.4)GO TO 1603
YU(J)=-YU(J)
Y4(J)=-Y4(J)
Y14(J)=-YM4(J)
1603 YJ(J)=YU(J)+Y51(J)
Y4(J)=Y4(J)+Y52(J)
1602 YM4(J)=YM4(J)+Y53(J)
GO TO 2000
1700 IF(UYCMD.LT.1.) GO TO 1750
C*** UYCMD=1. * RC78 +MIRROR IMAGE OF (RC61+RC40)/2.*
CALL FITS(78)
DO 1701 J=1,6
Y51(J)=Y0(J)
Y52(J)=Y4(J)
1701 Y53(J)=YM4(J)
CALL FITS(40)
DO 1702 J=1,6
YZ=.5
IF(J.GT.3)YZ=-.5
Y51(J)=(Y51(J)+YZ*Y0(J)
Y52(J)=Y52(J)+YZ*YM4(J)
1702 Y53(J)=Y53(J)+YZ*Y4(J)
CALL FITS(61)
DO 1703 J=1,6
YZ=.5
IF(J.GT.3)YZ=-.5
Y0(J)=Y51(J)+YZ*Y0(J)
Y4(J)=Y52(J)+YZ*YM4(J)
1703 YM4(J)=Y53(J)+YZ*Y4(J)
GO TO 2000
1750 IF(JYCMD.LT.0.) GO TO 1800
C*** UYCMD=0 *RC94 DATA *
CALL FITS(94)
GO TO 2000
C*** IF(UYCMD=-3. * USE RC55 DATA *
1800 IF(UYCMD.LT.-1.) GO TO 1250
C*** UYCMD=-1 * RC78+RC06/3+MIRROR IMAGE OF (RC40-RC11)2/3
CALL FITS(78)
DO 1801 J=1,6
Y51(J) = Y0(J)
Y52(J)=Y4(J)
1801 Y53(J)=YM4(J)
```

```

XMR=XMR/3.
CALL FITS(6)
DO 1802 J=1,6
Y51(J)=Y51(J)+Y0(J)
Y52(J)=Y52(J)+Y4(J)
1802 Y53(J)=Y53(J)+YM4(J)
XMR=2.*XMR
CALL FITS(40)
DO 1803 J=1,6
YZ=1.
IF(J.GE.4) YZ=-1.
Y51(J)=Y51(J)+YZ*Y0(J)
Y52(J)=Y52(J)+YZ*YM4(J)
1803 Y53(J)=Y53(J)+YZ*Y4(J)
CALL FITS(11)
DO 1804 J=1,6
YZ=1.
IF(J.GE.4) YZ=-1.
Y0(J)=Y51(J)-YZ*Y0(J)
Y4(J)=Y52(J)-YZ*YM4(J)
1804 YM4(J)=Y53(J)-YZ*Y4(J)
2000 CONTINUE
C*** CORRECT FOR YAW ANGLE
DO 2222 J=1,6
C3=1.0025*Y0(J)-.02632*Y4(J)+.02381*YM4(J)
BX=(Y4(J)-YM4(J))/8.
AX=.02970*YM4(J)+.03289*Y4(J)-.06266*Y0(J)
YCOR=C3+BETA*(BX+BETA*AX)
GO TO(2001,2002,2003,2004,2005,2006),J
2001 CZ=-YCOR
GO TO 2222
2002 CX=-YCOR
GO TO 2222
2003 CM=YCOR
GO TO 2222
2004 CL=YCOR
GO TO 2222
2005 CN=YCOR
GO TO 2222
2006 CY=YCOR
2222 CONTINUE
RETURN
END

```

DATA(A02(3,II,4),II=1,14)/
 1 .110389E+01,-.882300E+00,-.265939E+01,-.324618E+01,-.336770E+01,
 2-.311097E+01,-.218912E+01,-.896242E+00,.689333E+00,.252668E+01,
 3 .403530E+01,.388370E+01,.113148E+01,.402799E+00/
 DATA(A00(3,II,5),II=1,14)/
 1 .595079E-03,.400526E-03,.271464E-03,.311439E-03,.226113E-03,
 2 .106304E-03,.731899E-04,.462446E-04,.206781E-04,-.233652E-04,
 3 .175703E-04,.176300E-04,-.720219E-04,-.180422E-03/
 DATA(A01(3,II,5),II=1,14)/
 1 .426361E-01,.739093E-02,.147119E-02,-.400191E-02,.554214E-02,
 2 .283023E-01,.816933E-01,.132208E+00,.192184E+00,.253058E+00,
 3 .280350E+00,.254658E+00,.139115E+00,.136505E+00/
 DATA(A02(3,II,5),II=1,14)/
 1-.247337E+01,.314083E+00,.236821E+01,.305365E+01,.307728E+01,
 2 .270492E+01,.727152E+00,-.154586E+01,-.420149E+01,-.699122E+01,
 3-.858166E+01,-.804523E+01,-.404201E+01,-.407583E+01/
 DATA(A00(3,II,6),II=1,14)/
 1 .143331E-02,.917802E-03,.758071E-03,.728641E-03,.228576E-03,
 2 .189830E-04,-.273598E-03,-.353181E-03,-.382292E-03,-.687535E-03,
 3-.721543E-03,-.923479E-03,-.115900E-02,-.138913E-02/
 DATA(A01(3,II,6),II=1,14)/
 1-.192154E+00,-.634863E-01,.549718E-01,.719794E-01,.114382E+00,
 2 .864579E-01,.622033E-01,-.347390E-01,-.144397E+00,-.272963E+00,
 3-.351841E+00,-.297325E+00,-.655395E-01,.157940E-01/
 DATA(A02(3,II,6),II=1,14)/
 1 .374874E+01,-.276952E+01,-.101642E+02,-.101003E+02,-.112808E+02,
 2-.105917E+02,-.969988E+01,-.598887E+01,-.121384E+01,.479465E+01,
 3 .100263E+02,.956010E+01,.375247E+01,.161227E+01/
 DATA(A00(4,II,1),II=1,14)/
 1-.568458E-02,-.569730E-02,-.518222E-02,-.531197E-02,-.567565E-02,
 2-.508138E-02,-.550724E-02,-.604592E-02,-.546119E-02,-.535059E-02,
 3-.465518E-02,-.491112E-02,-.488242E-02,-.500490E-02/
 DATA(A01(4,II,1),II=1,14)/
 1-.469929E+01,-.410142E+01,-.323426E+01,-.279221E+01,-.280087E+01,
 2-.295159E+01,-.269250E+01,-.240269E+01,-.211041E+01,-.186558E+01,
 3-.167890E+01,-.147359E+01,-.138445E+01,-.187635E+01/
 DATA(A02(4,II,1),II=1,14)/
 1-.474350E+01,-.204066E+02,-.469895E+02,-.618817E+02,-.579836E+02,
 2-.448172E+02,-.478652E+02,-.549511E+02,-.646451E+02,-.720056E+02,
 3-.770703E+02,-.800539E+02,-.599822E+02,-.299712E+02/
 DATA(A00(4,II,2),II=1,14)/
 1-.468553E-02,-.490260E-02,-.507157E-02,-.509733E-02,-.497531E-02,
 2-.507031E-02,-.514824E-02,-.525831E-02,-.539738E-02,-.552278E-02,
 3-.501391E-02,-.562662E-02,-.555845E-02,-.535083E-02/
 DATA(A01(4,II,2),II=1,14)/
 1-.319294E+01,-.331404E+01,-.327271E+01,-.304070E+01,-.312704E+01,
 2-.326914E+01,-.346460E+01,-.352909E+01,-.350950E+01,-.367308E+01,
 3-.381746E+01,-.397227E+01,-.429225E+01,-.468602E+01/
 DATA(A02(4,II,2),II=1,14)/
 1 .721151E+02,.778627E+02,.798417E+02,.767470E+02,.800091E+02,


```

2-.665962E+00,-.610833E+00,-.557961E+00,-.414467E+00,-.264760E+00,
3-.878538E-01,.377911E-01,.247128E+00,.247143E+00/
DATA(A02( 2,II,6),II=1,14)/
1-.223511E+02,-.977261E+01,-.115138E+01,.589839E+01,.712130E+01,
2 .136677E+02,.153106E+02,.167995E+02,.125870E+02,.800221E+01,
3 .121960E+01,-.351833E+01,-.126354E+02,-.115053E+02/
DATA(A00( 3,II,1),II=1,14)/
1-.554847E-02,-.558786E-02,-.507520E-02,-.519144E-02,-.558425E-02,
2-.501228E-02,-.544600E-02,-.595758E-02,-.536553E-02,-.522158E-02,
3-.454240E-02,-.479886E-02,-.478671E-02,-.490355E-02/
DATA(A01( 3,II,1),II=1,14)/
1-.748179E+00,-.795536E+00,-.730830E+00,-.566836E+00,-.571617E+00,
2-.599287E+00,-.627583E+00,-.512231E+00,-.499114E+00,-.438325E+00,
3-.539607E+00,-.632938E+00,-.928827E+00,-.107839E+01/
DATA(A02( 3,II,1),II=1,14)/
1 .146076E+02,.170759E+02,.157736E+02,.107221E+02,.109729E+02,
2 .108404E+02,.987840E+01,.456760E+01,.248056E+01,-.114688E+01,
3-.412977E+00,.316674E+00,.654816E+01,.108042E+02/
DATA(A00( 3,II,2),II=1,14)/
1-.472416E-02,-.492139E-02,-.508089E-02,-.509973E-02,-.497688E-02,
2-.506320E-02,-.514344E-02,-.524502E-02,-.538526E-02,-.551540E-02,
3-.561679E-02,-.563085E-02,-.555831E-02,-.535615E-02/
DATA(A01( 3,II,2),II=1,14)/
1-.341126E+00,-.248423E+00,-.227413E+00,-.292374E+00,-.309053E+00,
2-.329728E+00,-.390281E+00,-.456419E+00,-.505920E+00,-.518838E+00,
3-.472155E+00,-.362579E+00,-.198141E+00,-.285844E+00/
DATA(A02( 3,II,2),II=1,14)/
1 .217406E+01,-.214335E+01,-.345111E+01,-.326030E+00,-.705210E+00,
2-.122252E+01,.384641E-01,.256838E+01,.567568E+01,.828393E+01,
3 .929221E+01,.685873E+01,-.130454E+01,-.351761E-02/
DATA(A00( 3,II,3),II=1,14)/
1-.915593E-03,-.107615E-02,-.880807E-03,-.108779E-02,-.138855E-02,
2-.115275E-02,-.127071E-02,-.144677E-02,-.123651E-02,-.120859E-02,
3-.103730E-02,-.114498E-02,-.124437E-02,-.128562E-02/
DATA(A01( 3,II,3),II=1,14)/
1 .304154E+00,.328568E+00,.292734E+00,.245009E+00,.198624E+00,
2 .173184E+00,.149347E+00,.140817E+00,.561681E-01,.291886E-01,
3 .343317E-01,.144916E+00,.272417E+00,.154000E+00/
DATA(A02( 3,II,3),II=1,14)/
1-.189869E+01,-.348054E+01,-.377148E+01,-.209789E+01,-.616115E+00,
2-.523480E+00,.241761E+00,.112348E+01,.466711E+01,.685975E+01,
3 .755265E+01,.372429E+01,-.314225E+01,-.665694E+00/
DATA(A00( 3,II,4),II=1,14)/
1-.298730E-03,-.204150E-03,-.169117E-03,-.206406E-03,-.190418E-03,
2-.151512E-03,-.142278E-03,-.134545E-03,-.132277E-03,-.129048E-03,
3-.153360E-03,-.168086E-03,-.167883E-03,-.148153E-03/
DATA(A01( 3,II,4),II=1,14)/
1-.118094E-01,.200581E-01,.373714E-01,.471143E-01,.448235E-01,
2 .293248E-01,-.232258E-03,-.332466E-01,-.703558E-01,-.108634E+00,
3-.131688E+00,-.113461E+00,-.284468E-01,-.917419E-02/

```

DATA(A01(2,II,2),II=1,14)/
1-.101084E+01,-.106450E+01,-.108489E+01,-.114688E+01,-.120585E+01,
2-.123628E+01,-.123517E+01,-.121151E+01,-.116197E+01,-.986743E+00,
3-.800259E+00,-.684279E+00,-.798094E+00,-.958919E+00/
DATA(A02(2,II,2),II=1,14)/
1-.100236E+01, .294126E+01, .745469E+01, .146263E+02, .181851E+02,
2 .204603E+02, .215569E+02, .227242E+02, .232879E+02, .184666E+02,
3 .131711E+02, .901891E+01, .111459E+02, .165190E+02/
DATA(A00(2,II,3),II=1,14)/
1-.905217E-03,-.107508E-02,-.884100E-03,-.108838E-02,-.139080E-02,
2-.116270E-02,-.128492E-02,-.146437E-02,-.125501E-02,-.122656E-02,
3-.104772E-02,-.114000E-02,-.123611E-02,-.128820E-02/
DATA(A01(2,II,3),II=1,14)/
1-.499092E-02,-.159553E-01,-.433181E-01,-.584655E-01,-.741168E-01,
2-.721055E-01, .147523E-01, .617255E-01, .123989E+00, .266317E+00,
3 .406082E+00, .502052E+00, .355029E+00, .137099E+00/
DATA(A02(2,II,3),II=1,14)/
1 .922617E+01, .103115E+02, .109560E+02, .146946E+02, .159073E+02,
2 .154175E+02, .116900E+02, .101017E+02, .711886E+01, .393878E+00,
3-.697067E+01,-.127204E+02,-.103439E+02,-.354601E+01/
DATA(A00(2,II,4),II=1,14)/
1-.284430E-03,-.200491E-03,-.164552E-03,-.200798E-03,-.190609E-03,
2-.156218E-03,-.151016E-03,-.144340E-03,-.143558E-03,-.140346E-03,
3-.101079E-03,-.171184E-03,-.165475E-03,-.145571E-03/
DATA(A01(2,II,4),II=1,14)/
1 .844717E-01, .218278E-02,-.727010E-01,-.966779E-01,-.112557E+00,
2-.171790E+00,-.173397E+00,-.151610E+00,-.102361E+00,-.482149E-01,
3 .338120E-02, .318769E-01, .587776E-01, .108988E-01/
DATA(A02(2,II,4),II=1,14)/
1-.617931E+01,-.265354E+01, .283710E+00, .303068E+01, .421773E+01,
2 .624037E+01, .720696E+01, .727196E+01, .561676E+01, .368258E+01,
3 .150129E+01, .463835E+00,-.132078E+01, .119930E+00/
DATA(A00(2,II,5),II=1,14)/
1 .576292E-03, .401314E-03, .269667E-03, .306177E-03, .229882E-03,
2 .116504E-03, .909363E-04, .639392E-04, .403275E-04,-.575267E-05,
3 .282010E-04, .215370E-04,-.742243E-04,-.181798E-03/
DATA(A01(2,II,5),II=1,14)/
1 .609528E-01, .180602E+00, .295257E+00, .320042E+00, .339600E+00,
2 .420480E+00, .400894E+00, .346619E+00, .254155E+00, .195082E+00,
3 .153973E+00, .151817E+00, .117427E+00, .163083E+00/
DATA(A02(2,II,5),II=1,14)/
1 .601010E+01, .973015E+00,-.362971E+01,-.716349E+01,-.853941E+01,
2-.117135E+02,-.120861E+02,-.114349E+02,-.774239E+01,-.547248E+01,
3-.330201E+01,-.317653E+01,-.108016E+01,-.254991E+01/
DATA(A00(2,II,6),II=1,14)/
1 .147233E-02, .941916E-03, .777220E-03, .741516E-03, .223325E-03,
2-.348741E-05,-.304829E-03,-.382207E-03,-.413479E-03,-.713469E-03,
3-.740681E-03,-.929309E-03,-.114749E-02,-.136441E-02/
DATA(A01(2,II,6),II=1,14)/
1-.606455E-01,-.317178E+00,-.499579E+00,-.521634E+00,-.490323E+00,

```

2-.155427E-03,-.147407E-03,-.139569E-03,-.136851E-03,-.131644E-03,
3-.153751E-03,-.167342E-03,-.166038E-03,-.146346E-03/
  DATA(A01( 1,II,4),II=1,14)/
1 .219730E-02, .127224E-01, .287615E-01, .284429E-01, .139027E-01,
2 .809622E-02, .637186E-02, .173937E-01, .160959E-01, .213124E-01,
3 .188775E-01, .142723E-01, .209510E-01, .255670E-01/
  DATA(A02( 1,II,4),II=1,14)/
1 .110666E+01, .548385E+00,-.454303E+00,-.364772E-01, .840367E+00,
2 .113219E+01, .123320E+01, .758490E+00, .811183E+00, .663528E+00,
3 .644580E+00, .756550E+00, .381119E+00, .228709E+00/
  DATA(A00( 1,II,5),II=1,14)/
1 .593177E-03, .401470E-03, .269814E-03, .306321E-03, .225436E-03,
2 .110004E-03, .820944E-04, .548538E-04, .281989E-04,-.218822E-04,
3 .156907E-04, .131945E-04,-.773312E-04,-.183292E-03/
  DATA(A01( 1,II,5),II=1,14)/
1-.797215E-01,-.618430E-01,-.547188E-01,-.108624E-01, .242817E-01,
2 .270009E-01, .147113E-01,-.757727E-02,-.270166E-01,-.202705E-01,
3-.143181E-01, .476864E-02,-.180761E-02, .514184E-02/
  DATA(A02( 1,II,5),II=1,14)/
1 .107098E+01, .273969E+00,-.429496E-01,-.181361E+01,-.300356E+01,
2-.303678E+01,-.245452E+01,-.167860E+01,-.354988E+00,-.376073E+00,
3-.188620E+00,-.105451E+01,-.760017E+00,-.672705E+00/
  DATA(A00( 1,II,6),II=1,14)/
1 .143377E-02, .927317E-03, .766578E-03, .738051E-03, .231833E-03,
2 .304986E-05,-.297238E-03,-.381916E-03,-.409811E-03,-.705795E-03,
3-.728342E-03,-.924276E-03,-.115457E-02,-.138496E-02/
  DATA(A01( 1,II,6),II=1,14)/
1 .209414E+00, .342867E+00, .282182E+00, .119713E+00, .143316E+00,
2 .180902E+00, .263413E+00, .335655E+00, .468485E+00, .522672E+00,
3 .596292E+00, .587308E+00, .635618E+00, .560933E+00/
  DATA(A02( 1,II,6),II=1,14)/
1-.365599E+01,-.623460E+01,-.193249E+01, .478061E+01, .293719E+01,
2 .144544E+01,-.210702E+01,-.439231E+01,-.991021E+01,-.122395E+02,
3-.144898E+02,-.131953E+02,-.154348E+02,-.133016E+02/
  DATA(A00( 2,II,1),II=1,14)/
1-.555403E-02,-.558884E-02,-.505139E-02,-.515261E-02,-.553402E-02,
2-.495601E-02,-.538859E-02,-.591565E-02,-.532658E-02,-.518637E-02,
3-.450976E-02,-.477085E-02,-.477553E-02,-.489938E-02/
  DATA(A01( 2,II,1),II=1,14)/
1 .255477E+00, .221996E+00, .279215E+00, .260608E+00, .318391E+00,
2 .277493E+00, .279074E+00, .117630E+00, .627089E-01,-.269490E+00,
3-.636813E+00,-.107103E+01,-.163243E+01,-.169227E+01/
  DATA(A02( 2,II,1),II=1,14)/
1-.272942E+02,-.250938E+02,-.277105E+02,-.271202E+02,-.317683E+02,
2-.314307E+02,-.369901E+02,-.351237E+02,-.392109E+02,-.288914E+02,
3-.170588E+02,-.158710E+01, .200767E+02, .250393E+02/
  DATA(A00( 2,II,2),II=1,14)/
1-.473303E-02,-.493974E-02,-.510951E-02,-.512868E-02,-.501077E-02,
2-.510187E-02,-.519130E-02,-.529266E-02,-.542869E-02,-.555213E-02,
3-.563396E-02,-.563342E-02,-.556088E-02,-.536680E-02/

```

```

SUBROUTINE FITS(ID)
  DIMENSION JD(15),KD(11),LD(7),A00(15,14,6),A01(15,14,6),A02(15,14,
16),AP0(11,14,6),AP1(11,14,6),AP2(11,14,6),AM0(7,14,6),AM1(7,14,6),
2AM2(7,14,6),AL(14)
  DIMENSION AU(6),A1(6),A2(6),A4(6),A41(6),A42(6),AM4(6),AM41(6),
1AM42(6)
  COMMON/FIT/ALPH,XMR,Y0(6),Y4(6),YM4(6)
  DATA JD/6,11,37,38,40,51,55,61,62,77,78,82,87,89,94/
  DATA KD/6,11,37,38,40,55,61,62,78,89,94/
  DATA LD/ 38,40,55,61,78,89,94/
  DATA AL/-14.,-12.,-9.,-6.,-4.5,-3.,-1.5,0.,1.5,3.,4.5,6.,9.,12.35/
C**** CURVE FIT TABLES ****
  DATA(A00( 1,II,1),II=1,14)/
1-.556728E-02,-.558975E-02,-.506998E-02,-.517178E-02,-.554991E-02,
2-.497718E-02,-.538776E-02,-.589547E-02,-.529653E-02,-.517635E-02,
3-.451214E-02,-.475444E-02,-.472840E-02,-.485576E-02/
  DATA(A01( 1,II,1),II=1,14)/
1-.301838E+01,-.339735E+01,-.225953E+01,-.200105E+01,-.227949E+01,
2-.273415E+01,-.297627E+01,-.328021E+01,-.334595E+01,-.348895E+01,
3-.349190E+01,-.356541E+01,-.329821E+01,-.327994E+01/
  DATA(A02( 1,II,1),II=1,14)/
1 .102744E+02, .165761E+02,-.384040E+02,-.560651E+02,-.534176E+02,
2-.428578E+02,-.357407E+02,-.220907E+02,-.179108E+02,-.894916E+01,
3-.833557E+01,-.664444E+01,-.258359E+02,-.325296E+02/
  DATA(A00( 1,II,2),II=1,14)/
1-.478063E-02,-.497540E-02,-.514091E-02,-.514331E-02,-.501552E-02,
2-.510388E-02,-.518468E-02,-.528643E-02,-.542831E-02,-.555348E-02,
3-.564953E-02,-.566178E-02,-.559142E-02,-.539364E-02/
  DATA(A01( 1,II,2),II=1,14)/
1-.378487E+01,-.412836E+01,-.379276E+01,-.351127E+01,-.355573E+01,
2-.360965E+01,-.366313E+01,-.370190E+01,-.382321E+01,-.393696E+01,
3-.401052E+01,-.399993E+01,-.398674E+01,-.417241E+01/
  DATA(A02( 1,II,2),II=1,14)/
1 .438674E+02, .562186E+02, .413972E+02, .275778E+02, .291527E+02,
2 .317841E+02, .330481E+02, .325776E+02, .353675E+02, .374011E+02,
3 .381869E+02, .357784E+02, .318521E+02, .346090E+02/
  DATA(A00( 1,II,3),II=1,14)/
1-.909107E-03,-.106853E-02,-.874215E-03,-.109655E-02,-.138901E-02,
2-.115110E-02,-.126312E-02,-.144681E-02,-.123823E-02,-.121379E-02,
3-.103997E-02,-.114253E-02,-.125014E-02,-.129882E-02/
  DATA(A01( 1,II,3),II=1,14)/
1 .140302E+01, .158098E+01, .120463E+01, .980725E+00, .107440E+01,
2 .110393E+01, .111008E+01, .108151E+01, .115193E+01, .125709E+01,
3 .132219E+01, .132571E+01, .135430E+01, .143267E+01/
  DATA(A02( 1,II,3),II=1,14)/
1 .351543E+01,-.233856E+01, .128978E+02, .221923E+02, .199636E+02,
2 .211181E+02, .233810E+02, .260552E+02, .227509E+02, .163796E+02,
3 .115527E+02, .110190E+02, .125760E+02, .112061E+02/
  DATA(A00( 1,II,4),II=1,14)/
1-.301304E-03,-.205757E-03,-.167777E-03,-.205476E-03,-.192252E-03,

```

```

2 .820468E+02, .867472E+02, .868990E+02, .875770E+02, .904554E+02,
3 .935530E+02, .953005E+02, .969827E+02, .108736E+03/
DATA(A00( 4,II,3),II=1,14)/
1-.878543E-03,-.104792E-02,-.863539E-03,-.108079E-02,-.138632E-02,
2-.115126E-02,-.127474E-02,-.145323E-02,-.123690E-02,-.119821E-02,
3-.101143E-02,-.111830E-02,-.122364E-02,-.126498E-02/
DATA(A01( 4,II,3),II=1,14)/
1-.882111E+00,-.976125E+00,-.958442E+00,-.671746E+00,-.454623E+00,
2-.254839E+00,-.131326E+00, .402226E-01, .240064E+00, .442902E+00,
3 .470639E+00, .505284E+00, .119442E+01, .178905E+01/
DATA(A02( 4,II,3),II=1,14)/
1 .587431E+02, .688021E+02, .756481E+02, .749761E+02, .697344E+02,
2 .635962E+02, .600474E+02, .542055E+02, .471787E+02, .399040E+02,
3 .404345E+02, .419746E+02, .226652E+02, .313058E+01/
DATA(A00( 4,II,4),II=1,14)/
1-.302023E-03,-.208991E-03,-.177361E-03,-.204985E-03,-.189646E-03,
2-.156215E-03,-.154493E-03,-.148950E-03,-.150277E-03,-.152581E-03,
3-.189554E-03,-.208665E-03,-.196904E-03,-.161124E-03/
DATA(A01( 4,II,4),II=1,14)/
1 .215340E+00, .112718E+00, .592598E-01, .562496E-02,-.503062E-01,
2-.810016E-01,-.101690E+00,-.122263E+00,-.189105E+00,-.202787E+00,
3-.421154E-01, .233273E+00, .391940E+00, .165890E+00/
DATA(A02( 4,II,4),II=1,14)/
1-.203183E+02,-.155334E+02,-.122394E+02,-.909362E+01,-.598185E+01,
2-.411386E+01,-.349431E+01,-.286522E+01, .378608E+00, .136267E+01,
3-.683799E+01,-.202050E+02,-.253587E+02,-.149609E+02/
DATA(A00( 4,II,5),II=1,14)/
1 .604056E-03, .419214E-03, .296055E-03, .318614E-03, .233571E-03,
2 .120547E-03, .976027E-04, .722506E-04, .526695E-04, .146867E-04,
3 .750457E-04, .770776E-04,-.329719E-04,-.171256E-03/
DATA(A01( 4,II,5),II=1,14)/
1-.604211E+00,-.545684E+00,-.517745E+00,-.371785E+00,-.267501E+00,
2-.225582E+00,-.214956E+00,-.209995E+00,-.148701E+00,-.167509E+00,
3-.463157E+00,-.888330E+00,-.109368E+01,-.755444E+00/
DATA(A02( 4,II,5),II=1,14)/
1 .191720E+02, .135120E+02, .109238E+02, .368709E+01,-.114530E+01,
2-.357018E+01,-.414955E+01,-.641325E+01,-.115644E+02,-.123202E+02,
3 .353924E+01, .250250E+02, .326807E+02, .183408E+02/
DATA(A00( 4,II,6),II=1,14)/
1 .141958E-02, .889455E-03, .773274E-03, .697763E-03, .181084E-03,
2-.497782E-04,-.343817E-03,-.429862E-03,-.448938E-03,-.751460E-03,
3-.807017E-03,-.103838E-02,-.123044E-02,-.139513E-02/
DATA(A01( 4,II,6),II=1,14)/
1 .198174E+01, .147292E+01, .757754E+00, .169990E+00,-.185280E-01,
2 .627149E-01, .174003E+00, .209494E+00,-.923296E-02,-.615388E-01,
3 .557169E+00, .157889E+01, .307983E+01, .292577E+01/
DATA(A02( 4,II,6),II=1,14)/
1-.884667E+02,-.674515E+02,-.332048E+02, .297314E+00, .912008E+01,
2 .340378E+01,-.487289E+01,-.595815E+01, .690199E+01, .129511E+02,
3-.155406E+02,-.602298E+02,-.113181E+03,-.104585E+03/

```

```

DATA(A00( 5,II,1),II=1,14)/
1-.566894E-02,-.566500E-02,-.510746E-02,-.517081E-02,-.552432E-02,
2-.490845E-02,-.532570E-02,-.581110E-02,-.519580E-02,-.504275E-02,
3-.436285E-02,-.459176E-02,-.453847E-02,-.465435E-02/
DATA(A01( 5,II,1),II=1,14)/
1-.340459E+00,-.961230E+00,-.112712E+01,-.150231E+01,-.206174E+01,
2-.289960E+01,-.369987E+01,-.460630E+01,-.522919E+01,-.591014E+01,
3-.649211E+01,-.731917E+01,-.876195E+01,-.877502E+01/
DATA(A02( 5,II,1),II=1,14)/
1-.108197E+03,-.760450E+02,-.596023E+02,-.355765E+02,-.848398E+01,
2 .327150E+02, .730021E+02, .115179E+03, .142943E+03, .171831E+03,
3 .198206E+03, .238974E+03, .318568E+03, .326156E+03/
DATA(A00( 5,II,2),II=1,14)/
1-.464310E-02,-.484858E-02,-.501392E-02,-.501563E-02,-.490423E-02,
2-.501841E-02,-.512538E-02,-.523544E-02,-.538053E-02,-.550317E-02,
3-.559669E-02,-.560844E-02,-.555080E-02,-.534770E-02/
DATA(A01( 5,II,2),II=1,14)/
1-.440645E+01,-.445991E+01,-.431426E+01,-.441806E+01,-.442461E+01,
2-.426845E+01,-.413641E+01,-.399544E+01,-.384794E+01,-.356822E+01,
3-.329272E+01,-.309233E+01,-.302997E+01,-.317960E+01/
DATA(A02( 5,II,2),II=1,14)/
1 .135243E+03, .138198E+03, .136825E+03, .148567E+03, .149588E+03,
2 .141265E+03, .133092E+03, .125654E+03, .119731E+03, .109180E+03,
3 .962587E+02, .848517E+02, .739381E+02, .762553E+02/
DATA(A00( 5,II,3),II=1,14)/
1-.985019E-03,-.114243E-02,-.942571E-03,-.113591E-02,-.143078E-02,
2-.120314E-02,-.133603E-02,-.151557E-02,-.130352E-02,-.126560E-02,
3-.108080E-02,-.116349E-02,-.123704E-02,-.128038E-02/
DATA(A01( 5,II,3),II=1,14)/
1 .189076E+01, .175013E+01, .135607E+01, .111408E+01, .104688E+01,
2 .106514E+01, .123956E+01, .137136E+01, .150203E+01, .156074E+01,
3 .156350E+01, .142708E+01, .909102E+00, .567560E+00/
DATA(A02( 5,II,3),II=1,14)/
1-.799239E+02,-.685937E+02,-.466669E+02,-.283821E+02,-.226991E+02,
2-.219546E+02,-.285206E+02,-.340322E+02,-.393591E+02,-.416352E+02,
3-.412464E+02,-.334900E+02,-.436256E+01, .126720E+02/
DATA(A00( 5,II,4),II=1,14)/
1-.285141E-03,-.197155E-03,-.157046E-03,-.188312E-03,-.178653E-03,
2-.152477E-03,-.150160E-03,-.140242E-03,-.131235E-03,-.119881E-03,
3-.141306E-03,-.153314E-03,-.148935E-03,-.139205E-03/
DATA(A01( 5,II,4),II=1,14)/
1 .966805E-01,-.435294E-01,-.147146E+00,-.219173E+00,-.259597E+00,
2-.322824E+00,-.320581E+00,-.329560E+00,-.367416E+00,-.394415E+00,
3-.387931E+00,-.360482E+00,-.292499E+00,-.175330E+00/
DATA(A02( 5,II,4),II=1,14)/
1-.732950E+01,-.136552E+01, .375778E+01, .737333E+01, .940721E+01,
2 .126525E+02, .131479E+02, .144470E+02, .173001E+02, .197866E+02,
3 .210206E+02, .205832E+02, .158412E+02, .679344E+01/
DATA(A00( 5,II,5),II=1,14)/
1 .602849E-03, .422477E-03, .293899E-03, .328710E-03, .250963E-03,

```

```

2 .148065E-03, .120807E-03, .858055E-04, .491957E-04, -.562905E-05,
3 .349537E-04, .342041E-04, -.557445E-04, -.150694E-03/
DATA(A01( 5,II,5),II=1,14)/
1-.784204E+00, -.670087E+00, -.602134E+00, -.559709E+00, -.532911E+00,
2-.477333E+00, -.490724E+00, -.434151E+00, -.325215E+00, -.256098E+00,
3-.307128E+00, -.397036E+00, -.596026E+00, -.813060E+00/
DATA(A02( 5,II,5),II=1,14)/
1 .373467E+02, .328646E+02, .302186E+02, .285948E+02, .271709E+02,
2 .237691E+02, .228296E+02, .176498E+02, .104379E+02, .527458E+01,
3 .616689E+01, .951632E+01, .218325E+02, .365509E+02/
DATA(A00( 5,II,6),II=1,14)/
1 .143763E-02, .877632E-03, .714893E-03, .702201E-03, .181879E-03,
2-.832149E-04, -.404001E-03, -.473115E-03, -.475782E-03, -.748003E-03,
3-.767326E-03, -.959291E-03, -.117875E-02, -.142639E-02/
DATA(A01( 5,II,6),II=1,14)/
1 .174534E+01, .153222E+01, .135763E+01, .127275E+01, .132657E+01,
2 .138295E+01, .169590E+01, .185107E+01, .180937E+01, .161696E+01,
3 .145079E+01, .138417E+01, .160652E+01, .213160E+01/
DATA(A02( 5,II,6),II=1,14)/
1-.711350E+02, -.632140E+02, -.532736E+02, -.456489E+02, -.478647E+02,
2-.521354E+02, -.664678E+02, -.705721E+02, -.632682E+02, -.494041E+02,
3-.369413E+02, -.296366E+02, -.404477E+02, -.728685E+02/
DATA(A00( 6,II,1),II=1,14)/
1-.555917E-02, -.559036E-02, -.509457E-02, -.516574E-02, -.555629E-02,
2-.497953E-02, -.541735E-02, -.594294E-02, -.534554E-02, -.520732E-02,
3-.451636E-02, -.479243E-02, -.481386E-02, -.491167E-02/
DATA(A01( 6,II,1),II=1,14)/
1-.459816E+01, -.376478E+01, -.263302E+01, -.254651E+01, -.262673E+01,
2-.256689E+01, -.214599E+01, -.165246E+01, -.141751E+01, -.146224E+01,
3-.180163E+01, -.209314E+01, -.143124E+01, -.178297E+01/
DATA(A02( 6,II,1),II=1,14)/
1 .193567E+02, -.133940E+01, -.262253E+02, -.198636E+02, -.171115E+02,
2-.157837E+02, -.257179E+02, -.358441E+02, -.380759E+02, -.316716E+02,
3-.127059E+02, .890114E+01, .101982E+02, .283992E+02/
DATA(A00( 6,II,2),II=1,14)/
1-.470939E-02, -.492028E-02, -.509077E-02, -.514180E-02, -.502282E-02,
2-.510409E-02, -.517750E-02, -.527841E-02, -.541752E-02, -.554264E-02,
3-.563222E-02, -.564331E-02, -.557989E-02, -.538181E-02/
DATA(A01( 6,II,2),II=1,14)/
1-.252128E+01, -.274253E+01, -.240840E+01, -.153676E+01, -.127774E+01,
2-.129652E+01, -.153005E+01, -.165353E+01, -.162410E+01, -.146245E+01,
3-.135645E+01, -.130314E+01, -.158901E+01, -.185938E+01/
DATA(A02( 6,II,2),II=1,14)/
1 .303140E+02, .417738E+02, .340796E+02, .971918E+01, .366032E+01,
2 .546262E+01, .134424E+02, .163358E+02, .160160E+02, .104725E+02,
3 .568315E+01, .562095E+00, .569672E+01, .155979E+02/
DATA(A00( 6,II,3),II=1,14)/
1-.923691E-03, -.108981E-02, -.909187E-03, -.113255E-02, -.143328E-02,
2-.119710E-02, -.131007E-02, -.148376E-02, -.126458E-02, -.123255E-02,
3-.104279E-02, -.114736E-02, -.124536E-02, -.128660E-02/

```

DATA(A01(6,II,3),II=1,14)/
1-.968672E+00,-.970301E+00,-.913064E+00,-.486896E+00,-.177185E+00,
2 .205665E-01, .124398E+00, .210259E+00, .335062E+00, .546000E+00,
3 .715037E+00, .851593E+00, .143311E+01, .216015E+01/
DATA(A02(6,II,3),II=1,14)/
1 .352970E+02, .400334E+02, .402506E+02, .317284E+02, .244291E+02,
2 .205515E+02, .171213E+02, .132356E+02, .777875E+01,-.498374E+00,
3-.626049E+01,-.915850E+01,-.214436E+02,-.470025E+02/
DATA(A00(6,II,4),II=1,14)/
1-.297055E-03,-.190607E-03,-.154513E-03,-.198927E-03,-.183501E-03,
2-.152581E-03,-.144742E-03,-.129015E-03,-.119166E-03,-.110049E-03,
3-.149211E-03,-.172309E-03,-.126453E-03,-.141933E-03/
DATA(A01(6,II,4),II=1,14)/
1-.873119E-02, .269797E-01,-.854199E-01,-.135617E+00,-.106358E+00,
2-.102067E+00,-.177409E+00,-.219850E+00,-.250890E+00,-.270572E+00,
3-.378550E+00,-.402803E+00,-.640437E+00,-.609005E+00/
DATA(A02(6,II,4),II=1,14)/
1-.858539E+01,-.981076E+01,-.143990E+01, .334164E+01, .199042E+01,
2 .137279E+01, .475177E+01, .656134E+01, .722003E+01, .884214E+01,
3 .159945E+02, .205118E+02, .306553E+02, .234310E+02/
DATA(A00(6,II,5),II=1,14)/
1 .610770E-03, .402991E-03, .274813E-03, .313171E-03, .225347E-03,
2 .111650E-03, .809060E-04, .428663E-04, .140870E-04,-.396631E-04,
3 .231408E-04, .224745E-04,-.146771E-03,-.193960E-03/
DATA(A01(6,II,5),II=1,14)/
1 .365945E+00, .352543E+00, .548714E+00, .531855E+00, .412829E+00,
2 .334638E+00, .416840E+00, .480797E+00, .516997E+00, .538392E+00,
3 .569821E+00, .498269E+00, .937031E+00, .998327E+00/
DATA(A02(6,II,5),II=1,14)/
1-.205600E+01, .108507E+01,-.607486E+01,-.722713E+01,-.218942E+01,
2 .942139E+00,-.406082E+01,-.851363E+01,-.959791E+01,-.126169E+02,
3-.179723E+02,-.209285E+02,-.369462E+02,-.277125E+02/
DATA(A00(6,II,6),II=1,14)/
1 .137768E-02, .909253E-03, .789913E-03, .719091E-03, .212325E-03,
2-.169784E-04,-.282284E-03,-.334809E-03,-.339933E-03,-.647891E-03,
3-.700583E-03,-.904257E-03,-.101800E-02,-.136819E-02/
DATA(A01(6,II,6),II=1,14)/
1-.733359E+00,-.127943E+01,-.198070E+01,-.196349E+01,-.165382E+01,
2-.136738E+01,-.154024E+01,-.182606E+01,-.206053E+01,-.186772E+01,
3-.149426E+01,-.112384E+01,-.169268E+01,-.692894E+00/
DATA(A02(6,II,6),II=1,14)/
1-.282456E+02,-.137015E+02, .187731E+02, .299161E+02, .170521E+02,
2 .260878E+01, .116461E+02, .301475E+02, .464154E+02, .480506E+02,
3 .453003E+02, .440729E+02, .783759E+02, .394299E+02/
DATA(A00(7,II,1),II=1,14)/
1-.554246E-02,-.557369E-02,-.503291E-02,-.513726E-02,-.554915E-02,
2-.500416E-02,-.544372E-02,-.592198E-02,-.529321E-02,-.516631E-02,
3-.448371E-02,-.474506E-02,-.474168E-02,-.487984E-02/
DATA(A01(7,II,1),II=1,14)/
1-.211603E+01,-.147698E+01,-.517725E+00,-.609482E+00,-.848842E+00,


```

2-.102169E+01,-.111956E+01,-.141956E+01,-.171305E+01,-.219883E+01,
3-.258022E+01,-.287493E+01,-.358774E+01,-.350973E+01/
  DATA(A02( 7,II,1),II=1,14)/
1-.365922E+02,-.607751E+02,-.877485E+02,-.949053E+02,-.100445E+03,
2-.105912E+03,-.110926E+03,-.102873E+03,-.950949E+02,-.764831E+02,
3-.595705E+02,-.462922E+02,-.239554E+02,-.478799E+02/
  DATA(A00( 7,II,2),II=1,14)/
1-.477872E-02,-.497685E-02,-.513447E-02,-.514792E-02,-.502092E-02,
2-.510651E-02,-.518905E-02,-.530130E-02,-.544483E-02,-.557147E-02,
3-.565712E-02,-.566293E-02,-.558732E-02,-.539813E-02/
  DATA(A01( 7,II,2),II=1,14)/
1-.518334E+01,-.546005E+01,-.524713E+01,-.490220E+01,-.476419E+01,
2-.470093E+01,-.461766E+01,-.456889E+01,-.457172E+01,-.457828E+01,
3-.464048E+01,-.474370E+01,-.492906E+01,-.486919E+01/
  DATA(A02( 7,II,2),II=1,14)/
1 .900296E+02, .964655E+02, .878254E+02, .787452E+02, .749063E+02,
2 .726585E+02, .679980E+02, .639737E+02, .625949E+02, .617848E+02,
3 .624776E+02, .634972E+02, .657792E+02, .611104E+02/
  DATA(A00( 7,II,3),II=1,14)/
1-.914586E-03,-.108424E-02,-.894215E-03,-.109562E-02,-.139135E-02,
2-.110039E-02,-.128479E-02,-.145903E-02,-.124007E-02,-.121316E-02,
3-.103878E-02,-.115099E-02,-.124837E-02,-.129530E-02/
  DATA(A01( 7,II,3),II=1,14)/
1 .840712E+00, .749778E+00, .458072E+00, .580164E+00, .666127E+00,
2 .734019E+00, .788574E+00, .878191E+00, .986626E+00, .106540E+01,
3 .113304E+01, .112998E+01, .114435E+01, .115007E+01/
  DATA(A02( 7,II,3),II=1,14)/
1 .208669E+02, .244980E+02, .327159E+02, .304675E+02, .308149E+02,
2 .322591E+02, .337521E+02, .321808E+02, .279943E+02, .243656E+02,
3 .204692E+02, .202167E+02, .183773E+02, .140969E+02/
  DATA(A00( 7,II,4),II=1,14)/
1-.301199E-03,-.201249E-03,-.164774E-03,-.207142E-03,-.195327E-03,
2-.158480E-03,-.152380E-03,-.144915E-03,-.142406E-03,-.136259E-03,
3-.161164E-03,-.176105E-03,-.168374E-03,-.145534E-03/
  DATA(A01( 7,II,4),II=1,14)/
1-.724725E-01, .112094E+00, .175894E+00, .131298E+00, .140419E+00,
2 .117391E+00, .680188E-01,-.473657E-02,-.584309E-01,-.121505E+00,
3-.160363E+00,-.197718E+00,-.210012E+00,-.248467E+00/
  DATA(A02( 7,II,4),II=1,14)/
1-.195777E+00,-.543055E+01,-.561467E+01,-.327629E+01,-.361112E+01,
2-.270604E+01,-.877126E+00, .161114E+01, .325414E+01, .503970E+01,
3 .617438E+01, .698964E+01, .717938E+01, .894942E+01/
  DATA(A00( 7,II,5),II=1,14)/
1 .605190E-03, .401606E-03, .270369E-03, .316510E-03, .238697E-03,
2 .120739E-03, .861586E-04, .558833E-04, .299032E-04,-.169124E-04,
3 .197863E-04, .163491E-04,-.766973E-04,-.188795E-03/
  DATA(A01( 7,II,5),II=1,14)/
1 .500963E+00, .643197E+00, .747712E+00, .678074E+00, .547999E+00,
2 .457710E+00, .471311E+00, .556121E+00, .622040E+00, .635568E+00,
3 .617086E+00, .573943E+00, .568371E+00, .591818E+00/

```

DATA(A02(7,II,5),II=1,14)/
1-.571957E+01,-.951553E+01,-.113829E+02,-.894386E+01,-.403842E+01,
2-.941917E+00,-.131456E+01,-.458345E+01,-.679444E+01,-.677956E+01,
3-.587149E+01,-.439074E+01,-.462356E+01,-.751349E+01/
DATA(A00(7,II,6),II=1,14)/
1 .141180E-02, .909107E-03, .749902E-03, .707939E-03, .200358E-03,
2-.148060E-04,-.297541E-03,-.357916E-03,-.379204E-03,-.678363E-03,
3-.709834E-03,-.905462E-03,-.113686E-02,-.130124E-02/
DATA(A01(7,II,6),II=1,14)/
1-.216580E+00,-.781009E+00,-.759306E+00,-.480350E+00,-.142079E+00,
2 .175515E+00, .355597E+00, .499439E+00, .714274E+00, .982435E+00,
3 .118794E+01, .136113E+01, .154916E+01, .154894E+01/
DATA(A02(7,II,6),II=1,14)/
1 .904222E+01, .256796E+02, .213023E+02, .107358E+02,-.197981E+01,
2-.115068E+02,-.158979E+02,-.174094E+02,-.238067E+02,-.317234E+02,
3-.367700E+02,-.396737E+02,-.421381E+02,-.508708E+02/
DATA(A00(8,II,1),II=1,14)/
1-.554531E-02,-.559011E-02,-.506497E-02,-.515804E-02,-.553949E-02,
2-.497040E-02,-.539473E-02,-.592035E-02,-.533940E-02,-.519018E-02,
3-.451417E-02,-.474763E-02,-.475453E-02,-.490475E-02/
DATA(A01(8,II,1),II=1,14)/
1-.115880E+01,-.121629E+01,-.844025E+00,-.721012E+00,-.975209E+00,
2-.115449E+01,-.146149E+01,-.160707E+01,-.166892E+01,-.170015E+01,
3-.175455E+01,-.198556E+01,-.223148E+01,-.237925E+01/
DATA(A02(8,II,1),II=1,14)/
1-.812602E+01,-.137942E+02,-.313342E+02,-.385609E+02,-.324354E+02,
2-.302976E+02,-.226230E+02,-.195732E+02,-.202656E+02,-.221659E+02,
3-.228330E+02,-.177099E+02,-.128547E+02,-.618840E+01/
DATA(A00(8,II,2),II=1,14)/
1-.475087E-02,-.495713E-02,-.510512E-02,-.511569E-02,-.499618E-02,
2-.508533E-02,-.516381E-02,-.526256E-02,-.539963E-02,-.553483E-02,
3-.563825E-02,-.565765E-02,-.557524E-02,-.537163E-02/
DATA(A01(8,II,2),II=1,14)/
1-.249497E+01,-.249399E+01,-.234769E+01,-.235677E+01,-.241552E+01,
2-.254862E+01,-.270507E+01,-.288359E+01,-.295040E+01,-.291547E+01,
3-.285042E+01,-.274672E+01,-.263068E+01,-.273151E+01/
DATA(A02(8,II,2),II=1,14)/
1 .216695E+02, .197225E+02, .115808E+02, .108406E+02, .136087E+02,
2 .191436E+02, .246447E+02, .312412E+02, .347243E+02, .345155E+02,
3 .332781E+02, .292659E+02, .213351E+02, .210981E+02/
DATA(A00(8,II,3),II=1,14)/
1-.902479E-03,-.106929E-02,-.884056E-03,-.108795E-02,-.137939E-02,
2-.114798E-02,-.126693E-02,-.145077E-02,-.124796E-02,-.121345E-02,
3-.104449E-02,-.114320E-02,-.124491E-02,-.129054E-02/
DATA(A01(8,II,3),II=1,14)/
1 .742822E+00, .788280E+00, .607749E+00, .590791E+00, .560919E+00,
2 .610267E+00, .608683E+00, .604805E+00, .603411E+00, .610105E+00,
3 .673344E+00, .721511E+00, .836415E+00, .726918E+00/
DATA(A02(8,II,3),II=1,14)/
1-.689981E+00,-.148564E+01, .566260E+01, .513125E+01, .662620E+01,

2 .584798E+01, .716384E+01, .881854E+01, .916052E+01, .889080E+01,
 3 .663075E+01, .520339E+01, -.219117E+00, .244936E+01/
 DATA(A00(8,II,4),II=1,14)/
 1-.303481E-03, -.208590E-03, -.171112E-03, -.201900E-03, -.186083E-03,
 2-.148046E-03, -.143312E-03, -.137453E-03, -.137804E-03, -.134103E-03,
 3-.157993E-03, -.172795E-03, -.171149E-03, -.149152E-03/
 DATA(A01(8,II,4),II=1,14)/
 1 .114477E-01, .555893E-01, .123452E+00, .672196E-01, -.728612E-02,
 2-.677439E-01, -.109643E+00, -.139841E+00, -.164089E+00, -.196480E+00,
 3-.220793E+00, -.226453E+00, -.165108E+00, -.163144E+00/
 DATA(AU2(8,II,4),II=1,14)/
 1-.910788E+00, -.470620E+01, -.950995E+01, -.702716E+01, -.385519E+01,
 2-.203026E+01, -.103309E+01, -.777172E-01, .928412E+00, .238401E+01,
 3 .350949E+01, .389374E+01, .193025E+01, .200022E+01/
 DATA(A00(8,II,5),II=1,14)/
 1 .599770E-03, .403854E-03, .274108E-03, .304646E-03, .218786E-03,
 2 .102021E-03, .760403E-04, .531004E-04, .294707E-04, -.165150E-04,
 3 .215302E-04, .214796E-04, -.711467E-04, -.181620E-03/
 DATA(AU1(8,II,5),II=1,14)/
 1-.303212E+00, -.348209E+00, -.403832E+00, -.345870E+00, -.263609E+00,
 2-.216213E+00, -.184641E+00, -.170368E+00, -.135764E+00, -.800024E-01,
 3-.275719E-01, -.374676E-01, -.159487E+00, -.190694E+00/
 DATA(A02(8,II,5),II=1,14)/
 1-.227893E+01, .132571E+01, .607867E+01, .394071E+01, .301192E+00,
 2-.116680E+01, -.183393E+01, -.201453E+01, -.303735E+01, -.494920E+01,
 3-.704583E+01, -.689589E+01, -.323529E+01, -.296471E+01/
 DATA(A00(8,II,6),II=1,14)/
 1 .143745E-02, .917288E-03, .756797E-03, .743239E-03, .240049E-03,
 2 .182675E-04, -.281517E-03, -.356277E-03, -.389200E-03, -.692708E-03,
 3-.729780E-03, -.933734E-03, -.116762E-02, -.138669E-02/
 DATA(A01(8,II,6),II=1,14)/
 1 .872913E+00, .976989E+00, .117102E+01, .114086E+01, .106766E+01,
 2 .994679E+00, .101614E+01, .100029E+01, .988033E+00, .899602E+00,
 3 .829566E+00, .814458E+00, .111703E+01, .124838E+01/
 DATA(A02(8,II,6),II=1,14)/
 1 .603799E+01, -.567602E+00, -.123403E+02, -.879081E+01, -.365719E+01,
 2-.136681E+01, -.409305E+01, -.449315E+01, -.532057E+01, -.322422E+01,
 3-.163455E+01, -.768065E+00, -.954064E+01, -.106891E+02/
 DATA(A00(9,II,1),II=1,14)/
 1-.500912E-02, -.562798E-02, -.511778E-02, -.520924E-02, -.557995E-02,
 2-.501801E-02, -.546491E-02, -.599166E-02, -.539782E-02, -.525982E-02,
 3-.458048E-02, -.483146E-02, -.482596E-02, -.495596E-02/
 DATA(AU1(9,II,1),II=1,14)/
 1-.309707E+01, -.248636E+01, -.169157E+01, -.125238E+01, -.898472E+00,
 2-.969380E+00, -.466459E+00, -.922633E-01, .182415E+00, .335139E+00,
 3 .299904E+00, .382062E+00, .590550E+00, .337965E+00/
 DATA(A02(9,II,1),II=1,14)/
 1 .955261E+01, -.713356E+01, -.296933E+02, -.368912E+02, -.433664E+02,
 2-.334187E+02, -.432456E+02, -.505489E+02, -.580241E+02, -.614943E+02,
 3-.578434E+02, -.518671E+02, -.365363E+02, -.199146E+02/

DATA(A00(9,II,2),II=1,14)/
1-.470737E-02,-.491851E-02,-.507856E-02,-.509430E-02,-.497491E-02,
2-.506991E-02,-.515345E-02,-.525744E-02,-.539085E-02,-.550822E-02,
3-.560154E-02,-.561755E-02,-.555756E-02,-.535714E-02/
DATA(A01(9,II,2),II=1,14)/
1-.600813E+00,-.581774E+00,-.434043E+00,-.268242E+00,-.325531E+00,
2-.337784E+00,-.412241E+00,-.390100E+00,-.395241E+00,-.457965E+00,
3-.575284E+00,-.720421E+00,-.108374E+01,-.139841E+01/
DATA(A02(9,II,2),II=1,14)/
1-.312975E+01,-.166948E+01,-.249008E+01,-.942675E+00, .162884E+01,
2 .641958E-01,-.245737E+00,-.247185E+01,-.244135E+01, .717124E+00,
3 .308846E+01, .542697E+01, .112335E+02, .197655E+02/
DATA(A00(9,II,3),II=1,14)/
1-.899655E-03,-.106230E-02,-.877045E-03,-.108599E-02,-.138548E-02,
2-.116142E-02,-.128391E-02,-.146450E-02,-.124770E-02,-.121512E-02,
3-.103308E-02,-.113230E-02,-.123090E-02,-.128029E-02/
DATA(A01(9,II,3),II=1,14)/
1-.978841E+00,-.994528E+00,-.991850E+00,-.726048E+00,-.516860E+00,
2-.501246E+00,-.358510E+00,-.184138E+00, .585523E-01, .246477E+00,
3 .293202E+00, .350540E+00, .986480E+00, .156235E+01/
DATA(A02(9,II,3),II=1,14)/
1 .328660E+02, .392937E+02, .450750E+02, .441814E+02, .401231E+02,
2 .402452E+02, .348206E+02, .275649E+02, .177316E+02, .106316E+02,
3 .906647E+01, .970408E+01,-.615372E+01,-.249211E+02/
DATA(A00(9,II,4),II=1,14)/
1-.293462E-03,-.200071E-03,-.164337E-03,-.199357E-03,-.187877E-03,
2-.152461E-03,-.146814E-03,-.140165E-03,-.141408E-03,-.142070E-03,
3-.170493E-03,-.183339E-03,-.177970E-03,-.151589E-03/
DATA(A01(9,II,4),II=1,14)/
1-.506887E-01,-.985843E-01,-.110373E+00,-.141123E+00,-.143622E+00,
2-.133527E+00,-.162223E+00,-.210388E+00,-.285973E+00,-.305982E+00,
3-.247925E+00,-.683369E-01, .262750E+00, .187795E+00/
DATA(A02(9,II,4),II=1,14)/
1-.117713E+01, .926896E+00, .243354E+01, .454631E+01, .504676E+01,
2 .518133E+01, .684712E+01, .974795E+01, .142560E+02, .166512E+02,
3 .160002E+02, .960908E+01,-.550662E+01,-.728211E+01/
DATA(A00(9,II,5),II=1,14)/
1 .583841E-03, .395976E-03, .266684E-03, .300057E-03, .221735E-03,
2 .106350E-03, .795792E-04, .541920E-04, .374910E-04,-.129617E-05,
3 .422056E-04, .325132E-04,-.618305E-04,-.179534E-03/
DATA(A01(9,II,5),II=1,14)/
1 .379437E+00, .429073E+00, .410921E+00, .497041E+00, .544291E+00,
2 .580562E+00, .633521E+00, .687063E+00, .746966E+00, .752676E+00,
3 .646964E+00, .404856E+00, .185374E-01, .195803E+00/
DATA(A02(9,II,5),II=1,14)/
1-.854424E+01,-.101173E+02,-.915751E+01,-.125314E+02,-.146594E+02,
2-.167991E+02,-.203353E+02,-.255571E+02,-.311624E+02,-.340075E+02,
3-.310210E+02,-.214906E+02,-.148731E+01,-.177763E+01/
DATA(A00(9,II,6),II=1,14)/
1 .143455E-02, .936074E-03, .794232E-03, .731641E-03, .221098E-03,

```

2-.947763E-05,-.300668E-03,-.376708E-03,-.397013E-03,-.709633E-03,
3-.749547E-03,-.956676E-03,-.117295E-02,-.136357E-02/
  DATA(A01( 9,II,6),II=1,14)/
  1 .459967E+00, .983520E-01,-.366196E+00,-.738841E+00,-.783290E+00,
  2-.679771E+00,-.624434E+00,-.765031E+00,-.114921E+01,-.128975E+01,
  3-.997607E+00,-.245293E+00, .150823E+01, .170131E+01/
  DATA(A02( 9,II,6),II=1,14)/
  1-.215453E+02,-.844865E+01, .128843E+02, .327346E+02, .349426E+02,
  2 .286419E+02, .245849E+02, .323655E+02, .534475E+02, .665101E+02,
  3 .614044E+02, .373629E+02,-.330076E+02,-.552229E+02/
  DATA(A00(10,II,1),II=1,14)/
  1-.554883E-02,-.556750E-02,-.505475E-02,-.516659E-02,-.553128E-02,
  2-.497098E-02,-.540521E-02,-.595141E-02,-.537098E-02,-.524151E-02,
  3-.456194E-02,-.481841E-02,-.479284E-02,-.491916E-02/
  DATA(A01(10,II,1),II=1,14)/
  1-.104878E+01,-.455581E+00, .336485E+00, .200561E+00, .112204E+00,
  2 .147443E+00, .352017E+00, .217887E+00, .810019E-01,-.293259E+00,
  3-.577098E+00,-.904236E+00,-.147753E+01,-.213229E+01/
  DATA(A02(10,II,1),II=1,14)/
  1 .700343E+01,-.858925E+01,-.245113E+02,-.175255E+02,-.180424E+02,
  2-.216162E+02,-.297039E+02,-.228233E+02,-.186311E+02,-.549050E+01,
  3 .129320E+01, .989881E+01, .173056E+02, .257223E+02/
  DATA(A00(10,II,2),II=1,14)/
  1-.474027E-02,-.494330E-02,-.510284E-02,-.511497E-02,-.499221E-02,
  2-.507332E-02,-.515558E-02,-.526035E-02,-.540800E-02,-.553556E-02,
  3-.562394E-02,-.563172E-02,-.556460E-02,-.537080E-02/
  DATA(A01(10,II,2),II=1,14)/
  1-.938097E+00,-.114638E+01,-.112620E+01,-.764553E+00,-.711837E+00,
  2-.744120E+00,-.790324E+00,-.736081E+00,-.684829E+00,-.618485E+00,
  3-.554052E+00,-.515347E+00,-.438167E+00,-.186816E+00/
  DATA(A02(10,II,2),II=1,14)/
  1 .119082E+02, .172930E+02, .163720E+02, .907550E+01, .102761E+02,
  2 .130783E+02, .148151E+02, .122192E+02, .103746E+02, .871353E+01,
  3 .757487E+01, .788575E+01, .701918E+01,-.148984E+01/
  DATA(A00(10,II,3),II=1,14)/
  1-.923702E-03,-.108095E-02,-.886177E-03,-.108558E-02,-.137586E-02,
  2-.114818E-02,-.126833E-02,-.145901E-02,-.124886E-02,-.122186E-02,
  3-.103993E-02,-.114686E-02,-.124246E-02,-.127856E-02/
  DATA(A01(10,II,3),II=1,14)/
  1-.611683E-01,-.107683E+00,-.299335E+00,-.264529E+00,-.198645E+00,
  2-.210223E+00,-.179488E+00,-.178764E+00,-.159699E+00,-.159745E+00,
  3-.127874E+00,-.100596E+00,-.874047E-02, .571289E-01/
  DATA(A02(10,II,3),II=1,14)/
  1 .385317E+01, .335495E+01, .652835E+01, .641593E+01, .579124E+01,
  2 .805867E+01, .760870E+01, .774163E+01, .652648E+01, .683489E+01,
  3 .599830E+01, .571489E+01, .111209E+01,-.361545E+01/
  DATA(A00(10,II,4),II=1,14)/
  1-.300379E-03,-.200709E-03,-.163808E-03,-.203920E-03,-.190412E-03,
  2-.153298E-03,-.142711E-03,-.136317E-03,-.136825E-03,-.134972E-03,
  3-.164670E-03,-.177753E-03,-.164199E-03,-.148287E-03/

```

DATA(A01(10,II,4),II=1,14)/
1-.722659E-01, .111665E+00, .243853E+00, .179281E+00, .153126E+00,
2 .154354E+00, .125947E+00, .549620E-01,-.804237E-01,-.225407E+00,
3-.262427E+00,-.163141E+00,-.167200E+00,-.366383E+00/
DATA(A02(10,II,4),II=1,14)/
1-.305715E+00,-.651636E+01,-.968598E+01,-.658259E+01,-.551394E+01,
2-.647139E+01,-.733401E+01,-.639666E+01,-.110314E+01, .511639E+01,
3 .690571E+01, .155919E+01,-.200202E+01, .795117E+01/
DATA(A00(10,II,5),II=1,14)/
1 .601980E-03, .406098E-03, .274816E-03, .314193E-03, .232540E-03,
2 .115231E-03, .754153E-04, .477106E-04, .266385E-04,-.154643E-04,
3 .304228E-04, .254022E-04,-.812089E-04,-.187160E-03/
DATA(A01(10,II,5),II=1,14)/
1 .634519E+00, .715850E+00, .797838E+00, .782595E+00, .687913E+00,
2 .537639E+00, .486767E+00, .548054E+00, .703624E+00, .836827E+00,
3 .817922E+00, .655047E+00, .660031E+00, .862766E+00/
DATA(A02(10,II,5),II=1,14)/
1-.788460E+01,-.788574E+01,-.813340E+01,-.865199E+01,-.638351E+01,
2-.804433E+00, .256523E+01, .171074E+01,-.454000E+01,-.102911E+02,
3-.960280E+01,-.157403E+01, .100269E+01,-.115746E+02/
DATA(A00(10,II,6),II=1,14)/
1 .141106E-02, .898229E-03, .753180E-03, .722763E-03, .211334E-03,
2-.618817E-05,-.285556E-03,-.355724E-03,-.380409E-03,-.686255E-03,
3-.757875E-03,-.936994E-03,-.112554E-02,-.137764E-02/
DATA(A01(10,II,6),II=1,14)/
1-.100292E+01,-.140280E+01,-.137381E+01,-.113158E+01,-.812706E+00,
2-.338970E+00, .290100E-01, .304397E+00, .265659E+00, .201568E+00,
3 .337202E+00, .868442E+00, .990154E+00, .424809E+00/
DATA(A02(10,II,6),II=1,14)/
1 .279282E+02, .346355E+02, .263732E+02, .215616E+02, .143981E+02,
2-.111454E+01,-.149772E+02,-.245138E+02,-.162668E+02,-.617899E+01,
3-.566415E+01,-.261729E+02,-.331208E+02,-.688882E+01/
DATA(A00(11,II,1),II=1,14)/
1-.554766E-02,-.557182E-02,-.505479E-02,-.517330E-02,-.554929E-02,
2-.497991E-02,-.541923E-02,-.593502E-02,-.533945E-02,-.519830E-02,
3-.453450E-02,-.481000E-02,-.480873E-02,-.491472E-02/
DATA(A01(11,II,1),II=1,14)/
1-.959568E+00,-.418628E+00, .353593E+00, .179835E+00, .146348E-01,
2 .848703E-01, .189803E+00, .143687E+00,-.240605E-01,-.232434E+00,
3-.520664E+00,-.760272E+00,-.121648E+01,-.165195E+01/
DATA(A02(11,II,1),II=1,14)/
1 .168534E+02, .319251E+01,-.132736E+02,-.530271E+01,-.227874E+01,
2-.778562E+01,-.117154E+02,-.693642E+01,-.906254E+00, .642552E+01,
3 .135936E+02, .205162E+02, .285020E+02, .278637E+02/
DATA(A00(11,II,2),II=1,14)/
1-.476042E-02,-.496726E-02,-.513398E-02,-.514263E-02,-.501495E-02,
2-.509685E-02,-.517813E-02,-.528823E-02,-.543273E-02,-.556166E-02,
3-.565165E-02,-.565811E-02,-.557834E-02,-.538570E-02/
DATA(A01(11,II,2),II=1,14)/
1-.645185E+00,-.915488E+00,-.869640E+00,-.470938E+00,-.456517E+00,

```

2-.479796E+00,-.501843E+00,-.439782E+00,-.383759E+00,-.364959E+00,
3-.301285E+00,-.237287E+00,-.213345E+00,-.142232E+00/
  DATA(A02(11,II,2),II=1,14)/
  1 .116025E+02, .192794E+02, .165189E+02, .654772E+01, .943103E+01,
  2 .118525E+02, .133727E+02, .102946E+02, .793131E+01, .706613E+01,
  3 .425552E+01, .201930E+01, .144057E+01,-.170690E+00/
  DATA(A00(11,II,3),II=1,14)/
  1-.923599E-03,-.108431E-02,-.892756E-03,-.109603E-02,-.138766E-02,
  2-.115411E-02,-.127780E-02,-.145847E-02,-.124716E-02,-.121272E-02,
  3-.103643E-02,-.114151E-02,-.124394E-02,-.128865E-02/
  DATA(A01(11,II,3),II=1,14)/
  1-.391212E+00,-.467222E+00,-.584045E+00,-.519521E+00,-.441995E+00,
  2-.406932E+00,-.371435E+00,-.363491E+00,-.326509E+00,-.285916E+00,
  3-.226301E+00,-.178297E+00,-.207778E+00,-.193152E+00/
  DATA(A02(11,II,3),II=1,14)/
  1 .873940E+01, .103710E+02, .113466E+02, .101263E+02, .931788E+01,
  2 .100841E+02, .971285E+01, .103020E+02, .833022E+01, .664164E+01,
  3 .345639E+01, .133785E+01, .249233E+01, .140844E+01/
  DATA(A00(11,II,4),II=1,14)/
  1-.298674E-03,-.198724E-03,-.164412E-03,-.205366E-03,-.193404E-03,
  2-.157675E-03,-.150101E-03,-.141968E-03,-.139106E-03,-.133636E-03,
  3-.157411E-03,-.170602E-03,-.166579E-03,-.148094E-03/
  DATA(A01(11,II,4),II=1,14)/
  1-.667432E-01, .114276E+00, .248643E+00, .210080E+00, .188246E+00,
  2 .155047E+00, .106396E+00, .366468E-01,-.330309E-01,-.107976E+00,
  3-.165139E+00,-.191905E+00,-.195886E+00,-.195279E+00/
  DATA(A02(11,II,4),II=1,14)/
  1 .221946E+00,-.561145E+01,-.847230E+01,-.708533E+01,-.628767E+01,
  2-.531533E+01,-.401096E+01,-.231210E+01,-.539410E+00, .173564E+01,
  3 .376525E+01, .439465E+01, .337248E+01, .426127E+01/
  DATA(A00(11,II,5),II=1,14)/
  1 .599537E-03, .403777E-03, .275559E-03, .316240E-03, .237187E-03,
  2 .121241E-03, .886759E-04, .588675E-04, .323638E-04,-.158561E-04,
  3 .236264E-04, .200705E-04,-.746725E-04,-.181882E-03/
  DATA(A01(11,II,5),II=1,14)/
  1 .635048E+00, .735272E+00, .804201E+00, .720425E+00, .637934E+00,
  2 .561864E+00, .555288E+00, .599413E+00, .649109E+00, .677790E+00,
  3 .683836E+00, .665722E+00, .628852E+00, .577696E+00/
  DATA(A02(11,II,5),II=1,14)/
  1-.911505E+01,-.102555E+02,-.103678E+02,-.762037E+01,-.552832E+01,
  2-.376851E+01,-.403289E+01,-.536824E+01,-.654500E+01,-.697670E+01,
  3-.710255E+01,-.662551E+01,-.568602E+01,-.577011E+01/
  DATA(A00(11,II,6),II=1,14)/
  1 .141226E-02, .906130E-03, .754892E-03, .720844E-03, .208133E-03,
  2-.136431E-04,-.306074E-03,-.376154E-03,-.390698E-03,-.684254E-03,
  3-.710461E-03,-.912953E-03,-.113327E-02,-.136333E-02/
  DATA(A01(11,II,6),II=1,14)/
  1-.008030E+00,-.121616E+01,-.122865E+01,-.853136E+00,-.526839E+00,
  2-.152990E+00, .143148E+00, .373578E+00, .559808E+00, .805723E+00,
  3 .981675E+00, .110385E+01, .115384E+01, .102550E+01/

```

DATA(A02(11,II,6),II=1,14)/
1 .265169E+02, .341713E+02, .282557E+02, .166284E+02, .827283E+01,
2-.118930E+01,-.833965E+01,-.127347E+02,-.169796E+02,-.231785E+02,
3-.269923E+02,-.275101E+02,-.258705E+02,-.222963E+02/
DATA(A00(12,II,1),II=1,14)/
1-.558299E-02,-.561507E-02,-.509207E-02,-.519870E-02,-.555508E-02,
2-.497250E-02,-.541221E-02,-.593313E-02,-.535198E-02,-.521227E-02,
3-.454606E-02,-.480322E-02,-.481473E-02,-.494837E-02/
DATA(A01(12,II,1),II=1,14)/
1-.508480E+01,-.482789E+01,-.357769E+01,-.338589E+01,-.364324E+01,
2-.370910E+01,-.340693E+01,-.310596E+01,-.299265E+01,-.308073E+01,
3-.335053E+01,-.372407E+01,-.332504E+01,-.341723E+01/
DATA(A02(12,II,1),II=1,14)/
1 .385649E+01,-.144495E+02,-.455677E+02,-.498844E+02,-.384264E+02,
2-.306436E+02,-.331982E+02,-.392505E+02,-.406527E+02,-.369642E+02,
3-.194757E+02, .981175E+01, .240683E+02, .275234E+02/
DATA(A00(12,II,2),II=1,14)/
1-.467500E-02,-.488507E-02,-.506594E-02,-.510534E-02,-.499196E-02,
2-.507449E-02,-.515263E-02,-.524385E-02,-.537891E-02,-.550580E-02,
3-.561151E-02,-.562564E-02,-.554154E-02,-.534181E-02/
DATA(A01(12,II,2),II=1,14)/
1-.354280E+01,-.366491E+01,-.322456E+01,-.236026E+01,-.213958E+01,
2-.222442E+01,-.251627E+01,-.274978E+01,-.273536E+01,-.274092E+01,
3-.272950E+01,-.280889E+01,-.312244E+01,-.339706E+01/
DATA(A02(12,II,2),II=1,14)/
1 .227967E+02, .296263E+02, .155883E+02,-.114684E+02,-.177428E+02,
2-.136245E+02,-.301510E+01, .661744E+01, .694614E+01, .817446E+01,
3 .433878E+01, .156722E+01, .526583E+01, .154990E+02/
DATA(A00(12,II,3),II=1,14)/
1-.928245E-03,-.108972E-02,-.907420E-03,-.112907E-02,-.141938E-02,
2-.118108E-02,-.129920E-02,-.147789E-02,-.126738E-02,-.123350E-02,
3-.105807E-02,-.110103E-02,-.124283E-02,-.128141E-02/
DATA(A01(12,II,3),II=1,14)/
1-.495430E+00,-.587410E+00,-.541101E+00,-.750516E-01, .227061E+00,
2 .469703E+00, .648777E+00, .783443E+00, .968896E+00, .119613E+01,
3 .135420E+01, .155233E+01, .214333E+01, .268696E+01/
DATA(A02(12,II,3),II=1,14)/
1 .411815E+02, .500041E+02, .507334E+02, .417158E+02, .359293E+02,
2 .298899E+02, .226784E+02, .159317E+02, .796270E+01,-.151492E+01,
3-.787141E+01,-.149638E+02,-.265592E+02,-.433723E+02/
DATA(A00(12,II,4),II=1,14)/
1-.298479E-03,-.193278E-03,-.157443E-03,-.198772E-03,-.185299E-03,
2-.153129E-03,-.154829E-03,-.141912E-03,-.133221E-03,-.114121E-03,
3-.140703E-03,-.159517E-03,-.163936E-03,-.146762E-03/
DATA(A01(12,II,4),II=1,14)/
1 .644334E-01, .981049E-01,-.113597E-01,-.607068E-01,-.571066E-01,
2-.841223E-01,-.806793E-01,-.382128E-01,-.124363E-01,-.402294E-01,
3-.213042E+00,-.394010E+00,-.639391E+00,-.640895E+00/
DATA(A02(12,II,4),II=1,14)/
1-.128031E+02,-.139837E+02,-.620035E+01,-.242084E+01,-.294623E+01,


```

2-.185822E+01,-.303894E+01,-.703472E+01,-.113556E+02,-.122965E+02,
3-.561519E+01,.226523E+01,.147145E+02,.196673E+02/
DATA(A00(12,II,5),II=1,14)/
1 .620930E-03,.411440E-03,.286990E-03,.327666E-03,.245753E-03,
2 .130370E-03,.985762E-04,.467896E-04,.350840E-05,-.589203E-04,
3-.949571E-05,-.308533E-06,-.771706E-04,-.189429E-03/
DATA(A01(12,II,5),II=1,14)/
1-.103271E+00,-.891673E-01,.507567E-01,-.475810E-01,-.176064E+00,
2-.236061E+00,-.201463E+00,-.149461E+00,-.683798E-01,.417597E-01,
3 .236719E+00,.394453E+00,.577178E+00,.582018E+00/
DATA(A02(12,II,5),II=1,14)/
1 .391271E+00,.314117E+01,-.199840E+00,.466624E+01,.109713E+02,
2 .134132E+02,.133893E+02,.130857E+02,.128450E+02,.906770E+01,
3 .129021E+01,-.523173E+01,-.134945E+02,-.187600E+02/
DATA(A00(12,II,6),II=1,14)/
1 .133092E-02,.871224E-03,.752975E-03,.694733E-03,.182254E-03,
2-.306704E-04,-.341432E-03,-.388174E-03,-.386205E-03,-.646481E-03,
3-.668318E-03,-.884484E-03,-.114451E-02,-.137820E-02/
DATA(A01(12,II,6),II=1,14)/
1 .240269E+00,-.225862E+00,-.992331E+00,-.890260E+00,-.647115E+00,
2-.481244E+00,-.507677E+00,-.599529E+00,-.713661E+00,-.608168E+00,
3-.452447E+00,-.387790E+00,-.537974E+00,.616607E+00/
DATA(A02(12,II,6),II=1,14)/
1-.236125E+02,-.158905E+02,.171409E+02,.240262E+02,.136612E+02,
2 .420394E+01,.466114E+01,.987809E+01,.159138E+02,.132259E+02,
3 .895165E+01,.874512E+01,.228626E+02,.556943E+01/
DATA(A00(13,II,1),II=1,14)/
1-.556167E-02,-.558730E-02,-.506182E-02,-.517401E-02,-.555374E-02,
2-.498555E-02,-.541678E-02,-.595457E-02,-.536045E-02,-.523119E-02,
3-.453403E-02,-.479028E-02,-.478759E-02,-.493106E-02/
DATA(A01(13,II,1),II=1,14)/
1-.209348E+01,-.119369E+01,-.656356E+00,-.996780E+00,-.110593E+01,
2-.112857E+01,-.102204E+01,-.125213E+01,-.134536E+01,-.207059E+01,
3-.265547E+01,-.367974E+01,-.472426E+01,-.488453E+01/
DATA(A02(13,II,1),II=1,14)/
1-.189428E+02,-.530562E+02,-.635491E+02,-.550068E+02,-.596272E+02,
2-.666108E+02,-.759542E+02,-.719523E+02,-.741554E+02,-.495480E+02,
3-.289505E+02,.981598E+01,.475784E+02,.452958E+02/
DATA(A00(13,II,2),II=1,14)/
1-.470240E-02,-.490840E-02,-.506537E-02,-.509429E-02,-.498050E-02,
2-.506239E-02,-.514718E-02,-.524900E-02,-.539612E-02,-.551534E-02,
3-.560008E-02,-.561714E-02,-.555707E-02,-.534671E-02/
DATA(A01(13,II,2),II=1,14)/
1-.319482E+01,-.356043E+01,-.369871E+01,-.325028E+01,-.312556E+01,
2-.317703E+01,-.319245E+01,-.314672E+01,-.306133E+01,-.295396E+01,
3-.275545E+01,-.255226E+01,-.245081E+01,-.237705E+01/
DATA(A02(13,II,2),II=1,14)/
1 .334761E+02,.487741E+02,.595163E+02,.518905E+02,.511080E+02,
2 .549020E+02,.553891E+02,.552577E+02,.548094E+02,.533790E+02,
3 .458075E+02,.367917E+02,.296021E+02,.273193E+02/

```

DATA(A00(13,II,3),II=1,14)/
1-.909369E-03,-.107336E-02,-.888340E-03,-.110282E-02,-.140303E-02,
2-.117159E-02,-.128651E-02,-.146444E-02,-.124693E-02,-.122248E-02,
3-.104240E-02,-.114858E-02,-.124039E-02,-.129279E-02/
DATA(A01(13,II,3),II=1,14)/
1 .755094E-02,-.977840E-01,-.255719E+00,-.129468E+00,-.176739E-01,
2 .717844E-02, .868276E-01, .133451E+00, .311984E+00, .452501E+00,
3 .759723E+00, .810520E+00, .725358E+00, .585622E+00/
DATA(A02(13,II,3),II=1,14)/
1 .228418E+02, .279640E+02, .342912E+02, .337795E+02, .317945E+02,
2 .322043E+02, .296843E+02, .282584E+02, .213610E+02, .149017E+02,
3 .461481E+00,-.337207E+01,-.373214E+01,-.182221E+01/
DATA(A00(13,II,4),II=1,14)/
1-.302649E-03,-.203511E-03,-.164783E-03,-.209312E-03,-.203410E-03,
2-.107418E-03,-.159455E-03,-.150761E-03,-.150110E-03,-.148197E-03,
3-.157760E-03,-.159021E-03,-.163953E-03,-.153993E-03/
DATA(A01(13,II,4),II=1,14)/
1-.339651E-01, .143407E+00, .181501E+00, .150581E+00, .100392E+00,
2 .280614E-03,-.280643E+00,-.310849E+00,-.223822E+00,-.161531E+00,
3-.236761E+00,-.445158E+00,-.765696E+00,-.496820E+00/
DATA(A02(13,II,4),II=1,14)/
1-.339765E+01,-.101285E+02,-.105906E+02,-.103791E+02,-.888902E+01,
2-.566850E+01, .526462E+01, .407422E+01,-.214511E+01,-.761929E+01,
3-.587346E+01, .295102E+01, .202572E+02, .118808E+02/
DATA(A00(13,II,5),II=1,14)/
1 .604069E-03, .409131E-03, .275675E-03, .318022E-03, .246204E-03,
2 .129784E-03, .100567E-03, .741713E-04, .504842E-04,-.248795E-05,
3 .778790E-05,-.115603E-04,-.764409E-04,-.172608E-03/
DATA(A01(13,II,5),II=1,14)/
1 .327078E+00, .476474E+00, .673037E+00, .586027E+00, .519230E+00,
2 .500370E+00, .761085E+00, .623702E+00, .374345E+00, .196520E+00,
3 .359965E+00, .738896E+00, .116777E+01, .655482E+00/
DATA(A02(13,II,5),II=1,14)/
1-.712065E+01,-.108158E+02,-.142682E+02,-.957353E+01,-.775772E+01,
2-.811727E+01,-.199845E+02,-.106028E+02, .419502E+01, .167371E+02,
3 .108380E+02,-.651091E+01,-.327939E+02,-.175792E+02/
DATA(A00(13,II,6),II=1,14)/
1 .139674E-02, .882691E-03, .738730E-03, .704424E-03, .174747E-03,
2-.434822E-04,-.335403E-03,-.404368E-03,-.427800E-03,-.726897E-03,
3-.717724E-03,-.886331E-03,-.114472E-02,-.139946E-02/
DATA(A01(13,II,6),II=1,14)/
1-.317703E-01,-.675021E+00,-.957036E+00,-.563063E+00,-.311597E+00,
2-.120331E+00,-.457706E+00, .218899E-01, .771501E+00, .133882E+01,
3 .131145E+01, .878213E+00, .323723E+00, .144177E+01/
DATA(A02(13,II,6),II=1,14)/
1 .268579E+02, .462289E+02, .448698E+02, .281121E+02, .230607E+02,
2 .203832E+02, .412729E+02, .229670E+02,-.710015E+01,-.318401E+02,
3-.285198E+02,-.520259E+01, .352496E+02,-.636434E+01/
DATA(A00(14,II,1),II=1,14)/
1-.552295E-02,-.555216E-02,-.503248E-02,-.518003E-02,-.556488E-02,

```

2-.499032E-02,-.542439E-02,-.593520E-02,-.534031E-02,-.518003E-02,
3-.450223E-02,-.475251E-02,-.475624E-02,-.489725E-02/
DATA(AU1(14,II,1),II=1,14)/
1-.701205E+00,-.807521E-01,.411864E+00,.135437E+00,-.743529E-01,
2-.256313E-02,-.490551E-01,-.194425E+00,-.696736E+00,-.109281E+01,
3-.154415E+01,-.172808E+01,-.254500E+01,-.329555E+01/
DATA(AO2(14,II,1),II=1,14)/
1-.386354E+02,-.557759E+02,-.622908E+02,-.569765E+02,-.570485E+02,
2-.654618E+02,-.646022E+02,-.602241E+02,-.442070E+02,-.342475E+02,
3-.218076E+02,-.210061E+02,.391861E+00,.132377E+02/
DATA(AO0(14,II,2),II=1,14)/
1-.477204E-02,-.496576E-02,-.511577E-02,-.512415E-02,-.500174E-02,
2-.507789E-02,-.515372E-02,-.525497E-02,-.540015E-02,-.553040E-02,
3-.562564E-02,-.563766E-02,-.556377E-02,-.536196E-02/
DATA(AU1(14,II,2),II=1,14)/
1-.126211E+01,-.154651E+01,-.165280E+01,-.137709E+01,-.132262E+01,
2-.137411E+01,-.142021E+01,-.141450E+01,-.136769E+01,-.136554E+01,
3-.134454E+01,-.134829E+01,-.129981E+01,-.111603E+01/
DATA(AO2(14,II,2),II=1,14)/
1.329712E+00,.734381E+01,.988849E+01,.490444E+01,.513553E+01,
2.753655E+01,.888049E+01,.820849E+01,.788267E+01,.776745E+01,
3.769896E+01,.743200E+01,.402208E+01,-.243977E+01/
DATA(AO0(14,II,3),II=1,14)/
1-.913194E-03,-.107426E-02,-.877873E-03,-.109545E-02,-.138910E-02,
2-.115140E-02,-.126765E-02,-.144945E-02,-.123844E-02,-.120839E-02,
3-.103510E-02,-.114572E-02,-.124246E-02,-.128581E-02/
DATA(AO1(14,II,3),II=1,14)/
1.391225E+00,.369927E+00,.258963E+00,.360398E+00,.400118E+00,
2.438505E+00,.502504E+00,.568377E+00,.498507E+00,.578699E+00,
3.670189E+00,.836458E+00,.822718E+00,.809458E+00/
DATA(AO2(14,II,3),II=1,14)/
1.967683E+01,.925682E+01,.974925E+01,.801577E+01,.952863E+01,
2.108842E+02,.106732E+02,.917696E+01,.120648E+02,.843292E+01,
3.446314E+01,-.239147E+01,-.338542E+01,-.487449E+01/
DATA(AO0(14,II,4),II=1,14)/
1-.304029E-03,-.202588E-03,-.163321E-03,-.203526E-03,-.191982E-03,
2-.154830E-03,-.142490E-03,-.133410E-03,-.134170E-03,-.133374E-03,
3-.166865E-03,-.178754E-03,-.162873E-03,-.148940E-03/
DATA(AO1(14,II,4),II=1,14)/
1.116775E-01,.193491E+00,.270619E+00,.174574E+00,.163645E+00,
2.157628E+00,.754584E-01,-.587778E-01,-.214463E+00,-.348081E+00,
3-.352535E+00,-.252799E+00,-.327071E+00,-.493550E+00/
DATA(AO2(14,II,4),II=1,14)/
1-.492052E+01,-.115984E+02,-.130417E+02,-.956425E+01,-.102347E+02,
2-.114267E+02,-.977122E+01,-.512240E+01,.122233E+01,.653463E+01,
3.591698E+01,.154308E+00,.409968E+00,.891588E+01/
DATA(AO0(14,II,5),II=1,14)/
1.610064E-03,.411576E-03,.272794E-03,.313852E-03,.233236E-03,
2.112444E-03,.733157E-04,.440497E-04,.235482E-04,-.184599E-04,
3.336482E-04,.269698E-04,-.838842E-04,-.184526E-03/

```

```

DATA(A01(14,II,5),II=1,14)/
1 .171979E+00, .289827E+00, .446768E+00, .427808E+00, .309547E+00,
2 .150743E+00, .145019E+00, .241129E+00, .400502E+00, .492662E+00,
3 .422830E+00, .269142E+00, .421016E+00, .573608E+00/
DATA(A02(14,II,5),II=1,14)/
1-.529113E+01,-.646067E+01,-.918828E+01,-.858313E+01,-.375606E+01,
2 .291060E+01, .420144E+01, .397205E+00,-.643848E+01,-.948005E+01,
3-.486845E+01, .377935E+01,-.839789E+00,-.117231E+02/
DATA(A00(14,II,6),II=1,14)/
1 .138886E-02, .872952E-03, .731490E-03, .716211E-03, .206763E-03,
2-.751076E-05,-.281148E-03,-.352747E-03,-.383057E-03,-.694633E-03,
3-.750593E-05,-.948478E-03,-.112840E-02,-.138231E-02/
DATA(A01(14,II,6),II=1,14)/
1 .922676E-01,-.336476E+00,-.517496E+00,-.318994E+00, .114001E+00,
2 .579030E+00, .882657E+00, .103516E+01, .101762E+01, .108995E+01,
3 .132630E+01, .179006E+01, .164527E+01, .116973E+01/
DATA(A02(14,II,6),II=1,14)/
1 .280028E+02, .371740E+02, .344778E+02, .270008E+02, .134560E+02,
2-.175785E+01,-.108831E+02,-.114192E+02,-.405202E+01,-.201861E+01,
3-.115209E+02,-.319298E+02,-.282280E+02,-.659312E+01/
DATA(A00(15,II,1),II=1,14)/
1-.554891E-02,-.556998E-02,-.505473E-02,-.516105E-02,-.556111E-02,
2-.500437E-02,-.543184E-02,-.594308E-02,-.534610E-02,-.523747E-02,
3-.456016E-02,-.480211E-02,-.475407E-02,-.491290E-02/
DATA(AU1(15,II,1),II=1,14)/
1-.188831E+01,-.111384E+01, .565427E-02,-.277287E+00,-.436484E+00,
2-.247447E+00,-.275084E+00,-.663460E+00,-.117988E+01,-.158476E+01,
3-.185387E+01,-.220697E+01,-.326246E+01,-.387820E+01/
DATA(A02(15,II,1),II=1,14)/
1-.126211E+02,-.310176E+02,-.667175E+02,-.609514E+02,-.647981E+02,
2-.808450E+02,-.824494E+02,-.677838E+02,-.521857E+02,-.432749E+02,
3-.394888E+02,-.299899E+02, .210646E+01, .167458E+02/
DATA(A00(15,II,2),II=1,14)/
1-.476538E-02,-.496606E-02,-.513104E-02,-.513226E-02,-.500510E-02,
2-.508755E-02,-.516974E-02,-.527350E-02,-.541288E-02,-.552790E-02,
3-.562773E-02,-.565134E-02,-.558002E-02,-.536787E-02/
DATA(A01(15,II,2),II=1,14)/
1-.126384E+01,-.150394E+01,-.128599E+01,-.886543E+00,-.866617E+00,
2-.955544E+00,-.100433E+01,-.959801E+00,-.896000E+00,-.869956E+00,
3-.827014E+00,-.821106E+00,-.841484E+00,-.799599E+00/
DATA(A02(15,II,2),II=1,14)/
1 .164659E+00, .586933E+01,-.360427E+01,-.139888E+02,-.115467E+02,
2-.675719E+01,-.5323685+01,-.838481E+01,-.103927E+02,-.976216E+01,
3-.986501E+01,-.978377E+01,-.109282E+02,-.135472E+02/
DATA(A00(15,II,3),II=1,14)/
1-.916497E-03,-.107601E-02,-.877790E-03,-.108852E-02,-.138602E-02,
2-.114966E-02,-.127349E-02,-.145965E-02,-.125046E-02,-.122385E-02,
3-.104923E-02,-.115975E-02,-.124436E-02,-.128605E-02/
DATA(A01(15,II,3),II=1,14)/
1 .509000E+00, .496508E+00, .156623E+00, .166652E+00, .224354E+00,

```

ORIGINAL PAGE IS
OF POOR QUALITY

```

2 .243434E+00, .288657E+00, .389934E+00, .457688E+00, .531930E+00,
3 .584222E+00, .613411E+00, .791914E+00, .805644E+00/
DATA(A02(15,II,3),II=1,14)/
1 .398218E+01, .356992E+01, .138735E+02, .160634E+02, .174867E+02,
2 .202666E+02, .219166E+02, .190883E+02, .163575E+02, .128017E+02,
3 .113199E+02, .110411E+02, .262233E+01, -.157342E+01/
DATA(A00(15,II,4),II=1,14)/
1-.298001E-03, -.197229E-03, -.160425E-03, -.205375E-03, -.191071E-03,
2-.151101E-03, -.141221E-03, -.137886E-03, -.143797E-03, -.141520E-03,
3-.162642E-03, -.167493E-03, -.159328E-03, -.145212E-03/
DATA(AU1(15,II,4),II=1,14)/
1-.794564E-01, .102851E+00, .203365E+00, .172222E+00, .187397E+00,
2 .207344E+00, .199984E+00, .171880E+00, .132317E+00, .649331E-01,
3 .978216E-02, -.163116E-01, -.704479E-01, -.210654E+00/
DATA(A02(15,II,4),II=1,14)/
1 .102479E+01, -.422593E+01, -.460412E+01, -.160552E+01, -.224564E+01,
2-.389367E+01, -.551981E+01, -.561963E+01, -.435467E+01, -.160536E+01,
3 .502324E+00, .117802E+01, .191192E+01, .861206E+01/
DATA(A00(15,II,5),II=1,14)/
1 .606083E-03, .403634E-03, .274288E-03, .317535E-03, .235963E-03,
2 .114953E-03, .729757E-04, .461656E-04, .307629E-04, -.830466E-05,
3 .235642E-04, .569974E-05, -.888595E-04, -.188191E-03/
DATA(AU1(15,II,5),II=1,14)/
1 .823008E+00, .977717E+00, .109789E+01, .104928E+01, .910152E+00,
2 .740170E+00, .707652E+00, .777264E+00, .876931E+00, .947201E+00,
3 .987392E+00, .969410E+00, .105277E+01, .113389E+01/
DATA(A02(15,II,5),II=1,14)/
1-.147880E+01, -.569405E+01, -.853974E+01, -.780400E+01, -.226852E+01,
2 .519976E+01, .885055E+01, .684229E+01, .269416E+01, -.424849E+00,
3-.296240E+01, -.227981E+01, -.510758E+01, -.112599E+02/
DATA(A00(15,II,6),II=1,14)/
1 .140808E-02, .890896E-03, .739243E-03, .709765E-03, .202218E-03,
2-.745968E-05, -.275011E-03, -.344082E-03, -.381609E-03, -.693357E-03,
3-.717375E-03, -.886805E-03, -.110203E-02, -.137130E-02/
DATA(A01(15,II,6),II=1,14)/
1-.147906E+01, -.192493E+01, -.202437E+01, -.177890E+01, -.125723E+01,
2-.664671E+00, -.313904E+00, -.152372E+00, -.819969E-01, .340806E-01,
3 .409822E-01, .123949E+00, -.741517E-01, -.354947E+00/
DATA(A02(15,II,6),II=1,14)/
1 .696706E+01, .209558E+02, .195248E+02, .113548E+02, -.741781E+01,
2-.311743E+02, -.468694E+02, -.506958E+02, -.478968E+02, -.453614E+02,
3-.392249E+02, -.375513E+02, -.237946E+02, -.110894E+02/
DATA(AP0( 1,II,1),II=1,14)/
1 .521961E-02, .623843E-02, .555754E-02, .618534E-02, .631471E-02,
2 .726327E-02, .728902E-02, .723077E-02, .528050E-02, .368943E-02,
3 .343486E-02, .461459E-02, .462561E-02, .396666E-02/
DATA(AP1( 1,II,1),II=1,14)/
1-.467439E+01, -.473459E+01, -.459471E+01, -.486897E+01, -.490663E+01,
2-.501494E+01, -.489268E+01, -.507467E+01, -.507648E+01, -.509519E+01,
3-.494886E+01, -.479528E+01, -.454733E+01, -.467535E+01/

```

DATA(AP2(1,II,1),II=1,14)/
1 .432277E+02, .370045E+02, .239799E+02, .271566E+02, .263658E+02,
2 .258730E+02, .197319E+02, .240039E+02, .246309E+02, .245731E+02,
3 .183577E+02, .924694E+01, -.206459E+00, -.110125E+01/
DATA(AP0(1,II,2),II=1,14)/
1 .210982E-01, .215362E-01, .218869E-01, .220545E-01, .207241E-01,
2 .220491E-01, .205574E-01, .217317E-01, .205495E-01, .221523E-01,
3 .211636E-01, .225461E-01, .224834E-01, .220169E-01/
DATA(AP1(1,II,2),II=1,14)/
1-.659250E+01, -.663246E+01, -.674390E+01, -.680581E+01, -.669154E+01,
2-.676752E+01, -.657709E+01, -.663163E+01, -.646967E+01, -.670357E+01,
3-.668854E+01, -.691579E+01, -.697782E+01, -.690635E+01/
DATA(AP2(1,II,2),II=1,14)/
1 .124480E+03, .123675E+03, .126275E+03, .126694E+03, .123357E+03,
2 .123565E+03, .117345E+03, .117184E+03, .111895E+03, .117586E+03,
3 .117105E+03, .121957E+03, .118569E+03, .115324E+03/
DATA(AP0(1,II,3),II=1,14)/
1 .219162E-02, .256527E-02, .240221E-02, .202049E-02, .217558E-02,
2 .251373E-02, .285792E-02, .285098E-02, .222542E-02, .142287E-02,
3 .139242E-02, .168211E-02, .184285E-02, .198452E-02/
DATA(AP1(1,II,3),II=1,14)/
1 .129413E+01, .119522E+01, .122629E+01, .132496E+01, .129635E+01,
2 .117812E+01, .110841E+01, .106773E+01, .113948E+01, .122865E+01,
3 .123619E+01, .117622E+01, .112583E+01, .113454E+01/
DATA(AP2(1,II,3),II=1,14)/
1 .104015E+02, .144305E+02, .136238E+02, .939954E+01, .101709E+02,
2 .137965E+02, .169303E+02, .188825E+02, .181512E+02, .163231E+02,
3 .161200E+02, .181002E+02, .195071E+02, .195920E+02/
DATA(AP0(1,II,4),II=1,14)/
1 .103864E-04, .111619E-03, .147933E-03, .165423E-03, .137272E-03,
2 .138945E-03, .965821E-04, .895275E-04, .648529E-04, .105223E-03,
3 .109277E-03, .163031E-03, .107486E-03, .564632E-04/
DATA(AP1(1,II,4),II=1,14)/
1 .755100E-02, -.292705E-02, .274363E-01, .466499E-01, .443743E-01,
2 .405005E-01, .357287E-01, .316500E-01, .363095E-01, .381987E-01,
3 .527554E-01, .779659E-01, .133127E+00, .489809E-01/
DATA(AP2(1,II,4),II=1,14)/
1-.308155E+01, -.250892E+01, -.279133E+01, -.292048E+01, -.271003E+01,
2-.219212E+01, -.143734E+01, -.764722E+00, -.517193E+00, -.299246E+00,
3-.646272E+00, -.185483E+01, -.468440E+01, -.217321E+01/
DATA(AP0(1,II,5),II=1,14)/
1-.483573E-03, -.740034E-03, -.720389E-03, -.803316E-03, -.797003E-03,
2-.790064E-03, -.721635E-03, -.714438E-03, -.665746E-03, -.704388E-03,
3-.694466E-03, -.759711E-03, -.566056E-03, -.667181E-03/
DATA(AP1(1,II,5),II=1,14)/
1 .796475E-01, .638518E-01, .387567E-01, .442008E-01, .722428E-01,
2 .855872E-01, .945199E-01, .850941E-01, .547798E-01, .574126E-01,
3 .484725E-01, .641290E-01, .313529E-01, .720916E-01/
DATA(AP2(1,II,5),II=1,14)/
1-.266158E+01, -.238616E+01, -.245755E+01, -.276350E+01, -.350428E+01,

```

2-.399727E+01,-.492108E+01,-.499042E+01,-.400321E+01,-.343613E+01,
3-.258061E+01,-.282466E+01,-.122003E+01,-.142145E+01/
DATA(AP0( 1,II,6),II=1,14)/
1-.105141E-02,-.179339E-02,-.120518E-02,-.125136E-02,-.127023E-02,
2-.127380E-02,-.943807E-03,-.916059E-03,-.883696E-03,-.104024E-02,
3-.910208E-03,-.965309E-03,-.648347E-03,-.100972E-02/
DATA(AP1( 1,II,6),II=1,14)/
1 .392742E+00, .451854E+00, .272978E+00, .330346E+00, .389993E+00,
2 .421740E+00, .378816E+00, .362439E+00, .363176E+00, .417511E+00,
3 .417735E+00, .413136E+00, .356474E+00, .820258E+00/
DATA(AP2( 1,II,6),II=1,14)/
1-.628698E+01,-.383854E+01, .627987E+01, .402689E+01, .116133E+01,
2-.107312E+01, .934828E+00, .346874E+01, .579405E+01, .481974E+01,
3 .448276E+01, .526041E+01, .794807E+01,-.569320E+01/
DATA(AP0( 2,II,1),II=1,14)/
1 .523452E-02, .621058E-02, .558641E-02, .625497E-02, .638032E-02,
2 .739462E-02, .741874E-02, .739223E-02, .539040E-02, .381055E-02,
3 .354589E-02, .474111E-02, .470148E-02, .400520E-02/
DATA(AP1( 2,II,1),II=1,14)/
1-.196364E+01,-.196499E+01,-.185616E+01,-.193625E+01,-.174963E+01,
2-.183116E+01,-.174502E+01,-.209581E+01,-.228311E+01,-.272358E+01,
3-.313602E+01,-.353503E+01,-.391721E+01,-.382492E+01/
DATA(AP2( 2,II,1),II=1,14)/
1 .180149E+02, .171936E+02, .145108E+02, .184891E+02, .102077E+02,
2 .680872E+01,-.265252E+01, .482646E+01, .138266E+02, .334330E+02,
3 .504834E+02, .610070E+02, .710928E+02, .750820E+02/
DATA(AP0( 2,II,2),II=1,14)/
1 .214215E-01, .219196E-01, .221427E-01, .222897E-01, .209415E-01,
2 .223294E-01, .207537E-01, .219329E-01, .207043E-01, .223464E-01,
3 .213283E-01, .227629E-01, .227430E-01, .222230E-01/
DATA(AP1( 2,II,2),II=1,14)/
1-.339210E+01,-.353869E+01,-.363566E+01,-.352198E+01,-.348383E+01,
2-.386219E+01,-.386405E+01,-.397085E+01,-.365126E+01,-.358345E+01,
3-.319856E+01,-.313755E+01,-.304252E+01,-.302901E+01/
DATA(AP2( 2,II,2),II=1,14)/
1 .570051E+02, .650236E+02, .735529E+02, .686533E+02, .685907E+02,
2 .839522E+02, .902840E+02, .977034E+02, .917892E+02, .891466E+02,
3 .761996E+02, .708378E+02, .655267E+02, .667827E+02/
DATA(AP0( 2,II,3),II=1,14)/
1 .217225E-02, .253298E-02, .245595E-02, .206102E-02, .219229E-02,
2 .253623E-02, .288128E-02, .287200E-02, .223870E-02, .142838E-02,
3 .140181E-02, .170766E-02, .189750E-02, .202174E-02/
DATA(AP1( 2,II,3),II=1,14)/
1-.847525E-02,-.119610E+00,-.260950E+00,-.157986E+00,-.120299E+00,
2-.217054E+00,-.244328E+00,-.275015E+00,-.170192E+00,-.572733E-01,
3 .903608E-01, .180112E+00, .203660E+00, .514300E-01/
DATA(AP2( 2,II,3),II=1,14)/
1 .100064E+02, .140529E+02, .200757E+02, .141577E+02, .115101E+02,
2 .145725E+02, .159362E+02, .173634E+02, .152076E+02, .121126E+02,
3 .590579E+01, .391413E+00,-.514207E+01,-.154952E+01/

```

DATA(AP0(2,II,4),II=1,14)/
 1 .378773E-04, .127462E-03, .159020E-03, .189360E-03, .155737E-03,
 2 .157218E-03, .103221E-03, .888179E-04, .565379E-04, .913232E-04,
 3 .965609E-04, .148929E-03, .101816E-03, .554022E-04/
 DATA(AP1(2,II,4),II=1,14)/
 1 .244610E+00, .161082E-01, -.136944E+00, -.239718E+00, -.311217E+00,
 2 -.419307E+00, -.605892E+00, -.666686E+00, -.623199E+00, -.506513E+00,
 3 -.385339E+00, -.310007E+00, -.150307E+00, .251208E-02/
 DATA(AP2(2,II,4),II=1,14)/
 1 -.227420E+02, -.143705E+02, -.808958E+01, -.737318E+00, .413625E+01,
 2 .939149E+01, .187875E+02, .224529E+02, .218633E+02, .174211E+02,
 3 .125724E+02, .965685E+01, .501478E+01, -.366691E+00/
 DATA(AP0(2,II,5),II=1,14)/
 1 -.520698E-03, -.772509E-03, -.737824E-03, -.843818E-03, -.834858E-03,
 2 -.837739E-03, -.746002E-03, -.730550E-03, -.667901E-03, -.704478E-03,
 3 -.692693E-03, -.756603E-03, -.567870E-03, -.668067E-03/
 DATA(AP1(2,II,5),II=1,14)/
 1 -.216825E+00, .176226E+00, .393372E+00, .559153E+00, .683744E+00,
 2 .849635E+00, .111803E+01, .118243E+01, .108149E+01, .882969E+00,
 3 .683965E+00, .550969E+00, .300788E+00, .184454E+00/
 DATA(AP2(2,II,5),II=1,14)/
 1 .314568E+02, .172017E+02, .759091E+01, -.378814E+01, -.117014E+02,
 2 -.199539E+02, -.339357E+02, -.381675E+02, -.356389E+02, -.278028E+02,
 3 -.202339E+02, -.158291E+02, -.931659E+01, -.370408E+01/
 DATA(AP0(2,II,6),II=1,14)/
 1 -.101992E-02, -.179926E-02, -.118238E-02, -.118514E-02, -.119869E-02,
 2 -.118445E-02, -.908001E-03, -.912004E-03, -.909739E-03, -.107991E-02,
 3 -.922632E-03, -.973321E-03, -.682703E-03, -.103566E-02/
 DATA(AP1(2,II,6),II=1,14)/
 1 .523758E+00, -.893551E-01, -.658051E+00, -.932504E+00, -.116984E+01,
 2 -.154686E+01, -.211919E+01, -.211861E+01, -.169608E+01, -.103153E+01,
 3 -.439120E+00, .647896E-01, .767205E+00, .993434E+00/
 DATA(AP2(2,II,6),II=1,14)/
 1 -.658527E+02, -.410320E+02, -.170903E+02, .617181E+01, .257800E+02,
 2 .496453E+02, .840583E+02, .912201E+02, .787824E+02, .552574E+02,
 3 .335556E+02, .163379E+02, -.553132E+01, -.137311E+02/
 DATA(AP0(3,II,1),II=1,14)/
 1 .525659E-02, .621119E-02, .559287E-02, .622728E-02, .636057E-02,
 2 .737865E-02, .737660E-02, .734815E-02, .536450E-02, .381112E-02,
 3 .351904E-02, .468781E-02, .472135E-02, .403153E-02/
 DATA(AP1(3,II,1),II=1,14)/
 1 -.218496E+01, -.229282E+01, -.211789E+01, -.205968E+01, -.195356E+01,
 2 -.208288E+01, -.213641E+01, -.226038E+01, -.206488E+01, -.169660E+01,
 3 -.162360E+01, -.177804E+01, -.223628E+01, -.284848E+01/
 DATA(AP2(3,II,1),II=1,14)/
 1 .409390E+02, .460385E+02, .423368E+02, .385165E+02, .354465E+02,
 2 .372579E+02, .415098E+02, .439324E+02, .385349E+02, .222193E+02,
 3 .178328E+02, .179486E+02, .265390E+02, .503817E+02/
 DATA(AP0(3,II,2),II=1,14)/
 1 .214172E-01, .219218E-01, .221435E-01, .223016E-01, .209497E-01,

ORIGINAL PAGE IS -
 OF POOR QUALITY


```

2 .223238E-01, .207501E-01, .219402E-01, .207212E-01, .223839E-01,
3 .213715E-01, .228135E-01, .227615E-01, .222248E-01/
DATA(AP1( 3,II,2),II=1,14)/
1-.339367E+01,-.343778E+01,-.344910E+01,-.346064E+01,-.335872E+01,
2-.358672E+01,-.343295E+01,-.353981E+01,-.334434E+01,-.354653E+01,
3-.352821E+01,-.377672E+01,-.379019E+01,-.358384E+01/
DATA(AP2( 3,II,2),II=1,14)/
1 .788697E+02, .790447E+02, .786978E+02, .794149E+02, .767630E+02,
2 .827426E+02, .781367E+02, .812693E+02, .761977E+02, .828206E+02,
3 .849173E+02, .942612E+02, .960678E+02, .890360E+02/
DATA(AP0( 3,II,3),II=1,14)/
1 .215586E-02, .252142E-02, .245724E-02, .205834E-02, .219346E-02,
2 .252944E-02, .286817E-02, .286330E-02, .224609E-02, .146034E-02,
3 .141743E-02, .170777E-02, .188096E-02, .201146E-02/
DATA(AP1( 3,II,3),II=1,14)/
1 .154716E+00, .114318E+00, .814718E-01, .127017E+00, .116673E+00,
2 .657713E-01, .426444E-01, .390436E-01, .779612E-01, .173767E+00,
3 .807833E-01,-.259881E-01,-.320623E-01,-.281318E-01/
DATA(AP2( 3,II,3),II=1,14)/
1 .940126E+00, .122340E+01, .532704E+00,-.228891E+01,-.196558E+01,
2-.110952E+01, .258476E+00,-.597937E-03,-.524207E+00,-.377799E+01,
3 .659161E+00, .484064E+01, .476406E+01, .378479E+01/
DATA(AP0( 3,II,4),II=1,14)/
1 .715891E-05, .107391E-03, .143825E-03, .167590E-03, .134961E-03,
2 .128316E-03, .862507E-04, .821085E-04, .632459E-04, .107279E-03,
3 .111588E-03, .169091E-03, .119145E-03, .677095E-04/
DATA(AP1( 3,II,4),II=1,14)/
1 .831046E-04, .715232E-01, .144581E+00, .141298E+00, .143531E+00,
2 .158767E+00, .191081E+00, .213977E+00, .209845E+00, .170998E+00,
3 .120682E+00, .350395E-01,-.685714E-01,-.197590E+00/
DATA(AP2( 3,II,4),II=1,14)/
1 .166369E+01,-.286604E+01,-.756282E+01,-.768832E+01,-.777693E+01,
2-.881394E+01,-.111002E+02,-.130971E+02,-.136007E+02,-.124028E+02,
3-.102992E+02,-.617021E+01, .148918E+00, .625778E+01/
DATA(AP0( 3,II,5),II=1,14)/
1-.480176E-03,-.745411E-03,-.718396E-03,-.813134E-03,-.801618E-03,
2-.790257E-03,-.716445E-03,-.717695E-03,-.677106E-03,-.729390E-03,
3-.716610E-03,-.787858E-03,-.594340E-03,-.681621E-03/
DATA(AP1( 3,II,5),II=1,14)/
1 .929937E-01, .148106E-01,-.102843E+00,-.928511E-01,-.858660E-01,
2-.105424E+00,-.156527E+00,-.193398E+00,-.196821E+00,-.137970E+00,
3-.532084E-01, .936069E-01, .299128E+00, .534584E+00/
DATA(AP2( 3,II,5),II=1,14)/
1-.472216E+01, .148774E+01, .889492E+01, .897394E+01, .867203E+01,
2 .987087E+01, .132142E+02, .163012E+02, .174195E+02, .156595E+02,
3 .118697E+02, .481733E+01,-.666429E+01,-.161297E+02/
DATA(AP0( 3,II,6),II=1,14)/
1-.115130E-02,-.188498E-02,-.125078E-02,-.127005E-02,-.127419E-02,
2-.128665E-02,-.956254E-03,-.918497E-03,-.873164E-03,-.102139E-02,
3-.878462E-03,-.920552E-03,-.650141E-03,-.101807E-02/

```

DATA(AP1(3,II,6),II=1,14)/
 1-.120168E+00, .217652E+00, .428449E+00, .423345E+00, .480899E+00,
 2 .577506E+00, .676727E+00, .766921E+00, .733080E+00, .658315E+00,
 3 .461459E+00, .227789E+00,-.650520E-01,-.356227E+00/
 DATA(AP2(3,II,6),II=1,14)/
 1 .773594E+01,-.985504E+01,-.248358E+02,-.242318E+02,-.251092E+02,
 2-.292167E+02,-.354351E+02,-.414105E+02,-.408968E+02,-.364317E+02,
 3-.262029E+02,-.117492E+02, .897830E+01, .226220E+02/
 DATA(AP0(4,II,1),II=1,14)/
 1 .524990E-02, .623952E-02, .557491E-02, .622482E-02, .635623E-02,
 2 .736673E-02, .736547E-02, .734678E-02, .534993E-02, .376744E-02,
 3 .349071E-02, .463778E-02, .460531E-02, .399280E-02/
 DATA(AP1(4,II,1),II=1,14)/
 1-.560184E+01,-.569324E+01,-.504361E+01,-.413499E+01,-.395066E+01,
 2-.398119E+01,-.376800E+01,-.405998E+01,-.459925E+01,-.530123E+01,
 3-.582917E+01,-.604693E+01,-.536209E+01,-.472521E+01/
 DATA(AP2(4,II,1),II=1,14)/
 1 .828085E+01, .288734E+02, .244312E+02,-.600667E+01,-.868937E+01,
 2-.642100E+01,-.149589E+02,-.897878E+01, .122773E+02, .423479E+02,
 3 .706529E+02, .872689E+02, .779067E+02, .523508E+02/
 DATA(AP0(4,II,2),II=1,14)/
 1 .215332E-01, .220310E-01, .222548E-01, .224088E-01, .210290E-01,
 2 .224206E-01, .208117E-01, .220125E-01, .207800E-01, .224668E-01,
 3 .214415E-01, .229044E-01, .228519E-01, .223059E-01/
 DATA(AP1(4,II,2),II=1,14)/
 1-.125008E+01,-.155332E+01,-.187615E+01,-.192428E+01,-.169099E+01,
 2-.179305E+01,-.164344E+01,-.172171E+01,-.144558E+01,-.148454E+01,
 3-.147058E+01,-.199588E+01,-.278464E+01,-.274289E+01/
 DATA(AP2(4,II,2),II=1,14)/
 1-.278151E+02,-.158938E+02,-.174719E+01, .386300E+01,-.234757E+01,
 2-.100504E+01,-.417814E+01, .132349E-01,-.747984E+01,-.115078E+02,
 3-.179033E+02,-.713302E+01, .161699E+02, .196608E+02/
 DATA(AP0(4,II,3),II=1,14)/
 1 .217890E-02, .254925E-02, .245143E-02, .204643E-02, .217646E-02,
 2 .251061E-02, .286143E-02, .285911E-02, .223232E-02, .142939E-02,
 3 .139777E-02, .169027E-02, .188146E-02, .202353E-02/
 DATA(AP1(4,II,3),II=1,14)/
 1-.141365E+00,-.127056E+00, .472163E-01, .293238E+00, .472278E+00,
 2 .628855E+00, .851671E+00, .952692E+00, .111362E+01, .125719E+01,
 3 .144230E+01, .155553E+01, .194128E+01, .237785E+01/
 DATA(AP2(4,II,3),II=1,14)/
 1 .311738E+02, .374057E+02, .377117E+02, .343483E+02, .316453E+02,
 2 .271863E+02, .192616E+02, .148745E+02, .948268E+01, .503367E+01,
 3-.964505E+00,-.337861E+01,-.141412E+02,-.308954E+02/
 DATA(AP0(4,II,4),II=1,14)/
 1 .199853E-04, .114128E-03, .159677E-03, .189052E-03, .153285E-03,
 2 .157298E-03, .106379E-03, .939000E-04, .530296E-04, .832204E-04,
 3 .964225E-04, .157883E-03, .114030E-03, .579226E-04/
 DATA(AP1(4,II,4),II=1,14)/
 1 .516817E-02,-.209435E+00,-.269506E+00,-.261916E+00,-.241066E+00,

ORIGINAL PAGE IS
 OF POOR QUALITY

```

2-.373001E+00,-.586426E+00,-.783614E+00,-.668839E+00,-.362412E+00,
3-.123805E+00,-.206770E-01,-.117035E+00,-.178426E+00/
DATA(AP2( 4,II,4),II=1,14)/
1-.236905E+02,-.149519E+02,-.997188E+01,-.649542E+01,-.670389E+01,
2 .656739E-01, .106010E+02, .224234E+02, .203655E+02, .962524E+01,
3 .300636E-01,-.571896E+01,-.357809E+01, .174430E+01/
DATA(AP0( 4,II,5),II=1,14)/
1-.495231E-03,-.752461E-03,-.741545E-03,-.843009E-03,-.820774E-03,
2-.822716E-03,-.741142E-03,-.730661E-03,-.661086E-03,-.697448E-03,
3-.700505E-03,-.781122E-03,-.596267E-03,-.677655E-03/
DATA(AP1( 4,II,5),II=1,14)/
1-.520941E+00,-.314030E+00,-.363158E+00,-.269741E+00,-.176409E+00,
2 .147527E+00, .429025E+00, .608934E+00, .340706E+00,-.355974E-02,
3-.201185E+00,-.150198E+00, .355037E+00, .502288E+00/
DATA(AP2( 4,II,5),II=1,14)/
1 .240514E+02, .151260E+02, .112175E+02, .403055E+01, .239417E+01,
2-.107454E+02,-.236209E+02,-.347512E+02,-.255037E+02,-.110629E+02,
3-.907345E+00, .170215E+01,-.119230E+02,-.215229E+02/
DATA(AP0( 4,II,6),II=1,14)/
1-.104458E-02,-.178752E-02,-.115119E-02,-.118447E-02,-.120229E-02,
2-.117999E-02,-.933520E-03,-.970738E-03,-.987301E-03,-.118191E-02,
3-.972912E-03,-.995860E-03,-.656729E-03,-.107017E-02/
DATA(AP1( 4,II,6),II=1,14)/
1 .186248E+01, .111601E+01, .290123E+00,-.234397E+00,-.644844E+00,
2-.124352E+01,-.157373E+01,-.128729E+01,-.362265E+00, .795963E+00,
3 .175768E+01, .245700E+01, .305026E+01, .331253E+01/
DATA(AP2( 4,II,6),II=1,14)/
1-.720376E+02,-.421675E+02, .461892E-01, .288833E+02, .462601E+02,
2 .813172E+02, .111243E+03, .119071E+03, .890955E+02, .452309E+02,
3 .801897E+01,-.188935E+02,-.362091E+02,-.423183E+02/
DATA(AP0( 5,II,1),II=1,14)/
1 .530251E-02, .631149E-02, .567025E-02, .631063E-02, .642757E-02,
2 .745704E-02, .745765E-02, .744112E-02, .543319E-02, .384935E-02,
3 .357035E-02, .474813E-02, .470801E-02, .402577E-02/
DATA(AP1( 5,II,1),II=1,14)/
1-.301012E+01,-.314932E+01,-.288585E+01,-.297314E+01,-.294998E+01,
2-.312837E+01,-.340118E+01,-.400053E+01,-.434188E+01,-.476304E+01,
3-.511992E+01,-.546902E+01,-.547651E+01,-.518597E+01/
DATA(AP2( 5,II,1),II=1,14)/
1-.100648E+02,-.593339E+01,-.184647E+02,-.208230E+02,-.251396E+02,
2-.285884E+02,-.235854E+02,-.661103E+01, .753362E+01, .233436E+02,
3 .358109E+02, .459553E+02, .465630E+02, .428635E+02/
DATA(AP0( 5,II,2),II=1,14)/
1 .213332E-01, .218194E-01, .220445E-01, .221952E-01, .208641E-01,
2 .222302E-01, .206679E-01, .218300E-01, .206205E-01, .222535E-01,
3 .212559E-01, .226851E-01, .226631E-01, .221491E-01/
DATA(AP1( 5,II,2),II=1,14)/
1-.467113E+01,-.474781E+01,-.485782E+01,-.482485E+01,-.487106E+01,
2-.532801E+01,-.537106E+01,-.540965E+01,-.498594E+01,-.488863E+01,
3-.458118E+01,-.464718E+01,-.473707E+01,-.475070E+01/

```

```

DATA(AP2( 5,II,2),II=1,14)/
1 .698411E+02, .735278E+02, .823352E+02, .792117E+02, .820433E+02,
2 .101158E+03, .109639E+03, .113613E+03, .101394E+03, .959909E+02,
3 .851783E+02, .840265E+02, .848359E+02, .860579E+02/
DATA(AP0( 5,II,3),II=1,14)/
1 .216360E-02, .252613E-02, .243287E-02, .203505E-02, .217221E-02,
2 .250725E-02, .285231E-02, .283535E-02, .221442E-02, .140123E-02,
3 .138194E-02, .167447E-02, .185960E-02, .199958E-02/
DATA(AP1( 5,II,3),II=1,14)/
1 .364530E+00, .250058E+00, .200781E+00, .377914E+00, .369878E+00,
2 .253479E+00, .259664E+00, .354560E+00, .563812E+00, .724637E+00,
3 .801812E+00, .821855E+00, .736571E+00, .606486E+00/
DATA(AP2( 5,II,3),II=1,14)/
1 .253087E+02, .304180E+02, .329616E+02, .246167E+02, .245082E+02,
2 .290459E+02, .297750E+02, .267562E+02, .203967E+02, .147463E+02,
3 .105930E+02, .801220E+01, .867920E+01, .117571E+02/
DATA(AP0( 5,II,4),II=1,14)/
1 .369072E-04, .128811E-03, .163922E-03, .192224E-03, .158638E-03,
2 .162653E-03, .109089E-03, .950568E-04, .586500E-04, .937454E-04,
3 .100427E-03, .160815E-03, .117744E-03, .628725E-04/
DATA(AP1( 5,II,4),II=1,14)/
1 .269434E+00, .472355E-01, -.130341E+00, -.210564E+00, -.295596E+00,
2 -.453673E+00, -.626022E+00, -.644099E+00, -.551388E+00, -.457505E+00,
3 -.345800E+00, -.243649E+00, -.928545E-01, -.281686E-01/
DATA(AP2( 5,II,4),II=1,14)/
1 -.290603E+02, -.217578E+02, -.144133E+02, -.844142E+01, -.337291E+01,
2 .454385E+01, .147025E+02, .173877E+02, .145079E+02, .105081E+02,
3 .573590E+01, .175353E+01, -.300645E+01, -.566026E+01/
DATA(AP0( 5,II,5),II=1,14)/
1 -.522497E-03, -.773386E-03, -.742097E-03, -.847531E-03, -.840365E-03,
2 -.840460E-03, -.746045E-03, -.725839E-03, -.663766E-03, -.705439E-03,
3 -.699825E-03, -.776348E-03, -.590300E-03, -.678939E-03/
DATA(AP1( 5,II,5),II=1,14)/
1 -.536254E+00, -.214852E+00, .116850E-01, .169956E+00, .353377E+00,
2 .574830E+00, .766668E+00, .698594E+00, .504059E+00, .364324E+00,
3 .215474E+00, .774442E-01, -.173673E+00, -.181793E+00/
DATA(AP2( 5,II,5),II=1,14)/
1 .325260E+02, .209129E+02, .102066E+02, -.129502E+00, -.991051E+01,
2 -.203219E+02, -.318251E+02, -.309465E+02, -.243826E+02, -.185328E+02,
3 -.127457E+02, -.817586E+01, -.201863E+01, -.731361E+00/
DATA(AP0( 5,II,6),II=1,14)/
1 -.100174E-02, -.178080E-02, -.116912E-02, -.116251E-02, -.116919E-02,
2 -.115331E-02, -.878954E-03, -.882538E-03, -.883539E-03, -.105523E-02,
3 -.901150E-03, -.924318E-03, -.622875E-03, -.101294E-02/
DATA(AP1( 5,II,6),II=1,14)/
1 .161161E+01, .103208E+01, .543891E+00, .268468E+00, -.148376E-01,
2 -.457653E+00, -.731765E+00, -.464233E+00, .680324E-01, .518917E+00,
3 .938501E+00, .140114E+01, .198143E+01, .191822E+01/
DATA(AP2( 5,II,6),II=1,14)/
1 -.762421E+02, -.517156E+02, -.289176E+02, -.702261E+01, .134353E+02,

```

ORIGINAL PAGE IS
OF POOR QUALITY

```

2 .404272E+02, .642061E+02, .609648E+02, .434433E+02, .268001E+02,
3 .109760E+02, -.497362E+01, -.226163E+02, -.205202E+02/
  DATA(AP0( 6,II,1),II=1,14)/
1 .527971E-02, .625793E-02, .557256E-02, .625319E-02, .636886E-02,
2 .734971E-02, .736241E-02, .734101E-02, .535291E-02, .378069E-02,
3 .351779E-02, .472933E-02, .473741E-02, .404546E-02/
  DATA(AP1( 6,II,1),II=1,14)/
1-.481502E+01, -.485671E+01, -.438181E+01, -.472244E+01, -.490823E+01,
2-.469394E+01, -.437584E+01, -.434178E+01, -.442096E+01, -.472490E+01,
3-.491476E+01, -.543589E+01, -.610878E+01, -.667485E+01/
  DATA(AP2( 6,II,1),II=1,14)/
1 .245232E+01, .582979E+01, -.100820E+02, -.103138E+02, -.501241E+01,
2-.155328E+02, -.283029E+02, -.332152E+02, -.314598E+02, -.235615E+02,
3-.237162E+02, -.133771E+02, .145343E+01, .157228E+02/
  DATA(AP0( 6,II,2),II=1,14)/
1 .214485E-01, .219549E-01, .221758E-01, .223350E-01, .209724E-01,
2 .223505E-01, .207712E-01, .219703E-01, .207491E-01, .224220E-01,
3 .213983E-01, .228480E-01, .228127E-01, .222846E-01/
  DATA(AP1( 6,II,2),II=1,14)/
1-.334375E+01, -.370789E+01, -.372335E+01, -.365798E+01, -.345779E+01,
2-.349026E+01, -.314678E+01, -.316717E+01, -.304924E+01, -.328885E+01,
3-.327544E+01, -.351546E+01, -.364997E+01, -.356023E+01/
  DATA(AP2( 6,II,2),II=1,14)/
1 .426487E+02, .546952E+02, .554779E+02, .519109E+02, .465085E+02,
2 .449392E+02, .318595E+02, .296749E+02, .249968E+02, .300891E+02,
3 .282754E+02, .333243E+02, .346482E+02, .297463E+02/
  DATA(AP0( 6,II,3),II=1,14)/
1 .215542E-02, .253224E-02, .246398E-02, .205251E-02, .219072E-02,
2 .254855E-02, .289103E-02, .289000E-02, .225653E-02, .145637E-02,
3 .141352E-02, .170773E-02, .188509E-02, .202184E-02/
  DATA(AP1( 6,II,3),II=1,14)/
1 .132904E+01, .140985E+01, .141011E+01, .156361E+01, .158546E+01,
2 .156942E+01, .147641E+01, .141747E+01, .145470E+01, .146654E+01,
3 .148161E+01, .144464E+01, .148671E+01, .147571E+01/
  DATA(AP2( 6,II,3),II=1,14)/
1 .152181E+02, .108607E+02, .110241E+02, .874567E+01, .949418E+01,
2 .116176E+02, .171765E+02, .200786E+02, .183815E+02, .175538E+02,
3 .175711E+02, .192793E+02, .157268E+02, .128406E+02/
  DATA(AP0( 6,II,4),II=1,14)/
1 .801936E-05, .115346E-03, .155747E-03, .170193E-03, .136524E-03,
2 .133435E-03, .909093E-04, .826168E-04, .583829E-04, .961691E-04,
3 .100016E-03, .154684E-03, .106283E-03, .534968E-04/
  DATA(AP1( 6,II,4),II=1,14)/
1-.207844E+00, -.111886E+00, -.988954E-02, -.622048E-01, -.683477E-01,
2-.595258E-01, -.859803E-01, -.136211E+00, -.173741E+00, -.222154E+00,
3-.267076E+00, -.299106E+00, -.183313E+00, -.103884E+00/
  DATA(AP2( 6,II,4),II=1,14)/
1-.222146E+01, -.324499E+01, -.463439E+01, -.342448E+01, -.268396E+01,
2-.201096E+01, .188654E+00, .270030E+01, .418855E+01, .571651E+01,
3 .728674E+01, .830979E+01, .411063E+01, .769141E+00/

```

DATA(APU(6,II,5),II=1,14)/
 1-.471401E-03,-.741545E-03,-.716226E-03,-.800356E-03,-.793895E-03,
 2-.786719E-03,-.716533E-03,-.712729E-03,-.668161E-03,-.717308E-03,
 3-.706730E-03,-.776854E-03,-.587360E-03,-.677585E-03/
 DATA(AP1(6,II,5),II=1,14)/
 1 .599718E+00, .645236E+00, .685913E+00, .737854E+00, .742114E+00,
 2 .718366E+00, .709403E+00, .717267E+00, .707289E+00, .730758E+00,
 3 .742838E+00, .769986E+00, .696121E+00, .618032E+00/
 DATA(AP2(6,II,5),II=1,14)/
 1-.559807E+01,-.808631E+01,-.787414E+01,-.898815E+01,-.988137E+01,
 2-.926432E+01,-.887606E+01,-.890055E+01,-.845648E+01,-.891935E+01,
 3-.920098E+01,-.105422E+02,-.867323E+01,-.345713E+01/
 DATA(AP0(6,II,6),II=1,14)/
 1-.114959E-02,-.190303E-02,-.126274E-02,-.128627E-02,-.128993E-02,
 2-.128946E-02,-.961471E-03,-.933265E-03,-.894791E-03,-.104951E-02,
 3-.898313E-03,-.943046E-03,-.640229E-03,-.100671E-02/
 DATA(AP1(6,II,6),II=1,14)/
 1 .813491E-02, .415575E-01,-.431792E-01,-.294801E+00,-.257872E+00,
 2-.440991E-01, .141762E+00, .437339E+00, .704338E+00, .913545E+00,
 3 .102595E+01, .117374E+01, .139356E+01, .127861E+01/
 DATA(AP2(6,II,6),II=1,14)/
 1 .262149E+01,-.186732E+00,-.191720E+01, .781068E+01, .789526E+01,
 2 .116059E+01,-.538165E+01,-.142219E+02,-.204025E+02,-.245607E+02,
 3-.261950E+02,-.302096E+02,-.340085E+02,-.265349E+02/
 DATA(AP0(7,II,1),II=1,14)/
 1 .524400E-02, .623395E-02, .559404E-02, .623173E-02, .637114E-02,
 2 .740905E-02, .741374E-02, .738124E-02, .537570E-02, .381362E-02,
 3 .354699E-02, .472920E-02, .469975E-02, .404337E-02/
 DATA(AP1(7,II,1),II=1,14)/
 1-.286206E+01,-.260807E+01,-.262220E+01,-.300581E+01,-.294977E+01,
 2-.311855E+01,-.309206E+01,-.321198E+01,-.313952E+01,-.314810E+01,
 3-.319840E+01,-.339332E+01,-.383559E+01,-.388157E+01/
 DATA(AP2(7,II,1),II=1,14)/
 1 .585472E+01,-.908989E+01,-.906853E+01, .161115E+01,-.217693E+01,
 2-.134720E+00,-.357149E+01,-.571969E+01,-.115653E+02,-.140927E+02,
 3-.147731E+02,-.116473E+02, .275441E+01, .860462E+01/
 DATA(AP0(7,II,2),II=1,14)/
 1 .214304E-01, .219287E-01, .221664E-01, .223247E-01, .209625E-01,
 2 .223475E-01, .207639E-01, .219557E-01, .207392E-01, .224116E-01,
 3 .213839E-01, .228118E-01, .227747E-01, .222490E-01/
 DATA(AP1(7,II,2),II=1,14)/
 1-.499621E+01,-.500211E+01,-.491334E+01,-.488661E+01,-.488405E+01,
 2-.518621E+01,-.512355E+01,-.520872E+01,-.510640E+01,-.541664E+01,
 3-.544594E+01,-.564190E+01,-.555003E+01,-.551627E+01/
 DATA(AP2(7,II,2),II=1,14)/
 1 .955659E+02, .935227E+02, .896974E+02, .865713E+02, .867104E+02,
 2 .949652E+02, .934741E+02, .947462E+02, .938368E+02, .105395E+03,
 3 .109755E+03, .115653E+03, .111661E+03, .111680E+03/
 DATA(AP0(7,II,3),II=1,14)/
 1 .217310E-02, .254370E-02, .246152E-02, .205985E-02, .219354E-02,

ORIGINAL PAGE IS
 OF POOR QUALITY

```

2 .253735E-02, .287904E-02, .287613E-02, .225064E-02, .146012E-02,
3 .141751E-02, .171093E-02, .188842E-02, .201737E-02/
DATA(AP1( 7,II,3),II=1,14)/
1 .508685E+00, .475706E+00, .395959E+00, .410897E+00, .435692E+00,
2 .355978E+00, .386869E+00, .378792E+00, .438168E+00, .440690E+00,
3 .423327E+00, .386267E+00, .406001E+00, .412686E+00/
DATA(AP2( 7,II,3),II=1,14)/
1 .193477E+02, .200188E+02, .216682E+02, .203411E+02, .189352E+02,
2 .209524E+02, .196126E+02, .201504E+02, .202238E+02, .227905E+02,
3 .247994E+02, .261162E+02, .237777E+02, .214072E+02/
DATA(AP0( 7,II,4),II=1,14)/
1 .874687E-06, .101545E-03, .141208E-03, .166004E-03, .133702E-03,
2 .126426E-03, .839406E-04, .778230E-04, .578999E-04, .106754E-03,
3 .123008E-03, .187478E-03, .122457E-03, .618271E-04/
DATA(AP1( 7,II,4),II=1,14)/
1 .810200E-03, .809500E-01, .147670E+00, .146761E+00, .146262E+00,
2 .149307E+00, .148151E+00, .134194E+00, .119454E+00, .487498E-01,
3 -.736349E-01, -.192086E+00, -.282205E+00, -.318439E+00/
DATA(AP2( 7,II,4),II=1,14)/
1 -.410135E+01, -.982986E+01, -.144214E+02, -.146713E+02, -.149621E+02,
2 -.156340E+02, -.160715E+02, -.158085E+02, -.160275E+02, -.139645E+02,
3 -.904788E+01, -.318984E+01, .343716E+01, .517350E+01/
DATA(AP0( 7,II,5),II=1,14)/
1 -.471456E-03, -.735654E-03, -.710456E-03, -.810312E-03, -.802672E-03,
2 -.792284E-03, -.716703E-03, -.714745E-03, -.670998E-03, -.729766E-03,
3 -.730175E-03, -.808467E-03, -.591711E-03, -.674988E-03/
DATA(AP1( 7,II,5),II=1,14)/
1 -.192374E+00, -.295685E+00, -.456639E+00, -.435131E+00, -.406803E+00,
2 -.397305E+00, -.397614E+00, -.395991E+00, -.404808E+00, -.317207E+00,
3 -.141135E+00, .567512E-01, .224490E+00, .327244E+00/
DATA(AP2( 7,II,5),II=1,14)/
1 -.113422E+01, .610229E+01, .148447E+02, .148230E+02, .145585E+02,
2 .152072E+02, .159556E+02, .161460E+02, .173443E+02, .150258E+02,
3 .785021E+01, -.202137E+01, -.136716E+02, -.172965E+02/
DATA(AP0( 7,II,6),II=1,14)/
1 -.111256E-02, -.185564E-02, -.122383E-02, -.124546E-02, -.126132E-02,
2 -.126850E-02, -.950041E-03, -.917687E-03, -.879268E-03, -.100998E-02,
3 -.833612E-03, -.853532E-03, -.619679E-03, -.102261E-02/
DATA(AP1( 7,II,6),II=1,14)/
1 .148000E+01, .190446E+01, .215578E+01, .226595E+01, .237310E+01,
2 .239467E+01, .241680E+01, .239250E+01, .239004E+01, .227001E+01,
3 .191171E+01, .158658E+01, .116680E+01, .854634E+00/
DATA(AP2( 7,II,6),II=1,14)/
1 -.159313E+02, -.360899E+02, -.518456E+02, -.560365E+02, -.606113E+02,
2 -.627160E+02, -.649437E+02, -.634394E+02, -.644730E+02, -.602771E+02,
3 -.449626E+02, -.265687E+02, -.132308E-01, .134099E+02/
DATA(AP0( 8,II,1),II=1,14)/
1 .523099E-02, .620971E-02, .554165E-02, .619789E-02, .636025E-02,
2 .737751E-02, .739463E-02, .735210E-02, .535428E-02, .375150E-02,
3 .348256E-02, .464256E-02, .460523E-02, .400411E-02/

```

```

DATA(AP1( 8,II,1),II=1,14)/
1-.492820E+01,-.460993E+01,-.374192E+01,-.296366E+01,-.266078E+01,
2-.250080E+01,-.225429E+01,-.227503E+01,-.278523E+01,-.341637E+01,
3-.394582E+01,-.409999E+01,-.349618E+01,-.285335E+01/
DATA(AP2( 8,II,1),II=1,14)/
1 .648791E+02, .683567E+02, .587025E+02, .357218E+02, .294361E+02,
2 .265945E+02, .216878E+02, .167824E+02, .364024E+02, .607197E+02,
3 .903967E+02, .103680E+03, .964398E+02, .715477E+02/
DATA(AP0( 8,II,2),II=1,14)/
1 .214233E-01, .219209E-01, .221491E-01, .222820E-01, .209147E-01,
2 .222909E-01, .207217E-01, .219159E-01, .206959E-01, .223561E-01,
3 .213400E-01, .227753E-01, .227319E-01, .222073E-01/
DATA(AP1( 8,II,2),II=1,14)/
1-.653013E+00,-.104546E+01,-.133068E+01,-.130233E+01,-.105465E+01,
2-.111247E+01,-.865187E+00,-.943992E+00,-.722946E+00,-.825152E+00,
3-.768174E+00,-.121158E+01,-.173059E+01,-.161280E+01/
DATA(AP2( 8,II,2),II=1,14)/
1-.252308E+02,-.878917E+01, .421814E+01, .864731E+01, .313755E+01,
2 .271671E+01,-.525293E+01,-.138038E+01,-.585995E+01,-.453025E+01,
3-.104012E+02,-.113803E+01, .113663E+02, .935969E+01/
DATA(APU( 8,II,3),II=1,14)/
1 .216472E-02, .253786E-02, .243857E-02, .203389E-02, .217676E-02,
2 .251203E-02, .286128E-02, .285507E-02, .223586E-02, .143032E-02,
3 .139497E-02, .168425E-02, .186721E-02, .201566E-02/
DATA(AP1( 8,II,3),II=1,14)/
1-.102912E+01,-.111005E+01,-.110232E+01,-.849783E+00,-.689352E+00,
2-.500810E+00,-.265448E+00,-.600086E-01, .928886E-02, .103791E+00,
3 .209799E+00, .362122E+00, .888524E+00, .135758E+01/
DATA(AP2( 8,II,3),II=1,14)/
1 .223881E+02, .323421E+02, .393758E+02, .355633E+02, .335278E+02,
2 .265898E+02, .171832E+02, .703692E+01, .561347E+01, .327090E+01,
3 .148591E+01,-.234396E+01,-.183110E+02,-.359758E+02/
DATA(AP0( 8,II,4),II=1,14)/
1 .243451E-04, .116495E-03, .162944E-03, .195734E-03, .157446E-03,
2 .159689E-03, .112717E-03, .102478E-03, .588302E-04, .813112E-04,
3 .921556E-04, .157923E-03, .107518E-03, .520516E-04/
DATA(AP1( 8,II,4),II=1,14)/
1 .110694E+00,-.123884E+00,-.207752E+00,-.223303E+00,-.165703E+00,
2-.235742E+00,-.419461E+00,-.661937E+00,-.640836E+00,-.396510E+00,
3-.120686E+00, .293085E-01, .158251E-01, .184428E-02/
DATA(AP2( 8,II,4),II=1,14)/
1-.240734E+02,-.137479E+02,-.698999E+01,-.130478E+01,-.231484E+01,
2 .219554E+01, .110141E+02, .242728E+02, .264459E+02, .193852E+02,
3 .885587E+01, .168010E+01, .938144E+00, .411169E+01/
DATA(AP0( 8,II,5),II=1,14)/
1-.503052E-03,-.751566E-03,-.740747E-03,-.843438E-03,-.819373E-03,
2-.819047E-03,-.747596E-03,-.740297E-03,-.666454E-03,-.688379E-03,
3-.690052E-03,-.773094E-03,-.581442E-03,-.669527E-03/
DATA(AP1( 8,II,5),II=1,14)/
1 .362717E-01, .307578E+00, .351230E+00, .453310E+00, .505981E+00,

```

ORIGINAL PAGE IS
OF POOR QUALITY


```

2 .737701E+00, .100038E+01, .128478E+01, .117222E+01, .895482E+00,
3 .640847E+00, .637425E+00, .973808E+00, .109096E+01/
DATA(AP2( 8,II,5),II=1,14)/
1 .289379E+02, .164855E+02, .786588E+01,-.153907E+01,-.265539E+01,
2-.121718E+02,-.236789E+02,-.391453E+02,-.372360E+02,-.277296E+02,
3-.159971E+02,-.120348E+02,-.186796E+02,-.260762E+02/
DATA(AP0( 8,II,6),II=1,14)/
1-.103519E-02,-.178994E-02,-.115619E-02,-.118024E-02,-.119604E-02,
2-.118230E-02,-.923415E-03,-.969388E-03,-.992930E-03,-.122011E-02,
3-.100164E-02,-.100936E-02,-.699393E-03,-.110448E-02/
DATA(AP1( 8,II,6),II=1,14)/
1 .181194E+01, .844292E+00,-.346396E+00,-.987271E+00,-.127940E+01,
2-.169569E+01,-.202815E+01,-.192084E+01,-.125578E+01,-.191868E+00,
3 .814185E+00, .159056E+01, .254472E+01, .282937E+01/
DATA(AP2( 8,II,6),II=1,14)/
1-.973141E+02,-.559730E+02, .465163E+01, .423355E+02, .572479E+02,
2 .842939E+02, .113383E+03, .128432E+03, .111918E+03, .741411E+02,
3 .364765E+02, .855711E+01,-.221640E+02,-.282930E+02/
DATA(AP0( 9,II,1),II=1,14)/
1 .524108E-02, .621925E-02, .556820E-02, .623727E-02, .637988E-02,
2 .739765E-02, .740448E-02, .737846E-02, .537703E-02, .379788E-02,
3 .352470E-02, .471728E-02, .468428E-02, .401115E-02/
DATA(AP1( 9,II,1),II=1,14)/
1-.164791E+01,-.132667E+01,-.108664E+01,-.116397E+01,-.934867E+00,
2-.800137E+00,-.633458E+00,-.663464E+00,-.774441E+00,-.116423E+01,
3-.141471E+01,-.189784E+01,-.216262E+01,-.265581E+01/
DATA(AP2( 9,II,1),II=1,14)/
1 .293288E+02, .209421E+02, .215411E+02, .217549E+02, .137713E+02,
2 .105980E+02, .890487E+01, .885943E+01, .110226E+02, .211515E+02,
3 .255128E+02, .376068E+02, .405798E+02, .496748E+02/
DATA(AP0( 9,II,2),II=1,14)/
1 .214426E-01, .219329E-01, .221754E-01, .223264E-01, .209666E-01,
2 .223489E-01, .207701E-01, .219655E-01, .207509E-01, .224232E-01,
3 .213982E-01, .228358E-01, .228024E-01, .222711E-01/
DATA(AP1( 9,II,2),II=1,14)/
1-.248768E+00,-.426986E+00,-.346148E+00,-.253276E+00,-.537806E-01,
2-.204410E+00, .243614E-01,-.927958E-01, .150431E-01,-.191871E+00,
3-.106567E+00,-.249634E+00,-.171413E+00, .295519E-01/
DATA(AP2( 9,II,2),II=1,14)/
1 .134426E+01, .583155E+01, .273437E+01, .933526E+00,-.460780E+01,
2-.724133E+00,-.786734E+01,-.399233E+01,-.658263E+01,-.892481E+00,
3-.353412E+01,-.624485E+00,-.397490E+01,-.111543E+02/
DATA(AP0( 9,II,3),II=1,14)/
1 .216384E-02, .252685E-02, .244488E-02, .205651E-02, .218628E-02,
2 .252326E-02, .286924E-02, .286894E-02, .224331E-02, .144740E-02,
3 .141657E-02, .171764E-02, .188794E-02, .202065E-02/
DATA(AP1( 9,II,3),II=1,14)/
1-.236751E+00,-.289709E+00,-.363544E+00,-.237384E+00,-.204209E+00,
2-.250211E+00,-.280117E+00,-.278982E+00,-.255438E+00,-.240894E+00,
3-.159491E+00,-.127442E+00,-.224752E+00,-.394108E+00/

```

```

DATA(AP2( 9,II,3),II=1,14)/
1 .132018E+01, .301873E+01, .528440E+01, .222072E+01, .224516E+01,
2 .470343E+01, .655248E+01, .643541E+01, .571929E+01, .502114E+01,
3 .148800E+01, -.724872E+00, .179522E+01, .764766E+01/
DATA(APU( 9,II,4),II=1,14)/
1 .454031E-05, .111308E-03, .150332E-03, .167039E-03, .134429E-03,
2 .127433E-03, .829716E-04, .766125E-04, .571135E-04, .982494E-04,
3 .104298E-03, .160825E-03, .114789E-03, .564711E-04/
DATA(API( 9,II,4),II=1,14)/
1-.107315E+00, -.118949E-01, .117247E+00, .540109E-01, .484608E-01,
2 .583664E-01, .343186E-01, .112277E-01, -.186125E-01, -.761927E-01,
3-.123899E+00, -.165442E+00, -.999932E-01, -.120928E+00/
DATA(AP2( 9,II,4),II=1,14)/
1 .127631E+01, -.120662E+01, -.425534E+01, -.241679E+01, -.224955E+01,
2-.243993E+01, -.133910E+01, -.853725E+00, -.334862E+00, .101680E+01,
3 .200211E+01, .304557E+01, .380468E+00, .165388E+01/
DATA(APU( 9,II,5),II=1,14)/
1-.472969E-03, -.747085E-03, -.720542E-03, -.808005E-03, -.798932E-03,
2-.787616E-03, -.713264E-03, -.711330E-03, -.669733E-03, -.719150E-03,
3-.706689E-03, -.776766E-03, -.587447E-03, -.680392E-03/
DATA(API( 9,II,5),II=1,14)/
1 .599942E+00, .663214E+00, .670662E+00, .670105E+00, .628092E+00,
2 .579198E+00, .585804E+00, .599637E+00, .609299E+00, .621574E+00,
3 .632170E+00, .657024E+00, .668867E+00, .625934E+00/
DATA(AP2( 9,II,5),II=1,14)/
1-.825793E+01, -.941618E+01, -.828155E+01, -.766575E+01, -.621656E+01,
2-.470782E+01, -.533589E+01, -.557190E+01, -.581656E+01, -.576261E+01,
3-.572764E+01, -.651231E+01, -.747309E+01, -.518420E+01/
DATA(AP0( 9,II,6),II=1,14)/
1-.112448E-02, -.186445E-02, -.121723E-02, -.126333E-02, -.127524E-02,
2-.127741E-02, -.946352E-03, -.918212E-03, -.887059E-03, -.103831E-02,
3-.887785E-03, -.922481E-03, -.636010E-03, -.100255E-02/
DATA(API( 9,II,6),II=1,14)/
1-.142877E+00, -.295053E+00, -.139787E+00, -.451356E-01, .113711E+00,
2 .344344E+00, .541952E+00, .724431E+00, .883266E+00, .112866E+01,
3 .123444E+01, .132745E+01, .136467E+01, .126672E+01/
DATA(AP2( 9,II,6),II=1,14)/
1 .101772E+02, .130301E+02, .248404E+01, -.122348E+01, -.597473E+01,
2-.118007E+02, -.161444E+02, -.189090E+02, -.205817E+02, -.263452E+02,
3-.279854E+02, -.300083E+02, -.319953E+02, -.226789E+02/
DATA(AP0(10,II,1),II=1,14)/
1 .526639E-02, .627883E-02, .563007E-02, .627866E-02, .640955E-02,
2 .742119E-02, .742314E-02, .738594E-02, .536875E-02, .377998E-02,
3 .351577E-02, .472499E-02, .474042E-02, .405207E-02/
DATA(API(10,II,1),II=1,14)/
1-.292158E+01, -.263945E+01, -.218385E+01, -.236740E+01, -.236321E+01,
2-.247131E+01, -.237453E+01, -.252026E+01, -.258077E+01, -.287170E+01,
3-.324240E+01, -.380200E+01, -.438199E+01, -.496683E+01/
DATA(AP2(10,II,1),II=1,14)/
1-.148668E+02, -.232558E+02, -.303077E+02, -.257211E+02, -.270245E+02,

```

ORIGINAL PAGE IS
OF POOR QUALITY

```

2-.244941E+02,-.277670E+02,-.244469E+02,-.251122E+02,-.200355E+02,
3-.131768E+02,.607036E-01,.141436E+02,.284202E+02/
DATA(AP0(10,II,2),II=1,14)/
1 .214693E-01,.219748E-01,.222131E-01,.223675E-01,.209979E-01,
2 .223834E-01,.207865E-01,.219851E-01,.207661E-01,.224485E-01,
3 .214189E-01,.228621E-01,.228200E-01,.222897E-01/
DATA(AP1(10,II,2),II=1,14)/
1-.788760E+00,-.990327E+00,-.108009E+01,-.102738E+01,-.889866E+00,
2-.980965E+00,-.773799E+00,-.829263E+00,-.797075E+00,-.110784E+01,
3-.115755E+01,-.140981E+01,-.124063E+01,-.968499E+00/
DATA(AP2(10,II,2),II=1,14)/
1-.182902E+02,-.133116E+02,-.102437E+02,-.113733E+02,-.151463E+02,
2-.155093E+02,-.230538E+02,-.226026E+02,-.221444E+02,-.121492E+02,
3-.772075E+01,.181053E+01,-.379952E+01,-.135633E+02/
DATA(APU(10,II,3),II=1,14)/
1 .215883E-02,.252651E-02,.245592E-02,.206860E-02,.220176E-02,
2 .253879E-02,.287779E-02,.287026E-02,.224418E-02,.144321E-02,
3 .141091E-02,.170323E-02,.188064E-02,.201651E-02/
DATA(AP1(10,II,3),II=1,14)/
1 .847381E+00,.844704E+00,.787897E+00,.863238E+00,.925879E+00,
2 .923105E+00,.951404E+00,.100163E+01,.105397E+01,.102016E+01,
3 .946887E+00,.917438E+00,.918961E+00,.820817E+00/
DATA(AP2(10,II,3),II=1,14)/
1 .521032E+01,.455223E+01,.494630E+01,.548225E+01,.477713E+01,
2 .447065E+01,.297594E+01,.104698E+01,-.379399E+00,.183194E+01,
3 .487058E+01,.591342E+01,.412443E+01,.645825E+01/
DATA(APU(10,II,4),II=1,14)/
1 .553696E-05,.110716E-03,.148194E-03,.168756E-03,.134557E-03,
2 .124912E-03,.827948E-04,.783427E-04,.604413E-04,.104831E-03,
3 .111579E-03,.176626E-03,.131037E-03,.617224E-04/
DATA(AP1(10,II,4),II=1,14)/
1-.153381E+00,-.354989E-02,.168232E+00,.974254E-01,.604760E-01,
2 .574537E-01,.559478E-01,.167523E-01,-.518460E-01,-.138770E+00,
3-.214413E+00,-.320725E+00,-.480995E+00,-.498950E+00/
DATA(AP2(10,II,4),II=1,14)/
1-.340361E+01,-.991434E+01,-.166088E+02,-.155943E+02,-.144159E+02,
2-.141649E+02,-.145314E+02,-.138114E+02,-.121807E+02,-.103169E+02,
3-.912924E+01,-.551559E+01,.394467E+01,.582265E+01/
DATA(AP0(10,II,5),II=1,14)/
1-.473844E-03,-.742636E-03,-.716541E-03,-.809229E-03,-.800927E-03,
2-.788439E-03,-.715943E-03,-.716818E-03,-.677457E-03,-.734895E-03,
3-.720925E-03,-.800688E-03,-.607417E-03,-.678404E-03/
DATA(AP1(10,II,5),II=1,14)/
1 .259829E+00,.242632E+00,.199373E+00,.230619E+00,.235197E+00,
2 .214702E+00,.182482E+00,.192928E+00,.228792E+00,.302982E+00,
3 .359948E+00,.488118E+00,.783637E+00,.782529E+00/
DATA(AP2(10,II,5),II=1,14)/
1-.450439E+01,-.157338E+00,.562413E+01,.659456E+01,.696038E+01,
2 .784133E+01,.970092E+01,.103129E+02,.100400E+02,.871299E+01,
3 .825135E+01,.308474E+01,-.134580E+02,-.137965E+02/

```

```

DATA(AP0(10,II,6),II=1,14)/
1-.114330E-02,-.188605E-02,-.123744E-02,-.125180E-02,-.126398E-02,
2-.127437E-02,-.945386E-03,-.906207E-03,-.862908E-03,-.100998E-02,
3-.855435E-03,-.872211E-03,-.597857E-03,-.101189E-02/
DATA(AP1(10,II,6),II=1,14)/
1 .836367E+00, .858297E+00, .107527E+01, .100315E+01, .102363E+01,
2 .119215E+01, .139665E+01, .164246E+01, .177618E+01, .187424E+01,
3 .182004E+01, .169683E+01, .128017E+01, .107082E+01/
DATA(AP2(10,II,6),II=1,14)/
1 .583099E+01,-.453747E+01,-.230280E+02,-.232237E+02,-.248752E+02,
2-.303053E+02,-.375614E+02,-.448536E+02,-.479219E+02,-.503696E+02,
3-.482365E+02,-.398689E+02,-.114930E+02, .732256E+01/
DATA(AP0(11,II,1),II=1,14)/
1 .527761E-02, .625613E-02, .559692E-02, .626762E-02, .640846E-02,
2 .740718E-02, .737337E-02, .731972E-02, .533221E-02, .378788E-02,
3 .354187E-02, .474862E-02, .476271E-02, .405454E-02/
DATA(AP1(11,II,1),II=1,14)/
1-.293982E+01,-.282130E+01,-.215223E+01,-.220542E+01,-.229764E+01,
2-.224804E+01,-.200479E+01,-.203899E+01,-.193441E+01,-.212220E+01,
3-.227345E+01,-.291319E+01,-.377554E+01,-.465898E+01/
DATA(AP2(11,II,1),II=1,14)/
1 .202431E+02, .176866E+02,-.186710E+01,-.547276E+01,-.247880E+01,
2-.553044E+01,-.148330E+02,-.169167E+02,-.239350E+02,-.245984E+02,
3-.311651E+02,-.205918E+02,-.386798E+01, .259664E+02/
DATA(AP0(11,II,2),II=1,14)/
1 .214949E-01, .219984E-01, .222288E-01, .223916E-01, .210161E-01,
2 .224004E-01, .208024E-01, .220127E-01, .207911E-01, .224751E-01,
3 .214372E-01, .228852E-01, .228437E-01, .222959E-01/
DATA(AP1(11,II,2),II=1,14)/
1-.142340E+01,-.166364E+01,-.169959E+01,-.169748E+01,-.151020E+01,
2-.156890E+01,-.130845E+01,-.136107E+01,-.129598E+01,-.154935E+01,
3-.158593E+01,-.182223E+01,-.187460E+01,-.159666E+01/
DATA(AP2(11,II,2),II=1,14)/
1-.123647E+02,-.631412E+01,-.441477E+01,-.321100E+01,-.859546E+01,
2-.899490E+01,-.179560E+02,-.166427E+02,-.177996E+02,-.908434E+01,
3-.552721E+01, .358084E+01, .686035E+01,-.358112E+01/
DATA(AP0(11,II,3),II=1,14)/
1 .216646E-02, .253527E-02, .246271E-02, .206727E-02, .220311E-02,
2 .255118E-02, .287936E-02, .286639E-02, .223533E-02, .144557E-02,
3 .140798E-02, .169749E-02, .186758E-02, .201034E-02/
DATA(AP1(11,II,3),II=1,14)/
1 .632074E+00, .649137E+00, .508320E+00, .613965E+00, .661120E+00,
2 .561466E+00, .471190E+00, .412323E+00, .455627E+00, .478486E+00,
3 .476434E+00, .419101E+00, .519416E+00, .626673E+00/
DATA(AP2(11,II,3),II=1,14)/
1-.343996E+01,-.481981E+01,-.368486E+00,-.207004E+01,-.222847E+01,
2 .315725E+01, .862205E+01, .118168E+02, .105895E+02, .100812E+02,
3 .114853E+02, .151608E+02, .110445E+02, .442938E+01/
DATA(AP0(11,II,4),II=1,14)/
1 .480379E-05, .110862E-03, .152614E-03, .171211E-03, .137811E-03,

```

ORIGINAL PAGE IS
OF POOR QUALITY

2 .134193E-03, .898346E-04, .802594E-04, .585042E-04, .109932E-03,
 3 .123284E-03, .184550E-03, .114165E-03, .548188E-04/
 DATA(AP1(11,II,4),II=1,14)/
 1-.105378E+00, .839890E-01, .262454E+00, .214660E+00, .231005E+00,
 2 .260962E+00, .301560E+00, .310294E+00, .276707E+00, .143547E+00,
 3-.452969E-01,-.177507E+00,-.155307E+00,-.634479E-01/
 DATA(AP2(11,II,4),II=1,14)/
 1 .214621E+01,-.483156E+01,-.100287E+02,-.782819E+01,-.804138E+01,
 2-.821900E+01,-.978143E+01,-.112138E+02,-.116063E+02,-.770041E+01,
 3 .253337E-01, .660542E+01, .996692E+01, .608891E+01/
 DATA(AP0(11,II,5),II=1,14)/
 1-.477112E-03,-.751394E-03,-.725987E-03,-.814814E-03,-.803744E-03,
 2-.791323E-03,-.715302E-03,-.709403E-03,-.668715E-03,-.734064E-03,
 3-.735416E-03,-.815277E-03,-.596124E-03,-.674845E-03/
 DATA(AP1(11,II,5),II=1,14)/
 1 .887707E+00, .849501E+00, .766267E+00, .777039E+00, .745986E+00,
 2 .703360E+00, .616334E+00, .557436E+00, .546530E+00, .685400E+00,
 3 .905779E+00, .109479E+01, .122678E+01, .113004E+01/
 DATA(AP2(11,II,5),II=1,14)/
 1-.793950E+01,-.333326E+01, .295515E+01, .234344E+01, .331536E+01,
 2 .440277E+01, .882916E+01, .128151E+02, .150506E+02, .105094E+02,
 3 .978365E+00,-.884411E+01,-.203481E+02,-.162235E+02/
 DATA(AP0(11,II,6),II=1,14)/
 1-.115311E-02,-.188187E-02,-.123361E-02,-.126349E-02,-.127988E-02,
 2-.129872E-02,-.976004E-03,-.948904E-03,-.902009E-03,-.102367E-02,
 3-.844518E-03,-.864381E-03,-.623791E-03,-.102423E-02/
 DATA(AP1(11,II,6),II=1,14)/
 1-.951800E+00,-.920370E+00,-.640108E+00,-.604132E+00,-.519572E+00,
 2-.235569E+00, .127371E+00, .556789E+00, .784323E+00, .720334E+00,
 3 .343751E+00, .571678E-01,-.213069E+00,-.278662E+00/
 DATA(AP2(11,II,6),II=1,14)/
 1 .575171E+01,-.246626E+01,-.206360E+02,-.218431E+02,-.241403E+02,
 2-.321737E+02,-.461115E+02,-.623753E+02,-.696289E+02,-.641129E+02,
 3-.432521E+02,-.242312E+02, .343302E+01, .148559E+02/
 DATA(AM0(1,II,1),II=1,14)/
 1 .326590E-02, .248931E-02, .310986E-02, .359460E-02, .356298E-02,
 2 .492329E-02, .337290E-02, .239619E-02, .108551E-02, .336949E-03,
 3 .605945E-03, .165957E-02, .253203E-02, .258097E-02/
 DATA(AM1(1,II,1),II=1,14)/
 1-.626948E+01,-.536432E+01,-.432798E+01,-.355441E+01,-.355496E+01,
 2-.378816E+01,-.376858E+01,-.355237E+01,-.355998E+01,-.382229E+01,
 3-.436626E+01,-.476869E+01,-.456739E+01,-.421495E+01/
 DATA(AM2(1,II,1),II=1,14)/
 1 .880602E+02, .651187E+02, .356295E+02, .113856E+02, .135254E+02,
 2 .229891E+02, .253907E+02, .137658E+02, .118781E+02, .210708E+02,
 3 .476937E+02, .737905E+02, .860642E+02, .671135E+02/
 DATA(AM0(1,II,2),II=1,14)/
 1-.183644E-03,-.982898E-03,-.565165E-03,-.202875E-03,-.481570E-03,
 2-.681361E-03,-.674225E-03,-.625867E-03,-.730615E-03,-.900126E-03,
 3-.108453E-02,-.119913E-02,-.118887E-02,-.116225E-02/

DATA(AM1(1,II,2),II=1,14)/
 1-.317026E+01,-.310011E+01,-.357414E+01,-.350535E+01,-.330617E+01,
 2-.330018E+01,-.337779E+01,-.340500E+01,-.318396E+01,-.297331E+01,
 3-.297670E+01,-.323152E+01,-.376581E+01,-.401038E+01/
 DATA(AM2(1,II,2),II=1,14)/
 1 .415192E+02, .424693E+02, .617099E+02, .630629E+02, .552960E+02,
 2 .533221E+02, .566771E+02, .622962E+02, .570131E+02, .491371E+02,
 3 .444787E+02, .483424E+02, .599650E+02, .664322E+02/
 DATA(AM0(1,II,3),II=1,14)/
 1 .901625E-03, .514678E-03, .478507E-03, .874695E-03, .855738E-03,
 2 .124660E-02, .558353E-03, .159074E-03,-.209762E-03,-.410157E-03,
 3-.214659E-03, .165274E-03, .323055E-03, .121095E-03/
 DATA(AM1(1,II,3),II=1,14)/
 1-.260660E+00,-.135045E+00, .382922E-01, .991239E-01, .289575E+00,
 2 .457184E+00, .625462E+00, .752999E+00, .928163E+00, .111732E+01,
 3 .120105E+01, .129523E+01, .185061E+01, .234541E+01/
 DATA(AM2(1,II,3),II=1,14)/
 1 .222686E+02, .250284E+02, .244566E+02, .290905E+02, .247415E+02,
 2 .190222E+02, .145023E+02, .116093E+02, .679954E+01, .228434E+00,
 3-.277688E+01,-.509949E+01,-.190894E+02,-.338605E+02/
 DATA(AM0(1,II,4),II=1,14)/
 1 .926630E-04, .107148E-03, .174296E-03, .215872E-03, .166948E-03,
 2 .143758E-03, .141181E-03, .151554E-03, .160021E-03, .184138E-03,
 3 .200648E-03, .241150E-03, .212966E-03, .225503E-03/
 DATA(AM1(1,II,4),II=1,14)/
 1-.181360E+00, .119191E-01,-.142049E-01,-.605881E-01,-.801190E-01,
 2-.238136E-03, .163286E+00, .312185E+00, .295737E+00, .121557E+00,
 3-.860812E-01,-.246554E+00,-.162633E+00,-.598997E-01/
 DATA(AM2(1,II,4),II=1,14)/
 1 .175451E+02, .900991E+01, .760955E+01, .672921E+01, .654784E+01,
 2 .172234E+01,-.729709E+01,-.158726E+02,-.173799E+02,-.115755E+02,
 3-.323380E+01, .490184E+01, .402236E+01,-.212005E+01/
 DATA(AM0(1,II,5),II=1,14)/
 1-.100914E-03,-.145037E-03,-.217618E-03,-.350576E-03,-.284192E-03,
 2-.269104E-03,-.267734E-03,-.287183E-03,-.308093E-03,-.346876E-03,
 3-.413667E-03,-.497072E-03,-.439508E-03,-.631323E-03/
 DATA(AM1(1,II,5),II=1,14)/
 1 .295332E-01,-.197574E+00,-.130446E+00,-.266501E-01,-.926974E-01,
 2-.342819E+00,-.667999E+00,-.890172E+00,-.892019E+00,-.734268E+00,
 3-.576296E+00,-.481957E+00,-.889431E+00,-.131819E+01/
 DATA(AM2(1,II,5),II=1,14)/
 1-.326946E+02,-.222800E+02,-.203919E+02,-.219919E+02,-.196185E+02,
 2-.897663E+01, .627398E+01, .165754E+02, .172479E+02, .102271E+02,
 3 .283144E+01,-.427261E+01, .461901E+01, .219178E+02/
 DATA(AM0(1,II,6),II=1,14)/
 1-.360324E-04,-.379771E-03,-.431323E-03,-.739758E-03,-.932922E-03,
 2-.116926E-02,-.131703E-02,-.133440E-02,-.134241E-02,-.127842E-02,
 3-.137055E-02,-.138048E-02,-.121819E-02,-.135390E-02/
 DATA(AM1(1,II,6),II=1,14)/
 1-.559300E+00, .644030E-01, .349964E+00, .687480E+00, .101333E+01,

ORIGINAL PAGE IS
 OF POOR QUALITY

2 .125690E+01, .148321E+01, .120314E+01, .520069E+00, -.432735E+00,
 3-.112358E+01, -.156123E+01, -.215177E+01, -.238607E+01/
 DATA(AM2(1, II, 6), II=1, 14)/
 1 .476141E+02, .192701E+02, -.563143E+01, -.282002E+02, -.439339E+02,
 2-.612440E+02, -.826692E+02, -.849683E+02, -.651974E+02, -.301286E+02,
 3-.495317E+01, .992606E+01, .306117E+02, .447419E+02/
 DATA(AMU(2, II, 1), II=1, 14)/
 1 .335026E-02, .260371E-02, .323377E-02, .370300E-02, .362512E-02,
 2 .495963E-02, .342045E-02, .246560E-02, .117223E-02, .453919E-03,
 3 .722375E-03, .179825E-02, .262373E-02, .263256E-02/
 DATA(AM1(2, II, 1), II=1, 14)/
 1-.351767E+01, -.325751E+01, -.302454E+01, -.346825E+01, -.339144E+01,
 2-.312826E+01, -.288379E+01, -.302628E+01, -.342627E+01, -.367136E+01,
 3-.431660E+01, -.483228E+01, -.545243E+01, -.554765E+01/
 DATA(AM2(2, II, 1), II=1, 14)/
 1 .558112E+02, .406484E+02, .256822E+02, .413330E+02, .316935E+02,
 2 .104506E+02, -.613245E+01, -.583860E+01, .615208E+01, .150621E+02,
 3 .379001E+02, .540769E+02, .763582E+02, .841407E+02/
 DATA(AM0(2, II, 2), II=1, 14)/
 1-.108329E-03, -.903028E-03, -.477133E-03, -.102653E-03, -.387720E-03,
 2-.573022E-03, -.591827E-03, -.537209E-03, -.654815E-03, -.813256E-03,
 3-.101560E-02, -.111607E-02, -.108471E-02, -.107575E-02/
 DATA(AM1(2, II, 2), II=1, 14)/
 1-.236007E+01, -.237023E+01, -.254726E+01, -.264037E+01, -.274044E+01,
 2-.291677E+01, -.301457E+01, -.298865E+01, -.280613E+01, -.256114E+01,
 3-.219057E+01, -.193189E+01, -.186143E+01, -.198928E+01/
 DATA(AM2(2, II, 2), II=1, 14)/
 1 .405615E+01, .778535E+01, .167176E+02, .174071E+02, .225541E+02,
 2 .342860E+02, .434565E+02, .468083E+02, .435201E+02, .353903E+02,
 3 .225512E+02, .121319E+02, .730120E+01, .112135E+02/
 DATA(AM0(2, II, 3), II=1, 14)/
 1 .923555E-03, .523104E-03, .491698E-03, .887399E-03, .871304E-03,
 2 .127704E-02, .587617E-03, .176224E-03, -.210474E-03, -.430596E-03,
 3-.228340E-03, .163712E-03, .327171E-03, .117260E-03/
 DATA(AM1(2, II, 3), II=1, 14)/
 1 .358279E+00, .277258E+00, .175915E+00, .304144E+00, .292425E+00,
 2 .147215E+00, .134291E+00, .171526E+00, .241984E+00, .508756E+00,
 3 .647087E+00, .781328E+00, .781775E+00, .685602E+00/
 DATA(AM2(2, II, 3), II=1, 14)/
 1 .111182E+02, .163115E+02, .226810E+02, .162339E+02, .158591E+02,
 2 .229516E+02, .269523E+02, .287064E+02, .271911E+02, .163973E+02,
 3 .888694E+01, .142356E+01, -.163726E+01, .417346E+00/
 DATA(AM0(2, II, 4), II=1, 14)/
 1 .978418E-04, .110671E-03, .182057E-03, .234033E-03, .183846E-03,
 2 .159324E-03, .149299E-03, .153687E-03, .157470E-03, .181141E-03,
 3 .205572E-03, .249229E-03, .216577E-03, .227190E-03/
 DATA(AM1(2, II, 4), II=1, 14)/
 1-.287349E+00, -.147184E+00, -.397518E-01, -.966243E-01, -.419389E-01,
 2 .131682E+00, .306081E+00, .379194E+00, .367257E+00, .283129E+00,
 3 .175802E+00, .814846E-01, -.348990E-01, -.125325E+00/

DATA(AM2(2,II,4),II=1,14)/
 1 .195348E+02, .138123E+02, .803785E+01, .900838E+01, .541401E+01,
 2-.271345E+01,-.114342E+02,-.155586E+02,-.162818E+02,-.131877E+02,
 3-.823770E+01,-.406430E+01,-.428056E+00, .246210E+01/
 DATA(AM0(2,II,5),II=1,14)/
 1-.107428E-03,-.151457E-03,-.229341E-03,-.359286E-03,-.294446E-03,
 2-.279566E-03,-.273776E-03,-.284133E-03,-.301859E-03,-.341955E-03,
 3-.418840E-03,-.501606E-03,-.447110E-03,-.636130E-03/
 DATA(AM1(2,II,5),II=1,14)/
 1 .225991E+00, .357984E-01,-.124337E+00,-.148278E+00,-.260312E+00,
 2-.502701E+00,-.733164E+00,-.817478E+00,-.775344E+00,-.639865E+00,
 3-.484873E+00,-.368716E+00,-.252051E+00,-.143863E+00/
 DATA(AM2(2,II,5),II=1,14)/
 1-.297134E+02,-.231643E+02,-.159532E+02,-.124697E+02,-.602338E+01,
 2 .500829E+01, .163382E+02, .208608E+02, .203079E+02, .147651E+02,
 3 .778065E+01, .317754E+01, .487477E+00,-.333288E+01/
 DATA(AM0(2,II,6),II=1,14)/
 1-.172000E-04,-.356843E-03,-.440082E-03,-.752051E-03,-.976377E-03,
 2-.126857E-02,-.139379E-02,-.144017E-02,-.143559E-02,-.137248E-02,
 3-.138754E-02,-.137875E-02,-.124629E-02,-.137104E-02/
 DATA(AM1(2,II,6),II=1,14)/
 1 .357459E-03, .473476E+00, .879225E+00, .109904E+01, .141943E+01,
 2 .199397E+01, .241654E+01, .240679E+01, .214658E+01, .172079E+01,
 3 .133000E+01, .944654E+00, .509174E+00, .429421E+00/
 DATA(AM2(2,II,6),II=1,14)/
 1 .536573E+02, .388702E+02, .219293E+02, .867091E+01,-.110078E+02,
 2-.408268E+02,-.663181E+02,-.709807E+02,-.650537E+02,-.504029E+02,
 3-.348932E+02,-.195644E+02,-.634561E+01,-.340669E+01/
 DATA(AM0(3,II,1),II=1,14)/
 1 .331459E-02, .259183E-02, .325234E-02, .369401E-02, .361413E-02,
 2 .496720E-02, .341830E-02, .244043E-02, .111081E-02, .369630E-03,
 3 .633330E-03, .173072E-02, .263822E-02, .262682E-02/
 DATA(AM1(3,II,1),II=1,14)/
 1-.375370E+01,-.258797E+01,-.218642E+01,-.307125E+01,-.351543E+01,
 2-.385410E+01,-.400208E+01,-.420825E+01,-.454888E+01,-.489361E+01,
 3-.547608E+01,-.596315E+01,-.636579E+01,-.553578E+01/
 DATA(AM2(3,II,1),II=1,14)/
 1 .475540E+00,-.368803E+02,-.362311E+02,-.647235E+01,-.124168E+01,
 2 .229337E+00,-.498300E+01,-.714022E+01,-.340897E+01, .475323E+01,
 3 .247251E+02, .424129E+02, .548978E+02, .846162E+01/
 DATA(AM0(3,II,2),II=1,14)/
 1-.176459E-03,-.970657E-03,-.542300E-03,-.175991E-03,-.458156E-03,
 2-.658386E-03,-.651213E-03,-.585979E-03,-.674513E-03,-.816928E-03,
 3-.102371E-02,-.114438E-02,-.112987E-02,-.109855E-02/
 DATA(AM1(3,II,2),II=1,14)/
 1-.402635E+01,-.467696E+01,-.465985E+01,-.420549E+01,-.386534E+01,
 2-.369278E+01,-.353823E+01,-.343287E+01,-.329390E+01,-.323738E+01,
 3-.322080E+01,-.332662E+01,-.356127E+01,-.340768E+01/
 DATA(AM2(3,II,2),II=1,14)/
 1 .744119E+02, .719129E+02, .662734E+02, .531048E+02, .438248E+02,

ORIGINAL PAGE IS
 OF POOR QUALITY

2 .403892E+02, .357240E+02, .316026E+02, .252610E+02, .218077E+02,
 3 .211569E+02, .235946E+02, .287655E+02, .266318E+02/
 DATA(AM0(3,II,3),II=1,14)/
 1 .912329E-03, .504247E-03, .477759E-03, .879200E-03, .861556E-03,
 2 .125786E-02, .573679E-03, .173143E-03, -.204269E-03, -.408314E-03,
 3 -.215478E-03, .173271E-03, .333317E-03, .117999E-03/
 DATA(AM1(3,II,3),II=1,14)/
 1 .710964E+00, .477333E+00, .355093E+00, .547576E+00, .749532E+00,
 2 .852241E+00, .938169E+00, .883985E+00, .852018E+00, .957060E+00,
 3 .103865E+01, .112911E+01, .110573E+01, .100375E+01/
 DATA(AM2(3,II,3),II=1,14)/
 1 .241638E+02, .317816E+02, .321784E+02, .258018E+02, .206164E+02,
 2 .190389E+02, .184755E+02, .226471E+02, .256975E+02, .231421E+02,
 3 .204041E+02, .159222E+02, .139999E+02, .171766E+02/
 DATA(AM0(3,II,4),II=1,14)/
 1 .101941E-03, .116468E-03, .189409E-03, .242717E-03, .195254E-03,
 2 .180184E-03, .166401E-03, .169337E-03, .160600E-03, .178051E-03,
 3 .192590E-03, .231643E-03, .208735E-03, .226451E-03/
 DATA(AM1(3,II,4),II=1,14)/
 1 .851889E-01, .264706E+00, .331875E+00, .236092E+00, .123460E+00,
 2 .912094E-02, -.509918E-01, -.103061E+00, -.137063E+00, -.163177E+00,
 3 -.162699E+00, -.178473E+00, -.310821E+00, -.244568E+00/
 DATA(AM2(3,II,4),II=1,14)/
 1 .567480E-01, -.579749E+01, -.812065E+01, -.423251E+01, -.697765E+00,
 2 .215694E+01, .280887E+01, .387295E+01, .525971E+01, .642758E+01,
 3 .594363E+01, .532403E+01, .973218E+01, .762179E+01/
 DATA(AM0(3,II,5),II=1,14)/
 1 -.111508E-03, -.160615E-03, -.239465E-03, -.367341E-03, -.311297E-03,
 2 -.320754E-03, -.302122E-03, -.309331E-03, -.305747E-03, -.331694E-03,
 3 -.396788E-03, -.474113E-03, -.439088E-03, -.639549E-03/
 DATA(AM1(3,II,5),II=1,14)/
 1 .715401E+00, .886206E+00, .104700E+01, .931743E+00, .784007E+00,
 2 .604000E+00, .563769E+00, .554369E+00, .572577E+00, .623701E+00,
 3 .642605E+00, .645526E+00, .542864E+00, .350677E+00/
 DATA(AM2(3,II,5),II=1,14)/
 1 -.110911E+02, -.157559E+02, -.184924E+02, -.162920E+02, -.126427E+02,
 2 -.920145E+01, -.506222E+01, -.354119E+01, -.301134E+01, -.460612E+01,
 3 -.571744E+01, -.635904E+01, -.348397E+01, .859340E+00/
 DATA(AM0(3,II,6),II=1,14)/
 1 -.212706E-04, -.372557E-03, -.438251E-03, -.739067E-03, -.955834E-03,
 2 -.121742E-02, -.136012E-02, -.140113E-02, -.142661E-02, -.138283E-02,
 3 -.142776E-02, -.142600E-02, -.126801E-02, -.135920E-02/
 DATA(AM1(3,II,6),II=1,14)/
 1 -.729826E+00, -.151909E+01, -.220498E+01, -.153377E+01, -.874091E+00,
 2 -.230243E+00, .220322E+00, .568713E+00, .751645E+00, .924027E+00,
 3 .101941E+01, .111938E+01, .176583E+01, .180110E+01/
 DATA(AM2(3,II,6),II=1,14)/
 1 .193997E+02, .396394E+02, .563187E+02, .345269E+02, .141039E+02,
 2 -.438428E+01, -.147371E+02, -.230076E+02, -.264332E+02, -.311133E+02,
 3 -.318396E+02, -.326661E+02, -.607863E+02, -.707490E+02/

DATA(AM0(4,II,1),II=1,14)/
1 .338344E-02, .261116E-02, .323349E-02, .371108E-02, .363436E-02,
2 .497579E-02, .342378E-02, .245678E-02, .115696E-02, .455602E-03,
3 .748207E-03, .183757E-02, .269119E-02, .267269E-02/
DATA(AM1(4,II,1),II=1,14)/
1-.179175E+01,-.153337E+01,-.133675E+01,-.178893E+01,-.176640E+01,
2-.165854E+01,-.131805E+01,-.129778E+01,-.131484E+01,-.130076E+01,
3-.144150E+01,-.177503E+01,-.240124E+01,-.280862E+01/
DATA(AM2(4,II,1),II=1,14)/
1 .187902E+02, .285319E+01,-.864881E+01, .690783E+01, .235147E+01,
2-.634607E+01,-.198033E+02,-.211863E+02,-.253909E+02,-.277998E+02,
3-.297860E+02,-.213708E+02,-.554821E+01, .127522E+02/
DATA(AM0(4,II,2),II=1,14)/
1-.101453E-03,-.891718E-03,-.470138E-03,-.977329E-04,-.394706E-03,
2-.590376E-03,-.602271E-03,-.533693E-03,-.640056E-03,-.779024E-03,
3-.986426E-03,-.108223E-02,-.107172E-02,-.105990E-02/
DATA(AM1(4,II,2),II=1,14)/
1-.150294E+01,-.135590E+01,-.139632E+01,-.158195E+01,-.153511E+01,
2-.147702E+01,-.140184E+01,-.135117E+01,-.132315E+01,-.142181E+01,
3-.149849E+01,-.158305E+01,-.156872E+01,-.144418E+01/
DATA(AM2(4,II,2),II=1,14)/
1-.888150E+01,-.156325E+02,-.173299E+02,-.129550E+02,-.151149E+02,
2-.168398E+02,-.194336E+02,-.210970E+02,-.210643E+02,-.166779E+02,
3-.108844E+02,-.546762E+01,-.529841E+01,-.117325E+02/
DATA(AM0(4,II,3),II=1,14)/
1 .911349E-03, .515570E-03, .493206E-03, .892088E-03, .874895E-03,
2 .127171E-02, .581596E-03, .173431E-03,-.203312E-03,-.411474E-03,
3-.210819E-03, .169207E-03, .322583E-03, .112562E-03/
DATA(AM1(4,II,3),II=1,14)/
1 .662072E+00, .596239E+00, .495351E+00, .571904E+00, .563946E+00,
2 .505558E+00, .599064E+00, .639140E+00, .628544E+00, .641497E+00,
3 .576884E+00, .502070E+00, .574638E+00, .731264E+00/
DATA(AM2(4,II,3),II=1,14)/
1-.416880E+00, .353929E+01, .791518E+01, .328417E+01, .360436E+01,
2 .673272E+01, .560293E+01, .558306E+01, .605650E+01, .719274E+01,
3 .100363E+02, .135020E+02, .922333E+01, .174315E+01/
DATA(AM0(4,II,4),II=1,14)/
1 .959719E-04, .112009E-03, .186653E-03, .242747E-03, .195701E-03,
2 .185088E-03, .169041E-03, .173708E-03, .165081E-03, .177277E-03,
3 .186270E-03, .222815E-03, .208298E-03, .216832E-03/
DATA(AM1(4,II,4),II=1,14)/
1-.251159E-01,-.468616E-02,-.259290E-01,-.749908E-01,-.822796E-01,
2-.996307E-01,-.150415E+00,-.202440E+00,-.239291E+00,-.217337E+00,
3-.163529E+00,-.142141E+00,-.153364E+00,-.385475E-01/
DATA(AM2(4,II,4),II=1,14)/
1 .101133E+01,-.113532E+01,-.155269E+01, .286142E+00, .558632E+00,
2 .131918E+01, .374034E+01, .634330E+01, .826151E+01, .744417E+01,
3 .523835E+01, .397432E+01, .312111E+01,-.199825E+01/
DATA(AM0(4,II,5),II=1,14)/
1-.110150E-03,-.160080E-03,-.239638E-03,-.378440E-03,-.318325E-03,

ORIGINAL PAGE IS
OF POOR QUALITY

2-.325456E-03,-.306755E-03,-.313214E-03,-.309711E-03,-.329928E-03,
 3-.389798E-03,-.463864E-03,-.434825E-03,-.624269E-03/
 DATA(AM1(4,II,5),II=1,14)/
 1-.228958E+00,-.213214E+00,-.166647E+00,-.160272E+00,-.174181E+00,
 2-.142253E+00,-.535761E-01,.527640E-02,.291519E-01,-.542303E-01,
 3-.158334E+00,-.215241E+00,-.245063E+00,-.407823E+00/
 DATA(AM2(4,II,5),II=1,14)/
 1-.355495E+01,-.343846E+01,-.474085E+01,-.465209E+01,-.444243E+01,
 2-.621993E+01,-.105209E+02,-.135066E+02,-.148693E+02,-.114258E+02,
 3-.696889E+01,-.410518E+01,-.124680E+01,.603952E+01/
 DATA(AM0(4,II,6),II=1,14)/
 1-.527453E-05,-.349867E-03,-.416585E-03,-.710086E-03,-.924854E-03,
 2-.117256E-02,-.133965E-02,-.139459E-02,-.143815E-02,-.140760E-02,
 3-.146409E-02,-.145917E-02,-.125848E-02,-.139163E-02/
 DATA(AM1(4,II,6),II=1,14)/
 1 .990160E+00,.107703E+01,.106753E+01,.119410E+01,.118869E+01,
 2 .114717E+01,.988079E+00,.860637E+00,.813063E+00,.978970E+00,
 3 .121766E+01,.134665E+01,.121146E+01,.157403E+01/
 DATA(AM2(4,II,6),II=1,14)/
 1-.567497E+00,-.288338E+01,-.252227E+01,-.571030E+01,-.477991E+01,
 2-.197165E+01,.561371E+01,.116249E+02,.125008E+02,.377683E+01,
 3-.775119E+01,-.154661E+02,-.170106E+02,-.347687E+02/
 DATA(AM0(5,II,1),II=1,14)/
 1 .339770E-02,.265574E-02,.328014E-02,.374291E-02,.366572E-02,
 2 .502220E-02,.345255E-02,.248721E-02,.116627E-02,.440784E-03,
 3 .691871E-03,.177668E-02,.264406E-02,.264104E-02/
 DATA(AM1(5,II,1),II=1,14)/
 1-.434904E+00,.439896E+00,.135946E+01,.122593E+01,.817474E+00,
 2 .401690E+00,.354610E-01,-.255297E+00,-.489749E+00,-.797209E+00,
 3-.115044E+01,-.140618E+01,-.171286E+01,-.164241E+01/
 DATA(AM2(5,II,1),II=1,14)/
 1-.167749E+01,-.240344E+02,-.422515E+02,-.336878E+02,-.205515E+02,
 2-.783335E+01,.540182E+01,.130350E+02,.179282E+02,.277952E+02,
 3 .385655E+02,.428626E+02,.394748E+02,.288521E+02/
 DATA(AM0(5,II,2),II=1,14)/
 1-.106130E-03,-.904663E-03,-.475353E-03,-.105788E-03,-.401587E-03,
 2-.592209E-03,-.606869E-03,-.545197E-03,-.645689E-03,-.783210E-03,
 3-.984958E-03,-.109064E-02,-.107277E-02,-.104998E-02/
 DATA(AM1(5,II,2),II=1,14)/
 1-.247782E+00,-.423794E+00,-.545865E+00,-.233648E-01,.379334E+00,
 2 .580566E+00,.715222E+00,.833947E+00,.985249E+00,.993023E+00,
 3 .104437E+01,.100739E+01,.930447E+00,.126968E+01/
 DATA(AM2(5,II,2),II=1,14)/
 1 .105931E+00,.531616E+01,.706176E+01,-.653183E+01,-.171077E+02,
 2-.206178E+02,-.239927E+02,-.279819E+02,-.337856E+02,-.337753E+02,
 3-.350919E+02,-.333518E+02,-.305453E+02,-.397578E+02/
 DATA(AM0(5,II,3),II=1,14)/
 1 .901935E-03,.507261E-03,.486960E-03,.878503E-03,.862534E-03,
 2 .126025E-02,.577159E-03,.175259E-03,-.203382E-03,-.412207E-03,
 3-.221227E-03,.170830E-03,.340897E-03,.120931E-03/

```

DATA(AM1(5,II,3),II=1,14)/
1-.461732E+00,-.651524E+00,-.809499E+00,-.720549E+00,-.564554E+00,
2-.466605E+00,-.418549E+00,-.415175E+00,-.365350E+00,-.334899E+00,
3-.338974E+00,-.309792E+00,-.168286E+00,-.144907E+00/
DATA(AM2(5,II,3),II=1,14)/
1.945500E+01,.148706E+02,.163799E+02,.143378E+02,.107095E+02,
2.832965E+01,.865182E+01,.891481E+01,.650775E+01,.584170E+01,
3.651190E+01,.623471E+01,.107252E+01,-.394607E+00/
DATA(AM0(5,II,4),II=1,14)/
1.103327E-03,.120071E-03,.193167E-03,.242337E-03,.194141E-03,
2.183436E-03,.166374E-03,.170271E-03,.162334E-03,.178080E-03,
3.191930E-03,.229948E-03,.210832E-03,.225699E-03/
DATA(AM1(5,II,4),II=1,14)/
1.137251E+00,.322986E+00,.377921E+00,.312255E+00,.214995E+00,
2.104479E+00,.254209E-01,-.317025E-01,-.769318E-01,-.133581E+00,
3-.186665E+00,-.235339E+00,-.241812E+00,-.146299E+00/
DATA(AM2(5,II,4),II=1,14)/
1-.443534E+01,-.113545E+02,-.124134E+02,-.911354E+01,-.612770E+01,
2-.325907E+01,-.160285E+01,-.654974E+00,.379540E+00,.217909E+01,
3.393012E+01,.514896E+01,.475235E+01,.170176E+01/
DATA(AM0(5,II,5),II=1,14)/
1-.102855E-03,-.151954E-03,-.236032E-03,-.372302E-03,-.313259E-03,
2-.320765E-03,-.301773E-03,-.308452E-03,-.304481E-03,-.332082E-03,
3-.396926E-03,-.478504E-03,-.441940E-03,-.635487E-03/
DATA(AM1(5,II,5),II=1,14)/
1.768753E+00,.908785E+00,.103406E+01,.925211E+00,.826585E+00,
2.760062E+00,.701387E+00,.673532E+00,.666475E+00,.691611E+00,
3.722761E+00,.739889E+00,.574685E+00,.307989E+00/
DATA(AM2(5,II,5),II=1,14)/
1-.118214E+02,-.145465E+02,-.152868E+02,-.134467E+02,-.118630E+02,
2-.103599E+02,-.829961E+01,-.640542E+01,-.532805E+01,-.565026E+01,
3-.708075E+01,-.816539E+01,-.388299E+01,.364573E+01/
DATA(AM0(5,II,6),II=1,14)/
1-.245304E-04,-.372888E-03,-.432364E-03,-.728331E-03,-.941173E-03,
2-.118603E-02,-.135060E-02,-.140112E-02,-.143675E-02,-.138963E-02,
3-.142398E-02,-.141131E-02,-.123881E-02,-.136124E-02/
DATA(AM1(5,II,6),II=1,14)/
1-.988860E+00,-.167264E+01,-.205538E+01,-.137455E+01,-.902284E+00,
2-.425237E+00,.412491E-01,.481535E+00,.836508E+00,.110867E+01,
3.130041E+01,.139466E+01,.163961E+01,.171428E+01/
DATA(AM2(5,II,6),II=1,14)/
1.290474E+02,.454322E+02,.486614E+02,.299003E+02,.185213E+02,
2.718639E+01,-.503883E+01,-.165829E+02,-.252311E+02,-.312388E+02,
3-.352041E+02,-.352407E+02,-.360032E+02,-.360610E+02/
DATA(AM0(6,II,1),II=1,14)/
1.338778E-02,.262791E-02,.325397E-02,.369854E-02,.360692E-02,
2.495501E-02,.339499E-02,.241822E-02,.111645E-02,.398050E-03,
3.701661E-03,.178845E-02,.264856E-02,.264056E-02/
DATA(AM1(6,II,1),II=1,14)/
1-.257721E+01,-.154964E+01,-.537655E+00,-.100952E+01,-.163152E+01,

```

```

2-.201049E+01,-.212104E+01,-.210928E+01,-.227618E+01,-.254890E+01,
3-.301639E+01,-.356403E+01,-.493694E+01,-.495652E+01/
DATA(AM2(6,II,1),II=1,14)/
1 .187245E+02,-.101864E+02,-.361930E+02,-.203298E+02,-.183687E+01,
2 .655882E+01, .542069E+01,-.407103E+01,-.630564E+01,-.415885E+01,
3 .718231E+01, .200935E+02, .613709E+02, .553231E+02/
DATA(AM0(6,II,2),II=1,14)/
1-.160058E-03,-.960569E-03,-.550530E-03,-.172817E-03,-.448493E-03,
2-.648450E-03,-.643636E-03,-.584498E-03,-.678204E-03,-.821918E-03,
3-.103009E-02,-.114702E-02,-.113129E-02,-.109050E-02/
DATA(AM1(6,II,2),II=1,14)/
1-.388391E+01,-.405115E+01,-.412750E+01,-.360084E+01,-.318426E+01,
2-.297767E+01,-.279826E+01,-.272233E+01,-.266783E+01,-.272501E+01,
3-.265523E+01,-.259454E+01,-.244658E+01,-.229369E+01/
DATA(AM2(6,II,2),II=1,14)/
1 .698369E+02, .724132E+02, .707370E+02, .557882E+02, .450272E+02,
2 .408140E+02, .351481E+02, .324032E+02, .309782E+02, .343943E+02,
3 .331905E+02, .316618E+02, .253206E+02, .211794E+02/
DATA(AM0(6,II,3),II=1,14)/
1 .904860E-03, .509332E-03, .497887E-03, .879852E-03, .858279E-03,
2 .125555E-02, .574119E-03, .173703E-03,-.197720E-03,-.404779E-03,
3-.209533E-03, .164680E-03, .325048E-03, .116325E-03/
DATA(AM1(6,II,3),II=1,14)/
1 .308002E+00, .170809E+00,-.387187E-01, .197293E-01, .133705E+00,
2 .223828E+00, .278674E+00, .309853E+00, .346603E+00, .380389E+00,
3 .371415E+00, .442744E+00, .687419E+00, .663358E+00/
DATA(AM2(6,II,3),II=1,14)/
1 .712052E+01, .995565E+01, .134089E+02, .131423E+02, .116856E+02,
2 .103385E+02, .127687E+02, .138565E+02, .139485E+02, .123682E+02,
3 .131585E+02, .985269E+01,-.147868E+01,-.234948E+01/
DATA(AM0(6,II,4),II=1,14)/
1 .104843E-03, .122099E-03, .194791E-03, .241580E-03, .191450E-03,
2 .179481E-03, .160969E-03, .158298E-03, .147873E-03, .163368E-03,
3 .187806E-03, .231445E-03, .210160E-03, .222075E-03/
DATA(AM1(6,II,4),II=1,14)/
1 .108379E+00, .232455E+00, .213146E+00, .690013E-01,-.540148E-01,
2-.152943E+00,-.200389E+00,-.194584E+00,-.200739E+00,-.194707E+00,
3-.209145E+00,-.257646E+00,-.401805E+00,-.286309E+00/
DATA(AM2(6,II,4),II=1,14)/
1-.485279E+01,-.913004E+01,-.775317E+01,-.647846E+00, .390020E+01,
2 .638466E+01, .725982E+01, .576912E+01, .506187E+01, .199525E+01,
3-.497381E-01,-.606233E+00, .485894E+01, .209635E+01/
DATA(AM0(6,II,5),II=1,14)/
1-.115143E-03,-.157665E-03,-.238466E-03,-.366398E-03,-.304410E-03,
2-.311123E-03,-.291645E-03,-.290841E-03,-.283903E-03,-.314367E-03,
3-.397348E-03,-.485969E-03,-.443446E-03,-.632493E-03/
DATA(AM1(6,II,5),II=1,14)/
1 .524783E+00, .753471E+00, .956670E+00, .844114E+00, .725644E+00,
2 .599396E+00, .442787E+00, .284258E+00, .184972E+00, .139276E+00,
3 .149867E+00, .177951E+00, .150750E+00,-.963906E-01/

```

C-5

```

DATA(AM2(6,II,5),II=1,14)/
1-.101425E+02,-.221900E+02,-.266754E+02,-.269421E+02,-.254836E+02,
2-.217007E+02,-.159507E+02,-.864334E+01,-.288497E+01, .301015E+01,
3 .575250E+01, .698654E+01, .620233E+01, .113766E+02/
DATA(AM0(6,II,6),II=1,14)/
1-.319909E-04,-.376249E-03,-.440577E-03,-.740588E-03,-.968182E-03,
2-.122580E-02,-.137875E-02,-.143930E-02,-.147474E-02,-.142000E-02,
3-.141983E-02,-.139231E-02,-.123041E-02,-.135762E-02/
DATA(AM1(6,II,6),II=1,14)/
1-.390492E+00,-.124080E+01,-.181522E+01,-.121621E+01,-.717006E+00,
2-.126791E+00, .484817E+00, .119080E+01, .176293E+01, .216275E+01,
3 .235251E+01, .239589E+01, .241586E+01, .261598E+01/
DATA(AM2(6,II,6),II=1,14)/
1 .408300E+02, .634745E+02, .748682E+02, .635095E+02, .532551E+02,
2 .374399E+02, .227810E+02, .167520E+01,-.173712E+02,-.381263E+02,
3-.512806E+02,-.577121E+02,-.558101E+02,-.591014E+02/
DATA(AM0(7,II,1),II=1,14)/
1 .342116E-02, .266125E-02, .329332E-02, .372842E-02, .364093E-02,
2 .498702E-02, .341032E-02, .242685E-02, .110722E-02, .400649E-03,
3 .688688E-03, .179371E-02, .264489E-02, .265499E-02/
DATA(AM1(7,II,1),II=1,14)/
1-.207442E+01,-.109500E+01,-.515314E+00,-.753750E+00,-.136599E+01,
2-.176149E+01,-.183777E+01,-.187837E+01,-.213578E+01,-.273265E+01,
3-.330453E+01,-.405089E+01,-.509586E+01,-.446118E+01/
DATA(AM2(7,II,1),II=1,14)/
1-.219163E+02,-.471764E+02,-.514954E+02,-.413046E+02,-.219258E+02,
2-.114574E+02,-.120642E+02,-.193231E+02,-.211504E+02,-.902791E+01,
3 .527454E+01, .282141E+02, .576029E+02, .299136E+02/
DATA(AM0(7,II,2),II=1,14)/
1-.174940E-03,-.964183E-03,-.526491E-03,-.157722E-03,-.440416E-03,
2-.637902E-03,-.633904E-03,-.566607E-03,-.661755E-03,-.816127E-03,
3-.103301E-02,-.115307E-02,-.111883E-02,-.108888E-02/
DATA(AM1(7,II,2),II=1,14)/
1-.259395E+01,-.266568E+01,-.276735E+01,-.237158E+01,-.204357E+01,
2-.193694E+01,-.185550E+01,-.185440E+01,-.179332E+01,-.178065E+01,
3-.107467E+01,-.157546E+01,-.160425E+01,-.137715E+01/
DATA(AM2(7,II,2),II=1,14)/
1 .391290E+02, .376917E+02, .376105E+02, .276744E+02, .196593E+02,
2 .188453E+02, .164114E+02, .168279E+02, .163775E+02, .185831E+02,
3 .104742E+02, .122655E+02, .115321E+02, .713237E+01/
DATA(AM0(7,II,3),II=1,14)/
1 .893980E-03, .493666E-03, .478203E-03, .884489E-03, .865485E-03,
2 .125929E-02, .567201E-03, .161654E-03,-.215403E-03,-.424432E-03,
3-.226568E-03, .168832E-03, .335396E-03, .121812E-03/
DATA(AM1(7,II,3),II=1,14)/
1 .713989E-01,-.283390E-01,-.204546E+00,-.147960E+00,-.773846E-01,
2-.452777E-01, .600213E-01, .529526E-01, .563463E-01, .130802E+00,
3 .311546E+00, .518134E+00, .667092E+00, .518053E+00/
DATA(AM2(7,II,3),II=1,14)/
1 .225172E+02, .236150E+02, .248197E+02, .230749E+02, .229822E+02,

```

```

2 .236795E+02, .215385E+02, .230914E+02, .254846E+02, .252284E+02,
3 .193963E+02, .102846E+02, .187626E+01, .493028E+01/
  DATA(AM0(7,II,4),II=1,14)/
1 .105109E-03, .121792E-03, .195639E-03, .241439E-03, .188340E-03,
2 .174235E-03, .159521E-03, .159561E-03, .149034E-03, .162173E-03,
3 .187323E-03, .234341E-03, .212783E-03, .223391E-03/
  DATA(AM1(7,II,4),II=1,14)/
1 .174631E-01, .180347E+00, .247761E+00, .184183E+00, .995514E-01,
2 .927905E-02, -.394623E-02, .349851E-01, .923677E-01, .905275E-01,
3 .512132E-01, -.200655E-01, -.130219E+00, -.706290E-01/
  DATA(AM2(7,II,4),II=1,14)/
1 .129921E+01, -.323047E+01, -.335527E+01, .195683E+01, .559977E+01,
2 .826289E+01, .753309E+01, .416903E+01, .440596E+00, -.115919E+01,
3 -.921049E+00, .576199E+00, .459841E+01, .385019E+01/
  DATA(AM0(7,II,5),II=1,14)/
1 -.122914E-03, -.164482E-03, -.243747E-03, -.366158E-03, -.300938E-03,
2 -.302666E-03, -.288937E-03, -.293649E-03, -.287226E-03, -.314784E-03,
3 -.394864E-03, -.488559E-03, -.450652E-03, -.636745E-03/
  DATA(AM1(7,II,5),II=1,14)/
1 .128858E+01, .147817E+01, .165186E+01, .153312E+01, .135488E+01,
2 .123456E+01, .105902E+01, .944029E+00, .832784E+00, .847335E+00,
3 .903821E+00, .985409E+00, .983973E+00, .647021E+00/
  DATA(AM2(7,II,5),II=1,14)/
1 -.157272E+02, -.227041E+02, -.277343E+02, -.286509E+02, -.251276E+02,
2 -.220992E+02, -.148223E+02, -.760817E+01, .309044E+00, .281011E+01,
3 .173421E+01, -.160557E+01, -.575718E+01, .288473E+01/
  DATA(AM0(7,II,6),II=1,14)/
1 -.598838E-05, -.365989E-03, -.430245E-03, -.746576E-03, -.973158E-03,
2 -.122925E-02, -.138309E-02, -.143850E-02, -.147676E-02, -.142077E-02,
3 -.142550E-02, -.138194E-02, -.120539E-02, -.134420E-02/
  DATA(AM1(7,II,6),II=1,14)/
1 -.227569E+01, -.316479E+01, -.378087E+01, -.306798E+01, -.253080E+01,
2 -.201021E+01, -.140112E+01, -.701372E+00, -.130051E+00, .991820E-01,
3 .137886E+00, .570033E-01, -.400623E-01, .382389E+00/
  DATA(AM2(7,II,6),II=1,14)/
1 .198724E+02, .512204E+02, .702886E+02, .569803E+02, .449827E+02,
2 .319272E+02, .130778E+02, -.115480E+02, -.330573E+02, -.416456E+02,
3 -.417445E+02, -.353300E+02, -.205340E+02, -.332344E+02/

```

C**** COMPUTE ANGLE OF ATTACK INDEX ****

```

DO 3 JCK=1,14
  IF(ALPH.LE.AL(JCK)) GO TO 4
3 CONTINUE
  JCK=14
4 IA=JCK-1
  IF(IA.LE.0) IA=1
  IB = IA+1
  DALPH=AL(IB)-AL(IA)
  IF(DALPH.EQ.0.) DALPH=1.
  RATIO = (ALPH-AL(IA))/DALPH

```

C**** BETA = 0 FITS ****

```

DO 5 ICK=1,15
IF(ID.EQ.JD(ICK)) GO TO 7
5 CONTINUE
PRINT 1000, ID
1000 FORMAT (28H0 ID NOT IN TABLE JD, ID =, I5)
CALL EXIT
7 I=ICK
DO 10 J=1,6
C**** INTERPOLATE LINEARLY FOR ALPHA ****
C I CONFIGURATION IDENTIFICATION NUMBER
C IA, IB ANGLE OF ATTACK IDENTIFICATION
C J COEFFICIENT IDENTIFICATION
A0(J)=A00(I, IA, J)+(A00(I, IB, J)-A00(I, IA, J))*RATIO
A1(J)=A01(I, IA, J)+(A01(I, IB, J)-A01(I, IA, J))*RATIO
A2(J)=A02(I, IA, J)+(A02(I, IB, J)-A02(I, IA, J))*RATIO
10 CONTINUE
C****BETA = +4 COEFFIECENTS ****
DO 20 ICK=1,11
IF(ID.EQ.KD(ICK)) GO TO 27
20 CONTINUE
PRINT 1001, ID
1001 FORMAT (28H0 ID NOT IN TABLE KD, ID =, I5)
27 I=ICK
DO 30 J=1,6
A4 (J)=AP0(I, IA, J)+(AP0(I, IB, J)-AP0(I, IA, J))*RATIO
A41(J)=AP1(I, IA, J)+(AP1(I, IB, J)-AP1(I, IA, J))*RATIO
A42(J)=AP2(I, IA, J)+(AP2(I, IB, J)-AP2(I, IA, J))*RATIO
30 CONTINUE
C**** BETA = -4 CURVE FITS
DO 40 ICK=1,7
IF(ID.EQ.LD(ICK)) GO TO 45
40 CONTINUE
PRINT 1002, ID
1002 FORMAT (28H0 ID NOT IN TABLE LD, ID =, I5)
DO 41 ICK=1,8
AM4(ICK)=-A4(ICK)
AM41(ICK)=-A41(ICK)
41 AM42(ICK)=-A42(ICK)
GO TO 51
45 I=ICK
DO 50 J=1,6
AM4(J)=AM0(I, IA, J)+(AM0(I, IB, J)-AM0(I, IA, J))*RATIO
AM41(J)=AM1(I, IA, J)+(AM1(I, IB, J)-AM1(I, IA, J))*RATIO
AM42(J)=AM2(I, IA, J)+(AM2(I, IB, J)-AM2(I, IA, J))*RATIO
50 CONTINUE
51 CONTINUE
100 DO 120 I=1,6
Y0(I)=A0(I)+XMR*(A1(I)+XMR*A2(I))
Y4(I)=A4(I)+XMR*(A41(I)+XMR*A42(I))
YM4(I)=AM4(I)+XMR*(AM41(I)+XMR*AM42(I))

```


120 CONTINUE
RETURN
END

GENERAL DYNAMICS
Convair Division